Alma Mater Studiorum Università degli Studi di Bologna
Dottorato di Ricerca in Meccanica delle Strutture
XVIII ciclo - a.a. 2005/2006

Theoretical and Numerical Analysis of a New Class of Exponential-Based Integration Algorithms for Elastoplasticity

Ph.D. candidate: Edoardo Artioli
Advisor: Professor Erasmo Viola
Co-Advisor: Professor Ferdinando Auricchio

"We are all faced throughout our lives with agonizing decisions, moral choices. Some are on a grand scale. Most of these choices are on lesser points.
But we define ourselves by the choices we have made.
We are in fact the sum total of our choices.
Events unfold so unpredictably, so unfairly, human happiness does not seem to have been included in the design of creation. It is only we with our capacity to love that give meaning to the indifferent universe.
And yet most human beings seem to have the ability to keep trying and even to find joy from simple things like their family, their work, and from the hope that future generations might understand more."
-Dr. Levy

Woody Allen's "Crimes and Misdemeanors", 1989

ACKNOWLEDGEMENTS

I would like to thank Professor Erasmo Viola who gave me the chance of continuing studying after graduating and of attending the Ph.D. program in Structural Mechanics at the University of Bologna.
I am deeply indebted to Professor Ferdinando Auricchio and I sincerely thank him for the support and scientific tuition he has been giving to me. I would like to thank him for he has taught me the meaning of excellence in research.
I would like to thank Professor Franco Brezzi, Professor Donatella Marini and Professor Carlo Lovadina for their unique kindness in accepting me within the academic environment of the Institute of Applied Mathematics and Information Technology and of the Department of Mathematics in Pavia.
I would like to thank Professor Fiorella Sgallari for the unvaluable support she has provided to let me visit and work in Pavia.
I also would like to thank Professor Phillip L. Gould of the Civil Engineering Department of the Washington University in St. Louis for the many useful scientific discussions and for being such a good friend to me since I was a simple undergraduate student.
A deep feeling of gratitude goes to my friend Lourenço Beirão da Veiga who has worked shoulder-to-shoulder with me since I first came to Pavia in January 2004.

Pavia, March 13th, 2006

Sommario

Il tema di ricerca su cui verte questa tesi è connesso alla modellazione costitutiva di materiali a comportamento inelastico non lineare. Il filone che si è scelto di approfondire riguarda lo studio, lo sviluppo e l'implementazione di nuovi algoritmi di integrazione per problemi algebrico-differenziali non lineari, inerenti la modellazione costitutiva di materiali elastoplastici tipo von-Mises con incrudimento.

La teoria della plasticità è, come noto, un argomento classico della Meccanica dei continui e si caratterizza per essere una disciplina che attrae l'interesse sia di ingegneri che di matematici. Tale caratteristica è sostanzialmente dovuta a ragioni di carattere storico e, nella fattispecie, allo sviluppo della teoria delle equazioni differenziali a derivate parziali e della teoria delle disequazioni variazionali riscontrato nella seconda metà del secolo scorso. Tale sviluppo ha infatti permesso una più profonda comprensione dei caratteri fisici fondamentali dei fenomeni elastoplastici ed ha messo a disposizione strumenti idonei alla analisi dei modelli costitutivi e delle formulazioni variazionali dei problemi meccanici di interesse ingegneristico.

È nota la elevata complessità ed il carattere prettamente nonlineare dei modelli matematici in discorso. Un filone di ricerca ormai di rilievo in questo settore è quindi quello dello sviluppo di robusti schemi di integrazione di tali modelli, in grado di fornire un'accurata approssimazione numerica del comportamento del materiale. Detti metodi risultano infatti essenziali nell' implementazione di codici di calcolo (ad esempio codici commerciali agli elementi finiti) per la risoluzione approssimata di problemi a valori iniziali e dati al bordo per materiali a comportamento elastoplastico.

Questo lavoro si colloca all'interno di questo ultimo settore di ricerca ed è strutturato in modo da fornire una introduzione al problema elastoplastico quanto più completa possibile. Il primo capitolo propone alcuni richiami essenziali di Meccanica dei solidi deformabili e di teoria dell'elasticità. Il secondo capitolo riguarda la cosiddetta teoria classica o teoria matematica della plasticità e si concentra sulla formulazione della legge costitutiva per materiali a comportamento elastoplastico di tipo von-Mises con incrudimento lineare e non lineare.

Il terzo capitolo propone la formulazione variazionale del problema a valori iniziali e dati al bordo dell'equilibrio di un continuo tridimensionale costituito da materiale elastoplastico. In tale capitolo sono forniti alcuni risultati di buona posizione del problema. Il quarto capitolo introduce alla risoluzione numerica del problema variazionale, utilizzando il metodo degli elementi finiti per la discretizzazione spaziale e schemi basati su metodi alle differenze finite

per la discretizzazione temporale.

Il capitolo quinto costituisce la parte innovativa della tesi ed è incentrato sulla famiglia di metodi d'integrazione cosiddetta a base esponenziale. La tecnica alla base di questi metodi prevede la riscrittura del modello costitutivo di von-Mises a partire dalla sua formulazione classica, mediante l'adozione di un opportuno fattore integrante scalare, che governa l'evoluzione temporale del flusso plastico. Il sistema dinamico governante, così riformulato, ammette una forma evolutiva caratteristica di tipo quasi-lineare e, sotto opportune ipotesi, può essere integrato nel tempo e risolto al passo, utilizzando la tecnica delle mappe esponenziali. I vantaggi offerti dalla nuova classe di metodi esponenziali sono evidenziati dall'analisi delle proprietà numeriche e dal confronto con i classici metodi alle differenze finite su esempi numerici. Il capitolo sesto presenta una serie di test numerici che hanno lo scopo di valutare la precisione e l'accuratezza dei nuovi algoritmi e quindi validarne l'applicabilità nella simulazione di problemi di interesse ingegneristico.

Completano la tesi due brevi appendici inerenti elementi introduttivi di Analisi funzionale e di teoria delle disequazioni variazionali. I contenuti delle appendici possono risultare utili nello studio della teoria matematica della plasticità affrontato nei Capitoli 2,3 e 4.

Abstract

The research theme upon which this thesis is based regards the constitutive modeling of nonlinear inelastic materials. The main topic is concerned with the analysis, the development and the implementation of a new class of integration algorithms for differential-algebraic nonlinear problems arising in the constitutive modeling of von-Mises elastoplastic hardening materials.

The theory of plasticity, as it is well known, is a classical part of continuum Mechanics and is characterized by being a discipline which attracts both the scientific interest of engineer scientists and mathematicians. This fact is mainly due to historical reasons and, in particular, to the development of the theory of partial differential equations and of the theory of variational inequalities taken place in the second half of the last century. This development has in fact made it possible a deeper comprehension of the fundamental physical meanings of elastoplastic phenomena and has provided useful theoretical tools for the analysis of the constitutive models and of the variational formulation of the mechanical problems of interest.

Given the high complexity and the preeminent nonlinear nature of such mathematical models, another relevant research challenge in this area is the development of rubust numerical methods for the integration of such models.

The numerical schemes in argument need to be as precise as possible in order to accurately reproduce the constitutive response of real elastoplastic materials in computational enviroments (such as commercial finite element codes).

This work is set within this last research field and is structured in such a way that the introduction of the elastoplastic constitutive problem remains as complete as possible, in order to carry out both the engineering and the mathematical aspects of the problem. The first chapter proposes some fundamental concepts of Mechanics of deformable material bodies and of theory of elasticity. The second chapter is centred on the so-called classical or mathematical theory of plasticity. This chapter focuses in particular on the formulation of the von-Mises constitutive law for elastoplastic materials with linear and nonlinear hardening.

The third chapter proposes the analysis of the variational formulation of the initial boundary value problem of equilibrium for three-dimensional continuum bodies constituted of elastoplastic material. In this chapter also some theoretical results on the well-posedness of the variational problem are exposed. The fourth chapter introduces to the numerical solution of the variational problem of elastoplastic equilibrium, within the context of a finite element space discretization and of classical finite difference time discretization schemes.

Chapter 5 constitutes the innovative part and, being the core of the thesis, focuses on the new class of exponential-based integration schemes for von-Mises elastoplastic models. The basic technique underneath the application of these schemes prescribes the rewriting of the original constitutive model using a suitable integration factor which governs the evolution of plastic flow. The ensuing differential-algebraic dynamical system results in a characteristic quasi-linear evolutive equation which, under proper hypotheses, may be integrated and solved stepwise, using exponential maps. The advantages granted by the new family of methods are made evident by the theoretical analysis of their numerical properties and by the comparison on numerical tests with the classical finite difference schemes. Chapter 6 presents an extensive series of numerical tests which aim to evaluate the precision and the order of accuracy of the new exponential-based algorithms and hence to validate them as feasible tools in practical simulation of problems of engineering interest.

The thesis is completed by two brief appendices concerning mathematical elements of functional analysis and of theory of variational inequalities. The contents of these last two sections may be of some value in the study of the mathematical theory of plasticity carried out in chapters 2, 3 and 4.

Contents

Chapter 1

Continuum Mechanics and Elasticity

Introduzione

Questo capitolo è dedicato ai concetti fondamentali della Meccanica dei solidi deformabili e della elasticità lineare. Segue un breve sommario dei contenuti del capitolo.

La Sezione 1.2 richiama gli elementi di algebra vettoriale e tensoriale che vengono utilizzati nella tesi. La Sezione 1.3 riguarda la Cinematica del corpo materiale. In detta sezione si definiscono le fondamentali misure di deformazione e viene messo in evidenza il caso delle deformazioni infinitesime. La Sezione 1.4 riguarda la formulazione dell'equilibrio per un corpo materiale. Vengono qui presentati gli assiomi dell'equilibrio statico e dell'equilibrio dinamico, le leggi di bilancio del momento lineare ed angolare, la forma locale dell'equazione di equilibrio. La Sezione 1.5 costituisce una breve presentazione della legge costitutiva per materiali a comportamento elastico lineare isotropo con un accenno alle proprietà fondamentali del tensore dei moduli elastici.

La Sezione 1.6 è incentrata sulla prima e sulla seconda legge della Termodinamica e tratta, in particolare, il caso di solidi costituiti da materiale elastico lineare isotropo soggetti a trasformazioni isoterme. La Sezione 1.7 presenta la formulazione locale negli spostamenti per il problema a valori iniziali e dati al bordo dell'equilibrio, per solidi deformabili di materiale elastico lineare isotropo. Da ultimo, la Sezione 1.8 introduce i concetti utilizzati nel capitolo seguente riguardante la teoria classica della plasticità. In tale sezione si presenta una trattazione termodinamica generale, adatta allo studio di materiali a comportamento inelastico non lineare. In particolare viene introdotta la cosiddetta teoria termodinamica a variabili interne. Per ovvie ragioni, la

trattazione di questa sezione si limita al caso della elasticità lineare.

Gli elementi di Meccanica del continuo ed elasticità richiamati nel presente capitolo sono tratti preminentemente da [14, 20], mentre gli argomenti di Termodinamica seguono principalmente la trattazione in [41].

1.1 Introduction

This chapter is devoted to fundamental concepts of Mechanics of deformable solids and of linear elasticity. In what follows we give a brief outline of the contents of the chapter.

In Section 1.2 we recall the elements of vector and tensor algebra that are used throughout the thesis. Section 1.3 is concerned with the kinematics of a deformable material body. In this section the fundamental strain measures are defined and special emphasis is given to the small deformation case. Section 1.4 regards the formulation of equilibrium for a material body. Here we present the axioms of static and dynamic equilibrium, the balance laws of linear and angular momentum and the local form of the equilibrium equation. Section 1.5 is a concise review of the constitutive law for linear elastic isotropic materials. In this section we briefly examine the basic properties of the elastic tensor and the form of the linear elastic constitutive law.

Section 1.6 focuses on the first and second laws of Thermodynamics and particularly on the special case of linear elastic bodies undergoing isothermal transformations. Section 1.7 presents the classical displacement local formulation of the equilibrium boundary value problem for a deformable body constituted of linear elastic material. Finally, Section 1.8 sets the stage for the later developments on the elastoplastic theory developed in Chapter 2. In fact, in this section, we give a general framework which is particularly suitable for studying nonlinear inelastic materials. For obvious reasons the treatment is momentarily dedicated to linear elasticity. In particular the so-called thermodynamic theory with interval variables is addressed. In this chapter the elements of continuum Mechanics and elasticity are basically taken from [14, 20], while the Thermodynamics arguments are presented following [41].

1.2 Preliminaries and notation

Vectors and tensors

In this work, we deal with different types of mathematical objects, namely with scalars, second-order tensors and fourth-order tensors as well as with

generalized vector and matrix operators. Scalars are indicated by italic letters like

$$a, \ \alpha, \ A$$

Vectors, second-order tensors and generalized vector operators are denoted by boldface letters like

$$\mathbf{a}, \ \boldsymbol{\alpha}, \ \mathbf{A}, \ \boldsymbol{\Sigma}$$

while fourth-order tensors and generalized matrix operators are indicated with uppercase boldblackboard letters like

$$\mathbb{A}, \ \mathbb{G}$$

The summation convention for repeated indices, or Einstein convention, will be used in our developments[1]

We refer to a three dimensional Euclidean space $\mathcal{R}^3$ and thus make use of a Cartesian coordinate system equipped with an orthonormal basis $(\mathbf{e}_1, \mathbf{e}_2, \mathbf{e}_3)$ chosen once and for all. Components of vectors and tensors are systematically referred to such a basis. The vector $\mathbf{a}$ of the space $\mathcal{R}^3$ is identified by the ordered set $\{a_i\}^T$, $1 \leq i \leq 3$, which defines its coordinates with respect to the above canonical basis and where i is the free index varying between 1 and 3, such that

$$\mathbf{a} = a_i \mathbf{e}_i$$

In the following we adopt the following *notations* for vectors of $\mathcal{R}^3$:

- Compact

$$\mathbf{a}$$

- Indicial

$$a_i = \mathbf{a}|_i$$

- Engineering

$$\{\mathbf{a}\} = \{a_1, a_2, a_3\}^T$$

The *scalar product* of two vectors $\mathbf{a}$ and $\mathbf{b}$ is denoted by $\mathbf{a} \cdot \mathbf{b}$ and is defined by:

$$\mathbf{a} \cdot \mathbf{b} = a_i b_i$$

[1]The summation convention requires that a repeated index in a multiplicative term implies the presence of a summation over the possible index range. Consistently, a non-repeated index in a multiplicative term implies that it may assume indifferently any value in the possible index range.

The *Euclidean norm* of a vector $\mathbf{a}$ is defined according to:

$$\| \mathbf{a} \| = (\mathbf{a} \cdot \mathbf{a})^{1/2}$$

The Euclidean space $\mathcal{R}^3$ with the natural operations introduced above forms a vector space, indicated in the following as $\mathbf{l}$in.

The cross product or vector product $\mathbf{c}$ of two vectors $\mathbf{a}$ and $\mathbf{b}$ is a vector $\mathbf{c} = \mathbf{a} \times \mathbf{b}$, orthogonal to both $\mathbf{a}$ and $\mathbf{b}$, with length equal to the area of the parallelogram defined by the vectors $\mathbf{a}$ and $\mathbf{b}$ and direction defined according to the right-hand rule. We then have the following expression in terms of components

$$\mathbf{c} = \mathbf{a} \times \mathbf{b} = (a_i \mathbf{e}_i) \times (a_j \mathbf{e}_j) = a_i b_j (\mathbf{e}_i \times \mathbf{e}_j) = a_i b_j \mathcal{E}_{ijk} \mathbf{e}_k$$

where, for $1 \leq i, j, k \leq 3$, $\mathcal{E}_{ijk}$ is the permutation symbol, i.e. $\mathcal{E}_{ijk} = +1$ for (i, j, k) a cyclic permutation, $\mathcal{E}_{ijk} = -1$ for (i, j, k) an anticyclic permutation and $\mathcal{E}_{ijk} = 0$ otherwise. The cross product returns a vector which is orthogonal to the plane containing the two original vectors. Second-order tensor are objects defined to generalized such a property in the sense that they operate on a vector returning a vector.

A second-order tensor $\boldsymbol{\tau}$ is defined as a linear operator mapping vectors into vectors. Clearly, dealing with a three-dimensional space, to completely define the action of a second-order tensor, it is necessary to consider at least the action on three independent vectors of $\mathbf{l}$in, such as the three basis vectors. Since the action of the second-order tensor on the three basis vectors is to return three new vectors, we may conclude that second-order tensors are in general identified through a set of nine scalar components. The space of second-order tensors with the natural operation defined in the following form a vector space, indicated in the sequel as $\mathbf{L}$in

The fundamental operation to construct the space of second-order tensor is the tensor product of two vectors $\mathbf{a}$ and $\mathbf{b}$, indicated as $\mathbf{a} \otimes \mathbf{b}$ and defined as

$$(\mathbf{a} \otimes \mathbf{b})\mathbf{c} = (\mathbf{b} \cdot \mathbf{c})\mathbf{a} \qquad \forall \mathbf{a}, \mathbf{b}, \mathbf{c} \in \mathbf{l}\text{in}$$

The tensor products $\mathbf{e}_i \otimes \mathbf{e}_j$ of the basis vectors of $\mathbf{l}$in are a set of second-order tensors, providing a suitable basis for expressing the components of a second-order tensor of the space $\mathbf{L}$in. In particular we define the ijth component of a tensor $\boldsymbol{\tau}$ as

$$\tau_{ij} = \mathbf{e}_i \cdot \boldsymbol{\tau} \mathbf{e}_j$$

which implies that the second-order tensor $\boldsymbol{\tau}$ can be expressed in component form as

$$\boldsymbol{\tau} = \tau_{ij}(\mathbf{e}_i \otimes \mathbf{e}_j)$$

In this work we adopt the following *notations* for a second-order tensor of the space $\mathbf{L}$in:

- Compact

$$\boldsymbol{\tau}$$

- Indicial

$$\tau_{ij} = \boldsymbol{\tau}|_{ij}$$

- Engineering

$$[\boldsymbol{\tau}] = \begin{bmatrix} \tau_{11} & \tau_{12} & \tau_{13} \\ \tau_{21} & \tau_{22} & \tau_{23} \\ \tau_{31} & \tau_{32} & \tau_{33} \end{bmatrix}$$

The transpose of a second-order tensor $\boldsymbol{\tau}$ is indicated in compact notation by $\boldsymbol{\tau}^T$ and defined by the following relation

$$\boldsymbol{\tau}^T|_{ij} = \tau_{ji}$$

The *trace* of a second-order tensor $\boldsymbol{\tau}$ is a scalar-valued function defined as

$$\mathrm{tr}(\boldsymbol{\tau}) = \tau_{ii}$$

We use the symbol $\mathbf{L}\mathrm{in}^{\mathrm{sym}}$ to indicate the subspace of $\mathbf{L}$in of symmetric second-order tensors, i.e.

$$\mathbf{L}\mathrm{in}^{\mathrm{sym}} = \{\boldsymbol{\tau} \in \mathbf{L}\mathrm{in} : \ \boldsymbol{\tau} = \boldsymbol{\tau}^T\} \tag{1.1}$$

We use the symbol $\mathbf{L}\mathrm{in}_0^{\mathrm{sym}}$ to indicate the subspace of $\mathbf{L}$in of symmetric second-order traceless tensors, i.e.

$$\mathbf{L}\mathrm{in}_0^{\mathrm{sym}} = \{\boldsymbol{\tau} \in \mathbf{L}\mathrm{in}^{\mathrm{sym}} : \ \mathrm{tr}(\boldsymbol{\tau}) = 0\} \tag{1.2}$$

The action of a second-order tensor $\boldsymbol{\tau}$ onto a vector $\mathbf{a}$ is a vector $\mathbf{b} \in \mathbf{l}$in

$$\mathbf{b} = \boldsymbol{\tau}\mathbf{a}$$

defined according to

$$\begin{aligned} b_i = (\boldsymbol{\tau}\mathbf{a}) \cdot \mathbf{e}_i &= [(\tau_{lm}\mathbf{e}_l \otimes \mathbf{e}_m)(a_k\mathbf{e}_k)] \cdot \mathbf{e}_i = \tau_{lm}a_k[(\mathbf{e}_l \otimes \mathbf{e}_m)\mathbf{e}_k] \cdot \mathbf{e}_i \\ &= \tau_{lm}a_k[\mathbf{e}_l(\mathbf{e}_m \cdot \mathbf{e}_k)] \cdot \mathbf{e}_i = \tau_{lm}a_k(\mathbf{e}_l \cdot \mathbf{e}_i)\delta_{mk} = \tau_{lk}a_k\delta_{li} = \tau_{ik}a_k \end{aligned}$$

The scalar product or double-dot product of two second-order tensors $\boldsymbol{\sigma}$ and $\boldsymbol{\tau}$

$$\boldsymbol{\sigma} : \boldsymbol{\tau}$$

is a scalar defined by

$$\boldsymbol{\sigma} : \boldsymbol{\tau} = \sigma_{ij}\tau_{ij}$$

It is noted that

$$\boldsymbol{\sigma} : \boldsymbol{\tau} = \mathrm{tr}(\boldsymbol{\tau}^T\boldsymbol{\sigma})$$

The multiplication or combination of two second-order tensors $\boldsymbol{\sigma}$ and $\boldsymbol{\tau}$ is a second-order tensor $\boldsymbol{\eta}$

$$\boldsymbol{\eta} = \boldsymbol{\sigma}\boldsymbol{\tau}$$

defined in the following manner

$$\eta_{ij} = \sigma_{ik}\tau_{kj}$$

The Euclidean norm of a second-order tensor $\boldsymbol{\tau}$ induced by the above scalar product is

$$\| \boldsymbol{\tau} \| = (\boldsymbol{\tau} : \boldsymbol{\tau})^{1/2}$$

The second-order identity tensor $\mathbf{I}$ is defined by the relation $\mathbf{Ia} = \mathbf{a}, \forall \mathbf{a} \in \mathbf{l}\mathrm{in}$. The components of the identity tensor are the Kronecker delta, that is

$$\delta_{ij} = \begin{cases} 1 & \text{if } \ j = i \\ 0 & \text{otherwise} \end{cases}$$

A unique additive decomposition of any second-order tensor $\boldsymbol{\tau}$ is given by the sum of its *deviatoric* part $\boldsymbol{\tau}_{\mathrm{dev}}$ and its *volumetric* or *spherical* part $\boldsymbol{\tau}_{\mathrm{vol}}$, respectively defined as

$$\boldsymbol{\tau}_{\mathrm{vol}} = \frac{1}{3}\mathrm{tr}(\boldsymbol{\tau})\mathbf{I} \qquad \boldsymbol{\tau}_{\mathrm{dev}} = \boldsymbol{\tau} - \frac{1}{3}\mathrm{tr}(\boldsymbol{\tau}) \tag{1.3}$$

This definition implies

$$\boldsymbol{\tau} = \boldsymbol{\tau}_{\mathrm{vol}} + \boldsymbol{\tau}_{\mathrm{vol}} \tag{1.4}$$

A fourth-order tensor is defined as a linear operator mapping the space of second-order tensors $\mathbf{L}\mathrm{in}$ onto itself. To properly define the action of a fourth-order tensor, it is necessary to consider the action on a second-order tensor

basis; since the action of a fourth-order tensor on a second-order tensor is to return a second-order tensor, we may conclude that fourth-order tensors are in general defined by a set of eighty-one scalar components. The space of fourth-order tensors with the natural operations introduced in the following form a vector space, indicated in the sequel by $\mathbb{L}\mathrm{in}$.

The fundamental operation to construct the space of fourth-order tensor is the *dyadic* product of two second-order tensors $\boldsymbol{\tau}$ and $\boldsymbol{\sigma}$, indicated as $\boldsymbol{\tau} \otimes \boldsymbol{\sigma}$ and defined as to return a fourth-order tensor:

$$\mathbb{D} = (\boldsymbol{\tau} \otimes \boldsymbol{\sigma}) \tag{1.5}$$

with $\mathbb{D} \in \mathbb{L}\mathrm{in}$ and such that

$$\mathbb{D}\boldsymbol{\eta} = (\boldsymbol{\tau} \otimes \boldsymbol{\sigma})\boldsymbol{\eta} = (\boldsymbol{\sigma} : \boldsymbol{\eta})\boldsymbol{\tau} = \mathrm{tr}(\boldsymbol{\eta}^T \boldsymbol{\sigma})\boldsymbol{\tau} \qquad \forall \boldsymbol{\eta} \in \mathbb{L}\mathrm{in} \tag{1.6}$$

The tensor products between the second-order basis tensor provide a suitable basis for expressing the components of a fourth-order tensor of the space $\mathbb{L}\mathrm{in}$. In particular we define the $ijkl$th component of a tensor $\mathbb{D}$ as

$$\mathbb{D}_{ijkl} = (\mathbf{e}_i \otimes \mathbf{e}_j) : \mathbb{D}(\mathbf{e}_k \otimes \mathbf{e}_l)$$

such that the fourth-order tensor $\mathbb{D}$ can be expressed in component form as

$$\mathbb{D} = \mathbb{D}_{ijkl}(\mathbf{e}_i \otimes \mathbf{e}_j) \otimes (\mathbf{e}_k \otimes \mathbf{e}_l)$$

In the following we will adopt the following *notations* for fourth-order tensor of the space $\mathbb{L}\mathrm{in}$:

- Compact

$$\mathbb{D}$$

- Indicial

$$\mathbb{D}_{ijkl} = \mathbb{D}|_{ijkl}$$

The action of a fourth-order tensor $\mathbb{D}$ on a second-order tensor $\boldsymbol{\tau}$ is denoted by

$$\boldsymbol{\sigma} = \mathbb{D}\boldsymbol{\tau} \tag{1.7}$$

with the following indicial representation

$$\begin{aligned} \sigma_{ij} &= [\mathbb{D}\boldsymbol{\tau}] : (\mathbf{e}_i \otimes \mathbf{e}_j) = [(\mathbb{D}_{abcd}\, \mathbf{e}_a \otimes \mathbf{e}_b \otimes \mathbf{e}_c \otimes \mathbf{e}_d)\, (\tau_{kl}\, \mathbf{e}_k \otimes \mathbf{e}_l)] : (\mathbf{e}_i \otimes \mathbf{e}_j) \\ &= [(\mathbb{D}_{abkl}\, \tau_{kl})\, \mathbf{e}_a \otimes \mathbf{e}_b] : (\mathbf{e}_i \otimes \mathbf{e}_j) = \mathbb{D}_{abkl}\, \tau_{kl} \end{aligned} \tag{1.8}$$

Besides the *dyadic tensor product* between second-order tensors, the so-called *square tensor products* can be also introduced as:

$$\mathbb{E} = \mathbf{A} \boxtimes \mathbf{B}$$
$$\mathbb{F} = \mathbf{A} \,\widehat{\boxtimes}\, \mathbf{B}$$

defined, according to Del Piero [29], such that:

$$\begin{aligned} (\mathbf{A} \boxtimes \mathbf{B})\mathbf{C} &= \mathbf{A}\mathbf{C}\mathbf{B}^T \\ (\mathbf{A} \,\widehat{\boxtimes}\, \mathbf{B})\mathbf{C} &= \mathbf{A}\mathbf{C}^T\mathbf{B}^T \end{aligned} \qquad \forall \mathbf{C} \in \mathbf{L}\text{in}$$

or, equivalently,

$$\begin{aligned} (\mathbf{A} \boxtimes \mathbf{B})|_{ijkl} &= \mathbf{A}_{ik}\mathbf{B}_{jl} \\ (\mathbf{A} \,\widehat{\boxtimes}\, \mathbf{B})|_{ijkl} &= \mathbf{A}_{il}\mathbf{B}_{jk} \end{aligned} \qquad \forall \mathbf{A}, \mathbf{B} \in \mathbf{L}\text{in}$$

The fourth-order identity tensor $\mathbb{I}$, is defined to satisfy the relation $\mathbb{I}\boldsymbol{\tau} = \boldsymbol{\tau}$, for any second-order tensor $\boldsymbol{\tau}$. The fourth-order identity tensor, in components form, can be shown to be given by

$$\mathbb{I} = \mathbf{e}_i \otimes \mathbf{e}_i \otimes \mathbf{e}_i \otimes \mathbf{e}_i$$

or, equivalently

$$\mathbb{I} = \delta_{ik}\delta_{jl}\mathbf{e}_i \otimes \mathbf{e}_j \otimes \mathbf{e}_k \otimes \mathbf{e}_l$$

Therefore we have

$$\mathbb{I}_{ijkl} = \delta_{ik}\delta_{jl}$$

The fourth-order symmetrized identity tensor $\mathbb{I}^I$, is defined to satisfy the relation $\mathbb{I}^I\boldsymbol{\tau} = \frac{1}{2}(\boldsymbol{\tau} + \boldsymbol{\tau}^T)$, for any second-order tensor $\boldsymbol{\tau}$. Accordingly, $\mathbb{I}^I$ is defined as:

$$\mathbb{I}^I = \frac{1}{2}\left[\mathbf{I} \boxtimes \mathbf{I} + \mathbf{I} \,\widehat{\boxtimes}\, \mathbf{I}\right]$$

or, in indicial notation as:

$$\mathbb{I}^I_{ijkl} = \frac{1}{2}\left[\mathbf{I}_{ik}\mathbf{I}_{jl} + \mathbf{I}_{il}\mathbf{I}_{jk}\right]$$

Therefore we have

$$\mathbb{I}^I\mathbf{A} \quad = \tfrac{1}{2}(\mathbf{A} + \mathbf{A}^T) \qquad \forall \mathbf{A} \in \mathbf{L}\text{in}$$

A splitting into volumetric and deviatoric parts of the fourth-order identity tensor of the form

$$\mathbb{I} = \mathbb{I}_{\text{vol}} + \mathbb{I}_{\text{dev}} \tag{1.9}$$

is achievable by setting

$$\begin{aligned} \mathbb{I}_{\text{vol}} &= \frac{1}{3}\left(\mathbf{I} \otimes \mathbf{I}\right) \\ \mathbb{I}_{\text{dev}} &= \mathbb{I} - \frac{1}{3}\left(\mathbf{I} \otimes \mathbf{I}\right) \end{aligned} \tag{1.10}$$

With the above positions, the volumetric and deviatoric part $\boldsymbol{\tau}_{\text{vol}}$ and $\boldsymbol{\tau}_{\text{dev}}$ of any second-order tensor $\boldsymbol{\tau}$ are respectively given by:

$$\begin{aligned} \boldsymbol{\tau}_{\text{vol}} &= \mathbb{I}_{\text{vol}}\boldsymbol{\tau} = \frac{1}{3}\,\text{tr}(\boldsymbol{\tau})\,\mathbf{I} = \frac{1}{3}\left(\boldsymbol{\tau} : \mathbf{I}\right)\mathbf{I} \\ \boldsymbol{\tau}_{\text{vol}} &= \mathbb{I}_{\text{dev}}\boldsymbol{\tau} = \boldsymbol{\sigma} - \boldsymbol{\tau}_{\text{vol}} \end{aligned} \tag{1.11}$$

Other than vectors and second-order tensor defined over the Euclidean space $\mathcal{R}^3$, in some selected cases we make use of algebraic vectors or m-tuples. For instance, the m-component algebraic vector $\boldsymbol{\xi}$ can be equivalently indicated in compact notation or in algebraic notation as $\boldsymbol{\xi} = (\boldsymbol{\xi}_k) = (\boldsymbol{\xi}_1, ..., \boldsymbol{\xi}_k, ...\boldsymbol{\xi}_m)$. It is noted that the components $\boldsymbol{\xi}_k$ $(1 \leq k \leq m)$ of such a vector may be objects of different type, namely scalars, vectors or tensors. The use of algebraic vectors will be specified whenever needed in order to avoid confusion. Similarly, in some cases, use will be made of algebraic or matrix operators. Such matrix operators will be in general represented in engineering notation as

$$[\mathbb{G}] = \begin{bmatrix} \mathbb{G}_{11} & \mathbb{G}_{12} \\ \mathbb{G}_{21} & \mathbb{G}_{22} \end{bmatrix}$$

It is noted that the components $\mathbb{G}_{ij}$ of a matrix operator may be objects of different type, namely scalars, second-order tensors or fourth-order tensors. The use of matrix operators will be specified whenever needed in order to avoid confusion.

Invariants of second-order tensors

The algebraic problem of finding every scalar λ and every nonzero vector $\mathbf{q}$ such that

$$\boldsymbol{\tau}\mathbf{q} = \lambda\mathbf{q}$$

leads to the standard eigenvalue problem. This consists of solving the characteristic equation

$$\det(\lambda \mathbf{I} - \boldsymbol{\tau}) = 0$$

This equation can be written equivalently as

$$\lambda^3 - I_1\lambda^2 + I_2\lambda - I_3 = 0$$

where $I_1(\boldsymbol{\tau})$, $I_2(\boldsymbol{\tau})$ and $I_3(\boldsymbol{\tau})$ are the *principal scalar invariants* of $\boldsymbol{\tau}$. The principal scalar invariants are respectively defined by

$$\begin{aligned}
I_1 &= \mathrm{tr}(\boldsymbol{\tau}) = \lambda_1 + \lambda_2 + \lambda_3 \\
I_2 &= \frac{1}{2}\left[\mathrm{tr}(\boldsymbol{\tau})^2 - \mathrm{tr}\left(\boldsymbol{\tau}^2\right)\right] = \frac{1}{2}(\tau_{ii}\tau_{jj} - \tau_{ij}\tau_{ji}) = \lambda_1\lambda_2 + \lambda_2\lambda_3 + \lambda_3\lambda_1 \\
I_3 &= \det \boldsymbol{\tau} = \lambda_1\lambda_2\lambda_3
\end{aligned}$$

where the scalars λ_1, λ_2 and λ_3 are the eigenvalues of $\boldsymbol{\tau}$ as well as the roots of the characteristic equation (a multiple root is counted repeatedly according to its multiplicity). The eigenvalues of a matrix $\boldsymbol{\tau}$ are often referred to as the *principal components* of $\boldsymbol{\tau}$.

The gradient of a scalar field $\phi(\mathbf{x})$ defined on $\mathbf{l}$in is denoted by $\nabla\phi$ and it is the vector defined by

$$\nabla\phi = \frac{\partial \phi}{\partial x_i}\mathbf{e}_i$$

The divergence div$\mathbf{u}$ and the gradient $\nabla\mathbf{u}$ of a vector field $\mathbf{u}(\mathbf{x})$ defined on $\mathbf{l}$in are respectively a scalar and a second-order tensor field defined by

$$\begin{aligned}
\mathrm{div}\mathbf{u} &= \frac{\partial u_i}{\partial x_i} \\
\nabla\mathbf{u} &= \frac{\partial u_i}{\partial x_j}\,\mathbf{e}_i \otimes \mathbf{e}_j
\end{aligned}$$

The divergence of a second-order tensor $\boldsymbol{\tau}$ defined on $\mathbf{l}$in is a vector defined by

$$\mathrm{div}\boldsymbol{\tau} = \frac{\partial \tau_{ij}}{\partial x_j}\,\mathbf{e}_i$$

For a scalar-valued function $f(\boldsymbol{\tau})$ defined on $\mathbf{L}$in, the derivative with respect to $\boldsymbol{\tau}$ is defined as a second-order tensor of the following form

$$\frac{\partial f(\boldsymbol{\tau})}{\partial \boldsymbol{\tau}} = \frac{\partial f(\boldsymbol{\tau})}{\partial \tau_{ij}} \, \mathbf{e}_i \otimes \mathbf{e}_j$$

For a time-dependent quantity z, we will denote with $\dot{z}$ its partial derivative with respect to time t.

1.3 Kinematics

Material body

We consider a body $\mathfrak{B}$ that at the macroscopic level may be regarded as composed of material that is continuously distributed in space. Assume that at any time instant t the body $\mathfrak{B}$ can be *identified* with a closed subset, Ω, of the tridimensional real space $\mathcal{R}^3$:

$$\mathfrak{B} \equiv \Omega \subset \mathcal{R}^3 \tag{1.12}$$

Accordingly, it is possible to associate any material point $X \in \mathfrak{B}$ with a point $\mathbf{X} \in \Omega \subset \mathcal{R}^3$:

$$X \in \mathfrak{B} \rightarrow \mathbf{X} \in \Omega \subset \mathcal{R}^3 \tag{1.13}$$

The above *identification* procedure allows to treat the material body as a *continuum*, that is, as a mathematical entity which inherents the *continuum power* property of the $\mathcal{R}^3$ space [38]. In particular, we may define functions of position and time over the configuration, perform real analysis, differential calculus operations on such functions and so on. It is also possible to construct a mathematical model corresponding to experimental observations, that is, perform experimental observations and assign the measured averaged properties to a point of the body.

In the present context we start by addressing the kinematics of the body which is the common starting point to describe the behavior of general continuous media. As it is well known, this framework remains independent of what acts on the body and of the constitution of the body itself.

Change of configuration

Let us consider two distinct time instants t_0 and t, such that $t_0 < t$. We refer t_0 as the *initial time instant*, while we refer t as the *current time instant*. At time t_0 the material body $\mathfrak{B}$ can be identified with a subset $\Omega_0 \in \mathcal{R}^3$, indicated

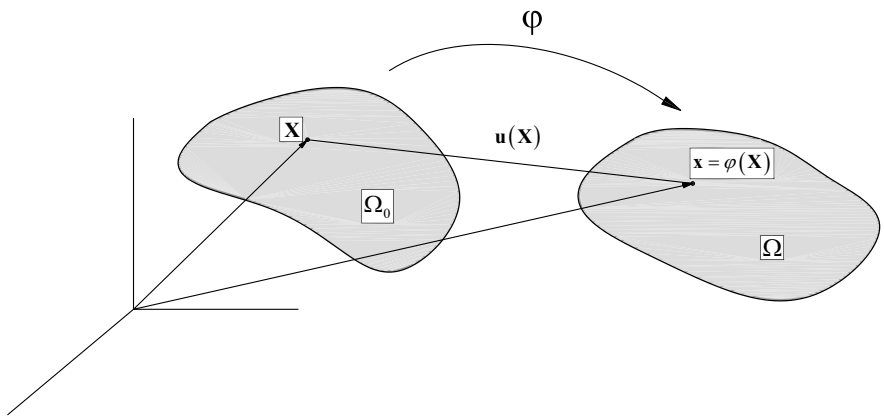

Figure 1.1: Current and reference configurations of a material body

as *initial* or *reference configuration*, such that at the same time instant the generic material point $X \in \mathfrak{B}$ can be identified with a corresponding point $\mathbf{X} \in \Omega_0$. At time t, the material body $\mathfrak{B}$ can be identified with a subset $\Omega \in \mathcal{R}^3$, indicated as *current configuration*, such that at the same time instant the generic material point $X \in \mathfrak{B}$ can be identified with a corresponding point $\mathbf{x} \in \boldsymbol{\Omega}$. In the above specifications we have set the convention of indicating the reference position vector, $\mathbf{X}$, with an upper case boldface letter and the current position vector, $\mathbf{x}$, with a lower case boldface letter. More generally, either using a compact or an indicial notation, quantities relative to the reference configuration are indicated with upper case letters and quantities relative to the current configuration are indicated with lower case letters.

In view of the identification represented by relation (1.13), it is possible to construct a map between the reference and the current configuration, indicated, in general, as *change of configuration* or *deformation map* $\boldsymbol{\varphi}$. Adopting in the following both a compact and an indicial notation, we can express the deformation map $\boldsymbol{\varphi}$ as follows:

$$\begin{aligned} \mathbf{x} &= \boldsymbol{\varphi}(\mathbf{X}) \\ x_i &= \varphi_i(X_J) \end{aligned} \tag{1.14}$$

or more precisely as:

$$\boldsymbol{\varphi} : \mathbf{X} \in \Omega_0 \subset \mathcal{R}^3 \rightarrow \mathbf{x} \in \boldsymbol{\Omega} \subset \mathcal{R}^{\mathbf{3}}$$

Observing Equation (1.14) it is noted that the conventions on the use of upper and lower case letters to denote respectively reference and current configura-

tions quantities is applied also to the subscript relative to the components of the reference position vector (indicated with an upper case index (J)) and to the components of the current position vector (indicated with a lower case index (i)).

The analytical requirement on the deformation map is that it has to respect the body continuity. This condition can be split in *external requirements* and *internal requirements*, i.e. in requirements relative to the body boundary and to the body interior. In particular, if the body configuration is assigned on a portion of the boundary, indicated as $\partial\Omega_0^{\boldsymbol{\varphi}}$ (for example, $\mathbf{x} = \mathbf{X}$ on $\partial\Omega_0^{\boldsymbol{\varphi}}$, $\forall t \geq t_0$), then the map should respect such an assignment on such a boundary portion. Moreover, in the body interior the map should respect the body continuity; from a mathematical point of view this is expressed through the following conditions:

- the map $\boldsymbol{\varphi}$ is a function
- the map $\boldsymbol{\varphi}$ is continuous
- the map $\boldsymbol{\varphi}$ is differentiable with continuous derivatives (class C^2)
- the map $\boldsymbol{\varphi}$ is invertible

The gradient of the deformation map, or *deformation gradient*, $\mathbf{F}$, is defined as:

$$\begin{aligned} \mathbf{F} &= \nabla_{\mathbf{X}}\boldsymbol{\varphi} \\ F_{iJ} &= \frac{\partial \varphi_i}{\partial X_J} \end{aligned} \tag{1.15}$$

and, without distinguishing between the deformation map, $\boldsymbol{\varphi}$, and the current position, $\mathbf{x}$, (i.e. $\mathbf{x} \equiv \boldsymbol{\varphi}$) the deformation gradient can be also written as:

$$\begin{aligned} \mathbf{F} &= \nabla_{\mathbf{X}}\mathbf{x} = \frac{\partial \mathbf{x}}{\partial \mathbf{X}} \\ F_{iJ} &= \frac{\partial x_i}{\partial X_J} \end{aligned} \tag{1.16}$$

It can be shown that $\boldsymbol{\varphi}$ maps an infinitesimal vector $d\mathbf{X}$, with origin in $\mathbf{X}$, into a vector, $d\mathbf{x}$, with origin in $\mathbf{x}$, as follows:

$$\begin{aligned} d\mathbf{x} &= \mathbf{F}d\mathbf{X} \\ dx_i &= F_{iJ}dX_J \end{aligned} \tag{1.17}$$

Accordingly, the deformation gradient is a *two-point* second-order tensor; in fact, it is a second-order tensor since it maps vectors into vectors, but it is

two-point since one component is relative to the reference configuration and one component is relative to the current configuration. This is consistent with the fact that $\mathbf{F}$ operates on vectors defined in the reference configuration and it returns vectors defined in the current configuration. In fact, the indices of $\mathbf{F}$ are still indicated with a lower case letter and with an upper case letter respectively.

The deformation gradient $\mathbf{F} = \mathbf{F}(\mathbf{X})$ is in general function of position, since the deformation map is in general non uniform. Likewise, $\boldsymbol{\varphi}$ is in general a nonlinear map in space and $\mathbf{F}$ results as its pointwise linearization.

Strain

It is possible to prove that the deformation gradient $\mathbf{F} = \mathbf{F}(\mathbf{X})$, being a pointwise-defined second-order tensor, characterizes the *strain status* of the point $\mathbf{X}$ neighborhood. In particular, given $\mathbf{F}$ it is possible two compute the relative change in length of a generic fiber emanating from $\mathbf{X}$, as well as the change in angle between two fibers emanating from $\mathbf{X}$.

The above statement can be derived with the following reasoning. Consider an infinitesimal vector $d\mathbf{S}$, with origin in $\mathbf{X}$ and expressed as $d\mathbf{S} = \mathbf{N}dS$ with $\mathbf{N}$ unit vector (i.e. $\|\mathbf{N}\| = 1$). Let us indicate with $d\mathbf{s}$ the vector with origin in $\mathbf{x}$, obtained from $d\mathbf{S}$ through the deformation map $\boldsymbol{\varphi}$, that is: $d\mathbf{s} = \mathbf{F}d\mathbf{S} = \mathbf{F}\mathbf{N}dS$. Defining the *stretch* of the vector $d\mathbf{S}$ as the elongation of the vector through the deformation map, that is, as the ratio between the norm of the vector after and before the mapping:

$$\lambda = \frac{\|d\mathbf{s}\|}{\|d\mathbf{S}\|} \tag{1.18}$$

and recalling that $\|\mathbf{N}\| = 1$, it holds:

$$\lambda^2 = \frac{d\mathbf{s} \cdot d\mathbf{s}}{d\mathbf{S} \cdot d\mathbf{S}} = \frac{(\mathbf{F}\mathbf{N}dS) \cdot (\mathbf{F}\mathbf{N}dS)}{(\mathbf{N}dS) \cdot (\mathbf{N}dS)} = \frac{(\mathbf{F}\mathbf{N}) \cdot (\mathbf{F}\mathbf{N})}{\mathbf{N} \cdot \mathbf{N}} = \mathbf{C}\mathbf{N} \cdot \mathbf{N} = \lambda^2(\mathbf{N}) \tag{1.19}$$

where $\mathbf{C}$ is the *right Cauchy-Green deformation* tensor, defined as:

$$\begin{aligned} \mathbf{C} &= \mathbf{F}^T\mathbf{F} \\ C_{IJ} &= F_{aI}F_{aJ} \end{aligned} \tag{1.20}$$

Accordingly:

$$\lambda = \lambda(\mathbf{N}) = \|\mathbf{F}\mathbf{N}\| = \sqrt{\mathbf{C}\mathbf{N} \cdot \mathbf{N}} \tag{1.21}$$

that is, given $\mathbf{F}$ and hence $\mathbf{C}$, we can compute the elongation of any fiber with origin in $\mathbf{X}$ and extremum in a sufficiently small neighborhood of $\mathbf{X}$. Such

an elongation is just a function of the direction $\mathbf{N}$. Consider two infinitesimal vectors, $d\mathbf{S}_1$ and $d\mathbf{S}_2$, with origin in $\mathbf{X}$ and expressed as

$$\begin{aligned} d\mathbf{S}_1 &= \mathbf{N}_1 dS_1 \\ d\mathbf{S}_2 &= \mathbf{N}_1 dS_2 \end{aligned} \tag{1.22}$$

with $\mathbf{N}_1$ and $\mathbf{N}_2$ unit vectors. Then, indicate with $d\mathbf{s}_1$ and $d\mathbf{s}_2$ the vectors with origin in $\mathbf{x}$, defined through the deformation map:

$$\begin{aligned} d\mathbf{s}_1 &= \mathbf{F} d\mathbf{S}_1 = \mathbf{F}\mathbf{N}_1 dS_1 \\ d\mathbf{s}_2 &= \mathbf{F} d\mathbf{S}_2 = \mathbf{F}\mathbf{N}_2 dS_2 \end{aligned}$$

If θ_0 is the angle between $d\mathbf{S}_1$ and $d\mathbf{S}_2$ and θ is the angle between $d\mathbf{s}_1$ and $d\mathbf{s}_2$, the difference $\gamma = \theta - \theta_0$ represents the angle variation. We may note that also this quantity can be expressed in terms of $\mathbf{F}$ since:

$$\cos(\theta) = \frac{d\mathbf{s}_1 \cdot d\mathbf{s}_2}{\|d\mathbf{s}_1\|\|d\mathbf{s}_2\|} = \frac{\mathbf{F}\mathbf{N}_1 \cdot \mathbf{F}\mathbf{N}_2}{\|\mathbf{F}\mathbf{N}_1\|\|\mathbf{F}\mathbf{N}_2\|} = \frac{\mathbf{C}\mathbf{N}_1 \cdot \mathbf{N}_2}{\lambda(\mathbf{N}_1)\lambda(\mathbf{N}_2)}$$

Despite the fact that $\mathbf{F}$ and $\mathbf{C}$ represent a correct tool to calculate the local state of strain, neither of them is an appropriate strain measures. In fact, in the undeformed configuration $\mathbf{F} = \mathbf{C} = \mathbf{I}$, while one would expect a proper strain measure to be zero in the undeformed configuration. This lacking can be avoided by introducing the *Lagrangian* or *Green strain* tensor $\mathbf{E}$, defined as:

$$\begin{aligned} \mathbf{E} &= \frac{1}{2}\left(\mathbf{C} - \mathbf{I}\right) = \frac{1}{2}\left(\mathbf{F}^T\mathbf{F} - \mathbf{I}\right) \\ E_{IJ} &= \frac{1}{2}\left(C_{IJ} - I_{IJ}\right) = \frac{1}{2}\left(F_{aI}F_{aJ} - I_{IJ}\right) \end{aligned} \tag{1.23}$$

This definition is suggested in a straightforward manner by considering the following change in scalar product:

$$\begin{aligned} d\mathbf{s}_1 \cdot d\mathbf{s}_2 - d\mathbf{S}_1 \cdot d\mathbf{S}_2 &= \left(\mathbf{F} d\mathbf{S}_1 \cdot \mathbf{F} d\mathbf{S}_2\right) - d\mathbf{S}_1 \cdot d\mathbf{S}_2 \\ &= \mathbf{F}^T\mathbf{F} d\mathbf{S}_1 \cdot d\mathbf{S}_2 - d\mathbf{S}_1 \cdot d\mathbf{S}_2 \\ &= \left(\mathbf{F}^T\mathbf{F} - \mathbf{I}\right) d\mathbf{S}_1 \cdot d\mathbf{S}_2 \\ &= 2\mathbf{E} d\mathbf{S}_1 \cdot d\mathbf{S}_2 \end{aligned}$$

which is also amenable of the following representation :

$$\begin{aligned} d\mathbf{s}_1 \cdot d\mathbf{s}_2 - d\mathbf{S}_1 \cdot d\mathbf{S}_2 &= d\mathbf{s}_1 \cdot d\mathbf{s}_2 - \left(\mathbf{F}^{-1} d\mathbf{s}_1 \cdot \mathbf{F}^{-1} d\mathbf{s}_2\right) \\ &= d\mathbf{s}_1 \cdot d\mathbf{s}_2 - \mathbf{F}^{-T}\mathbf{F}^{-1} d\mathbf{s}_1 \cdot d\mathbf{s}_2 \\ &= \left(\mathbf{I} - \mathbf{F}^{-T}\mathbf{F}^{-1}\right) d\mathbf{s}_1 \cdot d\mathbf{s}_2 \\ &= 2\mathbf{e} d\mathbf{s}_1 \cdot d\mathbf{s}_2 \end{aligned}$$

The second-order tensor $\mathbf{e}$ is called *Eulerian* or *Almansi strain* tensor and is defined as:

$$\begin{aligned} \mathbf{e} &= \frac{1}{2}\left(\mathbf{I} - \mathbf{b}^{-1}\right) \\ e_{ij} &= \frac{1}{2}\left(I_{ij} - b_{ij}^{-1}\right) \end{aligned} \tag{1.24}$$

where the second-order tensor $\mathbf{b}$ is the *left Cauchy-Green* or *Finger deformation* tensor, defined as:

$$\begin{aligned} \mathbf{b} &= \mathbf{F}\mathbf{F}^T \\ b_{ij} &= F_{iA}F_{jA} \end{aligned} \tag{1.25}$$

such that:

$$\begin{aligned} \mathbf{b}^{-1} &= \mathbf{F}^{-T}\mathbf{F}^{-1} \\ b_{ij}^{-1} &= F_{iA}^{-T}F_{jA}^{-1} \end{aligned} \tag{1.26}$$

The scalar product can still be takes as a measure of deformation. Take for example $d\mathbf{S}_1 = d\mathbf{S}_2 = d\mathbf{S}$, such that $d\mathbf{S} = \mathbf{N}dS$, with $\mathbf{N}$ unit vector in the direction of $d\mathbf{S}$. Similarly, $d\mathbf{s} = \mathbf{n}ds$, with $\mathbf{n}$ unit vector in the direction of $d\mathbf{s}$. With these positions, the initial (material) length dS and the current (spatial) length ds are respectively:

$$\begin{aligned} dS^2 &= d\mathbf{S} \cdot d\mathbf{S} \\ ds^2 &= d\mathbf{s} \cdot d\mathbf{s} \end{aligned}$$

Hence:

$$\begin{aligned} \frac{ds^2 - dS^2}{dS^2} &= 2\,\mathbf{E}\mathbf{N} \cdot \mathbf{N} \\ \frac{ds^2 - dS^2}{ds^2} &= 2\,\mathbf{e}\mathbf{n} \cdot \mathbf{n} \end{aligned}$$

which respectively return the change in square length of the fiber $d\mathbf{S}$ with respect to the initial and current length.

Particular choices of the unit vectors $\mathbf{N}_1$ and $\mathbf{N}_2$ appearing in (1.22) together with the above calculations induce to recognize the geometrical meaning of the components of the Lagrangian and Eulerian tensors relative to the local state of deformation. For instance, taking $\mathbf{N}_1 = \mathbf{N}_2 = \mathbf{e}_i$ $(i = 1, 2, 3)$ it is found that the components E_{ii}, e_{ii} $(i = 1, 2, 3)$, respectively, represent the relative elongation of a fiber initially oriented along the ith basis vector with respect to the initial and to the current length. Similarly, taking $\mathbf{N}_1 = \mathbf{e}_i$ and $\mathbf{N}_2 = \mathbf{e}_j$ $(i, j = 1, 2, 3)$ it is found that the components E_{ij}, e_{ij} $(i, j = 1, 2, 3)$

with $i \neq j$, respectively, represent the relative change in angle between the fibers initially oriented along the ith and jth reference axis with respect to the initial and to the current angle between them.

It is convenient to describe the change of configuration introducing the displacement field $\mathbf{u}$, defined as the pointwise difference between the current and the reference vector position:

$$\mathbf{u}(\mathbf{X}) = \mathbf{x}(\mathbf{X}) - \mathbf{X} \tag{1.27}$$

Then the current position vector is given by the sum of the reference position vector and of the displacement vector:

$$\mathbf{x} = \boldsymbol{\varphi}(\mathbf{X}) = \mathbf{X} + \mathbf{u}(\mathbf{X})$$

The expression of the deformation map in terms of displacement gives rise to alternative expressions of the strain tensors introduced previously. For example, the deformation gradient becomes:

$$\mathbf{F} = \frac{\partial \mathbf{x}}{\partial \mathbf{X}} = \frac{\partial}{\partial \mathbf{X}} (\mathbf{X} + \mathbf{u}) = \mathbf{I} + \nabla_{\mathbf{X}} \mathbf{u} \tag{1.28}$$

which, defining $\mathbf{H} = \nabla_{\mathbf{X}} \mathbf{u}$, can be written as:

$$\mathbf{F} = \mathbf{I} + \mathbf{H} \tag{1.29}$$

Moreover, we may write:

$$\begin{aligned} \mathbf{C} &= \mathbf{F}^T \mathbf{F} = \mathbf{I} + \mathbf{H} + \mathbf{H}^T + \mathbf{H}^T \mathbf{H} \\ \mathbf{E} &= \frac{1}{2} (\mathbf{C} - \mathbf{I}) = \frac{1}{2} \left(\mathbf{H} + \mathbf{H}^T + \mathbf{H}^T \mathbf{H} \right) \end{aligned} \tag{1.30}$$

The Eulerian strain tensor $(1.30)_2$ admits the splitting:

$$\mathbf{E} = \mathbf{E}_1 + \mathbf{E}_2 = \boldsymbol{\varepsilon} + \mathbf{E}_2$$

which identifies the linear and the nonlinear parts of $\mathbf{E}$, respectively as $\mathbf{E}_1 = \boldsymbol{\varepsilon} = (\mathbf{H} + \mathbf{H}^T)/2$ and $\mathbf{E}_2 = (\mathbf{H}^T \mathbf{H})/2$.

Small displacement gradient

In many structural engineering problems the deformations can be regarded as *small* in some sense. This assumption, which is rigorously formalized, obviously introduces an approximation in the treatment but, nevertheless, permits to simplify the problem formulation and thus remains of notable interest.

Consider the case of a motion with a *small displacement gradient* $\nabla\mathbf{u}$, that is:

$$\|\nabla_{\mathbf{X}}\mathbf{u}\| = \varepsilon \qquad \text{with} \qquad \varepsilon \ll 1$$

Recalling (1.30), the additive decomposition of the strain tensor $\mathbf{E}$ in a linear and a nonlinear term, we may prove the following theorem [37].

Theorem 1.3.1 *Assume* $||\nabla\mathbf{u}|| = \varepsilon \ll 1$. *Then:*

$$2\mathbf{E} = \mathbf{C} - \mathbf{I} + \mathcal{O}(\varepsilon) = \mathbf{b} - \mathbf{I} + \mathcal{O}(\varepsilon) = 2\mathbf{E}_1 = 2\boldsymbol{\varepsilon}$$

Furthermore, if $\mathbf{F}$ *corresponds to a rigid motion, then:*

$$\nabla\mathbf{u} = -\nabla\mathbf{u}^T + \mathcal{O}(\varepsilon)$$

This proposition asserts that to within an error of order $\mathcal{O}(\varepsilon)$:

- if the displacement gradient $\nabla_{\mathbf{X}}\mathbf{u}$ is *sufficiently small* then the nonlinear term in (1.30) can be neglected
- the tensors $\mathbf{E}$ and $\boldsymbol{\varepsilon}$ coincide as well as the tensors $\mathbf{C}$ and $\mathbf{b}$ coincide
- the displacement gradient corresponding to a rigid deformation is skew

Under the same assumptions it is also possible to prove that:

$$\det(\mathbf{F}) - 1 = \text{div}\ (\mathbf{u}) + \mathcal{O}(\varepsilon) \tag{1.31}$$

In the following we indicate a deformation map characterized by a small displacement gradient field as a *small deformation map* or simply we talk about *small deformations*, that is:

$$\textbf{Small deformation} \qquad \Leftrightarrow \qquad \begin{cases} \|\nabla_{\mathbf{X}}\mathbf{u}\| \ll 1 \\ \\ \boldsymbol{\varepsilon} = \frac{1}{2}\left[\nabla_{\mathbf{X}}\mathbf{u} + (\nabla_{\mathbf{X}}\mathbf{u})^T\right] \end{cases}$$

Volume change

We are now interested in the evaluation of the unit volume change produced in the change of configuration of the body by means of the deformation map. To begin with it is worth recalling that the volume V of a parallelepiped defined by the vectors $\mathbf{a}$, $\mathbf{b}$ and $\mathbf{c}$ is given by:

$$V(\mathbf{a}, \mathbf{b}, \mathbf{c}) = (\mathbf{a} \times \mathbf{b}) \cdot \mathbf{c}$$

Moreover, the following theorem holds:

Theorem 1.3.2 *Let* $\{\mathbf{a}, \mathbf{b}, \mathbf{c}\}$ *be any triad of non-collinear vectors in the three-dimensional space and let* $\mathbf{T}$ *be any second-order tensor. Then, the following identities hold:*

$$[(\mathbf{Ta}) \times (\mathbf{Tb})] \cdot \mathbf{Tc} = \det(\mathbf{T}) \, [(\mathbf{a} \times \mathbf{b}) \cdot \mathbf{c}]$$

$$\mathbf{T}^T \, [(\mathbf{Ta}) \times (\mathbf{Tb})] = \det(\mathbf{T}) \, (\mathbf{a} \times \mathbf{b})$$

Let us consider a parallelepiped of material described by a triad of infinitesimal vectors $\{d\mathbf{S}_1, d\mathbf{S}_2, d\mathbf{S}_3\}$, expressed respectively as a product of the unit vectors $\mathbf{N}_1, \mathbf{N}_2, \mathbf{N}_3$ and of the infinitesimal lengths dS_1, dS_2, dS_3. Accordingly, the volume dV of the parallelepiped is given by:

$$dV = [(\mathbf{N}_1 \times \mathbf{N}_2) \cdot \mathbf{N}_3] \, dS_1 dS_2 dS_3$$

The deformed parallelepiped is described by the vectors $\{\mathbf{FN}_1, \mathbf{FN}_2, \mathbf{FN}_3\}$ multiplied respectively by the quantities dS_1, dS_2, dS_3. Accordingly, the corresponding volume dv is given by:

$$dv = [(\mathbf{FN}_1 \times \mathbf{FN}_2) \cdot \mathbf{FN}_3] \, dS_1 dS_2 dS_3$$

which can also be rewritten as:

$$dv = \det(\mathbf{F}) \, [(\mathbf{N}_1 \times \mathbf{N}_2) \cdot \mathbf{N}_3] \, dS_1 dS_2 dS_3$$

Hence, we get:

$$\frac{dv}{dV} = \det(\mathbf{F}) = J \tag{1.32}$$

where we also used the classical notation $J = \det(\mathbf{F})$ indicating the *Jacobian* of the deformation gradient.

The above formula can be specialized in the case of small deformations [25]. Recalling (1.31) and omitting higher order terms, it holds:

$$J = \det(\mathbf{F}) = \det(\mathbf{I} + \nabla \mathbf{u}) = 1 + \mathrm{div}\mathbf{u} \tag{1.33}$$

A body transformation such that it produces no volume change is said top be *isochoric* and observing (1.32) in this case one has

$$J = 1 \quad \forall \mathbf{x} \in \Omega \tag{1.34}$$

Accordingly, for an isochoric infinitesimal deformation process and to within an error of $O(\varepsilon)$, the displacement field satisfies the condition

$$\mathrm{tr}(\boldsymbol{\varepsilon}(\mathbf{u}(\mathbf{x}))) = \mathrm{div}\mathbf{u}(\mathbf{x}) = 0 \quad \forall \mathbf{x} \in \Omega \tag{1.35}$$

A material that cannot undergo any transformation that is accompanied by change in volume is called *incompressible*. For such a material, relations (1.34) and (1.35) represent a constraint on the admissible deformation field.

1.4 Equilibrium

1.4.1 Static equilibrium

This section investigates body static equilibrium conditions, relative either to the whole body or to body subsets. In particular, the equilibrium is comprehensive of the relations introducing proper quantities measuring internal forces, i.e. actions exchanged between neighborhood body subsets.

Given a body $\mathfrak{B}$ in a configuration Ω, we postulate that the interaction between the external world and the body can be described through two force fields:

- a surface force field, or *contact force* field, $\mathbf{t}$, with dimension of force by unit area and defined on a portion of the current boundary surface, $\partial\Omega^{\mathbf{t}}$ [2];
- a volume force field, or *body force* field, $\mathbf{b}$, with dimension of force by unit volume and defined on the current configuration, Ω.

We also postulate that:

- the interaction between any portion of the body Ω' internal to the body (i.e. such that $\Omega' \subset \overset{\circ}{\Omega}$) and the remaining part of the body $\Omega \setminus \Omega'$ can be described through a surface force field, indicated also as *traction force* field, with dimension of force by unit area and defined on $\partial\Omega'$. These interaction forces are assumed to be function of the local outward normal to Ω', and, accordingly, we indicate this field with $\mathbf{t_n}$, with the subscript to express the dependency from the normal $\mathbf{n}$.

Given any portion Ω' of the body in the current configuration Ω, we can define the force resultant, $\mathbf{r}$, and the moment resultant, $\mathbf{m}$, relative to $\Omega' \subseteq \Omega$ as:

$$\begin{aligned} \mathbf{r}(\Omega') &= \int_{\Omega'} \mathbf{b} dv + \int_{\partial\Omega'} \mathbf{t_n} da \\ \mathbf{m}(\Omega') &= \int_{\Omega'} (\mathbf{x} \times \mathbf{b})\, dv + \int_{\partial\Omega'} (\mathbf{x} \times \mathbf{t_n})\, da \end{aligned} \tag{1.36}$$

where $\mathbf{x}$ is the current position vector and where the resultant momentum is computed with respect to a generic origin $\mathbf{o}$.

Now, defined the force and moment resultants, we may state the

[2] In general, we set $\partial\Omega^{\mathbf{t}} = \partial\Omega \setminus \partial\Omega^{\varphi}$ with $\partial\Omega^{\varphi}$ the part of the boundary where we assign the deformation map φ; accordingly, we have: $\partial\Omega = \partial\Omega^{\mathbf{t}} \cup \partial\Omega^{\varphi}$.

Static Equilibrium Axiom. A deformable body is in equilibrium if and only if the **force resultant** and the **force momentum** on each portion of the body are zero, that is, a body $\mathfrak{B}$ in a configuration Ω is in equilibrium if and only if:

$$\begin{aligned} \mathbf{r}(\Omega') &= \mathbf{0} \qquad \forall \Omega' \subseteq \Omega \\ \mathbf{m}(\Omega') &= \mathbf{0} \qquad \forall \Omega' \subseteq \Omega \end{aligned} \tag{1.37}$$

or, in a more explicit format, a body $\mathfrak{B}$ in a configuration Ω is in equilibrium if and only if:

$$\begin{aligned} &\int_{\Omega'} \mathbf{b} dv + \int_{\partial\Omega'} \mathbf{t_n} da = \mathbf{0} \qquad \forall \Omega' \subseteq \Omega \\ &\int_{\Omega'} (\mathbf{x} \times \mathbf{b})\, dv + \int_{\partial\Omega'} (\mathbf{x} \times \mathbf{t_n})\, da = \mathbf{0} \qquad \forall \Omega' \subseteq \Omega \end{aligned} \tag{1.38}$$

Equation (1.38) are also indicated as *linear momentum* and *angular momentum* balance laws. Moreover, for the case $\Omega' \equiv \Omega$, the above equations specialize as:

$$\begin{aligned} \mathbf{r}(\Omega) &= \int_{\Omega} \mathbf{b} dv + \int_{\partial\Omega^{\boldsymbol{\varphi}}} \mathbf{t_n} da + \int_{\partial\Omega^{\mathbf{t}}} \mathbf{t} da = \mathbf{0} \\ \mathbf{m}(\Omega) &= \int_{\Omega} (\mathbf{x} \times \mathbf{b})\, dv + \int_{\partial\Omega^{\boldsymbol{\varphi}}} (\mathbf{x} \times \mathbf{t_n})\, da + \int_{\partial\Omega^{\mathbf{t_n}}} (\mathbf{x} \times \mathbf{t})\, da = \mathbf{0} \end{aligned} \tag{1.39}$$

where we note that the quantity $\mathbf{t_n}$ in the surface integral on $\partial\Omega^{\boldsymbol{\varphi}}$ is unknown.

We now want to investigate the actions that internal parts of the body mutually exchange. To do so, let us introduce a surface Σ, ideally dividing the body Ω in two parts, Ω'_1 and Ω'_2, such that $\Omega'_1 \cup \Omega'_2 = \Omega$, and let us also define: $\Gamma_1 = \partial\Omega'_1 \setminus \Sigma$ and $\Gamma_2 = \partial\Omega'_2 \setminus \Sigma$, such that: $\partial\Omega'_1 = \Gamma_1 \cup \Sigma$ and $\partial\Omega'_2 = \Gamma_2 \cup \Sigma$. Assuming that the whole body is in equilibrium, by the equilibrium axiom, we have that each single part of the body should be in equilibrium, hence, also Ω'_1 and Ω'_2. Without showing all the calculations (refer for instance to [14]) the last statement amounts to the following fundamental result:

$$\int_{\Sigma} (\mathbf{t_n} + \mathbf{t_{-n}})\, da = \mathbf{0}$$

which, recalling the arbitrariness of the surface Σ, implies

$$\mathbf{t_n} = -\mathbf{t_{-n}} \tag{1.40}$$

The above equation is known as *action-reaction principle* or as *Cauchy reciprocal principle* or as *first Cauchy theorem.*

Stress tensor

Let us introduce a right-angle tetrahedron $\mathcal{T}$ contained in the body ($\mathcal{T} \subset \overset{\circ}{\Omega}$) and a coordinate system with origin $\mathbf{o}$ in the tetrahedron right-angle vertex and axes given by the tetrahedron edges, respectively with lengths along the coordinate axes equal to $\varepsilon_1, \varepsilon_2, \varepsilon_3$. Moreover, let us indicate with $\mathbf{p}_i$ (with $i = 1, 2, 3$) the other tetrahedron vertices, with $\mathbf{e}_i$ the unit vector along the ith coordinate axis, with a_i the area of the face with unit normal $-\mathbf{e}_i$, and with a_n the fourth area describing the tetrahedron, having normal $\mathbf{n}$.

We now consider the tetrahedron equilibrium, taking into account the traction vector fields acting on the four sides and the body force field acting on the volume. This amounts to studying the following integral force balance:

$$\int_v \mathbf{b} dv + \sum_{i=1}^{3} \int_{a_i} \mathbf{t}_{-\mathbf{e}_i} da + \int_{a_n} \mathbf{t}_{\mathbf{n}} da = \mathbf{0}$$

Omitting, for brevity, the mathematical manipulations and using the action-reaction principle it is possible to state that the above equilibrium condition for the tetrahedron implies the following relation for the traction field

$$\mathbf{t}_{\mathbf{n}} = \sum_{i=1}^{3} (\mathbf{n} \cdot \mathbf{e}_i)\, \mathbf{t}_{\mathbf{e}_i} = \left[\sum_{i=1}^{3} (\mathbf{t}_{\mathbf{e}_i} \otimes \mathbf{e}_i) \right] \mathbf{n} \tag{1.41}$$

This relation shows how the traction vector acting on the oblique face is related to the traction vectors on the faces orthogonal to the coordinate axes; in particular, setting:

$$\boldsymbol{\sigma} = \left[\sum_{i=1}^{3} (\mathbf{t}_{\mathbf{e}_i} \otimes \mathbf{e}_i) \right] \tag{1.42}$$

we have:

$$\mathbf{t}_{\mathbf{n}} = \boldsymbol{\sigma} \mathbf{n} \tag{1.43}$$

which is known as *second Cauchy theorem*, valid for any point internal to the body (i.e. $\forall \mathbf{x} \in \overset{\circ}{\boldsymbol{\Omega}}$). It is interesting to emphasize how, starting from the assumption that the traction vector $\mathbf{t}_{\mathbf{n}}$ depends on $\mathbf{n}$, we prove that this dependency is linear through a second-order tensor $\boldsymbol{\sigma}$, known as *Cauchy stress tensor*. Accordingly, knowing $\boldsymbol{\sigma}$ in a point, it is possible to compute the stress vector $\mathbf{t}_{\mathbf{n}}$ acting on any surface of normal $\mathbf{n}$, which is equivalent to say that $\boldsymbol{\sigma}$ contains all the information relative to the local state of stress.

From Equation (1.43), it is possible to obtain a physical interpretation for the components of the stress tensor, noting that:

$$\sigma_{ij} = \mathbf{e}_i \cdot \boldsymbol{\sigma}\mathbf{e}_j = \mathbf{e}_i \cdot \left[\sum_{i=1}^{3} (\mathbf{t}_{\mathbf{e}_i} \otimes \mathbf{e}_i)\right] \mathbf{e}_j = \mathbf{e}_i \cdot \mathbf{t}_{\mathbf{e}_j} \tag{1.44}$$

Hence, the ijth component of $\boldsymbol{\sigma}$ is the ith component of the traction vector acting on the face with normal vector $\mathbf{e}_j$. The reader should be warned that some authors reverse the convention [3, 38, 53].

It is also interesting to note that Equation (1.42) indicates that $\boldsymbol{\sigma}$ is fully determined once we know the three vectors $\mathbf{t}_{\mathbf{e}_1}, \mathbf{t}_{\mathbf{e}_2}, \mathbf{t}_{\mathbf{e}_3}$; accordingly, $\boldsymbol{\sigma}$ is known once we know nine independent components, which are exactly the number of components in a second-order tensor.

Static equilibrium equations

We now want to transform the equilibrium requirements from the global integral format of Equation (1.38) to a local differential format. To do so, we start recalling that, given any tensor field $\mathbf{G}$ defined on a region Ω' with normal $\mathbf{n}$ and boundary $\partial\Omega'$, the divergence theorem of a tensor field states:

$$\int_{\partial\Omega'} \mathbf{G}\mathbf{n} da = \int_{\Omega'} \text{div } (\mathbf{G}) dv \tag{1.45}$$

Applying this equality to Equation $(1.38)_1$, we get:

$$\int_{\Omega'} \mathbf{b} dv + \int_{\partial\Omega'} \mathbf{t}_{\mathbf{n}} da = \int_{\Omega'} \mathbf{b} dv + \int_{\partial\Omega'} \boldsymbol{\sigma}\mathbf{n} da = \int_{\Omega'} (\mathbf{b} + \text{div } \boldsymbol{\sigma})\, dv = \mathbf{0}$$

and since this equality must hold for all $\Omega' \subseteq \Omega$, we get the corresponding local form of the equilibrium equation:

$$\begin{aligned} \text{div } \boldsymbol{\sigma} + \mathbf{b} &= \mathbf{0} \\ \sigma_{ij,j} + b_i &= 0 \end{aligned} \tag{1.46}$$

where the subscript comma indicates differentiation. Accordingly, this is a set of three linear partial differential equations.

To derive the local form of the angular momentum balance, we start multiplying Equation $(1.38)_2$ with an arbitrary and constant vector field $\mathbf{h}$:

$$\begin{aligned} &\int_{\Omega'} [(\mathbf{x} \times \mathbf{b}) \cdot \mathbf{h}]\, dv + \int_{\partial\Omega'} [(\mathbf{x} \times \mathbf{t}_{\mathbf{n}}) \cdot \mathbf{h}]\, da = \\ &\int_{\Omega'} [(\mathbf{x} \times \mathbf{b}) \cdot \mathbf{h}]\, dv + \int_{\partial\Omega'} [(\mathbf{x} \times \boldsymbol{\sigma}\mathbf{n}) \cdot \mathbf{h}]\, da = \mathbf{0} \end{aligned} \tag{1.47}$$

Now, recalling the cyclic nature of the triple product, the definition of transpose for a second-order tensor and the equality:

$$\text{div}\ \left(\mathbf{G}^T\mathbf{v}\right) = \mathbf{v}\cdot\text{div}\ \mathbf{G} + \mathbf{G} : \nabla\mathbf{v}$$

valid for any tensor field $\mathbf{G}$ and any vector field $\mathbf{v}$, we may note that:

$$\begin{aligned}
\int_{\partial\Omega'} [(\mathbf{x}\times\boldsymbol{\sigma}\mathbf{n})\cdot\mathbf{h}]\, da &= \int_{\partial\Omega'} [(\mathbf{h}\times\mathbf{x})\cdot\boldsymbol{\sigma}\mathbf{n}]\, da \\
&= \int_{\partial\Omega'} \left[\boldsymbol{\sigma}^T(\mathbf{h}\times\mathbf{x})\cdot\mathbf{n}\right] da \\
&= \int_{\Omega'} \text{div}\ \left[\boldsymbol{\sigma}^T(\mathbf{h}\times\mathbf{x})\right] dv \\
&= \int_{\Omega'} [(\mathbf{h}\times\mathbf{x})\cdot\text{div}\ \boldsymbol{\sigma} + \boldsymbol{\sigma} : \nabla(\mathbf{h}\times\mathbf{x})]\, dv \\
&= \int_{\Omega'} [(\mathbf{x}\times\text{div}\ \boldsymbol{\sigma})\cdot\mathbf{h} + \boldsymbol{\sigma} : \nabla(\mathbf{h}\times\mathbf{x})]\, dv
\end{aligned}$$

Accordingly, Equation (1.47) becomes:

$$\begin{aligned}
\int_{\Omega'} [(\mathbf{x}\times\mathbf{b})\cdot\mathbf{h}]\, dv + \int_{\Omega'} [(\mathbf{x}\times\text{div}\ \boldsymbol{\sigma})\cdot\mathbf{h} + \boldsymbol{\sigma} : \nabla(\mathbf{h}\times\mathbf{x})]\, dv = \\
\int_{\Omega'} [\mathbf{x}\times(\text{div}\ \boldsymbol{\sigma} + \mathbf{b})\cdot\mathbf{h} + \boldsymbol{\sigma} : \nabla(\mathbf{h}\times\mathbf{x})]\, dv = \\
\int_{\Omega'} [\boldsymbol{\sigma} : \nabla(\mathbf{h}\times\mathbf{x})]\, dv = \mathbf{0}
\end{aligned} \tag{1.48}$$

where we used the balance of linear momentum, i.e. $\text{div}\ \boldsymbol{\sigma} + \mathbf{b} = \mathbf{0}$. Noting that $\nabla\mathbf{x} = \mathbf{I}$, we have:

$$\nabla(\mathbf{h}\times\mathbf{x}) = \mathbf{H}$$

with $\mathbf{H}$ a skew-symmetric tensor such that: $\mathbf{H}\mathbf{v} = \mathbf{h}\times\mathbf{v}$ for any vector $\mathbf{v}$. Moreover,

$$\boldsymbol{\sigma} : \mathbf{H} = \text{tr}(\boldsymbol{\sigma}^T\mathbf{H}) = \mathbf{e}_i\cdot\boldsymbol{\sigma}^T\mathbf{H}\mathbf{e}_i$$

hence, Equation (1.48) reduces to:

$$\int_{\Omega'} [\mathbf{h}\cdot(\mathbf{e}_i\times\boldsymbol{\sigma}\mathbf{e}_i)]\, dv = \mathbf{0}$$

with an implied sum on i. Recalling that $\mathbf{h}$ and Ω' are arbitrary, we finally get:

$$\mathbf{e}_i\times\boldsymbol{\sigma}\mathbf{e}_i = \mathbf{0} \tag{1.49}$$

To understand the real implication of Equation (1.49), we may consider the kth component of the previous equation, expressing also the tensor $\boldsymbol{\sigma}$ in components:

$$\begin{aligned}\mathbf{e}_k \cdot [\mathbf{e}_i \times \boldsymbol{\sigma}\mathbf{e}_i] &= \mathbf{e}_k \cdot [\mathbf{e}_i \times (\sigma_{ab}\mathbf{e}_a \otimes \mathbf{e}_b)\,\mathbf{e}_i] = \mathbf{e}_k \cdot [\mathbf{e}_i \times \sigma_{ab}\mathbf{e}_a I_{ib}] \\ &= \mathbf{e}_k \cdot [\mathbf{e}_i \times \sigma_{ai}\mathbf{e}_a] = [\sigma_{ai}\,(\mathbf{e}_k \cdot \mathbf{e}_i \times \mathbf{e}_a)] = \sigma_{ai}\mathcal{E}_{kia}\end{aligned}$$

The above equaiton can be written in a more explicit format as:

$$\sigma_{ai} = \sigma_{ai} \quad (a \neq i) \tag{1.50}$$

or in compact notation as:

$$\boldsymbol{\sigma} = \boldsymbol{\sigma}^T \tag{1.51}$$

Therefore, the balance of angular momentum implies the *symmetry of stress tensor* $\boldsymbol{\sigma}$. In conclusion, the local form of the balance equations are respectively:

$$\begin{array}{lll} \operatorname{div}\boldsymbol{\sigma} + \mathbf{b} = \mathbf{0} & \text{in} & \Omega \\ \boldsymbol{\sigma} = \boldsymbol{\sigma}^T & \text{in} & \Omega \\ \mathbf{t} = \boldsymbol{\sigma}\mathbf{n} & \text{on} & \partial\Omega^{\mathbf{t}} \end{array} \tag{1.52}$$

or in indicial notation

$$\begin{array}{lll} \sigma_{ij,j} + b_i = 0 & \text{in} & \Omega \\ \sigma_{ij} = \sigma_{ji} & \text{in} & \Omega \\ t_i = \sigma_{ij}n_j & \text{on} & \partial\Omega^{\mathbf{t}} \end{array} \tag{1.53}$$

1.4.2 Dynamic equilibrium

Given a motion $\boldsymbol{\varphi}$ of a body $\mathfrak{B}$, the *linear momentum*, $\mathbf{l}$, and the *angular momentum*, $\mathbf{a}$, of any body portion $\Omega' \subseteq \Omega$ at time t are defined as:

$$\begin{aligned}\mathbf{l}(\Omega', t) &= \int_{\Omega'} \rho\dot{\mathbf{u}}dv \\ \mathbf{a}(\Omega', t) &= \int_{\Omega'} (\mathbf{x} \times \rho\dot{\mathbf{u}})\,dv\end{aligned} \tag{1.54}$$

where the angular momentum is computed with respect to a generic origin $\mathbf{o}$ and with the mass density ρ uniform at any point in the body.

Deriving in time it follows that for every portion Ω':

$$\begin{aligned}\dot{\mathbf{l}}(\Omega', t) &= \int_{\Omega'} \rho\ddot{\mathbf{u}}dv \\ \dot{\mathbf{a}}(\Omega', t) &= \int_{\Omega'} (\mathbf{x} \times \rho\ddot{\mathbf{u}})\,dv\end{aligned} \tag{1.55}$$

Recalling that for any portion $\Omega' \subseteq \Omega$ we can define a force resultant, $\mathbf{r}$, and a moment resultant, $\mathbf{m}$, given respectively by:

$$\begin{aligned} \mathbf{r}(\Omega') &= \int_{\Omega'} \mathbf{b} dv + \int_{\partial\Omega'} \mathbf{t_n} da \\ \mathbf{m}(\Omega') &= \int_{\Omega'} (\mathbf{x} \times \mathbf{b})\, dv + \int_{\partial\Omega'} (\mathbf{x} \times \mathbf{t_n})\, da \end{aligned} \tag{1.56}$$

it is possible to state the

Dynamic Equilibrium Axiom. A deformable body is in equilibrium if and only if the force resultant and the force momentum on each portion satisfy the linear and angular momentum balance laws. Accordingly, a body $\mathfrak{B}$ in a configuration Ω is in equilibrium if and only if:

$$\begin{aligned} \mathbf{r}(\Omega') &= \dot{\mathbf{l}}(\Omega') \quad \forall \Omega' \subseteq \Omega \\ \mathbf{m}(\Omega') &= \dot{\mathbf{a}}(\Omega') \quad \forall \Omega' \subseteq \Omega \end{aligned} \tag{1.57}$$

where we neglect to indicate time dependency and where $\dot{\mathbf{l}}$ and $\dot{\mathbf{a}}$ are the rate of the linear and of the angular momentum, as defined in (1.55). Accordingly, (1.57) can be rewritten as:

$$\begin{aligned} \int_{\Omega'} \mathbf{b} dv + \int_{\partial\Omega'} \mathbf{t_n} da &= \int_{\Omega'} \rho \ddot{\mathbf{u}} dv \qquad \forall \Omega' \subseteq \Omega \\ \int_{\Omega'} (\mathbf{x} \times \mathbf{b})\, dv + \int_{\partial\Omega'} (\mathbf{x} \times \mathbf{t_n})\, da &= \int_{\Omega'} (\mathbf{x} \times \rho \ddot{\mathbf{u}})\, dv \quad \forall \Omega' \subseteq \Omega \end{aligned} \tag{1.58}$$

Dynamic equilibrium equations

Consider first the law of balance of linear momentum $(1.58)_1$. Taking into consideration relationship (1.43) and using again the divergence theorem (1.45) one can rewrite the surface integral extended to the boundary $\partial\Omega'$ as

$$\int_{\partial\Omega'} \mathbf{t_n} da = \int_{\partial\Omega'} \boldsymbol{\sigma} \mathbf{n} da = \int_{\Omega'} \operatorname{div} \boldsymbol{\sigma} dv$$

so that Equation $(1.58)_1$ becomes

$$\int_{\Omega'} [\rho \ddot{\mathbf{u}} - \mathbf{b} - \operatorname{div} \boldsymbol{\sigma}]\, dv = \mathbf{0} \tag{1.59}$$

Since the portion Ω' is arbitrary, the integrand in (1.59) must vanish. This condition gives the local form of the *equation of motion*

$$\operatorname{div} \boldsymbol{\sigma} + \mathbf{b} = \rho \ddot{\mathbf{u}} \tag{1.60}$$

For the cases in which all the given data are independent of time, we have $\mathbf{u} = \mathbf{u}(\mathbf{x})$, $\boldsymbol{\sigma} = \boldsymbol{\sigma}(\mathbf{x})$ and the response of the body will be independent of time as well and the equation of motion recovers the *equation of static equilibrium* (1.46). Examining the law of balance for the angular momentum, we may perform similar manipulations to those that lead to Equation (1.60) and find again the symmetry of the Cauchy stress tensor:

$$\begin{aligned} \boldsymbol{\sigma}^T &= \boldsymbol{\sigma} \\ \sigma_{ij} &= \sigma_{ji} \end{aligned}$$

Remark 1.4.1 *All the equilibrium considerations presented so far are relative to the natural configuration where equilibrium should hold, hence they are all relative to the current configuration Ω and written in terms of geometrical quantities relative to the current configuration Ω. However, thanks to the invertibility of the map $\mathbf{x} = \boldsymbol{\varphi}(\mathbf{X})$ presented in Equation (1.14) and relating the current configuration Ω to the reference configuration Ω_0, we can also write:*

- *equilibrium equations relative to the current configuration Ω in term of geometrical quantities relative to the reference configuration Ω_0*
- *equilibrium equations relative to the reference configuration Ω_0 in term of geometrical quantities relative to the reference configuration Ω_0*

In particular, when a small deformation regime is considered, the distinction between reference and current configuration may be ignored. In this case the alternative forms of equilibrium listed above coincide.

1.5 Constitutive relation

Basic relations

We have so far described the equations of motion and the strain-displacements relations within the framework of infinitesimal deformation. In component form these equations are given by a set of nine partial differential equations: three from the balance law and six from the strain-displacement relation (admitting the symmetry of $\boldsymbol{\varepsilon}$). Correspondingly, we have a total of fifteen unknowns represented by the six independent components of the strain and of the stress and by the three displacement components. It is clear that six additional equations are needed in order to have a well defined problem.

From physical considerations we may infer that the missing equations should regard the behavior of the material constituting the body. This further

set of equations are the *constitutive equations*. In the present section we will be involved in summarizing the basic equations and properties related to linear elastic materials.

A material body is said to be *elastic* if the stress is entirely determined by the current state of deformation. Assuming the strain tensor $\boldsymbol{\varepsilon}$ as a measure of the local state of deformation we have

$$\begin{aligned} \boldsymbol{\sigma} &= \boldsymbol{\sigma}(\boldsymbol{\varepsilon}) \\ \sigma_{ij} &= \sigma_{ij}(\varepsilon_{ab}) \end{aligned} \tag{1.61}$$

This position implies that the stress cannot depend on the deformation history and, in particular, on the path followed to reach the actual state. However, introducing the density of internal work done in going from an initial strain, $\boldsymbol{\varepsilon}_i$, to a final strain, $\boldsymbol{\varepsilon}_f$, on a path $\Gamma_{\boldsymbol{\varepsilon}}$ as:

$$W^{\text{int}}_{\Gamma_{\boldsymbol{\varepsilon}}} = \int_{\Gamma_{\boldsymbol{\varepsilon}}} \boldsymbol{\sigma}(\boldsymbol{\varepsilon}) : \mathrm{d}\boldsymbol{\varepsilon}$$

it is in general possible that $W^{\text{int}}_{\Gamma_{\boldsymbol{\varepsilon}}}$ may depend on the specific strain path $\Gamma_{\boldsymbol{\varepsilon}}$.

In the absence of internal constraints and under proper mathematical conditions, Equation (1.61) can be inverted:

$$\begin{aligned} \boldsymbol{\varepsilon} &= \boldsymbol{\varepsilon}(\boldsymbol{\sigma}) \\ \varepsilon_{ij} &= \varepsilon_{ij}(\sigma_{ab}) \end{aligned} \tag{1.62}$$

It is also interesting to consider an incremental format of relation (1.61), in the form:

$$\dot{\boldsymbol{\sigma}} = \mathbb{C}^{\text{tg}}\dot{\boldsymbol{\varepsilon}} \tag{1.63}$$

where the superposed dot indicates a time derivative and $\mathbb{C}^{\text{tg}}$ is the tangent elastic tensor defined as:

$$\mathbb{C}^{\text{tg}} = \frac{\partial \boldsymbol{\sigma}}{\partial \boldsymbol{\varepsilon}} \tag{1.64}$$

An elastic material is said to be *linear* if the stress and the strain are related through a (linear) relation of the type:

$$\begin{aligned} \boldsymbol{\sigma} &= \mathbb{C}\boldsymbol{\varepsilon} \\ \sigma_{ij} &= \mathbb{C}_{ijkl}\varepsilon_{kl} \end{aligned} \tag{1.65}$$

where the fourth-order tensor $\mathbb{C}$ is termed the *elastic tensor*.

Given the symmetry of the second-order tensor $\boldsymbol{\varepsilon}$, we may write

$$\sigma_{ij} = \mathbb{C}_{ijkl}\varepsilon_{lk} = \mathbb{C}_{ijlk}\varepsilon_{kl}$$

Exploiting the symmetry of the stress tensor $\boldsymbol{\sigma}$, we have

$$\sigma_{ji} = \mathbb{C}_{jilk}\varepsilon_{lk} = \mathbb{C}_{jikl}\varepsilon_{kl}\varepsilon_{kl}$$

which implies the following equalities

$$\mathbb{C}_{ijkl} = \mathbb{C}_{ijlk} = \mathbb{C}_{jikl} = \mathbb{C}_{jilk}$$

The above relation states that the elastic tensor which by definition relates symmetric second-order tensors, possesses the the so-called *minor symmetries*

$$C_{ijkl} = C_{ijlk} = C_{jikl}$$

and thus presents, at most, 21 independent components.

In addition, the elastic tensor $\mathbb{C}$ is said to be *positive definite* if

$$\boldsymbol{\varepsilon} : \mathbb{C}\boldsymbol{\varepsilon} > 0 \qquad \forall \boldsymbol{\varepsilon} \in \mathbf{L}\mathrm{in}^{\mathrm{sym}} \tag{1.66}$$

while it is said to be *strongly elliptic* [60, 75] if

$$(\mathbf{a} \otimes \mathbf{b}) : \mathbb{C}\,(\mathbf{a} \otimes \mathbf{b}) > 0 \qquad \forall \mathbf{a}, \mathbf{b} \in \mathbf{l}\mathrm{in} \tag{1.67}$$

Finally, $\mathbb{C}$ is said to be *pointwise stable* [60] if there exists a constant $\alpha > 0$ such that

$$\boldsymbol{\varepsilon} : \mathbb{C}\boldsymbol{\varepsilon} \geq \alpha \parallel \boldsymbol{\varepsilon} \parallel^2 \qquad \forall \boldsymbol{\varepsilon} \in \mathbf{L}\mathrm{in}^{\mathrm{sym}} \tag{1.68}$$

Clearly pointwise stability implies, but is not implied, by strong ellipticity. Moreover, pointwise stability is equivalent to pointwise positive definiteness, under the assumption that $\mathbb{C}$ is continuous on $\bar{\Omega}$.

Inverting relationship (1.65), we may obtain the strain as a function of stress

$$\boldsymbol{\varepsilon} = \mathbb{A}\boldsymbol{\sigma} \tag{1.69}$$

and define the fourth-order *compliance tensor* $\mathbb{A}$, inverse of $\mathbb{C}$. Equivalently

$$\mathbb{A}\,(\mathbb{C}\boldsymbol{\varepsilon}) = \boldsymbol{\varepsilon} \qquad \forall \boldsymbol{\varepsilon},\ \boldsymbol{\varepsilon}^T = \boldsymbol{\varepsilon}$$

and

$$\mathbb{C}\,(\mathbb{A}\boldsymbol{\sigma}) = \boldsymbol{\varepsilon} \qquad \forall \boldsymbol{\sigma},\ \boldsymbol{\sigma}^T = \boldsymbol{\sigma}$$

Isotropic elasticity

A material that has no *preferred directions* in a way that it resists to external agencies independently of its orientation is said to be *isotropic* [41]. The property of isotropy for a linear elastic material reduces the twenty-one independent components of the elastic tensor to two and from a mathematical standpoint amounts to say that the elastic tensor $\mathbb{C}$ presents also the so-called *major symmetries*

$$\mathbb{C}_{ijkl} = \mathbb{C}_{klij}$$

In this hypothesis the elastic tensor admits the following representation [57]

$$\mathbb{C} = \lambda\,(\mathbf{I} \otimes \mathbf{I}) + 2\mu\mathbb{I}^I \tag{1.70}$$

where the constants λ and μ are called *Lamé moduli* and depend on the material. This corresponds to a linear elastic relation between stress and strain in the form:

$$\boldsymbol{\sigma} = \lambda(\mathrm{tr}(\boldsymbol{\varepsilon}))\mathbf{I} + 2\mu\boldsymbol{\varepsilon} \tag{1.71}$$

Bearing in mind the previous definition and recalling the volumetric/deviatoric splitting of the fourth-order identity tensor (cf. (1.10)), we may perform the decoupling into volumetric and deviatoric parts of the elastic tensor as well. Thus, the following relationship is derived

$$\begin{aligned}\mathbb{C} &= \left[\lambda\,(\mathbf{I} \otimes \mathbf{I}) + 2\mu\mathbb{I}^I\right] = [(3\lambda + 2\mu)\mathbb{I}_{\mathrm{vol}} + 2\mu\mathbb{I}_{\mathrm{dev}}] \\ &= [3K\mathbb{I}_{\mathrm{vol}} + 2\mu\mathbb{I}_{\mathrm{dev}}]\end{aligned}$$

with $3K = 3\lambda + 2\mu$, such that:

$$\begin{aligned}\boldsymbol{\sigma} = \mathbb{C}\boldsymbol{\varepsilon} &= [3K\mathbb{I}_{\mathrm{vol}} + 2\mu\mathbb{I}_{\mathrm{dev}}]\,\boldsymbol{\varepsilon} \\ &= 3K\mathbb{I}_{\mathrm{vol}}\boldsymbol{\varepsilon} + 2\mu\mathbb{I}_{\mathrm{dev}}\boldsymbol{\varepsilon}\end{aligned}$$

Recalling the split of a second-order tensor into its volumetric and deviatoric components (cf. (1.11)), we may write:

$$\begin{aligned}\boldsymbol{\sigma} &= p\mathbf{I} + \mathbf{s} \\ \boldsymbol{\varepsilon} &= \frac{1}{3}\theta\mathbf{I} + \mathbf{e}\end{aligned}$$

where $p = (1/3)\mathrm{tr}(\boldsymbol{\sigma})$ and $\theta = \mathrm{tr}(\boldsymbol{\varepsilon})$ are respectively the *pressure* and the *volumetric deformation*, while $\mathbf{s}$ and $\mathbf{e}$ are respectively the stress and strain

deviator. The uncoupled volumetric and deviatoric constitutive equations thus read:

$$\begin{aligned} p &= K\theta \\ \mathbf{s} &= 2\mu\mathbf{e} \end{aligned} \tag{1.72}$$

The scalar coefficient μ is referred to as the *shear modulus*, while the material coefficient $K = (\lambda + 2/3\mu)$ is called the *bulk modulus* and represents a measure of the ratio between the spherical stress and the change in volume [57]. The shear modulus μ is often denoted by G, especially in the engineering literature. With the above specifications, the isotropic linear elastic constitutive equations (1.72) can be rewritten as follows

$$p = K\theta \tag{1.73}$$

$$\mathbf{s} = 2G\mathbf{e} \tag{1.74}$$

where $\mathbf{s}$ and $\mathbf{e}$ are the deviatoric stress and strain, respectively. The quantities $p = 1/3\mathrm{tr}(\boldsymbol{\sigma})$ and $\theta = \mathrm{tr}(\boldsymbol{\varepsilon})$ are associated to the volumetric part of the stress and of the strain and are respectively called *pressure* and *volumetric deformation*.

It is worth trying to see if it is possible to find another choice of coefficients that define the linear isotropic elastic behavior of a material. We may try to find another set of parameters that play the same role as the Lamé moduli coefficients, from studying the mechanical behavior of an isotropic linear elastic rod subjected to uniaxial stress. Suppose that the rod lies aligned with the x_1 axis and that it is subjected to a uniform stress $\sigma_{11} \neq 0$, being the remaining stress components zero. Limiting our investigation to the ratios $\sigma_{11}/\varepsilon_{11}$ and $\varepsilon_{33}/\varepsilon_{11}$, or equivalently, $\varepsilon_{22}/\varepsilon_{11}$ we may define the following material parameters

$$\text{Young's modulus } E = \frac{\sigma_{11}}{\varepsilon_{11}}$$

$$\text{Poisson's ratio } \nu = -\frac{\varepsilon_{22}}{\varepsilon_{11}}$$

which measure, respectively, the slope of the stress-strain curve pertaining to the material which the rod is made of and the lateral contraction of the rod. Physical and experimental considerations suggest that the preceding are positive quantities. In what follows it will be seen how further restrictions, induced by thermodynamic considerations, hold on the quantities E and ν.

Using relation (1.70) and recalling the form of the stress and of the strain tensors in pure tension

$$[\boldsymbol{\sigma}] = \begin{bmatrix} \sigma_{11} & 0 & 0 \\ 0 & 0 & 0 \\ 0 & 0 & 0 \end{bmatrix} \quad [\boldsymbol{\varepsilon}] = \begin{bmatrix} \varepsilon_{11} & 0 & 0 \\ 0 & \varepsilon_{22} & 0 \\ 0 & 0 & \varepsilon_{33} \end{bmatrix}$$

it is possible to correlate the pairs $\{\lambda, \mu\}$ and $\{E, \nu\}$. Omitting the complete calculation, one obtains

$$E = \frac{\mu\,(3\lambda + 2\mu)}{(\mu + \lambda)} \tag{1.75}$$

$$\mu = \frac{\lambda}{2\,(\mu + \lambda)} \tag{1.76}$$

With the above relation, it is possible to invert relationship (1.71) and obtain a useful expression of strain in terms of stress involving E and μ

$$\boldsymbol{\varepsilon} = E^{-1}\left[(1+\nu)\,\boldsymbol{\sigma} - \nu \mathrm{tr}\,(\boldsymbol{\sigma})\,\mathbf{I}\right] \tag{1.77}$$

The above linear relationship between strain and stress, valid for isotropic media, is commonly referred to as Hooke's law. Applying the definitions of pointwise stability and of strong ellipticity to the fourth-order elastic tensor (see (1.67) and (1.68)), a set of bounds on the material parameters can be derived for the material parameter Young's modulus E [60]. These conditions allow to state that a linear elastic isotropic material is

- *pointwise stable* if and only if $\mu > 0$ and $3\lambda + 2\mu > 0$ or, equivalently, if and only if $E > 0$ and $-1 < \nu < \dfrac{1}{2}$
- *strongly elliptic* if and only if $\mu > 0$ and $\lambda + 2\mu > 0$ or, equivalently, if and only if $E > 0$ and $\nu < \dfrac{1}{2}$ or $\nu > 1$

1.6 Thermodynamic setting for elasticity

A common procedure in Mechanics of solids is to introduce a constitutive model as a set of relations that hold from a thermodynamic standpoint [4, 57, 41]. Precisely, the most favorable context is within a *thermodynamic theory with internal variables*. In this section, we present the linear elastic material behavior in this fashion. The treatment of the elastoplastic case is carried out in Chapter 2.

Suppose that a material body is subjected to a body force $\mathbf{b}$ in its interior and to a surface traction $\mathbf{t}$ upon its boundary. Analogously, the body will be acted by thermal equivalents of the previous mechanical sources: a *heat source* r per unit volume in the interior and a *heat flux* $\mathbf{q}$ across its boundary unit area. The first *law of Thermodynamics*, which essentially is a balance of energy statement, indicates that for any part Ω' of the body Ω, the rate of change of total energy plus kinetic energy equals the amount of work done on that part by the mechanical forces plus the heat supply. Mathematically, the law can be formulated in the form

$$\frac{d}{dt}\int_{\Omega'}(e+\frac{1}{2}\rho \parallel \dot{\mathbf{u}} \parallel^2)dv = \int_{\Omega'}\mathbf{b}\cdot\dot{\mathbf{u}}dv + \int_{\partial\Omega'}\mathbf{t_n}\cdot\dot{\mathbf{u}}da + \int_{\Omega'}rdv - \int_{\partial\Omega'}\mathbf{q}\cdot\dot{\mathbf{n}}da \tag{1.78}$$

where e is the internal energy density, $\dot{\mathbf{u}}$ is the velocity field, while $\partial\Omega'$ represents the boundary of Ω'. The minus sign before the last integral in (1.78) appears, since the heat flux vector $\mathbf{q}$ points outward the surface Ω' as well as $\mathbf{n}$. The preceding formulation can be simplified applying the divergence theorem to the term involving the surface traction which, invoking the symmetry of $\boldsymbol{\sigma}$, becomes (cf. $(1.52)_3$)

$$\begin{aligned}\int_{\partial\Omega'}\mathbf{t_n}\cdot\dot{\mathbf{u}}da = \int_{\partial\Omega'}\boldsymbol{\sigma}\mathbf{n}\cdot\dot{\mathbf{u}}da &= \int_{\Omega'}\boldsymbol{\sigma}:\nabla\dot{\mathbf{u}}dv + \int_{\Omega'}\mathrm{div}\boldsymbol{\sigma}\cdot\dot{\mathbf{u}}dv \\ &= \int_{\Omega'}\boldsymbol{\sigma}:\dot{\boldsymbol{\varepsilon}}dv + \int_{\Omega'}\mathrm{div}\boldsymbol{\sigma}\cdot\dot{\mathbf{u}}dv\end{aligned}$$

Substituting the last result in (1.78) and recalling the equation of balance of linear momentum (1.58), the first law can be rewritten as

$$\frac{d}{dt}\int_{\Omega'}edv = \int_{\Omega'}\boldsymbol{\sigma}:\dot{\boldsymbol{\varepsilon}}dv + \int_{\Omega'}rdv - \int_{\partial\Omega'}\mathbf{q}\cdot\mathbf{n}da \tag{1.79}$$

where it is implicitly assumed that $\dot{\boldsymbol{\varepsilon}} = \boldsymbol{\varepsilon}(\dot{\mathbf{u}})$. The *local* form of the above balance law follows from the requirement that all the involved field variables are sufficiently regular. This hypothesis allows to convert the surface integral on $\partial\Omega'$ appearing in (1.79) using the divergence theorem. Thus we are lead to

$$\int_{\Omega'}(\dot{e} - \boldsymbol{\sigma}:\dot{\boldsymbol{\varepsilon}} - r + \mathrm{div}\mathbf{q})dv = 0$$

which, for the arbitrariness of the portion Ω', gives

$$\dot{e} = \boldsymbol{\sigma}:\dot{\boldsymbol{\varepsilon}} + r - \mathrm{div}\mathbf{q} \tag{1.80}$$

It is useful to introduce also the notions of *entropy* η per unit volume or *entropy density*. This notion is given through the *absolute temperature* $\theta > 0$. Accordingly, it is assumed that the *entropy flux* across the bounding surface $\partial\Omega'$ into a material body Ω' is given by

$$\int_{\partial\Omega'} \theta^{-1}\mathbf{q}\cdot\mathbf{n}da$$

while the entropy supplied by the exterior is

$$\int_{\Omega'} \theta^{-1} r dv$$

The second law of Thermodynamics states that the rate of increase in entropy in the body is not less than the total entropy supplied to the body by the heat sources. The second law can thus be formalized as an integral inequality of the form

$$\frac{d}{dt}\int_{\Omega'} \eta dv \geq \int_{\Omega'} \theta^{-1} r dv - \int_{\partial\Omega'} \theta^{-1}\mathbf{q}\mathbf{n}da \tag{1.81}$$

The local form of the second law can be derived with some calculations of the same type of those carried out in finding the local form of the first law (1.80). Thus we have

$$\dot{\eta} \geq -\mathrm{div}(\theta^{-1}\mathbf{q}) + \theta^{-1} r \tag{1.82}$$

The inequalities (1.81) and (1.82) are known as the *Clausius-Duhem* form of the second law of Thermodynamics.

Introducing the *Helmoltz free energy* ψ, defined by

$$\psi = e - \eta\theta \tag{1.83}$$

and recalling the local form of the first law (1.80), we may rewrite (1.82) as

$$\dot{\psi} + \eta\dot{\theta} - \boldsymbol{\sigma} : \dot{\boldsymbol{\varepsilon}} + \theta^{-1}\mathbf{q}\cdot\nabla\theta \leq 0 \tag{1.84}$$

Relation (1.84) is known as the *local dissipation inequality*.

Since the arguments of the subsequent sections will always refer to isothermal processes, it is convenient to specialize the previous fundamental laws to such a case. Assume that the body temperature is uniformly constant and that the reference material body does not experience any exterior heat supply. Under these hypotheses, the local form of the dissipation inequality simplifies to

$$\dot{\psi} - \boldsymbol{\sigma} : \dot{\boldsymbol{\varepsilon}} \leq 0 \tag{1.85}$$

Linear elastic material

It is possible to give a characterization of the linear elastic material behavior in the thermodynamic framework developed hitherto. In this sense, it is customary to define a linear elastic material as one for which the constitutive equations take the form

$$\psi = \psi(\boldsymbol{\varepsilon}) \tag{1.86}$$

$$\boldsymbol{\sigma} = \sigma(\boldsymbol{\varepsilon}) \tag{1.87}$$

that is with the free energy and the stress field depending only on the strain. Dependence on time is also dropped. It is assumed that the functions appearing in (1.86) and in (1.87) are sufficiently regular with respect to their argument so that they can be differentiated as many times as required.

Substituting (1.86) into the local dissipation inequality, it is immediate to derive

$$\left(\frac{\partial \psi}{\partial \boldsymbol{\varepsilon}} - \boldsymbol{\sigma}\right) : \dot{\boldsymbol{\varepsilon}} \leq 0 \tag{1.88}$$

Hence, admitting that inequality (1.88) holds for all $\dot{\boldsymbol{\varepsilon}}$, the stress is expressed through the Helmoltz free energy ψ as

$$\boldsymbol{\sigma} = \frac{\partial \psi}{\partial \boldsymbol{\varepsilon}} \tag{1.89}$$

The stress-strain relationship (1.65), which is the characterizing feature of linear elastic materials, is obtained as a special case of Equation (1.89), when the free energy is a quadratic form of the strain, i.e.

$$\psi(\boldsymbol{\varepsilon}) = \frac{1}{2}\boldsymbol{\varepsilon} : \mathbb{C}\boldsymbol{\varepsilon} \tag{1.90}$$

According to the previous definition, ψ represents an *elastic potential* for the *state variable* $\boldsymbol{\sigma}$. In component form we may write

$$\psi(\boldsymbol{\varepsilon}) = \frac{1}{2}\mathbb{C}_{ijkl}\varepsilon_{ij}\varepsilon_{kl} \tag{1.91}$$

The above equation implies a relationship between the elastic tensor $\mathbb{C}$ and the elastic potential ψ. of the following type

$$\mathbb{C} = \frac{\partial^2 \psi}{\partial \boldsymbol{\varepsilon} \partial \boldsymbol{\varepsilon}} \tag{1.92}$$

which holds if the elastic tensor possesses the major symmetries, already introduced in Section 1.5 for discussing the symmetry properties of the isotropic elastic tensor. Namely, it is required that

$$C_{ijkl} = C_{klij} \tag{1.93}$$

The above condition grants the existence of the strain energy function [57] and must be fulfilled for relation (1.90) to be valid.

1.7 Initial boundary value problem of equilibrium in linear elasticity

Following the previous arguments, it is possible to formulate the mathematical problem that describes the deformation and the stress state of an isotropic linear elastic material body under an assigned set of external actions. For simplicity, the treatment is limited to isothermal static processes in which the effects of temperature variations and of heat flux exchanges are neglected. This problem is modeled by a set of partial differential equations posed on the domain Ω plus a set of boundary conditions assigned on the boundary $\partial\Omega$ of the body and a set of initial conditions.

Given a body with current configuration $\Omega \subset \mathcal{R}^3$, we indicate for compactness its boundary $\partial\Omega$ with Γ such that $\Gamma = \bar{\Gamma}_D \cup \bar{\Gamma}_S$, with $\bar{\Gamma}_D \cap \bar{\Gamma}_S = \varnothing$. Suppose that, for $t \in [0, T]$, a body force $\mathbf{b}(\mathbf{x}, t)$ is assigned in Ω, a displacement field $\bar{\mathbf{u}}(\mathbf{x}, t)$ is assigned on $\bar{\Gamma}_D$ and a surface traction $\bar{\mathbf{t}}(\mathbf{x}, t)$ is assigned on $\bar{\Gamma}_S$. Initial values for the displacement $\mathbf{u}(\mathbf{x}, 0) = \mathbf{u}_0$ and the velocity field $\mathbf{v}(\mathbf{x}, 0) = \mathbf{v}_0$ are known data as well. With the above specifications, the formulation of the *initial boundary value problem* for the isotropic linear elastic body under consideration is: find the displacement field $\mathbf{u}(\mathbf{x}, t)$ which, for any $\mathbf{x} \in \Omega$ and any $t \in [0, T]$, solves the

- *equation of dynamic equilibrium*

$$\mathrm{div}\boldsymbol{\sigma} + \mathbf{b} = \rho\ddot{\mathbf{u}} \tag{1.94}$$

- *strain-displacement relation*

$$\boldsymbol{\varepsilon}(\mathbf{u}) = \frac{1}{2}\left[\nabla\mathbf{u} + (\nabla\mathbf{u})^T\right] \tag{1.95}$$

- *constitutive relation*

$$\boldsymbol{\sigma} = \mathbb{C}\boldsymbol{\varepsilon} \tag{1.96}$$

and satisfies the

- *boundary conditions*

$$\mathbf{u} = \bar{\mathbf{u}} \quad \text{on} \quad \Gamma_D \quad \text{and} \quad \boldsymbol{\sigma}\mathbf{n} = \bar{\mathbf{t}} \quad \text{on} \quad \Gamma_S \tag{1.97}$$

- *initial conditions*

$$\mathbf{u}(\mathbf{x}, 0) = \mathbf{u}_0(\mathbf{x}) \quad \text{and} \quad \dot{\mathbf{u}}(\mathbf{x}, 0) = \dot{\mathbf{u}}_0(\mathbf{x}) \tag{1.98}$$

Equations (1.94)-(1.98) are known as *governing equations* of the linear elastic initial boundary value problem. Taking the displacement $\mathbf{u}$ as the primary unknown, the problem can be reduced to one singular partial differential equation, by solving successively for the stress and the strain. With these manipulations, the equation of motion becomes

$$\operatorname{div}(\mathbb{C}\boldsymbol{\varepsilon}(\mathbf{u})) + \mathbf{b} = \rho\ddot{\mathbf{u}} \tag{1.99}$$

while the second boundary condition in (1.97) is replaced by

$$(\mathbb{C}\boldsymbol{\varepsilon}(\mathbf{u}))\,\mathbf{n} = \bar{\mathbf{t}} \quad \text{on} \quad \Gamma_S \tag{1.100}$$

When the problem data $\bar{\mathbf{u}}(\mathbf{x}, t)$, $\mathbf{b}(\mathbf{x}, t)$ and $\bar{\mathbf{t}}(\mathbf{x}, t)$ are such that the acceleration term can be omitted in (1.99), the problem is defined as *quasi-static* [73]. Accordingly, the statement of this problem becomes: find a displacement field $\mathbf{u}(\mathbf{x}, t)$ that satisfies the *equation of equilibrium*

$$\operatorname{div}\boldsymbol{\sigma} + \mathbf{b} = \mathbf{0} \tag{1.101}$$

and Equations (1.95)-(1.97).

A formulation of equilibrium in terms of the displacement field $\mathbf{u}$ only can equally be obtained for the quasi-static initial boundary value problem, leading to Equation (1.99) with the right hand side equal to zero.

1.8 Thermodynamics with internal variables

The continuum thermodynamic theory briefly presented in Section 1.6 is a suitable tool for the discussion of elasticity and Thermoelasticity, but the same does not hold true when more "complicated" mechanic phenomena are taken into consideration. For example, in order to model physical processes involving chemical reactions, it often results necessary to equip the thermodynamic model with a finite number of *internal variables* that serve to account for the

evolution and advancement of each single reaction. These variables, which are intended to describe irreversible processes, may be regarded either as scalar or tensorial entities. A similar situation arises if the thermodynamic framework presented so far is extended to the mathematical modeling of mechanical elastoplastic phenomena. In this section a short introduction is given on the argument, in order to present an extension of the thermodynamic theory adopted in Section 1.6. In this case the theory is referred to as *Thermodynamics with internal variables* and may be conveniently adopted as a plasticity theory. More information regarding this kind of approach and its mathematical foundations may be found in [28, 36, 37, 40].

The first and second laws of Thermodynamics as stated in the forms (1.80) and (1.82) remain valid, as well as the thermodynamic hypotheses of isothermal process with no heat flux nor change in temperature in the body.

We consider a material for which the Helmoltz free energy and the stress are functions of the strain and of a particular set of strain-like internal variables, collected in the generalized m-component vector $\boldsymbol{\xi} = (\boldsymbol{\xi}_k)$, $(1 \leq k \leq m)$. These quantities may be regarded either as scalars or tensors, depending on the particular elastoplastic model under consideration. The constitutive equations are thus of the form

$$\psi = \psi(\boldsymbol{\varepsilon}, \boldsymbol{\xi}) = \psi(\boldsymbol{\varepsilon}, \boldsymbol{\xi}_1, ..., \boldsymbol{\xi}_m) \tag{1.102}$$

$$\boldsymbol{\sigma} = \boldsymbol{\sigma}(\boldsymbol{\varepsilon}, \boldsymbol{\xi}) = \boldsymbol{\sigma}(\boldsymbol{\varepsilon}, \boldsymbol{\xi}_1, ..., \boldsymbol{\xi}_m) \tag{1.103}$$

Differing from elasticity, in which the loading history of the material is not relevant, modeling inelastic phenomena implies introducing constitutive equations in rate form, i.e. involving time derivatives of the internal variables. These equations are intended to define the irreversible plastic effects in terms of the internal variables. Therefore, the model represented by Equations (1.102)-(1.103), is endowed with the following *evolutive constitutive equations*

$$\dot{\boldsymbol{\xi}}_k = \boldsymbol{\beta}_k(\boldsymbol{\varepsilon}, \boldsymbol{\xi}) = \boldsymbol{\beta}_k(\boldsymbol{\varepsilon}, \boldsymbol{\xi}_1, ..., \boldsymbol{\xi}_m) \tag{1.104}$$

In the next chapter, Equations (1.104) will be specialized for some significant case models. Introducing (1.102) and (1.103) into (1.84) it is easy to derive

$$\left(\frac{\partial \psi}{\partial \boldsymbol{\varepsilon}} - \boldsymbol{\sigma} \right) : \dot{\boldsymbol{\varepsilon}} + \frac{\partial \psi}{\partial \boldsymbol{\xi}_k} : \dot{\boldsymbol{\xi}}_k \leq 0 \tag{1.105}$$

which, recalling the arbitrariness of the strain rate $\dot{\boldsymbol{\varepsilon}}$, gives

$$\boldsymbol{\sigma} = \frac{\partial \psi}{\partial \boldsymbol{\varepsilon}} \tag{1.106}$$

In correspondence to the internal variables $\boldsymbol{\xi}_k$ $(1 \leq \ k \leq m)$, the *thermodynamic forces* or *thermodynamic affinities* $\boldsymbol{\chi}_k$ $(1 \leq \ k \leq m)$ are defined by

$$\boldsymbol{\chi}_k = -\frac{\partial \psi}{\partial \boldsymbol{\xi}_k} \quad 1 \leq \ k \leq m \tag{1.107}$$

and are said to be the *conjugate* to the internal variables $\boldsymbol{\xi}_k$. The thermodynamic forces are collected in the generalized m-component vector $\boldsymbol{\chi} = (\boldsymbol{\chi}_k)$, $(1 \leq k \leq m)$ and may be regarded either as scalars or tensors, depending on the particular elastoplastic model under consideration. Obviously, the kth internal variable $\boldsymbol{\xi}_k$ and the kth thermodynamic force $\boldsymbol{\chi}_k$ have the same algebraic dimension.

For later use we define the scalar product between the generalized internal variable and thermodynamic force vectors

$$\boldsymbol{\chi} \cdot \boldsymbol{\xi} = \boldsymbol{\chi}_k : \boldsymbol{\xi}_k \quad 1 \leq k \leq m \tag{1.108}$$

In agreement with relations (1.105) and (1.106), it is found that

$$\boldsymbol{\chi} \cdot \dot{\boldsymbol{\xi}} = \boldsymbol{\chi}_k : \dot{\boldsymbol{\xi}}_k \geq 0 \tag{1.109}$$

The l.h.s. quantity in the above inequality is a scalar product between force-like variables and strain rate-like variables, which can be interpreted as a rate of work dissipated in the time unit, acted by the thermodynamic forces and due to the time variation of those agencies modeled by the internal variables. In the following chapter, it is shown that inequality (1.109) plays a key role in the mathematical formulation of elastoplasticity.

Chapter 2

Elastoplasticity

Introduzione

Questo capitolo presenta i lineamenti essenziali del comportamento meccanico del materiale di tipo elastoplastico e della teoria matematica che modella tale comportamento. Il capitolo risulta suddiviso in tre distinte sezioni.

La Sezione 2.2 è dedicata al noto modello elastoplastico unidimensionale. La discussione è intesa, in questo contesto, ad affrontare i caratteri tipici del comportamento elastoplastico nel semplice caso di una provetta di materiale elastoplastico soggetta a prova di trazione monoassiale. Viene anche presentata, per il semplice caso monoassiale, la modellazione secondo la teoria termodinamica a variabili interne introdotta nel Capitolo 1.

Lo studio di un modello elastoplastico unidimensionale è presentato onde illustrare alcune caratteristiche fondamentali del comportamento elastoplastico riscontrabili nel caso tridimensionale, mantenendo pur sempre una semplice trattazione.

La Sezione 2.3 concerne il modello elastoplastico tridimensionale, che viene sviluppato mediante generalizzazione dei concetti introdotti nella sezione precedente. In particolare, vengono presentate le equazioni del modello elastoplastico tipo J_2, o di von-Mises, ad incrudimento lineare isotropo e cinematico e ad incrudimento non lineare cinematico.

La Sezione 2.5 può considerarsi come un capitolo a sè stante. È, infatti, dedicata alla riformulazione delle leggi costitutive della plasticità mediante gli strumenti matematici essenziali della Analisi convessa. I risultati e gli sviluppi analitici presentati in questa sezione costituiscono il punto fondamentale per la analisi del problema a valori iniziali e dati al bordo dell'equilibrio elastoplastico affrontata nel successivo Capitolo 3. I concetti matematici sviluppati nella Sezione 2.5 sono affiancati dai richiami di Analisi funzionale e di Teoria degli

spazi di funzioni fatti nella Appendice A.

La trattazione sulla teoria della elastoplasticità presentata in questo capitolo segue, tra gli altri, anche alcuni testi classici sull'argomento quali [41, 69, 70]. La dissertazione sulla riformulazione analitico-convessa è presentata traendo spunto da [41].

2.1 Introduction

This chapter is intended to present some fundamental concepts on the classical elastoplastic material behavior and on the mathematical modeling of such phenomenon. The chapter is divided in three main sections.

In Section 2.2 we address a well known one-dimensional elastoplastic model. The discussion in this context is intended to offer the basic features of the elastoplastic material response in the simple case of a uniaxial test. Also the first elements of the mathematical modeling of an elastoplastic phenomenon in terms of the thermodynamic theory with internal variables addressed in Chapter 1 are presented. The study of a uniaxial model is accomplished in order to illustrate peculiarities of the model at hand that are mirrored in the three-dimensional case yet maintaining the treatment as simple as possible. In Section 2.3 we address the three-dimensional elastoplastic model. The model is developed as a generalization of the concepts enlightened in the previous section. In particular, the J_2, or von-Mises, elastoplastic constitutive model with linear isotropic and kinematic and nonlinear kinematic hardening mechanisms is addressed in detail.

Section 2.5 represents a chapter of its own at some extents. It is in fact dedicated to the recasting of the mathematical theory of elastoplasticity analyzed so far within a convex-analytic context. The fundamental derivations presented in this section result the key point for the analysis of the initial boundary value problem of elatoplastic equilibrium that is the object of the next Chapter 3. The mathematical concepts used in this section are supported by the definitions and the fundamental results on functional analysis and function spaces which are reported in Appendix A at the end of the work.

The treatment of classical elastoplasticity exposed in this chapter follows [41, 69, 70]. The convex-analytic framework for the elastoplastic constitutive relations is derived by [41].

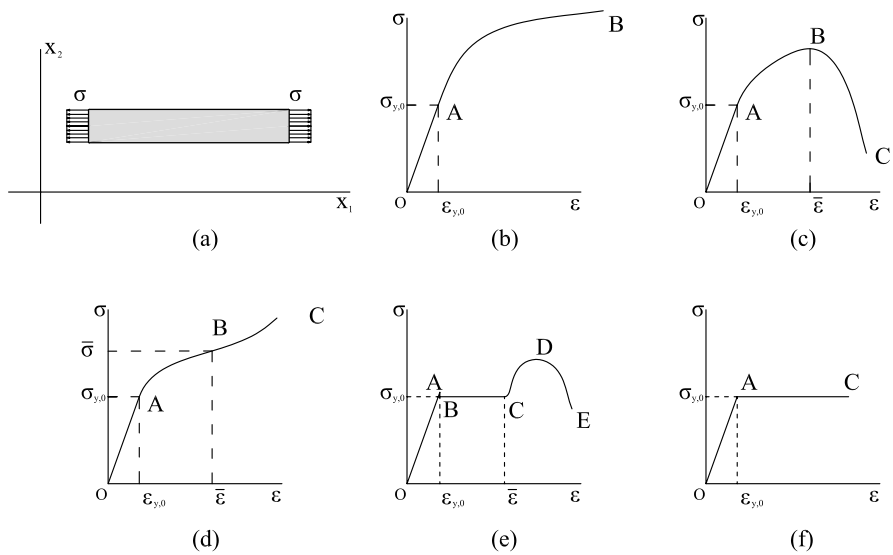

Figure 2.1: (a) Uniaxial tension of an elastoplastic rod; (b) Stress-strain curve with hardening; (c) Stress-strain curve with hardening and softening; (d) Stress-strain curve with hardening and stiffening; (e) Stress-strain curve for a typical mild steel; (f) Stress-strain curve for an elasto-perfectly-plastic material

2.2 A one-dimensional elastoplastic model

Basic features of a one-dimensional model

We begin with the study of a simple one-dimensional model which enlightens the basic features of the elastoplastic behavior. This makes it easier to discuss the three-dimensional case as a generalization of the concepts addressed in the one-dimensional context.

Let us consider for example the uniaxial stress state of the thin bar illustrated in Figure 2.1(a) subjected to uniform distributions of forces per unit area $\sigma \equiv \sigma_{11}$ applied at its ends. We suppose to report the graph of stress σ versus strain $\varepsilon \equiv \varepsilon_{11}$ in order to record the history of behavior during a loading in which, for instance, the applied force is gradually increased. The observer may thus encounter different situations as represented in Figures 2.1(b)-(d). All the cases illustrated in Figures 2.1(b)-(d)) have common peculiarities which characterize the elastoplastic behavior. In fact, a relationship between stress and strain of the form represented by the branch OA can be observed in Fig-

ures 2.1(b)-(d), up to a stress value $\sigma_{y,0}$, corresponding to a strain level $\varepsilon_{y,0}$. If the stress σ is reset to zero from any level $\sigma \leq \sigma_0$, the material recovers its strain completely. This part of the curve is known as the linear elastic path in that upon unloading the material returns to the unstressed and undeformed state and the relationship between stress and strain is linear.

Then, as the stress increases, one observes a deviation from the linear relation between stress and strain. This part of the curve represents the plastic or, more generally, the inelastic behavior of the material. A common feature along the path past the deviation is a decrease in the slope of the stress-strain curve as represented in Figure 2.1(b). Such a circumstance is known as *hardening behavior*. As the experiment proceeds, a variety of phenomena may be encountered. In Figure 2.1(c), for instance, one finds that, after a strain value $\bar{\varepsilon}$ is reached, the curve slope progressively diminishes up to a negative value and the plastic behavior is referred to as a *softening* one. This particular behavior is typically viewable in materials such as soil and concrete, which as it is well known are elastoplastic materials. In Figure 2.1(d), past a first path showing hardening, the slope of the stress-strain curve progressively increases. This behavior is known as *stiffening* and is typical of some metallic materials. The threshold between elastic and inelastic behavior is characterized by the stress level $\sigma_{y,0}$, known as *initial yield uniaxial stress*.

In practice, a material can show a stress-strain curve which encompasses more than one of the single effects analyzed above. For instance, consider the stress-strain curve of a typical mild steel, given in Figure 2.1(e). It is evident that such a material presents a complex series of elastoplastic features. In the range OA it shows linear elastic behavior which upon loading is followed by a sudden drop of the stress along AB, with no significant increase of elongation. After that, the stress-strain curve BC presents an almost zero slope which afterwards increases following CD and finally decreases along DE. In Figure 2.1(f) a simple idealization of the real behavior just illustrated is represented: the stress-strain curve in this case is usually referred as the one of an elasto-perfectly-plastic material in that it is the sequence of a pure linear elastic part followed by a purely plastic branch with no hardening.

A proper feature possessed by elastoplastic materials can be appreciated in Figure 2.2(a) which shows that the response in compression does not necessarily mirror the one observed in tension. In fact, the initial compressive uniaxial stress $\sigma'_{y,0}$ may differ in magnitude from the tensile value $\sigma_{y,0}$ as well as the post-elastic part of the stress-strain curve ($\sigma < \sigma'_{y,0}$) may not equal the curve pattern for $\sigma > \sigma_{y,0}$.

Another distinctive character of plastic materials is shown in Figure 2.2(b) and is *irreversibility* or *path-dependence*. By this it is meant that, unlike the

elastic materials, the original zero stress-strain state is not recovered upon removal of applied forces, once the yield threshold has been passed. As can be inspected in Figure 2.2(b), if the direction of loading is inverted at $\sigma_{y,1} > \sigma_{y,0}$ (point B), the path followed is not the original curve BAO (this case would actually imply simple nonlinear elastic behavior). Instead, the material behaves elastically, but on the stress path represented by the straight line BC, parallel to OA. This phase is referred to as *elastic unloading*; its peculiarity relies in the fact that after the loading has been completely removed the material shows a residual strain which is not elastically recovered (point B′). A new elastic behavior path is seen if the stress is further decreased down to the yield stress value $\sigma'_{y,1}$, which in general differs from the uniaxial compressive initial yield stress $\sigma'_{y,0}$. Finally, the curve follows the branch CD if the stress were to be decreased more.

Thus we may recognize an *initial elastic range*, i.e. the interval $\mathcal{E}_0 = (\sigma'_{y,0}, \sigma_{y,0})$, bounded by the *initial yield surface* given by the set $\mathcal{B}_0 = \{\sigma'_{y,0}, \sigma_{y,0}\}$. The initial elastic range $\mathcal{E}_0$ includes the unstressed, undeformed state (the origin). As a consequence of plastic flow, subsequent *expanded* and *shifted* elastic ranges, such as the interval $\mathcal{E}_1 = (\sigma'_{y,1}, \sigma_{y,1})$, bounded by the yield surface $\mathcal{B}_1 = \{\sigma'_{y,1}, \sigma_{y,1}\}$, can be observed. These new configurations of the elastic range are reached only as a result of plastic deformation having taken place, i.e. as a consequence of irreversible phenomena.

It is the above feature of irreversibility that sets elastoplastic materials apart from elastic ones, since it implies that no longer a one-to-one relationship exists between stress and strain. In order to compute the state of stress corresponding to a given strain level it is necessary to know the *loading history* prior to the actual state, as shown by Figure 2.2(b).

A further feature that is peculiar of the elastoplastic behavior is *rate-dependence*. Repeating the uniaxial test shown previously with different loading application rates, it is found that the elastic response is unchanged, while the plastic response ($\sigma > \sigma_{y,0}$) actually differs in a manner such as the one shown in Figure 2.3(a). Nevertheless, the elastoplastic theory that is developed in the following section in general omits to consider this effect. Thereby, in this work, attention is restricted to materials for which rate-dependence is not a significant phenomenon, or materials for which the loading histories occur at sufficiently low rates that rate-dependent effects can be neglected. The above considerations clearly indicate *material nonlinearity* as a fundamental quality of plastic behavior.

The irreversible phenomenon of plastic deformation analyzed at the microscopic scale enlightens two typical ways of material deformation, characterizing, respectively, a recoverable elastic part and an irreversible plastic part of

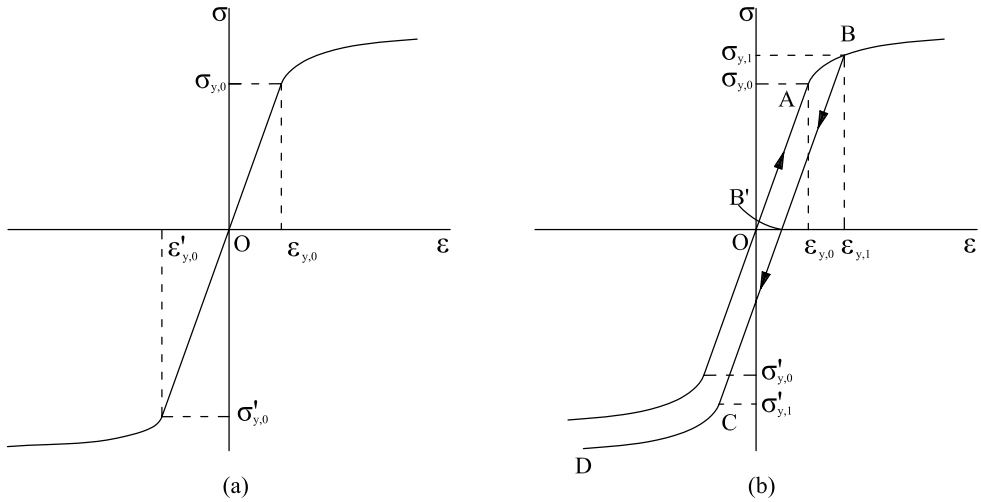

Figure 2.2: (a) Nonsymmetric uniaxial behavior in tension and compression; (b) Path dependence of the plastic behavior

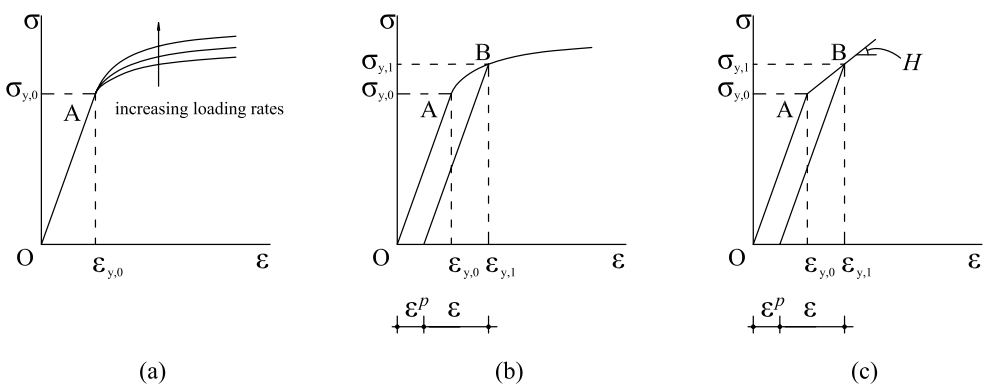

Figure 2.3: (a) Loading rate dependence of plastic behavior; (b) Additive strain decomposition into elastic and plastic parts for an elastoplastic material with nonlinear hardening; (c) Additive strain decomposition into elastic and plastic parts for an elastoplastic material with linear hardening

the total deformative effects [41]. Following this concept and the evidence of residual plastic strain (see Figures 2.3(b)-(c)), the material inelastic behavior is generally represented with an *additive strain decomposition* [14] of the form

$$\varepsilon = \varepsilon^e + \varepsilon^p$$

where

- ε^e is the so-called *elastic strain*, defined as the part of the strain related to the stress through an elastic relation or as the part of the strain which is function only of the stress, i.e. $\varepsilon^e = \varepsilon^e(\boldsymbol{\sigma})$
- ε^p is the so-called *plastic strain*, defined as the difference between the total strain and the elastic strain, i.e. $\varepsilon^p = \varepsilon - \varepsilon^e$

The elastic strain ε^e is still given by the Hooke's law

$$\sigma = E\varepsilon^e = E(\varepsilon - \varepsilon^p) \tag{2.1}$$

where E is the Young's modulus. The plastic strain ε^p is instead to be determined with account of the stress history. The elastoplastic problem can thus be formulated in the following way: given the stress state and the history of the material point, express the plastic strain rate as a function of stress and of the loading history. This approach induces a consistent representation of the elastoplastic behavior with the stress-strain curve of Figure 2.3(c) which shows the additive decomposition of the strain, the shifting of the elastic range in terms of stress (i.e. the hardening mechanism) and the path dependence of the plastic strain. In the following we present a simple uniaxial model able to describe this kind of elastoplastic behavior.

Constitutive law for the one-dimensional model

We initially refer to an elasto-perfectly-plastic material for which the initial tensile and compressive uniaxial yield stresses coincide in magnitude, i.e. $\sigma'_{y,0} = -\sigma_{y,0}$ (see Figure 2.4). Then it is assumed that ε, ε^p and σ are functions of time in the interval $[0, T] \subset \mathcal{R}$. In particular we let

$$\varepsilon^p : [0, T] \longrightarrow \mathcal{R}$$

An elastoplastic flow takes place only if $\dot{\varepsilon}^p \neq 0$. To characterize this circumstance, for the model represented in Figure 2.4, it is possible to draw the following considerations.

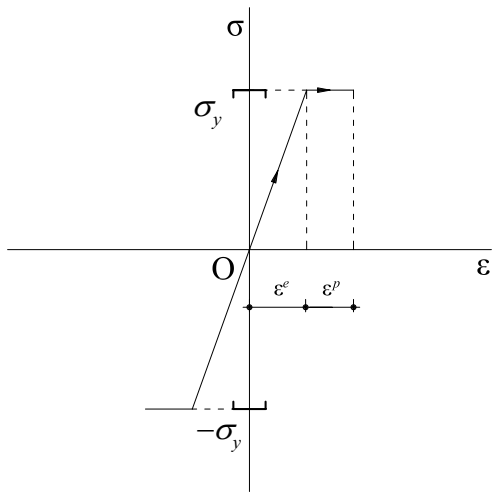

Figure 2.4: Stress-strain curve for an elasto-perfectly-plastic material

First, the stress is constrained within the closed interval $\mathcal{S} = [-\sigma_y, \sigma_y]$ which represents the union of the elastic region $\mathcal{E}$ plus the yield surface $\mathcal{B}$ and can be regarded as the *region of admissible stresses.* This set is defined through a scalar function $\phi = \phi(\sigma)$ known as the *yield function.* We have

$$\mathcal{S} = \{\sigma \in \mathcal{R} : \ \phi(\sigma) = |\sigma| - \sigma_y \leq 0\}$$

In general, ϕ depends on the stress and on the vector of thermodynamic forces (cf. (1.107)) and can be further modified to account for hardening phenomena. With the above definition at hand, we may distinguish between the following cases

$$\begin{aligned} \phi < 0 \quad &\Longleftrightarrow \quad \text{elastic range} \\ \phi = 0 \quad &\Longleftrightarrow \quad \text{elastoplastic threshold} \end{aligned}$$

Referring to the model illustrated in Figure 2.4, the plastic strain evolves according to

$$\dot{\varepsilon^p} = 0 \quad \text{if} \quad \begin{cases} \phi < 0 \\ \text{or} \\ \phi = 0 \quad \text{and} \ \dot{\phi} < 0 \end{cases} \tag{2.2}$$

and

$$\dot{\varepsilon^p} \neq 0 \quad \text{if} \quad \begin{cases} \phi = 0 \\ \text{and} \\ \dot{\phi} = 0 \end{cases} \tag{2.3}$$

Case (2.2) implies an elastic response of the material, according to which we have

$$\dot{\sigma} = E\dot{\varepsilon}$$

while the plastic strain rate is zero. Because, by assumption, stress states σ such that $\phi(\sigma) > 0$ are not admissible and $\dot{\varepsilon}^p = 0$ for $\phi(\sigma) < 0$, a change in ε^p can take place only if $\phi(\sigma) = 0$. When condition (2.3) is met the material experiences plastic flow in the direction of the applied stress, with constant rate. This equals to say that (see Figure 2.4)

$$\dot{\varepsilon^p} = \begin{cases} \dot{\gamma} \geq 0 \quad \text{if } \sigma = \sigma_y > 0 \\ \text{or} \\ -\dot{\gamma} \leq 0 \text{ if } \sigma = -\sigma_y < 0 \end{cases} \tag{2.4}$$

It is noted that the two cases shown by (2.4) can be recast into the following single equation

$$\dot{\varepsilon}^p = \dot{\gamma}\,\text{sign}\,(\sigma) \quad \text{iff} \quad \phi(\sigma) = |\sigma| - \sigma_y = 0 \tag{2.5}$$

where the scalar $\dot{\gamma}$, called the *plastic multiplier*, is always nonnegative. Whether $\dot{\gamma} \geq 0$ is actually positive or zero depends on further conditions involving the applied strain rate $\dot{\varepsilon}$ which are known as *loading/unloading conditions*.

It is possible, with the above positions, to show that the evaluation of $\varepsilon^p : [0, T] \to \mathcal{R}$ can be completely described, for any admissible stress state with the single evolutionary Equation (2.5) provided that $\dot{\gamma}$ and σ are restricted by certain unilateral constraints. First, it is noted that σ must be admissible, i.e. $\sigma \in \mathcal{S}$, and $\dot{\gamma}$ must be nonnegative by assumption. Consequently

$$\begin{aligned} \dot{\gamma} &\geq 0 \\ \phi(\sigma) &\leq 0 \end{aligned} \tag{2.6}$$

Second, by assumption, $\dot{\gamma} = 0$ if $\phi(\sigma) < 0$. On the other hand, $\dot{\varepsilon}^p \neq 0$ and, therefore, $\dot{\gamma} > 0$ only if $\phi(\sigma) = 0$. These observations imply the conditions

$$\begin{aligned} \phi(\sigma) \leq 0 \quad &\Rightarrow \quad \dot{\gamma} = 0 \\ \dot{\gamma} > 0 \quad &\Rightarrow \quad \phi(\sigma) = 0 \end{aligned}$$

and the requirement that

$$\dot{\gamma}\phi(\sigma) = 0 \tag{2.7}$$

The conditions (2.6)-(2.7) express the physical requirements for the model under consideration that the stress must be admissible and that the plastic flow, in the sense of nonzero plastic strain rate $\dot{\varepsilon}^p \neq 0$ can take place only when the stress lies on the yield surface $\mathcal{B}$. These conditions (i.e. (2.6)-(2.7)) are classical in the convex mathematical programming literature [58] and go by the name of Kuhn-Tucker conditions.

A further relation which enables to determine the actual value of $\dot{\gamma}$ at any given $t \in [0, T]$ is known as *consistency* or *persistency* condition. First, an introductory observation is in order. Let $\{\varepsilon(t), \varepsilon^p(t)\}$ be given at time $t \in [0, T]$, so that $\sigma(t)$ is also known by the elastic relationship (2.1), i.e. $\sigma(t) = E[\varepsilon(t) - \varepsilon^p(t)]$. Assume that we prescribe the total strain rate $\dot{\varepsilon}(t)$ at time t. Further, consider the case where $\sigma(t) \in \mathcal{B} \Longleftrightarrow \hat{\phi}(t) \equiv \phi(\sigma(t)) = 0$ at time t. Then, it follows that $\dot{\hat{\phi}}(t) \leq 0$, since should $\dot{\hat{\phi}}(t)$ be positive it would imply that $\hat{\phi}(t + \Delta t) > 0$ for some $\Delta t > 0$, which violates the admissibility condition $\phi \leq 0$. Further, we specify that $\dot{\gamma} > 0$ only if $\dot{\hat{\phi}}(t) = 0$ and set $\dot{\gamma} = 0$ if $\dot{\hat{\phi}}(t) < 0$, that is, dropping the hat to simplify the notation, we set

$$\begin{aligned} \dot{\gamma} > 0 \quad &\Rightarrow \quad \dot{\phi} = 0 \\ \dot{\phi} < 0 \quad &\Rightarrow \quad \dot{\gamma} = 0 \end{aligned}$$

We are left with the following condition

$$\dot{\gamma}\dot{\phi}(\sigma) = 0 \tag{2.8}$$

which is known as *consistency* condition in that it corresponds to the physical requirement that for $\dot{\varepsilon}^p$ to be nonzero (i.e. $\dot{\gamma} > 0$) the stress point $\sigma \in \mathcal{B}$ must "persist" on $\mathcal{B}$, so that $\dot{\phi}(\sigma(t)) = 0$.

For the constitutive model under examination, once the condition (2.8) holds, the expression of $\dot{\gamma}$ takes a particular simple form. Applying the chain rule and considering (2.1) and (2.5), we have

$$\dot{\phi} = \frac{\partial \phi}{\partial \sigma} E(\dot{\varepsilon} - \dot{\varepsilon}^p) = \frac{\partial \phi}{\partial \sigma} E\, \dot{\varepsilon} - \dot{\gamma} \frac{\partial \phi}{\partial \sigma} E \operatorname{sign}(\sigma) \tag{2.9}$$

It is noted that

$$\frac{\partial |\sigma|}{\partial \sigma} = \operatorname{sign}(\sigma) \Rightarrow \frac{\partial \phi}{\partial \sigma} = \operatorname{sign}(\sigma) \tag{2.10}$$

and that, being $[\text{sign}\,(\sigma)]^2 = 1$, (2.9) and (2.10) imply

$$\dot{\phi} = 0 \Rightarrow \dot{\gamma} = \dot{\varepsilon}\,\text{sign}\,(\sigma) \tag{2.11}$$

Substitution of (2.11) into (2.5) yields the result

$$\dot{\varepsilon}^p = \dot{\varepsilon} \quad \text{for} \quad \phi(\sigma) = \dot{\phi}(\sigma) = 0 \tag{2.12}$$

which essentially affirms that the plastic strain rate equals the applied strain leading to a rate form of the constitutive equation (cf. (1.63)) of the type

$$\dot{\sigma} = \begin{cases} E\dot{\varepsilon} & \text{if } \dot{\gamma} = 0 \\ 0 & \text{if } \dot{\gamma} > 0 \end{cases} \tag{2.13}$$

which allows to define the *continuous elastoplastic tangent modulus* as the constant scalar E.

The flow rule given by (2.5) is related to the yield condition expressed by the function $\phi = |\sigma| - \sigma_y$ through the potential relationship

$$\dot{\varepsilon}^p = \dot{\gamma}\,\frac{\partial \phi}{\partial \sigma} \tag{2.14}$$

since the second of (2.10). In the three-dimensional theory, for the case in which (2.14) holds, one speaks of an *associative* flow rule and of *associative* elastoplastic model.

As a next step in our presentation of the one-dimensional mathematical theory of elastoplasticity, we examine an enhancement of the model discussed so far which illustrates an effect experimentally observed in many metals, called *strain hardening*. For the perfectly plastic model, the plastic flow takes place at a constant value of the applied stress σ, such that $|\sigma| = \sigma_y$, leading to the stress-strain response shown in Figure 2.4. A strain-hardening model, on the other hand, leads to a stress-strain curve of the type idealized in Figure 2.5(a) or Figure 2.5(b). The essential difference between the two models lies in the fact that for perfectly plastic materials the closure of the elastic range, i.e. the yield surface $\mathcal{B}$, remains unchanged, whereas for the strain hardening model $\mathcal{B}$ expands with the amount of plastic flow in the system. A mathematical model that capture this effect is considered here.

Our basic assumptions on the additive strain decomposition and on a Hooke-type elastic relation are still valid. To illustrate the mathematical structure of strain-hardening we consider the simplest situation illustrated in Figure 2.5(a), which shows an expansion of the elastic range that obeys two conditions:

(a) The hardening is *isotropic* in the sense that at any state of loading, the center of $\mathcal{E}$ remains at the origin.

(b) The hardening is *linear* in the amount of plastic flow (i.e. linear in $|\dot{\varepsilon}^p|$) and independent of sign $(\dot{\varepsilon}^p)$.

The first condition leads to a new yield function of the form

$$\phi(\sigma, \chi) = |\sigma| - \sigma_y(\chi) = |\sigma| - (\sigma_{y,0} + H_{iso}\bar{e}^p) \tag{2.15}$$

where the thermodynamic force $\chi = -H_{iso}\bar{e}^p$. The constant H_{iso} depends on the material and is called the *isotropic hardening modulus*. The variable $\bar{e}^p$ is a nonnegative function of the amount of the plastic flow called *accumulated plastic strain* and is defined according to $\dot{\bar{e}}^p = |\dot{\varepsilon}^p|$. The variable $\bar{e}^p$ plays the role of a strain-type internal hardening variable. The flow rule in terms of plastic strain, the Kuhn-Tucker complementarity conditions and the consistency conditions expressed respectively in the forms (2.11), (2.6)-(2.8) remain unchanged. With some developments analogous to the ones carried out for the perfectly plastic constitutive model, it is possible to express the plastic rate parameter $\dot{\gamma}$ in terms of the total strain rate. Thus we have

$$\phi = \dot{\phi} = 0 \Rightarrow \dot{\gamma} = \frac{\text{sign}\,(\sigma) E \dot{\varepsilon}}{E + H_{iso}} \tag{2.16}$$

while the rate form of the constitutive relation becomes

$$\dot{\sigma} = \begin{cases} E\dot{\varepsilon} & \text{if } \dot{\gamma} = 0 \\ \dfrac{EH_{iso}}{E + H_{iso}}\dot{\varepsilon} & \text{if } \dot{\gamma} > 0 \end{cases} \tag{2.17}$$

In this case the continuous elastoplastic tangent modulus consists of the scalar $\dfrac{EH_{iso}}{E + H_{iso}}$.

A further refinement of the hardening mechanism is concerned with *kinematic hardening*. This effect which is of particular interest for metals can be used alone or in conjunction with isotropic hardening and provides an improved means of representing the behavior of metals under cyclic loading. The basic phenomenological law is credited to Prager [66] with subsequent improvements of Ziegler [78]. Within the present one-dimensional context the model can be illustrated as follows. In many metals subjected to cyclic loading, it is experimented a shifting of the yield surface in the direction of the plastic flow. Figure 2.5(b) reproduces an idealization of this hardening behavior closely related to a phenomenon known as the Bauschinger effect [57].

A simple phenomenological model that captures the aforementioned effect is constructed by introducing an additional internal variable which is indeed the plastic strain to which it corresponds a thermodynamic force α referred to as the *backstress*. The backstress defines the actual location of the center of the yield surface and enters the form of the yield function as a shifting stress term, i.e.

$$\phi = \phi(\sigma, \alpha) = |\sigma - \alpha| - \sigma_y \tag{2.18}$$

According to Ziegler, the evolution of α is defined by

$$\dot{\alpha} = H_{kin}\dot{\varepsilon}^p \tag{2.19}$$

where H_{kin} is called the *kinematic hardening modulus* and is a constant depending on the material. Usually the variable $\Sigma = \sigma - \alpha$ is introduced and called *relative stress*. In this way the yield function takes the form

$$\phi(\Sigma) = |\Sigma| - \sigma_y \tag{2.20}$$

which will be recalled in the following section in the three-dimensional context. The addition of the Kuhn-Tucker conditions of the form (2.11) along with a consistency condition analogous to (2.6)-(2.8) completes the formulation of the model with linear kinematic hardening under consideration. In the present case it is found that

$$\phi = \dot{\phi} = 0 \Rightarrow \dot{\gamma} = \frac{\text{sign}\,(\Sigma)E\dot{\varepsilon}}{E + H_{kin}} \tag{2.21}$$

which implies the following rate constitutive equation

$$\dot{\sigma} = \begin{cases} E\dot{\varepsilon} & \text{if } \dot{\gamma} = 0 \\ \dfrac{EH_{kin}}{E + H_{kin}}\dot{\varepsilon} & \text{if } \dot{\gamma} > 0 \end{cases} \tag{2.22}$$

admitting $\dfrac{EH_{kin}}{E + H_{kin}}$ as the continuous elastoplastic tangent modulus.

In the case where both linear isotropic and kinematic hardening mechanisms are considered, we obtain a yield function of the form

$$\phi(\Sigma, \chi) = |\Sigma| - (\sigma_{y,0} + H_{iso}\bar{e}^p) \tag{2.23}$$

with a combined relations for the plastic multiplier given by:

$$\phi = \dot{\phi} = 0 \Rightarrow \dot{\gamma} = \frac{\text{sign}\,(\Sigma)E\dot{\varepsilon}}{E + H_{iso} + H_{kin}} \tag{2.24}$$

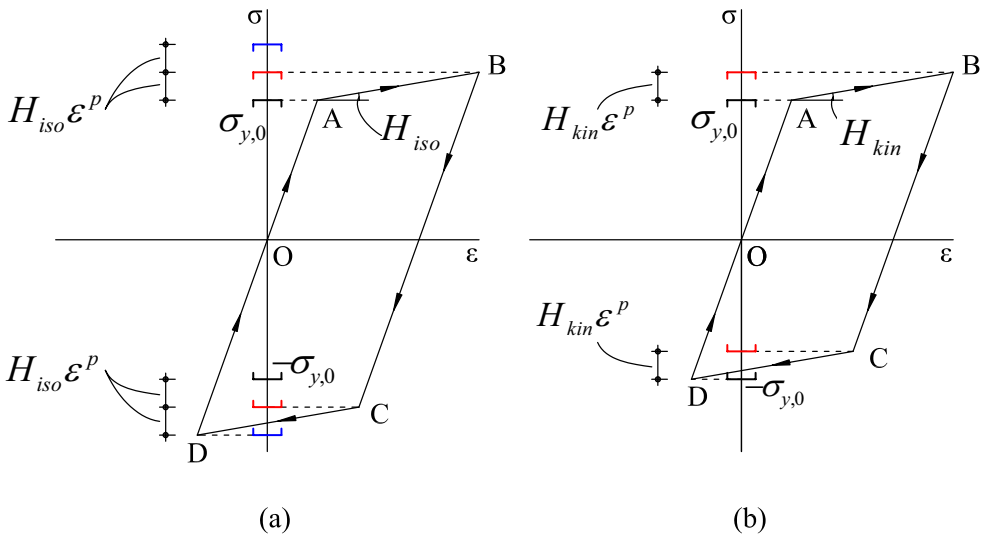

Figure 2.5: (a) Stress-strain curve for linear isotropic hardening; (b) Stress-strain curve for linear kinematic hardening

The rate form of the constitutive equation reads

$$\dot{\sigma} = \begin{cases} E\dot{\varepsilon} & \text{if } \dot{\gamma} = 0 \\ \dfrac{E(H_{iso} + H_{kin})}{E + H_{iso} + H_{kin}}\dot{\varepsilon} & \text{if } \dot{\gamma} > 0 \end{cases} \tag{2.25}$$

and the continuous elastoplastic tangent modulus becomes $\dfrac{E(H_{iso} + H_{kin})}{E + H_{iso} + H_{kin}}$.

2.3 Three-dimensional elastoplastic behavior

2.3.1 Thermodynamic foundations of elastoplasticity

The stage is ready for presenting the theory of elastoplasticity in the three-dimensional case. This is achieved by setting up a generalization of the basic features of the one-dimensional elastoplastic behavior discussed in the previous section. There are more complex features, not appearing in the uniaxial situation, that are appropriately incorporated in this part of the development. Since we are "constructing" the constitutive model, in what follows we present each specific feature as an independent ingredient. The aim is to cast the elasto-

plasticity theory within the Thermodynamics with internal variables setting initially presented for elastic materials in Section 1.8.

Isothermal behavior

In the theory in argument it is assumed that all transformations are isothermal, i.e. such that thermal effects as temperature variation or flux of heat are negligible.

Rate-independence

The theory of plasticity developed in the following sections refers to a quasi-static transformation (see Section 1.7) of a material body. In other words, the material body transformation considered takes place sufficiently slow so that the inertial term appearing in Equation (1.94) is negligible. Moreover, our discussion is here limited to the case of a body undergoing a sufficiently slow process such that the rate independent material response can be taken as a good approximation of the real behavior.

Primary variables

In order to apply the internal variables thermodynamic theory (see Section 1.8) to the context of elastoplasticity herein studied, it is appropriate to identify the variables used to describe the constitutive behavior of the material. A distinction following from the theoretical framework is also made between *primary* variables and *internal* variables which, in turn, may have a kinematic nature or a force-like nature.

The primary or fundamental kinematic variable is the strain $\boldsymbol{\varepsilon}$, which, as already pointed out in Section 2.2, can be decomposed into two parts: the elastic strain $\boldsymbol{\varepsilon}^e$, due to the elastic behavior of the material and the plastic strain $\boldsymbol{\varepsilon}^p$, which represents the inelastic or irreversible part of the deformation process. Along with these variables, the theory accounts for a set of internal variables $\boldsymbol{\xi} = (\boldsymbol{\xi}_k)$ $(1 \leq k \leq m)$ which are intended to describe internal kinematic irreversible phenomena such as, for instance, material hardening. It is to be remarked that the vector of strain-like internal variable can be in general constituted of objects of different nature, namely second-order tensors and scalars. For example, in the case in which the model presents three internal variables which are, in order, two scalars and a second-order tensor, the generalized vector of the internal variable is defined as $\boldsymbol{\xi} = (\xi_1, \xi_2, \boldsymbol{\xi}_3)$. In general we may define the space of the generalized vectors $\boldsymbol{\xi}$ as

$$\Xi = \{\boldsymbol{\xi} = (\boldsymbol{\xi}_k) : \ \boldsymbol{\xi}_k \in \mathbf{Lin}^{\mathrm{sym}}, \ 1 \leq k \leq m\}$$

In compact notation and generalizing the above definition, one may refer to the kinematic variables representing irreversible internal phenomena with the ordered pair $\mathbf{P} = (\boldsymbol{\varepsilon}^p, \boldsymbol{\xi})$ called *generalized plastic strain.*

The choice of not grouping the plastic strain within the internal variables class turns out to be a consequence of the thermodynamic theory adopted, even if there are instances in which the specific model is so simple that $\boldsymbol{\varepsilon}^p$ can be identified as an internal variable. This is for instance the case of pure linear kinematic hardening behavior (see Section 2.3.2).

Following thermodynamic arguments, the stress-like primary and internal variables are the thermodynamically conjugates of the kinematic variables. Then, we assume as stress-like primary and internal variables, respectively, the stress $\boldsymbol{\sigma}$ and the *internal forces* $\boldsymbol{\chi} = (\boldsymbol{\chi}_k)$ $(1 \leq k \leq m)$. According to the above reasonings developed for the variables $\boldsymbol{\xi}$, the forces $\boldsymbol{\chi}$ are defined in the space

$$\Upsilon = \{\boldsymbol{\chi} = (\boldsymbol{\chi}_k) : \ \boldsymbol{\chi}_k \in \mathbf{Lin}^{\mathrm{sym}}, \ 1 \leq k \leq m\}$$

Hence, the ordered pair $\mathbf{S} = (\boldsymbol{\sigma}, \boldsymbol{\chi})$ is collectively referred to as *generalized stress.* In this fashion, it is found that the scalar product $\mathbf{S} \cdot \dot{\mathbf{P}}$, defined as:

$$\mathbf{S} \cdot \dot{\mathbf{P}} = \boldsymbol{\sigma} : \dot{\boldsymbol{\varepsilon}}^p + \boldsymbol{\chi} \cdot \dot{\boldsymbol{\xi}} = \boldsymbol{\sigma} : \dot{\boldsymbol{\varepsilon}}^p + \boldsymbol{\chi}_k : \dot{\boldsymbol{\xi}}_k \tag{2.26}$$

represents either a rate of work done or the *dissipation* taking place as a result of plastic deformation. In this sense we consider $\mathbf{S}$ and $\mathbf{P}$ *thermodynamically* conjugate variables of the model under consideration.

Thermodynamic assumptions

As explained in Section 1.8, we assume in our developments that the free energy and the stress are functions of the strain and of the strain-like internal variables, which are thus regarded, in the following, as driving variables

$$\psi = \psi(\boldsymbol{\varepsilon}, \boldsymbol{\xi}) \tag{2.27}$$

$$\boldsymbol{\sigma} = \boldsymbol{\sigma}(\boldsymbol{\varepsilon}, \boldsymbol{\xi}) \tag{2.28}$$

Moreover, in what follows, it is deduced that the free energy can be equivalently written in terms of the elastic strain and of the internal variables.

In order to account for nonlinear irreversible effects, the model takes into account an *evolution law* of the strain-like internal variables in terms of the dependent variables

$$\dot{\boldsymbol{\xi}} = \boldsymbol{\beta}(\boldsymbol{\varepsilon}, \boldsymbol{\xi}) \tag{2.29}$$

Recalling again the derivations of Section 1.8 it is found that, as a consequence of the second law of Thermodynamics, the stress is related to the free energy function as

$$\boldsymbol{\sigma} = \frac{\partial \psi}{\partial \boldsymbol{\varepsilon}} \tag{2.30}$$

Furthermore, the internal forces $\boldsymbol{\chi} = (\boldsymbol{\chi}_k)$ are defined as *conjugate* quantities to the internal variables in the following sense

$$\boldsymbol{\chi}_k = -\frac{\partial \psi}{\partial \boldsymbol{\xi}_k}, \qquad 1 \leq k \leq m \tag{2.31}$$

or, by recognizing that these variables enter the expressions $\boldsymbol{\chi}_k : \dot{\boldsymbol{\xi}}_k$, appearing in the second law of Thermodynamics (1.105), as internal dissipation contributions. The variation

$$\boldsymbol{\chi} : \dot{\boldsymbol{\xi}} = \boldsymbol{\chi}_k : \dot{\boldsymbol{\xi}}_k \quad 1 \leq k \leq m \tag{2.32}$$

which is defined as *internal dissipation* results nonnegative (cf. (1.109)).

Additive decomposition of strain

It is possible to show that the strain decomposition into elastic and plastic parts can be viewed as a consequence of the thermodynamic framework herein adopted. The approach followed is similar to the one presented in [56]. We start by introducing the *Gibbs free energy* function

$$h(\boldsymbol{\sigma}, \boldsymbol{\xi}) = \boldsymbol{\sigma} : \boldsymbol{\varepsilon} - \psi \tag{2.33}$$

defined through a Legendre transformation of the Helmoltz free energy, assuming the stress as the independent variable. The relation conjugate to (2.30) is

$$\boldsymbol{\varepsilon} = \frac{\partial h}{\partial \boldsymbol{\sigma}} \tag{2.34}$$

Defining the fourth-order tensors

$$\mathbb{A} = \frac{\partial \boldsymbol{\varepsilon}}{\partial \boldsymbol{\sigma}}; \quad \mathbb{B}_k = \frac{\partial \boldsymbol{\varepsilon}}{\partial \boldsymbol{\xi}_k}, \qquad 1 \leq k \leq m \tag{2.35}$$

the strain rate is given by

$$\dot{\boldsymbol{\varepsilon}} = \mathbb{A}\dot{\boldsymbol{\sigma}} + \mathbb{B}_k \dot{\boldsymbol{\xi}}_k \quad 1 \leq k \leq m \tag{2.36}$$

It is known that for crystalline materials the elastic compliance matrix $\mathbb{A}$ is independent of irreversible processes and hence its dependence on the variables $\boldsymbol{\xi}$ can be neglected [57]. Assuming $\mathbb{A} = \mathbb{A}(\sigma)$, it follows that $\mathbb{B}_k = \mathbb{B}_k(\boldsymbol{\xi})$, $1 \leq k \leq m$, since

$$\mathbf{0} = \frac{\partial}{\partial \boldsymbol{\xi}_k}\frac{\partial \boldsymbol{\varepsilon}}{\partial \boldsymbol{\sigma}} = \frac{\partial}{\partial \boldsymbol{\sigma}}\frac{\partial \boldsymbol{\varepsilon}}{\partial \boldsymbol{\xi}_k} = \frac{\partial \mathbb{B}_k}{\partial \boldsymbol{\sigma}} \qquad 1 \leq k \leq m$$

It is then possible to decompose additively the strain tensor in the form

$$\boldsymbol{\varepsilon} = \boldsymbol{\varepsilon}^e(\boldsymbol{\sigma}) + \boldsymbol{\varepsilon}^p(\boldsymbol{\xi}) \tag{2.37}$$

in which the *elastic strain* $\boldsymbol{\varepsilon}^e$ depends only on the stress and the *plastic strain* $\boldsymbol{\varepsilon}^p$ is a function of the internal variables only. Integrating in time Equation (2.36), we obtain the above strain quantities as

$$\boldsymbol{\varepsilon}^e(\boldsymbol{\sigma})(t) = \int_0^t \mathbb{A}(\boldsymbol{\sigma}(s))\dot{\boldsymbol{\sigma}}(s)ds \equiv \int_0^{\boldsymbol{\sigma}(t)} \mathbb{A}(\boldsymbol{\sigma})d\boldsymbol{\sigma}$$

and

$$\boldsymbol{\varepsilon}^p(\boldsymbol{\xi}_k)(t) = \int_0^t \mathbb{B}_k(\boldsymbol{\xi}_k(s))\dot{\boldsymbol{\xi}}_k(s)ds \equiv \int_0^{\boldsymbol{\xi}_k(t)} \mathbb{B}_k(\boldsymbol{\xi})d\boldsymbol{\xi}_k$$

In the case where $\mathbb{A}$ is independent of $\boldsymbol{\sigma}$, the elastic strain is given as a linear function of the stress by

$$\boldsymbol{\varepsilon}^e = \mathbb{A}\boldsymbol{\sigma} \quad \text{or} \quad \boldsymbol{\sigma} = \mathbb{C}\boldsymbol{\varepsilon}^e \tag{2.38}$$

and it is clear from the inspection of relation (1.69) that the fourth-order *compliance* tensor $\mathbb{A}$ is the inverse of the elastic tensor $\mathbb{C}$.

Free energy as a function of elastic strain and internal variables

Since Equations (2.30) and (2.37) imply that

$$\frac{\partial \boldsymbol{\varepsilon}^e}{\partial \boldsymbol{\sigma}} = \frac{\partial \boldsymbol{\varepsilon}}{\partial \boldsymbol{\sigma}} = \frac{\partial \boldsymbol{\varepsilon}^T}{\partial \boldsymbol{\sigma}} = \frac{\partial (\boldsymbol{\varepsilon}^e)^T}{\partial \boldsymbol{\sigma}}$$

recalling a multivariable calculus theorem [41], we may assert the existence of a scalar potential function $h^e = h^e(\boldsymbol{\sigma})$ such that

$$\boldsymbol{\varepsilon}^e = \frac{\partial h^e}{\partial \boldsymbol{\sigma}} \tag{2.39}$$

The above potential function in turn admits the Legendre transform ψ^e defined by

$$\psi^e = \boldsymbol{\sigma} : \boldsymbol{\varepsilon}^e - h^e \tag{2.40}$$

which satisfies the following relation

$$\boldsymbol{\sigma} = \frac{\partial \psi^e}{\partial \boldsymbol{\varepsilon}^e} \tag{2.41}$$

Since (cf. (2.40))

$$\boldsymbol{\sigma} : \boldsymbol{\varepsilon}^e = \psi^e(\boldsymbol{\varepsilon}^e) + h^e(\boldsymbol{\sigma})$$

we have the following representation of the Gibbs free energy

$$h(\boldsymbol{\sigma}, \boldsymbol{\xi}) = \boldsymbol{\sigma} : (\boldsymbol{\varepsilon}^e + \boldsymbol{\varepsilon}^p) - \psi(\boldsymbol{\varepsilon}, \boldsymbol{\xi}) = h^e(\boldsymbol{\sigma}) + \boldsymbol{\sigma} : \boldsymbol{\varepsilon}^p(\boldsymbol{\xi}) - \psi^p(\boldsymbol{\xi}) \tag{2.42}$$

by which the inelastic part of the free energy ψ^p results defined as

$$\psi^p(\boldsymbol{\xi}) = \psi(\boldsymbol{\varepsilon}, \boldsymbol{\xi}) - \psi^e(\boldsymbol{\varepsilon}^e)$$

It is noted that the function ψ^p depends only on the internal variables, since

$$\boldsymbol{\varepsilon} = \frac{\partial h}{\partial \boldsymbol{\sigma}} = \frac{\partial h^e}{\partial \boldsymbol{\sigma}} + \boldsymbol{\varepsilon}^p(\boldsymbol{\xi}) - \frac{\partial \psi^p}{\partial \boldsymbol{\sigma}}$$

whence it results that $\partial \psi^p / \partial \boldsymbol{\sigma} = \mathbf{0}$. In conclusion, the Helmoltz energy function ψ and the Gibbs energy function h can be additively decomposed into elastic and plastic parts, respectively, as

$$\psi(\boldsymbol{\varepsilon}, \boldsymbol{\xi}) = \psi^e(\boldsymbol{\varepsilon}^e) + \psi^p(\boldsymbol{\xi}) \equiv \hat{\psi}(\boldsymbol{\varepsilon}^e, \boldsymbol{\xi}) \tag{2.43}$$

$$h(\boldsymbol{\sigma}, \boldsymbol{\xi}) = h^e(\boldsymbol{\sigma}) + h^p(\boldsymbol{\xi}) \tag{2.44}$$

where $\boldsymbol{\varepsilon}^e = \boldsymbol{\varepsilon} - \boldsymbol{\varepsilon}^p$.

Recalling the second law of Thermodynamics (1.85) and using definition (2.43), we obtain (2.41) which leads to the reduced dissipation inequality in the alternative form

$$\boldsymbol{\sigma} : \dot{\boldsymbol{\varepsilon}}^p + \boldsymbol{\chi}_k : \dot{\boldsymbol{\xi}}_k \geq 0 \quad 1 \leq k \leq m \tag{2.45}$$

The above inequality, in view of (2.26), can be written in compact notation as

$$\mathbf{S} \cdot \dot{\mathbf{P}} \geq 0 \tag{2.46}$$

Plastic incompressibility

The physical evidence shows that, for metallic materials, volume changes occur almost exclusively as a consequence of elastic deformation [14]. Hence, it is reasonable to assume that the plastic part of the deformation is only of deviatoric or shearing type. Following the development of Section 1.3 and recalling relation (1.35) we are lead to assume that the quantity

$$\mathrm{tr}\,(\boldsymbol{\varepsilon}^p) = \varepsilon^p_{ii} \tag{2.47}$$

is zero which implies that the tensor $\boldsymbol{\varepsilon}^p$ coincides with its deviatoric part. In the rest of the work we then refer to the plastic strain tensor as the *traceless* deviatoric tensor $\mathbf{e}^p$.

Using the above arguments on the additive decomposition of strain into an elastic and a plastic part and the assumption on plastic incompressibility, it is possible to generalize the linear elastic relations (1.73)-(1.74) developed in Section 1.5 for the isotropic elastic material response. We have, in fact

$$p = K\theta \tag{2.48}$$

$$\mathbf{s} = 2G(\mathbf{e} - \mathbf{e}^p) = 2G\mathbf{e}^e \tag{2.49}$$

where, $\mathbf{e}^e$ is the elastic strain deviatoric part, that is

$$\mathbf{e}^e = \mathbf{e} - \mathbf{e}^p$$

Elastic region and yield surface

Here we generalize to a three-dimensional context the basic concepts regarding the elastoplastic behavior presented in Section 2.2 for the one-dimensional case. In order to introduce the concepts of *elastic region* $\mathcal{E}$ and *yield surface* $\mathcal{B}$ within the three-dimensional framework, it is worth recalling Equation (2.18) which represents the form of the yield function for the uniaxial elastoplastic constitutive model with linear kinematic and isotropic hardening. Such a limit function was shown to represent a constraint on the evolution of the stress and of the thermodynamic forces, i.e. a constraint on the generalized stress evolution.

The above discussion can be extended to the three-dimensional case stating that at all times, the generalized stress $\mathbf{S}$ must lie in the closed connected set $\mathcal{S}$, the *admissible generalized stress region.* The interior of this set is called the *elastic region* and is denoted by $\mathcal{E}$, while its boundary is denoted by $\mathcal{B}$ and is known as the *yield surface.* The set $\mathcal{S}^c$ represents the complement of the set of the admissible stresses domain and is not attainable by the generalized stress.

Whenever $\mathbf{S}$ lies within the interior of $\mathcal{S}$, purely elastic behavior takes place, while plastic loading may be observed only if $\mathbf{S}$ evolves on the boundary of $\mathcal{S}$.

A convenient way to represent the constrained evolution mechanism of the generalized stress tensor is to assume the yield surface to be described by a scalar function ϕ such that

$$\mathcal{E} = \{\mathbf{S} : \phi(\mathbf{S}) < 0\}$$
$$\mathcal{B} = \{\mathbf{S} : \phi(\mathbf{S}) = 0\}$$

With the above formalism we may collect a total of three possible cases in regard to the evolution of the generalized stress $\mathbf{S}$ with respect to the region of admissible generalized stresses. The first one, named *purely elastic loading*, takes place when the evolution of $\mathbf{S}$ is such that $\mathbf{S} \in \mathcal{E}$; the second case refers to $\mathbf{S}$ moving from $\mathcal{B}$ to $\mathcal{E}$ and is referred to as *elastic unloading*. In both the above cases the material response is elastic. The third case refers to an evolution of the generalized stress according to which $\mathbf{S} \in \mathcal{B}$ and goes by the name of *plastic loading*. Clearly, the different kinds of movements described above and characterizing the material point loading history can be subsequently coupled leading to a sequence of loading and unloading phases, which are referred in the sequel as *elastoplastic* or *mixed phases*.

With the above definitions, recalling the simple uniaxial case discussed in Section 2.2 (cf. (2.2)-(2.3)), we can make the following assumptions about the rate of change of generalized plastic strain

$$\begin{aligned} \dot{\mathbf{P}} = \mathbf{0} \quad \text{if} \quad & \begin{cases} \phi(\mathbf{S}) < 0 \\ \text{or} \\ \phi(\mathbf{S}) = 0 \text{ and } \dot{\phi} < 0 \end{cases} \\ \dot{\mathbf{P}} \neq 0 \quad \text{if} \quad & \begin{cases} \phi(\mathbf{S}) = 0 \\ \text{and} \\ \dot{\phi}(\mathbf{S}) = 0 \end{cases} \end{aligned} \tag{2.50}$$

The above positions implies that during plastic loading

$$\phi = \dot{\phi} = 0$$

which is a fundamental requirement known as the *plastic consistency condition*. Another interesting feature characterizing the three-dimensional plasticity theory here developed is achievable with the following reasoning. Let us consider the yield surface projection onto the stress space, i.e. the function

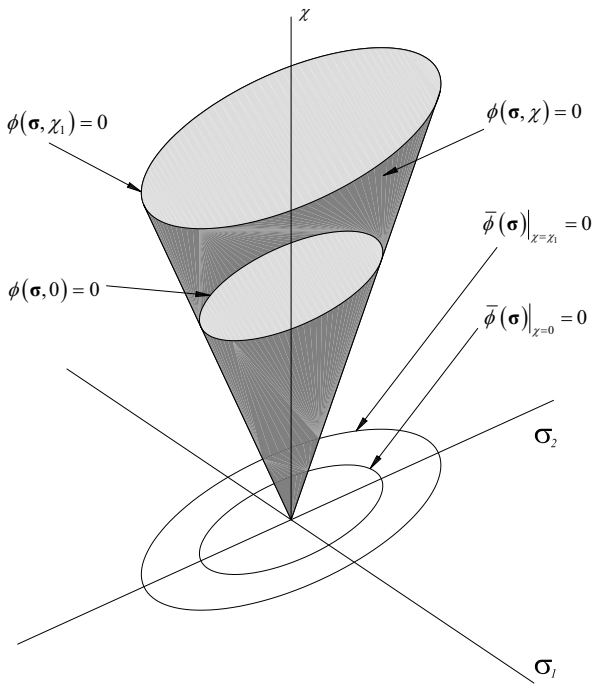

Figure 2.6: The yield surface $\phi(\boldsymbol{\sigma},\chi)=0$ and its projection on the stress space

$\bar{\phi}(\boldsymbol{\sigma}) \equiv \phi(\boldsymbol{\sigma},\boldsymbol{\chi})$ for fixed $\boldsymbol{\chi}$. Assume, for instance, that $\phi(\boldsymbol{\sigma},\boldsymbol{\chi})=0$ and that the stress rate is such that

$$\frac{\partial\phi}{\partial\boldsymbol{\sigma}} : \dot{\boldsymbol{\sigma}} > 0 \tag{2.51}$$

Since for plastic loading it is

$$\dot{\phi} = \frac{\partial\phi}{\partial\boldsymbol{\sigma}} : \dot{\boldsymbol{\sigma}} + \frac{\partial\phi}{\partial\boldsymbol{\chi}} \cdot \dot{\boldsymbol{\chi}} = 0 \tag{2.52}$$

it is clear that both a time variation of the forces $\boldsymbol{\chi}$ and of the projection of the yield surface onto the stress space must occur. This change is interpreted as the *evolution* of the yield surface in generalized stress space (see Figure 2.6 for a visualization of this argument in the case where $\boldsymbol{\chi} \equiv \chi$ is a single scalar variable). On the other hand, if $\phi(\boldsymbol{\sigma},\boldsymbol{\chi})=0$ and elastic unloading takes place, then by the definition of elastic behavior there is no change in the internal variables, nor in the forces conjugate to these variables. Consequently, from

(2.50), it is found that

$$\dot{\phi} = \frac{\partial \phi}{\partial \boldsymbol{\sigma}} : \dot{\boldsymbol{\sigma}} < 0 \tag{2.53}$$

meaning that the yield surface does not modify and that all $\dot{\boldsymbol{\chi}}_k$ $(1 \leq k \leq m)$ are zero.

In Section 2.3.2, in relation to specific kinds of hardening mechanisms, we present a geometric interpretation of the evolution of the surface $\bar{\phi} = 0$ under conditions of plastic loading. For completeness, it should be added that the proper nature of a *perfectly plastic material* is that the yield surface depends on the stress only. Hence, in this case, we have $\phi(\boldsymbol{\sigma}) = \bar{\phi}(\boldsymbol{\sigma})$. When $\phi(\boldsymbol{\sigma}) = 0$, plastic behavior takes place when

$$0 = \dot{\phi} = \frac{\partial \phi}{\partial \boldsymbol{\sigma}} : \dot{\boldsymbol{\sigma}} \tag{2.54}$$

which implies that the stress evolves lying on the yield surface, while the yield surface remains unchanged in the stress space. Such a behavior is known as *neutral loading* to distinguish it by the situations in which, due to hardening, the surface $\bar{\phi} = 0$ changes during plastic deformation.

The above considerations readily apply to the one-dimensional example discussed earlier. In fact, as can be seen in Figure 2.2(b), the initial elastic region in the stress space is simply the interval $(\sigma'_{y,0}, \sigma_{y,0})$, but upon plastic loading the elastic boundary expands to the new interval $(\sigma'_{y,1}, \sigma_{y,1})$.

We can thus admit the double interpretation of the yield surface as a fixed region in the generalized stress space or equivalently as an evolving closed convex set in the space of stress.

Principle of maximum plastic work

The last law that is needed to complete the theory has its origin in the work of von-Mises, Taylor, Bishop and Hill [56] and can be justified from the physical point of view by appealing to the behavior of crystals undergoing plastic deformations. In its original version it can be stated as follows: given a stress state $\boldsymbol{\sigma}$ such that $\bar{\phi}(\boldsymbol{\sigma}) = 0$ and a plastic rate $\dot{\mathbf{e}}^p$ associated with $\boldsymbol{\sigma}$, then

$$\boldsymbol{\sigma} : \dot{\mathbf{e}}^p \geq \boldsymbol{\tau} : \dot{\mathbf{e}}^p \tag{2.55}$$

for all admissible stresses $\boldsymbol{\tau}$ satisfying the yield constraint $\bar{\phi}(\boldsymbol{\tau}) \leq 0$. An alternative form of the postulate of maximum plastic work follows by the

definition of *rate of plastic work* $W(\dot{\mathbf{e}}^p) = \boldsymbol{\sigma} : \dot{\mathbf{e}}^p$ associated with a plastic strain rate $\dot{\mathbf{e}}^p$ and reads

$$W(\dot{\mathbf{e}}^p) = \max\{\boldsymbol{\tau} : \dot{\mathbf{e}}^p : \ \bar{\phi}(\boldsymbol{\tau}) \leq 0\} \tag{2.56}$$

The principle of maximum plastic work is a key point of the theory of plasticity. Depending on the viewpoint adopted, it may be regarded as a postulate, as stated by (2.56), or as a consequence of the classical stability postulate by Drucker (for such a deduction, see for example [30, 57, 61]).

In the present context, the postulate of maximum plastic work is presented in a more general fashion [41], which incorporates the *dissipation function* D due to the internal variables, defined by

$$D = D(\dot{\mathbf{P}}) = \mathbf{S} \cdot \dot{\mathbf{P}} \tag{2.57}$$

First, we assume that the zero generalized stress point $\mathbf{S} = \mathbf{0}$ belongs to $\mathcal{S}$ and second we extend the classical form of the postulate of maximum plastic work by stating the following: given a generalized stress state $\mathbf{S} \in \mathcal{S}$ and an associated generalized strain rate $\dot{\mathbf{P}}$, the inequality

$$\mathbf{S} \cdot \dot{\mathbf{P}} \geq \mathbf{T} \cdot \dot{\mathbf{P}} \tag{2.58}$$

holds for all the admissible generalized stresses $\mathbf{T} \in \mathcal{S}$. Choosing $\mathbf{T} = \mathbf{0}$, which is an admissible state by assumption, (2.58) gives

$$\mathbf{S} \cdot \dot{\mathbf{P}} \geq 0$$

or, in terms of *dissipation* D,

$$D \geq 0 \tag{2.59}$$

It is noted that the reduced dissipation inequality in the form (2.46) is recovered by (2.59). A mathematical proof of the principle of maximum plastic dissipation, as stated by relation (2.59), is presented in Section 2.5, where it is carried out in the framework of a convex-analytic recasting of the fundamental equations of elastoplasticity.

There are two major consequences arising from the above postulate. First, it can be shown that the plastic strain rate $\dot{\mathbf{P}}$ associated with a generalized stress $\mathbf{S}$ lying on the yield surface $\mathcal{B}$ is normal to the tangent hyperplane at the point $\mathbf{S}$ to the the yield surface $\mathcal{B}$. This result is generally referred to as *normality law* which, in the case of a non-smooth limit surface, states that $\dot{\mathbf{P}}$ belongs to the cone of normals at $\mathbf{S}$. Second, it results that the region $\mathcal{E}$ (or $\mathcal{S}$)

is convex. A rigorous mathematical proof of these two properties is presented in Section 2.5.

For the time being, following [41], we present a deduction of the normality law in the simple case of a smooth yield surface. Let $\mathbf{S}'$ be a unit tangent vector of the tangent hyperplane of the yield surface at $\mathbf{S}$. Consider a sequence of generalized stresses $\mathbf{T} = \mathbf{S} + \mathbf{S}'_\varepsilon$ that lie on the yield surface and satisfy the property

$$\mathbf{S}'_\varepsilon \to \mathbf{0} \quad \text{and} \quad \frac{\mathbf{S}'_\varepsilon}{\| \mathbf{S}'_\varepsilon \|} \to \mathbf{S}' \quad \text{as} \quad \boldsymbol{\varepsilon} \to \mathbf{0}$$

Applying (2.58) to the above relation one finds

$$\mathbf{S}'_\varepsilon \cdot \dot{\mathbf{P}} \leq 0$$

which, dividing by $\| \mathbf{S}'_\varepsilon \|$, gives

$$\frac{\mathbf{S}'_\varepsilon}{\| \mathbf{S}'_\varepsilon \|} \cdot \dot{\mathbf{P}} \leq 0$$

Taking the limit of the above expression for $\boldsymbol{\varepsilon} \to 0$, shows that

$$\mathbf{S}' \cdot \dot{\mathbf{P}} \leq 0$$

which, observing that $-\mathbf{S}'$ is also a unit tangent vector, implies

$$-\mathbf{S}' \cdot \dot{\mathbf{P}} \leq 0$$

From the last two conditions, it is concluded that

$$\mathbf{S}' \cdot \dot{\mathbf{P}} = 0$$

for any vector $\mathbf{S}'$ tangent to the yield surface at $\mathbf{S}$. The above equation states that $\dot{\mathbf{P}}$ is normal to the yield surface at $\mathbf{S}$.

To demonstrate that $\mathcal{S}$ is a convex set we must show that $\mathcal{S}$ lies to one side of the tangent plane at any point $\mathbf{S} \in \mathcal{B}$, as illustrated in Figure 2.7. Equivalently, given the normality law, it suffices to show that the product $(\mathbf{S} - \mathbf{T}) \cdot \dot{\mathbf{P}}$ is always non-negative for any $\mathbf{T} \in \mathcal{S}$, which is easily derived from (2.58)

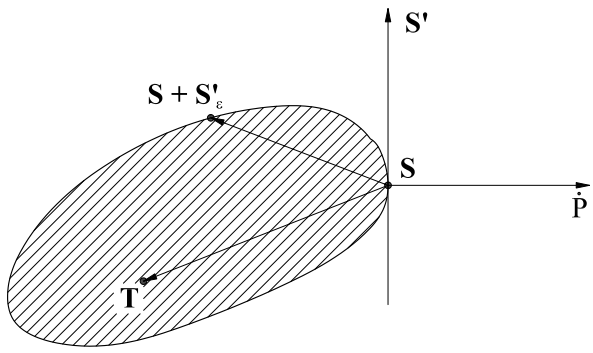

Figure 2.7: Convexity of the yield surface and normality law

Associative plasticity

When the yield surface is smooth, i.e. it presents a well-defined gradient at each point, recalling that $\dot{\mathbf{P}}$ lies parallel to the normal to $\mathcal{B}$ at $\mathbf{S}$, we may write the following important form of the normality law [57, 69, 79]

$$\dot{\mathbf{P}} = \dot{\gamma}\nabla\phi(\mathbf{S}) \tag{2.60}$$

where $\dot{\gamma}$ is the non-negative scalar *plastic multiplier*. Separating the tensorial components of the above evolution equation we obtain [4]

$$\dot{\mathbf{e}}^p = \dot{\gamma}\frac{\partial\phi}{\partial\boldsymbol{\sigma}} \tag{2.61}$$

$$\dot{\boldsymbol{\xi}} = \dot{\gamma}\frac{\partial\phi}{\partial\boldsymbol{\chi}} \tag{2.62}$$

Equations (2.61)-(2.62) state that ϕ represents a *flow potential* for $\mathbf{e}^p$ and $\boldsymbol{\xi}$. The above flow rule is said to be *associated* with the yield function in generalized stress space. For convenience, we report here Equation (2.31), written in compact form

$$\boldsymbol{\chi} = -\frac{\partial\hat{\psi}}{\partial\boldsymbol{\xi}} = -\frac{\partial\psi^p}{\partial\boldsymbol{\xi}} \tag{2.63}$$

which, in rate form, reads

$$\dot{\boldsymbol{\chi}} = -\frac{\partial^2\psi^p}{\partial\boldsymbol{\xi}^2}\dot{\boldsymbol{\xi}} \tag{2.64}$$

Introducing the evolutive relation (2.62) into (2.64) and defining the fourth-order tensors

$$\mathbb{D}_k = \frac{\partial^2 \psi^p}{\partial \boldsymbol{\xi}_k^2} \quad 1 \leq k \leq m \tag{2.65}$$

we can recast the rate form of the hardening law (2.64) in the form

$$\dot{\boldsymbol{\chi}}_k = -\dot{\gamma}\mathbb{D}_k \frac{\partial \phi}{\partial \boldsymbol{\chi}_k} \tag{2.66}$$

or, equivalently

$$\dot{\boldsymbol{\chi}} = -\dot{\gamma}\mathbb{D} \frac{\partial \phi}{\partial \boldsymbol{\chi}} \tag{2.67}$$

where $\mathbb{D}$ is the (diagonal) generalized matrix operator containing the tensors $\mathbb{D}_k$. In view of the previous definitions, (2.66) can be regarded as a hardening law associated with the function ψ^p, which clearly reveals to be a hardening potential. Equivalently, (2.64) represents the rate form of the mentioned hardening law which, admitting the normality law, leads to the generalized associative hardening law in stress space (2.66). A constitutive model characterized by the flow rule (2.61) and by the two evolutive Equations (2.62) and (2.67) regarding the internal hardening variables is then referred to as *associative plasticity* [17]. In the following sections we present a yield function and a set of hardening laws which readily satisfy the above notion of associative elastoplastic model.

To complete the statement of our problem we need only to give the conditions on the plastic multiplier $\dot{\gamma}$ and on the yield function ϕ in concise form. We have

$$\dot{\gamma} \geq 0, \quad \phi \leq 0 \quad \dot{\gamma}\phi = 0 \tag{2.68}$$

which are known as *complementarity conditions* or *Kuhn-Tucker* conditions [4, 57, 69]. The first two conditions in (2.68) constrain the signs of $\dot{\gamma}$ and ϕ, while the third one states that the above quantities are not simultaneously nonzero; positive values for $\dot{\gamma}$ require $\phi = 0$, in which case plastic deformation takes place, while negative values for ϕ imply that $\dot{\gamma}$ is zero, that is the plastic deformation rate is zero. In the case where $\phi = 0$, the consistency condition (2.68) can be equivalently formulated in terms of time derivative of the yield function as

$$\text{When } \phi = 0, \quad \dot{\gamma} \geq 0, \quad \dot{\phi} \leq 0, \quad \dot{\gamma}\dot{\phi} \leq 0 \tag{2.69}$$

since by the second inequality appearing in (2.68) the generalized stress is always constraint to evolve towards the interior of $\mathcal{S}$ or at most to remain on the yield surface, that is to say $\dot{\phi} \leq 0$ [69]. The above consistency formulation results of great importance in the derivation of integration schemes for the elastoplastic model under consideration. These schemes are addressed in detail in Chapter 4 and Chapter 5.

2.3.2 von-Mises yield criterion

Perfect plasticity

In this paragraph we first introduce the definition of the *von-Mises yield function*, indicated henceforth with F, for the simplest case of perfect plasticity. Hence we choose $F = F(\boldsymbol{\sigma})$. In the subsequent section, when different hardening mechanisms are described, we generalize the expression of the von-Mises yield criterion and of the relative flow and hardening laws to the case of hardening materials. In this context, we also draw some considerations on the ensuing form assumed by the flow rule and by the elastic and plastic potentials.

The primary consideration that needs to be drawn on the outset is that, regardless of the type of hardening, the von-Mises yield function is independent of the mean stress or pressure $p = 1/3\text{tr}(\boldsymbol{\sigma})$ and is an isotropic function. The first assumption implies that the F depends on the stress deviator only:

$$F = F(\mathbf{s})$$

while the second hypothesis indicates that, given any proper orthogonal second-order tensor $\mathbf{Q} \in \mathbf{L}\text{in}$, it holds

$$F(\mathbf{s}) = F(\mathbf{Q}\mathbf{s}\mathbf{Q}^T)$$

The von-Mises yield function then is defined by

$$F(\mathbf{s}) = \| \mathbf{s} \| - \sigma_y \tag{2.70}$$

with σ_y the *yield stress*. Equivalently, denoting by $J_2 = \frac{1}{2}(\mathbf{s} : \mathbf{s})$ the second scalar invariant of $\mathbf{s}$, the von-Mises yield function may be expressed as

$$F(\mathbf{s}) = \sqrt{2J_2} - \sigma_y \tag{2.71}$$

In view of the last expression, a perfect elastoplastic model with a von-Mises yield surface is usually referred to as J_2 *plasticity model*. In the above expression the scalar quantity σ_y represents the initial uniaxial yield stress and is therefore a quantity depending on the material.

Applying (2.61), we can derive the plastic flow rule, which reads

$$\dot{\mathbf{e}}^p = \dot{\gamma}\frac{\partial F(\mathbf{s})}{\partial \boldsymbol{\sigma}} = \dot{\gamma}\frac{\partial F(\mathbf{s})}{\partial \mathbf{s}} = \dot{\gamma}\mathbf{n} \tag{2.72}$$

where $\mathbf{n}$ indicates the second-order normal tensor to the yield surface at $\mathbf{s}$, which with simple considerations [17], results

$$\mathbf{n} = \frac{\mathbf{s}}{\parallel \mathbf{s} \parallel} \tag{2.73}$$

In the case of perfect J_2 plasticity just presented the strain-like internal variable can be identified with the plastic strain $\mathbf{e}^p$.

Linear isotropic hardening

This type of hardening is characterized by a single scalar strain-like internal variable, denoted here by ξ and by a single scalar thermodynamically conjugate force indicated with χ. In most cases, ξ represents a measure of accumulated plastic deformation. A typical choice is the *accumulated plastic strain*, defined as [57]

$$\bar{e}^p(t) = \int_0^t \parallel \dot{\mathbf{e}}^p(\tau) \parallel d\tau \tag{2.74}$$

The above quantity indicates the total plastic strain accumulated from the beginning of the loading history. The von-Mises yield function becomes

$$F(\mathbf{s}, \chi) = \parallel \mathbf{s} \parallel - \sigma_y(\chi) \tag{2.75}$$

where σ_y is not constant, rather it depends on the internal variable χ through a relation of the form

$$\sigma_y = \sigma_{y,0} + G(\chi) \tag{2.76}$$

where $\sigma_{y,0}$ is as usual the uniaxial initial yield stress, while $G(\chi)$ is a monotonically increasing function satisfying $G(0) = 0$. According to this rule, isotropic hardening is viewable as the yield surface projection on the stress space which expands retaining its original shape by an amount which is proportional to the accumulated plastic deformation through the function $G(\chi)$. Setting

$$\psi^p(\xi) = \psi^p(\bar{e}^p) = \frac{1}{2} H_{iso}(\bar{e}^p)^2 \tag{2.77}$$

where the material constant H_{iso} is known as the isotropic hardening modulus, the expression of the free energy is thus

$$\psi(\boldsymbol{\varepsilon}^e, \mathbf{e}^p) = \frac{1}{2}\boldsymbol{\varepsilon}^e : \mathbb{C}\boldsymbol{\varepsilon}^e + \frac{1}{2}H_{iso}(\bar{e}^p)^2 \tag{2.78}$$

Invoking the definition (2.63), we immediately derive χ as

$$\chi = -\frac{\partial \psi^p}{\partial \xi} = -\frac{\partial \psi^p}{\partial \bar{e}^p} = -H_{iso}\bar{e}^p \tag{2.79}$$

Admitting, for simplicity, that $G = -\chi$, (2.75) becomes

$$F(\mathbf{s}, \chi) = \| \mathbf{s} \| - \sigma_{y,0} - H_{iso}\bar{e}^p \tag{2.80}$$

The associated flow rule and hardening laws thus read

$$\dot{\mathbf{e}}^p = \dot{\gamma}\frac{\partial F(\mathbf{s}, \chi)}{\partial \boldsymbol{\sigma}} = \dot{\gamma}\frac{\partial F(\mathbf{s}, \chi)}{\partial \mathbf{s}} = \dot{\gamma}\mathbf{n} \tag{2.81}$$

$$\dot{\bar{e}}^p = \| \dot{\mathbf{e}}^p \| \tag{2.82}$$

$$\dot{\chi} = -H_{iso}\dot{\bar{e}}^p \tag{2.83}$$

As a possible further generalization, we may take into consideration the case of a yield surface that expands isotropically with a nonlinear dependence on χ. This possibility is anyway beyond the scope of this work and then is not studied in detail.

Linear kinematic hardening

The kinematic hardening mechanism has been briefly presented for the one-dimensional situation in Section 2.3.1. It was stated that, differing from isotropic hardening which causes the yield domain to expand homogenously, kinematic hardening produces a *shifting* of the initial yield surface in stress space. Such a characteristic is still valid in the three-dimensional context. We start by the case of linear kinematic hardening, whose description implies a single internal tensorial variable $\boldsymbol{\xi}$. Usually, $\boldsymbol{\xi}$ is taken to be the plastic strain tensor $\mathbf{e}^p$, with an expression of the free energy in the form

$$\psi(\boldsymbol{\varepsilon}^e, \mathbf{e}^p) = \frac{1}{2}\boldsymbol{\varepsilon}^e : \mathbb{C}\boldsymbol{\varepsilon}^e + \frac{1}{2}\mathbf{e}^p : \mathbb{D}\mathbf{e}^p \tag{2.84}$$

where

$$\mathbb{D} = H_{kin}\mathbb{I} \tag{2.85}$$

The term H_{kin} is the linear kinematic hardening modulus, a material property. In correspondence to the internal variable $\boldsymbol{\xi} = \mathbf{e}^p$, we have the conjugate force

$$\boldsymbol{\chi} = -\frac{\partial \psi^p}{\partial \boldsymbol{\xi}} = -\frac{\partial \psi^p}{\partial \mathbf{e}^p} = -H_{kin}\mathbf{e}^p \tag{2.86}$$

The yield condition is obtained by introducing the thermodynamic force $\boldsymbol{\chi}$ in the yield function [41], according to

$$F(\mathbf{s}, \boldsymbol{\chi}) = \| \mathbf{s} + \boldsymbol{\chi} \| - \sigma_y \tag{2.87}$$

Introducing the new internal stress variable

$$\boldsymbol{\alpha} = -\boldsymbol{\chi} \tag{2.88}$$

a deviatoric tensor defined in stress space called *backstress*, the yield function (2.87) becomes

$$F(\mathbf{s}, \boldsymbol{\alpha}) = \| \mathbf{s} - \boldsymbol{\alpha} \| - \sigma_y = \| \boldsymbol{\Sigma} \| - \sigma_y \tag{2.89}$$

The backstress tensor $\boldsymbol{\alpha}$ represents the shifting of the center of the yield surface in stress space due to the kinematic hardening effect. The tensor $\boldsymbol{\Sigma} = \mathbf{s} - \boldsymbol{\alpha}$ appearing in the yield function (2.89) is called the *relative stress* and, de facto, defines the *generalized stress space* also referred to as the *relative stress space*. Applying (2.61) we can easily derive the plastic flow rule, which reads

$$\dot{\mathbf{e}}^p = \dot{\gamma}\frac{\partial F(\mathbf{s}, \boldsymbol{\alpha})}{\partial \boldsymbol{\sigma}} = \dot{\gamma}\frac{\partial F(\mathbf{s}, \boldsymbol{\alpha})}{\partial \mathbf{s}} = \dot{\gamma}\mathbf{n} \tag{2.90}$$

where $\mathbf{n}$ indicates the second-order normal tensor to the yield surface in stress space. With some algebra, it can be shown that

$$\mathbf{n} = \frac{\mathbf{s} - \boldsymbol{\alpha}}{\| \mathbf{s} - \boldsymbol{\alpha} \|} = \frac{\boldsymbol{\Sigma}}{\| \boldsymbol{\Sigma} \|} \tag{2.91}$$

The associated flow rule and the hardening law are easily determined to be

$$\dot{\mathbf{e}}^p = \dot{\gamma}\frac{\partial F(\mathbf{s}, \boldsymbol{\alpha})}{\partial \boldsymbol{\sigma}} = \dot{\gamma}\frac{\partial F(\boldsymbol{\Sigma})}{\partial \boldsymbol{\Sigma}} = \dot{\gamma}\mathbf{n} \tag{2.92}$$

$$\dot{\boldsymbol{\alpha}} = H_{kin}\dot{\mathbf{e}}^p = \dot{\gamma}H_{kin}\mathbf{n} \tag{2.93}$$

Combined linear isotropic and kinematic hardening

To assemble the effects of both linear kinematic and linear isotropic hardening into a single model, it is necessary to sum up the hardening potential, in terms of internal variables, relative to each single mechanism. The ensuing form of the free energy is given by

$$\psi(\boldsymbol{\varepsilon}^e, \mathbf{e}^p, \bar{e}^p) = \frac{1}{2}\boldsymbol{\varepsilon}^e : \mathbb{C}\boldsymbol{\varepsilon}^e + \frac{1}{2}H_{iso}(\bar{e}^p)^2 + \frac{1}{2}\mathbf{e}^p : \mathbb{D}\mathbf{e}^p \tag{2.94}$$

which depends in an uncoupled manner on the internal variables $\mathbf{e}^p, \bar{e}^p$. The conjugate forces are derived as done previously and are exactly the same ones found in the case of pure isotropic and kinematic linear hardening mechanisms as well as the flow rule which is still expressed by (2.90). The form of the hardening law remains unchanged and, in compact notation, reads

$$\boldsymbol{\chi} = -\mathbb{H}\boldsymbol{\xi} \tag{2.95}$$

or, adopting the engineering notation also for the internal variables vectors and for the hardening moduli operator,

$$\{\boldsymbol{\chi}\} = \left\{ \begin{array}{c} -\chi \\ -\boldsymbol{\alpha} \end{array} \right\}; \quad [\mathbb{H}] = \left[\begin{array}{cc} H_{iso} & 0 \\ 0 & H_{kin} \end{array} \right]; \quad \{\boldsymbol{\xi}\} = \left\{ \begin{array}{c} \bar{e}^p \\ \mathbf{e}^p \end{array} \right\} \tag{2.96}$$

The diagonal 2×2 matrix operator $\mathbb{H}$ appearing in (2.95) is known as *linear hardening operator* or briefly *linear hardening moduli* and (cf. (2.96)) allows to rewrite the total potential energy (2.94) as

$$\psi(\boldsymbol{\varepsilon}^e, \mathbf{e}^p, \bar{e}^p) = \frac{1}{2}\boldsymbol{\varepsilon}^e : \mathbb{C}\boldsymbol{\varepsilon}^e + \frac{1}{2}\boldsymbol{\xi} \cdot \mathbb{H}\boldsymbol{\xi} \tag{2.97}$$

With the above specifications, the yield function takes the form

$$F(\mathbf{s}, \boldsymbol{\alpha}, \boldsymbol{\chi}) = F(\boldsymbol{\Sigma}, \boldsymbol{\chi}) = \| \boldsymbol{\Sigma} \| - \sigma_{y,0} - H_{iso}\bar{e}^p \tag{2.98}$$

with the flow rule and the hardening laws still given by

$$\dot{\mathbf{e}}^p = = \dot{\gamma}\frac{\partial F(\boldsymbol{\Sigma}, \boldsymbol{\chi})}{\partial \boldsymbol{\Sigma}} = \dot{\gamma}\mathbf{n} \tag{2.99}$$

$$\dot{\bar{e}}^p = \| \dot{\mathbf{e}}^p \| = \dot{\gamma} \tag{2.100}$$

$$\dot{\boldsymbol{\alpha}} = H_{kin}\dot{\mathbf{e}}^p = \dot{\gamma}H_{kin}\mathbf{n} \tag{2.101}$$

For the combined linear isotropic and kinematic hardening model under discussion the dissipation function (2.57) takes the following form

$$\begin{aligned} D &= \mathbf{S} \cdot \dot{\mathbf{P}} = \boldsymbol{\sigma} : \dot{\mathbf{e}}^p + \boldsymbol{\chi} \cdot \dot{\boldsymbol{\xi}} \\ &= \boldsymbol{\sigma} : \dot{\mathbf{e}}^p - \bar{e}^p H_{iso}\dot{\bar{e}}^p - \boldsymbol{\alpha} : H_{kin}\dot{\mathbf{e}}^p \end{aligned} \tag{2.102}$$

Combined linear isotropic and linear/nonlinear kinematic hardening

The Thermodynamics with internal variables framework adopted so far needs to be slightly generalized in order to include a nonlinear kinematic hardening mechanism. The treatment, however, remains general inasmuch the preceding case is perfectly recovered by canceling the nonlinear kinematic hardening term. The thermodynamic setting that is presented mainly follows the work of Chaboche and Jung [23] which applies to a wider class of viscoplasticity models.

We begin by specifying the general form of the total Helmoltz free energy which, in isothermal conditions, is still

$$\psi = \psi(\boldsymbol{\varepsilon}^e, \boldsymbol{\xi}) \tag{2.103}$$

In the present case the internal variables vector is not represented by (2.96) but in a more general form

$$\{\boldsymbol{\xi}\} = \left\{ \begin{array}{c} \bar{e}^p \\ \bar{\boldsymbol{\xi}} \end{array} \right\} \tag{2.104}$$

where $\bar{\boldsymbol{\xi}}$ is a tensorial strain-like variable that corresponds to the thermodynamic force $\boldsymbol{\alpha}$ and in this case is distinguished by the traceless plastic strain tensor $\mathbf{e}^p$. The above potential gives the stress and the thermodynamic forces by means of the usual definitions

$$\boldsymbol{\sigma} = \frac{\partial \psi}{\partial \boldsymbol{\varepsilon}^e} \tag{2.105}$$

$$\boldsymbol{\chi} = -\frac{\partial \psi}{\partial \boldsymbol{\xi}} \tag{2.106}$$

The basic assumption, at this point, regards the thermodynamic forces $\boldsymbol{\chi}$. These are taken to be the entities corresponding to the hardening variables that, in stress space, describe the present elastic domain and the relative (nonlinear) plastic potential. According to the quasi-standard material theory [24, 40], the von-Mises yield function F remains unchanged, while a new elastoplastic potential $\Psi^p = \Psi^p(F, \boldsymbol{\chi})$ is introduced [23] in order to establish a *generalized normality rule* in the form

$$\dot{\mathbf{e}}^p = \dot{\gamma} \frac{\partial \Psi^p}{\partial \boldsymbol{\sigma}} \tag{2.107}$$

$$\dot{\boldsymbol{\xi}} = \dot{\gamma} \frac{\partial \Psi^p}{\partial \boldsymbol{\chi}} \tag{2.108}$$

The total potential, corresponding to elastic deformation and plastic deformation taking place due to linear hardening only reads

$$\psi(\boldsymbol{\varepsilon}^e, \mathbf{e}^p, \bar{e}^p) = \frac{1}{2}\boldsymbol{\varepsilon}^e : \mathbb{C}\boldsymbol{\varepsilon}^e + \frac{1}{2}\boldsymbol{\xi} \cdot \mathbb{H}\boldsymbol{\xi} \tag{2.109}$$

by which we infer the classical constitutive equations

$$\boldsymbol{\sigma} = \mathbb{C}\boldsymbol{\varepsilon}^e \tag{2.110}$$

$$\boldsymbol{\chi} = -\mathbb{H}\boldsymbol{\xi} \tag{2.111}$$

The plastic potential, according to the nonlinear kinematic hardening mechanism by Armstrong and Frederick [5] is expressed by

$$\begin{aligned} \Psi^p &= F(\boldsymbol{\Sigma}, \chi) + \frac{1}{2}\boldsymbol{\alpha} : \left(\frac{H_{nl}}{H_{kin}}\right)\boldsymbol{\alpha} \\ &= \| \boldsymbol{\Sigma} \| - \sigma_{y,0} - H_{iso}\bar{e}^p + \frac{1}{2}\boldsymbol{\alpha} : \left(\frac{H_{nl}}{H_{kin}}\right)\boldsymbol{\alpha} \end{aligned} \tag{2.112}$$

where H_{nl} is a nondimensional material parameter known as *nonlinear kinematic hardening modulus*. The choice for the plastic potential Ψ^p leads to the following evolutive equations (cf. (2.107)-(2.108))

$$\dot{\mathbf{e}}^p = \dot{\gamma}\frac{\partial \Psi^p}{\partial \boldsymbol{\sigma}} = \dot{\gamma}\mathbf{n} \tag{2.113}$$

$$\dot{\bar{e}}^p = \| \dot{\mathbf{e}}^p \| = \dot{\gamma} \tag{2.114}$$

$$\dot{\bar{\boldsymbol{\xi}}} = \dot{\gamma}\mathbf{n} - \dot{\gamma}\frac{H_{nl}}{H_{kin}}\boldsymbol{\alpha} \tag{2.115}$$

The evolution of the backstress tensor $\boldsymbol{\alpha}$ can be found by taking the rate form of (2.111). We have:

$$\dot{\boldsymbol{\alpha}} = H_{kin}\dot{\bar{\boldsymbol{\xi}}} = H_{kin}\dot{\mathbf{e}}^p - H_{nl}\dot{\gamma}\boldsymbol{\alpha} = \dot{\gamma}(H_{kin}\mathbf{n} - H_{nl}\boldsymbol{\alpha}) \tag{2.116}$$

As observed at the outset, whenever the nonlinear hardening modulus H_{nl} is zero, the tensor $\bar{\boldsymbol{\xi}}$ coincides with $\mathbf{e}^p$ and the linear hardening mechanisms presented above are recovered by the previous combined model.

2.3.3 General von-Mises plasticity model

It is convenient to resume here the general version of the von-Mises constitutive model analyzed hitherto. Combining the three hardening mechanisms, the

equations which define the model are the following [17]

$$
\begin{aligned}
p &= K\theta && (2.117)\\
\mathbf{s} &= 2G[\mathbf{e} - \mathbf{e}^p] && (2.118)\\
\boldsymbol{\Sigma} &= \mathbf{s} - \boldsymbol{\alpha} && (2.119)\\
F &= \|\boldsymbol{\Sigma}\| - \sigma_y && (2.120)\\
\dot{\mathbf{e}}^p &= \dot{\gamma}\mathbf{n} && (2.121)\\
\sigma_y &= \sigma_{y,0} + H_{iso}\gamma && (2.122)\\
\dot{\boldsymbol{\alpha}} &= \dot{\gamma}(H_{kin}\mathbf{n} - H_{nl}\boldsymbol{\alpha}) && (2.123)\\
\dot{\gamma} &\geq 0\ , \quad F \leq 0\ , \quad \dot{\gamma}F = 0 && (2.124)
\end{aligned}
$$

where p is the pressure and θ the volumetric part of the strain tensor, K is the material bulk elastic modulus, G is the material shear modulus, $\mathbf{e}^p$ is the traceless plastic strain, $\boldsymbol{\Sigma}$ is the relative stress in terms of the backstress $\boldsymbol{\alpha}$, the latter introduced to describe a kinematic hardening mechanism. Moreover, F is the von-Mises yield function, $\mathbf{n}$ is the normal to the yield surface, σ_y is the yield surface radius, $\sigma_{y,0}$ the initial yield stress, H_{iso} and H_{kin} are the linear isotropic and kinematic hardening moduli, H_{nl} is the nonlinear kinematic hardening modulus. Finally, Equations (2.124) are the Kuhn-Tucker conditions; in particular, the second equation limits the relative stress within the boundary defined by the yield surface $F = 0$, while the other two are necessary to determine the plastic behavior. With a slight over-simplification of the model complexity, we may say that when $\dot{\gamma} = 0$ the system is in an elastic phase, while when $\dot{\gamma} > 0$ we say that the system is in a plastic phase.

For later convenience, we fix some labeling conventions taken from [17]. The above constitutive model, when encompassing all the three kinds of hardening mechanisms, namely linear isotropic/kinematic hardening and nonlinear kinematic hardening is labeled as NLK model. Instead, whenever the term corresponding to nonlinear kinematic hardening is zero, the model is briefly addressed as LP model.

Rate form of the stress-strain relation

The rate form of the stress-strain relation plays a key role in the discrete approximation of the variational problem of elastoplastic equilibrium that is addressed in Chapter 3. We find it appropriate to present such a form here, for the associative models studied in Section 2.3.1.

Recall the flow rule in the form

$$\dot{\mathbf{P}} = \dot{\gamma}\nabla\phi(\mathbf{S}) \tag{2.125}$$

where the plastic multiplier $\dot{\gamma}$ and the yield function ϕ are related through the complementarity conditions

$$\dot{\gamma} \geq 0\,, \quad \phi \leq 0\,, \quad \dot{\gamma}\phi = 0 \tag{2.126}$$

and satisfy the consistency condition that when $\phi = 0$

$$\dot{\gamma} \geq 0\,, \quad \dot{\phi} \leq 0\,, \quad \dot{\gamma}\dot{\phi} = 0 \tag{2.127}$$

Consider the rate form of the constitutive law (2.38) and (2.95) which read

$$\dot{\mathbf{e}}^p = \boldsymbol{\varepsilon}(\dot{\mathbf{u}}) - \mathbb{C}^{-1}\dot{\boldsymbol{\sigma}} \tag{2.128}$$

$$\dot{\boldsymbol{\xi}} = -\mathbb{H}^{-1}\dot{\chi} \tag{2.129}$$

The inverse of the elastic tensor is guaranteed by its positive-definiteness and the same holds true for $\mathbb{H}$, in view of its definition (2.96). Combining (2.125), (2.128) and (2.129) it is found that

$$\dot{\boldsymbol{\varepsilon}}(\mathbf{u}) - \mathbb{C}^{-1}\dot{\boldsymbol{\sigma}} = \dot{\gamma}\frac{\partial\phi}{\partial\boldsymbol{\sigma}} \tag{2.130}$$

$$-\mathbb{H}^{-1}\dot{\chi} = \dot{\gamma}\frac{\partial\phi}{\partial\boldsymbol{\chi}} \tag{2.131}$$

Checking (2.126) and (2.127), it is evident that $\dot{\gamma} = 0$ if $\phi < 0$ or, if $\phi = 0$ and $\dot{\phi} < 0$. The aim is then to deduce an expression for the plastic rate parameter $\dot{\gamma}$ in the case $\phi = \dot{\phi} = 0$. In such a case it is

$$\dot{\phi}(\mathbf{S}) = \frac{\partial\phi}{\partial\boldsymbol{\sigma}} : \dot{\boldsymbol{\sigma}} + \frac{\partial\phi}{\partial\boldsymbol{\chi}} \cdot \dot{\boldsymbol{\chi}} = 0$$

which, introducing (2.128) and (2.129), implies

$$\dot{\gamma} = \frac{\dfrac{\partial\phi}{\partial\boldsymbol{\sigma}} : \mathbb{C}\boldsymbol{\varepsilon}(\mathbf{u})}{\dfrac{\partial\phi}{\partial\boldsymbol{\sigma}} : \mathbb{C}\dfrac{\partial\phi}{\partial\boldsymbol{\sigma}} + \dfrac{\partial\phi}{\partial\boldsymbol{\chi}} \cdot \mathbb{H}\dfrac{\partial\phi}{\partial\boldsymbol{\chi}}} \tag{2.132}$$

The preceding formula is derived under the assumption that $\dot{\gamma} \geq 0$. Being the tensors $\mathbb{C}$ and $\mathbb{H}$ positive definite this correspond to check if the numerator in (2.132)

$$\frac{\partial\phi}{\partial\boldsymbol{\sigma}} : \mathbb{C}\boldsymbol{\varepsilon}(\mathbf{u}) \geq 0$$

is nonnegative. There are three cases that may arise:

Case 1. The numerator is negative. Then $\dot{\gamma}$ can only be zero. In fact, it is

$$\dot{\phi}(\mathbf{S}) = \frac{\partial \phi}{\partial \boldsymbol{\sigma}} : \dot{\boldsymbol{\sigma}} + \frac{\partial \phi}{\partial \boldsymbol{\chi}} \cdot \dot{\boldsymbol{\chi}} = \frac{\partial \phi}{\partial \boldsymbol{\sigma}} : \mathbb{C}\boldsymbol{\varepsilon}(\mathbf{u}) - \dot{\gamma} \left(\frac{\partial \phi}{\partial \boldsymbol{\sigma}} : \mathbb{C}\frac{\partial \phi}{\partial \boldsymbol{\sigma}} + \frac{\partial \phi}{\partial \boldsymbol{\chi}} \cdot \mathbb{H}\frac{\partial \phi}{\partial \boldsymbol{\chi}} \right) < 0$$

and, by the consistency condition (2.127), $\dot{\gamma} = 0$.

Case 2. The numerator is positive. Then $\dot{\gamma} > 0$. This can be shown supposing by contradiction that $\dot{\gamma} = 0$. Then

$$\dot{\phi}(\mathbf{S}) = \frac{\partial \phi}{\partial \boldsymbol{\sigma}} : \dot{\boldsymbol{\sigma}} + \frac{\partial \phi}{\partial \boldsymbol{\chi}} \cdot \dot{\boldsymbol{\chi}} = \frac{\partial \phi}{\partial \boldsymbol{\sigma}} : \mathbb{C}\boldsymbol{\varepsilon}(\mathbf{u}) > 0$$

which is not allowed, since $\phi = 0$.

Case 3. The numerator is zero. Then $\dot{\gamma} = 0$ obviously in view of (2.132).

The above discussion, in which the consistency conditions plays a key role in the determination of the plastic multiplier λ, amounts to the following formula

$$\dot{\gamma} = \begin{cases} \left(\dfrac{\partial \phi}{\partial \boldsymbol{\sigma}} : \mathbb{C}\boldsymbol{\varepsilon}(\mathbf{u}) \right)_+ \Big/ \left(\dfrac{\partial \phi}{\partial \boldsymbol{\sigma}} : \mathbb{C}\dfrac{\partial \phi}{\partial \boldsymbol{\sigma}} + \dfrac{\partial \phi}{\partial \boldsymbol{\chi}} \cdot \mathbb{H}\dfrac{\partial \phi}{\partial \boldsymbol{\chi}} \right) & \text{if } \ \phi(\boldsymbol{\sigma}, \boldsymbol{\chi}) = 0 \\ 0 & \text{if } \ \phi(\boldsymbol{\sigma}, \boldsymbol{\chi}) < 0 \end{cases} \tag{2.133}$$

where $(\cdot)_+ = \max\{0, \cdot\}$. This formula, which has a general validity, was mentioned but not proved in [68] and is reported here following [41].

Recalling relations (2.133) and (2.130), is is found that when $\phi(\boldsymbol{\sigma}, \boldsymbol{\chi}) < 0$ or when $\phi(\boldsymbol{\sigma}, \boldsymbol{\chi}) = 0$ and $\dfrac{\partial \phi}{\partial \boldsymbol{\sigma}} : \dot{\boldsymbol{\sigma}} \leq 0$, then

$$\dot{\boldsymbol{\varepsilon}}(\mathbf{u}) = \mathbb{C}^{-1}\dot{\boldsymbol{\sigma}}$$

whilst, when $\phi(\boldsymbol{\sigma}, \boldsymbol{\chi}) = 0$ and $\dfrac{\partial \phi}{\partial \boldsymbol{\sigma}} : \dot{\boldsymbol{\sigma}} > 0$, then

$$\dot{\boldsymbol{\varepsilon}}(\mathbf{u}) = \tilde{\mathbb{C}}^{-1}\dot{\boldsymbol{\sigma}}$$

where

$$\tilde{\mathbb{C}} = \mathbb{C} - \frac{\mathbb{C}\dfrac{\partial \phi}{\partial \boldsymbol{\sigma}} \otimes \mathbb{C}\dfrac{\partial \phi}{\partial \boldsymbol{\sigma}}}{\dfrac{\partial \phi}{\partial \boldsymbol{\sigma}} : \mathbb{C}\dfrac{\partial \phi}{\partial \boldsymbol{\sigma}} + \dfrac{\partial \phi}{\partial \boldsymbol{\chi}} \cdot \mathbb{H}\dfrac{\partial \phi}{\partial \boldsymbol{\chi}}}$$

is an invertible fourth-order tensor, given the assumptions on $\mathbb{C}$ and $\mathbb{H}$. The rate form of the stress-strain relation is

$$\dot{\boldsymbol{\sigma}} = \mathbb{C}^{\mathrm{ep}}_{cont}\boldsymbol{\varepsilon}(\dot{\mathbf{u}}) \tag{2.134}$$

with

$$\mathbb{C}^{\mathrm{ep}}_{cont} = \begin{cases} \mathbb{C} & \text{if } \phi(\boldsymbol{\sigma},\boldsymbol{\chi}) < 0 \text{ or } \phi(\boldsymbol{\sigma},\boldsymbol{\chi}) = 0 \text{ and } \dfrac{\partial\phi}{\partial\boldsymbol{\sigma}} : \dot{\boldsymbol{\sigma}} \leq 0 \\ \tilde{\mathbb{C}} & \text{if } \phi(\boldsymbol{\sigma},\boldsymbol{\chi}) = 0 \text{ and } \dfrac{\partial\phi}{\partial\boldsymbol{\sigma}} : \dot{\boldsymbol{\sigma}} \geq 0 \end{cases} \tag{2.135}$$

The *continuous elastoplastic tangent operator* $\mathbb{C}^{\mathrm{ep}}_{cont}$ can be computed in compact explicit expression following [17], for the J_2 elastoplastic model with hardening under examination. It holds:

$$\mathbb{C}^{\mathrm{ep}}_{cont} = K(\mathbf{1}\otimes\mathbf{1}) + 2G[\mathbb{I}_{\mathrm{dev}} - A_{cont}(\mathbf{n}\otimes\mathbf{n})] \tag{2.136}$$

The fourth-order tensor $\mathbb{C}^{\mathrm{ep}}_{cont}$ is specialized with a distinction between the LP model and the NLK model

- LP model

$$A_{cont} = A^{LP}_{cont} = \frac{G}{G_1} \tag{2.137}$$

- NLK model

$$A_{cont} = A^{NLK}_{cont} = \frac{2G}{2G_1 - H_{nl}[\mathbf{n}:\boldsymbol{\alpha}]} \tag{2.138}$$

where

$$2G_1 = 2G + H_{iso} + H_{kin}$$

2.4 Initial boundary value problem of equilibrium in J_2 elastoplasticity

In the same fashion adopted in Section 1.7, it is possible to formulate the initial boundary value problem of quasi-static equilibrium for an isotropic material body characterized by a J_2 elastoplastic model. This problem is modeled by a set of partial differential equations posed on the domain Ω plus a set of

boundary conditions assigned on the boundary $\partial\Omega$ of the body and a set of initial conditions.

Given a body with current configuration $\Omega \subset \mathcal{R}^3$, we indicate for compactness its boundary $\partial\Omega$ with Γ such that $\Gamma = \bar{\Gamma}_D \cup \bar{\Gamma}_S$, with $\bar{\Gamma}_D \cap \bar{\Gamma}_S = \varnothing$. Suppose that, for $t \in [0, T]$, a body force $\mathbf{b}(\mathbf{x}, t)$ is assigned in Ω, a displacement field $\bar{\mathbf{u}}(\mathbf{x}, t)$ is assigned on $\bar{\Gamma}_D$ and a surface traction $\bar{\mathbf{t}}(\mathbf{x}, t)$ is assigned on $\bar{\Gamma}_S$. Initial values for the displacement $\mathbf{u}(\mathbf{x}, 0) = \mathbf{u}_0$ and the velocity field $\mathbf{v}(\mathbf{x}, 0) = \mathbf{v}_0$ are known data as well. With the above specifications, the formulation of the problem in argument for the material body under consideration is: find the displacement field $\mathbf{u}(\mathbf{x}, t)$ which, for any $\mathbf{x} \in \Omega$ and any $t \in [0, T]$, solves the

- *equation of equilibrium*

$$\mathrm{div}\boldsymbol{\sigma} + \mathbf{b} = \mathbf{0} \tag{2.139}$$

- *strain-displacement relation*

$$\boldsymbol{\varepsilon}(\mathbf{u}) = \frac{1}{2}\left[\nabla\mathbf{u} + (\nabla\mathbf{u})^T\right] \tag{2.140}$$

- *constitutive relation* represented by relations (2.117)-(2.124) together with the rate form of the stress-strain relationship (2.134)

and satisfies the

- *boundary conditions*

$$\mathbf{u} = \bar{\mathbf{u}} \quad \text{on} \quad \Gamma_D \quad \text{and} \quad \boldsymbol{\sigma}\mathbf{n} = \bar{\mathbf{t}} \quad \text{on} \quad \Gamma_S \tag{2.141}$$

- *initial conditions*

$$\mathbf{u}(\mathbf{x}, 0) = \mathbf{u}_0(\mathbf{x}) \tag{2.142}$$

It is observed that this problem results highly nonlinear for two main reasons. First, the (time-)integration of the rate constitutive equations requires careful consideration of the loading/unloading conditions relative to the choice of the correct tangent operator. Second, the stress and the internal variables are constrained during their evolution by the yield limit. The object of investigation of the next chapters is mainly concerned with the numerical solution of the above stated problem, posed in variational form.

2.5 Elastoplasticity in a convex-analytic setting

2.5.1 Results from convex analysis

Let X be a normed vector space, with its topological dual X', the space of the linear continuous functionals on X. For $x \in X$ and $x^* \in X'$, the action of x^* on x is denoted by $\langle x^*, x\rangle$. In the finite dimensional case the space X' is isomorphic to X and thus can be identified with X itself. This is indeed the case, for instance, of the Euclidean space $\mathcal{R}^d$ for which the action of a vector $\mathbf{v} \in (\mathcal{R}^d)'$ on a vector $\mathbf{u} \in \mathcal{R}^d$ is usually defined to be the scalar product

$$\langle \mathbf{v}, \mathbf{u}\rangle = \mathbf{v} \cdot \mathbf{u}$$

Examples of infinite dimensional spaces and their duals, in particular function spaces, are given in Appendix A.

Convex sets

Let Y be a subset of X. The interior and the boundary of Y are denoted respectively by $\mathrm{int}(Y)$ and $\mathrm{bdy}(Y)$. The subset Y is said to be *convex* if

$$\text{for any } x, y \in Y \text{ and } 0 < \theta < 1, \;\; \theta x + (1-\theta) y \in Y \tag{2.143}$$

that is to say if and only if any line segment joining any two elements of Y lies entirely in Y.

The *normal cone* to a convex set Y at its point x is a set in X' defined as

$$N_Y(x) = \{x^* \in X' : \;\; \langle x^*, y - x\rangle \leq 0 \;\; \forall y \in Y\} \tag{2.144}$$

The set $N_Y(x)$ is indeed a *cone* since for any $x^* \in N_Y(x)$ and any $\lambda > 0$, $\lambda x^* \in N_Y(x)$. When the point x belongs to the interior of Y the normal cone clearly reduces to the null set, while at least in the finite-dimensional case, $x \in \mathrm{bdy}(Y)$ identifies $N_Y(x)$ as the cone of normals at x in the space X. These definitions are illustrated in Figure 2.8, where the two cases of smooth boundary point x and non-smooth boundary point y are presented. In the former case the normal cone degenerates to the one-dimensional set spanned by the outward normal at x, while in the latter $N_Y(y)$ is a non-trivial cone.

Convex functions

In what follows it is admitted for a function f to attain the values $\pm\infty$. Let f be a function on X, with values in $\bar{\mathcal{R}} \equiv \mathcal{R} \cup \{\pm\infty\}$, the extended real line. The *effective domain* of f, denoted by $\mathrm{dom}(f)$ is defined by

$$\mathrm{dom}(f) = \{x \in X : \;\; f(x) < \infty\}$$

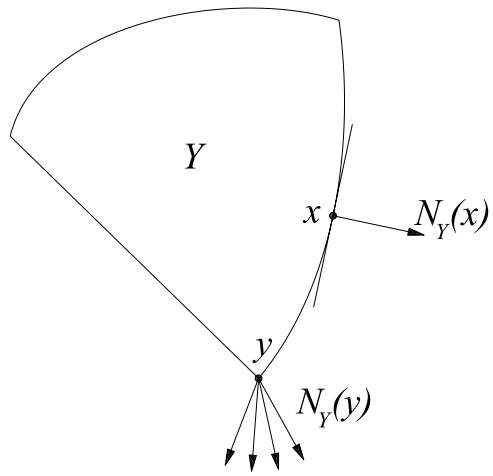

Figure 2.8: Normal cone to a convex set

The *epigraph* of f, denoted by epi(f), is the set formed by ordered pairs in $X \times \mathcal{R}$ defined by

$$\text{epi}(f) = \{(x, \alpha) \in X \times \mathcal{R} : \ f(x) \leq \alpha\}$$

that is the set of points that lie above the graph of f.

A function f is said to be *convex* if

$$f(\theta x + (1-\theta)y) \leq \theta f(x) + (1-\theta) f(y) \ \forall x, y \in X, \quad \forall \theta \in (0,1) \tag{2.145}$$

and it is said to be *strictly convex* if the strict inequality in (2.145) holds whenever $x \neq y$. We note that a function is convex if and only if its epigraph is a convex set.

Also the following definitions, regarding functions defined on normed spaces, will be of notable importance in subsequent paragraphs. A function f is said to be *positively homogeneous* if

$$f(\alpha x) = \alpha f(x) \quad \forall x \in X, \ \forall \alpha > 0$$

proper if

$$f(x) < +\infty \text{ for at least one } x \in X \text{ and } f(x) > -\infty \quad \forall x \in X$$

and *lower semicontinuous* (l.s.c.) if

$$\lim_{n \to \infty} f(x_n) \geq f(x) \tag{2.146}$$

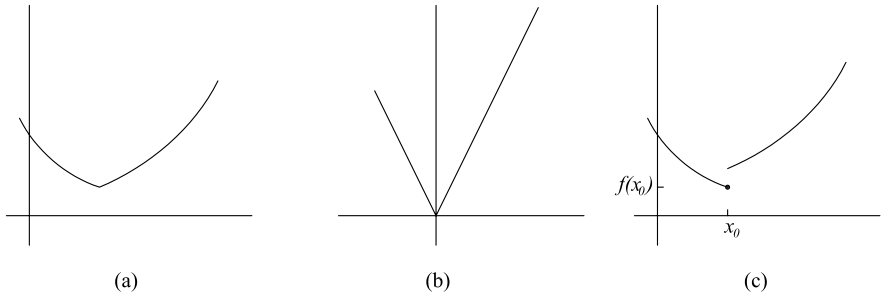

Figure 2.9: (a) Strictly convex function; (b) Positively homogeneous function; (c) Lower semicontinuous function

for any sequence $\{x_n\}$ converging to x. The last notions are illustrated in Figure 2.9 where the space X coincides with $\mathcal{R}$. We observe that a continuous functions is lower semicontinuous, but the converse is not true.

It can be seen that a function f is l.s.c. if and only if its epigraph is closed and that every proper convex function in a finite-dimensional space is continuous on the interior of its effective domain.

A sequence $\{x_n\}$ in a normed space X converges *weakly* to an element $x \in X$ if and only if

$$\lim_{n\to\infty} \langle x^*, x_n \rangle = \langle x^*, x \rangle \quad \forall x^* \in X'$$

The concepts of weak and strong convergence coincide whenever X is a finite-dimensional space. Moreover a function is said to be *weakly lower semicontinuous* (weakly l.s.c.) if the inequality (2.146) holds for any sequence $\{x_n\}$ converging weakly to x. Obviously, a weakly l.s.c. function is l.s.c. Inversely, the following statement holds: if f is convex and l.s.c., then it is weakly l.s.c.

With a slight extension of the classical definition, which does not include lower semicontinuity, we call a function $g : X \to [0, \infty]$ a *gauge* if

$$\begin{aligned} &g(x) \geq 0 \quad \forall x \in X \\ &g(x) = 0 \\ &g(x) \text{ is convex, positively homogeneous and l.s.c.} \end{aligned} \tag{2.147}$$

For any set $S \subset X$, we define the *indicator function* I_S of S as

$$I_S(x) = \begin{cases} 0 & x \in S \\ +\infty & x \notin S \end{cases} \tag{2.148}$$

The *support function* of S, σ_S, is a function on X' defined by

$$\sigma_S(x^*) = \sup\{\langle x^*, x\rangle : \ x \in S\} \tag{2.149}$$

If f is a function on X with values in $\bar{\mathcal{R}}$, the Legendre-Fenchel conjugate (or simply conjugate) function f^* of f is defined by

$$f^*(x^*) = \sup_{x\in X}\{\langle x^*, x_n\rangle - f(x) \quad x^* \in X'\} \tag{2.150}$$

which allows to establish the equivalence

$$I_S^* = \sigma_S \tag{2.151}$$

between the support function and the conjugate to the indicator function. Moreover, if f is proper, convex and l.s.c. then so is f^*, i.e.

$$(f^*)^* \equiv f^{**} = f \tag{2.152}$$

In particular, if S is nonempty, convex and closed, its indicator function I_S is proper, convex and l.s.c.. For such a set, we then have

$$I_S = \sigma_S^* = I_S^{**} \tag{2.153}$$

Given a convex function f on X, the *subdifferential* $\partial f(x)$ of f at any $x \in X$ is defined as the (possibly empty) following subset of X'

$$\partial f(x) = \{x* \in X' : \ f(y) \geq f(x) + \langle x^*, y - x\rangle \quad \forall y \in X\} \tag{2.154}$$

An element of $\partial f(x)$ is called a *subgradient* of f at x. According to the definition, when $f(x) = +\infty$, $\partial f(x) = \varnothing$. In f is a functions defined on $\mathcal{R}^d$ and differentiable at x, then

$$\partial f(x) = \{\nabla f(x)\}$$

At a corner point $(x_0, f(x_0))$, the subdifferential $\partial f(x_0)$ results in the set of the slopes of all the lines lying below the graph of f and passing through the point $(x_0, f(x_0))$ (see Figure 2.10). It is clear from (2.144) that the subdifferential of the indicator function is given by

$$\partial I_S(x) = N_S(x) \quad \forall x \in S \tag{2.155}$$

A result of great importance in later developments is that, for a proper, convex and l.s.c. function f it holds true that

$$x^* \in \partial f(x) \text{ iff } x \in \partial f^*(x^*) \tag{2.156}$$

We have the following fundamental results.

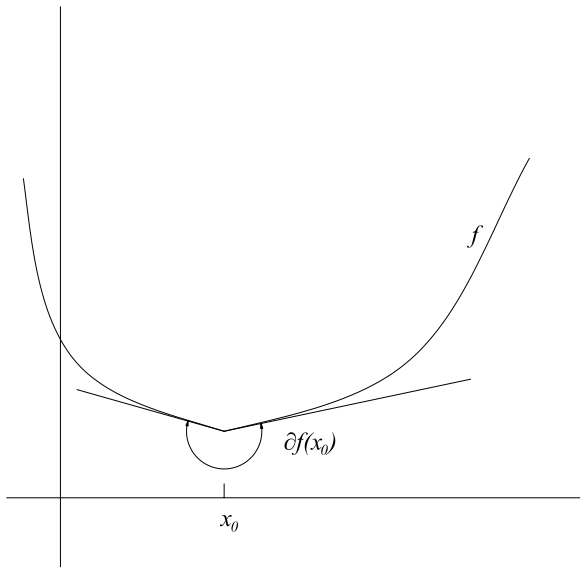

Figure 2.10: Subgradient of a nonsmooth, convex function of a single variable

Lemma 2.5.1 *Let f be a proper, convex, l.s.c. function defined on a normed space X. Define*

$$\mathrm{dom}(\partial f) = \{x \in X : \ \partial f(x) \neq \varnothing\}$$

Then

(a) $\mathrm{dom}(\partial f) \neq \varnothing$ *and* $\mathrm{dom}(\partial f)$ *is dense in* $\mathrm{dom}(f)$

(b) for any proper, convex, l.s.c. functions f and g, defined on X

$$\partial f(x) = \partial g(x) \quad \forall x \in X$$

if and only if

$$f(x) = g(x) + \ \textit{constant}$$

Lemma 2.5.2 *Let g be a gauge on a reflexive Banach space X. Define a closed convex set K in X' by*

$$K = \{x^* \in X' : \ \langle x^*, x\rangle \leq g(x) \ \forall x \in X\}$$

Then

(a) g is the support function of K

(b) the function g^* conjugate of g is the indicator function of K:

$$g^*(x^*) = \begin{cases} 0 & x^* \in K \\ +\infty & \text{otherwise} \end{cases}$$

(c) $K = \partial g(0)$

(d) $x^* \in \partial g(x) \;\Leftrightarrow\; x \in \partial g^*(x^*) = N_K(x^*)$

Maximal responsive relations

It is proper to consider and analyze the properties shared by a special class of multivalued maps. Thanks to the concept exposed herein it will be possible to cast the basic flow rules of elastoplasticity in the present analytic setting. Let us consider a map $G : x \mapsto G(x)$ that associates with each $x \in X$ a (possibly empty) set in X'. The map G is said to be

- *responsive* if

$$0 \in G(0) \tag{2.157}$$

  and if for any $x_1, x_2 \in X$

$$\langle y_1 - y_2, x_1 \rangle \geq 0 \text{ and } \langle y_2 - y_1, x_2 \rangle \geq 0 \tag{2.158}$$

  whenever $y_1 \in G(x_1)$ and $y_2 \in G(x_2)$.

- *maximal responsive* if the following condition

$$\langle y_1 - y_2, x_1 \rangle \geq 0 \text{ and } \langle y_2 - y_1, x_2 \rangle \geq 0 \quad \forall y_2 \in G(x_2),\ \forall x_2 \in X \tag{2.159}$$

  implies that $y_1 \in G(x_1)$ or equivalently if there is no other responsive map whose graph properly include the graph of G (see Figure 2.11).

We have the following important theorem regarding the significance of maximal responsive maps in the present framework

Theorem 2.5.3 [33] If G is a multivalued map on X, with $G(x) \subset X'$ for any $x \in X$, then the following statements are equivalent

(a) the mapping G is maximal responsive

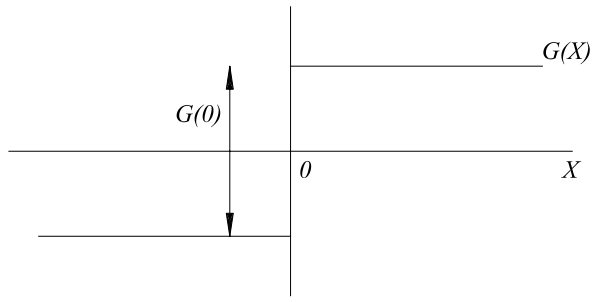

Figure 2.11: Example of a maximal responsive map

(b) there exists a gauge g on X such that

$$G(x) = \partial g(x) \quad \forall x \in X$$

Furthermore, when G is maximal responsive, it determines g uniquely. Setting $\mathrm{dom}(G) = \{x \in X : \ G(x) \neq \varnothing\}$, $g(x)$ is given by

$$G(x) = \begin{cases} \langle x^*, x \rangle & \forall x^* \in G(x), \ \ x \in \mathrm{dom}(G) \\ +\infty & \forall x \notin \mathrm{dom}(G) \end{cases} \tag{2.160}$$

Polar functions

From the viewpoint of convex analysis herein adopted, the admissible elastic region can be conveniently interpreted as a closed convex set K whose boundary (the yield surface) is the level set of a convex function g. K is hence defined by

$$K = \{x^* \in X' : \ g(x^*) \leq c_0\}$$

with c_0 a positive scalar. It results possible to construct g in a way that this function is a gauge such that its epigraph is a closed convex set containing the origin. Furthermore, it is found that the function g has an evident connection to the support function σ_S. Thus, g is defined according to

$$g_K(x^*) = \inf\{\mu > 0 : \ x^* \in \mu K\} \tag{2.161}$$

where $\mu K = \{\mu y : y \in K\}$. Lemma 2.5.2(a) and definition (2.161) suggest the following alternative form for g_K

$$g_K(x^*) = \inf\{\mu > 0 : \langle x^*, x \rangle \leq \mu \sigma_K(x) \quad \forall x \in X\} \tag{2.162}$$

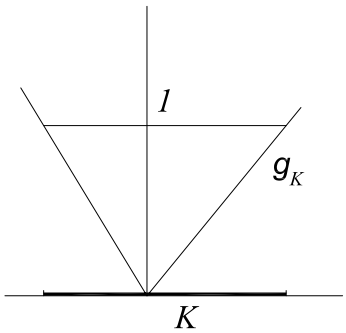

Figure 2.12: Representation of the gauge g_K corresponding to a set $K \subset \mathcal{R}$

An illustration of the function g_K is provided in Figure 2.12. Note that when $x^* \notin \mu K$, for any $\mu > 0$, then $g_K(x^*)$ can take the value $+\infty$. Assuming also that $\sigma_k(x) = 0$ if and only if $x = 0$, the following relationship is derived

$$g_K(x^*) = \sup_{x \in \mathrm{dom}(\sigma_K)\setminus\{0\}} \frac{\langle x^*, x\rangle}{\sigma_K(x)} \tag{2.163}$$

or, equivalently, we are left with the following inequality relating g_K and σ_k

$$\langle x^*, x\rangle \leq g_K(x^*)\sigma_K(x) \quad \forall x \in \mathrm{dom}(\sigma_K), \;\; x^* \in \mathrm{dom}(g_K) \tag{2.164}$$

Taking $x^* \in \mathrm{bdy}(K)$, one finds that

$$\sup_{y \in \mathrm{dom}(\sigma_K)\setminus\{0\}} \frac{\langle x^*, y\rangle}{\sigma_K(x)} = 1 \tag{2.165}$$

which properly returns the supremum if $y = x$, the conjugate to x^* according to Lemma 2.5.2 (d). Relation (2.163), for $x^* \in K$ and $x^* \in \partial\sigma_K(x), \;\; x \neq 0$, then gives

$$\langle x^*, x\rangle = g_K(x^*)\sigma_K(x) \tag{2.166}$$

The functions σ_K and g_K are defined as *polar conjugates* of each other whenever the relationships (2.164) and (2.166) hold, whereas I_K and σ_K are conjugate according to (2.151). With the symbolism $g_K = \sigma_K^\circ$ it is meant that g_K is the *polar function* of σ_K. Moreover, when $\sigma_K^{**} = \sigma_K$ with σ_K a l.s.c. function, it also holds that $\sigma_K^{\circ\circ} = \sigma_K$. The previous notions of polar conjugate functions between pairs of functions have already been investigated by Hill [43] who referred to such pairs as dual potentials.

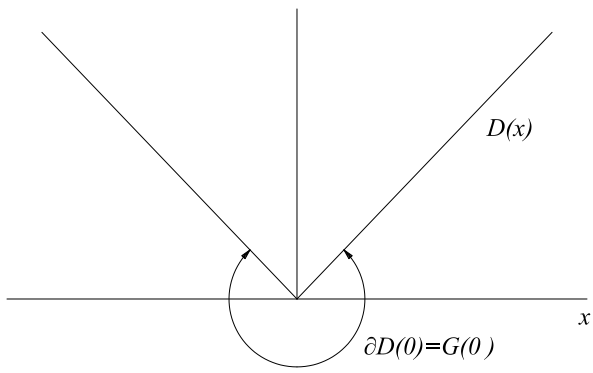

Figure 2.13: Support function D corresponding to the map G shown in Figure 2.11

We have the following important result which, in the next section, will allow to state the normality law in a form involving the yield function (for the proof refer to [41]).

Lemma 2.5.4 *Let g be nonnegative and convex, with $g(0) = 0$ and $x \in$* int(dom(g)) *such that $g(x) > 0$. Set $C = \{z : g(z) \leq g(x)\}$. Then $y \in N_C(x)$ if and only if there exists a scalar $\dot{\gamma} \geq 0$ such that $y \in \dot{\gamma}\partial g(x)$.*

2.5.2 Basic flow relations of elastoplasticity

With the mathematical instruments introduced in the previous section available, it is possible to re-examine the elastoplastic thermodynamic theory studied hitherto. In particular, adopting the standpoint of convex analysis we are able to derive basic results like the yield function convexity, the normality law in a more rigorous and more general fashion. As a result the yield surface smoothness constraint can be avoided, permitting to obtain a set of alternative forms of the plastic flow law, which become of great importance for the analysis of the variational problem of elastoplasticity carried out in Chapter 3.

For later developments and in view of the previous section notation we

convene to establish the following substitutions

$$\begin{array}{ccl} X & \longleftrightarrow & \text{set of generalized plastic strain rates} \\ & \Updownarrow & \\ x & \longleftrightarrow & \dot{\mathbf{P}} = \left(\dot{\mathbf{e}}^p, \dot{\boldsymbol{\xi}}\right) \\ \\ X' & \longleftrightarrow & \text{set of generalized stresses} \\ & \Updownarrow & \\ x^* & \longleftrightarrow & \mathbf{S} = (\boldsymbol{\sigma}, \boldsymbol{\chi}) \end{array}$$

Moreover, it is assumed that K represents a closed set in the space of generalized stresses $\mathbf{S}$ such that it admits the following representation

$$K = \{\mathbf{S} : \ \phi(\mathbf{S}) \leq 0\}$$

through the yield function ϕ. As done in Section 2.3.1, we refer the zone for which $\phi < 0$ as the *elastic domain*, while those points of K satisfying $\phi = 0$ constitute the *yield surface*.

With these positions we are able to apply the results on maximal responsiveness and convex sets to the existence of a convex yield surface. Let us recall Theorem 2.5.3 and consider a maximal responsive map G having as its values subsets of X'. First, it is found by (2.157) that the zero generalized stress is contained within the set of thermodynamic forces $\mathbf{S}$ corresponding to zero generalized plastic strain rate. Second, relation (2.158) constitutes a generalization of the *maximum plastic work* inequality (2.58) in the case of perfectly plastic materials and, admitting $\boldsymbol{\sigma}_0 \in G(\dot{\mathbf{e}}_0^p)$ and $\boldsymbol{\sigma}_1 \in G(\dot{\mathbf{e}}_1^p)$, becomes

$$(\boldsymbol{\sigma}_0 - \boldsymbol{\sigma}_1) : \dot{\mathbf{e}}_0^p \geq 0 \ \text{ and } \ (\boldsymbol{\sigma}_1 - \boldsymbol{\sigma}_0) : \dot{\mathbf{e}}_1^p \geq 0$$

that parallels (2.55).

Going a step further, we may inquire whether the maximal responsiveness condition which permits deducing yield surface convexity can be derived as a consequence of the Principle of maximum plastic dissipation inequality (2.59). Apply Theorem 2.5.3 and Lemma 2.5.2. By the maximal responsiveness condition we are led to recognize the existence of a closed convex set K of admissible generalized stresses and of a generalized normality rule stated in the form

$$\dot{\mathbf{P}} \in N_K(\mathbf{S}) \tag{2.167}$$

Theorem 2.5.3, moreover, implies the equivalence between the normality rule (2.167) and the following

$$\mathbf{S} \in G(\dot{\mathbf{P}}) \tag{2.168}$$

Since

$$\mathbf{S} \in \mathrm{int}(K) \Rightarrow N_K(\mathbf{S}) = \{\mathbf{0}\}$$

it is clear from (2.167) that in the elastic region $\dot{\mathbf{P}} = \mathbf{0}$. Hence, it is stated the equivalence between the existence of a convex yield surface satisfying the normality rule and the property of maximal responsiveness.

At this point it is possible to draw some considerations on the dissipation function. The dissipation function D, defined by (2.57) in Section 2.3.1, in the present context becomes the function g that appears in Lemma 2.5.2 and is characterized by being the support function of the set K. With this association and inspecting (2.59) we are left with

$$D(\dot{\mathbf{P}}) = \sup\{\mathbf{T} : \mathbf{P} : \ \mathbf{T} \in K\} = \mathbf{S} : \dot{\mathbf{P}} \tag{2.169}$$

which indicates that $\mathbf{S}$ represents the point which returns the supremum of the set of admissible plastic work rates.

If we consider the Legendre-Fenchel conjugate D^* of the function D, that is the indicator function of the set K; applying Lemma 2.5.2(d), we arrive at the equivalent condition

$$\mathbf{S} \in \partial D(\dot{\mathbf{P}}) \tag{2.170}$$

which provides the connection existing between the support function D and the maximal responsive map G through Theorem 2.5.3.

Going back for a moment to the example presented in Figure 2.11 which shows the support function corresponding to G, we can derived the relationship

$$G = \partial D \tag{2.171}$$

The last equation qualifies D as a *pseudopotential* for $\mathbf{S}$ [23].

The analytical considerations carried out in Section 2.5.1 make it possible to derive the following equivalent formulations of the flow law in plasticity

(a) G maximal responsive
$\mathbf{S} \in G(\dot{\mathbf{P}})$
$\Updownarrow$

(b) G convex, positively homogeneous, l.s.c.
$D(\dot{\mathbf{P}}) \geq 0, \quad D(\mathbf{0}) = 0$
$\mathbf{S} \in \partial D(\dot{\mathbf{P}})$
$\Updownarrow$

(c) K closed, convex, containing $\mathbf{0}$
$D^* =$ indicator function of K
$\dot{\mathbf{P}} \in \partial D^*(\mathbf{S}) = N_K(\mathbf{S})$

Relationship between the yield and dissipation functions

The analysis on polar functions presented in Section 2.5.1 permits to recognize an enlightening relationship between the yield and dissipation function. Equation (2.161) authorizes to define a gauge function g (we omit for brevity the subscript K with no ambiguity) corresponding to which the set of admissible generalized stress can be expressed as

$$K = \{\mathbf{S} : g(\mathbf{S}) \leq c_0\}$$

The above representation of the yield function through a gauge is usually termed the *canonical yield function.* The gauge g is defined according to

$$g(\mathbf{S}) = \inf\{\mu > 0 : \mathbf{S} \in \mu K\}$$

and, by generalization, we infer that any yield surface may be represented in this manner. In the sequel it is be assumed that f represents an arbitrary representation of the yield function, while g refers to the canonical representation.

Assume that the dissipation $D(\mathbf{\Lambda}) = 0$ (for convenience, we indicate momentarily the argument of D by $\mathbf{\Lambda}$, a generalized plastic strain rate) if and only if $\mathbf{\Lambda} = \mathbf{0}$. It results clear from (2.163) that g and D are related by

$$g(\mathbf{S}) = \sup_{\mathbf{\Lambda} \in \mathrm{dom}(D) \setminus \{\mathbf{0}\}} \frac{\mathbf{S} : \mathbf{\Lambda}}{D(\mathbf{\Lambda})}$$

In the case where $\mathbf{S} \in \partial K$, the boundary of K, then

$$\sup_{\mathbf{\Lambda} \in \mathrm{dom}(D) \setminus \{\mathbf{0}\}} \frac{\mathbf{S} : \mathbf{\Lambda}}{D(\mathbf{\Lambda})} = 1$$

The above expression reaches the supremum when $\mathbf{\Lambda} = \dot{\mathbf{P}}$, being $\dot{\mathbf{P}}$ conjugate to $\mathbf{S}$ in the sense of an equality in (2.169). Hence, for $\mathbf{S} \in K \cap \partial D(\dot{\mathbf{P}})$ and $\dot{\mathbf{P}} \neq \mathbf{0}$, it holds

$$\mathbf{S} : \dot{\mathbf{P}} = g(\mathbf{S}) D(\dot{\mathbf{P}}) \tag{2.172}$$

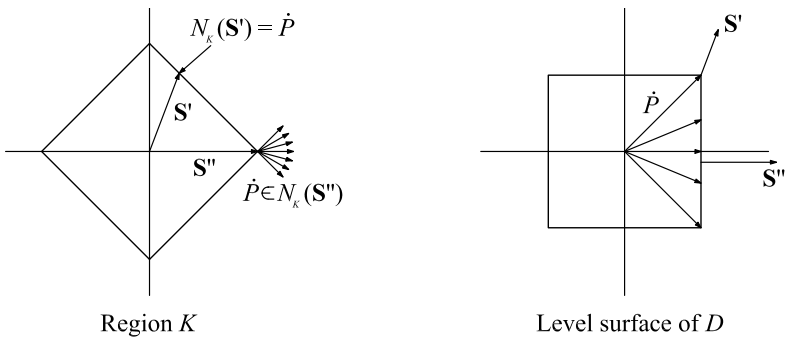

Figure 2.14: Relationship between the admissible set K and its support function D

by which when D and D^* are Legendre-Fenchel conjugate, D and g are polar in the sense of (2.172).

The above polarity condition for the canonical form of the yield function g enables to derive a generalized version of the classical flow rule (2.60), using Lemma 2.5.4. Consider the following

Lemma 2.5.5 *Let g be non-negative and convex, with $g(0) = 0$ and $\boldsymbol{S}$ a point in the interior of* $\mathrm{dom}(g)$ *such that $g(\boldsymbol{S}) > 0$. Set $K = \{\boldsymbol{T} : g(\boldsymbol{T}) \leq g(\boldsymbol{S})\}$. Then $\dot{\boldsymbol{P}} \in N_K(\boldsymbol{S})$ if and only if there exists a constant $\dot{\gamma} \geq 0$ such that*

$$\dot{\boldsymbol{P}} \in \dot{\gamma}\partial g(\boldsymbol{S}) \tag{2.173}$$

Equation (2.60) is readily seen to coincide with (2.173) as soon as g is smooth. Moreover, we can write

$$\dot{\mathbf{P}} \in \dot{\gamma}\partial g(\mathbf{S}) \Leftrightarrow \dot{\gamma} g(\mathbf{T}) \geq \dot{\gamma} g(\mathbf{S}) + \dot{\mathbf{P}} : (\mathbf{T} - \mathbf{S}) \ \ \forall \mathbf{T}$$

Considering sequentially the cases $\mathbf{T} = \mathbf{0}$ and $\mathbf{T} = 2\mathbf{S}$ and using the properties of the gauge g, yields the following characterization of the plastic multiplier

$$\dot{\gamma} = D(\dot{\mathbf{P}})$$

The above fundamental relation simply qualifies the scalar quantity $\dot{\gamma}$ as the dissipation corresponding with a particular generalized plastic strain rate. Indeed, Lemma 2.5.5 also applies to the particular case $g = D$. Setting

$$C = \{\mathbf{Q} : \ \ D(\mathbf{Q}) \leq D(\dot{\mathbf{P}})\}$$

for $\dot{\mathbf{P}} \neq \mathbf{0}$, it is readily found that there exists a strictly positive $\dot{\gamma}$ (excluding $\dot{\gamma} = 0$ since $\mathbf{S} \neq \mathbf{0}$ by hypothesis) such that

$$\mathbf{S} \in N_C(\dot{\mathbf{P}}) \ \textit{or} \ \mathbf{S} \in \dot{\gamma}\partial D(\dot{\mathbf{P}})$$

whenever a relation like (2.170) insists between $\mathbf{S}$ and $\dot{\mathbf{P}}$. A clear visualization of the previous concept can be seen in Figure 2.14 which shows the pair $(\mathbf{S}, \dot{\mathbf{P}}) \in X'$ such that the rate $\dot{\mathbf{P}}$ is in the normal cone to K (the level set $g(\mathbf{S}) \leq 1$) at $\mathbf{S}$. Instead, it is evident that in X, the point $\mathbf{S}$ lies in the normal cone to C (the level set $D(\mathbf{Q}) \leq D(\dot{\mathbf{P}})$ at $\dot{\mathbf{P}}$).

Chapter 3

Variational Formulation of the Elastoplastic Equilibrium Problem

Introduzione

Il presente capitolo è incentrato sulla formulazione variazionale o formulazione debole del problema a valori iniziali e dati al bordo dell'equilibrio per solidi di materiale elastoplastico. Il capitolo è strutturato in maniera da soddisfare due istanze. La prima è quella di presentare le due classiche formulazioni variazionali del problema elastoplastico, cosiddette primale e duale. La seconda è quella di fornire, senza addentrarsi eccessivamente nella dimostrazione matematica, i risultati essenziali sulla buona posizione del problema variazionale in discorso. Il capitolo è suddiviso in due sezioni.

La Sezione 3.2 riguarda la cosiddetta formulazione primale del problema dell'equilibrio elastoplastico. La caratteristica di tale formulazione risiede nella adozione di una particolare forma della legge costitutiva. Detta scelta si riflette sul tipo di spazi funzionali su cui il problema è formulato. In particolare, le grandezze incognite, secondo la formulazione primale, risultano essere lo spostamento ed il tensore di deformazione plastica generalizzato. In riferimento al modello elastoplastico trattato tipo von-Mises, sono presentati i risultati classici di buona posizione del problema primale.

La Sezione 3.3 riguarda la cosiddetta formulazione variazionale duale del problema dell'equilibrio elastoplastico. Tale problema si dimostra equivalente al problema in forma primale, eccetto che per la forma della legge costitutiva adottata. Tale scelta induce una posizione del problema su spazi funzionali differenti rispetto a quelli su cui è posto il problema in forma primale. In questo

caso, infatti, le grandezze incognite sono rispettivamente lo spostamento ed il tensore delle tensioni generalizzato.

La forma duale del problema dell'equilibrio elastoplastico rappresenta la versione più comune di formulazione debole per tale problema riscontrabile in letteratura. Essa costituisce infatti l'oggetto del capitolo successivo che ne affronta la approssimazione numerica.

Le definizioni fondamentali sulle disequazioni variazionali ellittiche e paraboliche e relative proprietà di esistenza ed unicità della soluzione sono brevemente richiamate nella Appendice B.

La trattazione matematica svolta in questo capitolo trae maggiormente spunto da [41].

3.1 Introduction

The present chapter is devoted to the variational or weak formulation of the initial boundary value equilibrium problem of elastoplastic material bodies or simply elastoplastic equilibrium problem. The chapter has two main purposes. The first one is to present the structure of the classical weak formulations of elastoplastic problems. The second one is to provide the basic results on well-posedness for the above problems. This latter part is carried out without going into the mathematical details of the theoretical results. The chapter is subdivided in two sections.

Section 3.2 regards the so-called primal variational formulation of the elastoplastic equilibrium problem. The characterizing feature of this formulation is the form of the flow rule which is adopted. This choice reflects also the spaces on which the problem is posed. Particularly, the unknowns of the problem are the displacement and the generalized plastic strain. Following [41], we present the fundamental results on the well-posedness of the problem under consideration for the relevant case of von-Mises plasticity with linear hardening.

Section 3.3 regards the so-called dual variational formulation of the elastoplastic equilibrium problem. This is by any means the same physical problem but with a different choice of the flow rule. In this way the space on which the problem is formulated results different than that of the primal formulation. In this case, in fact, the unknowns are respectively the displacement and the generalized stress. The results on well-posedness of the dual problem are still derived from [41] in a very sharp manner. The dual variational problem is probably the most common version of the elastoplastic equilibrium weak formulation and remains of primary importance. Indeed, it is the one which is

addressed in the following chapter where its numerical solution is considered.

The basic definitions on elliptic and parabolic variational inequalities together with the elementary properties of existence and uniqueness of solution used in this chapter are collected briefly in Appendix B.

The mathematical arguments presented in this chapter mainly derive from [41].

3.2 The primal variational formulation

Basic relations

We briefly recollect here all the "ingredients" necessary in order to obtain a variational formulation of the boundary value problem of quasi-static equilibrium for an elastoplastic solid. It is assumed in the following developments that all the governing equations are given on a Lipschitz domain Ω with boundary Γ.

The unknown variables of the problem are respectively the displacement vector $\mathbf{u}$, the plastic strain tensor $\mathbf{e}^p$ and the internal variables $\boldsymbol{\xi}$. The equations governing the problem in the domain Ω at any instant $t \in [0, T]$ (cf. Section 1.7) are the

- equilibrium equation
$$\mathrm{div}\boldsymbol{\sigma} + \mathbf{b} = \mathbf{0} \tag{3.1}$$
- the strain-displacement relation
$$\boldsymbol{\varepsilon}(\mathbf{u}) = \frac{1}{2}\left[\nabla\mathbf{u} + (\nabla\mathbf{u})^T\right] \tag{3.2}$$
- the constitutive law
$$\boldsymbol{\sigma} = \mathbb{C}(\boldsymbol{\varepsilon}(\mathbf{u}) - \mathbf{e}^p) \tag{3.3}$$
$$\boldsymbol{\chi} = -\mathbb{H}\boldsymbol{\xi} \tag{3.4}$$

with the flow rule and the maximum plastic dissipation inequality in the form (cf. (2.167) and (2.58))

$$\begin{aligned} &(\dot{\mathbf{e}}^p, \dot{\boldsymbol{\xi}}) \in K_p \\ &D(\mathbf{q}, \boldsymbol{\eta}) \geq D(\dot{\mathbf{e}}^p, \dot{\boldsymbol{\xi}}) + \boldsymbol{\sigma} : (\mathbf{q} - \dot{\boldsymbol{\varepsilon}}) + \boldsymbol{\chi} : (\boldsymbol{\eta} - \dot{\boldsymbol{\xi}}) \quad \forall (\mathbf{q}, \boldsymbol{\eta}) \in K_p \end{aligned} \tag{3.5}$$

where $K_p = \mathrm{dom}(D)$ ([1]). The dissipation D, due to the considerations made in the previous chapter, is a gauge, i.e. it is a nonnegative, convex, positively homogeneous and l.s.c. function with $D(\mathbf{0}) = 0$.

[1]For a detailed derivation of the expression $(3.5)_2$ refer to [41]

Material parameters

Some assumptions on the material parameters are necessary for the well posedness of the problem and to assure a realistic representation of elastoplastic materials.

The elastic tensor $\mathbb{C}$ has the following symmetries

$$\mathbb{C}_{ijkl} = \mathbb{C}_{jikl} = \mathbb{C}_{klij} \tag{3.6}$$

and it is pointwise stable, that is, for some constant $C_0 > 0$ it holds

$$\boldsymbol{\zeta} : \mathbb{C}(\mathbf{x})\boldsymbol{\zeta} \geq C_0 \parallel \boldsymbol{\zeta} \parallel^2 \quad \forall \boldsymbol{\zeta} \in \mathbf{L}\mathrm{in}^{\mathrm{sym}}, \text{ a.e. in } \Omega \tag{3.7}$$

For obvious reasons, $\mathbb{C}$ has bounded and measurable components,

$$\mathbb{C}_{ijkl} \in L^\infty(\Omega) \tag{3.8}$$

The hardening moduli matrix $\mathbb{H}$, which can be viewed as a linear operator from the space of the internal variables $\boldsymbol{\xi}$ into itself (cf. 2.95), is taken to be symmetric in the sense that

$$\boldsymbol{\xi} \cdot \mathbb{H}\boldsymbol{\lambda} = \boldsymbol{\lambda} \cdot \mathbb{H}\boldsymbol{\xi} \tag{3.9}$$

for any couple of vectors of internal variables $\boldsymbol{\xi}$ and $\boldsymbol{\lambda}$. Finally, we admit that $\mathbb{H}$ has bounded and measurable components which satisfy

$$\mathbb{H}_{ij} \in L^\infty(\Omega) \tag{3.10}$$

and it is positive definite, in the sense that there exists a constant H_0 such that

$$\boldsymbol{\xi} \cdot \mathbb{H}\boldsymbol{\xi} \geq H_0 \parallel \boldsymbol{\xi} \parallel^2 \tag{3.11}$$

for all the vectors of internal variables $\boldsymbol{\xi} = (\boldsymbol{\xi}_k)$ s.t. $\boldsymbol{\xi}_k \in \mathbf{L}\mathrm{in}^{\mathrm{sym}}$, $(1 \leq k \leq m)$. In addition, we admit that the compliance tensor $\mathbb{C}^{-1}$ exists, it possesses the same symmetry properties as $\mathbb{C}$ and it is also pointwise stable. This implies that there exists a constant C_0 such that

$$\boldsymbol{\zeta} : \mathbb{C}^{-1}(\mathbf{x})\boldsymbol{\zeta} \geq C_0 \parallel \boldsymbol{\zeta} \parallel^2 \quad \forall \boldsymbol{\zeta} \in \mathbf{L}\mathrm{in}^{\mathrm{sym}}, \text{ a.e. in } \Omega \tag{3.12}$$

Indeed, the inverse $\mathbb{H}^{-1}$ of the hardening moduli matrix exists and it shares the same properties of $\mathbb{H}$, i.e. it is symmetric, it has bounded measurable components and it satisfies the pointwise stability property:

$$\boldsymbol{\xi} \cdot \mathbb{H}^{-1}\boldsymbol{\xi} \geq H_0' \parallel \boldsymbol{\xi} \parallel^2 \tag{3.13}$$

for all the vectors $\boldsymbol{\xi}$.

Initial and boundary conditions

For brevity, we only consider homogeneous Dirichlet-type boundary conditions for the problem under consideration. This choice does not affect the generality of treatment by any means and the results presented in the following sections can readily be extended to mixed type of boundary conditions [41]. Hence, we assume that

$$\mathbf{u} = \mathbf{0} \quad \text{on} \quad \Gamma \tag{3.14}$$

The initial condition on the displacement is of the form

$$\mathbf{u}(\mathbf{x}, 0) = \mathbf{0} \quad \text{in} \quad \Omega \tag{3.15}$$

Function spaces

The variables of the problem need be collocated within appropriate function spaces. Accordingly, we define the space of admissible displacements by

$$V = \left[H_0^1(\Omega)\right]^3$$

The space of plastic strains is taken as

$$Q_0 = \{\mathbf{q} \in Q : \ \operatorname{tr}(\mathbf{q}) = 0 \ \text{ a.e. in } \Omega\}$$

a closed subspace of the space Q defined by

$$Q = \left\{\mathbf{q} : \ \mathbf{q} \in \mathbf{L}\mathrm{in}^{\mathrm{sym}}, \ q_{ij} \in L^2(\Omega)\right\}$$

The space Q is endowed with the inner product and the norm of the space $[L^2(\Omega)]^{3\times 3}$. We have then the space M of internal variables, defined by

$$M = \left\{\boldsymbol{\eta} = (\boldsymbol{\eta}_k) : \ \boldsymbol{\eta}_k \in \mathbf{L}\mathrm{in}^{\mathrm{sym}}, \ \boldsymbol{\eta}_k|_{ij} \in L^2(\Omega), \ 1 \le k \le m\right\}$$

which is endowed with the usual $L^2(\Omega)$-based inner product and norm.

The statement of the problem makes use of the following space

$$Z = V \times Q_0 \times M$$

which becomes a Hilbert space with the inner product

$$(\mathbf{w}, \mathbf{z})_Z = (\mathbf{u}, \mathbf{v})_V + (\mathbf{e}^p, \mathbf{q})_Q + (\boldsymbol{\xi}, \boldsymbol{\eta})_M$$

and the norm $\| \mathbf{z} \|_Z = (\mathbf{z}, \mathbf{z})_Z^{1/2}$, where $\mathbf{w} = (\mathbf{u}, \mathbf{e}^p, \boldsymbol{\xi})$ and $\mathbf{z} = (\mathbf{v}, \mathbf{q}, \boldsymbol{\eta})$. Letting $K_p = \operatorname{dom}(D)$, it is also defined the set

$$Z_p = \{\mathbf{z} = (\mathbf{v}, \mathbf{q}, \boldsymbol{\eta}) \in Z : (\mathbf{q}, \boldsymbol{\eta}) \in K_p \ \text{ a.e. in } \Omega\} \tag{3.16}$$

which is a nonempty, closed, convex cone in Z.

Bilinear form and functionals

We introduce the bilinear form $a : Z \times Z \to R$, defined by

$$a(\mathbf{w}, \mathbf{z}) = \int_\Omega [\mathbb{C}(\boldsymbol{\varepsilon}(\mathbf{u}) - \mathbf{e}^p) : (\boldsymbol{\varepsilon}(\mathbf{v}) - \mathbf{q}) + \boldsymbol{\xi} \cdot \mathbb{H}\boldsymbol{\eta}]\, dv \tag{3.17}$$

the linear functional $\ell(t) : Z \to \mathcal{R}$ given by

$$\langle \ell(t), \mathbf{z} \rangle = \int_\Omega \mathbf{b} \cdot \mathbf{v} dv \tag{3.18}$$

and the functional $j : Z \to \mathcal{R}$ such that

$$j(\mathbf{z}) = \int_\Omega D(\mathbf{q}, \boldsymbol{\eta}) dv \tag{3.19}$$

where $\mathbf{w} = (\mathbf{u}, \mathbf{e}^p, \boldsymbol{\xi})$ and $\mathbf{z} = (\mathbf{v}, \mathbf{q}, \boldsymbol{\eta})$.

Due to the symmetry properties of $\mathbb{C}$ and $\mathbb{H}$, the bilinear form $a(\cdot, \cdot)$ is symmetric as well. By the definition and properties of the dissipation D, the functional $j(\cdot)$ is a convex, positively homogeneous, nonnegative and l.s.c. functional. It is noted that in general j is not differentiable.

Primal formulation

First, integrating relation $(3.5)_2$ over the domain Ω and substituting in the ensuing integral inequality respectively (3.3) and (3.4) we obtain

$$\int_\Omega D(\mathbf{q}, \boldsymbol{\eta}) dv \geq \int_\Omega D(\dot{\mathbf{e}}^p, \dot{\boldsymbol{\xi}}) dv + \int_\Omega \left[\mathbb{C}\left(\boldsymbol{\varepsilon}(\mathbf{u}) - \mathbf{e}^p\right) : (\mathbf{q} - \dot{\mathbf{e}}^p) - \mathbb{H}\boldsymbol{\xi} \cdot (\boldsymbol{\eta} - \dot{\boldsymbol{\xi}}) \right] dv \quad \forall (\mathbf{q}, \boldsymbol{\eta}) \in Z_p \tag{3.20}$$

Next, taking the scalar product of relation (3.1) with $\mathbf{v} - \dot{\mathbf{u}}$ for an arbitrary $\mathbf{v} \in V$, integrating over Ω and performing sequentially an integration by parts and the substitution of expression (3.3) for the stress $\boldsymbol{\sigma}$, we arrive at the following equation

$$\int_\Omega \mathbb{C}\left[\boldsymbol{\varepsilon}(\mathbf{u}) - \mathbf{e}^p\right] : \left[\boldsymbol{\varepsilon}(\mathbf{v}) - \boldsymbol{\varepsilon}(\dot{\mathbf{u}})\right] dv = \int_\Omega \mathbf{b} \cdot (\mathbf{v} - \dot{\mathbf{u}}) dv \quad \forall \mathbf{v} \in V \tag{3.21}$$

Summing relations (3.20) and (3.21), we obtain the variational inequality

$$a(\mathbf{w}(t), \mathbf{z} - \dot{\mathbf{w}}(t)) + j(\mathbf{z}) - j(\dot{\mathbf{w}}(t)) \geq \langle \boldsymbol{\ell}(t), \mathbf{z} - \dot{\mathbf{w}}(t) \rangle \tag{3.22}$$

which holds on the space Z_p. Formally, the primal variational formulation of the elastoplastic initial boundary value problem of equilibrium can thus be stated as [41]

PROBLEM PRIM. Given a linear functional $\boldsymbol{\ell} \in H^1(0,T;Z')$, $\boldsymbol{\ell}(0) = \mathbf{0}$, find $\mathbf{w} = (\mathbf{u}, \mathbf{e}^p, \boldsymbol{\xi}) : [0,T] \to Z$, $\mathbf{w}(0) = \mathbf{0}$, such that for almost all $t \in (0,T)$, $\dot{\mathbf{w}} \in Z_p$ and

$$a(\mathbf{w}(t), \mathbf{z} - \dot{\mathbf{w}}(t)) + j(\mathbf{z}) - j(\dot{\mathbf{w}}(t)) \geq \langle \boldsymbol{\ell}(t), \mathbf{z} - \dot{\mathbf{w}}(t) \rangle \quad \forall \mathbf{z} \in Z_p \tag{3.23}$$

It is noted that if $\mathbf{w}$ is a classical solution of the problem defined by (3.1)-(3.5) and (3.14)-(3.15), then it is a solution of the problem PRIM (See Appendix B). Conversely, inverting the developments which leads to the inequality (3.23) it is possible to recognize that if $\mathbf{w}$ is a smooth solution to problem PRIM, then it is also a classical solution of the problem posed in local form. Hence the two formulation are formally equivalent.

For the applicability of theoretical results in the analysis of the initial boundary value problem in argument, it is more convenient to view the inequality (3.23) as one posed on the whole space Z, instead than on its subspace Z_p. Recalling that $j(\mathbf{z}) = \infty$ when $\mathbf{z} \notin Z_p$ and invoking the requirement $\dot{\mathbf{w}} \in Z_p$, (3.23) can be rewritten equivalently in the form

$$a(\mathbf{w}(t), \mathbf{z} - \dot{\mathbf{w}}(t)) + j(\mathbf{z}) - j(\dot{\mathbf{w}}(t)) \geq \langle \boldsymbol{\ell}(t), \mathbf{z} - \dot{\mathbf{w}}(t) \rangle \quad \forall \mathbf{z} \in Z \tag{3.24}$$

The subdifferential of $j(\cdot)$ is defined as

$$\partial j(\dot{\mathbf{w}}) = \left\{ \mathbf{w}^* \in Z' : \; j(\mathbf{z}) \geq j(\dot{\mathbf{w}}) + \langle \mathbf{w}^*, \mathbf{z} - \dot{\mathbf{w}} \rangle \; \forall \mathbf{z} \in Z \right\} \tag{3.25}$$

and with the aid of (3.24) it is possible to restate the original problem (3.23) as an equation and an inclusion. Setting the new auxiliary variable $\mathbf{w}^*$, we are lead to the new problem of finding a couple of functions $\mathbf{w} : [0,T] \to Z$ and $\mathbf{w}^* : [0,T] \to Z'$ satisfying, for almost all $t \in (0,T)$ the following relations

$$a(\mathbf{w}(t), \mathbf{z}) + \langle \mathbf{w}^*(t), \mathbf{z} \rangle = \langle \boldsymbol{\ell}(t), \mathbf{z} \rangle \quad \forall \mathbf{z} \in Z \tag{3.26}$$

$$\mathbf{w}^*(t) \in \partial j(\dot{\mathbf{w}}(t)) \tag{3.27}$$

Consequently, noting that j is positively homogeneous, it follows that Equation (3.27) is equivalent to the couple of conditions

$$\langle \mathbf{w}^*(t), \mathbf{z} \rangle \leq j(\mathbf{z}) \quad \forall \mathbf{z} \in Z \tag{3.28}$$

and

$$\langle \mathbf{w}^*(t), \dot{\mathbf{w}}(t) \rangle = j(\dot{\mathbf{w}}(t)) \tag{3.29}$$

Ultimately, we can see that, setting to zero all the above plastic and hardening variables appearing in the formulation of problem PRIM, one is left with the following variational equation

$$\int_\Omega \mathbb{C}\boldsymbol{\varepsilon}(\mathbf{u}) : \boldsymbol{\varepsilon}(\mathbf{v})dv = \int_\Omega \mathbf{b}\cdot\mathbf{v}dv \quad \forall \mathbf{v} \in \left[H_0^1(\Omega)\right]^3$$

which recovers exactly the boundary value problem of linear elasticity (B.14) examined in Appendix B, i.e.

$$\int_\Omega \mathbb{C}\boldsymbol{\varepsilon}(\mathbf{v}) : \boldsymbol{\varepsilon}(\mathbf{v})dv = \int_\Omega \mathbf{b}\cdot\mathbf{v}dv \quad \forall \mathbf{v} \in \left[H_0^1(\Omega)\right]^3$$

with Dirichlet homogeneous boundary conditions on the whole boundary.

Combined linear kinematic and isotropic hardening with von-Mises yield function

We now address the formulation of the problem PRIM in the special case of combined linear kinematic and isotropic hardening with the von-Mises yield function. In this context the unknowns of the problem can be identified by the triplets $\mathbf{u}, \mathbf{e}^p, \bar{e}^p$, namely the displacement, the plastic strain and the accumulated plastic stain. The spaces V and Q_0 remain unchanged, while the space of internal variables M reduces to $L^2(\Omega)$. With this position, we may write the admissible set Z_p as

$$Z_p = \{\mathbf{z} = (\mathbf{v}, \mathbf{q}, \mu) \in Z : \parallel \mathbf{q} \parallel \leq \mu \text{ a.e. in } \Omega\}$$

The bilinear form $a(\cdot,\cdot) : Z \times Z \to \mathcal{R}$ becomes

$$a(\mathbf{w}, \mathbf{z}) = \int_\Omega \left[\mathbb{C}(\boldsymbol{\varepsilon}(\mathbf{u}) - \mathbf{e}^p) : (\boldsymbol{\varepsilon}(\mathbf{v}) - \mathbf{q}) + H_{kin}\mathbf{e}^p : \mathbf{q} + H_{iso}\bar{e}^p\mu\right] dv \tag{3.30}$$

where, obviously, $\mathbf{w} = (\mathbf{u}, \mathbf{e}^p, \bar{e}^p)$ and $\mathbf{z} = (\mathbf{v}, \mathbf{q}, \mu)$. The functional j is defined according to (3.19) and reads

$$j(\mathbf{z}) = \int_\Omega D(\mathbf{q}, \mu)dv$$

whilst the dissipation D, in the case of the von-Mises yield criterion, can be expressed in the following alternative form (cf. (2.102) and refer to [41] for a detailed explanation of this expression)

$$D(\mathbf{q}, \mu) = \begin{cases} c_0 \parallel \mathbf{q} \parallel & \text{if } \parallel \mathbf{q} \parallel \leq \mu \\ +\infty & \text{if } \parallel \mathbf{q} \parallel > \mu \end{cases} \tag{3.31}$$

The linear functional $\boldsymbol{\ell}(t)$ simply remains as in (3.18). The above specifications produce the following formulation of the problem with combined linear kinematic-isotropic hardening [41].

PROBLEM PRIM1. Given a linear functional $\boldsymbol{\ell} \in H^1(0,T;Z')$, $\boldsymbol{\ell}(0) = \mathbf{0}$, find $\mathbf{w} = (\mathbf{u}, \mathbf{e}^p, \bar{e}^p) : [0,T] \to Z$, with $\mathbf{w}(0) = \mathbf{0}$, such that for almost all $t \in (0,T)$, $\dot{\mathbf{w}} \in Z_p$ and

$$a(\mathbf{w}(t), \mathbf{z} - \dot{\mathbf{w}}(t)) + j(\mathbf{z}) - j(\dot{\mathbf{w}}(t)) \geq \langle \boldsymbol{\ell}(t), \mathbf{z} - \dot{\mathbf{w}}(t) \rangle \quad \forall \mathbf{z} \in Z_p \tag{3.32}$$

The problem just formulated, being a special case, shares with its general counterpart PROBLEM PRIM. all of its properties, in particular it results equivalent to its local form.

Linear kinematic hardening with von-Mises yield function

The elastoplastic problem of a material experiencing purely linear kinematic hardening and characterized by a von-Mises type yield function can be formalized as a degenerate case of Problem PRIM1, with $H_{iso} = 0$. The solution space is now simply $Z = V \times Q_0$ with the inner product

$$(\mathbf{w}, \mathbf{z})_Z = (\mathbf{u}, \mathbf{v})_V + (\mathbf{e}^p, \mathbf{q})_Q$$

and the usual norm $\| \mathbf{z} \|_Z = (\mathbf{z}, \mathbf{z})_Z^{1/2}$. Here, $\mathbf{w} = (\mathbf{u}, \mathbf{e}^p)$ and $\mathbf{z} = (\mathbf{v}, \mathbf{q})$. The dissipation function D becomes

$$D = c_0 \| \mathbf{q} \| \quad \forall \mathbf{q} \in Q_0$$

so that the function

$$j(\mathbf{z}) = \int_\Omega D(\mathbf{q}) dv \quad \text{for } \mathbf{z} = (\mathbf{v}, \mathbf{q}) \in Z$$

is finite on the entire space Z. The bilinear form is now

$$a(\mathbf{w}, \mathbf{z}) = \int_\Omega [\mathbb{C}(\boldsymbol{\varepsilon}(\mathbf{u}) - \mathbf{e}^p) : (\boldsymbol{\varepsilon}(\mathbf{v}) - \mathbf{q}) + H_{kin} \mathbf{e}^p : \mathbf{q}] \, dv \tag{3.33}$$

The linear functional $\boldsymbol{\ell}(t)$ is still given by (3.18). The statement of the initial boundary value problem is then

PROBLEM PRIM2. Given a linear functional $\boldsymbol{\ell} \in H^1(0,T;Z')$, $\boldsymbol{\ell}(0) = \mathbf{0}$, find $\mathbf{w} = (\mathbf{u}, \mathbf{e}^p) : [0,T] \to Z$, with $\mathbf{w}(0) = \mathbf{0}$, such that for almost all $t \in (0,T)$, $\dot{\mathbf{w}} \in Z_p$ and

$$a(\mathbf{w}(t), \mathbf{z} - \dot{\mathbf{w}}(t)) + j(\mathbf{z}) - j(\dot{\mathbf{w}}(t)) \geq \langle \boldsymbol{\ell}(t), \mathbf{z} - \dot{\mathbf{w}}(t) \rangle \quad \forall \mathbf{z} \in Z \tag{3.34}$$

Existence, uniqueness and stability of the primal formulation

In this short section we aim to give a hint at the properties of existence, uniqueness and stability of the solutions to the variational problems given hitherto in the so called primal formulation. For brevity's sake the proofs of the properties herein exposed are not presented and the reader is referred again to [41] for the complete derivation of results. Following [41], it is seen that the proper way to study the primal variational formulation of the elastoplastic equilibrium problem is that of recasting the ensuing variational inequality into a more general framework which may be stated as follows:

Problem ABS. Find $w : [0,T] \to H$, $w(0) = 0$, such that for almost all $t \in (0,T)$, $\dot{w}(t) \in K$ and

$$a(w(t), z - \dot{w}(t)) + j(z) - j(\dot{w}(t)) \geq \langle \ell(t), z - \dot{w}(t) \rangle \quad \forall z \in K \tag{3.35}$$

where H denotes a Hilbert space and K a nonempty, closed, convex cone in H. As can be checked in Appendix B, (3.35) is a variational inequality of the mixed kind because it shows peculiarities of both variational inequalities of the first kind (convex set K on which the test functions are taken) and of the second kind (nondifferentiable term j).

The suitable hypotheses under which the above problem shows unique solvability and stability have been studied by Han, Reddy and Schroeder [42] for the elastoplastic problem with combined linear isotropic and kinematic hardening. These hypotheses concern, respectively, the bilinear form $a(\cdot,\cdot)$ which is required to be H-elliptic and the functional ℓ which must be a $H^1(0,T;H')$, function with $j(0) = 0$. Moreover, the functional j is required to be nonnegative, convex, positively homogeneous and Lipschitz continuous (even if not necessarily differentiable). When the above conditions are fulfilled, it is possible, with some mathematical manipulations, to show that the original abstract variational inequality (3.35) is equivalent to

$$a(w(t), z - \dot{w}(t)) + j(z) - j(\dot{w}(t)) \geq \langle \ell(t), z - \dot{w}(t) \rangle \quad \forall z \in H$$

The preceding relation implies that it is possible to choose the test functions z in H instead of K. In this way, Theorem B.2.3, the standard solvability result, is applicable.

We are now in a position to introduce the following fundamental result which plays a key role in the subsequent specializations of the abstract problem in argument to its elastoplasticity counterpart in the vest of the primal formulation. Under a proper set of fundamental assumptions on the bilinear form a and on the linear functional it results possible to state general results

of existence, uniqueness and stability of the solution to the problem ABS. As a special case we may have the problem PRIM and its specializations PRIM1 and PRIM2. It is therefore possible to extend the results on the abstract problem to the practical elastoplastic problems examined hitherto.

Theorem 3.2.1 EXISTENCE AND UNIQUENESS OF PROBLEM ABS. *[41] Let H a Hilbert space; $K \subset H$ a nonempty, closed, convex cone; $a : H \times H \to \mathcal{R}$ a bilinear form that is symmetric, bounded and H-elliptic; $\ell \in H^1(0,T;H')$ with $\ell(0) = 0$ and $j : K \to \mathcal{R}$ a nonnegative, convex, positively homogeneous and Lipschitz-continuous function. Then, there exists a unique solution w of Problem* ABS *satisfying $w \in H^1(0,T;H)$. Furthermore, $w : [0,T] \to H$ is the solution to problem* ABS *if and only if there is a function $w^*(t) : [0,T] \to H'$ such that for almost all $t \in (0,)$*

$$a(w(t),z) + \langle w^*(t), z\rangle = \langle \ell(t), z\rangle \quad \forall z \in H \tag{3.36}$$

$$w^*(t) \in \partial j(\dot{w}(t)) \tag{3.37}$$

Following [41] we are also provided of the following stability result

Theorem 3.2.2 STABILITY OF PROBLEM ABS. *[41] Under the assumptions of Theorem 3.2.1, the solution of Problem* ABS *depends continuously on ℓ. In particular, given two linear functionals $\ell^{(1)}$, $\ell^{(2)} \in H^1(0,T;H')$ with $\ell^{(1)}(0) = \ell^{(2)}(0) = 0$, the corresponding solutions $w^{(1)}$ and $w^{(2)}$ are related by the following estimate*

$$\| w^{(1)} - w^{(2)} \|_{L^\infty(0,T;H)} \leq c \, \| \dot{\ell}^{(1)} - \dot{\ell}^{(2)} \|_{L^1(0,T;H')} \tag{3.38}$$

The preceding theorems permit to extend the results made clear for the abstract variational problem (3.35) to the physical problem under consideration, i.e. the primal variational formulation PRIM together with its particular cases PRIM1 and PRIM2. Relatively to the definition (3.17), we first note that in general the bilinear form $a(\cdot,\cdot)$ cannot be expected to be Z-elliptic, since

$$a(\mathbf{z},\mathbf{z}) = \int_\Omega [\mathbb{C}(\boldsymbol{\varepsilon}(\mathbf{v}) - \mathbf{q}) : (\boldsymbol{\varepsilon}(\mathbf{v}) - \mathbf{q}) + \boldsymbol{\eta} \cdot \mathbb{H}\boldsymbol{\eta}] \, dv$$

for $\mathbf{z} = (\mathbf{v}, \mathbf{q}, \boldsymbol{\eta}) \in Z$ and since it is at most

$$a(\mathbf{z},\mathbf{z}) \geq c \left(\| \boldsymbol{\varepsilon}(\mathbf{v}) - \mathbf{q} \|^2_{[L^2(\Omega)]^{3\times 3}} + \| \boldsymbol{\eta} \|^2_{[L^2(\Omega)]^m} \right)$$

On the other hand, the variational inequality (3.23) is posed on the set Z_p, defined by (3.16) and the requirement $\mathbf{z} \in Z_p$ produces a constraint on the

relation between the components $\mathbf{q}$ and $\boldsymbol{\eta}$. We are then lead to make the following assumption

$$\mathbf{z} = (\mathbf{v}, \mathbf{q}, \boldsymbol{\eta}) \in K_p \Rightarrow \beta \parallel \mathbf{q} \parallel^2 \leq \boldsymbol{\eta} \cdot \mathbb{H}\boldsymbol{\eta} \quad \text{for some constant} \quad \beta > 0 \tag{3.39}$$

This crucial assumption can be shown, with an application of the Korn's inequality, to make the bilinear form $a(\cdot,\cdot)$ Z-elliptic on Z_p [41], in the sense that there exists a constant $c_0 > 0$ such that

$$\begin{aligned} a(\mathbf{z},\mathbf{z}) = \int_\Omega [\mathbb{C}(\boldsymbol{\varepsilon}(\mathbf{v}) - \mathbf{q}) : (\boldsymbol{\varepsilon}(\mathbf{v}) - \mathbf{q}) + \boldsymbol{\eta} \cdot \mathbb{H}\boldsymbol{\eta}]\, dv \geq \\ c_0 \left(\parallel \mathbf{v} \parallel_V^2 + \parallel \mathbf{q} \parallel_Q^2 + \parallel \boldsymbol{\eta} \parallel_M^2 \right) \end{aligned} \tag{3.40}$$

The last result is of great importance since in the practical cases analyzed previously the assumption (3.39) is satisfied. Thus we have the following result.

Theorem 3.2.3 *[41] Under the assumption (3.39), the problem* PRIM *has a solution*

The proof of this last statement, which is omitted here for brevity's reasons, parallels the existence proof of the abstract problem (3.35), but makes use of Proposition B.1.2, instead of Theorem B.2.3, which results unapplicable here since the bilinear form is not elliptic on the whole space.

In conclusion, it is to be pointed out that lacking the ellipticity of $a(\cdot,\cdot)$ over the whole space Z, uniqueness and stability of a problem solution cannot be proved. In the two particular cases seen above regarding combined linear isotropic and kinematic hardening and of pure linear kinematic hardening, it is found that the bilinear form ellipticity is granted on the entire space Z. The remainder of this section is devoted to important results valid in such two situations. We have then the following theorems

Theorem 3.2.4 EXISTENCE AND UNIQUENESS - PROBLEM PRIM1. *[41] Under the assumptions made on the data for Problem* PRIM*, the quasi-static elastoplastic equilibrium problem* PRIM1 *has a unique solution* $\mathbf{w} = (\mathbf{u}, \mathbf{e}^p, \bar{e}^p) \in H^1(0,T;Z)$*. Furthermore, if* $\mathbf{w}^{(1)}$ *and* $\mathbf{w}^{(2)}$ *are the solutions corresponding to* $\boldsymbol{\ell}^{(1)}$, $\boldsymbol{\ell}^{(2)} \in H^1(0,T,Z')$*, with* $\boldsymbol{\ell}^{(1)}(0) = \boldsymbol{\ell}^{(2)}(0) = 0$*, then the following estimate holds*

$$\parallel \mathbf{w}^{(1)} - \mathbf{w}^{(2)} \parallel_{L^\infty(0,T;Z)} \leq c \parallel \dot{\boldsymbol{\ell}}^{(1)} - \dot{\boldsymbol{\ell}}^{(2)} \parallel_{L^1(0,T;Z')} \tag{3.41}$$

A similar result holds for the other special case of the primal problem. Indeed, we have

Theorem 3.2.5 EXISTENCE AND UNIQUENESS - PROBLEM PRIM2. *[41] Under the assumptions made on the data for Problem* PRIM*, the quasi-static elastoplastic equilibrium problem* PRIM2 *has a unique solution* $\mathbf{w} = (\boldsymbol{u}, \mathbf{e}^p) \in H^1(0,T;Z)$*. Furthermore, if* $\mathbf{w}^{(1)}$ *and* $\mathbf{w}^{(2)}$ *are the solutions corresponding to* $\boldsymbol{\ell}^{(1)}$*,* $\boldsymbol{\ell}^{(2)} \in H^1(0,T,Z')$*, with* $\boldsymbol{\ell}^{(1)}(0) = \boldsymbol{\ell}^{(2)}(0) = 0$*, then the following estimate holds*

$$\| \mathbf{w}^{(1)} - \mathbf{w}^{(2)} \|_{L^\infty(0,T;Z)} \leq c \, \| \dot{\boldsymbol{\ell}}^{(1)} - \dot{\boldsymbol{\ell}}^{(2)} \|_{L^1(0,T;Z')} \tag{3.42}$$

3.3 The dual variational formulation

The variational formulation examined in this section makes use of the flow law in the form (2.167). This choice leads to a problem in which the unknown variables are the displacement vector $\mathbf{u}$ and the generalized stress vector $\mathbf{S} = (\boldsymbol{\sigma}, \boldsymbol{\chi})$. We begin, as done in Section 3.2 with the proper space setting of the fields involved in the formulation. The space of admissible displacement is still indicated by

$$V = \left[H_0^1(\Omega)\right]^3$$

while the space of stresses is defined as

$$S = \left\{\boldsymbol{\tau} : \ \boldsymbol{\tau} \in \mathbf{L}\mathrm{in}^{\mathrm{sym}}, \ \tau_{ij} \in L^2(\Omega)\right\}$$

The space of conjugate forces is given by

$$M = \left\{\boldsymbol{\mu} = (\boldsymbol{\mu}_k) : \ \ \boldsymbol{\mu}_k \in \mathbf{L}\mathrm{in}^{\mathrm{sym}}, \ \boldsymbol{\mu}_k|_{ij} \in L^2(\Omega), \ \ 1 \leq k \leq m\right\}$$

For later purposes, we set

$$\mathcal{T} = S \times M$$

and implicitly endow this space with the inner products naturally induced by the inner products defined respectively on S and M. Recalling that the admissible generalized stresses are those belonging to the set K pointwise, we may define the following convex subset

$$\mathcal{P} = \{\mathbf{T} = (\boldsymbol{\tau}, \boldsymbol{\mu}) \in \mathcal{T} : \ (\boldsymbol{\tau}, \boldsymbol{\mu}) \in K \text{ a.e. in } (\Omega)\} \tag{3.43}$$

We are now in a position to introduce the following bilinear forms which define the elastoplastic dual problem

$$\bar{a} : S \times S \to \mathcal{R}, \quad \bar{a}(\boldsymbol{\sigma}, \boldsymbol{\tau}) = \int_\Omega \boldsymbol{\sigma} : \mathbb{C}^{-1} \boldsymbol{\tau} dv \tag{3.44}$$

$$b : V \times S \to \mathcal{R}, \quad b(\mathbf{v}, \boldsymbol{\tau}) = -\int_\Omega \boldsymbol{\varepsilon}(\mathbf{v}) : \boldsymbol{\tau} dv \tag{3.45}$$

$$c : M \times M \to \mathcal{R}, \quad c(\boldsymbol{\chi}, \boldsymbol{\mu}) = \int_\Omega \boldsymbol{\chi} \cdot \mathbb{H}^{-1} \boldsymbol{\mu} dv \tag{3.46}$$

together with the bilinear form

$$A : \mathcal{T} \times \mathcal{T} \to \mathcal{R}, \quad A(\mathbf{S}, \mathbf{T}) = \bar{a}(\boldsymbol{\sigma}, \boldsymbol{\tau}) + c(\boldsymbol{\chi}, \boldsymbol{\mu}) \tag{3.47}$$

with $\mathbf{S} = (\boldsymbol{\sigma}, \boldsymbol{\chi})$ and $\mathbf{T} = (\boldsymbol{\tau}, \boldsymbol{\mu})$. It is remarked that both the compliance tensor $\mathbb{C}^{-1}$ and the inverse of the hardening moduli operator $\mathbb{H}^{-1}$ possess the same material properties of symmetry, pointwise stability and boundedness stated in the previous section. Moreover, in view of the above properties, the bilinear form $A(\cdot, \cdot)$ results symmetric, continuous and $\mathcal{T}$-elliptic, i.e. there exist two positive constants α_A and β_A such that

$$|A(\mathbf{S}, \mathbf{T})| \leq \alpha_A \parallel \mathbf{S} \parallel_{\mathcal{T}} \parallel \mathbf{T} \parallel_{\mathcal{T}} \quad \forall \mathbf{S}, \mathbf{T} \in \mathcal{T} \tag{3.48}$$

$$A(\mathbf{T}, \mathbf{T}) \geq \beta_A \parallel \mathbf{T} \parallel_{\mathcal{T}}^2 \quad \forall \mathbf{T} \in \mathcal{T} \tag{3.49}$$

The bilinear form $b(\cdot, \cdot)$ is continuous or equivalently, there exists a positive constant α_b such that

$$|b(\mathbf{v}, \boldsymbol{\tau})| \leq \alpha_b \parallel \mathbf{v} \parallel_V \parallel \boldsymbol{\tau} \parallel_S \quad \forall \mathbf{v} \in V, \boldsymbol{\tau} \in S \tag{3.50}$$

Moreover, for some constant $\beta_b > 0$, it holds

$$\sup_{\boldsymbol{\tau} \in S \setminus 0} \frac{|b(\mathbf{v}, \boldsymbol{\tau})|}{\parallel \boldsymbol{\tau} \parallel_S} \geq \beta_b \parallel \mathbf{v} \parallel_V \quad \forall \mathbf{v} \in V \tag{3.51}$$

The above bound can be easily proved taking $\boldsymbol{\tau} = \boldsymbol{\varepsilon}(\mathbf{v})$ and applying Korn's inequality (A.18). The linear functional of the load is as usual defined by

$$\boldsymbol{\ell}(t) : V \to \mathcal{R}, \quad \langle \boldsymbol{\ell}(t), \mathbf{v} \rangle = -\int_\Omega \mathbf{b}(t) \cdot \mathbf{v} dv \tag{3.52}$$

It is then possible to derive the dual formulation of the elastoplastic problem by applying the standard procedure and recalling, respectively, the local form of the equilibrium equation

$$\operatorname{div} \boldsymbol{\sigma} + \mathbf{b} = \mathbf{0} \quad \text{in } \Omega$$

and the flow law in the form

$$(\dot{\boldsymbol{\sigma}}_E - \dot{\boldsymbol{\sigma}}) : \mathbb{C}^{-1}(\boldsymbol{\tau} - \boldsymbol{\sigma}) - \dot{\boldsymbol{\chi}} \cdot \mathbb{H}^{-1}(\boldsymbol{\mu} - \boldsymbol{\chi}) \leq 0 \quad \forall (\boldsymbol{\tau}, \boldsymbol{\mu}) \in K$$

derived from (2.167) in which $\dot{\boldsymbol{\sigma}}_E = \mathbb{C}\boldsymbol{\varepsilon}(\dot{\mathbf{u}})$ is the elastic stress rate. The variational statement reads as follows:

PROBLEM DUAL. Given a linear functional $\boldsymbol{\ell} \in H^1(0,T;V')$, with $\boldsymbol{\ell}(0) = \mathbf{0}$, find $(\mathbf{u},\mathbf{S}) = (\mathbf{u},\boldsymbol{\sigma},\boldsymbol{\chi}) : [0,T] \to V \times \mathcal{P}$, with $(\mathbf{u}(0),\mathbf{S}(0)) = (\mathbf{0},\mathbf{0})$, such that for almost all $t \in (0,T)$

$$\begin{aligned} b(\mathbf{v},\boldsymbol{\sigma}(t)) &= \langle \boldsymbol{\ell}(t),\mathbf{v}\rangle \quad \forall \mathbf{v} \in V && (3.53)\\ A(\dot{\mathbf{S}}(t),\mathbf{T}-\mathbf{S}(t)) + b(\dot{\mathbf{u}}(t),\boldsymbol{\tau}-\boldsymbol{\sigma}(t)) &\geq 0 \quad \forall \mathbf{T} = (\boldsymbol{\tau},\boldsymbol{\mu}) \in \mathcal{P} && (3.54)\end{aligned}$$

The formal equivalence of Problem DUAL to the classical problem can be easily established. It is also immediate to show that the above problem, setting to zero all the elastoplastic internal forces $\boldsymbol{\chi}$ and letting $\boldsymbol{\sigma},\boldsymbol{\tau} \in \mathcal{S}$, reduces to the linear elastic initial boundary value equilibrium problem (B.20)-(B.21) with homogeneous displacement boundary conditions.

The issue of proving existence and uniqueness of the solution of the dual form is addressed in detail in [41]. Here, for brevity, we give just a brief clue of the concepts necessary to pose such a result.

First, we may observe that the bilinear form $b(\cdot,\cdot) : V \times S \to \mathcal{R}$, appearing in (3.53) and defined by (3.45), satisfies the Babuska-Brezzi condition by means of (3.51). Hence, this bilinear form induces two bounded linear operators $B : S \to V'$ and $B' : V \to S'$ defined as

$$b(\mathbf{v},\boldsymbol{\tau}) = \langle B\boldsymbol{\tau},\mathbf{v}\rangle = \langle B'\mathbf{v},\boldsymbol{\tau}\rangle \quad \text{for } \mathbf{v} \in V,\ \boldsymbol{\tau} \in S \tag{3.55}$$

The above properties lead to the following

Lemma 3.3.1 *The operator B defined by the bilinear form $b(\cdot,\cdot)$ through relation (3.55) is an isomorphism from $(\mathrm{Ker}B)^\perp$ onto V' and the operator B' is an isomorphism from V onto $(\mathrm{Ker}B)^\circ$, where*

$$\begin{aligned} \mathrm{Ker}B &= \{\boldsymbol{\tau} \in S :\ b(\boldsymbol{v},\boldsymbol{\tau}) = 0 \quad \forall \boldsymbol{v} \in V\}\\ (\mathrm{Ker}B)^\circ &= \{f \in S' :\ \langle f,\boldsymbol{\tau}\rangle = 0 \quad \forall \boldsymbol{\tau} \in \mathrm{Ker}B\}\end{aligned}$$

Thus, we have the following important equivalence result

Theorem 3.3.2 *Assume $\boldsymbol{b} \in H^1(0,T;V')$. Then $(\boldsymbol{u},\mathbf{e}^p,\boldsymbol{\xi}) \in H^1(0,T;Z)$ is a solution of the problem* PRIM *if and only if $(\boldsymbol{u},\boldsymbol{\sigma},\boldsymbol{\chi}) \in H^1(0,T;V \times \mathcal{T})$ is a solution of the problem* DUAL*, where $(\boldsymbol{u},\mathbf{e}^p,\boldsymbol{\xi})$ and $(\boldsymbol{u},\boldsymbol{\sigma},\boldsymbol{\chi})$ are related by the (constitutive) equations*

$$\begin{aligned} \boldsymbol{\sigma} &= \mathbb{C}(\boldsymbol{\varepsilon}(\boldsymbol{u}) - \mathbf{e}^p)\\ \boldsymbol{\chi} &= -\mathbb{H}\boldsymbol{\xi}\end{aligned}$$

or

$$\begin{aligned} \mathbf{e}^p &= \boldsymbol{\varepsilon}(\boldsymbol{u}) - \mathbb{C}^{-1}\boldsymbol{\sigma} \\ \boldsymbol{\xi} &= -\mathbb{H}^{-1}\boldsymbol{\chi} \end{aligned}$$

The well-posedness of the dual variational formulation of the elastoplastic problem is then inferred by that of the primal problem.

If we are not to follow this route for proving well-posedness of Problem DUAL, we can instead follow another argument which can be regarded as independent of the developments carried out with respect to the primal formulation to the equivalence result, Theorem 3.3.2. Again, in the same fashion adopted for the primal version of the elastoplastic variational problem, some apriori assumptions have to be taken, in order to show existence and uniqueness "ab initio". The first assumption concerns the set $\mathcal{P}$ and requires that there exists a constant $c > 0$ such that for any generalized stress $\mathbf{S}_1 = (\boldsymbol{\sigma}_1, \boldsymbol{\chi}_1) \in \mathcal{P}$ and any $\boldsymbol{\sigma}_2 \in S$, it corresponds a $\boldsymbol{\chi}_2 \in M$ which satisfies

$$\| \boldsymbol{\chi}_2 \| \leq c \, \| \boldsymbol{\sigma}_2 \| \quad \text{and} \quad \mathbf{S}_1 + \mathbf{S}_2 \in \mathcal{P}$$

with $\mathbf{S}_2 = (\boldsymbol{\sigma}_2, \boldsymbol{\chi}_2)$. This assumption is satisfied in practical situations as that of combined linear isotropic and kinematic hardening. With some mathematical manipulations and recalling Lemma 3.3.1, it is found that the above assumptions grants nonemptyness, convexity and closedness of the set $\mathcal{P}(t)$. The previous requirement is accompanied by an hypothesis on the structure of the set K, whose definition is recalled here for convenience

$$K = \{\mathbf{S} \in S \times M : \ \phi(\mathbf{S}) \leq 0\}$$

It is then assumed that for any $\mathbf{S} \in K$ and any scalar $\kappa \in [0, 1)$, it follows that $\kappa\mathbf{S} \in K$ and

$$\inf_{\mathbf{x}\in\Omega} \operatorname{dist}(\kappa\mathbf{S}(\mathbf{x}), \partial K) > 0$$

The last statement is satisfied for materials characterized by combined linear isotropic and kinematic hardening as soon as the function ϕ is positively homogeneous and Lipschitz continuous.

Under the above assumptions, the following result [41] holds true.

Theorem 3.3.3 *[41] The variational problem* DUAL *has a unique solution* $(\boldsymbol{u}, \boldsymbol{S})$*, with* $\boldsymbol{u} \in H^1(0, T; V)$ *and* $\boldsymbol{S} \in H^1(0, T; \mathcal{T})$*.*

Remark 3.3.4 *The cases of the primal and dual variationals formulation for a constitutive model including nonlinear kinematic hardening are omitted here for brevity. The same results on existence, uniqueness and stability apply also to such cases and can be deduced with similar reasonings starting from the principle of maximum dissipation (see, for instance, [4, 69, 70, 79]).*

Chapter 4

Discrete Variational Formulation of the Elastoplastic Equilibrium Problem

Introduzione

Il tema trattato dal presente capitolo riguarda la risoluzione del problema variazionale dell'equilibrio elastoplastico in forma duale attraverso un metodo numerico. Nella letteratura scientifica è possibile trovare, per diversi casi particolari del problema in discorso, soluzioni in forma chiusa [57]. Si osserva, tuttavia, che tali casi riguardano geometrie regolari, condizioni al bordo estremamente semplici e comportamento del materiale di tipo semplificato. È quindi evidente che tali situazioni risultano di minore interesse pratico. La soluzione approssimata per via numerica, per problemi inerenti modelli maggiormente aderenti al vero, ovvero meno semplificati, risulta quindi la via da seguire onde ottenere risultati ingegneristicamente significativi.

Un notevole impulso alla ricerca in questo senso è venuto anche dallo sviluppo di calcolatori elettronici sempre più potenti.

L'approssimazione del problema in esame implica, come ben noto, sia una discretizzazione rispetto alla variabile spaziale che una discretizzazione temporale. Nel seguito del capitolo, maggiore attenzione è rivolta al secondo punto, dato che questo costituisce l'argomento fondamentale di questo lavoro. Nell'immediato vengono presentati brevemente i concetti generali riguardanti il primo tipo di discretizzazione spaziale per mezzo del metodo degli elementi

finiti. Questo permette di introdurre la terminologia standard dell'analisi per elementi finiti senza entrare nel dettaglio degli aspetti matematici inerenti tale tecnica numerica applicata alla Meccanica dei solidi. La scelta emerge dalla necessità di introdurre alcuni concetti di base della discretizzazione spaziale, che vengono richiamati brevemente nella trattazione relativa alla discretizzazione temporale che constituisce l'argomento principale di questo capitolo.

Nella Sezione 4.2 viene presentata la discretizzazione spaziale e temporale del problema elastoplastico posto in forma duale, insieme ai risultati inerenti l'esistenza della soluzione per il problema così approssimato ed inerenti la convergenza del metodo numerico. Nella Sezione 4.3 vengono introdotti alcuni tra i più comuni schemi di integrazione temporale basati rispettivamente sulla formula di Eulero all'indietro e sulla formula generalizzata di punto medio. Gli schemi di integrazione temporali, specializzati al caso del legame costitutivo elastoplastico in esame, generano una famiglia di metodi che possono essere caratterizzati come metodi alle differenze finite. In relazione a tali metodi sono presentati i principali risultati inerenti stabilità e ordine di accuratezza.

Nella Sezione 4.4 vengono infine proposti due classici algoritmi risolutori del problema elastoplastico nella forma discretizzata rispetto alla variabile temporale. I due algoritmi in esame sono basati sullo schema a doppio passo denominato "predictor-corrector" (previsione-correzione). Il primo adotta un passo di previsione semplicemente elastico, mentre il secondo adotta un passo di previsione tangente.

Il presente capitolo trae spunto principalmente da [41, 70].

4.1 Introduction

The subject of this chapter is the numerical solution of the elastoplastic equilibrium boundary value problem posed in the dual weak form (see Section 3.3). In the literature it is possible to find a number of solutions to such a problem in closed form (see for instance [57]). It is noted, however, that these situations involve only extremely simple cases consisting of highly regular body shape, simple boundary conditions and idealized material behavior. Models that approximate the behavior of real bodies are mostly feasible for approximate solutions which, especially in the recent past, have increasingly become the focus of research due to the development of high-speed digital computers.

As it is well known, the approximation of the problem under consideration involves both a space discretization issue and a time discretization issue. In what follows we focus the discussion on the second issue, since it constitutes the central theme of this work. In the immediate following a brief hint of

what concerns the first discretization issue is proposed, referring to one of the most commonly used tool in this context: the finite element method. This is done in order to provide the minimum necessary familiarity with the standard terminology of finite element analysis without entering into a detailed presentation of the mathematical aspects of the finite element technique in Mechanics of solids. This choice emerges from the necessity of having a basic knowledge of the space discretization when dealing with the time discretization issue which remains the centre of this chapter

In Section 4.2 the space and time (fully) discretization of the dual weak form of the elastoplastic equilibrium is presented and general results on existence of the solution and on convergence are provided. In Section 4.3 we introduce the most common time integration schemes based on the backward Euler's rule and on the generalized midpoint rule. The integration rules are specialized to the case under consideration stemming into a family of integrators which may be grouped into a set of finite difference-based methods. Results on stability and order of convergence are also given. In Section 4.4 we propose two solution algorithms for the discrete variational formulation of the elastoplastic dual problem based on the predictor-corrector philosophy. The first one adopt a purely elastic predictor, while the second one, the Newton's method, adopts a tangent predictor.

The present chapter basically follows the treatment of [41, 70].

4.1.1 Basics of the finite element method

In the following sections we deal with different general solution strategies of the elastoplastic equilibrium problem. As it will be made more evident, a key point of such strategies is the spatial discretization of the weak formulation of the problem. This is assumed to be carried out by the finite element method. Accordingly, since this part of the problem discretization does not represent the center of our discussion, it proves useful to provide some basic notions on the method together with some elementar terminology. This is indeed the target of this paragraph. By no means this introductory excursion claims to be mathematically rigorous or theoretically exhaustive and the interested reader is referred to fundamental standard books on the argument.

The development of a finite element scheme for solving an initial boundary value problem involves four main steps. First, the boundary value problem is reformulated into an equivalent variational problem. Second, the domain of the independent variables (or usually the spatial variables, for a time-dependent problem as the one under consideration) is partitioned into subdomains called finite elements and then a finite-dimensional space, called the finite element

space, is constructed as a collection of piecewise smooth functions with a certain degree of global smoothness. Third, the variational problem is projected to the finite element space and in this way a finite element system is formed. Finally, the solution of the system is searched, say with a proper iterative method, and various consideration are drawn from the solution of the finite element system.

The mathematical theory of the finite element method addresses many other issues such as a priori and a posteriori error estimation, convergence, stability and so on. Here we are not interested in entering within such details. With the following lines we simply aim to introduce basic notations and operational aspects that will be recalled in the later developments regarding the time discretization issue. A reader familiar with the basic terminology and theoretical results of the finite element method may skip this section *in toto*. For detailed information on the finite element method the reader may refer to the standard textbooks and among others [19, 26, 48, 62, 79].

Let us now consider, as an example, the finite element method discretization of the weak formulation associated to a linear elliptic boundary value problem defined on a Lipschitz domain Ω:

$$u \in V, \quad a(u, v) = \langle \ell, v \rangle \quad \forall v \in V \tag{4.1}$$

where V is a Sobolev space on Ω. For a second-order differential equation problem, $V = H^1(\Omega)$ if the given boundary condition is natural and $V = H^1_0(\Omega)$ if the homogeneous Dirichlet boundary condition is specified over the whole boundary. As it is shown in Appendix B, a problem with a nonhomogeneous boundary Dirichlet condition on a part of the boundary $\Gamma_D \subset \partial\Omega$ can be converted to one with the homogeneous Dirichlet boundary condition on Γ_D after a change of the dependent variable. In this case, then, the space $V = H^1_{\Gamma_D}(\Omega)$. The form $a(\cdot, \cdot)$ is assumed to be bilinear, continuous, V-elliptic, while ℓ is a given linear continuous operator on V.

Since V is infinite-dimensional, it is usually impossible to find the solution of the problem (4.1) in closed form. The idea of the Galerkin method is to approximate the weak formulation expressed by (4.1) by its discrete analogue

$$u_N \in V_N, \quad a(u_N, v) = \langle \ell, v \rangle \quad \forall v \in V_N \tag{4.2}$$

where $V_N \subset V$ is a finite-dimensional space and is used to approximate the space V. When V_N consists of piecewise polynomials associated with a partition of the domain Ω, the Galerkin method (4.2) becomes the classical Galerkin finite element method.

Convergence of the finite element method may be achieved by progressively refining the mesh or by increasing polynomial degrees or by doing both simultaneously: then we get the h-version, the p-version or the h-p-version of the finite element method, respectively. It is customary to use h as the parameter for the mesh-size and p as the parameter for the polynomial degree. An efficient selection among the three versions of the method depends on the a priori knowledge about the regularity of the exact solution of the problem.

In the following sections we consider only the h-version of the method, mainly because the solution of an initial boundary value problem of equilibrium in elastoplasticity does not show high regularity. Conventionally, for the h-version finite element method, we use V^h instead of V_N to denote the finite element space. Thus, with a finite element space V^h chosen, the finite element method is

$$u^h \in V^h, \quad a(u^h, v^h) = \langle \ell, v^h \rangle \quad \forall v \in V^h \tag{4.3}$$

Expressing the *trial function* u^h in terms of a basis of the space V^h and taking each of the basis functions for the test function v^h, we obtain an equivalent linear system, called the finite element system, from (4.3) for the coefficients in the expansion of u^h with respect to the basis. Once the finite element system is solved, we can resort to the finite element solution u^h.

The quality of the finite element solution u^h, i.e. the degree of accuracy in the approximation of the exact solution u granted by u^h relies on the regularity of the exact solution u, the construction of the finite element space V^h and eventually on the solver we adopt for the system resulting from (4.3). Again, we do not get into deep discussion on these details for they do not represent our aim at this stage.

For the moment it results useful to examine the basic notions and relative terminology of the construction of the finite-dimensional space V^h. We start by defining a partition $\mathcal{T}_h = \{\Omega_e\}$ $(1 \leq e \leq N_{el})$ of the domain $\bar{\Omega}$ into a finite number N_{el} of closed subsets, called *elements*. By this it is meant that the following properties are satisfied:

- Each Ω_e is a closed nonempty set, with a polygonal continuous boundary
- $\bar{\Omega} = \bigcup_{e=1}^{N_{el}} \Omega_e$
- $\overset{\circ}{\Omega}_{e_1} \cap \overset{\circ}{\Omega}_{e_2} = \varnothing \quad \forall e_1 \neq e_2$

Over each element Ω_e we associate a finite-dimensional function space X_e such that each function $v \in X_e$ is uniquely determined by its values at a finite number of points in Ω_e : $\mathbf{x}_i^{(e)}$ $1 \leq i \leq I$, called the local nodal points. For

example, in the two-dimensional case, if Ω_e is a triangle and X_e is the space of linear functions on Ω_e, then we may choose the three vertices of the triangle as the nodal points; if X_e consists of all the quadratic polynomials on Ω_e, then we can use the three vertices and the three side midpoints as the nodal points. It is required that any two neighboring elements Ω_{e_1} and Ω_{e_2} share the same nodal points on $\Omega_{e_1} \cap \Omega_{e_2}$. This last requirement usually leads to a regularity condition on the finite element partition that the intersection of any two elements must be empty, a vertex or a common side (or face).

For convenience in practical implementation as well as in theoretical analysis it is assumed that there exists one (or sometimes more) closed polygonal domain, ambiguously represented by the symbol $\hat{\Omega}$, such that for each element Ω_e, there is a smooth mapping function F_e with $\Omega_e = F(\hat{\Omega})$. A finite dimensional function space $\hat{X}$ is introduced on $\hat{\Omega}$, together with the nodal points on $\hat{\Omega}$ used to uniquely determine functions in $\hat{X}$. Then the local function space X_e on Ω_e will be obtained through the mapping function F_e from $\hat{X}$ by $X_e \circ F_e = \hat{X}$. For example, $\hat{X}$ can be taken to be a space of polynomials of certain degrees. In the case of a two-dimensional polygonal domain Ω, the partition consists of triangles or quadrilaterals, while in the case of a three-dimensional domain, the partition consists of tetrahedrals or hexahedrals. Then, the finite element space can be defined as

$$V^h = \{v^h \in V : \ v^h \circ F_e \in \hat{X} \ \forall e : \ 1 \leq e \leq N_{el}\} \tag{4.4}$$

We observe that if $\hat{X}$ consists of polynomials, then a function from the space V^h is a piecewise image of polynomials. When F_e is linear, $v^h|_{\Omega_e}$, the restriction of a function $v^h \in V^h$ on Ω_e is a polynomial, while if F_e is nonlinear (e.g. bilinear for quadrilateral elements), $v^h|_{\Omega_e}$ is in general not a polynomial.

A few indications are in order on the requirements of $v^h \in V$. For simplicity, we consider the case of a second-order initial boundary value problem with $V \subseteq H(\Omega)$. Since the restriction of v^h on each element Ω_e is a smooth function, a necessary and sufficient condition that $v^h \in V$ is $v^h \in C(\bar{\Omega})$ and v^h satisfies any possible Dirichlet boundary condition specified in V [26].

As a consequence of the defining relations (4.1) and (4.3) for u and v^h, together with the continuity and V-ellipticity of the bilinear form $a(\cdot,\cdot)$, we have the following result (Cea's lemma [26]) which estimates the error of the finite element solution according to

$$\| u - u^h \|_V \leq c \inf_{v^h \in V^h} \| u - u^h \|_V \tag{4.5}$$

which informs that, up to a multiplicative constant, the finite element solution u^h is an optimal approximation to u among the functions from the finite

element space V^h. Thus, the problem of estimating the finite element solution error can be reduced to one of estimating the approximation error

$$\| u - u^h \|_V \leq c \| u - \Pi^h u \|_V \tag{4.6}$$

where $\Pi^h u$ is any finite element interpolant of u.

4.2 Fully discrete approximation of the dual problem

In this section a family of spatial and time (fully) discrete approximations to the problem DUAL (see Section 3.3) is presented. It is remarked that, under certain assumptions made clear in Chapter 3, the problem DUAL has a unique solution. For convenience the statement of the variational formulation under consideration is reported here:

PROBLEM DUAL. Given a linear functional $\boldsymbol{\ell} \in H^1(0,T;V')$, with $\boldsymbol{\ell}(0) = \mathbf{0}$, find $(\mathbf{u}, \mathbf{S}) = (\mathbf{u}, \boldsymbol{\sigma}, \boldsymbol{\chi}) : [0,T] \to V \times \mathcal{P}$, with $(\mathbf{u}(0), \mathbf{S}(0)) = (\mathbf{0}, \mathbf{0})$, such that for almost all $t \in (0,T)$

$$b(\mathbf{v}, \boldsymbol{\sigma}(t)) = \langle \boldsymbol{\ell}(t), \mathbf{v} \rangle \quad \forall \mathbf{v} \in V \tag{4.7}$$

$$A(\dot{\mathbf{S}}(t), \mathbf{T} - \mathbf{S}(t)) + b(\dot{\mathbf{u}}(t), \boldsymbol{\tau} - \boldsymbol{\sigma}(t)) \geq 0 \quad \forall \mathbf{T} = (\boldsymbol{\tau}, \boldsymbol{\mu}) \in \mathcal{P} \tag{4.8}$$

with

$$\begin{aligned}
V &= [H_0^1(\Omega)]^3 \\
\mathcal{P} &= \{\mathbf{T} = (\boldsymbol{\tau}, \boldsymbol{\mu}) \in \mathcal{T} : \ (\boldsymbol{\tau}, \boldsymbol{\mu}) \in K \text{ a.e. in } \Omega\} \\
S &= \left\{\boldsymbol{\tau} \in \mathbf{Lin}^{\mathrm{sym}} : \ \tau_{ij} \in L^2(\Omega)\right\} \\
M &= \left\{\boldsymbol{\mu} = (\boldsymbol{\mu}_k) : \ \boldsymbol{\mu}_k \in \mathbf{Lin}^{\mathrm{sym}}, \ \boldsymbol{\mu}_k|_{ij} \in L^2(\Omega), \ 1 \leq k \leq m\right\}
\end{aligned}$$

and

$$\mathcal{T} = S \times M$$

The bilinear forms $A(\cdot,\cdot)$ and $b(\cdot,\cdot)$ are defined according to:

$$\begin{aligned}
A : \mathcal{T} \times \mathcal{T} \to \mathcal{R}, \qquad & A(\mathbf{S}, \mathbf{T}) = \int_\Omega \boldsymbol{\sigma} : \mathbb{C}^{-1} \boldsymbol{\tau} dv + \int_\Omega \boldsymbol{\chi} \cdot \mathbb{H}^{-1} \boldsymbol{\mu} dv \\
b : V \times S \to \mathcal{R}, \qquad & b(\mathbf{v}, \boldsymbol{\tau}) = -\int_\Omega \boldsymbol{\varepsilon}(\mathbf{v}) : \boldsymbol{\tau} dv
\end{aligned}$$

while the linear form $\boldsymbol{\ell}(t)$ reads:

$$\boldsymbol{\ell}(t) : V \to \mathcal{R}, \qquad \langle \boldsymbol{\ell}(t), \mathbf{v} \rangle = -\int_\Omega \mathbf{b}(t) \cdot \mathbf{v} dv$$

Assume that a uniform partition of the reference time interval $[0, T]$ into N subintervals is given, with constant step size $\Delta t = T/N$. Assume also that a finite element mesh $\mathcal{T}_h = \{\Omega_e\}$ $(1 \leq e \leq N_{el})$ of the spatial domain is constructed in the usual way, with the mesh-size parameter defined by $h = \max_{1 \leq e \leq E}(h_e)$, where h_e is the diameter of the element Ω_e, a general element of the triangulation. It is also assumed that the finite element subspace V^h consists of piecewise linear functions in V, while S^h and M^h are the subspaces of S and M, respectively, comprising piecewise constants. Define:

$$\mathcal{T}^h = S^h \times M^h$$

and

$$\mathcal{P}^h = \left\{ \mathbf{T}^h = (\boldsymbol{\tau}^h, \boldsymbol{\mu}^h) \in \mathcal{T}^h : \ \mathbf{T}^h \in K \text{ a.e. in } \Omega \right\}$$

by which it is recalled that admissible generalized stress states are those that belong to the set K pointwise.

Next we have a family of fully discrete schemes for the problem Dual [41].

Scheme Dual$^{h\Delta t}$. Let $\alpha \in \left[\frac{1}{2}, 1\right]$ be a scalar parameter. As before, we divide the time interval $[0, T]$ into N steps of equal size $\Delta t = T/N$. The partition nodes are $t_n = n\Delta t$, the midpoints are $t_{n+\alpha} = (n+\alpha)\Delta t$, with $n = 0, ..., N-1$. Find $(\mathbf{w}^{h\Delta t}, \mathbf{S}^{h\Delta t}) = \{(\mathbf{w}^{h\Delta t}_{n+1}, \mathbf{S}^{h\Delta t}_{n+1}), \ 0 \leq n \leq N-1\} \subset V^h \times \mathcal{P}^h$, with $(\mathbf{w}^{h\Delta t}_0, \mathbf{S}^{h\Delta t}_0) = (\mathbf{0}, \mathbf{0})$ such that for $n = 0, ..., N-1$

$$b(\mathbf{v}^h, \boldsymbol{\sigma}^{h\Delta t}_{n+\alpha}) = \langle \boldsymbol{\ell}(t_{n+\alpha}), \mathbf{v}^h \rangle \quad \forall \mathbf{v}^h \in V^h \tag{4.9}$$

$$A_h(\Delta \mathbf{S}^{h\Delta t}_{n+1}, \mathbf{T}^h - \mathbf{S}^{h\Delta t}_{n+\alpha}) + b(\mathbf{w}^{h\Delta t}_{n+\alpha}, \boldsymbol{\tau}^h - \boldsymbol{\sigma}^{h\Delta t}_{n+\alpha}) \geq 0 \quad \forall \mathbf{T}^h = (\boldsymbol{\tau}^h, \boldsymbol{\mu}^h) \in \mathcal{P}^h \tag{4.10}$$

In the above statement we have defined $\Delta \mathbf{S}^{h\Delta t}_{n+1} = \Delta \mathbf{S}^{h\Delta t}_{n+1} - \Delta \mathbf{S}^{h\Delta t}_n$ and have introduced the *generalized midpoint* formula

$$\mathbf{S}^{h\Delta t}_{n+\alpha} = \alpha \mathbf{S}^{h\Delta t}_{n+1} + (1-\alpha)\mathbf{S}^{h\Delta t}_n$$

used to approximate the time derivatives. The symbol $\mathbf{w}^{h\Delta t}_{n+\alpha} \in V^h$ is used to denote the approximation of the velocity $\mathbf{w}(t) = \dot{\mathbf{u}}(t)$ at $t = t_{n+\alpha}$. Likewise,

the bilinear form $A_h : \mathcal{T} \times \mathcal{T} \to \mathcal{R}$ represents an approximation to $A(\cdot,\cdot)$ defined by:

$$A_h(\mathbf{S},\mathbf{T}) = \int_\Omega \boldsymbol{\sigma} : \mathbb{C}_h^{-1}\boldsymbol{\tau} dv + \int_\Omega \boldsymbol{\chi} \cdot \mathbb{H}_h^{-1}\boldsymbol{\mu} dv \tag{4.11}$$

in which the approximate moduli $\mathbb{C}_h^{-1}$ and $\mathbb{H}_h^{-1}$ are piecewise constant approximations of $\mathbb{C}^{-1}$ and $\mathbb{H}^{-1}$ over each element. Also $\mathbb{C}_h^{-1}$ and $\mathbb{H}_h^{-1}$ are assumed to satisfy the material properties requirements possessed by $\mathbb{C}^{-1}$ and $\mathbb{H}^{-1}$, given in Section 3.2, with the constant there independent of h (cf. (3.12)-(3.13)).

It is found that under the discrete counterpart of the assumptions required in Section 3.3 to show the uniqueness of solution property for the problem DUAL, it is possible to show that the discrete problem DUAL$^{h\Delta t}$ has a solution. Without going into further details and referring to [41] for a complete derivation of the result, we give here two basic theorems respectively regarding the error order estimate and the stability of the previously presented schemes under minimal regularity conditions.

Theorem 4.2.1 *Assume* $\mathbf{S} \in W^{2,1}(0,T;\mathcal{T})$, $\mathbf{w} \in L^\infty(0,T;[H^2(\Omega)]^3)$, $\mathbb{C}_{ijkl} \in W^{1,\infty}(\Omega)$ *and* $\mathbb{H}_{ij} \in W^{1,\infty}(\Omega)$ $(1 \le i,j,k,l \le 3)$. *Then for the fully discrete solutions defined in* SCHEME DUAL$^{h\Delta t}$, *the following estimate holds:*

$$\max_{0\le n\le N} \| \mathbf{S}(t_n) - \mathbf{S}_n^{h\Delta t} \|_{\mathcal{T}} = O(h+\Delta t)$$

Additionally, if $\alpha = \frac{1}{2}$ *and* $\mathbf{S} \in W^{3,1}(0,T;\mathcal{T})$ *it holds:*

$$\max_{0\le n\le N} \| \mathbf{S}(t_n) - \mathbf{S}_n^{h\Delta t} \|_{\mathcal{T}} = O[h+(\Delta t)^2]$$

Theorem 4.2.2 *Under the basic regularity condition* $(\mathbf{u},\mathbf{S}) \in H^1(0,T;V \times \mathcal{T})$, *the fully discrete solution defined in the* SCHEME DUAL$^{h\Delta t}$ *converges:*

$$\max_{0\le n\le N} \| \mathbf{S}(t_n) - \mathbf{S}_n^{h\Delta t} \|_{\mathcal{T}} \to 0 \quad \textit{as } \Delta t, h \to 0$$

4.3 Time integration schemes for the dual problem based on finite difference methods

We now focus our attention only on the time discretization of the dual problem. The extension of the discussion to fully discrete schemes as the one presented in the previous section is straightforward and requires only to change infinite-dimensional spaces or their subsets to corresponding finite element spaces or their subsets in the argument.

The following schemes can be generally casted within the set of generalized midpoint integration schemes in that time derivatives are approximated stepwise using a generalized midpoint rule with respect to time. In the following we present three time integration schemes. The first is the well established backward Euler's scheme which results a particular case of the general integration scheme for a specific choice of the scalar integration parameter. The other two integration schemes are properly based on the generalized midpoint integration rule and form two distinct families since we have a variable integration parameter for each one of them.

For convenience and to make notation lighter we omit the dependence of the nodal variables on the time step Δt which, unless differently specified, is assumed constant for each time step of the interval $[0, T]$ and equal to T/N. Accordingly, we admit the identification $(\cdot)_n^{\Delta t} = (\cdot)_n$ for the generic nodal variable.

Scheme Dual$_1$ (Backward Euler's rule).
Find $(\mathbf{w}, \mathbf{S}) = \{(\mathbf{w}_{n+1}, \mathbf{S}_{n+1}),\ 0 \leq n \leq N-1\} \subset V \times \mathcal{P}$, with $(\mathbf{w}_0, \mathbf{S}_0) = (\mathbf{0}, \mathbf{0})$, such that for $n = 0, ..., N-1$

$$b(\mathbf{v}, \boldsymbol{\sigma}_{n+1}) = \langle \boldsymbol{\ell}(t_{n+1}), \mathbf{v} \rangle \quad \forall \mathbf{v} \in V \tag{4.12}$$

$$A(\Delta \mathbf{S}_{n+1}, \mathbf{T} - \mathbf{S}_{n+1}) + b(\mathbf{w}_{n+1}, \boldsymbol{\tau} - \boldsymbol{\sigma}_{n+1}) \quad \geq \quad 0 \quad \forall \mathbf{T} \in \mathcal{P} \tag{4.13}$$

More generally, it is possible to form a family of generalized midpoint integration schemes, based on the following generalized midpoint formula

$$\mathbf{S}_{n+\alpha} = \alpha \mathbf{S}_{n+1} + (1-\alpha)\mathbf{S}_n$$
$$\mathbf{w}_{n+\alpha} = \alpha \mathbf{w}_{n+1} + (1-\alpha)\mathbf{w}_n$$

where $\alpha \in \left[\frac{1}{2}, 1\right]$ is the scalar discretization parameter. Accordingly we have the following family of integration procedures [69, 71].

Scheme Dual$_2$ (One-stage Generalized Midpoint Rule).
Find $(\mathbf{w}, \mathbf{S}) = \{(\mathbf{w}_{n+1}, \mathbf{S}_{n+1}),\ 0 \leq n \leq N-1\} \subset V \times \mathcal{P}$, with $(\mathbf{w}_0, \mathbf{S}_0) = (\mathbf{0}, \mathbf{0})$, such that for $n = 0, ..., N-1$

$$b(\mathbf{v}, \boldsymbol{\sigma}_{n+\alpha}) = \langle \boldsymbol{\ell}(t_{n+\alpha}), \mathbf{v} \rangle \quad \forall \mathbf{v} \in V \tag{4.14}$$

$$A(\Delta \mathbf{S}_{n+1}, \mathbf{T} - \mathbf{S}_{n+\alpha}) + b(\mathbf{w}_{n+\alpha}, \boldsymbol{\tau} - \boldsymbol{\sigma}_{n+\alpha}) \quad \geq \quad 0 \quad \forall \mathbf{T} \in \mathcal{P} \tag{4.15}$$

It is noted that such a scheme grants that, since $\mathcal{P}$ is a convex set and since $\mathbf{S}_n, \mathbf{S}_{n+1} \in \mathcal{P}$, it results $\mathbf{S}_{n+\alpha} \in \mathcal{P}$. In other words, the scheme Dual$_2$ results both midpont ($t = t_{n+\alpha}$) and endpoint ($t = t_{n+1}$) *yield-consistent*, i.e. it returns a solution in terms of generalized stress which results consistent with

the yield surface limit. Obviously, in the case $\alpha = 1$ the scheme DUAL_2 reduces to the scheme DUAL_1. This implies that the also the scheme DUAL_1 is end-point *yield consistent*. Yield-consistency of the numerical solution is a desirable property of a numerical time integration scheme since it avoids possible undesired instabilities of the solution [72].

It is possible to carry out an error analysis of the above schemes in terms of the error norm $\max_n \parallel \mathbf{S}(t_n) - \mathbf{S}_n \parallel_{\mathcal{T}}$ [41]. If the solution is sufficiently smooth (i.e. $\mathbf{S} \in W^{2,1}(0,T;\mathcal{T})$), the scheme DUAL_2 and hence also the scheme DUAL_1 are of first-order when $\alpha \in \left(\frac{1}{2}, 1\right]$

$$\max_n \parallel \mathbf{S}(t_n) - \mathbf{S}_n \parallel_{\mathcal{T}} \leq c\Delta t \parallel \mathbf{S} \parallel_{W^{2,1}(0,T;\mathcal{T})}$$

while the scheme DUAL_2 is second-order accurate, i.e.:

$$\max_n \parallel \mathbf{S}(t_n) - \mathbf{S}_n \parallel_{\mathcal{T}} \leq c\Delta t^2 \parallel \mathbf{S} \parallel_{W^{3,1}(0,T;\mathcal{T})}$$

when $\alpha = \frac{1}{2}$ and $\mathbf{S} \in W^{3,1}(0,T;\mathcal{T})$.

A third family of discretization procedures is based on a generalized midpoint method proposed by Simo [69], still based on the generalized midpoint integration technique but with a double stage procedure.

SCHEME DUAL_3 (TWO-STAGE GENERALIZED MIDPOINT RULE). [69]
Let $(\mathbf{w}_0, \mathbf{S}_0) = (\mathbf{0}, \mathbf{0})$.

- STEP 1.

  For $n = 0, ..., N-1$, first compute $(\mathbf{w}_{n+\alpha}, \mathbf{S}_{n+\alpha}) \subset V \times \mathcal{P}$, satisfying

$$b(\mathbf{v}, \boldsymbol{\sigma}_{n+\alpha}) = \langle \boldsymbol{\ell}(t_{n+\alpha}), \mathbf{v} \rangle \ \ \forall \mathbf{v} \in V \tag{4.16}$$

$$\begin{aligned} &A(\mathbf{S}_{n+\alpha} - \mathbf{S}_n, \mathbf{T} - \mathbf{S}_{n+\alpha}) \\ &+(\alpha\Delta t) b(\mathbf{w}_{n+\alpha}, \boldsymbol{\tau} - \boldsymbol{\sigma}_{n+\alpha}) \geq 0 \ \ \forall \mathbf{T} \in \mathcal{P} \end{aligned} \tag{4.17}$$

  set

$$\mathbf{w}_{n+1} = \frac{1}{\alpha}\mathbf{w}_{n+\alpha} + \left(1 - \frac{1}{\alpha}\right)\mathbf{w}_n \tag{4.18}$$

- STEP 2.

  Find $\mathbf{S}_{n+1} \in \mathcal{P}$ such that

$$\begin{aligned} &A(\mathbf{S}_{n+1} - \mathbf{S}_n, \mathbf{T} - \mathbf{S}_{n+1}) \\ &+\Delta t b(\mathbf{w}_{n+1}, \boldsymbol{\tau} - \boldsymbol{\sigma}_{n+1}) \geq 0 \quad \forall \mathbf{T} \in \mathcal{P} \end{aligned} \tag{4.19}$$

The result on the existence of a solution of the time continuous problem DUAL introduced in Section 3.3 can be extended in the present context respectively to the discrete variational forms (4.14)-(4.15), (4.16)-(4.17) and (4.18)-(4.19) [41]. The variational problem expressed by the inequality (4.19) is equivalent to a constrained minimization problem of the form

$$\inf\left\{\frac{1}{2}A(\mathbf{T},\mathbf{T}) - A(\mathbf{S}_n,\mathbf{T}) + \Delta t b(\mathbf{w}_n,\boldsymbol{\tau}) :\ \mathbf{T}\in\mathcal{P}\right\}$$

which has a unique minimizer $\mathbf{S}_{n+1}\in\mathcal{P}$ [41]. In what follows we present two fundamental results on stability and convergence of the above semidiscrete schemes. The proof of the ensuing propositions may be found in [41].

We begin by first presenting a general property of contractivity of the solution.

Theorem 4.3.1 *Let* $(\mathbf{u}_1,\mathbf{S}_1)$ *and* $(\mathbf{u}_2,\mathbf{S}_2):[0,T]\to\mathcal{V}\times\mathcal{P}$ *satisfy the relations (4.7)-(4.8). Then:*

$$\|\ \mathbf{S}_1(t)-\mathbf{S}_2(t)\ \|_A \le \|\ \mathbf{S}_1(s)-\mathbf{S}_2(s)\ \|_A \quad \forall s,t,\ \ 0\le s\le t\le T \tag{4.20}$$

We thus say that a numerical scheme for PROBLEM DUAL is stable if its numerical solutions inherit the contractivity property of the solution of the continuous problem. More precisely we have the following definition.

Definition 4.3.2 *A numerical scheme for solving the* PROBLEM DUAL *is said to be stable if two numerical solutions* $(\boldsymbol{w}_1,\boldsymbol{S}_1)=\{(\boldsymbol{w}_{1,n+1},\boldsymbol{S}_{1,n+1}),\ 0\le n\le N-1\}$ *and* $(\boldsymbol{w}_2,\boldsymbol{S}_2)=$
$\{(\boldsymbol{w}_{2,n+1},\boldsymbol{S}_{2,n+1}),\ 0\le n\le N-1\}$ *generated by two initial values, satisfy the inequality:*

$$\|\ \boldsymbol{S}_{1,n+1}-\boldsymbol{S}_{2,n+1}\ \|_A \le \|\ \boldsymbol{S}_{1,m+1}-\boldsymbol{S}_{2,m+1}\ \|_A \quad \forall m,n,\ \ 0\le m\le n\le N \tag{4.21}$$

Stability is a desirable property for a numerical scheme. The estimate (4.21) shows that the propagation of the error to later steps is controlled with constant 1. With the above positions and definition we are able to state the following theorem (see [41] for a complete derivation of the result).

Theorem 4.3.3 *The schemes* DUAL_1 *and* DUAL_3 *are stable. If* $\alpha\in[\frac{1}{2},1]$, *the scheme* DUAL_2 *is also stable*

It is noted that the contractivity property implies uniqueness of a solution [41, 70]. Thus, in particular for both the continuous problem and discrete problem, the uniqueness of the generalized stress part of the solutions follows immediately.

4.4 Solution algorithms for the time integration schemes

In practical computations, usually the fully discrete schemes discussed above for the solution of the elastoplastic equilibrium variational problem are not implemented directly, because of the large size of the discrete problems. Commonly an iteration procedure is adopted in order to split the task of computing the generalized stress and the displacement. The iteration procedures used are all of the "predictor-corrector" type. In this section we present two of the most common predictor-corrector algorithms which apply to the discrete problems discussed in the previous section. Attention is focused on algorithms which are in common use in current computational practice [69]. The presentation, for brevity, is limited to the solution of the scheme DUAL_1 for a single time step. The treatment of the other time-discrete and fully discrete approximation involves the same basic steps and therefore it is omitted here.

For convenience, we first propose a re-formulation of the PROBLEM DUAL. Let

$$\mathbf{S}^e = (\mathbb{C}\boldsymbol{\varepsilon}, \mathbf{0})$$

where $\mathbb{C}$ represents as usual the elastic tensor. Then, the variational inequality (4.8) can be rewritten as

$$A(\dot{\mathbf{S}}^e(t) - \dot{\mathbf{S}}(t), \mathbf{T} - \mathbf{S}(t)) \leq 0 \quad \forall \mathbf{T} = (\boldsymbol{\tau}, \boldsymbol{\mu}) \in \mathcal{P} \tag{4.22}$$

Therefore, the scheme DUAL_1 can be restated as follows. Set $\boldsymbol{\ell}_{n+1} = \boldsymbol{\ell}(t_{n+1})$ and

$$\mathbf{u}_{n+1} = \Delta t \sum_{j=1}^{n} \mathbf{w}_j \quad n = 1, ..., N$$

SCHEME DUAL. Find $(\mathbf{u}_{n+1}, \mathbf{S}_{n+1}) = \{(\mathbf{u}_{n+1}, \boldsymbol{\sigma}_{n+1}, \boldsymbol{\chi}_{n+1}),\ 0 \leq n \leq N-1\} \subset V \times \mathcal{P}$, with $(\mathbf{u}_0, \mathbf{S}_0) = (\mathbf{0}, \mathbf{0})$, such that for $n = 0, ..., N-1$

$$b(\mathbf{v}, \boldsymbol{\sigma}_{n+1}) = \langle \boldsymbol{\ell}(t_{n+1}), \mathbf{v} \rangle \quad \forall \mathbf{v} \in V \tag{4.23}$$

$$A(\mathbf{S}^{TR}_{n+1} - \mathbf{S}_{n+1}, \mathbf{T} - \mathbf{S}_{n+1}) \leq 0 \quad \forall \mathbf{T} \in \mathcal{P} \tag{4.24}$$

in which

$$\mathbf{S}^{TR}_{n+1} = \mathbf{S}_n + \Delta \mathbf{S}^e_{n+1} \tag{4.25}$$

represents the generalized stress that results by a purely elastic evolution over the step, given in terms of the quantity

$$\Delta \mathbf{S}^e_{n+1} = (\mathbb{C}(\boldsymbol{\varepsilon}_{n+1} - \boldsymbol{\varepsilon}_n), \mathbf{0}) = (\mathbb{C}(\boldsymbol{\varepsilon}(\mathbf{u}_{n+1} - \mathbf{u}_n)), \mathbf{0})$$

Theorem 3.3.3, with its assumptions, grants that the Scheme Dual has a unique solution.

At this stage it may be noted that once $\mathbf{S}^{TR}_{n+1}$ is known, the variational inequality (4.24) is equivalent to the minimization problem

$$\text{Find } T \text{ s.t. } J(\mathbf{T}) = \frac{1}{2} \parallel \mathbf{S}^{TR}_{n+1} - \mathbf{T} \parallel_A \rightarrow \inf, \quad \mathbf{T} \in \mathcal{P} \tag{4.26}$$

where $\| \cdot \|_A$ is the norm induced by the bilinear form $A(\cdot, \cdot)$. Likewise, the above problem is formally equivalent to the following projection problem

$$\mathbf{S}_{n+1} = \Pi_{\mathcal{P},A} \mathbf{S}^{TR}_{n+1} \tag{4.27}$$

where $\Pi_{\mathcal{P},A}$ denotes the projection operator onto $\mathcal{P}$, with respect to the inner product $(\cdot, \cdot)_A$. In both views, the updating of the solution is set forth imposing the yield surface consistency constraint to the trial solution, calculated by (4.25).

The algorithms for solving the problem expressed by (4.23)-(4.24) that are discussed in the following paragraph and that are implemented in the subsequent section are of the predictor-corrector type.

By the predictor-corrector concept, we are lead to an iterative solution procedure in which each iteration consists of a predictor trial step, followed by a corrector step which returns a consistent solution. In the predictor step, in fact, the quantity $\mathbf{u}_{n+1}$ is first updated using Equation (4.23). Then an updated trial generalized stress value $\mathbf{S}^{TR}_{n+1}$ is computed. The corrector step, then, consists in solving Equation (4.24) (or equivalently (4.26) or (4.27)) in order to get a new iteration for $\mathbf{S}_{n+1}$. In general, a variety of solution algorithms can be developed by using different schemes to update $\mathbf{u}_{n+1}$ in the predictor step. In what follows we consider the so-called elastic predictor and the so-called tangent predictor [41]. Within the context of a finite element space discretization of the problem, the second algorithm refers to the well known Newton's iterative linearization procedure.

In the literature (see for instance [69, 71]) an implementation of the corrector step is usually referred to as a *return map* algorithm. Using an updated value for $\mathbf{u}_{n+1}$ from the predictor step, the algorithm computes the corresponding updated strain increment $\Delta\boldsymbol{\varepsilon}_{n+1}$ and, through Equation (4.25), an updated trial state $\mathbf{S}^{TR}_{n+1}$ for the generalized stress, assuming that no plastic

deformation takes place during the step $[t_n, t_{n+1}]$. If the trial state $\mathbf{S}_{n+1}^{TR}$ belongs to $\mathcal{P}$, i.e. if the trial state is admissible, then the solution updating is $\mathbf{S}_{n+1} = \mathbf{S}_{n+1}^{TR}$ and the procedure steps forward to the solution of equations (4.23)-(4.24) for the next time increment. Otherwise, if the updated trial state lies outside the admissible region $\mathcal{P}$, the corrector *returns* the iteration to a point on $\mathcal{P}$ which results close to the trial state in some sense. The architecture of the corrector step is also clear from the version of the projection problem, expressed by (4.27).

4.4.1 Elastic predictor

We begin by returning to Equation (4.7). As already specified one may think to work with a finite element strategy for the space discretization of the problem and to address the time integration by means of one of the presented time integration schemes. Accordingly, we solve a sequence of (consistently) linearized problems associated to the variational problem (4.7). In this exposition we adopt a superscript i as the iteration counter in the algorithm. We begin by assuming the stress $\boldsymbol{\sigma}$ as a function implicitly depending on the displacement $\mathbf{u}$. Then, for the $(i+1)$th iteration of the stress, let us introduce the following (elastic) approximation into (4.7) in the place of $\boldsymbol{\sigma}$

$$\boldsymbol{\sigma}^{i+1} = \boldsymbol{\sigma}(\boldsymbol{\varepsilon}(\mathbf{u}^{i+1})) \approx \boldsymbol{\sigma}(\boldsymbol{\varepsilon}(\mathbf{u}^{i})) + \mathbb{D}\boldsymbol{\varepsilon}(\mathbf{u}^{i+1} - \mathbf{u}^{i})$$

Accordingly, the predictor step is referred to as an *elastic predictor* by virtue of the fact that the modulus $\mathbb{D}$ is assumed to be time-independent and to be related to the elastic tensor $\mathbb{C}$ in an assigned way. Later, sufficient conditions on the tensor $\mathbb{D}$ are given in order to grant the convergence of the predictor-corrector method.

The above iterative form is then introduced into Equation (4.7) which, starting from the previous known iteration $(\mathbf{u}_{n+1}^{i}, \mathbf{S}_{n+1}^{i})$, is to be solved in order to update the displacement value $\mathbf{u}_{n+1}$ once at convergence. We have

$$\int_\Omega \mathbb{D}\boldsymbol{\varepsilon}(\mathbf{u}_{n+1}^{i+1} - \mathbf{u}_{n+1}^{i}) : \boldsymbol{\varepsilon}(\mathbf{v}) dv = b(\mathbf{v}, \boldsymbol{\sigma}_{n+1}^{i}) - \langle \boldsymbol{\ell}_{n+1}, \mathbf{v} \rangle \quad \forall \mathbf{v} \in V$$

The above equation may be regarded as an approximation to (4.7) at time $t = t_{n+1}$, in which $\boldsymbol{\sigma}(t_{n+1})$ is replaced by a first-order approximation $\boldsymbol{\sigma}(\boldsymbol{\varepsilon}(\mathbf{u}_{n+1}^{i+1})) \approx \boldsymbol{\sigma}(\boldsymbol{\varepsilon}(\mathbf{u}_{n+1}^{i})) + \mathbb{D}\boldsymbol{\varepsilon}(\mathbf{u}_{n+1}^{i+1} - \mathbf{u}_{n+1}^{i})$. Thus, once $(\mathbf{u}_n, \mathbf{S}_n)$ is known, a predictor corrector algorithm for computing $(\mathbf{u}_{n+1}, \mathbf{S}_{n+1})$ is provided by the following procedure.

- Initialization: $\mathbf{u}_{n+1}^{0} = \mathbf{u}_n$, $\mathbf{S}_{n+1}^{0} = \mathbf{S}_n$

- Iteration: for $i = 1, 2, ..., i_{\max}$
  - Predictor: compute $\mathbf{u}_{n+1}^{i+1} \in V$ satisfying

$$\int_\Omega \mathbb{D}\boldsymbol{\varepsilon}(\mathbf{u}_{n+1}^{i+1} - \mathbf{u}_{n+1}^{i}) : \boldsymbol{\varepsilon}(\mathbf{v})dv = b(\mathbf{v}, \boldsymbol{\sigma}_{n+1}^{i}) - \langle \boldsymbol{\ell}_{n+1}, \mathbf{v} \rangle \quad \forall \mathbf{v} \in V \tag{4.28}$$

    and a trial state for the generalized stress

$$\mathbf{S}_{n+1}^{TR,i+1} = \mathbf{S}_n + \Delta\mathbf{S}_{n+1}^{e,i+1} \tag{4.29}$$

    with

$$\Delta\mathbf{S}_{n+1}^{e,i+1} = (\mathbb{C}\boldsymbol{\varepsilon}(\mathbf{u}_{n+1}^{i+1} - \mathbf{u}_n), \mathbf{0})$$

  - Corrector: find $\mathbf{S}_{n+1}^{i+1} \in \mathcal{P}$ such that

$$A(\mathbf{S}_{n+1}^{TR,i+1} - \mathbf{S}_{n+1}^{i+1}, \mathbf{T} - \mathbf{S}_{n+1}^{i+1}) \leq 0 \quad \forall \mathbf{T} \in \mathcal{P} \tag{4.30}$$

The above elastic predictor-plastic corrector scheme is very popular in computational plasticity and is granted to be convergent [41, 69], provided some suitable requirements on the modulus $\mathbb{D}$ are satisfied. Namely, as soon as $\mathbb{D}$ is symmetric, uniformly bounded, pointwise stable and such that the inverse $\mathbb{D}^{-1}$ exists and is uniformly dominated by $\mathbb{C}^{-1}$, then the above iteration procedure converges to the exact solution. This fact is formalized by the following result.

Theorem 4.4.1 *Assume that the modulus $\mathbb{D}$ is chosen in such a way that it is symmetric, uniformly bounded, pointwise stable in the sense that for some constant $c > 0$*

$$\mathbb{D}(\boldsymbol{x})\boldsymbol{\tau} : \boldsymbol{\tau} \geq c \parallel \boldsymbol{\tau} \parallel^2 \quad \forall \boldsymbol{\tau} \in \mathbf{L}in^{\mathrm{sym}}, \ \ a.e. \ \boldsymbol{x} \in \Omega \tag{4.31}$$

and such that its inverse $\mathbb{D}^{-1}$ is uniformly dominated by $\mathbb{C}^{-1}$ (or equivalently $\mathbb{C}$ is uniformly dominated by $\mathbb{D}$) in the sense that for some constant $\alpha > 0$

$$\boldsymbol{\tau} : (\mathbb{C}^{-1}(\boldsymbol{x}) - \mathbb{D}^{-1}(\boldsymbol{x}))\boldsymbol{\tau} \geq \alpha \parallel \boldsymbol{\tau} \parallel^2 \quad \forall \boldsymbol{\tau} \in \mathbf{L}in^{\mathrm{sym}}, \ \ a.e. \ \boldsymbol{x} \in \Omega \tag{4.32}$$

Then

$$\boldsymbol{S}^i \to \boldsymbol{S} \text{ as } i \to \infty$$

and for some subsequence $\{\boldsymbol{u}^{i_j}\}_j$ of $\{\boldsymbol{u}^i\}_i$ and some element $\tilde{\boldsymbol{u}} \in V$

$$\boldsymbol{u}^{i_j} \rightharpoonup \tilde{\boldsymbol{u}} \text{ as } j \to \infty$$

The limits $\tilde{\boldsymbol{u}} \in V$ and $\boldsymbol{S} \in P$ together solve the problem (4.23)-(4.24) [41].

4.4.2 Tangent predictor

Another common approach in the application of the predictor-corrector type algorithms is the one that uses a tangent predictor. This choice produces an iterative solver based on Newton's method. This predictor takes as a starting point a first-order Taylor expansion of $\boldsymbol{\sigma}$, in which the modulus $\mathbb{D}$ introduced in the preceding section is replaced by an appropriate tangent modulus. We give here simply a brief illustration on the main idea underneath this choice and on the steps involved in the computation of the tangent predictor. The derivations are reported according to [69].

The procedure basically resemble the one of the elastic predictor, except that for the approximation of the stress tensor. As usual, we refer to the $(i+1)$th iteration, assuming that the data $(\mathbf{u}^i_{n+1}, \mathbf{S}^i_{n+1})$ is known. Again, Equation (4.23) is used to update $\mathbf{u}_{n+1}$. By a Taylor's expansion we may write

$$\boldsymbol{\sigma}(\boldsymbol{\varepsilon}(\mathbf{u}^{i+1}_{n+1})) \approx \boldsymbol{\sigma}(\boldsymbol{\varepsilon}(\mathbf{u}^{i}_{n+1})) + \frac{\partial \boldsymbol{\sigma}}{\partial \boldsymbol{\varepsilon}}(\boldsymbol{\varepsilon}(\mathbf{u}^{i}_{n+1})) : \boldsymbol{\varepsilon}(\mathbf{u}^{i+1}_{n+1} - \mathbf{u}^{i}_{n+1})$$

This leads to the task of finding an approximate value for the fourth-order tangent tensor $\frac{\partial \boldsymbol{\sigma}}{\partial \boldsymbol{\varepsilon}}(\boldsymbol{\varepsilon}(\mathbf{u}^{i}_{n+1}))$ consistent with the adopted time integration scheme. We start with the constitutive relations

$$\begin{aligned} \boldsymbol{\sigma} &= \mathbb{C}(\boldsymbol{\varepsilon}(\mathbf{u}) - \mathbf{e}^p) \\ \boldsymbol{\chi} &= -\mathbb{H}\boldsymbol{\xi} \end{aligned}$$

and make the following positions:

$$\begin{aligned} \boldsymbol{\varepsilon}_{n+1} &= \boldsymbol{\varepsilon}(\mathbf{u}_{n+1}) \\ \mathbf{E}_{n+1} &= (\boldsymbol{\varepsilon}_{n+1}, \mathbf{0}) \\ \mathbf{P}_{n+1} &= \mathbf{P}(\mathbf{u}_{n+1}) \\ \mathbf{S}_{n+1} &= \mathbf{S}(\boldsymbol{\varepsilon}_{n+1}) \end{aligned}$$

Thus we have

$$\mathbf{S}_{n+1} = \mathbb{G}(\mathbf{E}_{n+1} - \mathbf{P}_{n+1}) \tag{4.33}$$

with $\mathbb{G}$ the diagonal matrix operator given by

$$[\mathbb{G}] = \begin{bmatrix} \mathbb{C} & \\ & \mathbb{H} \end{bmatrix}$$

Differentiating both sides in (4.33) gives

$$d\mathbf{S}_{n+1} = \mathbb{G}(d\mathbf{E}_{n+1} - d\mathbf{P}_{n+1}) \tag{4.34}$$

We need an (approximate) expression for $d\mathbf{P}_{n+1}$ in terms of $d\mathbf{E}_{n+1}$. This is accomplished by recalling the associative flow rule examined in Section 2.3

$$\dot{\mathbf{P}} = \dot{\gamma}\nabla\phi(\mathbf{S})$$

which in incremental form becomes

$$\dot{\mathbf{P}}_{n+1} = \dot{\gamma}_{n+1}\nabla\phi(\mathbf{S}_{n+1})$$

Hence, integrating the above relation over the time step, one finds

$$\mathbf{P}_{n+1} - \mathbf{P}_n \approx \lambda_{n+1}\nabla\phi(\mathbf{S}_{n+1})$$

where $\lambda_{n+1} = \Delta t\dot{\gamma}_{n+1} = \Delta\gamma_{n+1}$. In the following sections, the increment of the plastic multiplier λ_{n+1} over the step $[t_n, t_{n+1}]$ will be simply indicated by λ for brevity's reasons.

Being $\mathbf{P}_n$ given, differentiating the preceding expression yields

$$d\mathbf{P}_{n+1} \approx d(\lambda_{n+1})\nabla\phi(\mathbf{S}_{n+1}) + \lambda_{n+1}\nabla^2\phi(\mathbf{S}_{n+1})d\mathbf{S}_{n+1}$$

which, upon substitution into (4.34), gives

$$d\mathbf{S}_{n+1} \approx \mathbb{G}(d\mathbf{E}_{n+1} - d(\lambda_{n+1})\nabla\phi(\mathbf{S}_{n+1}) - \lambda_{n+1}\nabla^2\phi(\mathbf{S}_{n+1})d\mathbf{S}_{n+1})$$

In conclusion it is found

$$d\mathbf{S}_{n+1} \approx \mathcal{G}_{n+1}[d\mathbf{E}_{n+1} - d(\lambda_{n+1})\nabla\phi(\mathbf{S}_{n+1})] \tag{4.35}$$

where

$$\mathcal{G}_{n+1} = [\mathbb{G}^{-1} - \lambda_{n+1}\nabla^2\phi(\mathbf{S}_{n+1})]^{-1} \tag{4.36}$$

In this way the problem is reduced to one of finding an (approximate) expression for the differential of the plastic multiplier increment $d(\lambda_{n+1})$ in terms of $d\mathbf{E}_{n+1}$. This task is achieved by imposing the consistency condition at the end of the step $t = t_{n+1}$

$$d\phi(\mathbf{S}_{n+1}) = \nabla\phi(\mathbf{S}_{n+1}) \cdot d\mathbf{S}_{n+1} = 0 \tag{4.37}$$

Combining (4.35) and (4.37) it results

$$d(\lambda_{n+1}) \approx \frac{\nabla\phi(\mathbf{S}_{n+1}) \cdot \mathcal{G}_{n+1}d\mathbf{E}_{n+1}}{\nabla\phi(\mathbf{S}_{n+1}) \cdot \mathcal{G}_{n+1}\nabla\phi(\mathbf{S}_{n+1})} \tag{4.38}$$

The above relation together with Equation (4.35) provides the following formula

$$d\mathbf{E}_{n+1} \approx [\mathcal{G}_{n+1} - \mathbb{N}_{n+1} \otimes \mathbb{N}_{n+1}] d\mathbf{E}_{n+1} \tag{4.39}$$

where the matrix operator $\mathbb{N}_{n+1}$ is defined as

$$\mathbb{N}_{n+1} = \frac{\mathcal{G}_{n+1} \nabla \phi(\mathbf{S}_{n+1})}{\sqrt{\nabla \phi(\mathbf{S}_{n+1}) \cdot \mathcal{G}_{n+1} \nabla \phi(\mathbf{S}_{n+1})}} \tag{4.40}$$

The relation (4.39) thus provides the formula

$$d\boldsymbol{\sigma}_{n+1} \approx \mathbb{C}^{ep}_{n+1} d\boldsymbol{\varepsilon}_{n+1} \tag{4.41}$$

in which $\mathbb{C}^{ep}_{n+1}$ can be viewed as an approximation of $\dfrac{\partial \boldsymbol{\sigma}}{\partial \boldsymbol{\varepsilon}}(\boldsymbol{\varepsilon}(\mathbf{u}_{n+1}))$. The fourth-order elastoplastic consistent algorithmic tangent operator $\mathbb{C}^{ep}_{n+1}$ can readily be viewed as the discrete counterpart of the continuous operator $\mathbb{C}^{ep}$ defined in Chapter 2 by Equation (2.134) for the case of J_2 plasticity with combined linear isotropic/kinematic and nonlinear kinematic hardening.

As pointed out in [71, 72] the use of a consistent tangent operator preserves the quadratic rate of convergence of the Newton's method adopted in the incremental solution of the finite element scheme. Moreover, as noted by [72] imposing consistency at the endpoint of each time steps, in relation to the previously studied backward Euler's method, produces a symmetric operator, while the same does not hold true for the midpoint family algorithms. The symmetry can anyway be obtained by enforcing consistency at the midpoint instant $t_{n+\alpha}$ [63].

The tangent predictor step is constructed as follows. Once an iteration $(\mathbf{u}^i_{n+1}, \mathbf{S}^i_{n+1})$ is known, the algorithm computes $\mathcal{G}^i_{n+1}$ from (4.36), with $\mathbf{S}_{n+1}$ there being replaced by $\mathbf{S}^i_{n+1}$. Then, the generalized matrix operator $\mathbb{N}^i_{n+1}$ is computed from its definition (4.40), again with $\mathbf{S}^i_{n+1}$ in the place of $\mathbf{S}_{n+1}$. Now, exploiting the relation between $d\mathbf{S}^i_{n+1}$ and $d\mathbf{E}^i_{n+1}$, given by (4.39), the algorithmic tangent modulus $\mathbb{C}^i_{n+1}$ can be calculated following (4.41). After the preceding predictor step is completed, the corrector (4.30) is applied to update $\mathbf{S}_{n+1}$. The unknown scalar λ_{n+1} appearing in (4.36) is computed imposing the consistency condition on the generalized stress at the end of the step.

From a theoretical standpoint it is not clear how to prove convergence for the tangent predictor constructed above [41]. However, in practice, it is known that the tangent predictor performs far more efficiently than the elastic predictor, particularly if a line search algorithm is implemented [69, 70, 79].

Closest point projection

It is observed that the key point of the corrector step in the predictor-corrector algorithms presented above is the solution of a variational inequality of the form (omitting all subscripts and superscripts for simplicity)

$$\mathbf{S} \in \mathcal{P} \quad A(\mathbf{S}^{TR} - \mathbf{S}, \mathbf{T} - \mathbf{S}) \leq 0 \quad \forall \mathbf{T} \in \mathcal{P} \tag{4.42}$$

Formally, this is an elliptic variational inequality of the first kind. Equivalently, the solution $\mathbf{S}$ can be shown to be the closest-point projection of the trial generalized stress $\mathbf{S}^{TR}$ (cf. (4.25)) onto the admissible convex set $\mathcal{P}$ [69]. This is a standard problem in convex programming that can be formulated as follows

Problem. Let $\mathcal{P}$ be a nonempty, closed, convex subset of a Hilbert space $\mathcal{T}$ and $\mathbb{G}^{-1}$ a symmetric, positive definite metric on $\mathcal{T}$. Given $\mathbf{S}^{TR} \in \mathcal{T}$, solve the problem

$$\min \left\{ \frac{1}{2}(\mathbf{S}^{TR} - \mathbf{S}) \cdot \mathbb{G}^{-1}(\mathbf{S}^{TR} - \mathbf{S}) \cdot \mathbf{S} \in \mathcal{P} \right\} \tag{4.43}$$

A possible solution algorithm for solving the constrained minimization problem (4.43) is presented in [69] and first needs the following equivalence result

Theorem 4.4.2 *$\boldsymbol{S} \in \mathcal{P}$ is the solution of the problem (4.43) if and only if there exists a scalar λ such that*

$$\begin{gathered} \boldsymbol{S} = \boldsymbol{S}^{TR} - \lambda \mathbb{G} \nabla \phi(\boldsymbol{S}) \\ \phi(\boldsymbol{S}) \leq 0, \;\; \lambda \geq 0, \;\; \lambda \phi(\boldsymbol{S}) = 0 \end{gathered} \tag{4.44}$$

The proof of the above assertion is straightforward. Let $\mathbf{S} \in \mathcal{P}$ be the solution of problem (4.43). The Lagrangian associated with the constrained minimization problem is

$$\mathcal{L}(\mathbf{S}, \lambda) = \frac{1}{2}(\mathbf{S}^{TR} - \mathbf{S}) \cdot \mathbb{G}^{-1}(\mathbf{S}^{TR} - \mathbf{S}) \cdot \mathbf{S} + \lambda \phi(\mathbf{S})$$

By the Kuhn-Tucker optimality condition, we get (4.44). On the other hand, assume that (4.44) is satisfied for some $\mathbf{S} \in \mathcal{P}$ and some scalar λ. Then, by the so-called second-order sufficiency condition [41, 58], $\mathbf{S} \in \mathcal{P}$ is the solution of the constrained minimization problem.

An application of Newton's iterative method to solve the system (4.44) results in a solution algorithm. This algorithm performs well on some numerical examples [69, 79], but from a theoretical point of view is not guaranteed to

have a consistent solution $\lambda \geq 0$. Also the convergence issue is still an open problem.

In some selected cases, nevertheless, the above algorithm results in the simple solution of a linear equation and thus the problem simplifies significantly. This case is addressed in detail in the following chapter when the case of J_2 plasticity with linear isotropic and kinematic hardening is approached adopting the backward Euler's integration scheme.

A return map algorithm for the one-dimensional elastoplastic model

In what follows we give a brief description of the classical return map algorithm [70], based on the backward Euler's rule for the integration of the one-dimensional contitutive model presented in Section 2.2. The one-dimensional constitutive model, recalled here for convenience, is governed by the following relations

$$\sigma = E\left(\varepsilon - \varepsilon^p\right) \tag{4.45}$$

$$\Sigma = \sigma - \alpha \tag{4.46}$$

$$\dot{\varepsilon}^p = \dot{\gamma}\,\mathrm{sign}\left(\Sigma\right) \tag{4.47}$$

$$\phi = |\Sigma| - \sigma_y \tag{4.48}$$

$$\dot{\bar{e}}^p = \dot{\gamma} \tag{4.49}$$

$$\sigma_y = \sigma_{y,0} + H_{iso}\bar{e}^p \tag{4.50}$$

$$\dot{\alpha} = \dot{\gamma} H_{kin}\,\mathrm{sign}\left(\Sigma\right) \tag{4.51}$$

$$\dot{\gamma} \geq 0\,, \quad F \leq 0\,, \quad \dot{\gamma}F = 0 \tag{4.52}$$

The aim of this paragraph is to provide an example of the specialization of the general algorithm enlightened previously to the simple one-dimensional case at hand. In the next chapter, the issue addressed by the following lines is generalized to the three-dimensional case and further investigated with particular emphasis on the exponential-based integration algorithms family which is the object of this thesis.

The problem to be solved in this context is purely local. We admit there exists a space discretization of the one-dimensional IBVP, carried out, for instance, with the finite element method. Let us then consider a material point $x \in \Omega$, the one-dimensional domain of interest. Assume that the local state at point x, represented by the set

$$\{\sigma_n(x), \varepsilon_n(x), \varepsilon_n^p(x), \bar{e}^p(x), \alpha(x)\} \tag{4.53}$$

is known at the time instant t_n. The stress is given by

$$\sigma_n(x) = E\left[\varepsilon_n(x) - \varepsilon_n^p(x)\right] \tag{4.54}$$

The problem we are dealing with may be stated as follows: given a strain increment $\Delta\varepsilon_{n+1} = \varepsilon_{n+1} - \varepsilon_n$ at x, which *drives* the local state to time t_{n+1}, update the state variables (4.53) to time t_{n+1}, in a manner consistent with the constitutive laws (4.45)-(4.52).

Note that the framework of the incremental integration problem over the time interval $[t_n, t_{n+1}]$ of the constitutive equations is purely local. Moreover, as already outlined in Section 4.4 with respect to the numerical solution of the IBVP of elastoplastic equilibrium, the process is regarded as *strain-driven* with the strain $\varepsilon = \partial u/\partial x$ playing the role of the independent variable.

We start by considering the incremental form of the flow rule (4.47) for the one-dimensional model. Using a backward's Euler integration rule, we obtain

$$\begin{aligned} \varepsilon^p_{n+1} &= \varepsilon^p_n + \lambda\,\mathrm{sign}(\Sigma_{n+1}) \\ \bar{e}^p_{n+1} &= \bar{e}^p_n + \lambda \end{aligned} \tag{4.55}$$

where the scalar λ is the plastic multiplier increment over the step and

$$\begin{aligned} \sigma_{n+1} &= E\left(\varepsilon_{n+1} - \varepsilon^p_{n+1}\right) \\ \varepsilon_{n+1} &= \varepsilon_n + \Delta\varepsilon_{n+1} \end{aligned} \tag{4.56}$$

The discrete couterpart of the Kuhn-Tucker optimality conditions are

$$\begin{aligned} \phi_{n+1} &= |\Sigma_{n+1}| - \left(\sigma_{y,n} + H_{iso}\bar{e}^p_{n+1}\right) \\ \lambda &\geq 0 \\ \lambda\phi_{n+1} &= 0 \end{aligned} \tag{4.57}$$

Note that integrating the contitutive model with the backward Euler's rule, we have transformed the initial constrained problem of evolution into a discrete constrained algebraic problem for the variables $\left\{\sigma_{n+1}, \varepsilon_{n+1}, \varepsilon^p_{n+1}, \bar{e}^p_{n+1}, \alpha_{n+1}\right\}$. As already pointed out, this problem may also be stated in the form of a discrete constrained optimization problem. We also observe that Equation (4.56), being $\Delta\varepsilon_{n+1}$ given, represents simply the definition for ε_{n+1}.

The integration algorithm starts by considering a *trial elastic state*, obtained by freezing plastic flow over the integration interval $[t_n, t_{n+1}]$. Thus we have

$$\begin{aligned} \sigma^{TR}_{n+1} &= E\left[\varepsilon_{n+1} - \varepsilon^p_n\right] = \sigma_n + E\Delta\varepsilon_{n+1} \\ \Sigma^{TR}_{n+1} &= \sigma^{TR}_{n+1} - \alpha_n \\ \varepsilon^{p,TR}_{n+1} &= \varepsilon^p_n \\ \bar{e}^{p,TR}_{n+1} &= \bar{e}^p_n \\ \alpha^{TR}_{n+1} &= \alpha_n \\ \phi^{TR}_{n+1} &= \left|\Sigma^{TR}_{n+1}\right| - \left(\sigma_{y,n} + H_{iso}\bar{e}^p_n\right) \end{aligned} \tag{4.58}$$

along with the algorithmic counterpart of the Kuhn-Tucker conditions

$$\phi_{n+1}^{TR} \begin{cases} \leq 0 & \text{elastic step} \quad \lambda = 0 \\ > 0 & \text{plastic step} \quad \lambda > 0 \end{cases} \tag{4.59}$$

If the step is elastic as in (4.59), then the trial state is taken as the actual state. Otherwise, if the step is plastic in the sense of (4.59), a correction to the trial state is introduced as follows by means of a return map algorithm.

Recalling Equation (4.54) and expressing the final stress σ_{n+1} in terms of σ_{n+1}^{TR} and λ we obtain

$$\begin{aligned} \sigma_{n+1} &= E\left(\varepsilon_{n+1} - \varepsilon_{n+1}^{p}\right) \\ &= E\left(\varepsilon_{n+1} - \varepsilon_{n}^{p}\right) - E\left(\varepsilon_{n+1}^{p} - \varepsilon_{n}^{p}\right) \\ &= \sigma_{n+1}^{TR} - E\lambda \operatorname{sign}\left(\sigma_{n+1}\right) \end{aligned} \tag{4.60}$$

Therefore, since $\lambda > 0$, Equations (4.55)-(4.57) are written, in view of (4.60) as

$$\begin{aligned} \sigma_{n+1} &= \sigma_{n+1}^{TR} - \lambda E \operatorname{sign}(\Sigma_{n+1}) \\ \varepsilon_{n+1}^{p} &= \varepsilon_{n+1}^{p,TR} + \lambda \operatorname{sign}(\Sigma_{n+1}) \\ \bar{e}_{n+1}^{p} &= \bar{e}_{n+1}^{p,TR} + \lambda \\ \alpha_{n+1} &= \alpha_{n+1}^{TR} + \lambda H_{kin} \operatorname{sign}(\Sigma_{n+1}) \\ \phi_{n+1} &= |\Sigma_{n+1}| - \left(\sigma_{y,n} + H_{iso}\bar{e}_{n+1}^{p}\right) = 0 \end{aligned} \tag{4.61}$$

where

$$\Sigma_{n+1} = \sigma_{n+1} - \alpha_{n+1} \tag{4.62}$$

Crucial to the above update is the computation of an expression for α_{n+1}, which can be obtained as follows. Subtract $(4.61)_4$ from $(4.61)_1$ and apply (4.62). One finds

$$\Sigma_{n+1} = \left(\sigma_{n+1}^{TR} - \alpha_n\right) - \lambda\left(H_{iso} + H_{kin}\right) \operatorname{sign}\left(\Sigma_{n+1}\right) \tag{4.63}$$

Exploiting the fact that $\Sigma_{n+1}^{TR} = \sigma_{n+1}^{TR} - \alpha_n$ and rearranging terms in (4.63), we have

$$\left[|\Sigma_{n+1}| + \lambda\left(H_{iso} + H_{kin}\right)\right] \operatorname{sign}\left(\Sigma_{n+1}\right) = \left|\sigma_{n+1}^{TR}\right| \operatorname{sign}\left(\Sigma_{n+1}^{TR}\right) \tag{4.64}$$

Being both λ and the sum $(H_{iso} + H_{kin})$ positive, it necessarily holds

$$\operatorname{sign}\left(\Sigma_{n+1}\right) = \operatorname{sign}\left(\Sigma_{n+1}^{TR}\right) \tag{4.65}$$

which implies

$$|\Sigma_{n+1}| + \lambda \left(H_{iso} + H_{kin}\right) = \left|\Sigma_{n+1}^{TR}\right| \tag{4.66}$$

The incremental plastic consistency parameter $\lambda > 0$ is determined from the discrete limit $(4.61)_5$ introducing in it Equations (4.66) and $(4.61)_3$:

$$\begin{aligned} \phi_{n+1} &= \left|\Sigma_{n+1}^{TR}\right| - \left(E + H_{kin}\right)\lambda - \left(\sigma_{y,n} + H_{iso}\bar{e}_{n+1}^{p}\right) \\ &= \left|\Sigma_{n+1}^{TR}\right| - \left(E + H_{kin}\right)\lambda - \left(\sigma_{y,n} + H_{iso}\bar{e}_{n}^{p}\right) - H_{iso}\left(\bar{e}_{n+1}^{p} - \bar{e}_{n}^{p}\right) \end{aligned} \tag{4.67}$$

The above equation is solved for λ in closed form and gives

$$\lambda = \frac{\phi_{n+1}^{TR}}{E + H_{iso} + H_{kin}} > 0 \tag{4.68}$$

The incremental plastic rate parameter given by Equation (4.68), together with (4.65) completes the plastic correction (4.61). As it is pointed out in the next chapter, where a wide set of integration algorithms for J_2 elastoplastic models are examined, the possibility of determining the plastic consistency parameter in closed form is not always granted a priori. In such cases particular solution strategies need to be actuated in order to compute the plastic rate parameter λ.

4.4.3 Finite element solution of the IBVP of elastoplastic equilibrium

In the preceding paragraph we have presented an integration algorithm for the one-dimensional elastoplastic constitutive model analyzed in Section 2.2, based on the backward Euler's rule. Before passing to the next chapter in which the generalization of the above case is made to three-dimensional J_2 plasticity, we find it convenient to present the sketch of the iterative solution of a general three-dimensional initial boundary value problem of elastoplastic equilibrium, within the context of a finite element strategy. The aim of the following lines is to introduce the general finite element strategy that is used by common finite element codes to solve elastoplastic equilibrium initial boundary value problems. The steps described here are the same followed by the FEAP code [73] used in the numerical tests Chapter 6 for the solution of our test problems. We briefly present here the procedure performed by the iterative solver for a general three-dimensional problem, while the next paragraph is devoted to the the one-dimensional case using the return map algorithm discussed above. Following [70] such a procedure is composed of the following steps:

i. Time discretization

(a) The reference time interval $[0, T]$ is discretized into a partition of N time subintervals, according to $[0, T] = \bigcup_{n=0}^{N-1}[t_n, t_{n+1}]$. The general interval $[t_n, t_{n+1}]$ has amplitude $\Delta t = t_{n+1} - t_n$. The relevant problem is reported to a typical time interval.

(b) The time derivatives arising in the weak form of the initial boundary value problem are approximated by suitable integration schemes, for instance, as the ones presented in Section 4.3. This step leads to the formulation of a global time integration algorithm and, to a large extent, is independent of the specific constitutive model.

(c) Attention is now restricted to a particular point $\mathbf{x} \in \Omega$ predetermined by the spatial discretization discussed below (in fact, a quadrature point of a typical finite element). The goal is to compute an approximation of the stress appearing in the weak form.

(d) At the point $\mathbf{x} \in \Omega$ of interest at time t_n, the (incremental) displacement (leading to t_{n+1}), denoted by $\Delta\mathbf{u}_{n+1}(\mathbf{x}) = \mathbf{u}_{n+1}(\mathbf{x}) - \mathbf{u}_n(\mathbf{x})$, is regarded as given.

(e) At time t_n, the state at $\mathbf{x} \in \Omega$ characterized by $\{\boldsymbol{\sigma}_n(\mathbf{x}), \boldsymbol{\varepsilon}_n(\mathbf{x}), \mathbf{e}^p_n(\mathbf{x}), \bar{e}^p_n(\mathbf{x}), \boldsymbol{\alpha}_n(\mathbf{x})\}$ is given and is assumed to be equilibrated, i.e. it satisfies Equation (4.12) evaluated at t_n.

(f) The problem at this stage is to update the state variables at $\mathbf{x} \in \Omega$ to the values $\left\{\boldsymbol{\sigma}_{n+1}(\mathbf{x}), \boldsymbol{\varepsilon}_{n+1}(\mathbf{x}), \mathbf{e}^p_{n+1}(\mathbf{x}), \bar{e}^p_{n+1}(\mathbf{x}), \boldsymbol{\alpha}_{n+1}(\mathbf{x})\right\}$ in a manner consistent with the constitutive equations examined in Section 2.2 for the von-Mises elastoplastic model.

ii. Space discretization

(a) The domain Ω is discretized as $\bar{\Omega} = \bigcup_{e=1}^{N_{el}} \Omega_e$ in order to arrive at the discrete counterpart of the weak form of the equilibrium equations (see Section 4.1).

(b) Attention is focused on a typical finite finite element Ω_e. For a given stress field $\boldsymbol{\sigma}_{n+1}(\mathbf{x})$ at predetermined points, one evaluates the weak form (4.12) restricted to Ω_e.

(c) Assemble the contributions of all elements and determine wether the system is equilibrated under the state $\{\mathbf{u}_{n+1}(\mathbf{x}), \boldsymbol{\sigma}_{n+1}(\mathbf{x})\}$.

(d) Determine a correction to the displacement field and return to step **i.** to evaluate the associated state $\{\boldsymbol{\sigma}_{n+1}(\mathbf{x}), \boldsymbol{\varepsilon}_{n+1}(\mathbf{x}), \mathbf{e}^p_{n+1}(\mathbf{x}), \bar{e}^p_{n+1}(\mathbf{x}), \boldsymbol{\alpha}_{n+1}(\mathbf{x})\}$

Finite element solution of a one-dimensional IBVP of elastoplastic equilibrium

To illustrate the above solution procedure and the use of the return map integration algorithm (4.58)-(4.61), we outline a typical numerical solution scheme for a one-dimensional elastoplastic equilibrium IBVP in the context of the finite element method. We aim at specializing the dual variational form of the problem presented in Section 2.4 for a one-dimensional material body.

The object of study is a one-dimensional body $\mathfrak{B}$, identified with the closed interval $\Omega \equiv \bar{\Omega} = [0, L]$, with material points labeled by their position $x \in \bar{\Omega}$. The boundary of $\bar{\Omega}$, denoted with Γ, is given by the interval extrema $\Gamma = \{0, L\}$. The interior of the domain is given by the open interval $\Omega =]0, L[$. Suppose that, for $t \in [0, T]$, a body force $b(x, t)$ is assigned in Ω, a displacement field $\bar{u}$ is assigned on $\Gamma_D = \{0\}$ as well as a traction $\bar{\sigma}$ is assigned on $\Gamma_S = \{L\}$.

For simplicity, it is assumed that the displacement boundary condition is homogeneous:

$$u|_{\Gamma_D} = \bar{u} = 0 \tag{4.69}$$

The loading is given in terms of body force

$$b : \Omega \times [0, T] \to \mathcal{R} \tag{4.70}$$

and traction

$$\bar{\sigma} : \Gamma_S \times [0, T] \to \mathcal{R} \tag{4.71}$$

The formulations of the problem (see Equations (2.139)-(2.142)) specializes to the present case as follows: find the displacement field $u(x, t)$ which, for any $x \in \Omega$ and any $t \in [0, T]$, solves the

- *equation of equilibrium*

$$\frac{\partial \sigma}{\partial x} + \rho b = 0 \tag{4.72}$$

- *strain-displacement relation*

$$\varepsilon(u) = \frac{\partial u}{\partial x} \tag{4.73}$$

- *constitutive relation* represented by relations (4.45)-(4.52) together with the rate form of the stress-strain relationship (2.25)

and satisfies the

- *boundary conditions*

$$u = \bar{u} \quad \text{on} \quad \Gamma_D \quad \text{and} \quad \sigma = \bar{\sigma} \quad \text{on} \quad \Gamma_S \tag{4.74}$$

- *initial conditions*

$$u(x, 0) = u_0(x) \tag{4.75}$$

Thus, in the spirit of the dual weak formulation of the elastoplastic problem of equilibrium we may set the following function spaces. The displacement solution space is defined as

$$V = \left\{ u : u \in H^1(\Omega),\, u|_{\Gamma_D} = \bar{u} \right\} \tag{4.76}$$

Then we have the following problem statement: find the displacement field $u(x, t) \subset V$ such that:

- the equilibrium equation holds:

$$G(\sigma, v) = 0 \quad \forall v \in V, \forall t \in [0, T] \tag{4.77}$$

- the constitutive equations (4.45)-(4.52) hold

where

$$G(\sigma, v) = \int_\Omega \sigma v' dx - \int_\Omega \rho b v dx - \bar{\sigma} v|_{\Gamma_S} \tag{4.78}$$

$$v' = \frac{\partial v}{\partial x} \tag{4.79}$$

With the above hypotheses, the problem solution concerns the numerical approximation of the displacement $u(x, t)$ appearing in (4.77) with $\sigma(x, t)$ satisfying the local elastoplastic constitutive equations.

In what follows we present a classical algorithmic scheme, for the solution of the exposed one-dimensional IBVP [48, 70].

Spatial discretization via finite element method

i. The domain $\Omega = [0, L]$ is discretized into a sequence of nonoverlapping elements

$$\Omega_e = [x_e, x_{e+1}] \tag{4.80}$$

such that

$$\Omega = \bigcup_{e=1}^{N_{el}} \Omega_e \tag{4.81}$$

where $x_1 = 0$ and $x_{N_{el}+1} = L$. We set $h_e = x_{e+1} - x_e$ the "mesh size", which for simplicity is assumed uniform.

ii. The simplest (conforming) finite-dimensional approximation to V, denoted as usual by V^h, is then constructed as follows. The restriction v_e^h to a typical element Ω_e of a test function $v^h \in V^h$ is locally interpolated linearly as

$$v_e^h = \sum_{a=1}^{2} N_e^a(x) v_e^a \tag{4.82}$$

where $N_e^a(x) : \Omega_e \to \mathcal{R}$, $a = 1, 2$ are the linear shape functions defined as

$$\begin{aligned} N_e^1 &= \frac{x_{e+1} - x}{h_e} \\ N_e^2 &= \frac{x - x_e}{h_e} \end{aligned} \tag{4.83}$$

With $\{\mathbf{v}_e\} = \left\{v_e^1, v_e^2\right\}^T$ and $\{\mathbf{N}_e\} = \left\{N_e^1, N_e^2\right\}^T$ we indicate, respectively, the vector containing the nodal values of the local element test functions and the element shape functions[1]. Then, a global, piecewise, continuous function $v^h \in V^h$ is obtained from the above element interpolation by matching the value of $\mathbf{v}_e$ at the nodes:

$$\begin{aligned} v_e &= v_e^1 = v_{e-1}^2 \\ v_{e+1} &= v_e^2 = v_{e+1}^1 \end{aligned} \tag{4.84}$$

[1]In this paragraph we admit a slight abuse of notation and indicate algebraic vectors as for instance $\{\mathbf{v}_e\}$, $\{\mathbf{N}_e\}$ and $\{\mathbf{B}_e\}$ with the engineering notation. This permits to mantain the treatment more compact.

iii. The computation of $G(\sigma^h, v^h)$, given by (4.77) with $v^h \in V^h$ (and u^h also in V^h since, by assumption $\bar{u} = 0$) is performed in an element-by-element fashion by setting, in view of (4.81)

$$G\left(\sigma^h, v^h\right) = \sum_{e=1}^{N_{el}} G_e\left(\sigma^h, v^h\right) \tag{4.85}$$

For a general element Ω_e it is first computed

$$\frac{\partial}{\partial x} v_e^h = \mathbf{B}_e \mathbf{v}_e \tag{4.86}$$

where, in the present case, from (4.83), it results

$$\{\mathbf{B}_e\} = \left\{\frac{\partial}{\partial x} N_e^1\ ,\ \frac{\partial}{\partial x} N_e^2\right\} = \left\{-\frac{1}{h_e},\ \frac{1}{h_e}\right\} \tag{4.87}$$

Therefore, recalling (4.77), it is found

$$G_e\left(\sigma^h, v^h\right) = \mathbf{v}_e^T\left[\mathbf{f}_e^{int}(\sigma^h) - \mathbf{f}_e^{ext}(t)\right] \tag{4.88}$$

where

$$\mathbf{f}_e^{int}\left(\sigma^h\right) = \int_{\Omega_e} \mathbf{B}_e^T\, \sigma^h(x,t) dx \tag{4.89}$$

is the *element internal force vector*. Note that $\mathbf{f}_e^{int}$ is implicitly a function of u^h along with $\varepsilon^p, \bar{e}^p$ and α through the constitutive equations. Moreover,

$$\mathbf{f}_e^{ext}\left(\sigma^h\right) = \int_{\Omega_e} \left[\mathbf{N}_e\, \rho b(x,t)\right] dx + \left[\bar{\sigma}(t)\, \mathbf{N}_e\right]\big|_{\Gamma_S \cap \Gamma_e} \tag{4.90}$$

is referred to as the *element external load vector*.

Using Equations (4.69) and (4.84), the expression (4.85) is assembled from the element contributions given by (4.89) and (4.90) as follows

$$G^h\left(\sigma^h, v^h\right) = \mathbf{v}^T\left[\mathbf{F}^{int}(\sigma^h) - \mathbf{F}^{ext}(t)\right] \tag{4.91}$$

where $\{\mathbf{v}\} = \left\{v^2, v^3, ..., v^{N_{el}+1}\right\}^T \in \mathcal{R}^{N_{el}}$. The global force vectors are computed from the element contributions as

$$\begin{aligned} \mathbf{F}^{int}(\sigma^h) &= \mathop{\mathbb{A}}_{e=1}^{N_{el}} \mathbf{f}_e^{int}(\sigma^h) \\ \mathbf{F}^{ext}(t) &= \mathop{\mathbb{A}}_{e=1}^{N_{el}} \mathbf{f}_e^{ext}(t) \end{aligned} \tag{4.92}$$

where $\underset{e=1}{\overset{N_{el}}{\mathbb{A}}}$ is the standard finite element assembly operator [48].

Thus, the finite element counterpart of the weak form (4.77) of the equilibrium equation takes the form

$$G\left(\sigma^h, v^h\right) = 0 \quad \forall v^h \in V^h \tag{4.93}$$

Since the test function v^h is arbitrary, it follows that $\mathbf{v} \in \mathcal{R}^{N_{el}}$ is also arbitrary and from (4.91) one arrives at the discrete system of (nonlinear) equations:

$$\mathbf{F}^{int}(\sigma^h) - \mathbf{F}^{ext}(t) = \mathbf{0} \tag{4.94}$$

The crucial step in the outline given above which remains to be addressed concerns the computation of the stress field $\sigma^h(x,t)$ within a typical element at time $t \in [0,T]$.

An important observation concerning *numerical quadrature* in the context of the finite element method is now in order. It is remarked that in general the expression for the element internal force vector is computed according to a formula of the following kind

$$\mathbf{f}_e^{int}(\sigma^h) = \sum_{\ell=1}^{n_{int}} \mathbf{B}_e^T \, \sigma^h(x,t)\Big|_{x=x_e^\ell} \omega^\ell h_e \tag{4.95}$$

where x_e^ℓ indicates a quadrature point in Ω_e, ω^ℓ represenets the corresponding weight and n_{int} is the number of quadrature points on Ω_e. It is noted that from (4.95), in general, in a finite element formulation, the stress is to be computed at a finite number of points over each element, typically the quadrature points of the element Ω_e.

Incremental solution procedure

Consider the usual partition of the time interval of interest

$$[0,T] = \bigcup_{n=1}^{N} [t_n, t_{n+1}] \tag{4.96}$$

Let $x_e^\ell \in \Omega_e$ be a quadrature point of a typical finite element and let $\{\varepsilon_n, \varepsilon_n^p, \bar{e}_n^p, \alpha_n\}$ be the internal variables at x_e^ℓ. Under the body force $b_n = b(t_n)$ and

the traction $\bar{\sigma}_n = \bar{\sigma}(t_n)$, the body is assumed to be equilibrated. Therefore, at $t = t_n$, the approximate stress field σ_n^h satisfies

$$\mathbf{F}^{int}(\sigma_n^h) - \mathbf{F}_n^{ext} = \mathbf{0} \tag{4.97}$$

The associated displacement field at t_n is $u_n^h \in V^h$. The load at t_{n+1} is given by

$$\begin{aligned} b_{n+1} &= b_n + \Delta b_{n+1} \\ \bar{\sigma}_{n+1} &= \bar{\sigma}_n + \Delta \bar{\sigma}_{n+1} \end{aligned} \tag{4.98}$$

with $\{\Delta b_{n+1}, \Delta \bar{\sigma}_{n+1}\}$ incremental loads, which define a discrete external force vector $\mathbf{F}_{n+1}^{ext}$. This is the known data.

The discrete equilibrium problem can be stated as follows: find the displacement field increment $\Delta u_{n+1}^h \subset V^h$, such that $u_{n+1}^h = u_n^h + \Delta u_{n+1}^h$, the updated internal variables $\left\{\varepsilon_{n+1}, \varepsilon_{n+1}^p, \bar{e}_{n+1}^p, \alpha_{n+1}\right\}$ and the stress field σ_{n+1}^h (at quadrature points x_e^ℓ) such that:

- $$\mathbf{F}^{int}(\sigma_{n+1}^h) - \mathbf{F}_{n+1}^{ext} = \mathbf{0} \tag{4.99}$$

- the discrete constitutive equations (4.58)-(4.61) hold

Iterative solution procedure

The solution of the above problem is carried out by an iterative solution procedure. In order to simplify the notation in the following we omit the superscript "h". We also fix the convention that $(\cdot)_{n+1}^i$ represents the value of a history variable $(\cdot)$ at the ith iteration during the time step $[t_n, t_{n+1}]$. The sketch of the algorithm is as follows:

i. Let $\Delta \mathbf{d}_{n+1}^i$ be the incremental nodal displacement vector at the ith iteration such that

$$\mathbf{d}_{n+1}^i = \mathbf{d}_n + \Delta \mathbf{d}_{n+1}^i \tag{4.100}$$

is the ith iteration nodal displacement vector. Following respectively (4.82) and (4.86) it is possible to calculate the displacement and strain fields over each element as

$$\varepsilon_{n+1}^i|_{\Omega_e} = \mathbf{B}_e \mathbf{d}_e|_{n+1}^i \tag{4.101}$$

ii. Given the strain field (4.101), the stress σ^i_{n+1} is computed (at each quadrature point over each element) using the algorithm (4.58)-(4.61).

iii. The element internal force vector $\mathbf{f}^{int}_e(\sigma^h_{n+1})$ (corresponding to the ith iteration) is evaluated according to (4.95) for each element and assembled applying (4.92).

iv. The convergence check is performed. If Equation (4.94) is satisfied for $\sigma = \sigma^i_{n+1}$ then $(\cdot)^i_{n+1}$ is the solution, otherwise go to the next step

v. Determine $\Delta\mathbf{d}^i_{n+1}$, set $i \leftarrow i+1$ and go to step **i**.

In the above sequence the calculation of the term $\Delta\mathbf{d}^i_{n+1}$ is addressed in the same fashion highlighted in Section 4.4.2, i.e. with a tangent predictor. Thus, determinating $\Delta\mathbf{d}^i_{n+1}$ involves the linearization of the term $\mathbf{f}^{int}(\sigma^i_{n+1})$ about the current configuration, represented by the vector $\mathbf{d}^i_{n+1}$. Inspecting Equation (4.92), by the linearity of the assembly operator, we may write

$$\begin{aligned}
\frac{\partial \mathbf{F}^{int}(\sigma^i_{n+1})}{\partial \mathbf{d}^i_{n+1}}\Delta\mathbf{d}^{i+1}_{n+1} &= \mathop{\mathbb{A}}_{e=1}^{N_{el}} \frac{\partial \mathbf{f}^{int}_e(\sigma^i_{n+1})}{\partial \mathbf{d}_e|^i_{n+1}}\Delta\mathbf{d}_e|^{i+1}_{n+1} \\
&= \mathop{\mathbb{A}}_{e=1}^{N_{el}} \int_{\Omega_e} \mathbf{B}^T_e \left[\frac{\partial \sigma^i_{n+1}}{\partial \varepsilon^i_{n+1}}\right] \frac{\partial \varepsilon^i_{n+1}}{\partial \mathbf{d}_e|^i_{n+1}}\Delta\mathbf{d}_e|^{i+1}_{n+1} dx \\
&= \mathop{\mathbb{A}}_{e=1}^{N_{el}} \left[\int_{\Omega_e} \mathbf{B}^T_e \left[\frac{\partial \sigma^i_{n+1}}{\partial \varepsilon^i_{n+1}}\right] \mathbf{B}_e \, dx\right] \Delta\mathbf{d}_e|^{i+1}_{n+1}
\end{aligned} \tag{4.102}$$

Defining the 2×2 *element stiffness matrix* $\mathbf{k}_e|^i_{n+1}$ as

$$\mathbf{k}_e|^i_{n+1} = \int_{\Omega_e} \mathbf{B}^T_e \left[\frac{\partial \sigma^i_{n+1}}{\partial \varepsilon^i_{n+1}}\right] \mathbf{B}_e \, dx \tag{4.103}$$

and assembling all the element contributions according to (4.102), we are left with an expression of the form

$$\frac{\partial \mathbf{F}^{\,int}(\sigma^i_{n+1})}{\partial \mathbf{d}^i_{n+1}}\Delta\mathbf{d}^{i+1}_{n+1} = \mathbf{K}^i_{n+1}\Delta\mathbf{d}^{i+1}_{n+1} \tag{4.104}$$

where

$$\mathbf{K}^i_{n+1} = \mathop{\mathbb{A}}_{e=1}^{N_{el}} \mathbf{k}_e|^i_{n+1} \tag{4.105}$$

is called the global stiffness matrix at time t_{n+1} and ith iteration. The evaluation of the next iteration incremental displacement $\Delta\mathbf{d}_{n+1}^{i+1}$ is achieved linearizing the equilibrium Equation (4.104), i.e.

$$\left[\mathbf{F}^{int}(\sigma_{n+1}^{i}) - \mathbf{F}_{n+1}^{ext}\right] + \frac{\partial \mathbf{F}^{int}(\sigma_{n+1}^{i})}{\partial \mathbf{d}_{n+1}^{i}} \Delta\mathbf{d}_{n+1}^{i+1} = \mathbf{0} \tag{4.106}$$

Note that all the terms appearing in the previous equation are known, except for $\Delta\mathbf{d}_{n+1}^{i+1}$, provided that the algorithmic tangent operator $\partial\sigma_{n+1}^{i}/\partial\varepsilon_{n+1}^{i}$ can be computed. If such is the case, one obtains the following expression

$$\Delta\mathbf{d}_{n+1}^{i+1} = -\left[\mathbf{K}_{n+1}^{i}\right]^{-1}\left[\mathbf{F}^{int}(\sigma_{n+1}^{i}) - \mathbf{F}_{n+1}^{ext}\right] \tag{4.107}$$

which, as already pointed out in Section 4.4.2, makes the above sequential procedure **i.** – **v.** equivalent to the classical Newton's method.

Algorithmic consistent tangent operator

The solution procedure addressed in the previous section is completed by specifying the explicit expression for the algorithmic tangent modulus

$$\mathbb{C}_{n+1}^{i} = \frac{\partial\sigma_{n+1}^{i}}{\partial\varepsilon_{n+1}^{i}} \tag{4.108}$$

appearing in (4.103). To obtain such operator it is necessary to differentiate the algorithm given by Equations (4.58)-(4.61).

For simplicity, in the following the superindex i is omitted. First from (4.58), we obtain (note that ε_n^p, $\bar{\varepsilon}_n^p$ and α_n are constant)

$$\begin{aligned} \frac{\partial\sigma_{n+1}^{TR}}{\partial\varepsilon_{n+1}} &= E \\ \frac{\partial\Sigma_{n+1}^{TR}}{\partial\varepsilon_{n+1}} &= \frac{\partial\sigma_{n+1}^{TR}}{\partial\varepsilon_{n+1}} = E \end{aligned} \tag{4.109}$$

With these results, differentiating (4.68), assuming that $\phi_{n+1}^{TR} > 0$, one finds

$$\begin{aligned} \frac{\partial\lambda}{\partial\varepsilon_{n+1}} &= \frac{1}{E + [H_{iso} + H_{kin}]}\frac{\partial\phi_{n+1}^{TR}}{\partial\varepsilon_{n+1}} \\ &= \frac{1}{E + [H_{iso} + H_{kin}]}\frac{\partial|\Sigma_{n+1}^{TR}|}{\partial\Sigma_{n+1}^{TR}}\,\frac{\partial\Sigma_{n+1}^{TR}}{\partial\varepsilon_{n+1}} = \\ &= \frac{E}{E + [H_{iso} + H_{kin}]}\,\mathrm{sign}\left(\Sigma_{n+1}^{TR}\right) \end{aligned} \tag{4.110}$$

Rearranging $(4.61)_2$, we may write

$$\begin{aligned}\sigma_{n+1} &= \left(\sigma_{n+1}^{TR} - \alpha_n\right) + \alpha_n - \lambda E \operatorname{sign}\left(\Sigma_{n+1}^{TR}\right) \\ &= \alpha_n + \Sigma_{n+1}^{TR} - \lambda E \operatorname{sign}\left(\Sigma_{n+1}^{TR}\right) \\ &= \alpha_n + \left(1 - \frac{\lambda E}{\left|\Sigma_{n+1}^{TR}\right|}\right)\Sigma_{n+1}^{TR}\end{aligned} \tag{4.111}$$

Differentiating the discrete constitutive Equation (4.111) with respect to the actual strain ε_{n+1} using the chain rule and recalling relations $(4.109)_2$ and (4.110) we obtain

$$\begin{aligned}\frac{\partial \sigma_{n+1}}{\partial \varepsilon_{n+1}} &= \left(1 - \frac{\lambda E}{|\Sigma_{n+1}^{TR}|}\right) E + \frac{\lambda E}{|\Sigma_{n+1}^{TR}|^2}\Sigma_{n+1}^{TR}\frac{\partial |\Sigma_{n+1}^{TR}|}{\partial \varepsilon_{n+1}} \\ &- \frac{E^2}{E + [H_{iso} + H_{kin}]} \\ &= \left(1 - \frac{\lambda E}{|\Sigma_{n+1}^{TR}|}\right) E + \frac{\lambda E^2}{|\Sigma_{n+1}^{TR}|^2}\Sigma_{n+1}^{TR} \operatorname{sign}\left(\Sigma_{n+1}^{TR}\right) \\ &- \frac{E}{|\Sigma_{n+1}^{TR}|}\frac{E}{E + [H_{iso} + H_{kin}]}\Sigma_{n+1}^{TR}\operatorname{sign}\left(\Sigma_{n+1}^{TR}\right) \\ &= \left(1 - \frac{\lambda E}{|\Sigma_{n+1}^{TR}|}\right) E + \frac{\lambda E^2}{|\Sigma_{n+1}^{TR}|} - \frac{E^2}{E + [H_{iso} + H_{kin}]} \\ &= \frac{E[H_{iso} + H_{kin}]}{E + [H_{iso} + H_{kin}]}\end{aligned} \tag{4.112}$$

Since $\sigma_{n+1} = \sigma_{n+1}^{TR}$ for $\phi_{n+1}^{TR} \leq 0$ by (4.109) and (4.112)

$$\mathbb{C}_{n+1}^{i} = \frac{\partial \sigma_{n+1}^{i}}{\partial \varepsilon_{n+1}^{i}} = \begin{cases} E & \text{if } \phi_{n+1}^{TR} \leq 0 \\ \dfrac{E[H_{iso} + H_{kin}]}{E + [H_{iso} + H_{kin}]} & \text{if } \phi_{n+1}^{TR} > 0 \end{cases} \tag{4.113}$$

Finally a comparison of (4.113) and (2.25) reveals that for the one-dimensional model the algorithmic tangent operator coincides with the elastoplastic tangent operator. In the next chapter, where three-dimensional integration algorithms for J_2 plasticity are presented it is found that closed-form return map algorithms are not always achievable and that the the plastic correction through the computation of the incremental plastic multiplier may be not even granted to have a solution.

Chapter 5

Time-integration schemes for J_2 plasticity

Introduzione

In questo capitolo vengono trattai in dettaglio la struttura e gli aspetti matematici fondamentali di una ampia gamma di algoritmi di integrazione per modelli elastoplastici di tipo J_2. Questo capitolo rappresenta il cuore della tesi dato che contiene gli sviluppi più recenti ed innovativi sugli algoritmi di integrazione a base esponenziale per plasticità von-Mises, oggetto della tesi.

Il capitolo risulta suddiviso in due macro-sezioni. La prima raggruppa gli algoritmi che si applicano al modello elastoplastico con incrudimento isotropo e cinematico lineare (modello LP). La seconda riunisce gli algoritmi applicabili al modelo elastoplastico con incrudimento lineare isotropo ed incrudimento cinematico lineare/nonlineare (modello NLK). L'organizzazione del capitolo è la seguente.

La Sezione 5.2 riporta brevemente il modello costitutivo LP. Nelle sezioni 5.3 e 5.4 sono introdotti gli algoritmi tipo return map per il modello LP, basati rispettivamente su regola di integrazione secondo Eulero all'indietro e di tipo midpoint generalizzato. Gli algoritmi suddetti, denominati rispettivamente BE ed MPT, vengo completati dalla derivazione dei rispettivi operatori tangenti per passo elastoplastico. Nelle sezioni 5.5 e 5.6 vengono presentati due algoritmi a base esponenziale basati su di una opportuna riscrittura del modello e sull'utilizzo delle mappe esponenziali per l'integrazione al passo. Detti algoritmi, denominati ENN ed ENC possono ritenersi i primi membri dlla famiglia degli algoritmi esponenziali.

La Sezione 5.7 presenta due innovativi algoritmi a base esponenziale, chiamati ESC and ESC^2. Tali schemi rappresentano l'evoluzione dei due schemi

precedenti in quanto posseggono caratteristiche numeriche avanzate e risultano globalmente più competitivi rispetto ai primi. Tutti gli algoritmi esponenziali vengono dettagliati con il rispettivo operatore tangente. La Sezione 5.8 fornisce una serie di risultati teorici sulle fondamentali proprità numeriche possedute dagli schemi innovativi ESC ed ESC^2.

La seconda parte del capitolo inizia con la Sezione 5.9 che richiama le equazioni governanti del modello elastoplastico NLK. La Sezione 5.10 è dedicata al classico algoritmo di integrazione di tipo return map per il modello NLK. L'algoritmo in parola, denominato BEnl è basato su integrazione mediante regola di Eulero all'indietro. La Sezione 5.11 tratta lo schema di integrazione basato su metodo midpoint generalizzato e applicabile allo stesso modello. Tale schema prende il nome di MPTnl.

Da ultimo, nella Sezione 5.12 viene introdotto il nuovo algoritmo ESC^{2}nl, basato sulla riformulazione del modello NLK tramite la scelta di un opportuno fattore integrante scalare e sull'uso delle mappe esponenziali.

I risultati teorici contenuti nel presente capitolo inerenti gli algoritmi ENN, ENC, ESC, ESC^2 ed ESC^{2}nl sono tratti precipuamente da [6, 7, 8, 11, 12, 13, 16].

5.1 Introduction

In this chapter we addres in detail the structure and the fundamental mathematical aspects of a wide set of integration algorithms which apply to J_2 elastoplastic models. The present chapter represents the core of the thesis as it contains the innovative developments on exponential-based integration algorithms for von-Mises plasticity: the object of this work.

The chapter is divided in two macro-sections. The first one groups algorithms which apply to linear isotropic and kinematic hardening materials (LP model), while the second one groups algorithms which apply to linear isotropic and linear/nonlinear kinematic hardening materials (NLK model). The arguments are exposed as follows.

Section 5.2 briefly reports the LP constitutive model. In Sections 5.3 and 5.4 we present the return map algorithms for the LP model respectively based on the backward Euler's rule and on the generalized midpoint rule. The algorithms are provided with the relative consistent elastoplastic tangent operators. In Sections 5.5 and 5.6 we present two exponential-based integration algorithms based on a proper time continuous model reformulation and on the use of exponential maps for the stepwise integration. These algorithms, labeled as ENN and ENC can be regarded as the first members of the exponential-based

family. Section 5.7 presents two innovative exponential-based integration algorithms, labeled as ESC and ESC^2. These schemes represent the evolution of the previous integration schemes since they show improved numerical properties and globally perform better than the previous two algorithms. All the exponential-based schemes are provided with the derivation of the consistent elastoplastic tengent operator. Section 5.8 is thus dedicated to the theoretical and numerical analysis of the relevant numerical properties presented by the ESC and ESC^2 integration procedures.

The second part of the chapter starts with Section 5.9 which recalls the governing equations for the NLK constitutive model. Section 5.10 is devoted to the backward Euler's integration algorithm for the NLK elastoplstic model. Section 5.11 addresses the treatment of the integration procedure based on the generalized midpoint integration rule for the NLK model. Finally, in Section 5.12 the newly developed ESC^{2}nl exponential-based integration algorithm for the NLK model is presented.

The theoretical results contained in this chapter concerning the exponential-based algorithms family are mainly taken from [6, 7, 8, 11, 12, 13, 16].

5.2 LP plasticity model

We start by recalling the associative von-Mises plasticity model under consideration, already examined in Section 2.3.3 and labeled as LP model. Splitting the strain and stress tensors, $\boldsymbol{\sigma}$ and $\boldsymbol{\varepsilon}$, in deviatoric and volumetric parts we have

$$\boldsymbol{\sigma} = \mathbf{s} + p\mathbf{I} \qquad \text{with} \qquad p = \frac{1}{3}\mathrm{tr}(\boldsymbol{\sigma}) \tag{5.1}$$

$$\boldsymbol{\varepsilon} = \mathbf{e} + \frac{1}{3}\theta\mathbf{I} \qquad \text{with} \qquad \theta = \mathrm{tr}(\boldsymbol{\varepsilon}) \tag{5.2}$$

where tr indicates the trace operator (sum of the first three components), while $\mathbf{I}$, $\mathbf{s}$, p, $\mathbf{e}$, θ are respectively the second-order identity tensor, the deviatoric and volumetric stress, the deviatoric and volumetric strain.

The equations for the model are

$$
\begin{aligned}
p &= K\theta && (5.3)\\
\mathbf{s} &= 2G[\mathbf{e} - \mathbf{e}^p] && (5.4)\\
\boldsymbol{\Sigma} &= \mathbf{s} - \boldsymbol{\alpha} && (5.5)\\
F &= \|\boldsymbol{\Sigma}\| - \sigma_y && (5.6)\\
\dot{\mathbf{e}}^p &= \dot{\gamma}\mathbf{n} && (5.7)\\
\sigma_y &= \sigma_{y,0} + H_{iso}\gamma && (5.8)\\
\dot{\boldsymbol{\alpha}} &= H_{kin}\dot{\gamma}\mathbf{n} && (5.9)\\
\dot{\gamma} &\geq 0\ , \quad F \leq 0\ , \quad \dot{\gamma}F = 0 && (5.10)
\end{aligned}
$$

where K is the material bulk elastic modulus, G is the material shear modulus, $\mathbf{e}^p$ is the traceless plastic strain, $\boldsymbol{\Sigma}$ is the relative stress in terms of the backstress $\boldsymbol{\alpha}$, the latter introduced to describe the kinematic hardening mechanism. Moreover, F is the von-Mises yield function, $\mathbf{n}$ is the normal to the yield surface, σ_y is the yield surface radius, $\sigma_{y,0}$ the initial yield stress, H_{kin} and H_{iso} are the kinematic and isotropic linear hardening moduli. Finally, Equations (5.10) are the Kuhn-Tucker conditions; in particular, the second equation limits the relative stress within the boundary defined by the yield surface $F = 0$, while the other two are necessary to determine the plastic behavior. With a slight over-simplification of the model complexity, we may say that when $\dot{\gamma} = 0$ the system is in an elastic phase, while when $\dot{\gamma} > 0$ we say that the system is in a plastic phase.

In the following sections a set of numerical schemes for the above problem is presented. The first two schemes are based respectively on the backward Euler's and on the generalized midpoint integration rules. The subsequent schemes belong to the exponential-based time integrators family.

Remark 5.2.1 *Due to the linear behavior of the volumetric part constitutive equations, in the following we treat only the deviatoric part of the model.*

5.3 Backward Euler's integration scheme for the LP model

The numerical method presented in this section for the solution of the LP plasticity model is based on a backward Euler's integration rule and on a return map algorithm. In the following this scheme is indicated as BE scheme. A more detailed description can be found in several articles and books [17, 69, 71, 79]; it is anyway worth recalling here the widespread success of such a method,

granted by its general good numerical performances and the well established numerical properties. In general, the method consists of the time-integration of the differential algebraic system, leading to an algebraic system and of the formulation of the solution algorithm for the obtained algebraic system. The method grants first-order accuracy and respect the yield consistency constraint. In the following chapter the BE scheme is used as a reference for testing the new exponential-based integration schemes which are suited for the LP elastoplastic model.

5.3.1 Integration scheme

In particular, for the model under investigation, adopting a first order backward Euler's time integration formula, the solution of the algebraic system returns a simple linear equation and, accordingly, the solution algorithm reduces to a radial return map. In the following we briefly review the method together with the form of the consistent elastoplastic tangent operator. It is assumed that the load history interval $[0, T]$ is divided into N sub-intervals defined by the points $0 = t_0 < t_1 < .... < t_n < t_{n+1} < .... < t_N < t_{N+1}$. If t_n is a generic time instant, we indicate by $\mathbf{e}_n$ the deviatoric strain at time t_n, by $\mathbf{s}_n$ the deviatoric stress at the same time, and so on for all the problem variables.

The strain history path is known and is taken as piecewise linear in time; we are then interested in the evolution of the other problem variables, in particular the stress, the plastic strain and the total strain.

As an example, assuming to know the values $\{\mathbf{s}_n, \mathbf{e}_n, \mathbf{e}^p_n, \gamma_n, \boldsymbol{\alpha}_n\}$ at time t_n, and the deviatoric strain $\mathbf{e}_{n+1}$ at time t_{n+1}, we search for the remaining variables at time t_{n+1}. Using a backward Euler's integration rule the discrete evolutionary equations for the plasticity model become

$$\begin{cases} \mathbf{e}^p_{n+1} = \mathbf{e}^p_n + \lambda \mathbf{n}_{n+1} \\ \boldsymbol{\alpha}_{n+1} = \boldsymbol{\alpha}_n + H_{kin}\lambda \mathbf{n}_{n+1} \\ \mathbf{s}_{n+1} = 2G[\mathbf{e}_{n+1} - \mathbf{e}^p_{n+1}] \\ \boldsymbol{\Sigma}_{n+1} = \mathbf{s}_{n+1} - \boldsymbol{\alpha}_{n+1} \\ \gamma_{n+1} = \gamma_n + \lambda \end{cases} \tag{5.11}$$

where λ represents the incremental plastic rate parameter, to be determined enforcing the plastic consistency condition (the subscript $n+1$ in λ is omitted for compactness).

Substituting $(5.11)_1$ into (5.4) yields:

$$\mathbf{s}_{n+1} = 2G[\mathbf{e}_{n+1} - \mathbf{e}^p_n] - 2G\lambda \mathbf{n}_{n+1} \tag{5.12}$$

and subtraction of $(5.11)_2$ gives

$$\mathbf{\Sigma}_{n+1} = \mathbf{s}_{n+1} - \boldsymbol{\alpha}_{n+1} = 2G[\mathbf{e}_{n+1} - \mathbf{e}_n^p] - \boldsymbol{\alpha}_n - H_{kin}\lambda\mathbf{n}_{n+1} \tag{5.13}$$

5.3.2 Solution algorithm

To solve the problem, we initially suppose the step to be elastic, and calculate the trial values at the final instant:

$$\begin{cases} \mathbf{e}_{n+1}^{p,TR} = \mathbf{e}_n^p \\ \mathbf{s}_{n+1}^{TR} = 2G[\mathbf{e}_{n+1} - \mathbf{e}_n^p] \\ \boldsymbol{\alpha}_{n+1}^{TR} = \boldsymbol{\alpha}_n \\ \mathbf{\Sigma}_{n+1}^{TR} = \mathbf{s}_{n+1}^{TR} - \boldsymbol{\alpha}_{n+1}^{TR} \\ \gamma_{n+1}^{TR} = \gamma_n \end{cases} \tag{5.14}$$

If the resulting stress is admissible, i.e.

$$\parallel \mathbf{\Sigma}_{n+1}^{TR} \parallel \leq \sigma_{y,0} + H_{iso}\gamma_{n+1}^{TR} \tag{5.15}$$

the variable values at the time step t_{n+1} are taken as the trial ones just calculated. On the other hand, if $\mathbf{\Sigma}_{n+1}^{TR}$ violates the yield limit (5.15), a plastic correction is introduced

$$\begin{cases} \mathbf{e}_{n+1}^{p} = \mathbf{e}_{n+1}^{p,TR} + \lambda\mathbf{n}_{n+1} \\ \mathbf{s}_{n+1} = \mathbf{s}_{n+1}^{TR} - 2G\lambda\mathbf{n}_{n+1} \\ \boldsymbol{\alpha}_{n+1} = \boldsymbol{\alpha}_{n+1}^{TR} + H_{kin}\lambda\mathbf{n}_{n+1} \\ \mathbf{\Sigma}_{n+1} = \mathbf{\Sigma}_{n+1}^{TR} - [2G + H_{kin}]\,\lambda\mathbf{n} \\ \gamma_{n+1} = \gamma_{n+1}^{TR} + \lambda \end{cases} \tag{5.16}$$

where the scalar λ represents the increment of the plastic consistency parameter i.e. $\int_{t_n}^{t_{n+1}} \dot{\gamma} dt$.

A graphical idealization of the return map algorithm applied to the BE integration scheme is provided in Figure 5.1, which represents in the deviatoric stress space the trial elastic predictor and the plastic corrector obtained applying the return map algorithm to the BE scheme.

The solution of the obtained algebraic system is approached solving initially for the scalar λ, enforcing the condition $F(\mathbf{\Sigma}_{n+1}) = 0$. This implicit equation is solved observing that $\mathbf{\Sigma}_{n+1}^{TR}$ and $\mathbf{\Sigma}_{n+1}$ are parallel, obtaining

$$\lambda = \frac{\parallel \mathbf{\Sigma}_{n+1}^{TR} \parallel - \left(\sigma_{y,0} + H_{iso}\gamma_{n+1}^{TR}\right)}{2G + H_{iso} + H_{kin}} \tag{5.17}$$

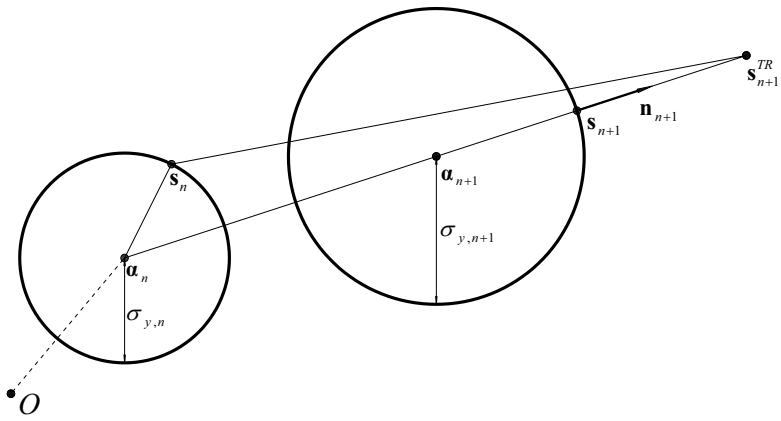

Figure 5.1: Application of the return map algorithm to the BE integration scheme. Plastic correction representation in deviatoric stress space.

Once the scalar λ is known, noting that

$$\mathbf{n}^{TR} = \frac{\boldsymbol{\Sigma}^{TR}_{n+1}}{\| \boldsymbol{\Sigma}^{TR}_{n+1} \|} = \mathbf{n} \tag{5.18}$$

it is possible to update all the problem variables.

5.3.3 BE scheme elastoplastic consistent tangent operator

For the reader convenience, we show here the consistent tangent operator for the BE scheme. For brevity's sake, only the final form of the operator corresponding to a plastic step (i.e. such that $\lambda \neq 0$) is reported without deriving it thoroughly. To make notation more clear, the subscripts of all variables are omitted and it is implicitly assumed that all quantities are evaluated at the final instant of the step t_{n+1}. The reader is referred to [17] for a complete derivation.

$$\mathbb{C}^{ep} = \frac{\partial \boldsymbol{\sigma}}{\partial \boldsymbol{\varepsilon}} = K\mathbf{I} \otimes \mathbf{I} + 2G\,(1 - C)\,\mathbb{I}_{\text{dev}} + [2G\,(C - A)]\,\mathbf{n} \otimes \mathbf{n} \tag{5.19}$$

with

$$\begin{aligned} A &= \frac{2G}{2G + H_{iso} + H_{kin}} \\ C &= \frac{2G\lambda}{\| \boldsymbol{\Sigma}^{\lambda}_{A} \|} \end{aligned}$$

5.4 Generalized midpoint integration scheme for the LP model

In this section we present the numerical method already proposed by Ortiz and Popov in 1985 [63] in the framework of elastoplastic constitutive models. The method is based on a generalized midpoint integration rule combined with a return map algorithm. In the following, this scheme is indicated as MPT scheme. The return map is achieved enforcing consistency at the end of the time step and projecting the trial solution onto the updated yield surface at the end of each elastoplastic step. This procedure results in solving a quadratic equation in the plastic consistency parameter. The method grants second-order accuracy as it is shown by the numerical tests carried out in the next chapter and is taken as a reference algorithm for testing the new exponential-based integration schemes in terms of accuracy and precision in stress and strain computation.

5.4.1 Integration scheme

Using a generalized midpoint rule the discrete evolutionary equations become

$$\begin{cases} \mathbf{e}^p_{n+1} = \mathbf{e}^p_n + \lambda \mathbf{n}_{n+\alpha} \\ \boldsymbol{\alpha}_{n+1} = \boldsymbol{\alpha}_n + \lambda H_{kin} \mathbf{n}_{n+\alpha} \\ \mathbf{s}_{n+1} = 2G[\mathbf{e}_{n+1} - \mathbf{e}^p_{n+1}] \\ \boldsymbol{\Sigma}_{n+1} = \mathbf{s}_{n+1} - \boldsymbol{\alpha}_{n+1} \\ \gamma_{n+1} = \gamma_n + \lambda \end{cases} \tag{5.20}$$

where λ may be regarded as the incremental plastic parameter to be determined enforcing the plastic consistency condition, while the scalar α is the algorithmic parameter such that the following the midpoint rule holds

$$\begin{cases} \mathbf{e}_{n+\alpha} = \alpha \mathbf{e}_{n+1} + (1-\alpha)\mathbf{e}_n \\ \mathbf{e}^p_{n+\alpha} = \alpha \mathbf{e}^p_{n+1} + (1-\alpha)\mathbf{e}^p_n \\ \boldsymbol{\alpha}_{n+\alpha} = \alpha \boldsymbol{\alpha}_{n+1} + (1-\alpha)\boldsymbol{\alpha}_n \\ \mathbf{s}_{n+\alpha} = 2G[\mathbf{e}_{n+\alpha} - \mathbf{e}^p_{n+\alpha}] \\ \boldsymbol{\Sigma}_{n+\alpha} = \mathbf{s}_{n+\alpha} - \boldsymbol{\alpha}_{n+\alpha} \end{cases} \tag{5.21}$$

In what follows we will assume $\alpha = 1/2$.

5.4.2 Solution algorithm

We initially suppose the step to be elastic, and calculate trial values at the final stage t_{n+1}:

$$\begin{cases} \mathbf{e}_{n+1}^{p,TR} = \mathbf{e}_n^p \\ \mathbf{s}_{n+1}^{TR} = 2G[\mathbf{e}_{n+1} - \mathbf{e}_n^p] \\ \boldsymbol{\alpha}_{n+1}^{TR} = \boldsymbol{\alpha}_n \\ \boldsymbol{\Sigma}_{n+1}^{TR} = \mathbf{s}_{n+1}^{TR} - \boldsymbol{\alpha}_{n+1}^{TR} \\ \gamma_{n+1}^{TR} = \gamma_n \end{cases} \tag{5.22}$$

If the resulting stress is admissible, i.e.

$$\| \boldsymbol{\Sigma}_{n+1}^{TR} \| \leq \sigma_{y,0} + H_{iso}\gamma_{n+1}^{TR} \tag{5.23}$$

the step is assumed to be elastic and the variable values at the final time instant are taken as the trial ones. On the other hand, if $\boldsymbol{\Sigma}_{n+1}^{TR}$ violates the yield limit, a plastic correction is introduced in two steps:

- Update of values at $t_{n+\alpha}$.

$$\begin{cases} \boldsymbol{\Sigma}_{n+\alpha} + (2G\alpha\lambda + \alpha\lambda H_{kin})\mathbf{n}_{n+\alpha} = 2G[\mathbf{e}_{n+\alpha} - \mathbf{e}_n^p - \dfrac{\boldsymbol{\alpha}_n}{2G}] \\ \boldsymbol{\alpha}_{n+\alpha} = \boldsymbol{\alpha}_n + \alpha\lambda H_{kin}\mathbf{n}_{n+\alpha} \\ \mathbf{s}_{n+\alpha} = \boldsymbol{\Sigma}_{n+\alpha} + \boldsymbol{\alpha}_{n+\alpha} \end{cases} \tag{5.24}$$

- Update of values at t_{n+1}.

$$\begin{cases} \mathbf{e}_{n+1}^p = \mathbf{e}_n^p + \lambda\mathbf{n}_{n+\alpha} \\ \boldsymbol{\alpha}_{n+1} = \boldsymbol{\alpha}_n + \lambda H_{kin}\mathbf{n}_{n+\alpha} \\ \mathbf{s}_{n+1} = 2G[\mathbf{e}_{n+1} - \mathbf{e}_{n+1}^p] \\ \boldsymbol{\Sigma}_{n+1} = \mathbf{s}_{n+1} - \boldsymbol{\alpha}_{n+1} \\ \gamma_{n+1} = \gamma_n + \lambda \end{cases} \tag{5.25}$$

A graphical idealization of the return map algorithm applied to the MPT integration scheme is provided in Figure 5.2 which represents in the deviatoric stress space the trial elastic predictor and the plastic corrector obtained applying the return map algorithm to the MPT scheme.

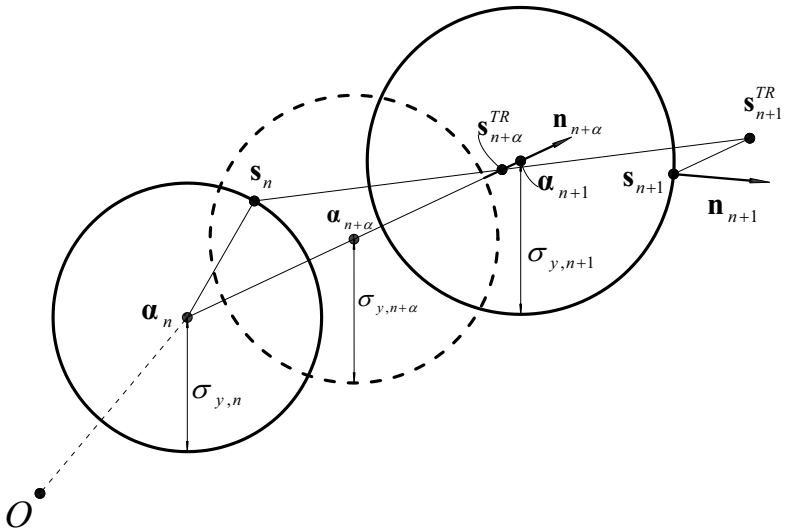

Figure 5.2: Application of the return map algorithm to the MPT integration scheme. Plastic correction representation in deviatoric stress space.

The above sequential update procedure is set forth by enforcing the plastic consistency condition at the end of the step and observing $(5.24)_1$ which states that $\mathbf{\Sigma}_{n+\alpha}$ and

$$\mathbf{\Sigma}_{n+\alpha}^{TR} = 2G[\mathbf{e}_{n+\alpha} - \mathbf{e}_n^p] - \boldsymbol{\alpha}_n \tag{5.26}$$

are parallel i.e.

$$\mathbf{n}_{n+\alpha} = \frac{\mathbf{\Sigma}_{n+\alpha}}{\parallel \mathbf{\Sigma}_{n+\alpha} \parallel} = \frac{\mathbf{\Sigma}_{n+\alpha}^{TR}}{\parallel \mathbf{\Sigma}_{n+\alpha}^{TR} \parallel} = \mathbf{n}_{n+\alpha}^{TR} \tag{5.27}$$

and using $(5.24)_{1-2}$ and $(5.25)_{1-4}$ to enforce the modified form of the discrete limit equation at the final instant t_{n+1}

$$\parallel \mathbf{\Sigma}_{n+1} \parallel^2 = \sigma_{y,n+1}^2 \tag{5.28}$$

This results in the following second order algebraic equation

$$a\lambda^2 + b\lambda + c = 0 \tag{5.29}$$

where

$$a = (2G + H_{kin})\mathbf{n}_{n+\alpha}^{TR} : \mathbf{n}_{n+\alpha}^{TR} - H_{iso}^2 \tag{5.30}$$

$$b = -2(2G + H_{kin})\mathbf{\Sigma}_{n+1}^{TR} : \mathbf{n}_{n+\alpha}^{TR} - 2(H_{iso}^2\gamma_n + H_{iso}^2\sigma_{y,0}) \tag{5.31}$$

$$c = \mathbf{\Sigma}_{n+1}^{TR} : \mathbf{\Sigma}_{n+1}^{TR} - \sigma_{y,0}^2 - H_{iso}^2\gamma_n^2 - 2H_{iso}\sigma_{y,0}\gamma_n \tag{5.32}$$

It is assumed that the plastic rate parameter λ which permits the updates (5.24) and (5.25) is given by the minimum positive root.

5.4.3 MPT scheme elastoplastic consistent tangent operator

The elastoplastic consistent tangent operator at t_{n+1} follows at once by a chain rule argument, once it is derived at $t_{n+\alpha}$. The reader can refer to [7, 13, 17, 72] for a detailed derivation of this part. For brevity's sake, we just report the final form of the operator for a plastic step (i.e. such that $\lambda \neq 0$) without deriving it thoroughly. To make notation more clear, the subscripts of all variables are omitted and it is implicitly assumed that all quantities are evaluated at the final instant of the step t_{n+1}. Recalling that

$$\frac{\partial \mathbf{s}}{\partial \boldsymbol{\varepsilon}} = \frac{\partial \mathbf{s}}{\partial \mathbf{e}} \frac{\partial \mathbf{e}}{\partial \boldsymbol{\varepsilon}} = \frac{\partial \mathbf{s}}{\partial \mathbf{e}} \mathbb{I}_{\text{dev}} \tag{5.33}$$

where

$$\mathbb{I}_{\text{dev}} = \mathbb{I} - \frac{1}{3} (\mathbf{I} \otimes \mathbf{I}) \tag{5.34}$$

and taking into account the volumetric part of the stress, from Equations (5.1), (5.2) and (5.3) we get

$$\mathbb{C}^{ep} = \frac{\partial \boldsymbol{\sigma}}{\partial \boldsymbol{\varepsilon}} = \frac{\partial \mathbf{s}}{\partial \mathbf{e}} \mathbb{I}_{\text{dev}} + K (\mathbf{I} \otimes \mathbf{I}) \tag{5.35}$$

The fourth-order tensor $\dfrac{\partial \mathbf{s}}{\partial \boldsymbol{\varepsilon}}$ can be computed as

$$\frac{\partial \mathbf{s}}{\partial \mathbf{e}} = \mathbf{m}_1 + \mathbf{m}_2 \tag{5.36}$$

where $\mathbf{m}_1$ and $\mathbf{m}_2$ are given by the following expressions

$$\mathbf{m}_1 = 2G \left(\mathbb{I} - \frac{\beta_1}{\beta_1 + \beta_2 + 1} \mathbb{I}_{\mathbf{n}} - \mathbf{n}_{n+\alpha} \otimes \frac{\partial \lambda}{\partial \mathbf{e}} \right) \tag{5.37}$$

$$\mathbf{m}_2 = \frac{\beta_1}{\beta_1 + \beta_2 + 1} \mathbb{I}_{\mathbf{n}} \left(\boldsymbol{\beta} \otimes \frac{\partial \lambda}{\partial \mathbf{e}} \right) \tag{5.38}$$

with

$$\begin{aligned}
\mathbb{I}_{\mathbf{n}} &= \mathbb{I} - \mathbf{n}_{n+\alpha} \otimes \mathbf{n}_{n+\alpha} && (5.39)\\
\frac{\partial \lambda}{\partial \mathbf{e}} &= -2G\theta_1^{-1}\left(\mathbb{I} - \frac{2G\lambda + H_{kin}\lambda/2}{2 \parallel \mathbf{s}_{n+\alpha}^{TR} - \boldsymbol{\alpha}_n \parallel}\mathbb{I}_{\mathbf{n}}\right)\boldsymbol{\Sigma}_{n+1} && (5.40)\\
\boldsymbol{\beta} &= \frac{1}{2}H_{kin}\mathbf{n}_{n+\alpha} && (5.41)\\
\theta_1 &= H_{iso}\sigma_{y,n+1} + (\boldsymbol{\beta} : \boldsymbol{\Sigma}_{n+1}) + 2G\left(\mathbf{n}_{n+\alpha} : \boldsymbol{\Sigma}_{n+1}\right) && (5.42)\\
\beta_1 &= \frac{2G\lambda}{2\|\Sigma_{n+\alpha}\|} && (5.43)\\
\beta_2 &= \frac{H_{kin}\lambda}{2\|\Sigma_{n+\alpha}\|} && (5.44)
\end{aligned}$$

5.5 ENN exponential-based integration scheme for the LP model

This section presents the first exponential-based integration algorithm for von-Mises plasticity with linear hardening, initially presented and implemented by Auricchio and Beirão da Veiga [16]. A similar idea had been developed by Hong and Liu [44, 45]. This algorithm which is labeled ENN (Exponential-based Non-symmetric Non-consistent method) constitutes the first member of the exponential-based family object of this work and is characterized by second-order accuracy, exactness in case of zero isotropic hardening, yet by not being yield-consistent.

The integration scheme is based on a model reformulation by a rewriting of the constitutive equations and on the choice for an integration factor. The resulting evolutive equation for a generalized stress tensor results of notable interest since it is quasi-linear. Under suitable hypotheses the time integration of the above quasi-linear dynamical system can be carried out with the exponential maps technique.

5.5.1 A new model formulation

Combining Equations (5.4) and (5.5), we obtain

$$\boldsymbol{\Sigma} + \boldsymbol{\alpha} + 2G\mathbf{e}^p = 2G\mathbf{e} \tag{5.45}$$

and, taking the derivative in time and applying Equation (5.9), Equation (5.45) becomes

$$\dot{\boldsymbol{\Sigma}} + (2G + H_{kin})\,\dot{\mathbf{e}}^p = 2G\dot{\mathbf{e}} \tag{5.46}$$

Now, recalling that in the plastic phase

$$\mathbf{n} = \frac{\mathbf{\Sigma}}{\parallel \mathbf{\Sigma} \parallel} = \frac{\mathbf{\Sigma}}{\sigma_{y,0} + H_{iso}\gamma} \tag{5.47}$$

we may apply (5.7) obtaining

$$\dot{\mathbf{\Sigma}} + (2G + H_{kin}) \frac{\mathbf{\Sigma}}{\sigma_{y,0} + H_{iso}\gamma}\dot{\gamma} = 2G\dot{\mathbf{e}} \tag{5.48}$$

which is a differential equation for $\mathbf{\Sigma}$. We now need an evolution law for γ, which in the elastic phase is simply

$$\dot{\gamma} = 0 \tag{5.49}$$

while in the plastic phase it is indirectly extracted from the Kuhn-Tucker condition $\dot{F} = 0$. Multiplying Equation (5.48) by $\mathbf{\Sigma}$ it follows

$$\mathbf{\Sigma} : \dot{\mathbf{\Sigma}} + (2G + H_{kin}) \frac{\parallel \mathbf{\Sigma} \parallel^2}{\sigma_{y,0} + H_{iso}\gamma}\dot{\gamma} = 2G\left[\dot{\mathbf{e}} : \mathbf{\Sigma}\right] \tag{5.50}$$

and, observing that in the plastic phase

$$\parallel \mathbf{\Sigma} \parallel^2 = (\sigma_{y,0} + H_{iso}\gamma)^2 \tag{5.51}$$

$$\mathbf{\Sigma} : \dot{\mathbf{\Sigma}} = \frac{1}{2}\frac{\mathrm{d}}{\mathrm{d}t} \parallel \mathbf{\Sigma} \parallel^2 = H_{iso}\left(\sigma_{y,0} + H_{iso}\gamma\right)\dot{\gamma} \tag{5.52}$$

it becomes

$$(\sigma_{y,0} + H_{iso}\gamma)\ (2G + H_{kin} + H_{iso})\,\dot{\gamma} = 2G\left[\dot{\mathbf{e}} : \mathbf{\Sigma}\right] \tag{5.53}$$

Now the idea is to rewrite the differential system formed by equations (5.48) and (5.49)-(5.53) introducing an integrating function. Accordingly, we set

$$X_0(\gamma) = \begin{cases} \left(1 + \dfrac{H_{iso}}{\sigma_{y,0}}\gamma\right)^{\dfrac{2G + H_{kin}}{H_{iso}}} & \text{if } \ H_{iso} \neq 0 \\ \exp\left(\dfrac{2G + H_{kin}}{\sigma_{y,0}}\gamma\right) & \text{if } \ H_{iso} = 0 \end{cases} \tag{5.54}$$

noting that such a function is continuous for fixed γ and $H_{iso} \to 0$. Multiplying Equation (5.48) by $X_0(\gamma)$, we have

$$\frac{\mathrm{d}}{\mathrm{d}t}\left[\mathbf{\Sigma}X_0(\gamma)\right] = 2G\dot{\mathbf{e}}X_0(\gamma) \tag{5.55}$$

At this stage, we define a new *generalized stress vector* $\mathbf{X}$ which, adopting the engineering notation reads

$$\{\mathbf{X}\} = \begin{Bmatrix} X_0 \mathbf{\Sigma} \\ X_0 \end{Bmatrix} = \begin{Bmatrix} \mathbf{X}^s \\ X_0 \end{Bmatrix} \tag{5.56}$$

from (5.55) we obtain

$$\dot{\mathbf{X}}^s = 2G X_0 \dot{\mathbf{e}} \tag{5.57}$$

We now search a similar differential equation for the last component X_0 of $\mathbf{X}$. Taking the derivative of $X_0(\gamma)$, we have

$$\dot{X}_0 = \frac{\mathrm{d}}{\mathrm{d}t} X_0(\gamma\,(t)) = (2G + H_{kin})\,\frac{X_0}{\sigma_{y,0} + H_{iso}\gamma}\dot{\gamma} \tag{5.58}$$

From (5.58) and (5.53) we obtain

$$\begin{aligned} \dot{X}_0 &= \frac{2G + H_{kin}}{\sigma_{y,0}^2\,(2G + H_{kin} + H_{iso})}\,\frac{X_0}{\left(1 + \dfrac{H_{iso}}{\sigma_{y,0}\gamma}\right)^2}\,[2G\dot{\mathbf{e}} : \mathbf{\Sigma}] = \\ &= \frac{2G + H_{kin}}{\sigma_{y,0}^2\,(2G + H_{kin} + H_{iso})}\,X_0^{-\dfrac{2H_{iso}}{2G + H_{kin}}}\,[2G\dot{\mathbf{e}} : \mathbf{X}^s] \end{aligned} \tag{5.59}$$

Introducing the position

$$\chi = \chi(X_0) = \frac{2G + H_{kin}}{\sigma_{y,0}^2\,(2G + H_{kin} + H_{iso})}\,X_0^{-\dfrac{2H_{iso}}{2G + H_{kin}}} \tag{5.60}$$

and, recalling Equation (5.49), we have

$$\dot{X}_0 = 0 \qquad \text{(elastic phase)} \tag{5.61}$$

$$\dot{X}_0 = 2G\,\chi\,\dot{\mathbf{e}} : \mathbf{X}^s \qquad \text{(plastic phase)} \tag{5.62}$$

We introduce now a linear space structure on the space of generalized stresses which is the key feature of the exponential-based formulation. Any element of the space of linear operators from the generalized stress space into itself can be written adopting the engineering notation as

$$[\mathbb{M}] = \begin{bmatrix} \mathbb{M}_{11} & \mathbf{M_{12}} \\ \mathbf{M_{21}} & M_{22} \end{bmatrix} \tag{5.63}$$

with $\mathbb{M}_{11}$ a fourth-order tensor, $\mathbf{M_{12}}, \mathbf{M_{21}}$ second-order tensors and M_{22} a scalar, under the convention that the formal expression

$$\mathbb{M}\mathbf{Y} \tag{5.64}$$

returns a generalized stress vector given by the following operation

$$[\mathbb{M}]\ \{\mathbf{Y}\} = \begin{bmatrix} \mathbb{M}_{11} & \mathbf{M_{12}} \\ \mathbf{M_{21}} & M_{22} \end{bmatrix} \begin{Bmatrix} \mathbf{Y}^s \\ Y_0 \end{Bmatrix} = \begin{Bmatrix} \mathbb{M}_{11}\mathbf{Y}^s + \mathbf{M_{12}}\, Y_{\mathbf{0}} \\ \mathbf{M_{21}} : \mathbf{Y^s} + \mathbf{M_{22}}\, Y_{\mathbf{0}} \end{Bmatrix} \tag{5.65}$$

for any couple $\{\mathbf{Y}\} = \{\mathbf{Y}^s, Y_0\}^T$ in the generalized stress space. The product by a scalar and the sum between vectors is defined in the obvious natural way. Accordingly, Equations (5.57) and (5.61)-(5.62) provide a system for the generalized stress vector $\mathbf{X}$

$$\dot{\mathbf{X}} = \mathbb{A}\mathbf{X} \tag{5.66}$$

with the matrix operator $\mathbb{A}$ depending on the actual phase

$$[\mathbb{A}] = [\mathbb{A}_e] = 2G \begin{bmatrix} \mathbb{O} & \dot{\mathbf{e}} \\ \mathbf{0} & 0 \end{bmatrix} \qquad \text{(elastic phase)} \tag{5.67}$$

$$[\mathbb{A}] = [\mathbb{A}_p] = 2G \begin{bmatrix} \mathbb{O} & \dot{\mathbf{e}} \\ \chi\dot{\mathbf{e}} & 0 \end{bmatrix} \qquad \text{(plastic phase)} \tag{5.68}$$

where $\mathbf{0}$ and $\mathbb{O}$ indicate respectively the second-order and fourth-order null tensors. Therefore, the original problem, represented by Equations (5.3)-(5.10), is replaced by a new one, where the relative stress $\mathbf{\Sigma}$ and the plastic rate γ are now represented in the form of vector $\mathbf{X}$. The main advantage of the new form is the quasi-linearity, both in the elastic and in the plastic phase.

As an example, let us consider the model with no isotropic hardening ($H_{iso} = 0$). Due to Equations (5.60) and (5.68), it is immediate to check that $\mathbb{A}$ depends only on $\dot{\mathbf{e}}$. This means that, if $\dot{\mathbf{e}}$ is constant in a certain time interval, $\mathbb{A}$ holds the same property: under such a hypothesis the solution of system (5.66) is known and the problem can be solved *exactly*.

However, in the general case, the matrix $\mathbb{A}$ depends on $\mathbf{X}$, and in this sense we say that the problem is quasi-linear. Anyway, the partial linearity arising in the problem is indeed of great value, allowing us to numerically approximate its solution with excellent results.

Time-continuous on-off switch

To properly convert the original problem in an equivalent but new differential algebraic format, we also need to introduce an elastic-plastic phase determination criteria expressed in the new generalized stress environment.

For a given phase to be plastic, the following two conditions hold:

1) The relative stress $\mathbf{\Sigma}$ must be on the yield surface

$$\| \mathbf{X}^s \|^2 = \| \mathbf{\Sigma} \|^2 X_0^2 = (\sigma_{y,0} + H_{iso}\gamma)^2 X_0^2 = \sigma_{y,0}^2 X_0 \frac{2(H_{iso} + H_{kin} + 2G)}{2G + H_{kin}} \tag{5.69}$$

2) The direction of the strain rate $\dot{\mathbf{e}}$ must be outward with respect to the yield surface

$$\mathbf{\Sigma} : \dot{\mathbf{e}} > 0 \iff \mathbf{X}^s : \dot{\mathbf{e}} > 0 \tag{5.70}$$

If such two conditions are not satisfied, the step is elastic.

5.5.2 Integration scheme

In the following we present a numerical scheme for the evolution of $\mathbf{X}$, governed by the dynamical law (5.66) with matrix $\mathbb{A}$ given by (5.67) or (5.68) respectively.

As usual, we assume that the time history interval $[0, T]$ is divided into N sub-intervals defined by the nodes $0 = t_0 < t_1 < .... < t_n < t_{n+1} < .... < t_N = T$ and indicate the general sub-interval amplitude as $\Delta t = t_{n+1} - t_n$. Given the values $\{\mathbf{s}_n, \mathbf{e}_n, \mathbf{e}_n^p, \gamma_n, \boldsymbol{\alpha}_n\}$ at time t_n and the deviatoric strain $\mathbf{e}_{n+1}$ at time t_{n+1}, we search for the remaining variables at time t_{n+1}, assuming the strain history to be piecewise linear. The strain is retained taken as a linear function in each time sub interval and, for simplicity, we consider the initial values of γ and $\boldsymbol{\alpha}$ to be zero, so that the initial generalized stress vector is

$$\{\mathbf{X}_0\} = \begin{Bmatrix} \mathbf{X}_0^s \\ X_0 \end{Bmatrix} = \begin{Bmatrix} \mathbf{\Sigma}_0 \\ 1 \end{Bmatrix} \tag{5.71}$$

Clearly, the initial values of the relative stress and the deviatoric strain must be consistent with the governing Equations (5.3)-(5.10).

The evolution of $\mathbf{X}$ is governed by the dynamical law (5.66) with matrix $\mathbb{A}$ given by (5.67) or (5.68). Due to the piecewise linearity of the strain path, $\dot{\mathbf{e}}$ is constant in each single time interval. Unluckily, due to the presence of χ in (5.68), this is not true for matrix $\mathbb{A}$; the scalar χ is a function of X_0, and so of $\mathbf{X}$, as shown in Equation (5.60). Therefore, we approximate the solution of the dynamical law (5.66) considering χ constant in each single time step. The discrete form of the evolution law (5.66) becomes

$$\dot{\mathbf{X}} = \bar{\mathbb{A}}\mathbf{X} \tag{5.72}$$

where the matrix $\bar{\mathbb{A}}$ is now constant along a single time interval

$$\left[\bar{\mathbb{A}}\right] = 2G \begin{bmatrix} \mathbb{O} & \dot{\mathbf{e}} \\ \mathbf{0} & 0 \end{bmatrix} \qquad \text{(elastic step)} \tag{5.73}$$

$$\left[\bar{\mathbb{A}}\right] = 2G \begin{bmatrix} \mathbb{O} & \dot{\mathbf{e}} \\ \chi_n \dot{\mathbf{e}} & 0 \end{bmatrix} \qquad \text{(plastic step)} \tag{5.74}$$

Under such an additional hypothesis, the matrix $\bar{\mathbb{A}}$ is constant in both phases, and so the evolution of Equation (5.72) is well known to be

$$\mathbf{X}_{n+1} = \exp\left[\bar{\mathbb{A}}\Delta t\right]\mathbf{X}_n \tag{5.75}$$

where $\Delta t = t_{n+1} - t_n$. Defining the tensor $\Delta\mathbf{e} = \mathbf{e}_{n+1} - \mathbf{e}_n$, we observe that the matrix $\bar{\mathbb{A}}\Delta t$ is equal to the matrix (5.67) or (5.68) after substituting $\dot{\mathbf{e}}$ with $\Delta\mathbf{e}$. Note that, being $\bar{\mathbb{A}}$ an element in the linear space of linear operators acting on couples, the exponential of $\bar{\mathbb{A}}\Delta t$ is naturally defined by the (converging) exponential serie

$$\bar{\mathbb{G}} = \exp\left[\bar{\mathbb{A}}\Delta t\right] = \sum_{n=0}^{+\infty} \frac{\left(\bar{\mathbb{A}}\Delta t\right)^n}{n!} \tag{5.76}$$

The linear operator $\bar{\mathbb{G}}$ appearing in Equation (5.75) can be derived calculating the shown exponential. Note that, for such purpose, it is convenient to reformulate the linear operator $\bar{\mathbb{A}}\Delta t$ as a $\mathcal{R}^{7\times 7}$ matrix, calculate the exponential, and finally write it back in the original form (5.63).

Hence, given the initial value $\mathbf{X}_n$, $\mathbf{X}_{n+1}$ can be now calculated as

$$\mathbf{X}_{n+1} = \bar{\mathbb{G}}\,\mathbf{X}_n \tag{5.77}$$

The matrix $\bar{\mathbb{G}}$ is the exponential appearing in (5.76), which is

$$\left[\bar{\mathbb{G}}_e\right] = \begin{bmatrix} \mathbb{I} & 2G\Delta\mathbf{e} \\ \mathbf{0} & 1 \end{bmatrix} \tag{5.78}$$

for an the elastic step, and

$$\left[\bar{\mathbb{G}}_p\right] = \begin{bmatrix} \mathbb{I} + \left[\dfrac{(a-1)}{\parallel \Delta\mathbf{e} \parallel^2}\right] \Delta\mathbf{e} \otimes \Delta\mathbf{e} & \dfrac{b}{\sqrt{\chi}} \dfrac{\Delta\mathbf{e}}{\parallel \Delta\mathbf{e} \parallel} \\ b\sqrt{\chi}\dfrac{\Delta\mathbf{e}}{\parallel \Delta\mathbf{e} \parallel} & a \end{bmatrix} \tag{5.79}$$

for a plastic step. The scalars a and b are

$$\begin{aligned} a &= \cosh\left(2G\sqrt{\chi} \parallel \Delta\mathbf{e} \parallel\right) \\ b &= \sinh\left(2G\sqrt{\chi} \parallel \Delta\mathbf{e} \parallel\right) \end{aligned}$$

while χ is given by (5.60) calculated in X_n^0, i.e. the last component of $\mathbf{X}_n$. Such a choice of χ is not only natural (we take its value at the start of the step) but also of simple application. More accurate and performing choices could be introduced, perhaps requiring some implicit calculation instead of the direct matrix product (5.77).

5.5.3 Solution algorithm

At every time step the numerical scheme is as follows:

1) suppose the step to be elastic and compute trial values following an elastic law

$$\mathbf{X}_{n+1}^{TR} = \bar{\mathbb{G}}_e \mathbf{X}_n \tag{5.80}$$

where the matrix $\bar{\mathbb{G}}_e$ is given by (5.78). If the trail solution is admissible, i.e.

$$\parallel \mathbf{X}_{n+1}^{TR} \parallel \leq \sigma_{y,0}\left(X_{0,n+1}^{TR}\right) \frac{H_{iso} + H_{kin} + 2G}{2G + H_{kin}} \tag{5.81}$$

then the history variables at the time step t_{n+1} are taken as the trial ones just calculated.

2) If the trail solution is not admissible, i.e. Equation (5.81) is violated, then the step is plastic. Being $\dot{\mathbf{e}}$ constant in each sub time interval, this means that the step can be divided into two parts: an elastic deformation followed by a plastic one. We represent with a scalar $\alpha \in [0, 1)$ the elastic time proportion of the step; for example $\alpha = 1/2$ means that the stress evolution is of elastic kind for the first half of the time interval, and plastic in the rest. Simple geometrical considerations allow us to compute α; without discussing the details, the obtained value is

$$\alpha = \frac{\sqrt{C^2 - DM} - C}{D} \tag{5.82}$$

where

$$\begin{cases} C = 2GX_{0,n}\left(\mathbf{X}_n^s\right) : \Delta\mathbf{e} \\ D = \left(2GX_{0,n} \parallel \Delta\mathbf{e} \parallel\right)^2 \\ M = \parallel \mathbf{X}_n^s \parallel^2 - \sigma_{y,0}^2 \left(X_{0,n}\right)^{2\varphi} \\ \varphi = \dfrac{2G + H_{kin} + H_{iso}}{2G + H_{kin}} \end{cases} \tag{5.83}$$

Computed α, $\mathbf{X}_{n+1}$ is updated in two steps.

- Calculate $\mathbf{X}_{n+1}^{TR}$ following an elastic law

$$\mathbf{X}_{n+1}^{TR} = \bar{\mathbb{G}}_e \mathbf{X}_n \tag{5.84}$$

with $\bar{\mathbb{G}}_e$ still given by (5.78), *but* where $\Delta\mathbf{e} = \alpha\,(\mathbf{e}_{n+1} - \mathbf{e}_n)$ instead of $\Delta\mathbf{e} = (\mathbf{e}_{n+1} - \mathbf{e}_n)$.

- Calculate $\mathbf{X}_{n+1}$ evolving from the new initial data $\mathbf{X}_{n+1}^{TR}$ following a plastic law:

$$\mathbf{X}_{n+1} = \bar{\mathbb{G}}_p \mathbf{X}_{n+1}^{TR} \tag{5.85}$$

with $\bar{\mathbb{G}}_p$ given by (5.78), where $\Delta\mathbf{e} = (1-\alpha)\,(\mathbf{e}_{n+1} - \mathbf{e}_n)$ instead of $\Delta\mathbf{e} = (\mathbf{e}_{n+1} - \mathbf{e}_n)$.
Observe that in such a framework purely plastic steps are simply those where the time proportion of elastic phase α is zero.

3) Whenever needed, calculate the relative stress and backstress as:

$$\boldsymbol{\Sigma} = \frac{\mathbf{X}^s}{X_0} \tag{5.86}$$

$$\boldsymbol{\alpha} = H_{kin}\mathbf{e}^p = H_{kin}\frac{2G\mathbf{e} - \boldsymbol{\Sigma}}{2G + H_{kin}} \tag{5.87}$$

The first one is immediately obtained from the definition of $\mathbf{X}$, while the second one follows from (5.4) and (5.5), observing that $\boldsymbol{\alpha} = H_{kin}\mathbf{e}^p$.

4) Finally, at the end of each step, update the constant $\chi = \chi(X_{0,n+1})$ used for the calculation of the matrix $\bar{\mathbb{G}}_p$.

Remark 3: Due to the approximation introduced assuming χ constant in each time step, during a plastic step Equation (5.69) is not exactly enforced (while in the BE method this is fulfilled). However, this discrepancy seems to resolve in very small numerical errors as shown in the examples that follow. A cure to this could be a radial projection of the solution on the yield surface at the end of each time step: this idea indeed leads to the development of the next algorithm (ENC algorithm). Nevertheless, it is observed that introducing such a correction does not change significantly the solution. In Section 5.7 two algorithms improved to be yield-consistent with no need of a radial projection at the end of plastic steps are presented.

5.5.4 ENN scheme elastoplastic consistent tangent operator

The algorithmically consistent tangent operator can be obtained properly linearizing the time-discrete procedure. To make notation more clear, the subscripts of all history variables evaluated at time t_{n+1} are omitted for brevity. Quantities evaluated at t_n are specified by the relative subscript.

From the definition of the generalized stress tensor $\mathbf{X}$ we get

$$\frac{\partial \mathbf{X}^s}{\partial \mathbf{e}} = \mathbf{\Sigma} \otimes \frac{\partial X_0}{\partial \mathbf{e}} + X_0 \frac{\partial \mathbf{\Sigma}}{\partial \mathbf{e}} \tag{5.88}$$

hence

$$\frac{\partial \mathbf{\Sigma}}{\partial \mathbf{e}} = \frac{1}{X_0} \left(\frac{\partial \mathbf{X}^s}{\partial \mathbf{e}} - \mathbf{\Sigma} \otimes \frac{\partial X_0}{\partial \mathbf{e}} \right) \tag{5.89}$$

For the elastic phase we immediately have

$$\frac{\partial \mathbf{X}^s}{\partial \mathbf{e}} = 2GX_0 \mathbb{I} \tag{5.90}$$

$$\frac{\partial X_0}{\partial \mathbf{e}} = \mathbf{0} \tag{5.91}$$

while in the plastic phase the result is slightly more complicated and can be found in the sequel.

For the deviatoric stress, Equation (5.5) provides

$$\frac{\partial \mathbf{s}}{\partial \mathbf{e}} = \frac{\partial \mathbf{\Sigma}}{\partial \mathbf{e}} + \frac{\partial \boldsymbol{\alpha}}{\partial \mathbf{e}} \tag{5.92}$$

and, recalling also Equation (5.87), it becomes

$$\frac{\partial \mathbf{s}}{\partial \mathbf{e}} = \frac{2G}{2G + H_{kin}} \frac{\partial \mathbf{\Sigma}}{\partial \mathbf{e}} + \frac{2GH_{kin}}{2G + H_{kin}} \mathbb{I} \tag{5.93}$$

We also have

$$\frac{\partial \mathbf{s}}{\partial \boldsymbol{\varepsilon}} = \frac{\partial \mathbf{s}}{\partial \mathbf{e}} \frac{\partial \mathbf{e}}{\partial \boldsymbol{\varepsilon}} = \frac{\partial \mathbf{s}}{\partial \mathbf{e}} \mathbb{I}_{\text{dev}} \tag{5.94}$$

Taking into account the volumetric part of the stress, from Equations (5.1), (5.2) and (5.3), we obtain the tangent operator

$$\mathbb{C}^{ep} = \frac{\partial \boldsymbol{\sigma}}{\partial \boldsymbol{\varepsilon}} = \frac{\partial \mathbf{s}}{\partial \boldsymbol{\varepsilon}} + K \left(\mathbf{I} \otimes \mathbf{I} \right) \tag{5.95}$$

Joining statements (5.89), (5.93), (5.94) and (5.95) we obtain

$$\frac{\partial \boldsymbol{\sigma}}{\partial \boldsymbol{\varepsilon}} = \frac{2G}{X_0(2G + H_{kin})} \left(\frac{\partial \mathbf{X}^s}{\partial \mathbf{e}} - \mathbf{\Sigma} \frac{\partial X_0}{\partial \mathbf{e}} \right) \mathbb{I}_{\text{dev}} + \frac{2GH_{kin}}{2G + H_{kin}} \mathbb{I}_{\text{dev}} + K \left(\mathbf{I} \otimes \mathbf{I} \right) \tag{5.96}$$

which in the elastic case simplifies to the usual

$$\frac{\partial \boldsymbol{\sigma}}{\partial \boldsymbol{\varepsilon}} = 2G\mathbb{I}_{\text{dev}} + K\left(\mathbf{I} \otimes \mathbf{I}\right) \tag{5.97}$$

and in the plastic one can be calculated substituting the fourth-order tensor $\partial \mathbf{X}^s/\partial \mathbf{e}$ and the second-order tensor $\partial X_0/\partial \mathbf{e}$, which can be deduced as follows. The fourth-order tangent tensor $\partial \mathbf{X}^s/\partial \mathbf{e}$ and the second-order tangent tensor $\partial X_0/\partial \mathbf{e}$ provide the tangent operator $\partial \boldsymbol{\sigma}/\partial \boldsymbol{\varepsilon}$ of the new algorithm during plastic or mixed elastoplastic steps (cf. Equation (5.96)). Remembering that purely plastic steps are a particular case within the range of mixed ones (see Section 5.5.3), we start analyzing the latter. We have, from (5.84)-(5.85),

$$\mathbf{X}_{n+1} = \bar{\mathbb{G}}_p \bar{\mathbb{G}}_e \mathbf{X}_n = \bar{\mathbb{G}}_p((1-\alpha)\Delta\mathbf{e})\, \bar{\mathbb{G}}_e(\alpha\Delta\mathbf{e})\, \mathbf{X}_n \tag{5.98}$$

where the tensors above are given by (5.78)-(5.79) and $\alpha = \alpha(\Delta\mathbf{e})$ is the "elastic step proportion" defined in (5.82). Consequently, following basic derivation rules, we have for mixed steps

$$\frac{\partial \mathbf{X}_{n+1}}{\partial \mathbf{e}} = \left[\tilde{\mathbb{A}}_1 + \tilde{\mathbb{A}}_2 + \tilde{\mathbb{A}}_3 + \tilde{\mathbb{A}}_4\right] \mathbf{X}_n \tag{5.99}$$

where the matrix operators

$$\begin{cases} \tilde{\mathbb{A}}_1 = \dfrac{\partial \bar{\mathbb{G}}_p}{\partial \Delta\mathbf{e}}[(1-\alpha)\Delta\mathbf{e}]\, \bar{\mathbb{G}}_e(\alpha\Delta\mathbf{e}) \\ \tilde{\mathbb{A}}_2 = \dfrac{\partial \bar{\mathbb{G}}_p}{\partial \alpha}[(1-\alpha)\Delta\mathbf{e}]\dfrac{\mathrm{d}\alpha}{\mathrm{d}\Delta\mathbf{e}}(\Delta\mathbf{e})\, \bar{\mathbb{G}}_e(\alpha\Delta\mathbf{e}) \\ \tilde{\mathbb{A}}_3 = \bar{\mathbb{G}}_p[(1-\alpha)\Delta\mathbf{e}]\, \dfrac{\partial \bar{\mathbb{G}}_e}{\partial \Delta\mathbf{e}}(\alpha\Delta\mathbf{e}) \\ \tilde{\mathbb{A}}_4 = \bar{\mathbb{G}}_p[(1-\alpha)\Delta\mathbf{e}]\, \dfrac{\partial \bar{\mathbb{G}}_e}{\partial\, \alpha}(\alpha\Delta\mathbf{e})\dfrac{\mathrm{d}\alpha}{\mathrm{d}\Delta\mathbf{e}}(\Delta\mathbf{e}) \end{cases} \tag{5.100}$$

From Equation (5.99) we can derive $\partial \mathbf{X}^s_{n+1}/\partial \mathbf{e}$ and $\partial \mathbf{X}_{0,n+1}/\partial \mathbf{e}$; in order to obtain the classical tangent operator, the obtained equations must be finally expressed as a linear function of the strain of the form (5.99), which is expressed as a linear function of $\mathbf{X}_n$. Doing so, we finally obtain that for mixed steps

$$\frac{\partial \mathbf{X}^s}{\partial \mathbf{e}} = (\mathbb{A}_1 + \mathbb{A}_2 + \mathbb{A}_3 + \mathbb{A}_4) \tag{5.101}$$

$$\frac{\partial X_0}{\partial \mathbf{e}} = (\mathbf{b}_1 + \mathbf{b}_2 + \mathbf{b}_3 + \mathbf{b}_4) \tag{5.102}$$

where the fourth-order tensors $\mathbb{A}$ and the second-order tensors $\mathbf{b}$ are described below without addressing the calculations.

For purely plastic steps, being α constantly equal to zero, we obtain the shorter formulation

$$\frac{\partial \mathbf{X}^s}{\partial \mathbf{e}} = \mathbb{A}_1 \tag{5.103}$$

$$\frac{\partial X_0}{\partial \mathbf{e}} = \mathbf{b}_1 \tag{5.104}$$

We start introducing (cf. (5.82) for M, D, C in each step) the $\boldsymbol{\upsilon} = \mathrm{d}\alpha/\mathrm{d}\Delta\mathbf{e}$ second-order tensor

$$\begin{cases} \boldsymbol{\upsilon} &= \phi_1 \dfrac{\mathrm{d}C}{\mathrm{d}\Delta\mathbf{e}} + \phi_2 \dfrac{\mathrm{d}D}{\mathrm{d}\Delta\mathbf{e}} \\ \phi_1 &= \dfrac{1}{D}\left(\dfrac{C}{\sqrt{C^2 - DM}} - 1\right) \\ \phi_2 &= -\dfrac{1}{D^2}\left(\dfrac{DM}{2\sqrt{C^2 - DM}} + \sqrt{C^2 - DM} - C\right) \\ \dfrac{\mathrm{d}C}{\mathrm{d}\Delta\mathbf{e}} &= 2GX_{0,n}\,\mathbf{X}_n^s \\ \dfrac{\mathrm{d}D}{\mathrm{d}\Delta\mathbf{e}} &= 2(2GX_{0,n})^2 \Delta\mathbf{e} \end{cases} \tag{5.105}$$

Let the scalars

$$\begin{cases} a = \cosh\left(2G(1-\alpha)\sqrt{\chi} \parallel \Delta\mathbf{e} \parallel\right) \\ b = \sinh\left(2G(1-\alpha)\sqrt{\chi} \parallel \Delta\mathbf{e} \parallel\right) \\ s = \dfrac{\Delta\mathbf{e} : \mathbf{X}_n^s}{\parallel \Delta\mathbf{e} \parallel} \\ k = 2G(1-\alpha)\sqrt{\chi} \\ \tilde{k} = -2G\sqrt{\chi} \parallel \Delta\mathbf{e} \parallel \end{cases} \tag{5.106}$$

and the operators

$$\begin{aligned} \mathbb{M}_1 = s\left(kb - 2\frac{a-1}{\parallel \Delta\mathbf{e} \parallel}\right)\left[\frac{\Delta\mathbf{e} \otimes \Delta\mathbf{e}}{\parallel \Delta\mathbf{e} \parallel^2}\right] \\ + \frac{(a-1)s}{\parallel \Delta\mathbf{e} \parallel}\,\mathbb{I} + \frac{a-1}{\parallel \Delta\mathbf{e} \parallel}\left[\frac{\Delta\mathbf{e} \otimes \mathbf{X}_n^s}{\parallel \Delta\mathbf{e} \parallel}\right] \end{aligned} \tag{5.107}$$

$$\mathbb{M}_2 = \left(ka - \frac{b}{\parallel \Delta\mathbf{e} \parallel}\right)\left[\frac{\Delta\mathbf{e} \otimes \Delta\mathbf{e}}{\parallel \Delta\mathbf{e} \parallel^2}\right] + \frac{b}{\parallel \Delta\mathbf{e} \parallel}\mathbb{I} \tag{5.108}$$

We then have, for the tensors in (5.101),

$$\begin{cases} \mathbb{A}_1 = \mathbb{M}_1 + \dfrac{X_{0,n}}{\sqrt{\chi}}\,\mathbb{M}_2 \\ \mathbb{A}_2 = \tilde{k}\left(bs + \dfrac{a}{\sqrt{\chi}}X_{0,n}\right)\left[\dfrac{\Delta\mathbf{e}\otimes\boldsymbol{\upsilon}}{\parallel \Delta\mathbf{e} \parallel}\right] \\ \mathbb{A}_3 = 2G\alpha X_{0,n}\left[\mathbb{I} + (a-1)\dfrac{\Delta\mathbf{e}\otimes\Delta\mathbf{e}}{\parallel \Delta\mathbf{e} \parallel^2}\right] \\ \mathbb{A}_4 = 2GaX_{0,n}\left[\,\Delta\mathbf{e}\otimes\boldsymbol{\upsilon}\right] \quad ; \end{cases} \tag{5.109}$$

and for the tensors appearing in (5.102)

$$\begin{cases} \mathbf{b}_1 = \sqrt{\chi}\;\mathbb{M}_2\mathbf{X}_n^s + kbX_{0,n}\dfrac{\Delta\mathbf{e}}{\parallel \Delta\mathbf{e} \parallel} \\ \mathbf{b}_2 = \tilde{k}\left(as\sqrt{\chi} + bX_{0,n}\right)\boldsymbol{\upsilon} \\ \mathbf{b}_3 = 2G\alpha bX_{0,n}\sqrt{\chi}\dfrac{\Delta\mathbf{e}}{\parallel \Delta\mathbf{e} \parallel} \\ \mathbf{b}_4 = 2GbX_{0,n}\sqrt{\chi}\parallel \Delta\mathbf{e} \parallel \boldsymbol{\upsilon} \end{cases} \tag{5.110}$$

5.6 ENC exponential-based integration scheme for the LP model

5.6.1 ENC scheme: an enforced consistency variant of the ENN scheme

As it is shown by the numerical tests carried out in the next chapter, when compared to the BE scheme and to the ESC algorithm which will be addressed in the next section, the ENN scheme shows far better precision properties and second-order accuracy. On the other hand, as already observed in [16], the ENN algorithm presented above is not consistent with the yield surface condition. In other words, at the end of plastic steps, condition (5.69) does not hold exactly for the numerical solution.

Apart from physical considerations, the above property is important also for the stability of the algorithm; whenever the numerical relative stress $\boldsymbol{\Sigma}$ falls out of the yield surface (i.e. $\parallel \boldsymbol{\Sigma}_{n+1} \parallel > \sigma_{y,n+1}$) this may lead to instabilities in the following time step. Therefore, in practical applications, it is recommendable to enforce the consistency at the end of each elastoplastic step. This can be achieved using a radial projection of the relative stress onto the yield surface in each time step in which $\parallel \boldsymbol{\Sigma}_{n+1} \parallel > \sigma_{y,n+1}$ by simply multiplying $\boldsymbol{\Sigma}_{n+1}$ by the rate $\sigma_{y,n+1}/\parallel \boldsymbol{\Sigma}_{n+1} \parallel$).

The ENC yield-consistent variant of the ENN scheme is implemented following this idea. The consistency check can be done either at the start of each step or at the end. It is to be pointed out that the algorithmical steps of this methods remain the same as the ones described in the previous section with respect to the ENN method. In particular, the enforced consistency variant ENC allows to use the same algorithmic consistent elastoplastic tangent operator calculated for the ENN scheme.

5.7 ESC-ESC^2 exponential-based integration schemes for the LP model

5.7.1 An innovative model formulation

In this section we present a new time-continuous model formulation for the differential algebraic problem under consideration [9, 10, 11]. This innovative statement of the problem represents a generalisation of the formulations presented in [6, 8] and thus constitutes an extension of the ones proposed in [44, 45, 16]. Such a formulation still allows to rewrite the system in the form

$$\dot{\mathbf{X}} = \mathbb{A}\mathbf{X} \tag{5.111}$$

which is the starting point for the numerical scheme developed in Section 5.7.2. As it will be cleared and substantiated on mathematical grounds by the theoretical analysis carried out in the next Section 5.8, one of the algorithms stemming from the present reformulation (ESC^2 algorithm) shows to be the "optimal" one within the exponential-based integration algorithms class for the LP elastoplastic model.

Combining Equations (5.4) and (5.5), we obtain

$$\mathbf{\Sigma} + \boldsymbol{\alpha} + 2G\mathbf{e}^p = 2G\mathbf{e} \tag{5.112}$$

which, taking the derivative in time, applying Equation (5.9) and rearranging terms gives

$$\dot{\mathbf{\Sigma}} = 2G\dot{\mathbf{e}} - (2G + H_{kin})\,\dot{\mathbf{e}}^p \tag{5.113}$$

Now, recalling the yield surface radius

$$\sigma_y = \sigma_{y,0} + H_{iso}\gamma \tag{5.114}$$

and that in the plastic phase

$$\mathbf{n} = \frac{\mathbf{\Sigma}}{\|\mathbf{\Sigma}\|} = \frac{\mathbf{\Sigma}}{\sigma_{y,0} + H_{iso}\gamma} = \frac{\mathbf{\Sigma}}{\sigma_y} \tag{5.115}$$

we may apply (5.7) obtaining

$$\dot{\mathbf{\Sigma}} + (2G + H_{kin}) \frac{\mathbf{\Sigma}}{\sigma_y} \dot{\gamma} = 2G\dot{\mathbf{e}} \tag{5.116}$$

which is a differential equation for $\mathbf{\Sigma}$ that is valid also during elastic phases ($\dot{\gamma} = 0$). Introducing the *scaled relative stress*

$$\bar{\mathbf{\Sigma}} = \frac{\mathbf{\Sigma}}{\sigma_y} \tag{5.117}$$

we observe that, whenever the relative stress $\mathbf{\Sigma}$ lays on the yield surface, then $\bar{\mathbf{\Sigma}} = \mathbf{n}$, while this is not true when $\mathbf{\Sigma}$ lays inside the yield surface. The time derivative of (5.117) and the use of relation (5.114) gives

$$\dot{\bar{\mathbf{\Sigma}}} = \frac{\dot{\mathbf{\Sigma}}}{\sigma_y} - \frac{H_{iso}}{\sigma_y} \dot{\gamma} \bar{\mathbf{\Sigma}} \tag{5.118}$$

Dividing Equation (5.116) by σ_y and using relationship (5.118), one obtains

$$\dot{\bar{\mathbf{\Sigma}}} + \frac{2G + H_{kin} + H_{iso}}{\sigma_y} \dot{\gamma} \bar{\mathbf{\Sigma}} = \frac{2G}{\sigma_y} \dot{\mathbf{e}} \tag{5.119}$$

The next goal is to introduce an *integration factor* for the above evolutionary equation. Accordingly, we set

$$X_0(\gamma) = \begin{cases} \left(1 + \dfrac{\gamma H_{iso}}{\sigma_{y,0}}\right)^{\dfrac{2G + H_{kin} + H_{iso}}{H_{iso}}} & \text{if } \; H_{iso} \neq 0 \\ \exp\left(\dfrac{2G + H_{kin} + H_{iso}}{\sigma_{y,0}} \gamma\right) & \text{if } \; H_{iso} = 0 \end{cases} \tag{5.120}$$

noting that such a function is continuous for fixed γ and $H_{iso} \to 0$ and that

$$\dot{X}_0 = \frac{2G + H_{kin} + H_{iso}}{\sigma_y} \dot{\gamma} X_0 \tag{5.121}$$

Multiplying Equation (5.119) by X_0 and using equation (5.121) the following relationship holds

$$\frac{\mathrm{d}}{\mathrm{d}t} \left[X_0 \bar{\mathbf{\Sigma}} \right] = X_0 \dot{\bar{\mathbf{\Sigma}}} + \dot{X}_0 \bar{\mathbf{\Sigma}} = \frac{2G}{\sigma_y} X_0 \dot{\mathbf{e}} \tag{5.122}$$

At this stage, defining the *generalized stress vector* $\mathbf{X}$ as

$$\{\mathbf{X}\} = \begin{Bmatrix} X_0\bar{\mathbf{\Sigma}} \\ X_0 \end{Bmatrix} = \begin{Bmatrix} \mathbf{X}^s \\ X_0 \end{Bmatrix} \tag{5.123}$$

Equation (5.122) can be rewritten as

$$\dot{\mathbf{X}}^s = \frac{2G}{\sigma_y} X_0 \dot{\mathbf{e}} \tag{5.124}$$

The evolution law for X_0 in terms of $\mathbf{X}$ in elastic phases follows immediately from (5.121):

$$\dot{X}_0 = 0 \qquad \text{(elastic phases)} \tag{5.125}$$

On the other hand, for $\dot{\gamma} \neq 0$, taking the scalar product of (5.122) with $\bar{\mathbf{\Sigma}}$, we have

$$X_0 \frac{1}{2}\frac{\mathrm{d}}{\mathrm{d}t}\|\bar{\mathbf{\Sigma}}\|^2 \; + \; \dot{X}_0\|\bar{\mathbf{\Sigma}}\|^2 = \frac{2G}{\sigma_y} X_0 \dot{\mathbf{e}} : \bar{\mathbf{\Sigma}} \tag{5.126}$$

which, noting that in plastic phases

$$\|\bar{\mathbf{\Sigma}}\| = \frac{\|\mathbf{\Sigma}\|}{\sigma_y} = 1 \tag{5.127}$$

and using (5.123), (5.126) gives

$$\dot{X}_0 = \frac{2G}{\sigma_y} \dot{\mathbf{e}} : \mathbf{X}^s \qquad \text{(plastic phases)} \tag{5.128}$$

Equations (5.124), (5.125) and (5.128) provide a system for the *generalized stress vector* $\mathbf{X}$, in the form

$$\dot{\mathbf{X}} = \mathbb{A}\mathbf{X} \tag{5.129}$$

with the matrix $\mathbb{A}$ depending on the actual phase as follows

$$[\mathbb{A}] = [\mathbb{A}_e] = \frac{2G}{\sigma_y} \begin{bmatrix} \mathbb{O} & \dot{\mathbf{e}} \\ \mathbf{O} & 0 \end{bmatrix} \qquad \text{(elastic phase)} \tag{5.130}$$

$$[\mathbb{A}] = [\mathbb{A}_p] = \frac{2G}{\sigma_y} \begin{bmatrix} \mathbb{O} & \dot{\mathbf{e}} \\ \dot{\mathbf{e}} & 0 \end{bmatrix} \qquad \text{(plastic phase)} \tag{5.131}$$

where $\mathbf{0}$ and $\mathbb{O}$ indicate respectively the second-order and fourth-order order null tensors. In the last statement, Equation (5.129), we have made use of the linear operator space structure introduced in the previous section (cf. Equations (5.63)-(5.65). Note that $\mathbb{A}$ is symmetric during plastic phases. Therefore

the original problem, expressed by Equations (5.4)-(5.9), has been substituted by a new one, expressed by Equations (5.129)-(5.131).

We also observe that in the case of no isotropic hardening ($H_{iso} = 0$) the yield radius σ_y is fixed and therefore $\mathbb{A}$ depends only on $\dot{\mathbf{e}}$. This means that, if $\dot{\mathbf{e}}$ is constant in a given time interval, $\mathbb{A}$ holds the same property: under such an hypothesis the solution of system (5.129) is known and the problem can be solved exactly.

However, in a general case ($H_{iso} \neq 0$) the matrix $\mathbb{A}$ depends on $\mathbf{X}$ and in this sense we say that the problem is quasi-linear. Anyway, the quasi-linearity arising in the problem is indeed of great value, allowing us to develop the numerical method of Section 5.7.2.

Time-continuous on-off switch

To properly convert the original problem in a new but equivalent differential algebraic format, we also need to introduce an elastoplastic phase determination criterium expressed in the new generalized stress environment.

For a given state to be plastic, the following two conditions must be fulfilled:

1) The relative stress $\mathbf{\Sigma}$ must be on the yield surface, in other words

$$\|\mathbf{\Sigma}\| = \sigma_y \tag{5.132}$$

Using (5.117) and (5.123) this can be easily rewritten as

$$\|\mathbf{X}^s\|^2 = \|\bar{\mathbf{\Sigma}}\|^2 X_0^2 = \frac{\|\mathbf{\Sigma}\|^2}{\sigma_y^2} X_0^2 = X_0^2 \tag{5.133}$$

2) The direction of the strain rate $\dot{\mathbf{e}}$ must be outward with respect to the yield surface, i.e.

$$\mathbf{\Sigma} : \dot{\mathbf{e}} > 0 \tag{5.134}$$

Again, recalling (5.117) and (5.123) it is immediate to check that (5.134) is equivalent to

$$\mathbf{X}^s : \dot{\mathbf{e}} > 0 \tag{5.135}$$

If the two conditions (5.133) and (5.135) are not satisfied, the step is elastic.

5.7.2 Integration scheme

We now want to develop a numerical scheme for the evolution of $\mathbf{X}$, governed by the dynamical law (5.129) with matrix $\mathbb{A}$ given by (5.130) or (5.131) respectively.

As usual, we assume that the time history interval $[0, T]$ is divided into N sub-intervals defined by the nodes $0 = t_0 < t_1 < .... < t_n < t_{n+1} < .... < t_N = T$ and indicate the general sub-interval amplitude as $\Delta t = t_{n+1} - t_n$. Given the values $\{\mathbf{s}_n, \mathbf{e}_n, \mathbf{e}_n^p, \gamma_n, \boldsymbol{\alpha}_n\}$ at time t_n and the deviatoric strain $\mathbf{e}_{n+1}$ at time t_{n+1}, we search for the remaining variables at time t_{n+1}, assuming the strain history to be piecewise linear. For simplicity, we consider the initial values (at $t = t_0$) of $\gamma, \mathbf{e}^p$ and $\boldsymbol{\alpha}$ to be zero, so that the initial *generalized stress vector* is

$$\{\mathbf{X}_0\} = \begin{Bmatrix} \boldsymbol{\Sigma}_0/\sigma_{y,0} \\ 1 \end{Bmatrix} \tag{5.136}$$

Due to the piecewise linearity of the strain path, $\dot{\mathbf{e}}$ is constant in each single time interval. Unluckily, due to the presence of σ_y in (5.131), during plastic phases, the matrix $\mathbb{A}$ is not constant in the same time interval; in fact the yield surface radius σ_y is a function of X_0, as shown by relation (5.121) and hence of $\mathbf{X}$. Therefore, we discretize the dynamical law (5.129), approximating σ_y stepwise. Along each time interval $[t_n, t_{n+1}]$, we choose $\sigma_y = R$, where R is now a constant value in each single time step. It is evident that for purely elastic steps R coincides with $\sigma_{y,n}$. The discrete form of the evolution law (5.129) becomes

$$\dot{\mathbf{X}} = \bar{\mathbb{A}}\mathbf{X} \tag{5.137}$$

where the matrix $\bar{\mathbb{A}}$ is now constant along a single time interval

$$[\bar{\mathbb{A}}] = \frac{2G}{\sigma_{y,n}} \begin{bmatrix} \mathbb{O} & \dot{\mathbf{e}} \\ \mathbf{0} & 0 \end{bmatrix} \qquad \text{(elastic step)} \tag{5.138}$$

$$[\bar{\mathbb{A}}] = \frac{2G}{R} \begin{bmatrix} \mathbb{O} & \dot{\mathbf{e}} \\ \dot{\mathbf{e}} & 0 \end{bmatrix} \qquad \text{(plastic step)} \tag{5.139}$$

Different choices for R are possible [11], for example

$$\begin{cases} R = \sigma_{y,n} & \text{(ESC } \textit{scheme}) \\ R = \dfrac{c\sigma_{y,n}}{\ln(1+c)} & \text{(ESC}^2 \textit{ scheme}) \end{cases} \tag{5.140}$$

where

$$c = \frac{2G\, q\, (1-\alpha) \left(\dfrac{\mathbf{X}_n^s}{X_{0,n}} : \dot{\mathbf{e}} \right)}{\sigma_{y,n}} \Delta t \tag{5.141}$$

with

$$q = \frac{H_{iso}}{2G + H_{kin} + H_{iso}} \tag{5.142}$$

The α scalar parameter represents the part of the step along which the stress remains within the limit surface (see Figure 5.3). Its calculation will be explained and discussed in detail in Section 5.7.3 for compactness reasons.

The first choice for R in (5.140) corresponds to the ESC scheme proposed in [8], the second one leads to the new ESC^2 scheme [11]. While the reasonings for the first choice for R are evident ("forward integration" scheme), the second choice for R comes from considerations regarding the improved numerical properties of the new exponential-based algorithm, discussed from the analytical standpoint in Section 5.8.

Due to the fact that R is computed using only quantities evaluated at the beginning of the step, the matrix $\bar{\mathbb{A}}$ is now constant in both elastic and plastic phases and so Equation (5.137) can be solved exactly, giving the following evolution for $\mathbf{X}$

$$\mathbf{X}_{n+1} = \exp\left[\bar{\mathbb{A}}\Delta t\right]\mathbf{X}_n = \bar{\mathbb{G}}\,\mathbf{X}_n \tag{5.143}$$

Note that, being $\bar{\mathbb{A}}$ an element in the linear space of linear operators acting on couples, the exponential of $\bar{\mathbb{A}}\Delta t$ is naturally defined by the (converging) exponential serie

$$\bar{\mathbb{G}} = \exp\left[\bar{\mathbb{A}}\Delta t\right] = \sum_{n=0}^{+\infty} \frac{\left(\bar{\mathbb{A}}\Delta t\right)^n}{n!} \tag{5.144}$$

Defining the tensor $\Delta\mathbf{e} = \mathbf{e}_{n+1} - \mathbf{e}_n$, we observe that the matrix $\bar{\mathbb{A}}\Delta t$ is equal to the matrix (5.138) or (5.139) after substituting $\dot{\mathbf{e}}$ with $\Delta\mathbf{e}$. The linear operator $\bar{\mathbb{G}}$ can be derived calculating the shown exponential. Note that, for such purpose, it is convenient to reformulate the linear operator $\bar{\mathbb{A}}\Delta t$ as a $\mathcal{R}^{7\times 7}$ matrix, calculate the exponential, and finally write it back in the original form (5.63). Without showing the calculations, one finds

$$\left[\bar{\mathbb{G}}\right] = \begin{cases} \left[\bar{\mathbb{G}}_e\right] = \begin{bmatrix} \mathbb{I} & \dfrac{2G}{\sigma_{y,n}}\Delta\mathbf{e} \\ \mathbb{O} & 1 \end{bmatrix} & \text{(elastic phase)} \\[2ex] \left[\bar{\mathbb{G}}_p\right] = \begin{bmatrix} \mathbb{I} + \left[\dfrac{(a-1)}{\|\Delta\mathbf{e}\|^2}\right]\Delta\mathbf{e}\otimes\Delta\mathbf{e} & b\dfrac{\Delta\mathbf{e}}{\|\Delta\mathbf{e}\|} \\ b\dfrac{\Delta\mathbf{e}}{\|\Delta\mathbf{e}\|} & a \end{bmatrix} & \text{(plastic phase)} \end{cases} \tag{5.145}$$

where the scalars a and b are

$$a = \cosh\left(\frac{2G}{R}\|\Delta\mathbf{e}\|\right) \tag{5.146}$$

$$b = \sinh\left(\frac{2G}{R}\|\Delta\mathbf{e}\|\right) \tag{5.147}$$

5.7.3 Solution algorithm

At every time step the exponential-based algorithm proceeds as follows:

1) suppose the step to be elastic and compute trial values following an elastic law

$$\mathbf{X}_{n+1}^{TR} = \bar{\mathbb{G}}_e \mathbf{X}_n \tag{5.148}$$

where the matrix $\bar{\mathbb{G}}_e$ is given by (5.145). If the trial solution is admissible, i.e.

$$\|\mathbf{X}_{n+1}^{s,TR}\| \leq \left(X_{0,n+1}^{TR}\right)^2 \tag{5.149}$$

then the history variables at the time step t_{n+1} are taken as the trial ones just calculated.

2) If the trial solution is not admissible, i.e. Equation (5.149) is violated, then the step is plastic or elastoplastic. Being $\dot{\mathbf{e}}$ constant in each time sub interval, the step can be divided into two parts: an elastic deformation taking place during $[t_n, t_{n+\alpha}]$, followed by a plastic one along $[t_{n+\alpha}, t_{n+1}]$. Hence, we represent with a scalar $\alpha \in [0, 1)$ the elastic time proportion of the step. The key consideration in order to calculate α is that the evolution during the partial elastic sub-step is linear in stress space. Accordingly, recalling (5.145), we search for an intermediate generalized stress vector

$$\mathbf{X}_{n+1}^{s,e} = \mathbf{X}_n^s + \frac{2GX_{0,n}}{\sigma_{y,n}}[\alpha\Delta\mathbf{e}] \tag{5.150}$$

such that $\mathbf{X}_{n+1}^{s,e}$ represents a relative stress tensor lying on the yield surface at time $t_{n+\alpha}$. In other words, we must request

$$\mathbf{X}_{n+1}^{s,e} : \mathbf{X}_{n+1}^{s,e} - X_{0,n}^2 = 0 \tag{5.151}$$

Note that the left hand side of the above equation is a second order polynomial in α. In stress space, the roots of such polynomial correspond to the intersections between a segment and the boundary of a sphere, where an extreme of the segment ($\mathbf{s}_n$) lays inside the sphere closure and the other extreme ($\mathbf{s}_n + 2G\Delta\mathbf{e}$) outside the sphere. As a consequence,

there is always one maximum (non-negative) root. Calculating therefore α from expression (5.151) we get

$$\alpha = \frac{\sqrt{C^2 - DM} - C}{D} \tag{5.152}$$

where

$$\begin{cases} C = \dfrac{2GX_{0,n}}{\sigma_{y,n}} \left(\mathbf{X}_n^s : \Delta\mathbf{e}\right) \\ D = \left(\dfrac{2GX_{0,n}\|\Delta\mathbf{e}\|}{\sigma_{y,n}}\right)^2 \\ M = \|\mathbf{X}_n^s\|^2 - \left(X_{0,n+1}^{TR}\right)^2 \end{cases} \tag{5.153}$$

Computed α, $\mathbf{X}_{n+1}$ is updated in two steps.

- Calculate a new $\mathbf{X}_{n+1}^e$ vector following an elastic law along an $\alpha\Delta t$ interval

$$\mathbf{X}_{n+1}^e = \bar{\mathbb{G}}_e[\alpha\Delta\mathbf{e}]\mathbf{X}_n \tag{5.154}$$

- Calculate $\mathbf{X}_{n+1}$ evolving from the new initial data $\mathbf{X}_{n+1}^e$ following a plastic law along the remaining part of the interval of amplitude $(1-\alpha)\Delta t$

$$\mathbf{X}_{n+1} = \bar{\mathbb{G}}_p[(1-\alpha)\Delta\mathbf{e}]\mathbf{X}_{n+1}^e \tag{5.155}$$

  Observe that in such a framework purely plastic steps are simply those where the time proportion of the elastic phase α is zero.

3) Update the yield surface radius

$$\sigma_{y,n+1} = \sigma_y(X_{0,n+1}) = \sigma_{y,0}\left(X_{0,n+1}\right)^q \tag{5.156}$$

which is easily obtained combining (5.114) and (5.120).

The updating procedure illustrated by steps 1) - 3) is represented in Figure 5.3 which refers to the space of tensors $\mathbf{X}^s$.

Remark 5.7.1 The relative stress and backstress can be calculated whenever needed as:

$$\mathbf{\Sigma} = \frac{\mathbf{X}^s}{X_0}\sigma_y \tag{5.157}$$

$$\boldsymbol{\alpha} = H_{kin}\frac{2G\mathbf{e} - \mathbf{\Sigma}}{2G + H_{kin}} \tag{5.158}$$

The first one is immediately obtained from the definition of $\mathbf{X}$, while the second one follows from (5.4) and (5.5), observing that $\boldsymbol{\alpha} = H_{kin}\mathbf{e}^p$.

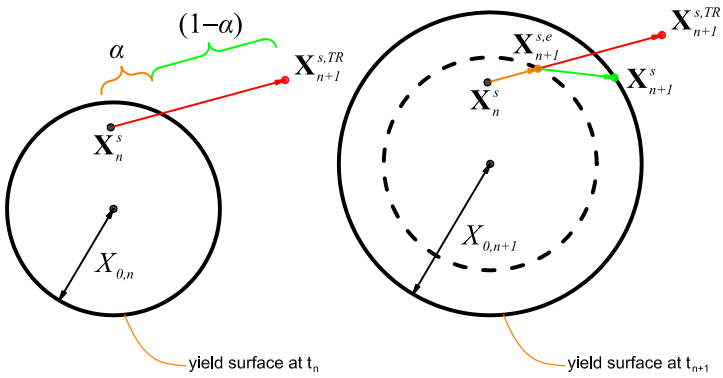

Figure 5.3: Updating procedure in generalized stress space for the ESC and ESC^2 scheme during a mixed elastoplastic step.

Remark 5.7.2 The variable X_0 is a local auxiliary variable and not an history variable. In other words, introducing an appropriate scaling of the vector $\mathbf{X}$ the variable X_0 does not need to be updated at every time step [8].

Remark 5.7.3 Whenever $H_{iso} = 0$, i.e. there is no isotropic hardening, the solution obtained with this scheme is exact. Other exact integrators can be found in the literature for the case $H_{iso} = 0$ [51, 67, 77]. A discussion of exponential-based exact integration schemes and other exact integrators can be found in [8].

5.7.4 ESC^2 scheme elastoplastic consistent tangent operator

In the following we present the tangent operator of the new optimal exponential-based ESC^2 integration scheme. For what concerns the ESC scheme, the reader is referred to [8] where a complete derivation of its tangent operator is developed. As it will be clear in the following, the tangent moduli operator corresponding to the ESC algorithm can be obtained in a straightforward manner by simply canceling the $\mathbb{A}_5$ and $\mathbf{e}_5$ terms arising in the new discrete formulation. To make notation more clear, the subscripts of all history variables evaluated at time t_{n+1} are omitted for brevity. Quantities evaluated either at t_n or at $t_{n+\alpha}$ are specified by the relative subscript.

We now present the tangent fourth-order tensor $\partial\mathbf{X}^s/\partial\mathbf{e}$ and the tangent second-order tensor $\partial X_0/\partial\mathbf{e}$ for plastic phases, which provide the elastoplastic consistent tangent operator $\mathbb{C}^{ep} = \dfrac{\partial\boldsymbol{\sigma}}{\partial\boldsymbol{\varepsilon}}$ of the new algorithm during plastic or

mixed elastoplastic steps.

Recalling that purely plastic steps are a particular case within the range of mixed ones (see Section 5.7.2), we start analyzing the latter. From (5.154)-(5.155), we have

$$\mathbf{X}_{n+1} = \bar{\mathbb{G}}_p \bar{\mathbb{G}}_e \mathbf{X}_n = \bar{\mathbb{G}}_p[(1-\alpha)\Delta\mathbf{e}, R]\, \bar{\mathbb{G}}_e[\alpha\Delta\mathbf{e}]\, \mathbf{X}_n \tag{5.159}$$

where the above matrix operators are given by (5.145) and α (which depends on $\Delta\mathbf{e}$) is the "elastic step proportion" defined in (5.152). Consequently, following basic differentiation rules, we have

$$\frac{\partial \mathbf{X}_{n+1}}{\partial \Delta\mathbf{e}} = \left[\tilde{\mathbb{A}}_1 + \tilde{\mathbb{A}}_2 + \tilde{\mathbb{A}}_3 + \tilde{\mathbb{A}}_4 + \tilde{\mathbb{A}}_5\right] \mathbf{X}_n \tag{5.160}$$

with

$$\begin{cases} \tilde{\mathbb{A}}_1 = \dfrac{\partial \bar{\mathbb{G}}_p}{\partial \Delta\mathbf{e}}[(1-\alpha)\Delta\mathbf{e}, R]\, \bar{\mathbb{G}}_e[\alpha\Delta\mathbf{e}] \\ \tilde{\mathbb{A}}_2 = \dfrac{\partial \bar{\mathbb{G}}_p}{\partial \alpha}[(1-\alpha)\Delta\mathbf{e}, R] \dfrac{\mathrm{d}\alpha}{\mathrm{d}\Delta\mathbf{e}}[\Delta\mathbf{e}]\, \bar{\mathbb{G}}_e[\alpha\Delta\mathbf{e}] \\ \tilde{\mathbb{A}}_3 = \bar{\mathbb{G}}_p[(1-\alpha)\Delta\mathbf{e}, R]\, \dfrac{\partial \bar{\mathbb{G}}_e}{\partial \Delta\mathbf{e}}[\alpha\Delta\mathbf{e}] \\ \tilde{\mathbb{A}}_4 = \bar{\mathbb{G}}_p[(1-\alpha)\Delta\mathbf{e}, R]\, \dfrac{\partial \bar{\mathbb{G}}_e}{\partial\, \alpha}[\alpha\Delta\mathbf{e}] \dfrac{\mathrm{d}\alpha}{\mathrm{d}\Delta\mathbf{e}}[\Delta\mathbf{e}] \\ \tilde{\mathbb{A}}_5 = \dfrac{\partial \bar{\mathbb{G}}_p}{\partial R}[(1-\alpha)\Delta\mathbf{e}, R] \dfrac{\partial R}{\partial \Delta\mathbf{e}}[\Delta\mathbf{e}, \sigma_{y,n}]\, \bar{\mathbb{G}}_e[\alpha\Delta\mathbf{e}] \end{cases} \tag{5.161}$$

From Equation (5.160) we derive $\partial \mathbf{X}^s_{n+1}/\partial\mathbf{e}$ and $\partial X_{0,n+1}/\partial\mathbf{e}$; in order to obtain the classical tangent operator, the obtained equations must be finally expressed as a linear function of the strain tensor instead of the form (5.160), which is expressed as a linear function of $\mathbf{X}_n$. Doing so, we finally obtain that for mixed steps

$$\frac{\partial \mathbf{X}^s}{\partial \mathbf{e}} = \mathbb{A}_1 + \mathbb{A}_2 + \mathbb{A}_3 + \mathbb{A}_4 + \mathbb{A}_5 \tag{5.162}$$

$$\frac{\partial \mathbf{X}_0}{\partial \mathbf{e}} = \mathbf{b}_1 + \mathbf{b}_2 + \mathbf{b}_3 + \mathbf{b}_4 + \mathbf{b}_5 \tag{5.163}$$

where the fourth-order tensors $\mathbb{A}$ and the second-order tensors $\mathbf{b}$ are described below without addressing the calculations.

For purely plastic steps, being α constantly equal to zero, we obtain the shorter formulation

$$\frac{\partial \mathbf{X}^s}{\partial \mathbf{e}} = \mathbb{A}_1 \tag{5.164}$$

$$\frac{\partial X_0}{\partial \mathbf{e}} = \mathbf{b}_1 \tag{5.165}$$

We start introducing (see again (5.152) for M, D, C in each step) the second-order tensor $\boldsymbol{\upsilon} = \mathrm{d}\alpha/\mathrm{d}\Delta\mathbf{e}$

$$\begin{cases} \boldsymbol{\upsilon} &= \phi_1 \dfrac{\mathrm{d}C}{\mathrm{d}\Delta\mathbf{e}} + \phi_2 \dfrac{\mathrm{d}D}{\mathrm{d}\Delta\mathbf{e}} \\ \phi_1 &= \dfrac{1}{D}\left(\dfrac{C}{\sqrt{C^2 - DM}} - 1\right) \\ \phi_2 &= -\dfrac{1}{D^2}\left(\dfrac{DM}{2\sqrt{C^2 - DM}} + \sqrt{C^2 - DM} - C\right) \\ \dfrac{\mathrm{d}C}{\mathrm{d}\Delta\mathbf{e}} &= \dfrac{2G}{\sigma_{y,n}} X_{0,n}\, \mathbf{X}_n^s \\ \dfrac{\mathrm{d}D}{\mathrm{d}\Delta\mathbf{e}} &= 2(\dfrac{2G}{\sigma_{y,n}} X_{0,n})^2 \Delta\mathbf{e} \end{cases} \tag{5.166}$$

and the second-order tensor $\mathbf{w}$

$$\begin{cases} \mathbf{w} &= p\,(\mathbf{w_1} + \mathbf{w_2}) \\ p &= \dfrac{-\sigma_{y,n}}{[c^{-1}\ln(1+c)]^2}\left[\dfrac{1}{c(1+c)} - \dfrac{\ln(1+c)}{c^2}\right] \\ p_1 &= \dfrac{2Gq}{\sigma_{y,n}}\,(\Delta\mathbf{e} : \mathbf{X}_n^s) \\ p_2 &= \left(\dfrac{2G}{\sigma_{y,n}}\right)^2 q(1-\alpha)\|\Delta\mathbf{e}\|^2 \\ \mathbf{w_1} &= (1-\alpha)\dfrac{2Gq}{\sigma_{y,n}}\mathbf{X}_n^s - p_1\boldsymbol{\upsilon} \\ \mathbf{w_2} &= p_2\boldsymbol{\upsilon} + \left(\dfrac{2G}{\sigma_{y,n}}\right)^2 q(1-\alpha)\Delta\mathbf{e} \end{cases} \tag{5.167}$$

Introducing the scalars

$$\begin{cases} a = \cosh\left(\dfrac{2G}{R}(1-\alpha)\|\Delta\mathbf{e}\|\right) \\ b = \sinh\left(\dfrac{2G}{R}(1-\alpha)\|\Delta\mathbf{e}\|\right) \\ s = \dfrac{\Delta\mathbf{e} : \mathbf{X}_n^s}{\|\Delta\mathbf{e}\|} \\ k = \dfrac{2G}{R}(1-\alpha) \\ \tilde{k} = -\dfrac{2G}{R}\|\Delta\mathbf{e}\| \end{cases} \tag{5.168}$$

and the fourth-order tensors

$$\begin{aligned}\mathbb{M}_1 = s\left(kb - 2\frac{a-1}{\parallel \Delta\mathbf{e} \parallel}\right)\left[\frac{\Delta\mathbf{e}\otimes\Delta\mathbf{e}}{\parallel \Delta\mathbf{e} \parallel^2}\right] \\ + \frac{(a-1)s}{\parallel \Delta\mathbf{e} \parallel}\,\mathbb{I} + \frac{a-1}{\parallel \Delta\mathbf{e} \parallel}\left[\frac{\Delta\mathbf{e}\otimes\mathbf{X}_n^s}{\parallel \Delta\mathbf{e} \parallel}\right]\end{aligned} \tag{5.169}$$

$$\mathbb{M}_2 = \left(ka - \frac{b}{\parallel \Delta\mathbf{e} \parallel}\right)\left[\frac{\Delta\mathbf{e}\otimes\Delta\mathbf{e}}{\parallel \Delta\mathbf{e} \parallel^2}\right] + \frac{b}{\parallel \Delta\mathbf{e} \parallel}\mathbb{I} \tag{5.170}$$

We can show that the tensors appearing in (5.162) are

$$\begin{cases}\mathbb{A}_1 = \mathbb{M}_1 + X_{0,n}\,\mathbb{M}_2 \\ \mathbb{A}_2 = \tilde{k}\,(bs + aX_{0,n})\left[\dfrac{\Delta\mathbf{e}\otimes\boldsymbol{v}}{\parallel \Delta\mathbf{e} \parallel}\right] \\ \mathbb{A}_3 = \dfrac{2G}{R}\alpha X_{0,n}\left[\mathbb{I} + (a-1)\dfrac{\Delta\mathbf{e}\otimes\Delta\mathbf{e}}{\parallel \Delta\mathbf{e} \parallel^2}\right] \\ \mathbb{A}_4 = \dfrac{2G}{R}aX_{0,n}\,[\,\Delta\mathbf{e}\otimes\boldsymbol{v}] \\ \mathbb{A}_5 = -\dfrac{k}{R}\left(\dfrac{bs}{\|\Delta\mathbf{e}\|^2} + a\right)[\,\Delta\mathbf{e}\otimes\mathbf{w}]\end{cases} \tag{5.171}$$

while the second-order tensors in (5.163) are

$$\begin{cases}\mathbf{b}_1 = \mathbb{M}_2\mathbf{X}_n^s + kbX_{0,n}\dfrac{\Delta\mathbf{e}}{\parallel \Delta\mathbf{e} \parallel} \\ \mathbf{b}_2 = \tilde{k}\,(as + bX_{0,n})\,\boldsymbol{v} \\ \mathbf{b}_3 = \dfrac{2G}{R}\alpha bX_{0,n}\dfrac{\Delta\mathbf{e}}{\parallel \Delta\mathbf{e} \parallel} \\ \mathbf{b}_4 = \dfrac{2G}{R}bX_{0,n}\parallel \Delta\mathbf{e} \parallel \boldsymbol{v} \\ \mathbf{b}_5 = -\dfrac{k}{R}\left(\dfrac{as}{\|\Delta\mathbf{e}\|} + b\|\Delta\mathbf{e}\|\right)\mathbf{w}\end{cases} \tag{5.172}$$

5.8 Theoretical analysis of algorithmical properties of the ESC and ESC^2 schemes

In this section we address from a theoretical point of view the following algorithmical properties for the ESC and ESC^2 methods: yield consistency, exactness under proportional loading, accuracy and convergence. In particular

we prove that the ESC scheme is yield consistent and converging with linear rate to the exact solution. The ESC^2 scheme is yield consistent, exact in the case of proportional loading and quadratically accurate. Moreover, limiting the proof to purely plastic load histories, we show that the ESC^2 scheme is quadratically convergent. Although purely plastic loadings are not uncommon in practical cases, a more complete approach should deal with generic loading histories; hence, this point is worth further investigation.

Finally, both schemes are exact in the case of materials with no isotropic hardening. Note that the word "exact" means that the algorithm introduces no error for strain driven load histories under the classical hypothesis $\dot{\mathbf{e}}$ piecewise constant. In practical applications this does not translate directly into exactness of the constitutive solver. This point will be cleared by the numerical tests and it will be briefly discussed in the following sections.

For basic results and definitions regarding the numerical integration of ordinary differential equations we refer for example to [39, 52].

5.8.1 Yield consistency

In the framework of the new formulation, recalling (5.117) and (5.123), the yield consistency condition

$$\|\mathbf{\Sigma}_{n+1}\| = \sigma_{y,n+1} \quad \text{at end of each plastic step} \tag{5.173}$$

becomes

$$\|\mathbf{X}^s_{n+1}\|^2 - X^2_{0,n+1} = 0 \quad \text{at end of each plastic step} \tag{5.174}$$

Both the ESC and ESC^2 schemes are yield consistent, in other words satisfy condition (5.174). The proof for the ESC^2 is identical to the one for the ESC method, which is shown in [8].

5.8.2 Exactness whenever $H_{iso} = 0$

Both the ESC and ESC^2 schemes are exact whenever there is no isotropic hardening. The proof of this property is immediate, considering that in such cases the matrix operators (5.130)-(5.131) are constant in each time step. For other methods with this property see References [51, 77].

5.8.3 Exactness under proportional loading

Assume as usual a piecewise linear strain history. We then say that a particular algorithmical time step develops under proportional loading if during the whole

step

$$\mathbf{\Sigma}(t) = r(t)\mathbf{\Sigma}_0 \tag{5.175}$$

where $\mathbf{\Sigma}_0$ is the initial stress and $r(t)$ is a scalar depending on time. It is easy to check that the definition above implies

$$\dot{\mathbf{e}} = \|\dot{\mathbf{e}}\|\frac{\mathbf{\Sigma}_0}{\|\mathbf{\Sigma}_0\|} = \|\dot{\mathbf{e}}\|\frac{\mathbf{\Sigma}}{\|\mathbf{\Sigma}\|} \tag{5.176}$$

during the time step. As noted in [8], the backward Euler method combined with a return map algorithm is exact in the case of proportional loading, while this same property in not shared by the ESC scheme. This means that, if a given time step develops under proportional loading, then the solution obtained with the return map will be identical to the continuous solution with the same initial step conditions. As shown in the following proposition, differently frmm the ESC scheme, the ESC^2 method has the advantage of being exact in the case of proportional loading.

We have the following

Proposition 5.8.1 *The* ESC^2 *algorithm is exact in the case of proportional loading.*

Proof: It is trivial to show that the scheme is exact during the elastic part of each time step; therefore what has to be proved is that the algorithm is exact also in the plastic part of each step. In the case of purely plastic steps ($\alpha = 0$) this follows from Lemma 5.8.2 below, while the general case ($\alpha > 0$) follows applying a trivial modification of the same Lemma.

□

In the sequel, we will call the *direction* of a vector $\mathbf{v} \in \mathcal{R}^n$ the normalized unit vector $\mathbf{v}/\|\mathbf{v}\|$.

Lemma 5.8.2 *Consider a purely plastic step under proportional loading. Then the solution obtained with the* ESC^2 *is identical to the continuous solution with the same initial step conditions.*

Proof: as usual we mark with the subindex n the values at the start of the step, which are assumed assigned. Note that, being the step purely plastic, the initial relative stress $\mathbf{\Sigma}_n$ lays on the yield surface. As already noted, the proportional loading assumption implies that during the step

$$\dot{\mathbf{e}} \;=\; \|\dot{\mathbf{e}}\|\frac{\mathbf{\Sigma}_n}{\|\mathbf{\Sigma}_n\|} \tag{5.177}$$

or equivalently

$$\Delta\mathbf{e} \;=\; \|\Delta\mathbf{e}\|\frac{\mathbf{\Sigma}_n}{\|\mathbf{\Sigma}_n\|} \tag{5.178}$$

In the case of proportional loading the continuous solution can be checked to be equal to

$$\mathbf{\Sigma}^{ex}_{n+1} \;=\; \frac{\mathbf{\Sigma}_n}{\|\mathbf{\Sigma}_n\|}\,\sigma^{ex}_{y,n+1} \tag{5.179}$$

$$\sigma^{ex}_{y,n+1} \;=\; \sigma_{y,n} + 2G\,q\|\Delta\mathbf{e}\| \tag{5.180}$$

where here and in the sequel the index e is used to indicate the exact solution.

The value of the backstress $\boldsymbol{\alpha}$ at any instant can be immediately derived from the value of $\mathbf{\Sigma}$ and relation (5.158); this is true both for the continuous and the numerical solution. Similarly, the remaining variables can be obtained from the usual relations (5.3)-(5.10). Therefore all that has to be checked in order to state the Lemma is that the value $\mathbf{\Sigma}_{n+1}$ obtained with the ESC^2 algorithm is equal to $\mathbf{\Sigma}^{ex}_{n+1}$.

This will be done in two steps. The first is to prove that the direction of $\mathbf{\Sigma}_{n+1}$ is the same as the one of $\mathbf{\Sigma}^{ex}_{n+1}$, in other words that the direction of $\mathbf{\Sigma}_{n+1}$ is equal to $\mathbf{\Sigma}_n/\|\mathbf{\Sigma}_n\|$. The second step is to show that the norm of $\mathbf{\Sigma}_{n+1}$ is the same as the one of $\mathbf{\Sigma}^{ex}_{n+1}$, in other words that the norm of $\mathbf{\Sigma}_{n+1}$ is equal to $\sigma^{ex}_{y,n+1}$.

Step1: by definition of $\mathbf{X}^s_n$ and recalling that $\|\mathbf{\Sigma}_n\| = \sigma_{y,n}$ we have

$$\mathbf{X}^s_n = X_{0,n}\frac{\mathbf{\Sigma}_n}{\|\mathbf{\Sigma}_n\|} \tag{5.181}$$

Applying the algorithm (see (5.145) and (5.155)), we get

$$\mathbf{X}^s_{n+1} = \mathbf{X}^s_n + \left(\left[\frac{(a-1)}{\|\Delta\mathbf{e}\|^2}\right]\,\Delta\mathbf{e} : \mathbf{X}^s_n + \frac{bX_{0,n}}{\|\Delta\mathbf{e}\|}\right)\Delta\mathbf{e} \tag{5.182}$$

where

$$a \;=\; \cosh\left(\frac{2G}{R}\|\Delta\mathbf{e}\|\right) \tag{5.183}$$

$$b \;=\; \sinh\left(\frac{2G}{R}\|\Delta\mathbf{e}\|\right) \tag{5.184}$$

with R defined in (5.140). Joining (5.182) with (5.178) and (5.181) immediately gives that $\mathbf{X}^s_{n+1}$ is of the form

$$\mathbf{X}^s_{n+1} = \psi\frac{\mathbf{\Sigma}_n}{\|\mathbf{\Sigma}_n\|} \qquad \psi \in \mathcal{R} \tag{5.185}$$

which immediately implies

$$\frac{\mathbf{X}^s_{n+1}}{\|\mathbf{X}^s_{n+1}\|} = \frac{\mathbf{\Sigma}_n}{\|\mathbf{\Sigma}_n\|} \tag{5.186}$$

First from definitions (5.117) and (5.123), then from (5.186) and finally using (5.179), we obtain

$$\frac{\mathbf{\Sigma}_{n+1}}{\|\mathbf{\Sigma}_{n+1}\|} = \frac{\mathbf{X}^s_{n+1}}{\|\mathbf{X}^s_{n+1}\|} = \frac{\mathbf{\Sigma}_n}{\|\mathbf{\Sigma}_n\|} = \frac{\mathbf{\Sigma}^{ex}_{n+1}}{\|\mathbf{\Sigma}^{ex}_{n+1}\|} \tag{5.187}$$

This completes the first part of the proof.

Step2: being the step plastic and due to the consistency of the scheme, we have

$$\|\mathbf{\Sigma}_{n+1}\| = \sigma_{y,n+1} \tag{5.188}$$

which, recalling relation (5.156) and with simple algebra, gives

$$\|\mathbf{\Sigma}_{n+1}\| = \sigma_{y,n+1} = \sigma_{y,0}\left(X_{0,n+1}\right)^q = \sigma_{y,0}\left(X_{0,n}\right)^q \left(\frac{X_{0,n+1}}{X_{0,n}}\right)^q = \sigma_{y,n}\left(\frac{X_{0,n+1}}{X_{0,n}}\right)^q \tag{5.189}$$

Again applying the algorithm (see (5.145) and (5.155)), we get

$$X_{0,n+1} = b\frac{\Delta\mathbf{e} : \mathbf{X}^s_n}{\|\Delta\mathbf{e}\|} + aX_{0,n} \tag{5.190}$$

Substituting (5.178) and (5.181) in (5.190) and dividing by $X_{0,n}$ gives immediately

$$\frac{X_{0,n+1}}{X_{0,n}} = b\|\Delta\mathbf{e}\|\frac{\dfrac{\mathbf{\Sigma}_n}{\|\mathbf{\Sigma}_n\|} : \dfrac{\mathbf{\Sigma}_n}{\|\mathbf{\Sigma}_n\|}}{\|\Delta\mathbf{e}\|} + a = b + a \tag{5.191}$$

which by definition of a and b gives

$$\frac{X_{0,n+1}}{X_{0,n}} = \exp\left(\frac{2G}{R}\|\Delta\mathbf{e}\|\right) \tag{5.192}$$

Substituting (5.192) into (5.189) we obtain

$$\|\mathbf{\Sigma}_{n+1}\| = \sigma_{y,n}\exp\left(\frac{2G\,q}{R}\|\Delta\mathbf{e}\|\right) \tag{5.193}$$

Due to (5.179)-(5.180) and (5.193), in order to show that

$$\|\mathbf{\Sigma}_{n+1}\| = \|\mathbf{\Sigma}^{ex}_{n+1}\| \tag{5.194}$$

and conclude the proof of the Lemma, it suffices to show that

$$\sigma_{y,n} \exp\left(\frac{2G\,q}{R}\|\Delta\mathbf{e}\|\right) = \sigma_{y,n} + 2G\,q\|\Delta\mathbf{e}\| \tag{5.195}$$

Identity (5.195) follows from a direct calculation and the definition of R in (5.140), observing that from (5.178) and (5.181)

$$c = \frac{2G\,q\,\|\Delta\mathbf{e}\|}{\sigma_{y,n}} \tag{5.196}$$

□

5.8.4 Accuracy

In this section we analyze the accuracy of the methods ESC and ESC^2.

It is easy to check that the function $R(\Delta t)$, defined in (5.140), is continuous even in $\Delta t = 0$. Moreover, it holds the following result which will be useful in the sequel.

Lemma 5.8.3 *Let $\alpha = 0$ (purely plastic step). Then the (right) derivative in $\Delta t = 0$ of the function $R(\Delta t)$ defined in (5.140) is well defined and equal to*

$$\dot{R}(0) = \frac{\dot{\sigma}_y(t_n)}{2} \tag{5.197}$$

Moreover, it exists the second (right) derivative in zero of $R(\Delta t)$.

Applying the definition of derivative and (5.140) we obtain

$$\begin{aligned}\dot{R}(0) &= \lim_{\Delta t\to 0}\frac{R(\Delta t)-R(0)}{\Delta t} = \sigma_{y,n}\lim_{\Delta t\to 0}\frac{c-\ln(1+c)}{\ln(1+c)\Delta t}\\ &= \sigma_{y,n}\lim_{\Delta t\to 0}\frac{c^2/2}{c\,\Delta t} = \frac{2G\,q}{2}\,\frac{\mathbf{X}_n^s}{X_{0,n}} : \dot{\mathbf{e}}\end{aligned} \tag{5.198}$$

where we also used the condition $\alpha = 0$. Due to definition (5.123), identity (5.198) gives

$$\dot{R}(0) = \frac{2G\,q}{2}\,\frac{\mathbf{\Sigma}_n}{\|\mathbf{\Sigma}_n\|} : \dot{\mathbf{e}} \tag{5.199}$$

Recalling that we are considering a plastic phase, a direct derivation gives

$$\dot{\sigma}_y = \frac{d}{dt}\|\mathbf{\Sigma}\| = \frac{\mathbf{\Sigma}}{\|\mathbf{\Sigma}\|} : \dot{\mathbf{\Sigma}} \tag{5.200}$$

Starting from the von-Mises constitutive equations, in Section 4 of [16] it is shown that in plastic phases

$$\dot{\mathbf{\Sigma}} + (2G + H_{kin}) \frac{\mathbf{\Sigma}}{\sigma_{y,0} + H_{iso}\gamma} \dot{\gamma} = 2G\dot{\mathbf{e}} \tag{5.201}$$

$$(\sigma_{y,0} + H_{iso}\gamma)\ (2G + H_{kin} + H_{iso})\, \dot{\gamma} = 2G\dot{\mathbf{e}} : \mathbf{\Sigma} \tag{5.202}$$

Extracting the expression for $\dot{\gamma}$ in (5.202) and using it in (5.201), we immediately obtain an equation for $\dot{\mathbf{\Sigma}}$; then, taking the scalar product with $\mathbf{\Sigma}/\|\mathbf{\Sigma}\|$ we get

$$\dot{\mathbf{\Sigma}} : \frac{\mathbf{\Sigma}}{\|\mathbf{\Sigma}\|} = 2G\dot{\mathbf{e}} : \frac{\mathbf{\Sigma}}{\|\mathbf{\Sigma}\|} - \frac{(2G + H_{kin})\, \mathbf{\Sigma} : \mathbf{\Sigma}}{\|\mathbf{\Sigma}\|\, (\sigma_{y,0} + H_{iso}\gamma)} \frac{2G\dot{\mathbf{e}} : \mathbf{\Sigma}}{(\sigma_{y,0} + H_{iso}\gamma)\ (2G + H_{kin} + H_{iso})} \tag{5.203}$$

Recalling that $\sigma_{y,0} + \gamma H_{iso} = \|\mathbf{\Sigma}\|$, Equation (5.203) immediately simplifies to

$$\dot{\mathbf{\Sigma}} : \frac{\mathbf{\Sigma}}{\|\mathbf{\Sigma}\|} = 2G\, q\, \dot{\mathbf{e}} : \frac{\mathbf{\Sigma}}{\|\mathbf{\Sigma}\|} \tag{5.204}$$

Equations (5.200) and (5.204) give at time t_n

$$\dot{\sigma}_y(t_n) = 2G\, q\, \dot{\mathbf{e}} : \frac{\mathbf{\Sigma}_n}{\|\mathbf{\Sigma}_n\|} \tag{5.205}$$

which joined with (5.199) proves (5.197).

Finally, the last statement of the Lemma can be derived from the definition of second order derivative

$$\ddot{R}(0) = \lim_{\Delta t \to 0^+} \frac{\dot{R}(\Delta t) - \dot{R}(0)}{\Delta t} \tag{5.206}$$

calculating the value of $\dot{R}(\Delta t)$ directly from (5.140), using (5.199) for the value of $\dot{R}(0)$ and then calculating the limit in (5.206).

□

We are now ready to present the following accuracy result.

Proposition 5.8.4 *The* ESC^2 *scheme holds quadratic accuracy, in other words the truncation error is of order* $(\Delta t)^2$ *with* Δt *size of the time step. The* ESC *scheme holds instead linear accuracy.*

Proof: We will show the proof only in the case of the ESC^2 method; the proof for the ESC scheme is simpler and follows similar steps. As usual, it is sufficient to show that the truncation error for the relative stress $\mathbf{\Sigma}$ is quadratic; the

result for the back stress $\boldsymbol{\alpha}$ follows from relation (5.158). Therefore, assuming all the variables at time t_n as given, we want to show that

$$T_n = \frac{\|\boldsymbol{\Sigma}^{ex}_{n+1} - \boldsymbol{\Sigma}_{n+1}\|}{\Delta t} \;=\; O(\Delta t^2) \tag{5.207}$$

where $\boldsymbol{\Sigma}^{ex}_{n+1}$ is the exact solution for the given initial data at time t_{n+1} and $\boldsymbol{\Sigma}_{n+1}$ the solution obtained with the ESC^2 scheme for the same initial data at time t_{n+1}.

We will start showing that

$$\|\mathbf{X}^{ex}_{n+1} - \mathbf{X}_{n+1}\| \;=\; O(\Delta t^3) \tag{5.208}$$

where again $\mathbf{X}^{ex}_{n+1}$ represents the exact generalized stress for the given initial data at time t_{n+1} and $\mathbf{X}_{n+1}$ the solution obtained with the ESC^2 algorithm for the same initial data.

Recalling that the scheme is exact during elastic phases, it is sufficient to prove the proposition for purely plastic steps. The result for mixed elastoplastic steps will then follow trivially considering the plastic part of the step as a purely plastic step with smaller Δt. We assume therefore a purely plastic step (i.e. $\alpha = 0$) with given initial data at time t_n.

Then, from (5.111), the exact value of the *generalized stress*

$$\mathbf{X}^{ex}_{n+1} = \mathbf{X}^{ex}(t_{n+1}) = \mathbf{X}^{ex}(t_n + \Delta t) \tag{5.209}$$

is the solution at time $t_n + \Delta t$ of the dynamical system

$$\begin{cases} \mathbf{X}^{ex}(t_n) = \mathbf{X}_n \\[2ex] \dot{\mathbf{X}}^{ex}(t) = \dfrac{2G}{\sigma_y}\,\mathbb{B}\,\mathbf{X}^{ex}(t) \qquad t \in [t_n, t_n + \Delta t] \end{cases} \tag{5.210}$$

where the matrix operator

$$[\mathbb{B}] = \begin{bmatrix} \mathbb{O} & \dot{\mathbf{e}} \\ \dot{\mathbf{e}} & 0 \end{bmatrix} \tag{5.211}$$

and where we recall that σ_y may vary in time. Following instead the scheme ESC^2, the value of the *generalized stress*

$$\mathbf{X}_{n+1} = \mathbf{X}(t_{n+1}) = \mathbf{X}(t_n + \Delta t) \tag{5.212}$$

is

$$\mathbf{X}(t_n + \Delta t) = \exp\left(\frac{2G}{R}\,\mathbb{B}\,\Delta t\right)\mathbf{X}_n \tag{5.213}$$

where $R = R(\Delta t)$ depends on Δt as shown in (5.140).

It can be checked after some calculation that both $\mathbf{X}^{ex}(t_n+\Delta t)$ and $\mathbf{X}(t_n+\Delta t)$ are C^3 regular as functions of Δt, even in $\Delta t = 0$. Therefore a truncated Taylor expansion immediately leads to

$$\mathbf{X}^{ex}(t_n+\Delta t) = \mathbf{X}^{ex}(t_n) + \frac{d\mathbf{X}^{ex}}{d\Delta t}(t_n)\Delta t + \frac{d^2\mathbf{X}^{ex}}{d\Delta t^2}(t_n)\frac{\Delta t^2}{2} + O(\Delta t^3) \tag{5.214}$$

$$\mathbf{X}(t_n+\Delta t) = \mathbf{X}(t_n) + \frac{d\mathbf{X}}{d\Delta t}(t_n)\Delta t + \frac{d^2\mathbf{X}}{d\Delta t^2}(t_n)\frac{\Delta t^2}{2} + O(\Delta t^3) \tag{5.215}$$

As a consequence, in order to prove (5.208), we must show that

$$\mathbf{X}^{ex}(t_n) = \mathbf{X}(t_n) \tag{5.216}$$

$$\frac{d\mathbf{X}^{ex}}{d\Delta t}(t_n) = \frac{d\mathbf{X}}{d\Delta t}(t_n) \tag{5.217}$$

$$\frac{d^2\mathbf{X}^{ex}}{d\Delta t^2}(t_n) = \frac{d^2\mathbf{X}}{d\Delta t^2}(t_n) \tag{5.218}$$

Using (5.210) and with direct derivations we easily obtain for the exact solution

$$\mathbf{X}^{ex}(t_n) = \mathbf{X}_n \tag{5.219}$$

$$\frac{d\mathbf{X}^{ex}}{d\Delta t}(t_n) = \dot{\mathbf{X}}^{ex}(t_n) = \frac{2G}{\sigma_{y,n}}\,\mathbb{B}\,\mathbf{X}^{ex}(t_n) = \frac{2G}{\sigma_{y,n}}\,\mathbb{B}\,\mathbf{X}_n \tag{5.220}$$

$$\begin{aligned}\frac{d^2\mathbf{X}^{ex}}{d\Delta t^2}(t_n) &= \ddot{\mathbf{X}}^{ex}(t_n) = \frac{2G}{\sigma_{y,n}}\,\mathbb{B}\,\dot{\mathbf{X}}^{ex}(t_n) - \frac{2G}{\sigma_{y,n}^2}\,\mathbb{B}\,\mathbf{X}^{ex}(t_n)\,\dot{\sigma}_y(t_n)\\ &= \left(\frac{2G}{\sigma_{y,n}}\,\mathbb{B}\right)^2\mathbf{X}_n - \frac{2G}{\sigma_{y,n}^2}\,\mathbb{B}\,\mathbf{X}_n\,\dot{\sigma}_y(t_n)\end{aligned} \tag{5.221}$$

For the discrete solution, from (5.213) we immediately have

$$\mathbf{X}(t_n) = \mathbf{X}_n \tag{5.222}$$

which joined with (5.219) gives (5.216).

Inspecting (5.213), a direct derivation leads to

$$\begin{aligned}\frac{d\mathbf{X}}{d\Delta t}(t_n) &= \left[\frac{d}{d\Delta t}\exp\left(\frac{2G}{R(\Delta t)}\,\mathbb{B}\,\Delta t\right)\right]_{\Delta t=0}\mathbf{X}_n\\ &= \left[\frac{2G}{R(\Delta t)}\mathbb{B} - \frac{2G}{R(\Delta t)^2}\mathbb{B}\,\Delta t\,\dot{R}(\Delta t)\right]_{\Delta t=0}\left[\exp\left(\frac{2G}{R(\Delta t)}\,\mathbb{B}\,\Delta t\right)\right]_{\Delta t=0}\mathbf{X}_n\\ &= \frac{2G}{R(0)}\mathbb{B}\,\mathbf{X}_n = \frac{2G}{\sigma_{y,n}}\mathbb{B}\,\mathbf{X}_n\end{aligned} \tag{5.223}$$

where we implicitly used that $\dot{R}(0)$ is well defined due to Lemma 5.8.3.

Identity (5.223) joined with (5.220) gives (5.217). Deriving (5.223) and omitting the manipulations we obtain

$$\frac{d^2\mathbf{X}}{d\Delta t^2}(t_n) = \left[\left(\frac{2G}{\sigma_{y,n}}\mathbb{B}\right)^2 - 2\,\frac{2G}{\sigma_{y,n}^2}\mathbb{B}\,\dot{R}(0)\right]\mathbf{X}_n \tag{5.224}$$

where we implicitly used that $\ddot{R}(0)$ is well defined due to Lemma 5.8.3.

Identity (5.218) then follows from (5.221), (5.224) and again Lemma 5.8.3. We have proven the three identities (5.216)-(5.218), therefore the proof of (5.208) follows as already discussed. First from definitions (5.117) and (5.123), then using relation (5.156) it follows the relation between relative and *generalized stress*

$$\mathbf{\Sigma} = \sigma_y \frac{\mathbf{X}^s}{X_0} = \sigma_{y,0}\, X_0^{q-1}\mathbf{X}^s \tag{5.225}$$

Using (5.225) and (5.208) and without showing all the calculations we finally get

$$\|\mathbf{\Sigma}_{n+1}^{ex} - \mathbf{\Sigma}_{n+1}\| = \|\sigma_{y,0}\left(X_{0,n+1}^{ex}\right)^{q-1}\mathbf{X}_{n+1}^{s,e} - \sigma_{y,0}\left(X_{0,n+1}\right)^{q-1}\mathbf{X}_{n+1}^{s}\| = O(\Delta t^3) \tag{5.226}$$

Bound (5.226) immediately implies (5.207) and proves the proposition.

□

5.8.5 Convergence

In this section we will make a first study of the convergence properties of the ESC and ESC^2 methods. In order to keep calculations simpler we will address the case with no kinematic hardening (i.e. $H_{kin} = 0$), otherwise also the norm introduced below should be modified accordingly. Note that this is not restrictive because, differently from isotropic hardening, an opportune translation in stress space shows that linear kinematic hardening does not generate additional difficulties from the numerical viewpoint.

We will consider convergence in the classical "complementary Helmholtz free energy" norm

$$\||\mathbf{\Sigma}, \sigma_y\||^2 = (2G)^{-1}\|\mathbf{\Sigma}\|^2 + (H_{iso})^{-1}\sigma_y^2 \tag{5.227}$$

Note that, although on a finite dimensional space all norms are equivalent, the choice of this norm is not arbitrary. This is in fact the norm in which the original continuous problem is contractive [68, 69]. Note also that we are

assuming $H_{iso} > 0$, otherwise both schemes are exact and there is nothing to prove.

Given a certain degree of accuracy, probably the best way to prove the convergence of a scheme in plasticity is to show that the scheme is B-stable, in other words that the method is contractive in the "complementary Helmholtz free energy" norm above [63]. On the other hand the aim of this section is not to address strong properties as the B-Stability [63, 68] which, considering the particular formulation under consideration, would require a deeper study. We will therefore prove convergence directly, essentially by showing that in the energy norm the error propagates at a controlled rate. In other words

- For the ESC scheme we prove linear convergence
- For the ESC^2 scheme we show quadratic convergence, but only for purely plastic load histories. On one hand, considering that during elastic phases there is virtually no additional error, an assumption of this kind, which is also addressed in the classical paper [63], can be reasonably accepted. On the other hand, in the presence of complicated histories with a large number of elasto-plastic switches, a result of this kind is not sufficient to guarantee convergence; the matter is surely worth further investigations.

In order to fix the notation, we note that in the sequel we will refer to the relative stress-radius couples $(\mathbf{\Sigma}, \sigma_y)$ simply as "couples". The convergence of the methods will derive from the accuracy results of the previous section and from the two following propositions, which state the stable behavior of the error propagation in the scheme.

Proposition 5.8.5 *Assume that two initial couples* $(\mathbf{\Sigma}_i, \sigma_{y,i})$ *and* $(\tilde{\mathbf{\Sigma}}_i, \tilde{\sigma}_{y,i})$ *and a strain increment* $\Delta \boldsymbol{e}$ *are assigned. Let* $(\mathbf{\Sigma}_f, \sigma_{y,f})$ *and* $(\tilde{\mathbf{\Sigma}}_f, \tilde{\sigma}_{y,f})$ *be the solutions obtained applying one step of the* ESC *algorithm with strain increment* $\Delta \boldsymbol{e}$*, respectively to* $(\mathbf{\Sigma}_i, \sigma_{y,i})$ *and* $(\tilde{\mathbf{\Sigma}}_i, \tilde{\sigma}_{y,i})$*. Then there exists a constant* K *such that*

$$|||\mathbf{\Sigma}_f - \tilde{\mathbf{\Sigma}}_f, \sigma_{y,f} - \tilde{\sigma}_{y,f}||| \;\leq\; \exp\left(K\|\Delta \boldsymbol{e}\|\right) |||\mathbf{\Sigma}_i - \tilde{\mathbf{\Sigma}}_i, \sigma_{y,i} - \tilde{\sigma}_{y,i}||| \qquad (5.228)$$

Moreover, the constant K *depends only on* $\|\Delta \boldsymbol{e}\|$ *and is bounded on all sets of the type*
$\{\Delta \boldsymbol{e} \in \mathbf{L}in,\ \|\Delta \boldsymbol{e}\| \leq c,\ c \in \mathcal{R}^+\}$.

Proof: In order to shorten the notation, during the proof an added index E will in general refer to the difference

$$\mathbf{\Sigma}^E = \mathbf{\Sigma} - \tilde{\mathbf{\Sigma}}\ , \qquad \sigma_y^E = \sigma_y - \tilde{\sigma}_y \qquad (5.229)$$

The proof can be divided into three separate cases, depending on which type of step (elastic or plastic) each of the two couples is following. It is not restrictive to assume that each couple is undergoing either a totally plastic or a totally elastic step; it is then trivial to check that the proof for mixed elastoplastic increments simply follows splitting the time step properly.

If both couples follow an elastic step, then both couples undergo the same identical transformation and the proposition is trivially true setting $K = 0$. If both couples are in plastic phase, or if one is in plastic and the other in elastic phase, the matter is more complicated. In both cases, Lemmas 5.8.10 and 5.8.11 respectively show that the error will evolve satisfying the bound

$$\frac{d}{dt}|||\mathbf{\Sigma}^E(t), \sigma_y^E(t)||| \;\leq\; \|\dot{\mathbf{e}}\|\Big[K_1|||\mathbf{\Sigma}^E(t_0), \sigma_y^E(t_0)||| + K_2|||\mathbf{\Sigma}^E(t), \sigma_y^E(t)|||\Big] \tag{5.230}$$

during the whole time step. In the present case, respectively at the beginning and at the end of an integration interval, it holds

$$(\mathbf{\Sigma}(t_0), \sigma_y(t_0)) = (\mathbf{\Sigma}_i, \sigma_{y,i}) \qquad (\mathbf{\Sigma}_f, \sigma_{y,f}) = (\mathbf{\Sigma}(t_0 + \Delta t), \sigma_y(t_0 + \Delta t)) \tag{5.231}$$

$$(\tilde{\mathbf{\Sigma}}(t_0), \tilde{\sigma}_y(t_0)) = (\tilde{\mathbf{\Sigma}}_i, \tilde{\sigma}_{y,i}) \qquad (\tilde{\mathbf{\Sigma}}_f, \tilde{\sigma}_{y,f}) = (\tilde{\mathbf{\Sigma}}(t_0 + \Delta t), \tilde{\sigma}_y(t_0 + \Delta t)) \tag{5.232}$$

$$(\mathbf{\Sigma}^E(t_0), \sigma_y^E(t_0)) = (\mathbf{\Sigma}_i^E, \sigma_{y,i}^E) \quad (\mathbf{\Sigma}_f^E, \sigma_{y,f}^E) = (\mathbf{\Sigma}^E(t_0 + \Delta t), \sigma_y^E(t_0 + \Delta t)) \tag{5.233}$$

assuming that the time-step has length Δt. We now have, for all $t \in [t_0, t_0+\Delta t]$

$$|||\mathbf{\Sigma}^E(t), \sigma_y^E(t)||| \;=\; |||\mathbf{\Sigma}^E(t_0), \sigma_y^E(t_0)||| + \int_{t_0}^{t_0+t} \frac{d}{ds}|||\mathbf{\Sigma}^E(s), \sigma_y^E(s)|||ds \tag{5.234}$$

Applying bound (5.231) in equation (5.234) now easily gives

$$\begin{aligned} |||\mathbf{\Sigma}^E(t), \sigma_y^E(t)||| \;&\leq\; \Big[1 + K_1\|\dot{\mathbf{e}}\|(t - t_0)\Big]|||\mathbf{\Sigma}^E(t_0), \sigma_y^E(t_0)||| \\ &+\|\dot{\mathbf{e}}\|K_2 \int_{t_0}^{t_0+t} |||\mathbf{\Sigma}^E(s), \sigma_y^E(s)|||ds \qquad \forall t \in [t_0, t_0 + \Delta t] \end{aligned} \tag{5.235}$$

which in turn, recalling that $t \in [t_0, t_0 + \Delta t]$, grants

$$\begin{aligned} |||\mathbf{\Sigma}^E(t), \sigma_y^E(t)||| \;&\leq\; \Big[1 + K_1\|\dot{\mathbf{e}}\|\Delta t\Big]|||\mathbf{\Sigma}^E(t_0), \sigma_y^E(t_0)||| \\ &+\|\dot{\mathbf{e}}\|K_2 \int_{t_0}^{t_0+t} |||\mathbf{\Sigma}^E(s), \sigma_y^E(s)|||ds \qquad \forall t \in [t_0, t_0 + \Delta t] \end{aligned} \tag{5.236}$$

A scalar function which satisfies a condition of this type must, due to the Gronwall Lemma [39, 52], satisfies on the same interval the bound

$$|||\mathbf{\Sigma}^E(t), \sigma_y^E(t)||| \leq \left[1 + K_1\|\dot{\mathbf{e}}\|\Delta t\right] |||\mathbf{\Sigma}^E(t_0), \sigma_y^E(t_0)||| \exp\left[K_2\|\dot{\mathbf{e}}\|(t - t_0)\right] \tag{5.237}$$

Using bound (5.237) for $t = t_0 + \Delta t$ and observing that $1 + x \leq \exp(x)$ for all $x \in \mathcal{R}$, it follows

$$|||\mathbf{\Sigma}_f^E, \sigma_{y,f}^E||| \leq \exp\left[K_1\|\dot{\mathbf{e}}\|\Delta t\right] |||\mathbf{\Sigma}_i^E, \sigma_{y,i}^E||| \exp\left[K_2\|\dot{\mathbf{e}}\|\Delta t\right] \tag{5.238}$$

where we also used the definitions (5.232) and (5.233). Finally, recalling that $\|\Delta\mathbf{e}\| = \|\dot{\mathbf{e}}\|\Delta t$ and setting $K = K_1 + K_2$, bound (5.238) gives

$$|||\mathbf{\Sigma}_f^E, \sigma_{y,f}^E||| \leq \exp\left[K\|\Delta\mathbf{e}\|\right] |||\mathbf{\Sigma}_i^E, \sigma_{y,i}^E||| \tag{5.239}$$

The proposition is proved.

□

The proof of the following result is identical to the previous one, the only difference being to limit the argument to plastic steps, therefore using only Lemma 5.8.10 instead of Lemma 5.8.11.

Proposition 5.8.6 *Assume that two initial couples* $(\mathbf{\Sigma}_i, \sigma_{y,i})$ *and* $(\tilde{\mathbf{\Sigma}}_i, \tilde{\sigma}_{y,i})$ *and a strain increment* $\Delta\boldsymbol{e}$ *are assigned. Let* $(\mathbf{\Sigma}_f, \sigma_{y,f})$ *and* $(\tilde{\mathbf{\Sigma}}_f, \tilde{\sigma}_{y,f})$ *be the solutions obtained applying one purely plastic step of the* ESC^2 *algorithm with strain increment* $\Delta\boldsymbol{e}$*, respectively to* $(\mathbf{\Sigma}_i, \sigma_{y,i})$ *and* $(\tilde{\mathbf{\Sigma}}_i, \tilde{\sigma}_{y,i})$*. Then there exists a constant* K *such that*

$$|||\mathbf{\Sigma}_f - \tilde{\mathbf{\Sigma}}_f, \sigma_{y,f} - \tilde{\sigma}_{y,f}||| \leq \exp\left(K\|\Delta\boldsymbol{e}\|\right) |||\mathbf{\Sigma}_i - \tilde{\mathbf{\Sigma}}_i, \sigma_{y,i} - \tilde{\sigma}_{y,i}||| \tag{5.240}$$

Moreover, the constant K *depends only on* $\|\Delta\boldsymbol{e}\|$ *and is bounded on all sets of the type*
$\{\Delta\boldsymbol{e} \in \mathbf{L}in,\ \|\Delta\boldsymbol{e}\| \leq c,\ c \in \mathcal{R}^+\}$.

Remark 5.8.7 Note that the second part of Lemma 5.8.11, i.e. proving that the scalar A_2 in the lemma is non positive, can be proved identically also for the ESC^2 scheme. The additional difficulty is instead given by bounding the scalar A_1 with terms which depend only on the present or past history. Note that following the same steps a conditional stability result could be obtained for the ESC^2 scheme in case of mixed elastoplastic evolution histories (i.e. a result as in Proposition 5.8.5 with the additional assumption that $\Delta\mathbf{e}$ is sufficiently small).

We can now state the convergence result for the ESC^2 method, which holds for purely plastic load histories. This is undoubtedly a non negligible limitation, as noted in the comments at the start of this section. The matter is therefore worth further investigation.

Proposition 5.8.8 *Let a piecewise linear strain history* $\boldsymbol{e}(t)$, $t \in [0, T]$ *and two starting couples* $(\boldsymbol{\Sigma}^{ex}(0), \sigma_y^{ex}(0))$ *and* $(\boldsymbol{\Sigma}(0), \sigma_y(0))$ *be assigned. Assume for simplicity that* $\|\dot{\boldsymbol{e}}\|$ *is constant during the whole history; due to the rate invariance of the problem, this is not restrictive. Let the time interval be divided into* N *uniform sub-intervals of length* $\Delta t = T/N$. *Let* $(\boldsymbol{\Sigma}^{ex}(T), \sigma_y^{ex}(T))$ *indicate the exact solution at time* T *following the strain history above with starting point* $(\boldsymbol{\Sigma}^{ex}(0), \sigma_y^{ex}(0))$*; let also* $(\boldsymbol{\Sigma}(T), \sigma_y(T))$ *indicate the solution at time* T *obtained with the* ESC^2 *scheme based on the above strain history and time stepping, with starting point* $(\boldsymbol{\Sigma}(0), \sigma_y(0))$. *Finally, assume that the strain history is such that the continuous and the discrete solutions undergo a purely plastic loading. Then*

$$\begin{aligned}
&|||(\boldsymbol{\Sigma}^{ex}(T), \sigma_y^{ex}(T)) - (\boldsymbol{\Sigma}(T), \sigma_y(T))||| \\
&\leq C_1 \|\dot{\boldsymbol{e}}\|^2 (\Delta t)^2 + C_2 |||(\boldsymbol{\Sigma}^{ex}(0), \sigma_y^{ex}(0)) - (\boldsymbol{\Sigma}(0), \sigma_y(0))|||
\end{aligned} \tag{5.241}$$

where C_1, C_2 *are independent of* N.

Proof: In the sequel a subindex n will indicate a variable calculated at time $t_n = n\Delta t$, $n = \{0, 1, 2...N-1\}$. Given any stress-radius couple $(\tilde{\boldsymbol{\Sigma}}, \tilde{\sigma}_y)$, let in the sequel $\Theta_n[\tilde{\boldsymbol{\Sigma}}, \tilde{\sigma}_y]$ indicate the couple obtained applying one step of the ESC^2 scheme to $(\tilde{\boldsymbol{\Sigma}}, \tilde{\sigma}_y)$ with $\Delta \mathbf{e} = \mathbf{e}_{n+1} - \mathbf{e}_n = \mathbf{e}(t_{n+1}) - \mathbf{e}(t_n)$. We have in particular for the discrete solution

$$(\boldsymbol{\Sigma}, \sigma_y)_{n+1} = \Theta_n[\boldsymbol{\Sigma}_n, \sigma_{y,n}] \tag{5.242}$$

Using the definition of the operator Θ and a triangle inequality, for the error at time t_{n+1} it holds

$$\begin{aligned}
E_{n+1} &:= |||(\boldsymbol{\Sigma}^{ex}, \sigma_y^{ex})_{n+1} - (\boldsymbol{\Sigma}, \sigma_y)_{n+1}||| \\
&\leq |||(\boldsymbol{\Sigma}^{ex}, \sigma_y^{ex})_{n+1} - \Theta_n[\boldsymbol{\Sigma}_n^{ex}, \sigma_{y,n}^{ex}]||| + |||\Theta_n[\boldsymbol{\Sigma}_n^{ex}, \sigma_{y,n}^{ex}] - \\
&\Theta_n[\boldsymbol{\Sigma}_n, \sigma_{y,n}]|||
\end{aligned} \tag{5.243}$$

The first member in the right hand side of (5.243) represents the local error generated at each time step, which can be controlled using the accuracy results of the previous section. The second member represents instead the propagation of the accumulated error, which must be dealt with essentially using the stability results of this section.

From Proposition 5.8.4 and bound (5.208), recalling that $\sigma_y = \sigma_{y,0} X_0^q$ both for the exact and the numerical solution, it follows

$$|||(\mathbf{\Sigma}^{ex}, \sigma_y^{ex})_{n+1} - \Theta_n[\mathbf{\Sigma}_n^{ex}, \sigma_{y,n}^{ex}]||| \leq \tilde{C}(\Delta t)^3 \tag{5.244}$$

where here and in the sequel $\tilde{C}$ will indicate a general constant independent of N. We want to rewrite bound (5.244) in rate invariant form. The error in Proposition 5.8.4 follows from the difference between the third order derivative of the numerical scheme and the exact solution. Therefore, it is easy to check that, bringing out the dependence of $\tilde{C}$ on $\|\dot{\mathbf{e}}\|$, bound (5.245) becomes

$$|||(\mathbf{\Sigma}^{ex}, \sigma_y^{ex})_{n+1} - \Theta_n[\mathbf{\Sigma}_n^{ex}, \sigma_{y,n}^{ex}]||| \leq \tilde{C}\|\dot{\mathbf{e}}\|^3(\Delta t)^3 = \tilde{C}\|\Delta\mathbf{e}\|^3 \tag{5.245}$$

where the new constant $\tilde{C}$ is now rate invariant. For the second member in the right hand side of (5.243), Proposition 5.8.6 gives

$$\begin{aligned} &|||\Theta_n[\mathbf{\Sigma}_n^{ex}, \sigma_{y,n}^{ex}] - \Theta_n[\mathbf{\Sigma}_n, \sigma_{y,n}]||| \leq \exp(K\|\Delta\mathbf{e}\|)|||(\mathbf{\Sigma}_n^{ex}, \sigma_{y,n}^{ex}) - (\mathbf{\Sigma}_n, \sigma_{y,n})||| \\ &= \exp(K\|\Delta\mathbf{e}\|)E_n \end{aligned} \tag{5.246}$$

with K fixed scalar independent of N. Therefore, applying the bounds (5.245) and (5.246) into the inequality (5.243), we get

$$E_{n+1} \leq \tilde{C}\|\Delta\mathbf{e}\|^3 + \exp(K\|\Delta\mathbf{e}\|)E_n \tag{5.247}$$

Iteration of (5.247) easily leads to

$$E_N \leq \tilde{C}\|\Delta\mathbf{e}\|^3[\sum_{n=0}^{N-1} \exp(Kn\|\Delta\mathbf{e}\|)] + \exp(KN\|\Delta\mathbf{e}\|)E_0 \tag{5.248}$$

From (5.248), using that $\Delta\mathbf{e} = \dot{\mathbf{e}}\,\Delta t$ and $T = N\Delta t$ we get

$$\begin{aligned} &E_N \leq \tilde{C}\|\Delta\mathbf{e}\|^3 N \exp(KN\|\Delta\mathbf{e}\|) + \exp(KN\|\Delta\mathbf{e}\|)E_0 \\ &\leq \tilde{C}(\|\dot{\mathbf{e}}\|^2(\Delta t)^2\|\dot{\mathbf{e}}\|T + E_0)\exp(K\|\dot{\mathbf{e}}\|T) \leq \tilde{C}'(\|\dot{\mathbf{e}}\|^2(\Delta t)^2 \\ &+E_0) \end{aligned} \tag{5.249}$$

where the scalar $\tilde{C}'$ is rate invariant and independent of N. Note that also the quantities $\|\dot{\mathbf{e}}\|^2(\Delta t)^2$ and $\|\dot{\mathbf{e}}\|T$ appearing in (5.249) are correctly rate invariant. Recalling the definition of E_n, $n \in \{0, 1, 2, ..., N\}$, the proposition is proved.

□

Remark 5.8.9 *The convergence result for the* ESC *method is not restricted to purely plastic load histories. The result is identic to that of Proposition 5.8.8 but holding for any type of loading history. The proof is essentially the same as for Proposition 5.8.8 but using the more general Proposition 5.8.5 instead of Proposition 5.8.6.*

In the following the reader is provided with the proofs of the lemmas recalled in Section 5.8.5 devoted to the numerical analysis of the exponential-based algorithms. The present results which play a key role in the derivations carried out in the previous section are taken from [11].

5.8.6 Two lemmas

We now introduce and prove the two lemmas mentioned in the previous sections by first recalling the following identities which can be derived from the new formulation of Section 5.7.1. At all time instants during plastic steps it holds:

$$\mathbf{X}^s = \sigma_{y,0}^{-1}\, X_0^{1-q}\, \mathbf{\Sigma} \tag{5.250}$$

$$\mathbf{\Sigma} = \sigma_{y,0}\, X_0^{q-1}\, \mathbf{X}^s \tag{5.251}$$

Lemma 5.8.10 *Let two initial couples* $(\mathbf{\Sigma}(t_0), \sigma_y(t_0))$, $(\tilde{\mathbf{\Sigma}}(t_0), \tilde{\sigma}_y(t_0))$ *and a strain increment* $\Delta \boldsymbol{e} = \dot{\boldsymbol{e}}\Delta t$ *be assigned. Assume to apply one step of the* ESC *or* ESC^2 *algorithm with strain increment* $\Delta \boldsymbol{e}$ *to both initial couples and assume that both steps are totally plastic. Then at all instants* $t \in [t_0, t_0 + \Delta t]$ *during the time step, it holds*

$$\begin{aligned}
&\frac{d}{dt}|||\mathbf{\Sigma}(t) - \tilde{\mathbf{\Sigma}}(t), \sigma_y(t) - \tilde{\sigma}_y(t)||| \\
&\leq \|\dot{\boldsymbol{e}}\| \Big[K_1|||\mathbf{\Sigma}(t_0) - \tilde{\mathbf{\Sigma}}(t_0), \sigma_y(t_0) - \tilde{\sigma}_y(t_0)||| \\
&+ K_2|||\mathbf{\Sigma}(t) - \tilde{\mathbf{\Sigma}}(t), \sigma_y(t) - \tilde{\sigma}_y(t)|||\Big]
\end{aligned} \tag{5.252}$$

where the positive constants K_1, K_2*, depending only on the material constants and* $\|\Delta \boldsymbol{e}\|$*, are bounded on all sets of the type* $\{\Delta \boldsymbol{e} \in \mathbf{L}in,\ \|\Delta \boldsymbol{e}\| \leq c,\ c \in \mathcal{R}^+\}$

Proof: The proof will be shown only in the case of the ESC^2 algorithm. The proof for the ESC scheme is a simpler version of the one that follows and can be trivially derived following the same steps. In the sequel, in order to

shorten the notation, the dependence of the variables on time will not be explicited; unless differently noted, the time dependent equations and identities that follow are valid for all $t \in [t_0, t_0 + \Delta t]$.

We will again adopt the notation introduced in (5.229). Direct derivation gives

$$\frac{d}{dt}|||\mathbf{\Sigma}^E, \sigma_y^E|||^2 = 2\left[(2G)^{-1}(\mathbf{\Sigma}^E, \dot{\mathbf{\Sigma}}^E) + (H_{iso})^{-1}\sigma_y^E \dot{\sigma}_y^E\right] \tag{5.253}$$

Deriving in time definition (5.251) and using (5.124)-(5.250) we easily get, without showing all the calculations,

$$\dot{\mathbf{\Sigma}}^E = \frac{d}{dt}(\mathbf{\Sigma} - \tilde{\mathbf{\Sigma}}) = \sigma_{y,0}\mathbf{T}_1 + \mathbf{T}_2 \tag{5.254}$$

$$\mathbf{T}_1 = \left[\frac{2G}{R}X_0^q - \frac{2G}{\tilde{R}}\tilde{X}_0^q\right]\dot{\mathbf{e}} \tag{5.255}$$

$$\mathbf{T}_2 = (q-1)\left[\frac{2G}{R}(\dot{\mathbf{e}} : \mathbf{\Sigma})\frac{\mathbf{\Sigma}}{\sigma_y} - \frac{2G}{\tilde{R}}\left(\dot{\mathbf{e}} : \tilde{\mathbf{\Sigma}}\right)\frac{\tilde{\mathbf{\Sigma}}}{\tilde{\sigma}_y}\right] \tag{5.256}$$

As a consequence, the first member in the right hand side of (5.253) can be bounded with

$$(2G)^{-1}\mathbf{\Sigma}^E : \dot{\mathbf{\Sigma}}^E = (2G)^{-1}\left[\sigma_{y,0}\,\mathbf{T}_1 + \mathbf{T}_2\right] : \mathbf{\Sigma}^E \leq C\left(\|\mathbf{T}_1\| + \|\mathbf{T}_2\|\right)\|\mathbf{\Sigma}^E\| \tag{5.257}$$

where here and in the sequel C indicates a general positive constant depending only on the material constants. We now have

$$\begin{aligned}
\|\mathbf{T}_1\| &\leq C\left[\left|\frac{\tilde{R} - R}{R\,\tilde{R}}X_0^q + \frac{1}{\tilde{R}}\left(X_0^q - \tilde{X}_0^q\right)\right|\right]\|\dot{\mathbf{e}}\| \\
&\leq C\left(\left|\frac{\tilde{R} - R}{R\,\tilde{R}}X_0^q\right| + \left|\frac{1}{\tilde{R}}(X_0^q - \tilde{X}_0^q)\right|\right)\|\dot{\mathbf{e}}\| \\
&= (A_1 + A_2)\|\dot{\mathbf{e}}\|
\end{aligned} \tag{5.258}$$

The definition of R, recalling that both couples are undergoing a purely plastic step, becomes

$$R = \frac{\|\mathbf{\Sigma}_i\|}{c^{-1}\ln(1+c)} \tag{5.259}$$

$$c = \frac{2G\,q\,\mathbf{\Sigma}_i : \Delta\mathbf{e}}{\|\mathbf{\Sigma}_i\|^2} \tag{5.260}$$

and the analogous for the barred variables. Therefore R is a real C^1 function of $\mathbf{\Sigma}_i$.

Recalling that both couples are in plastic phase, it follows immediately that both $\|\mathbf{\Sigma}_i\|$ and $\|\tilde{\mathbf{\Sigma}}_i\|$ are greater or equal to $\sigma_{y,0}$. It is therefore easy to check that it exists a smooth path $\boldsymbol{\gamma}$ in $\mathbf{Lin}^{\mathrm{sym}}$ from $\tilde{\mathbf{\Sigma}}_i$ to $\mathbf{\Sigma}_i$ such that

$$\boldsymbol{\gamma} \ : \ [0, L] \longrightarrow \mathbf{Lin}^{\mathrm{sym}} \tag{5.261}$$

$$\|\nabla\boldsymbol{\gamma}(s)\| = 1 \qquad \forall s \in [0, L] \tag{5.262}$$

$$\|\boldsymbol{\gamma}(s)\| \geq \sigma_{y,0} \qquad \forall s \in [0, L] \tag{5.263}$$

$$L \leq 4\|\mathbf{\Sigma}_i - \tilde{\mathbf{\Sigma}}_i\| \tag{5.264}$$

Note that the above conditions simply mean that $\boldsymbol{\gamma}$ is a C^1 path of length L lesser than $4\|\mathbf{\Sigma}_i - \tilde{\mathbf{\Sigma}}_i\|$, written with respect to its curvilinear abscissae and bounded outside a sphere of radius $\sigma_{y,0}$ centered at the origin.

From the Lagrange theorem applied to the function $R(\mathbf{\Sigma})$ along the path $\boldsymbol{\gamma}$, it follows the existence of $\beta \in [0, L]$ such that

$$R - \tilde{R} = L\, \nabla R|_{\mathbf{\Sigma}_i^*} : \nabla\boldsymbol{\gamma}|_\beta \tag{5.265}$$

where

$$\mathbf{\Sigma}_i^* = \boldsymbol{\gamma}(\beta) \qquad 0 \leq \beta \leq L \tag{5.266}$$

Using (5.262) and (5.264), from (5.265) we get

$$|R - \tilde{R}| \leq 4\|\nabla R|_{\mathbf{\Sigma}_i^*}\| \, \|\mathbf{\Sigma}_i - \tilde{\mathbf{\Sigma}}_i\| \tag{5.267}$$

Substituting (5.267) in the definition of A_1 and using the Cauchy-Schwartz inequality now leads to

$$A_1 \leq \frac{\|\nabla R|_{\mathbf{\Sigma}_i^*}\|}{\tilde{R}} \, \frac{X_0^q}{R} \, \|\mathbf{\Sigma}_i - \tilde{\mathbf{\Sigma}}_i\| \tag{5.268}$$

We now want to bound the pieces in (5.268). A direct calculation gives

$$\nabla R|_{\mathbf{\Sigma}_i^*} = \frac{1}{c^{-1}\ln(1+c)}\nabla\|\mathbf{\Sigma}\| - \|\mathbf{\Sigma}_i^*\| \frac{\dfrac{1}{c(1+c)} - \dfrac{\ln(1+c)}{c^2}}{\left(c^{-1}\ln(1+c)\right)^2} \left[\frac{\partial c}{\partial \mathbf{\Sigma}}\right] \tag{5.269}$$

where all the functions and derivatives are calculated in $\mathbf{\Sigma}_i^*$. We note that the functions

$$\frac{1}{c(1+c)} - \frac{\ln(1+c)}{c^2}\,, \qquad c^{-1}\ln(1+c) \tag{5.270}$$

are bounded from above on all the positive real line. Also, recalling (5.260), it is easy to check that the latter function $c^{-1}\ln(1+c)$ is bounded from below by a positive constant (independent of $\|\mathbf{\Sigma}_i^*\|$) on all sets of the type $\{\Delta\mathbf{e} \in \mathbf{L}\text{in},\ \|\Delta\mathbf{e}\| \leq c,\ c \in \mathcal{R}^+\}$. A direct calculation also easily gives

$$\| \left[\frac{\partial c}{\partial \mathbf{\Sigma}}\right] |_{\mathbf{\Sigma}_i^*} \| \leq C \frac{\|\Delta\mathbf{e}\|}{\|\mathbf{\Sigma}_i^*\|^2} \tag{5.271}$$

Joining the latter three statements with (5.269) and noting that the norm of $\nabla(\|\mathbf{\Sigma}\|)$ is equal to one, gives

$$\|\nabla R|_{\mathbf{\Sigma}_i^*}\| \leq K_3' \left(1 + \|\mathbf{\Sigma}_i^*\|^{-1}\right) \tag{5.272}$$

where K_3' depends only on $\|\Delta\mathbf{e}\|$ and is bounded on all sets of the type $\{\Delta\mathbf{e} \in \mathbf{L}\text{in},\ \|\Delta\mathbf{e}\| \leq c,\ c \in \mathcal{R}^+\}$. Finally, due to definition (5.266) and condition (5.263), the above bound becomes

$$\|\nabla R|_{\mathbf{\Sigma}_i^*}\| \leq K_3 \tag{5.273}$$

where K_3 depends only on $\|\Delta\mathbf{e}\|$ and is bounded on all sets of the type $\{\Delta\mathbf{e} \in \mathbf{L}\text{in},\ \|\Delta\mathbf{e}\| \leq c,\ c \in \mathcal{R}^+\}$.

Using again the boundedness from above of $c^{-1}\ln(1+c)$ and recalling (5.259), (5.156) we have

$$\frac{1}{\tilde{R}} \leq \frac{\tilde{c}^{-1}\ln(1+\tilde{c})}{\sigma_{y,0}} \leq C \tag{5.274}$$

$$\frac{1}{R} = \frac{c^{-1}\ln(1+c)}{\sigma_{y,0}X_{0,i}^q} \leq C\frac{1}{X_{0,i}^q} \tag{5.275}$$

Using (5.275) and recalling that X_0 never decreases during the step, we now have

$$\frac{X_0^q}{R} \leq C\left(\frac{X_0}{X_{0,i}}\right)^q \leq C\left(\frac{X_{0,f}}{X_{0,i}}\right)^q \tag{5.276}$$

We observe that, due to (5.143)-(5.145) and recalling that

$$\|\mathbf{X}^s\| = X_0 \qquad \text{during plastic phases} \tag{5.277}$$

it follows

$$X_{0,f} = b\frac{\dot{\mathbf{e}} : \mathbf{X}_i^s}{\|\dot{\mathbf{e}}\|} + aX_{0,i} \leq b\|\mathbf{X}_i^s\| + aX_{0,i} \leq (b+a)X_{0,i} \tag{5.278}$$

Therefore, from (5.276) and (5.278), it holds

$$\frac{X_0^q}{R} \leq C(b+a)^q \leq C \exp\left(\frac{2G\,q}{R}\|\Delta\mathbf{e}\|\right) \leq K_4 \tag{5.279}$$

with K_4 bounded on all sets of the type $\{\Delta\mathbf{e} \in \mathbf{L}\text{in},\ \|\Delta\mathbf{e}\| \leq c,\ c \in \mathcal{R}^+\}$.

Finally, simply applying the three bounds (5.273),(5.274) and (5.279) into (5.268), we obtain

$$A_1 \leq K_5\|\mathbf{\Sigma}_i - \tilde{\mathbf{\Sigma}}_i\| \tag{5.280}$$

with K_5 depending only on $\Delta\mathbf{e}$ and bounded on all sets of the type $\{\Delta\mathbf{e} \in \mathbf{L}\text{in},\ \|\Delta\mathbf{e}\| \leq c,\ c \in \mathcal{R}^+\}$. Using (5.274) and observing that any difference of tensor norms is bounded by the norm of the difference, we get for the second term in (5.258)

$$A_2 = \left|\frac{1}{\tilde{R}}\sigma_{y,0}^{-1}\left(\|\mathbf{\Sigma}\| - \|\tilde{\mathbf{\Sigma}}\|\right)\right| \leq C\left(\|\mathbf{\Sigma}\| - \|\tilde{\mathbf{\Sigma}}\|\right) \leq C\|\mathbf{\Sigma} - \tilde{\mathbf{\Sigma}}\| \tag{5.281}$$

Applying the bounds (5.280) and (5.281) to (5.258), it immediately follows

$$\|\mathbf{T}_1\| \leq \|\dot{\mathbf{e}}\|\left[K_5\|\mathbf{\Sigma}_i - \tilde{\mathbf{\Sigma}}_i\| + C\|\mathbf{\Sigma} - \tilde{\mathbf{\Sigma}}\|\right] \tag{5.282}$$

The second term $\mathbf{T}_2$ is bound following the same techniques; in the end we obtain a similar bound

$$\|\mathbf{T}_2\| \leq \|\dot{\mathbf{e}}\|\left[K_6\|\mathbf{\Sigma}_i - \tilde{\mathbf{\Sigma}}_i\| + K_7\|\mathbf{\Sigma} - \tilde{\mathbf{\Sigma}}\|\right] \tag{5.283}$$

where K_6, K_7 depend only on $\|\Delta\mathbf{e}\|$ and are bounded on all sets of the type $\{\Delta\mathbf{e} \in \mathbf{L}\text{in},\ \|\Delta\mathbf{e}\| \leq c,\ c \in \mathcal{R}^+\}$.

For the second term in (5.253), using the identities (5.156) and (5.128), it follows

$$|\sigma^E\dot{\sigma}^E| = |\sigma_y - \tilde{\sigma}_y|\,\sigma_{y,0}\,|X_0^{q-1}\dot{X}_0 - \tilde{X}_0^{q-1}\dot{\tilde{X}}_0| \tag{5.284}$$

which, recalling that in plastic phase $\sigma_y = \|\mathbf{\Sigma}\|$, becomes

$$|\sigma^E\dot{\sigma}^E| \leq C\|\mathbf{\Sigma} - \tilde{\mathbf{\Sigma}}\|\,\sigma_{y,0}\,|X_0^{q-1}\dot{X}_0 - \tilde{X}_0^{q-1}\dot{\tilde{X}}_0| \tag{5.285}$$

Applying identity (5.250), bound (5.285) becomes

$$|\sigma^E\dot{\sigma}^E| \leq C\|\mathbf{\Sigma} - \tilde{\mathbf{\Sigma}}\|\left(\frac{2G}{R}\dot{\mathbf{e}} : \mathbf{\Sigma} - \frac{2G}{\tilde{R}}\dot{\mathbf{e}} : \tilde{\mathbf{\Sigma}}\right) \tag{5.286}$$

where the term in parentheses can be bounded with the usual techniques. Thus it is found that

$$|\sigma^E \dot{\sigma}^E| \leq \|\mathbf{\Sigma} - \tilde{\mathbf{\Sigma}}\| \, \|\dot{\mathbf{e}}\| \, \left[K_{10}\|\mathbf{\Sigma}_i - \tilde{\mathbf{\Sigma}}_i\| + K_{11}\|\mathbf{\Sigma} - \tilde{\mathbf{\Sigma}}\|\right] \tag{5.287}$$

where K_{10}, K_{11} share the usual property of the previous cases.

Simply applying the four bounds (5.257), (5.282), (5.283) and (5.287) into (5.253), we obtain

$$\begin{aligned} &\frac{d}{dt}|||\mathbf{\Sigma}^E(t), \sigma_y(t)^E|||^2 \leq \|\dot{\mathbf{e}}\| \left[K_1\|\mathbf{\Sigma}_i - \tilde{\mathbf{\Sigma}}_i\| + K_2\|\mathbf{\Sigma} - \tilde{\mathbf{\Sigma}}\|\right] \|\mathbf{\Sigma}^E\| \\ &\leq C\|\dot{\mathbf{e}}\| \left[K_1\|\mathbf{\Sigma}_i - \tilde{\mathbf{\Sigma}}_i\| + K_2\|\mathbf{\Sigma} - \tilde{\mathbf{\Sigma}}\|\right] |||\mathbf{\Sigma}^E(t), \sigma_y(t)^E||| \end{aligned} \tag{5.288}$$

where K_1, K_2 depend only on $\|\Delta\mathbf{e}\|$ and are bounded on all sets of the type $\{\Delta\mathbf{e} \in \mathbf{L}\text{in}, \ \|\Delta\mathbf{e}\| \leq c, \ c \in \mathcal{R}^+\}$. Observing that

$$\frac{d}{dt}|||\mathbf{\Sigma}^E(t), \sigma_y(t)^E|||^2 = 2|||\mathbf{\Sigma}^E(t), \sigma_y(t)^E|||\frac{d}{dt}|||\mathbf{\Sigma}^E(t), \sigma_y(t)^E||| \tag{5.289}$$

bound (5.288) trivially proves the lemma.

□

Lemma 5.8.11 *Let two initial couples* $(\mathbf{\Sigma}(t_0), \sigma_y(t_0))$, $(\tilde{\mathbf{\Sigma}}(t_0), \tilde{\sigma}_y(t_0))$ *and a strain increment* $\Delta\boldsymbol{e} = \dot{\boldsymbol{e}}\Delta t$ *be assigned. Assume to apply one step of the* ESC *algorithm with strain increment* $\Delta\boldsymbol{e}$ *to both initial couples; assume also that the step for the first couple is totally plastic, while the step for the second couple is totally elastic. Then at all instants* $t \in [t_0, t_0 + \Delta t]$ *during the time step, it holds*

$$\begin{aligned} &\frac{d}{dt}|||\mathbf{\Sigma}(t) - \tilde{\mathbf{\Sigma}}(t), \sigma_y(t) - \tilde{\sigma}_y(t)||| \\ &\leq \ \|\dot{\boldsymbol{e}}\| \left[K_1|||\mathbf{\Sigma}(t_0) - \tilde{\mathbf{\Sigma}}(t_0), \sigma_y(t_0) - \tilde{\sigma}_y(t_0)||| \right. \\ &\left. + K_2 \ |||\mathbf{\Sigma}(t) - \tilde{\mathbf{\Sigma}}(t), \sigma_y(t) - \tilde{\sigma}_y(t)|||\right] \end{aligned} \tag{5.290}$$

where the positive constants K_1, K_2 *depend only on* $\|\Delta\boldsymbol{e}\|$ *and are bounded on all sets of the type* $\{\Delta\boldsymbol{e} \in \mathbf{L}in, \ \|\Delta\boldsymbol{e}\| \leq c, \ c \in \mathcal{R}^+\}$

Proof: As in the proof of Lemma 5.8.10, the dependence of the variables on time will not be explicited. Unless differently noted, the time dependent equations and identities that follow are valid for all $t \in [t_0, t_0 + \Delta t]$.

We will again adopt the notation introduced in (5.229). Following the same identical initial steps as in Lemma 5.8.10, we get

$$\frac{d}{dt}\|\|\mathbf{\Sigma}^E, \sigma_y^E\|\|^2 = 2\left[(2G)^{-1}\,\mathbf{\Sigma}^E : \dot{\mathbf{\Sigma}}^E + (H_{iso})^{-1}\sigma_y^E\dot{\sigma}_y\right] \tag{5.291}$$

where we implicitly used that $\dot{\sigma}_y^E = \dot{\sigma}_y$ because the second couple is in elastic phase. Note that for the time derivative of $\tilde{\mathbf{X}}$, which is in elastic phase, it holds

$$\frac{d}{dt}\tilde{\mathbf{X}}^s = \frac{2G}{\sigma_{y,i}}\tilde{X}_0\dot{\mathbf{e}} \tag{5.292}$$

$$\frac{d}{dt}\tilde{X}_0 = 0 \tag{5.293}$$

while the time derivative of $\mathbf{X}$ still follows (5.124)-(5.250). Deriving in time definition (5.251), then using (5.124)-(5.250) and (5.292)-(5.293), we easily get, without showing all the calculations,

$$\dot{\mathbf{\Sigma}}^E = \frac{d}{dt}(\mathbf{\Sigma} - \tilde{\mathbf{\Sigma}}) = \sigma_{y,0}\,\mathbf{T}_1 + \mathbf{T}_2 \tag{5.294}$$

$$\mathbf{T}_1 = \left[\frac{2G}{\sigma_{y,i}}X_0^q - \frac{2G}{\tilde{\sigma}_{y,i}}\tilde{X}_0^q\right]\,\dot{\mathbf{e}} \tag{5.295}$$

$$\mathbf{T}_2 = (q-1)\left[\frac{2G}{R}\,(\dot{\mathbf{e}} : \mathbf{\Sigma})\,\frac{\mathbf{\Sigma}}{\sigma_y}\right] \tag{5.296}$$

Joining (5.291) and (5.294) gives

$$\begin{aligned}\frac{d}{dt}\|\|\mathbf{\Sigma}^E, \sigma_y^E\|\|^2 &= 2(2G)^{-1}\sigma_{y,0}\,\mathbf{T}_1 : \mathbf{\Sigma}^E \\ &+2\left[(2G)^{-1}\mathbf{T}_2 : \mathbf{\Sigma}^E + (H_{iso})^{-1}\sigma_y^E\dot{\sigma}_y\right] =: A_1 + A_2\end{aligned} \tag{5.297}$$

Recalling the identity (5.156), which holds in all phases and using that $\tilde{\sigma}_y = \tilde{\sigma}_{y,i}$ during all the step, we get

$$A_1 = 2\left(\frac{\sigma_y}{\sigma_{y,i}} - 1\right)\,\dot{\mathbf{e}} : \mathbf{\Sigma}^E \leq \frac{2}{\sigma_{y,i}}|\sigma_y - \sigma_{y,i}|\,\|\mathbf{\Sigma}^E\|\,\|\dot{\mathbf{e}}\| \tag{5.298}$$

Observing that $\sigma_{y,i} \geq \sigma_{y,0}$ and $\tilde{\sigma}_y = \tilde{\sigma}_{y,i}$, due to a triangle inequality it follows

$$A_1 \leq \frac{2}{\sigma_{y,0}}(|\sigma_y - \tilde{\sigma}_y| + |\sigma_{y,i} - \tilde{\sigma}_{y,i}|)\,\|\mathbf{\Sigma}^E\|\,\|\dot{\mathbf{e}}\| \tag{5.299}$$

which, from definition (5.227), becomes

$$A_1 \leq C \left(|||\mathbf{\Sigma}_i^E, \sigma_{y,i}^E||| + |||\mathbf{\Sigma}^E, \sigma_y^E||| \right) |||\mathbf{\Sigma}^E, \sigma_y^E||| \, \|\dot{\mathbf{e}}\| \tag{5.300}$$

where the scalar C depends only on the material constants.

Deriving in time and applying (5.128) we get

$$\dot{\sigma}_y = \frac{d}{dt}\left[\sigma_{y,0} X_0^q\right] = q\, \sigma_{y,0}\, X_0^{q-1} \dot{X}_0 = q\, \sigma_{y,0}\, X_0^{q-1} \frac{2G}{\sigma_{y,i}} \dot{\mathbf{e}} : \mathbf{X}^s \tag{5.301}$$

Applying (5.156) and (5.250), the identity above easily gives

$$\dot{\sigma}_y = q \frac{2G}{\sigma_{y,i}} \dot{\mathbf{e}} : \mathbf{\Sigma} \tag{5.302}$$

From the definition of q (see (5.156)), identity (5.302) and rearranging the terms, the second member in (5.297) becomes

$$\begin{aligned} A_2 &= \left[-2 \frac{2G}{2G + H_{iso}} \frac{\mathbf{\Sigma}}{\sigma_y} : \mathbf{\Sigma}^E + 2 \frac{2G}{2G + H_{iso}} \sigma_y^E \right] \frac{\dot{\mathbf{e}} : \mathbf{\Sigma}}{\sigma_{y,i}} \\ &= 2 \frac{2G}{2G + H_{iso}} \left[-\frac{\mathbf{\Sigma}}{\sigma_y} : \mathbf{\Sigma}^E + \sigma_y - \tilde{\sigma}_y \right] \frac{\dot{\mathbf{e}} : \mathbf{\Sigma}}{\sigma_{y,i}} \end{aligned} \tag{5.303}$$

which we will show being lesser or equal than zero. Note that, being the first couple in purely plastic phase, $\dot{\mathbf{e}} : \mathbf{\Sigma} \geq 0$; as a consequence, in order to show

$$A_2 \leq 0 \tag{5.304}$$

it is sufficient to show

$$-\frac{\mathbf{\Sigma}}{\sigma_y} : \mathbf{\Sigma}^E + \sigma_y - \tilde{\sigma}_y \leq 0 \tag{5.305}$$

Multiplying and dividing by σ_y, then recalling that $\|\mathbf{\Sigma}\| = \sigma_y$, we get

$$\begin{aligned} -\frac{\mathbf{\Sigma}}{\sigma_y} : \mathbf{\Sigma}^E + \sigma_y - \tilde{\sigma}_y &= \frac{1}{\sigma_y} \left[-\|\mathbf{\Sigma}\|^2 + \mathbf{\Sigma} : \tilde{\mathbf{\Sigma}} + \sigma_y^2 - \sigma_y \tilde{\sigma}_y \right] \\ &= \frac{1}{\sigma_y} \left[\mathbf{\Sigma} : \tilde{\mathbf{\Sigma}} - \sigma_y \tilde{\sigma}_y \right] \end{aligned} \tag{5.306}$$

A Cauchy-Schwarz inequality and the Kuhn-Tucker conditions applied to (5.306) then give

$$-\frac{\mathbf{\Sigma}}{\sigma_y} : \mathbf{\Sigma}^E + \sigma_y - \tilde{\sigma}_y \leq \frac{1}{\sigma_y} [\|\mathbf{\Sigma}\| \|\tilde{\mathbf{\Sigma}}\| - \sigma_y \tilde{\sigma}_y] \leq 0 \tag{5.307}$$

which implies (5.304). Joining (5.300) and (5.304) with (5.297) implies

$$\frac{d}{dt} |||\mathbf{\Sigma}^E, \sigma_y^E|||^2 \leq C \left(|||\mathbf{\Sigma}_i^E, \sigma_{y,i}^E||| + |||\mathbf{\Sigma}^E, \sigma_y^E||| \right) |||\mathbf{\Sigma}^E, \sigma_y^E||| \, \|\dot{\mathbf{e}}\| \tag{5.308}$$

which recalling (5.289) easily proves the Lemma.

5.9 NLK plasticity model

We start by recalling the associative von-Mises plasticity model under consideration, already examined in Section 2.3.3 and labeled as NLK model. Splitting the strain and stress tensors, $\boldsymbol{\sigma}$ and $\boldsymbol{\varepsilon}$, in deviatoric and volumetric parts we have

$$\boldsymbol{\sigma} = \mathbf{s} + p\mathbf{I} \qquad \text{with} \qquad p = \frac{1}{3}\text{tr}(\boldsymbol{\sigma}) \tag{5.309}$$

$$\boldsymbol{\varepsilon} = \mathbf{e} + \frac{1}{3}\theta\mathbf{I} \qquad \text{with} \qquad \theta = \text{tr}(\boldsymbol{\varepsilon}) \tag{5.310}$$

where tr indicates the trace operator, while $\mathbf{I}$, $\mathbf{s}$, p, $\mathbf{e}$, θ are respectively the second-order identity tensor, the deviatoric and volumetric stress, the deviatoric and volumetric strain.

The equations for the model are

$$p = K\theta \tag{5.311}$$

$$\mathbf{s} = 2G[\mathbf{e} - \mathbf{e}^p] \tag{5.312}$$

$$\boldsymbol{\Sigma} = \mathbf{s} - \boldsymbol{\alpha} \tag{5.313}$$

$$F = \|\boldsymbol{\Sigma}\| - \sigma_y \tag{5.314}$$

$$\dot{\mathbf{e}}^p = \dot{\gamma}\mathbf{n} \tag{5.315}$$

$$\sigma_y = \sigma_{y,0} + H_{iso}\gamma \tag{5.316}$$

$$\dot{\boldsymbol{\alpha}} = H_{kin}\dot{\gamma}\mathbf{n} - H_{nl}\dot{\gamma}\boldsymbol{\alpha} \tag{5.317}$$

$$\dot{\gamma} \geq 0\,, \quad F \leq 0\,, \quad \dot{\gamma}F = 0 \tag{5.318}$$

where K is the material bulk elastic modulus, G is the material shear modulus, $\mathbf{e}^p$ is the traceless plastic strain, $\boldsymbol{\Sigma}$ is the relative stress in terms of the backstress $\boldsymbol{\alpha}$, the latter introduced to describe the nonlinear kinematic hardening mechanism. Moreover, F is the von-Mises yield function, $\mathbf{n}$ is the normal to the yield surface, σ_y is the yield surface radius, $\sigma_{y,0}$ the initial yield stress, H_{kin} and H_{iso} are the kinematic and isotropic linear hardening moduli. The constant H_{nl} is the nonlinear kinematic hardening modulus, introduced to represent a nonlinear kinematic hardening mechanism (see Section 2.3.2). Finally, Equations (5.318) are the Kuhn-Tucker conditions; in particular, the second equation limits the relative stress within the boundary defined by the yield surface $F = 0$, while the other two are necessary to determine the plastic behavior. With a slight over-simplification of the model complexity, we may say that when $\dot{\gamma} = 0$ the system is in an elastic phase, while when $\dot{\gamma} > 0$ we say that the system is in a plastic phase.

In the following sections a set of numerical schemes for the above problem is presented. The first two schemes are based respectively on the backward Euler's and on the generalized midpoint integration rules, while the third one is a newly developed exponential-based integration algorithm.

Remark 5.9.1 *Due to the linear behavior of the volumetric part constitutive equations, in the following we treat only the deviatoric part of the model.*

5.10 Backward Euler's integration scheme for the NLK model

In this section we present a numerical method which uses a backward Euler's integration rule and is combined with a return map algorithm. Originally proposed in the context of elasoplastic models by Maenchen and Sack [59] by Wilkins [76], by Auricchio and Taylor [17] in the framework of generalized plasticity, the return map algorithm is based on the elastic predictor- plastic corrector strategy. The return map is achieved enforcing consistency at the end of the time step and projecting the trial solution onto the updated yield surface at the end of each elastoplastic step. This procedure result in solving a fourth-order polynomial in the plastic consistency parameter. As usual, we present both the time integration and the solution algorithm together with the consistent elastoplastic tangent operator. In the following the present scheme is referred to as BEnl (Backward-Euler integration method for von-Mises plasticity with nonlinear hardening).

It is assumed that the time history interval $[0, T]$ is divided into N sub-intervals defined by the nodes $0 = t_0 < t_1 < .... < t_n < t_{n+1} < .... < t_N = T$. Given the values $\{\mathbf{s}_n, \mathbf{e}_n, \mathbf{e}_n^p, \gamma_n, \boldsymbol{\alpha}_n\}$ at time t_n, and the deviatoric strain $\mathbf{e}_{n+1}$ at time t_{n+1}, the scheme consists in computing the remaining variables at time t_{n+1}. The strain history is assumed to be piecewise linear and the initial values of $\gamma, \mathbf{e}^p$ and $\boldsymbol{\alpha}$ are equal to zero.

5.10.1 Integration scheme

Using a backward Euler's integration rule the discrete evolutionary equations for the plasticity model become

$$\begin{cases} \mathbf{e}^p_{n+1} = \mathbf{e}^p_n + \lambda \mathbf{n}_{n+1} \\ \boldsymbol{\alpha}_{n+1} = T^\lambda \boldsymbol{\alpha}_n + T^\lambda H_{kin} \lambda \mathbf{n}_{n+1} \\ \mathbf{s}_{n+1} = 2G\left(\mathbf{e}_{n+1} - \mathbf{e}^p_{n+1}\right) \\ \boldsymbol{\Sigma}_{n+1} = \mathbf{s}_{n+1} - \boldsymbol{\alpha}_{n+1} \\ \gamma_{n+1} = \gamma_n + \lambda \end{cases} \tag{5.319}$$

with

$$T^\lambda = \frac{1}{1 + H_{nl}\lambda} \tag{5.320}$$

and where λ represents the incremental plastic parameter to be determined enforcing the plastic consistency condition (the subscript $n+1$ in λ is omitted for compactness).

Substituting $(5.319)_1$ into (5.312) yields:

$$\mathbf{s}_{n+1} = 2G\left(\mathbf{e}_{n+1} - \mathbf{e}^p_n\right) - 2G\lambda \mathbf{n}_{n+1} \tag{5.321}$$

and subtraction of Equation $(5.319)_2$ gives

$$\boldsymbol{\Sigma}_{n+1} = \mathbf{s}_{n+1} - \boldsymbol{\alpha}_{n+1} = 2G\left(\mathbf{e}_{n+1} - \mathbf{e}^p_n\right) - T^\lambda \boldsymbol{\alpha}_n - U^\lambda \mathbf{n}_{n+1} \tag{5.322}$$

where

$$U^\lambda = \left(2G + H_{kin} T^\lambda\right)\lambda \tag{5.323}$$

5.10.2 Solution algorithm

We initially suppose the step to be elastic, and calculate trial values at the final stage t_{n+1}:

$$\begin{cases} \mathbf{e}^{p,TR}_{n+1} = \mathbf{e}^p_n \\ \mathbf{s}^{TR}_{n+1} = 2G\left(\mathbf{e}_{n+1} - \mathbf{e}^p_n\right) \\ \boldsymbol{\alpha}^{TR}_{n+1} = \boldsymbol{\alpha}_n \\ \boldsymbol{\Sigma}^{TR}_{n+1} = \mathbf{s}^{TR}_{n+1} - \boldsymbol{\alpha}^{TR}_{n+1} \\ \gamma^{TR}_{n+1} = \gamma_n \end{cases} \tag{5.324}$$

If the resulting stress is admissible, i.e.

$$\parallel \boldsymbol{\Sigma}^{TR}_{n+1} \parallel \leq \sigma_{y,0} + H_{iso}\gamma^{TR}_{n+1} \tag{5.325}$$

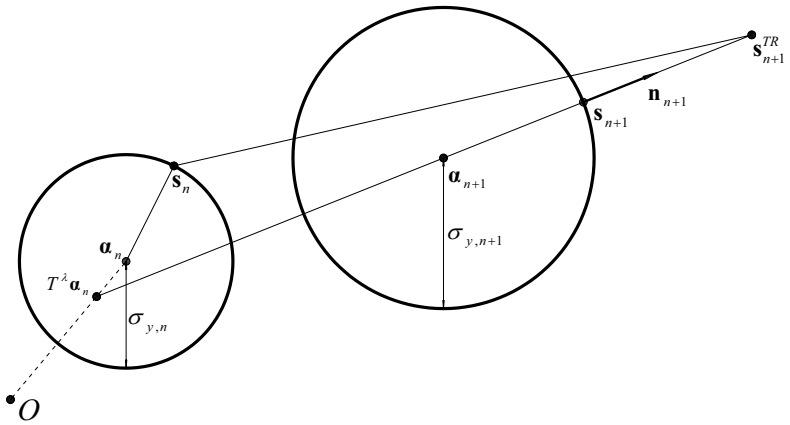

Figure 5.4: Application of the return map algorithm to the BEnl integration scheme. Plastic correction representation in deviatoric stress space.

the step is assumed to be elastic and the variable values at the final time instant are taken as the trial ones. On the other hand, if $\mathbf{\Sigma}^{TR}_{n+1}$ violates the yield limit, a plastic correction is introduced. Enforcing the satisfaction of the limit equation permits to compute λ and thus the discrete equantions (5.326) can be rewritten in terms of the trial state and λ:

$$\begin{cases} \mathbf{e}^{p}_{n+1} = \mathbf{e}^{p,TR}_{n} + \lambda \mathbf{n}_{n+1} \\ \mathbf{s}_{n+1} = \mathbf{s}^{TR}_{n+1} - 2G\lambda \mathbf{n}_{n+1} \\ \boldsymbol{\alpha}_{n+1} = T^{\lambda}\boldsymbol{\alpha}^{TR}_{n+1} + H_{kin}T^{\lambda}\lambda \mathbf{n}_{n+1} \\ \mathbf{\Sigma}_{n+1} = \mathbf{s}^{TR}_{n+1} - T^{\lambda}\boldsymbol{\alpha}^{TR}_{n+1} - U^{\lambda}\mathbf{n}_{n+1} \\ \gamma_{n+1} = \gamma^{TR}_{n+1} + \lambda \end{cases} \tag{5.326}$$

A graphical idealization of the return map algorithm applied to the BEnl integration scheme is provided in Figure 5.4 which represents in the deviatoric stress space the trial elastic predictor and the plastic corrector obtained applying the return map algorithm to the BEnl scheme.

It is noted that in Equations (5.319) and (5.326) the only unknown is represented by the consistency parameter λ which is to be computed imposing yield consistency at the end of the step. Therefore, the above sequential update procedure is set forth by enforcing the plastic consistency condition at t_{n+1} by means of a return map algorithm.

Observing that $(5.326)_4$ can be rewritten as

$$\mathbf{\Sigma}_{n+1} = \mathbf{\Sigma}^{\lambda}_{A} - U^{\lambda}\mathbf{n}_{n+1} \tag{5.327}$$

with

$$\mathbf{\Sigma}_A^\lambda = \mathbf{s}_{n+1}^{TR} - T^\lambda \boldsymbol{\alpha}_{n+1}^{TR}$$

we may conclude that $\mathbf{\Sigma}_{n+1}$ and $\mathbf{\Sigma}_A^\lambda$ are parallel i.e.

$$\| \mathbf{\Sigma}_{n+1} \| = \| \mathbf{\Sigma}_A^\lambda \| - U^\lambda$$

Using relation (5.327) we may write the discrete limit equation as

$$\|\mathbf{\Sigma}_A^\lambda\| - U^\lambda - \sigma_{y,n+1} = 0$$

Noting that:

$$\begin{aligned}
\|\mathbf{\Sigma}_A^\lambda\| &= \left[(\mathbf{\Sigma}_A^\lambda : \mathbf{\Sigma}_A^\lambda)\right]^{\frac{1}{2}} \\
&= \left[\left(\mathbf{s}_{n+1}^{TR} - T^\lambda \boldsymbol{\alpha}_{n+1}^{TR}\right) : \left(\mathbf{s}_{n+1}^{TR} - T^\lambda \boldsymbol{\alpha}_{n+1}^{TR}\right)\right]^{\frac{1}{2}} \\
&= \left[(\mathbf{s}_{n+1}^{TR} : \mathbf{s}_{n+1}^{TR}) - 2T^\lambda(\boldsymbol{\alpha}_{n+1}^{TR} : \mathbf{s}_{n+1}^{TR}) + (T^\lambda)^2(\boldsymbol{\alpha}_{n+1}^{TR} : \boldsymbol{\alpha}_{n+1}^{TR})\right]^{\frac{1}{2}} \\
&= \left[S_{ss} - 2S_{s\alpha}T^\lambda + S_{\alpha\alpha}(T^\lambda)^2\right]^{\frac{1}{2}}
\end{aligned}$$

where:

$$\begin{aligned}
S_{ss} &= (\mathbf{s}_{n+1}^{TR} : \mathbf{s}_{n+1}^{TR}) \\
S_{s\alpha} &= (\mathbf{s}_{n+1}^{TR} : \boldsymbol{\alpha}_{n+1}^{TR}) \\
S_{\alpha\alpha} &= (\boldsymbol{\alpha}_{n+1}^{TR} : \boldsymbol{\alpha}_{n+1}^{TR})
\end{aligned}$$

the limit equation becomes:

$$S_{ss}(R^\lambda)^2 - 2S_{s\alpha}R^\lambda + S_{\alpha\alpha} - \left[2G\lambda R^\lambda + H_{kin}\lambda + R^\lambda\sigma_{y,n} + H_{\text{iso}}\lambda R^\lambda\right]^2 = 0 \tag{5.328}$$

with

$$R^\lambda = 1 + H_{nl}\lambda \tag{5.329}$$

Equation (5.328) is a quartic equation in λ and may be expressed as:

$$g(\lambda) = C_1\lambda^4 + C_2\lambda^3 + C_3\lambda^2 + C_4\lambda + C_5 = 0$$

where:

$$\begin{aligned}
C_1 &= 4{H_{nl}}^2G_0^2 \\
C_2 &= 4{H_{nl}}^2G_0\sigma_{y,n} + 8G_0G_1H_{nl} \\
C_3 &= {H_{nl}}^2\left[(\sigma_{y,n})^2 - S_{ss}\right] + 4G_1^2 + 4H_{nl}\sigma_{y,n}\left[G_0 + G_1\right] \\
C_4 &= 2H_{nl}\left[(\sigma_{y,n})^2 + S_{s\alpha} - S_{ss}\right] + 4\sigma_{y,n}G_1 \\
C_5 &= (\sigma_{y,n})^2 - S_{\alpha\alpha} + 2S_{s\alpha} - S_{ss}
\end{aligned}$$

with:

$$2G_0 = 2G + H_{\text{iso}}$$

The solution of this equation, i.e. the search for the minimum positive root, is not an easy task, due to the order of the polynomial and to the dependence of the coefficients on the trial state. As observed in [17], an iterative algorithm of the Newton type may be easily implemented:

$$\begin{aligned} \lambda^{i+1} &= \lambda^i + \Delta\lambda^i \\ \Delta\lambda^i &= -\frac{g\left(\lambda^i\right)}{g^{'}\left(\lambda^i\right)} \end{aligned}$$

where: the superscript i refers to the i-th iteration, the superscript $'$ indicates first derivative; and where a starting value of $\lambda^0 = 0$ may be adopted. Unfortunately, this approach does not guarantee convergence to a positive root; in fact:

$$\begin{aligned} \Delta\lambda(0) &= -\frac{g(0)}{g^{'}(0)} = -\frac{C_5}{C_4} \\ &= \frac{\mathbf{\Sigma}^{TR} : \mathbf{\Sigma}^{TR} - (\sigma_{y,n})^2}{2H_{nl}\left[\mathbf{\Sigma}^{TR} : \mathbf{\Sigma}^{TR} - (\sigma_{y,n})^2\right] + 2H_{nl}(\mathbf{\Sigma}^{TR} : \boldsymbol{\alpha}^{TR}) - 4\sigma_{y,n}G_1} \end{aligned}$$

and the sign of $\Delta\lambda$ at zero depends on the sign of the denominator, which clearly depends on the trial state and on the previous solution. Consequently, it may happen that $\Delta\lambda(0) < 0$ and the Newton algorithm returns a negative value for λ. Attempts of starting the Newton iteration algorithm with different values of λ (such as $\lambda^0 = \lambda_n$) have been explored but generate the same pathology. Once the Newton algorithm has failed, the only robust approach is to perform a synthetic division of the quartic polynomial and compute in closed form the roots of the resulting cubic [14]; the roots should then be corrected using a Newton algorithm, since the synthetic division is sensitive to roundoff.

Remark 5.10.1 *The NLK model has been used to simulate the behavior of metals under cyclic loading, achieving an high degree of accuracy. Moreover, extensions of the model to include strain range memory, visco-plastic recovery properties, ratcheting effects have been presented in the literature [17, 23, 69, 70].*

However, difficulties arise to implement the model in a return map framework and they are all directly related to the non-linear kinematic hardening term. The discrete consistency condition yields a quartic equation, whose coefficients are function of the trial state and the previous solution, which makes

difficult the search of the minimum positive root. An approach based on a combination of Newton's algorithm and synthetic division is presented, which is robust but at the same time computationally expensive. Moreover, the elastoplastic tangent tensor consistent with the discrete model is non-symmetric and, as a result, an appropriate solver for non-symmetric linear systems must be used, plus the required memory storage is doubled.

5.10.3 BEnl scheme elastoplastic consistent tangent operator

We show here the consistent tangent operator for the BEnl scheme. For brevity's sake, only the final form of the operator corresponding to a plastic step (i.e. such that $\lambda \neq 0$) is reported without deriving it thoroughly. To make notation more clear, the subscripts of all history variables evaluated at time t_{n+1} are omitted for brevity. Quantities evaluated either at t_n are specified by the relative subscript. The reader is referred to [17] for a complete derivation.

$$\begin{aligned} \mathbb{C}^{ep} = \frac{\partial \boldsymbol{\sigma}}{\partial \boldsymbol{\varepsilon}} &= K\mathbf{I} \otimes \mathbf{I} + 2G\left(1 - C\right)\mathbb{I}_{\text{dev}} \\ &+ \left[2G\left(C - A\right) + B\left(\mathbf{n} : \boldsymbol{\alpha}\right)\right]\mathbf{n} \otimes \mathbf{n} - B\boldsymbol{\alpha} \otimes \mathbf{n} \end{aligned} \tag{5.330}$$

with

$$\begin{aligned} A &= \frac{2G}{2G_0 + T^{\lambda} H_{kin} - T^{\lambda}\left(\mathbf{n} : \boldsymbol{\alpha}\right)} \\ B &= A T^{\lambda} C H_{nl} \\ C &= \frac{2G\lambda}{\| \boldsymbol{\Sigma}_A^{\lambda} \|} \end{aligned}$$

5.11 Generalized midpoint integration scheme for the NLK model

In this section we present the numerical method already proposed by Ortiz and Popov [63] in the framework of linear hardening elastoplastic constitutive models. The method is based on a generalized midpoint integration rule combined with a return map algorithm. The return map is achieved enforcing consistency at the end of the time step and projecting the trial solution onto the updated yield surface at the end of each elastoplastic step. This procedure results in solving a 10th-order polynomial in the plastic consistency parameter which makes the computational effort quite significant. Again, this is still due to the nonlinear kinematic hardening term.

The present scheme is referred to as the MPTnl method (midpoint integration method for von-Mises plasticity with nonlinear hardening). In particular, the generalized midpoint integration rule investigated herein can be specialized to two different methods, namely the proper midpoint integration scheme [72] and the BEnl integration scheme analyzed in the preceding section. The method is outlined with its algorithmic solution sketch and consistent tangent operator.

To the author's knowledge, the literature does not report any detailed development or testing of the midpoint method MPTnl for the von-Mises plasticity model with nonlinear hardening as the one considered here (see [13] for a detailed comparison of generalized midpoint integration procedures applied to von-Mises plasticity with nonlinear hardening).

In the sequel it is assumed that the time history interval $[0, T]$ is divided into N sub-intervals defined by the nodes $0 = t_0 < t_1 < .... < t_n < t_{n+1} < .... < t_N = T$. Given the values $\{\mathbf{s}_n, \mathbf{e}_n, \gamma_n, \boldsymbol{\alpha}_n\}$ at time t_n, and the deviatoric strain $\mathbf{e}_{n+1}$ at time t_{n+1}, the scheme consists in computing the remaining variables at time t_{n+1}. The strain history is assumed to be piecewise linear and the initial values of $\gamma, \mathbf{e}^p$ and $\boldsymbol{\alpha}$ are zero.

5.11.1 Integration scheme

Using a generalized midpoint integration rule the discrete evolutionary equations can be written as:

$$\begin{cases} \mathbf{e}^p_{n+1} = \mathbf{e}^p_n + \lambda \mathbf{n}_{n+\alpha} \\ \boldsymbol{\alpha}_{n+1} = \boldsymbol{\alpha}_n + \lambda \left(H_{kin} \mathbf{n}_{n+\alpha} - H_{nl} \boldsymbol{\alpha}_{n+\alpha} \right) \\ \mathbf{s}_{n+1} = 2G \left(\mathbf{e}_{n+1} - \mathbf{e}^p_{n+1} \right) \\ \boldsymbol{\Sigma}_{n+1} = \mathbf{s}_{n+1} - \boldsymbol{\alpha}_{n+1} \\ \gamma_{n+1} = \gamma_n + \lambda \end{cases} \tag{5.331}$$

where λ represents the incremental plastic parameter to be determined enforcing the plastic consistency condition. The scalar α is the algorithmic parameter such that the following relations hold for quantities evaluated at the midpoint instant $t_{n+\alpha}$

$$\begin{cases} \mathbf{e}_{n+\alpha} = \alpha \mathbf{e}_{n+1} + (1-\alpha) \mathbf{e}_n \\ \mathbf{e}^p_{n+\alpha} = \alpha \mathbf{e}^p_{n+1} + (1-\alpha) \mathbf{e}^p_n \\ \boldsymbol{\alpha}_{n+\alpha} = \alpha \boldsymbol{\alpha}_{n+1} + (1-\alpha) \boldsymbol{\alpha}_n \\ \mathbf{s}_{n+\alpha} = 2G \left(\mathbf{e}_{n+\alpha} - \mathbf{e}^p_{n+\alpha} \right) \\ \boldsymbol{\Sigma}_{n+\alpha} = \mathbf{s}_{n+\alpha} - \boldsymbol{\alpha}_{n+\alpha} \end{cases} \tag{5.332}$$

Clearly, α can be arbitrarily chosen in the range $(0, 1]$. In particular, in the following we consider the possibility of $\alpha = 1/2$, leading to the midpoint integration rule (MPTnl). We remark that adopting $\alpha = 1$ leads to the backward Euler's integration rule (BEnl). The difference between the two schemes lays in fact only in the choice of the α parameter. The choice $\alpha = 1/2$ guarantees quadratic accuracy to the MPTnl, while the choice $\alpha = 1$ makes the BEnl method a simpler and more robust scheme with linear accuracy.

5.11.2 Solution algorithm

The elastic predictor-plastic corrector solution idea is applied again. Initially, the step is supposed to be elastic. This yields the following trial values at the final instant t_{n+1}:

$$\begin{cases} \mathbf{e}_{n+1}^{p,TR} = \mathbf{e}_n^p \\ \mathbf{s}_{n+1}^{TR} = 2G\left(\mathbf{e}_{n+1} - \mathbf{e}_n^p\right) \\ \boldsymbol{\alpha}_{n+1}^{TR} = \boldsymbol{\alpha}_n \\ \boldsymbol{\Sigma}_{n+1}^{TR} = \mathbf{s}_{n+1}^{TR} - \boldsymbol{\alpha}_{n+1}^{TR} \\ \gamma_{n+1}^{TR} = \gamma_n \end{cases} \tag{5.333}$$

If the resulting relative stress is admissible, i.e.

$$\| \boldsymbol{\Sigma}_{n+1}^{TR} \| \leq \sigma_{y,0} + H_{iso}\gamma_{n+1}^{TR} \tag{5.334}$$

then the step is purely elastic and the history variables are updated with their trial values. On the other hand, if $\boldsymbol{\Sigma}_{n+1}^{TR}$ lays outside the yield surface, a plastic correction is introduced in two steps:

- STEP 1: update at $t_{n+\alpha}$.

$$\begin{cases} \boldsymbol{\alpha}_{n+\alpha} = V^{\lambda}\boldsymbol{\alpha}_{n+1}^{TR} + \alpha H_{kin} V^{\lambda}\lambda\mathbf{n}_{n+\alpha} \\ \mathbf{s}_{n+\alpha} = \mathbf{s}_{n+\alpha}^{TR} - 2G\alpha\lambda\mathbf{n}_{n+\alpha} \\ \boldsymbol{\Sigma}_{n+\alpha} = \mathbf{s}_{n+\alpha} - \boldsymbol{\alpha}_{n+\alpha} \end{cases} \tag{5.335}$$

where

$$\begin{aligned} \mathbf{s}_{n+\alpha}^{TR} &= 2G\left(\mathbf{e}_{n+\alpha} - \mathbf{e}_n^p\right) \\ V^{\lambda} &= \frac{1}{1 + \alpha H_{nl}\lambda} \end{aligned}$$

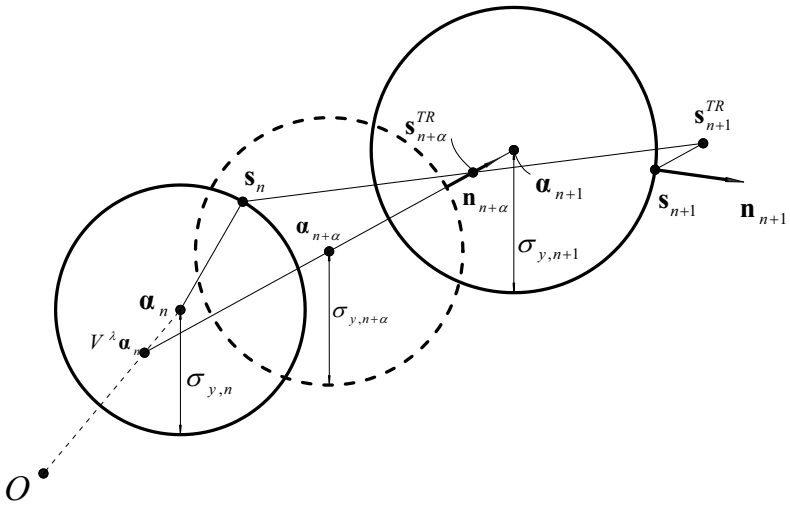

Figure 5.5: Application of the return map algorithm to the MPTnl integration scheme. Plastic correction representation in deviatoric stress space.

- STEP 2: update at t_{n+1}.

$$\begin{cases} \mathbf{e}^p_{n+1} = \mathbf{e}^p_n + \lambda \mathbf{n}_{n+\alpha} \\ \boldsymbol{\alpha}_{n+1} = W^{\lambda}\boldsymbol{\alpha}_n + H_{kin}V^{\lambda}\lambda\mathbf{n}_{n+\alpha} \\ \mathbf{s}_{n+1} = 2G\left(\mathbf{e}_{n+1} - \mathbf{e}^p_{n+1}\right) \\ \boldsymbol{\Sigma}_{n+1} = \mathbf{s}_{n+1} - \boldsymbol{\alpha}_{n+1} \\ \gamma_{n+1} = \gamma_n + \lambda \end{cases} \tag{5.336}$$

with

$$W^{\lambda} = \frac{1 + (\alpha - 1)\lambda H_{nl}}{1 + \alpha\lambda H_{nl}}$$

Remark 5.11.1 *In the case of the* BEnl *scheme, step (5.336) is equivalent to (5.335) and therefore is avoided in the procedure.*

A graphical idealization of the return map algorithm applied to the MPTnl integration scheme is provided in Figure 5.5, which represents in the deviatoric stress space the trial elastic predictor and the plastic corrector obtained applying the return map algorithm to the MPTnl scheme.

It is noted that in Equations (5.335) and (5.336) the only unknown is represented by the consistency parameter λ which is to be computed imposing

yield consistency at the end of the step. Therefore, the above sequential update procedure is set forth by enforcing the plastic consistency condition at t_{n+1}. Observing that $(5.335)_3$ can be rewritten as

$$\mathbf{\Sigma}_{n+\alpha} = \mathbf{\Sigma}_B^{\lambda} - Y^{\lambda}\mathbf{n}_{n+\alpha} \tag{5.337}$$

with

$$\begin{aligned} \mathbf{\Sigma}_B^{\lambda} &= \mathbf{s}_{n+\alpha}^{TR} - V^{\lambda}\boldsymbol{\alpha}_{n+1}^{TR} \\ Y^{\lambda} &= 2G\alpha\lambda + \alpha H_{kin}V^{\lambda}\lambda \end{aligned}$$

we may conclude that $\mathbf{\Sigma}_{n+\alpha}$ and $\mathbf{\Sigma}_B^{\lambda}$ are parallel i.e.

$$\| \mathbf{\Sigma}_{n+\alpha} \| = \| \mathbf{\Sigma}_B^{\lambda} \| - Y^{\lambda} \tag{5.338}$$

Using relation (5.338) we can finally write the consistency condition at t_{n+1} as follows

$$\| \mathbf{\Sigma}_{n+1} \| = \left\| \frac{1}{\alpha}\mathbf{\Sigma}_{n+\alpha} - \left(\frac{1-\alpha}{\alpha}\right)\mathbf{\Sigma}_n \right\| = [\sigma_{y,n} + \lambda H_{iso}] \tag{5.339}$$

Equation (5.339) is then solved searching for the minimum positive root. Note that, as an alternative in solving the above equation, the yield condition (5.339) can be rewritten as

$$\frac{1}{\alpha^2} \| \mathbf{\Sigma}_{n+\alpha} \|^2 - 2\left(\frac{1-\alpha}{\alpha^2}\right)(\mathbf{\Sigma}_{n+\alpha} : \mathbf{\Sigma}_n) + \left(\frac{1-\alpha}{\alpha}\right)^2 \| \mathbf{\Sigma}_n \|^2 = [\sigma_{y,n} + \lambda H_{iso}]^2 \tag{5.340}$$

which, with some algebra, results in a 10th-order polynomial in λ. For brevity, the expression of the polynomial coefficients is here omitted.

Remark 5.11.2 *In the case of the* BEnl *scheme, Equation (5.340) take a simpler form as the second and third term in the left hand side vanish. As a consequence, the relevant polynomial in λ is fourth degree and the coefficients have a shorter explicit form as discussed in Section 5.10.*

Remark 5.11.3 *Both th* MPTnl *and the* BEnl *scheme here presented are yield consistent and stable, as shown in [63] in a very general fashion. Moreover, the* BEnl *method is shown to be linearly accurate while the* MPTnl *method is quadratically accurate.*

Remark 5.11.4 *For the present model, the* MPTnl *midpoint scheme here detailed is not guaranteed to have a solution for every trial $\boldsymbol{s}_{n+1}^{TR}$. On the other hand, from all the numerical tests carried out in Chapter 6, it seems that a solution always exists for the values of strain increment $\| \Delta\boldsymbol{e} \|$ adopted throughout the testing.*

5.11.3 MPTnl scheme elastoplastic consistent tangent operator

We report here the elastoplastic tangent operator consistent with the MPTnl scheme. For brevity's sake, only the final form of the operator is given here for a plastic step (i.e. such that $\lambda \neq 0$) without deriving it thoroughly. To make notation more clear, the subscripts of all history variables evaluated at time t_{n+1} are omitted for brevity. Quantities evaluated either at t_n or at $t_{n+\alpha}$ are specified by the relative subscript.

Following the derivation procedure reported in [17, 63, 71], the consistent tangent operator $\dfrac{\partial \boldsymbol{\sigma}}{\partial \boldsymbol{\varepsilon}}$ for the MPTnl scheme is easily obtained. Recalling that

$$\frac{\partial \mathbf{s}}{\partial \boldsymbol{\varepsilon}} = \frac{\partial \mathbf{s}}{\partial \mathbf{e}} \frac{\partial \mathbf{e}}{\partial \boldsymbol{\varepsilon}} = \frac{\partial \mathbf{s}}{\partial \mathbf{e}} \mathbb{I}_{\text{dev}} \tag{5.341}$$

where

$$\mathbb{I}_{\text{dev}} = \mathbb{I} - \frac{1}{3} (\mathbf{I} \otimes \mathbf{I}) \tag{5.342}$$

and taking into account the volumetric part of the stress, from equations (5.309), (5.310) and (5.311) we get

$$\mathbb{C}^{ep} = \frac{\partial \boldsymbol{\sigma}}{\partial \boldsymbol{\varepsilon}} = \frac{\partial \mathbf{s}}{\partial \mathbf{e}} \mathbb{I}_{\text{dev}} + K (\mathbf{I} \otimes \mathbf{I}) \tag{5.343}$$

The fourth-order tensor $\dfrac{\partial \mathbf{s}}{\partial \mathbf{e}}$ may be computed as

$$\frac{\partial \mathbf{s}}{\partial \mathbf{e}} = \mathbb{M}_1 + \mathbb{M}_2 \tag{5.344}$$

where $\mathbb{M}_1$ and $\mathbb{M}_2$ are given by the following expressions

$$\mathbb{M}_1 = 2G \left(\mathbb{I} - \eta \, \mathbb{I}_{\mathbf{n}} - \mathbf{n}_{n+\alpha} \otimes \frac{\partial \lambda}{\partial \mathbf{e}} \right) \tag{5.345}$$

$$\mathbb{M}_2 = \eta \, \mathbb{I}_{\mathbf{n}} \left(\boldsymbol{\beta} \otimes \frac{\partial \lambda}{\partial \mathbf{e}} \right) \tag{5.346}$$

with

$$\eta = \lambda \frac{2G + H_{kin}V^{\lambda}}{2G\lambda + H_{kin}V^{\lambda}\lambda + 2\|\mathbf{\Sigma}_{n+\alpha}\|} \tag{5.347}$$

$$\mathbb{I}_{\mathbf{n}} = \mathbb{I} - \mathbf{n}_{n+\alpha} \otimes \mathbf{n}_{n+\alpha} \tag{5.348}$$

$$\frac{\partial \lambda}{\partial \mathbf{e}} = -2G(\theta_1 + \theta_2)^{-1} \left(\mathbb{I} - \frac{2G\lambda + H_{kin}V^{\lambda}\lambda/2}{2 \parallel \mathbf{s}^{TR}_{n+\alpha} - V^{\lambda}\boldsymbol{\alpha}_n \parallel} \mathbb{I}_{\mathbf{n}} \right) \mathbf{\Sigma} \tag{5.349}$$

$$\theta_1 = H_{iso}\sigma_{y,n+1} + (\boldsymbol{\beta} : \mathbf{\Sigma}) + 2G\left(\mathbf{n}_{n+\alpha} : \mathbf{\Sigma}\right) \tag{5.350}$$

$$\theta_2 = \frac{H_{nl}\left(2G\lambda + H_{kin}V^{\lambda}\lambda/2\right)}{2\left(V^{\lambda}\right)^2} \frac{\left(\mathbf{\Sigma} : \mathbb{I}_{\mathbf{n}}\boldsymbol{\alpha}_n\right)}{\parallel \mathbf{s}^{TR}_{n+\alpha} - V^{\lambda}\boldsymbol{\alpha}_n \parallel} \tag{5.351}$$

$$\boldsymbol{\beta} = \frac{1}{2}\frac{H_{nl}}{\left(V^{\lambda}\right)^2}\boldsymbol{\alpha}_n - \frac{1}{4}H_{kin}\frac{\lambda H_{nl}}{\left(V^{\lambda}\right)^2}\mathbf{n}_{n+\alpha} + \frac{1}{2}H_{kin}V^{\lambda}\mathbf{n}_{n+\alpha} \tag{5.352}$$

5.12 ESC^{2}nl exponential-based integration scheme for the NLK model

In this section we propose an exponential-based numerical scheme for the NLK model. The method is based on a different formulation of the constitutive relation and is developed following an ad-hoc rewriting of the time continuous model and on the application of exponential maps for the integration of the respective dynamical system [12]. A similar continuous formulation had been adopted earlier by Hong and Liu [44, 46, 47] in the case of von Mises plastic materials with no hardening. The new algorithm here presented, which will be referred as ESC^{2}nl, represents an extension of previous algorithms introduced by the author et al. in the case of linear hardening [16, 8, 9, 10, 11] and is a member of the "ESC" integration schemes family.

As will be pointed out within the numerical test chapter the new ESC^{2}nl scheme is yield consistent, quadratically accurate and grants exactness in case of no hardening.

5.12.1 A model reformulation

Combining Equations (5.312) and (5.313), we obtain

$$\mathbf{\Sigma} + \boldsymbol{\alpha} + 2G\mathbf{e}^p = 2G\mathbf{e} \tag{5.353}$$

which, taking the derivative in time, applying Equation (5.315), (5.317) and rearranging terms gives

$$\dot{\mathbf{\Sigma}} = 2G\dot{\mathbf{e}} - \left(2G + H_{kin}\right)\dot{\mathbf{e}}^p + H_{nl}\dot{\gamma}\boldsymbol{\alpha} \tag{5.354}$$

Now, recalling the yield surface radius

$$\sigma_y = \sigma_{y,0} + H_{iso}\gamma \tag{5.355}$$

and that in the plastic phase ($\dot{\gamma} > 0$)

$$\mathbf{n} = \frac{\mathbf{\Sigma}}{\|\mathbf{\Sigma}\|} = \frac{\mathbf{\Sigma}}{\sigma_{y,0} + H_{iso}\gamma} = \frac{\mathbf{\Sigma}}{\sigma_y} \tag{5.356}$$

we may apply (5.315) in (5.354) obtaining

$$\dot{\mathbf{\Sigma}} + (2G + H_{kin})\frac{\mathbf{\Sigma}}{\sigma_y}\dot{\gamma} = 2G\dot{\mathbf{\Psi}} \tag{5.357}$$

where we introduced the position

$$\dot{\mathbf{\Psi}} = \dot{\mathbf{e}} + \frac{H_{nl}}{2G}\dot{\gamma}\boldsymbol{\alpha} \tag{5.358}$$

Note that (5.357) is a differential equation for $\mathbf{\Sigma}$ that is valid also during elastic phases ($\dot{\gamma} = 0$). Introducing the *scaled relative stress*

$$\bar{\mathbf{\Sigma}} := \frac{\mathbf{\Sigma}}{\sigma_y} \tag{5.359}$$

we observe that, whenever the relative stress $\mathbf{\Sigma}$ lays on the yield surface, then $\bar{\mathbf{\Sigma}} = \mathbf{n}$, while this is not true when $\mathbf{\Sigma}$ lays inside the yield surface. The time derivative of (5.359) and the use of relation (5.355) gives

$$\dot{\bar{\mathbf{\Sigma}}} = \frac{\dot{\mathbf{\Sigma}}}{\sigma_y} - \frac{H_{iso}}{\sigma_y}\dot{\gamma}\bar{\mathbf{\Sigma}} \tag{5.360}$$

Using Equations (5.357) and (5.360), one obtains

$$\dot{\bar{\mathbf{\Sigma}}} + \frac{2G + H_{kin} + H_{iso}}{\sigma_y}\dot{\gamma}\bar{\mathbf{\Sigma}} = \frac{2G}{\sigma_y}\dot{\mathbf{\Psi}} \tag{5.361}$$

The next goal is to introduce an *integration factor* for the above evolutionary equation. In other words, we search for a scalar function depending on time X_0 such that

$$\frac{\mathrm{d}}{\mathrm{d}t}[X_0\bar{\mathbf{\Sigma}}] = X_0\dot{\bar{\mathbf{\Sigma}}} + \dot{X}_0\bar{\mathbf{\Sigma}} = X_0\dot{\bar{\mathbf{\Sigma}}} + X_0\frac{2G + H_{kin} + H_{iso}}{\sigma_y}\dot{\gamma}\bar{\mathbf{\Sigma}} \tag{5.362}$$

which, multiplying Equation (5.361) by X_0, would give

$$\frac{\mathrm{d}}{\mathrm{d}t}\left[X_0\bar{\mathbf{\Sigma}}\right] = \frac{2G}{\sigma_y}X_0\dot{\mathbf{\Psi}} \tag{5.363}$$

Accordingly, we set

$$X_0(\gamma) = \begin{cases} \left(1 + \dfrac{\gamma H_{iso}}{\sigma_{y,0}}\right)^{\dfrac{2G + H_{kin} + H_{iso}}{H_{iso}}} & \text{if } \; H_{iso} \neq 0 \\ \exp\left(\dfrac{2G + H_{kin} + H_{iso}}{\sigma_{y,0}}\gamma\right) & \text{if } \; H_{iso} = 0 \end{cases} \tag{5.364}$$

Noting that such a function is continuous for fixed γ and $H_{iso} \to 0$, and that

$$\dot{X}_0 = \frac{2G + H_{kin} + H_{iso}}{\sigma_y}\dot{\gamma}X_0 \tag{5.365}$$

we immediately obtain the target relationship (5.362) and therefore (5.363).

We now need an evolution law for X_0. In elastic phases, such law follows immediately from (5.365):

$$\dot{X}_0 = 0 \qquad \text{(elastic phases)} \tag{5.366}$$

On the other hand, for $\dot{\gamma} \neq 0$, taking the scalar product of (5.363) with $\bar{\mathbf{\Sigma}}$, we have

$$X_0 \frac{1}{2}\frac{\mathrm{d}}{\mathrm{d}t}\|\bar{\mathbf{\Sigma}}\|^2 \; + \; \dot{X}_0\|\bar{\mathbf{\Sigma}}\|^2 = \frac{2G}{\sigma_y}X_0\dot{\mathbf{\Psi}} : \bar{\mathbf{\Sigma}} \tag{5.367}$$

which, noting that in plastic phases

$$\|\bar{\mathbf{\Sigma}}\| = \frac{\|\mathbf{\Sigma}\|}{\sigma_y} = 1 \tag{5.368}$$

and using (5.367) gives

$$\dot{X}_0 = \frac{2G}{\sigma_y}\dot{\mathbf{\Psi}} : X_0\bar{\mathbf{\Sigma}} \qquad \text{(plastic phases)} \tag{5.369}$$

At this stage, we define the *generalized stress* $\mathbf{X}$ as the two component vector represented in engineering notation as

$$\{\mathbf{X}\} = \begin{Bmatrix} X_0\bar{\mathbf{\Sigma}} \\ X_0 \end{Bmatrix} = \begin{Bmatrix} \mathbf{X}^s \\ X_0 \end{Bmatrix} \tag{5.370}$$

As done for the ENN, ESC and ESC^2 schemes, we consider a linear space structure on the space of generalized stresses, the product by a scalar and the sum between vectors being defined in the obvious natural way. Moreover, any

element of the space of linear operators from the generalized stress space into itself can be written adopting the engineering notation as

$$[\mathbb{M}] = \begin{bmatrix} \mathbb{M}_{11} & \mathbf{M_{12}} \\ \mathbf{M_{21}} & M_{22} \end{bmatrix} \tag{5.371}$$

with $\mathbb{M}_{11}$ a fourth-order tensor, $\mathbf{M_{12}}, \mathbf{M_{21}}$ second-order tensors and M_{22} a scalar, under the convention that the formal expression

$$\mathbb{M}\mathbf{Y} \tag{5.372}$$

returns a generalized stress vector given by the following operation

$$[\mathbb{M}]\ \{\mathbf{Y}\} = \begin{bmatrix} \mathbb{M}_{11} & \mathbf{M_{12}} \\ \mathbf{M_{21}} & M_{22} \end{bmatrix} \begin{Bmatrix} \mathbf{Y}^s \\ Y_0 \end{Bmatrix} = \begin{Bmatrix} \mathbb{M}_{11}\mathbf{Y}^s + \mathbf{M_{12}}\, Y_0 \\ \mathbf{M_{21}} : \mathbf{Y^s} + \mathbf{M_{22}}\, Y_0 \end{Bmatrix} \tag{5.373}$$

for any couple $\{\mathbf{Y}\} = \{\mathbf{Y}^s, Y_0\}^T$ in the generalized stress space. In the sequel, we will consider a linear space structure also on the space of the linear operators acting on couples, again with the product by a scalar and the sum between such linear operators being defined in the obvious natural way.

Due to definition (5.370), Equation (5.363) can be rewritten as

$$\dot{\mathbf{X}}^s = \frac{2G}{\sigma_y} X_0 \dot{\mathbf{\Psi}} \tag{5.374}$$

while (5.369) becomes

$$\dot{X}_0 = \frac{2G}{\sigma_y} \dot{\mathbf{\Psi}} : \mathbf{X}^s \qquad \text{(plastic phases)} \tag{5.375}$$

Equations (5.374), (5.366) and (5.375) provide a system for the *generalized stress vector* $\mathbf{X}$, in the form

$$\dot{\mathbf{X}} = \mathbb{A}\mathbf{X} \tag{5.376}$$

where $\mathbb{A}$ represents a linear operator acting from the space of couples into itself, and depending on the actual phase as follows

$$[\mathbb{A}] = [\mathbb{A}_e] = \frac{2G}{\sigma_y} \begin{bmatrix} \mathbb{O} & \dot{\mathbf{\Psi}} \\ \mathbf{0} & 0 \end{bmatrix} \qquad \text{(elastic phase)} \tag{5.377}$$

$$[\mathbb{A}] = [\mathbb{A}_p] = \frac{2G}{\sigma_y} \begin{bmatrix} \mathbb{O} & \dot{\mathbf{\Psi}} \\ \dot{\mathbf{\Psi}} & 0 \end{bmatrix} \qquad \text{(plastic phase)} \tag{5.378}$$

where $\mathbf{0}$ and $\mathbb{O}$ indicate respectively the second-order and fourth-order null tensors.

Expression (5.376)-(5.378) is a formal compact notation to describe the action of the linear operator $\mathbb{A}$ on the couple $\mathbf{X}$, as introduced in (5.373).

Therefore the original problem, expressed by Equations (5.312)-(5.317), has been substituted by a new one, expressed by Equations (5.376)-(5.378). Note that $\dot{\mathbf{\Psi}}$ can be equivalently substituted by $\dot{\mathbf{e}}$ in (5.377), because $\dot{\gamma} = 0$ during elastic phases.

Remark 5.12.1 *Unless $H_{iso} = H_{nl} = 0$, the operator $\mathbb{A}$ is not constant in time, therefore our formulation* (5.376) *is nonlinear. Nevertheless, the particular form of the dynamical system* (5.376) *is useful, since it allows to develop the numerical method of Section 5.12.2.*

Time-continuous on-off switch

To properly convert the original problem in a new but equivalent differential algebraic format, we also need to introduce an elastoplastic phase determination criterion expressed in the new generalized stress environment.

For a given state to be plastic, the following two conditions must be fulfilled:

1) The relative stress $\mathbf{\Sigma}$ must be on the yield surface, i.e.

$$\|\mathbf{\Sigma}\| = \sigma_y \tag{5.379}$$

Using (5.359) and (5.370) this can be easily rewritten as

$$\|\mathbf{X}^s\|^2 = \|\bar{\mathbf{\Sigma}}\|^2 X_0^2 = \frac{\|\mathbf{\Sigma}\|^2}{\sigma_y^2} X_0^2 = X_0^2 \tag{5.380}$$

2) The direction of the strain rate $\dot{\mathbf{e}}$ must be outward with respect to the yield surface, i.e.

$$\mathbf{\Sigma} : \dot{\mathbf{e}} > 0 \tag{5.381}$$

Again recalling (5.359) and (5.370) it is immediate to check that (5.381) is equivalent to

$$\mathbf{X}^s : \dot{\mathbf{e}} > 0 \tag{5.382}$$

If the two conditions (5.380) and (5.382) are not satisfied, the step is elastic.

5.12.2 Integration scheme

It is assumed that the time history interval $[0, T]$ is divided into N sub-intervals defined by the points $0 = t_0 < t_1 < .... < t_n < t_{n+1} < .... < t_N = T$. Given the values $\{\mathbf{s}_n, \mathbf{e}_n, \gamma_n, \boldsymbol{\alpha}_n\}$ at time t_n, and the deviatoric strain $\mathbf{e}_{n+1}$ at time t_{n+1}, we search for the remaining variables at time t_{n+1}. As usual, the strain history is assumed to be piecewise linear. Equivalently, we may say that the piecewise linearity of the strain path makes $\dot{\mathbf{e}}$ constant within each single time interval. Moreover, we assume to start from an unstressed and undeformed state, i.e. characterized by zero initial values of the variables $\gamma, \mathbf{e}^p$ and $\boldsymbol{\alpha}$. Accordingly, the initial *generalized stress* is

$$\{\mathbf{X}_0\} = \begin{Bmatrix} \boldsymbol{\Sigma}_0/\sigma_{y,0} \\ 1 \end{Bmatrix} \tag{5.383}$$

Referring to the the dynamical law (5.376) with the operator $\mathbb{A}$ given respectively by (5.377) or (5.378), we aim to derive a numerical scheme for the discrete evolution of $\mathbf{X}$ along the general time step $[t_n, t_{n+1}]$.

It is immediate to observe that, if during the time interval $[t_n, t_{n+1}]$ the material behavior is purely elastic ($\dot{\gamma} = 0$ - elastic step), then the operator $\mathbb{A}_e$ is constant within this interval. In this case, the dynamical law (5.376) can be solved in closed form and the formula (5.384) returns the exact solution. In analogy to (5.376), the discrete evolution of the generalized stress will be in the form

$$\mathbf{X}_{n+1} = \exp\left[\bar{\mathbb{A}}\Delta t\right]\mathbf{X}_n = \bar{\mathbb{G}}\,\mathbf{X}_n \tag{5.384}$$

with $\bar{\mathbb{A}} = \mathbb{A}_e$ and $\Delta t = t_{n+1} - t_n$. Note that, being $\bar{\mathbb{A}}$ an element in the linear space of linear operators acting on couples, the exponential of $\bar{\mathbb{A}}\Delta t$ is naturally defined by the (converging) exponential serie

$$\exp\left[\bar{\mathbb{A}}\Delta t\right] = \sum_{n=0}^{+\infty} \frac{\left(\bar{\mathbb{A}}\Delta t\right)^n}{n!} \tag{5.385}$$

Instead, if during the step $[t_n, t_n + 1]$ purely plastic loading takes place, the linear operator $\mathbb{A}_p$ is not constant in time; in fact the yield surface radius σ_y and the "driving" tensor $\dot{\boldsymbol{\Psi}}$ cannot be expected to be constant whenever $\dot{\gamma} > 0$ (see Equations (5.316) and (5.358)). In such cases, therefore, the discrete solution of the dynamical system (5.376) is achieved by assuming that the above variables remain constant within the time step. As a consequence, an equation identic to (5.384) still holds, clearly with a different choice of $\bar{\mathbb{A}}$. This is equivalent to substitute the operator $\mathbb{A}_p$ with an operator $\bar{\mathbb{A}}_p$ which is constant during the time step. The respective constant values taken by σ_y

and $\dot{\mathbf{\Psi}}$, which depend on known quantities evaluated at the beginning of the step t_n, are still indicated by $\bar{\sigma}_y$ and $\bar{\dot{\mathbf{\Psi}}}$; we will specialize such constants in the immediate following. Then, we may introduce $\bar{\mathbb{A}}$ defined by

$$\left[\bar{\mathbb{A}}_e\right] = \frac{2G}{\sigma_{y,n}} \begin{bmatrix} \mathbb{O} & \dot{\mathbf{e}} \\ \mathbf{0} & 0 \end{bmatrix} \qquad \text{(elastic step)} \tag{5.386}$$

and

$$\left[\bar{\mathbb{A}}_p\right] = \frac{2G}{\bar{\sigma}_y} \begin{bmatrix} \mathbb{O} & \bar{\dot{\mathbf{\Psi}}} \\ \bar{\dot{\mathbf{\Psi}}} & 0 \end{bmatrix} \qquad \text{(plastic step)} \tag{5.387}$$

We are now in possess of all the ingredients for solving the Equation (5.376). In particular the choice of the parameters $\bar{\sigma}_y$ and $\bar{\dot{\mathbf{\Psi}}}$ for plastic steps is now addressed with emphasis on the effects this choices induces on the algorithmical properties.

The operator $\bar{\mathbb{A}}\Delta t$ is by definition equal to the original operator (5.377) or (5.378) after substituting $\bar{\dot{\mathbf{\Psi}}}$ with $\Delta\bar{\mathbf{\Psi}} = \Delta t\bar{\dot{\mathbf{\Psi}}}$ and σ_y with $\bar{\sigma}_y$. A possible choice is thus given by the following values

$$\left\{ \begin{array}{rcl} \bar{\sigma}_y & = & \dfrac{c\sigma_{y,n}}{\ln(1+c)} \\ \Delta\bar{\mathbf{\Psi}} & = & \Delta t\bar{\dot{\mathbf{\Psi}}} = \Delta\bar{\mathbf{\Psi}}_0 + \Delta\bar{\mathbf{\Psi}}_1 \end{array} \right. \tag{5.388}$$

where the constant and tensors appearing in (5.388) are given by

$$c = \frac{2G\,\bar{q}\,\left(\mathbf{n}_n : \Delta\mathbf{e}\right)}{\sigma_{y,n}} \tag{5.389}$$

$$\Delta\bar{\mathbf{\Psi}}_0 = \Delta\mathbf{e} + \frac{H_{nl}\left(\mathbf{n}_n : \Delta\mathbf{e}\right)}{2G_1 - H_{nl}\left(\mathbf{n}_n : \boldsymbol{\alpha}_n\right)}\boldsymbol{\alpha}_n \tag{5.390}$$

$$\Delta\bar{\mathbf{\Psi}}_1 = \frac{1}{2}\frac{H_{nl}}{2G}\left(\mathbf{D}_{\boldsymbol{\alpha}}D_\gamma + D'_\gamma\boldsymbol{\alpha}_n\right) \tag{5.391}$$

with

$$
\begin{aligned}
\Delta\mathbf{e} &= \dot{\mathbf{e}}\Delta t \\
\bar{q} &= \frac{H_{iso}}{2G_1 - H_{nl}\left(\mathbf{n}_n : \boldsymbol{\alpha}_n\right)} \\
\mathbf{n}_n &= \frac{\mathbf{X}_n^s}{X_{0,n}} \\
2G_1 &= 2G + H_{iso} + H_{kin} \\
D_\gamma &= \frac{2G}{2G_1 - H_{nl}\left(\mathbf{n}_n : \boldsymbol{\alpha}_n\right)}\left(\mathbf{n}_n : \Delta\mathbf{e}\right) \\
\mathbf{D}_{\boldsymbol{\alpha}} &= \left(H_{kin}\mathbf{n}_n - H_{nl}\boldsymbol{\alpha}\right) D_\gamma \\
D'_\gamma &= \frac{2G}{2G_1 - H_{nl}\left(\mathbf{n}_n : \boldsymbol{\alpha}_n\right)}\left(\mathbf{D}_{\mathbf{n}} : \Delta\mathbf{e}\right) \\
&+ \frac{H_{nl}D_\gamma}{2G_1 - H_{nl}\left(\mathbf{n}_n : \boldsymbol{\alpha}_n\right)}\left[\left(\mathbf{D}_{\mathbf{n}} : \boldsymbol{\alpha}_n\right) + \left(\mathbf{n}_n : \mathbf{D}_{\boldsymbol{\alpha}}\right)\right] \\
\mathbf{D}_{\mathbf{n}} &= \frac{2G}{\sigma_{y,n}}\Delta\mathbf{e} - \frac{2G_1 D_\gamma}{\sigma_{y,n}}\mathbf{n}_n + \frac{H_{nl}D_\gamma}{\sigma_{y,n}}\mathbf{D}_{\boldsymbol{\alpha}}
\end{aligned}
$$

The choice for $\bar{\sigma}_y$ in (5.388) corresponds to an extension of the ESC^2 scheme presented in Section 5.7 [9]. Instead, the value for $\Delta\bar{\boldsymbol{\Psi}}$ is essentially derived from a first order expansion of the tensor $\dot{\boldsymbol{\Psi}}$ in time. This choice guarantees a second-order scheme as well as other properties as discussed in the sequel (see [12] for further details on this issue).

The linear operator $\bar{\mathbb{G}}$ appearing in Equation (5.384) can be derived calculating the shown exponential. Note that, for such purpose, it is convenient to reformulate the linear operator $\bar{\mathbb{A}}\Delta t$ as a $\mathcal{R}^{7\times 7}$ matrix, calculate the exponential, and finally write it back in the original form (5.371). Without showing the calculations, we get

$$
\left[\bar{\mathbb{G}}\right] = \begin{cases}
\left[\bar{\mathbb{G}}_e\right] = \begin{bmatrix} \mathbb{I} & \dfrac{2G}{\bar{\sigma}_y}\Delta\mathbf{e} \\ \mathbf{0} & 1 \end{bmatrix} & \text{(elastic step)} \\[2ex]
\left[\bar{\mathbb{G}}_p\right] = \begin{bmatrix} \mathbb{I} + \left[\dfrac{(a-1)}{\|\Delta\bar{\boldsymbol{\Psi}}\|^2}\right]\Delta\bar{\boldsymbol{\Psi}} \otimes \Delta\bar{\boldsymbol{\Psi}} & b\dfrac{\Delta\bar{\boldsymbol{\Psi}}}{\|\Delta\bar{\boldsymbol{\Psi}}\|} \\ b\dfrac{\Delta\bar{\boldsymbol{\Psi}}^T}{\|\Delta\bar{\boldsymbol{\Psi}}\|} & a \end{bmatrix} & \text{(plastic step)}
\end{cases}
\tag{5.392}
$$

where $\mathbb{I}$ is the fourth-order identity tensor, while the scalars a and b are

$$a = \cosh\left(\frac{2G}{\bar{\sigma}_y}\|\Delta\bar{\boldsymbol{\Psi}}\|\right) \tag{5.393}$$

$$b = \sinh\left(\frac{2G}{\bar{\sigma}_y}\|\Delta\bar{\boldsymbol{\Psi}}\|\right) \tag{5.394}$$

Another point to be addressed is the update of the backstress tensor $\boldsymbol{\alpha}$. Due to the presence of the nonlinear kinematic hardening in the model, the tensor $\boldsymbol{\alpha}(t)$ is not a function of $\mathbf{e}(t)$ and $\boldsymbol{\Sigma}(t)$, $t \in [0, T]$, but must be recorded separately. As a consequence, the backstress $\boldsymbol{\alpha}$ needs to be updated at all time steps. An approximated integration in time of Equation (5.317) gives

$$\boldsymbol{\alpha}_{n+1} - \boldsymbol{\alpha}_n = \int_{t_n}^{t_{n+1}} (H_{kin}\dot{\gamma}\mathbf{n} - H_{nl}\dot{\gamma}\boldsymbol{\alpha})\, dt \simeq$$
$$\frac{\Delta\gamma}{2}\left[H_{kin}(\mathbf{n}_{n+1} + \mathbf{n}_n) - H_{nl}(\boldsymbol{\alpha}_{n+1} + \boldsymbol{\alpha}_n)\right] \tag{5.395}$$

From Equation (5.395) we get immediately

$$\boldsymbol{\alpha}_{n+1} \simeq \frac{H_{kin}\Delta\gamma(\mathbf{n}_{n+1} + \mathbf{n}_n)/2 + (1 - H_{nl}\Delta\gamma/2)\boldsymbol{\alpha}_n}{1 + H_{nl}\Delta\gamma/2} \tag{5.396}$$

where, as follows by definitions (5.370) and (5.359), the normal at time t_{n+1}

$$\mathbf{n}_{n+1} = \frac{\mathbf{X}^s_{n+1}}{X_{0,n+1}} \tag{5.397}$$

Moreover, we note that the value of $\Delta\gamma$ in (5.396) can be obtained directly from definition (5.364)

$$\Delta\gamma = \begin{cases} \dfrac{\sigma_{y,0}}{2G_1}\ln\left(X_{0,n+1}/X_{0,n}\right) & \text{if } H_{iso} = 0 \\[2ex] \dfrac{\sigma_{y,0}}{H_{iso}}\left(X^q_{0,n+1} - X^q_{0,n}\right) & \text{if } H_{iso} \neq 0 \end{cases} \tag{5.398}$$

where

$$q = \frac{H_{iso}}{2G + H_{iso} + H_{kin}} \tag{5.399}$$

5.12.3 Solution algorithm

At every time step the exponential-based ESC^{2}nl algorithm proceeds as follows:

1) Suppose the step to be elastic and compute trial values following an elastic law

$$\mathbf{X}_{n+1}^{TR} = \bar{\mathbb{G}}_e \mathbf{X}_n \tag{5.400}$$

where the operator $\bar{\mathbb{G}}_e$ is given by (5.392). If the trial solution is admissible, i.e.

$$\|\mathbf{X}_{n+1}^{s,TR}\| \leq \left(X_{0,n+1}^{TR}\right)^2 \tag{5.401}$$

then the variable values at the time step t_{n+1} are taken as the trial ones just calculated.

2) If the trial solution is non admissible, i.e. Equation (5.401) is violated, then the step is plastic or elastoplastic. Being $\dot{\mathbf{e}}$ constant in each time sub interval, the step can be divided into two parts: an elastic deformation followed by a plastic one. We represent with a scalar $\alpha \in [0, 1)$ the elastic time proportion of the step, which with simple geometrical considerations turns out to be

$$\alpha = \frac{\sqrt{C^2 - DM} - C}{D} \tag{5.402}$$

where

$$\begin{cases} C = \dfrac{2GX_{0,n}}{\sigma_{y,n}} \left(\mathbf{X}_n^s : \Delta\mathbf{e}\right) \\ D = \left(\dfrac{2GX_{0,n}\|\Delta\mathbf{e}\|}{\sigma_{y,n}}\right)^2 \\ M = \|\mathbf{X}_n^s\|^2 - \left(X_{0,n+1}^{TR}\right)^2 \end{cases} \tag{5.403}$$

Computed α, $\mathbf{X}_{n+1}$ is updated in two steps.

- Calculate a new $\mathbf{X}_{n+1}^e$ following an elastic law along an $\alpha\Delta t$ interval

$$\mathbf{X}_{n+1}^e = \bar{\mathbb{G}}_e[\alpha\Delta t]\mathbf{X}_n \tag{5.404}$$

- Calculate $\mathbf{X}_{n+1}$ evolving from the new initial data $\mathbf{X}_{n+1}^e$ following a plastic law along the remaining part of the interval of amplitude $(1-\alpha)\Delta t$

$$\mathbf{X}_{n+1} = \bar{\mathbb{G}}_p[(1-\alpha)\Delta t]\mathbf{X}_{n+1}^e \tag{5.405}$$

  Observe that in such a framework purely plastic steps are simply those where the time proportion of the elastic phase α is zero.

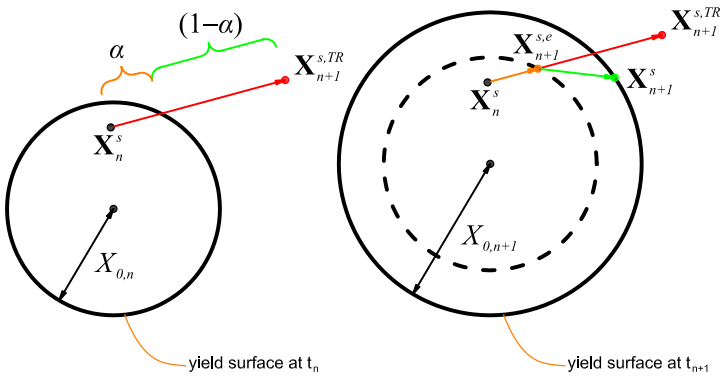

Figure 5.6: Updating procedure in generalized stress space for the ESC^{2}nl scheme during a mixed elastoplastic step.

3) Update the yield surface radius

$$\sigma_{y,n+1} = \sigma_y(X_{0,n+1}) = \sigma_{y,0}\,(X_{0,n+1})^q \tag{5.406}$$

which is easily obtained combining (5.355) and (5.364).

4) Update the backstress α as follows from (5.396)

$$\boldsymbol{\alpha}_{n+1} = \frac{H_{kin}\Delta\gamma(\mathbf{n}_{n+1} + \mathbf{n}_n)/2 + (1 - H_{nl}\Delta\gamma/2)\boldsymbol{\alpha}_n}{1 + H_{nl}\Delta\gamma/2} \tag{5.407}$$

where $\mathbf{n}_{n+1}$ and $\Delta\gamma$ can be calculated from (5.397) and (5.398) respectively. Note that, due to (5.355), in the case $H_{iso} \neq 0$ the scalar $\Delta\gamma$ can be simply computed as

$$\Delta\gamma = \frac{\sigma_{y,n+1} - \sigma_{y,n}}{H_{iso}} \tag{5.408}$$

where $\sigma_{y,n+1}$ has been already updated in (5.406).

The updating procedure illustrated by steps 1) - 3) is represented in Figure 5.6 which refers to the space of tensors $\mathbf{X}^s$.

Remark 5.12.2 *The relative stress can be calculated whenever needed as:*

$$\boldsymbol{\Sigma} \;=\; \frac{\boldsymbol{X}^s}{X_0}\sigma_y \tag{5.409}$$

which is immediately obtained from the definition of $\boldsymbol{X}$.

Remark 5.12.3 *The variable X_0 is a local auxiliary variable and not an history variable. In other words, introducing an appropriate scaling of the couple $\boldsymbol{X}$ the variable X_0 does not need to be updated at every time step [8].*

Remark 5.12.4 *The scalar α in the* ESC^{2}nl *scheme is not to be confused with the α parameter of the midpoint method presented in this same contribution. The author preferred to avoid renaming variables which already appear in the existing literature.*

5.12.4 ESC^{2}nl scheme elastoplastic consistent tangent operator

The algorithmically consistent tangent operator can be obtained properly linearizing the time-discrete procedure. To make notation more clear, the subscripts of all history variables evaluated at the end of the time interval t_{n+1} are omitted for brevity. Quantities evaluated either at t_n or at $t_{n+\alpha}$ are specified by the relative subscript.

For the total stress, from (5.343) and (5.313) it immediately follows

$$\mathbb{C}^{ep} = \frac{\partial \boldsymbol{\sigma}}{\partial \boldsymbol{\varepsilon}} = \left[\frac{\partial \boldsymbol{\Sigma}}{\partial \mathbf{e}} + \frac{\partial \boldsymbol{\alpha}}{\partial \mathbf{e}}\right] \mathbb{I}_{\text{dev}} + K\left(\mathbf{I} \otimes \mathbf{I}\right) \tag{5.410}$$

Then, a few calculations give

$$\frac{\partial \boldsymbol{\Sigma}}{\partial \mathbf{e}} = \frac{\sigma_y}{X_0}\left(\frac{\partial \mathbf{X}^s}{\partial \mathbf{e}} - \frac{1-q}{X_0}\mathbf{X}^s \frac{\partial X_0}{\partial \mathbf{e}}\right) \tag{5.411}$$

while a direct derivation of the update procedure (5.407) gives $\dfrac{\partial \boldsymbol{\alpha}}{\partial \mathbf{e}}$, which is shown in the sequel.

For the elastic phase we immediately have

$$\frac{\partial \mathbf{X}^s}{\partial \mathbf{e}} = 2GX_0\mathbb{I} \tag{5.412}$$

$$\frac{\partial X_0}{\partial \mathbf{e}} = \mathbf{0} \tag{5.413}$$

while in the plastic phase the result is more complicated and is achieved as follows. For the evaluation of the fourth-order tensors $\partial \mathbf{X}/\partial \mathbf{e}$ and $\partial \boldsymbol{\alpha}/\partial \mathbf{e}$, we start recalling that, for a general mixed elastoplastic step one has

$$\mathbf{X}^s = \mathbf{X}_n^{s,e} + \frac{a-1}{\|\Delta\hat{\boldsymbol{\Psi}}\|^2}(\Delta\hat{\boldsymbol{\Psi}} : \mathbf{X}_n^{s,e})\Delta\hat{\boldsymbol{\Psi}} + b\frac{X_{0,n}}{\|\Delta\hat{\boldsymbol{\Psi}}\|}\Delta\hat{\boldsymbol{\Psi}} \tag{5.414}$$

where

$$\mathbf{X}_n^{s,e} = \mathbf{X}_n^s + \alpha \frac{2G}{\sigma_{y,n}} X_{0,n} \Delta\mathbf{e} \tag{5.415}$$

$$a = \cosh\left[(1-\alpha)\frac{2G}{\bar{\sigma}_y}\|\Delta\hat{\mathbf{\Psi}}\|\right] \tag{5.416}$$

$$b = \sinh\left[(1-\alpha)\frac{2G}{\bar{\sigma}_y}\|\Delta\hat{\mathbf{\Psi}}\|\right] \tag{5.417}$$

$$\Delta\hat{\mathbf{\Psi}} = \Delta\bar{\mathbf{\Psi}}_0 + (1-\alpha)\Delta\bar{\mathbf{\Psi}}_1 \tag{5.418}$$

Above, $\mathbf{X}_n^{s,e}$ represents the value of the second-order tensor $\mathbf{X}^s$ updated at the end of the elastic part of the step. Moreover, $\Delta\hat{\mathbf{\Psi}}$ is the scaled driving tensor, introduced to take into account that the plastic proportion of the step amounts to $(1-\alpha)\Delta t$.

The fourth-order tensor $\partial\mathbf{X}^s/\partial\mathbf{e}$ is obtained deriving expression (5.414). Without presenting all the calculations, it is found that

$$\frac{\partial\mathbf{X}^s}{\partial\mathbf{e}} = \mathbb{T}_1 + \mathbb{T}_2 + \mathbb{T}_3 \tag{5.419}$$

In order to describe the three addenda $\mathbb{T}_1$, $\mathbb{T}_2$ and $\mathbb{T}_3$, a set of preliminary derivatives is necessary.

Thus, we start introducing the second-order tensor $\boldsymbol{\upsilon} = \mathrm{d}\alpha/\mathrm{d}\Delta\mathbf{e}$

$$\begin{cases} \boldsymbol{\upsilon} = \phi_1 \dfrac{\mathrm{d}C}{\mathrm{d}\Delta\mathbf{e}} + \phi_2 \dfrac{\mathrm{d}D}{\mathrm{d}\Delta\mathbf{e}} \\ \phi_1 = \dfrac{1}{D}\left(\dfrac{C}{\sqrt{C^2 - DM}} - 1\right) \\ \phi_2 = -\dfrac{1}{D^2}\left(\dfrac{DM}{2\sqrt{C^2 - DM}} + \sqrt{C^2 - DM} - C\right) \\ \dfrac{\mathrm{d}C}{\mathrm{d}\Delta\mathbf{e}} = 2GX_{0,n}\,\mathbf{X}_n^s \\ \dfrac{\mathrm{d}D}{\mathrm{d}\Delta\mathbf{e}} = 2(2GX_{0,n})^2\Delta\mathbf{e} \end{cases} \tag{5.420}$$

Indeed, the following relations hold

$$\frac{\partial \Delta\hat{\bar{\boldsymbol{\Psi}}}}{\partial \mathbf{e}} = \frac{\partial \Delta\bar{\boldsymbol{\Psi}}_0}{\partial \mathbf{e}} + (1-\alpha)\frac{\partial \Delta\bar{\boldsymbol{\Psi}}_1}{\partial \mathbf{e}} - \Delta\bar{\boldsymbol{\Psi}}_1 \otimes \boldsymbol{v} \tag{5.421}$$

$$\frac{\partial \Delta\bar{\boldsymbol{\Psi}}_0}{\partial \mathbf{e}} = \mathbb{I} + \frac{\tilde{q}}{X_{0,n}}\left(\boldsymbol{\alpha}_n \otimes \Delta\mathbf{e}\right) : \frac{\partial \mathbf{X}_n^{s,e}}{\partial \mathbf{e}} + \tilde{q}\,\boldsymbol{\alpha}_n \otimes \mathbf{n}_e \tag{5.422}$$

$$+\frac{H_{nl}}{H_{iso}}\left(\mathbf{n}_e : \Delta\mathbf{e}\right)\boldsymbol{\alpha}_n \otimes \frac{\partial \bar{q}}{\partial \mathbf{e}} \tag{5.423}$$

$$\frac{\partial \Delta\bar{\boldsymbol{\Psi}}_1}{\partial \mathbf{e}} = \frac{1}{2}\,\frac{H_{nl}}{2G}\left(\frac{\partial \mathbf{D}_{\boldsymbol{\alpha}}}{\partial \mathbf{e}} D_\gamma + \mathbf{D}_{\boldsymbol{\alpha}} \otimes \frac{\partial D_\gamma}{\partial \mathbf{e}} + \boldsymbol{\alpha}_n \otimes \frac{\partial D'_\gamma}{\partial \mathbf{e}}\right) \tag{5.424}$$

where

$$\tilde{q} = \frac{H_{nl}}{H_{iso}}\,\bar{q} = \frac{H_{nl}}{2G_1 - H_{nl}(\mathbf{n}_e : \boldsymbol{\alpha})} \tag{5.425}$$

$$\frac{\partial \bar{q}}{\partial \mathbf{e}} = \frac{H_{iso}H_{nl}}{(2G_1 - H_{nl}(\mathbf{n}_e : \boldsymbol{\alpha}_n))^2} X_{0,n}^{-1}\left(\frac{\partial \mathbf{X}_n^{s,e}}{\partial \mathbf{e}}\right)\boldsymbol{\alpha}_n \tag{5.426}$$

$$\frac{\partial \mathbf{D}_{\boldsymbol{\alpha}}}{\partial \mathbf{e}} = \left(H_{kin}\mathbf{n}_e - H_{nl}\boldsymbol{\alpha}_n\right) \otimes \frac{\partial D_\gamma}{\partial \mathbf{e}} + H_{kin}\frac{D_\gamma}{X_{0,n}}\frac{\partial \mathbf{X}_n^{s,e}}{\partial \mathbf{e}} \tag{5.427}$$

$$\frac{\partial D_\gamma}{\partial \mathbf{e}} = \left(\mathbf{n}_e : \Delta\mathbf{e}\right)\boldsymbol{\Phi} + \bar{q}\left(\mathbf{n}_e + X_{0,n}^{-1}\frac{\mathbf{X}_n^{s,e}}{\partial \mathbf{e}}\Delta\mathbf{e}\right) \tag{5.428}$$

$$\frac{\partial D'_\gamma}{\partial \mathbf{e}} = \mathbb{T}_4 + \mathbb{T}_5 + \mathbb{T}_6 \tag{5.429}$$

with $\mathbf{n}_e = \mathbf{X}_n^{s,e}/X_{0,n}$ the normalized stress at the end of the elastic part. The second-order tensors appearing in (5.428)-(5.429) are given by the following expressions

$$\boldsymbol{\Phi} = X_{0,n}^{-1}\frac{2GH_{nl}}{\left[2G_1 - H_{nl}(\mathbf{n}_e : \boldsymbol{\alpha}_n)\right]^2}\frac{\partial \mathbf{X}_n^{s,e}}{\partial \mathbf{e}}\boldsymbol{\alpha}_n \tag{5.430}$$

$$\mathbb{T}_4 = \left(\mathbf{n}_e : \Delta\mathbf{e}\right)\boldsymbol{\Phi} + \bar{q}\left(\mathbf{D}_{\mathbf{n}} + \frac{\partial \mathbf{D}_{\mathbf{n}}}{\partial \mathbf{e}}\Delta\mathbf{e}\right) \tag{5.431}$$

$$\mathbb{T}_5 = H_{nl}\left[(\mathbf{D}_{\mathbf{n}} : \boldsymbol{\alpha}) + (\mathbf{n}_e : \mathbf{D}_{\boldsymbol{\alpha}})\right]\left[\frac{2(\mathbf{n}_e : \Delta\mathbf{e})}{2G_1 - H_{nl}(\mathbf{n}_e : \boldsymbol{\alpha}_n)}\boldsymbol{\Phi}\right.$$

$$\left.+\frac{2G}{\left[2G_1 - H_{nl}(\mathbf{n}_e : \boldsymbol{\alpha}_n)\right]^2}\left(\mathbf{n}_e + X_{0,n}^{-1}\frac{\partial \mathbf{X}_n^{s,e}}{\partial \mathbf{e}}\Delta\mathbf{e}\right)\right] \tag{5.432}$$

$$\mathbb{T}_6 = \frac{2GH_{nl}}{(2G_1 - H_{nl}(\mathbf{n}_e : \boldsymbol{\alpha}_n))^2}(\mathbf{n}_e : \Delta\mathbf{e})\left[\frac{\partial \mathbf{D}_{\mathbf{n}}}{\partial \Delta\mathbf{e}}\boldsymbol{\alpha}_n\right.$$

$$\left.+X_{0,n}^{-1}\,\frac{\partial \mathbf{X}_n^{s,e}}{\partial \Delta\mathbf{e}}\mathbf{D}_{\boldsymbol{\alpha}} + \frac{\partial \mathbf{D}_{\boldsymbol{\alpha}}}{\partial \Delta\mathbf{e}}\mathbf{n}_e\right] \tag{5.433}$$

with

$$\frac{\partial \mathbf{D_n}}{\partial \Delta \mathbf{e}} = \frac{2G}{\sigma_{y,n}}\mathbb{I} - \frac{2G_1}{\sigma_{y,0}}\left[D_\gamma X_{0,n}^{-1}\frac{\partial \mathbf{X}_n^{s,e}}{\partial \Delta \mathbf{e}} + \mathbf{n}_e \otimes \frac{\partial D_\gamma}{\partial \Delta \mathbf{e}}\right] \tag{5.434}$$

$$+\frac{H_{nl}}{\sigma_{y,n}}\boldsymbol{\alpha}_n \otimes \frac{\partial D_\gamma}{\partial \Delta \mathbf{e}} \tag{5.435}$$

Let moreover

$$\frac{\partial \bar{\sigma}_y}{\partial \mathbf{e}} = \sigma_{y,n}\left(\frac{\log(1+c) - c/(1+c)}{2\log 1 + c}\right)\frac{\partial c}{\partial \mathbf{e}} \tag{5.436}$$

where

$$\frac{\partial c}{\partial \mathbf{e}} = \frac{2G\bar{q}}{\sigma_{y,n}}\left[-(\mathbf{n}_e : \Delta \mathbf{e})\,\boldsymbol{\upsilon} + \frac{(1-\alpha)}{X_{0,n}}\frac{\partial \mathbf{X}_n^{s,e}}{\partial \mathbf{e}}\Delta \mathbf{e}\right.$$

$$\left.+(1-\alpha)\mathbf{n}_e + \frac{1-\alpha}{\bar{q}}(\mathbf{n}_e : \Delta \mathbf{e})\frac{\partial \bar{q}}{\partial \mathbf{e}}\right] \tag{5.437}$$

$$\frac{\partial \mathbf{X}_n^{s,e}}{\partial \mathbf{e}} = \alpha\frac{2G}{\sigma_{y,n}}\mathbb{I} + \frac{2G}{\sigma_{y,n}}X_{0,n}(\Delta \mathbf{e} \otimes \boldsymbol{\upsilon}) \tag{5.438}$$

Let in addition

$$\frac{\partial \|\Delta \hat{\boldsymbol{\Psi}}\|}{\partial \mathbf{e}} = \frac{\partial \Delta \hat{\boldsymbol{\Psi}}}{\partial \mathbf{e}}\frac{\Delta \hat{\boldsymbol{\Psi}}}{\|\Delta \hat{\boldsymbol{\Psi}}\|} \tag{5.439}$$

$$\frac{\partial}{\partial \mathbf{e}}\left(\frac{\Delta \hat{\boldsymbol{\Psi}}}{\|\Delta \hat{\boldsymbol{\Psi}}\|}\right) = \|\Delta \hat{\boldsymbol{\Psi}}\|^{-2}\left(\|\Delta \hat{\boldsymbol{\Psi}}\|\frac{\partial \Delta \hat{\boldsymbol{\Psi}}}{\partial \mathbf{e}} - \Delta \hat{\boldsymbol{\Psi}} \otimes \frac{\partial \|\Delta \hat{\boldsymbol{\Psi}}\|}{\partial \mathbf{e}}\right) \tag{5.440}$$

$$\frac{\partial a}{\partial \mathbf{e}} = b\frac{2G}{\bar{\sigma}_y}\left[-\|\Delta \hat{\boldsymbol{\Psi}}\|\boldsymbol{\upsilon} - (1-\alpha)\frac{\|\Delta \hat{\boldsymbol{\Psi}}\|}{\bar{\sigma}_y}\frac{\partial \bar{\sigma}_y}{\partial \mathbf{e}} + (1-\alpha)\frac{\partial \|\Delta \hat{\boldsymbol{\Psi}}\|}{\partial \mathbf{e}}\right] \tag{5.441}$$

$$\frac{\partial b}{\partial \mathbf{e}} = a\frac{2G}{\bar{\sigma}_y}\left[-\|\Delta \hat{\boldsymbol{\Psi}}\|\boldsymbol{\upsilon} - (1-\alpha)\frac{\|\Delta \hat{\boldsymbol{\Psi}}\|}{\bar{\sigma}_y}\frac{\partial \bar{\sigma}_y}{\partial \mathbf{e}} + (1-\alpha)\frac{\partial \|\Delta \hat{\boldsymbol{\Psi}}\|}{\partial \mathbf{e}}\right] \tag{5.442}$$

The fourth-order tensors defined in (5.419) are thus:

$$\begin{aligned}
\mathbb{T}_1 &= \frac{\partial \mathbf{X}_n^{s,e}}{\partial \mathbf{e}} + \alpha \frac{2G}{\sigma_{y,n}} X_{0,n} \frac{a-1}{\|\Delta\hat{\boldsymbol{\Psi}}\|^2} \Delta\hat{\boldsymbol{\Psi}} \otimes \Delta\hat{\boldsymbol{\Psi}} \\
&\quad + \alpha \frac{2G}{\sigma_{y,n}} X_{0,n} \frac{a-1}{\|\Delta\hat{\boldsymbol{\Psi}}\|^2} \left(\Delta\hat{\boldsymbol{\Psi}} : \Delta\mathbf{e}\right) \Delta\hat{\boldsymbol{\Psi}} \otimes \boldsymbol{\upsilon} \qquad (5.443) \\
\mathbb{T}_2 &= \frac{\left(\Delta\hat{\boldsymbol{\Psi}} : \mathbf{X}_n^{s,e}\right)}{\|\Delta\hat{\boldsymbol{\Psi}}\|^2} \Delta\hat{\boldsymbol{\Psi}} \otimes \frac{\partial a}{\partial \mathbf{e}} + \frac{X_{0,n}}{\|\Delta\hat{\boldsymbol{\Psi}}\|} \Delta\hat{\boldsymbol{\Psi}} \otimes \frac{\partial b}{\partial \mathbf{e}} \qquad (5.444) \\
\mathbb{T}_3 &= (a-1) \left(\frac{\Delta\hat{\boldsymbol{\Psi}}}{\|\Delta\hat{\boldsymbol{\Psi}}\|} : \mathbf{X}_n^{s,e} \right) \frac{\partial}{\partial \mathbf{e}} \left(\frac{\Delta\hat{\boldsymbol{\Psi}}}{\|\Delta\hat{\boldsymbol{\Psi}}\|} \right) \\
&\quad + (a-1) \frac{\Delta\hat{\boldsymbol{\Psi}}}{\|\Delta\hat{\boldsymbol{\Psi}}\|} \otimes \left[\frac{\partial}{\partial \mathbf{e}} \left(\frac{\Delta\hat{\boldsymbol{\Psi}}}{\|\Delta\hat{\boldsymbol{\Psi}}\|} \right) \mathbf{X}_n^{s,e} \right] \\
&\quad + b X_{0,n} \frac{\partial}{\partial \mathbf{e}} \left(\frac{\Delta\hat{\boldsymbol{\Psi}}}{\|\Delta\hat{\boldsymbol{\Psi}}\|} \right) \qquad (5.445)
\end{aligned}$$

The scalar function X_0, following the algorithm of Section 5.12.2, is updated as

$$X_0 = b \frac{(\Delta\hat{\boldsymbol{\Psi}} : \mathbf{X}_n^{s,e})}{\|\Delta\hat{\boldsymbol{\Psi}}\|} + a X_{0,n} \qquad (5.446)$$

Therefore, a direct derivation gives

$$\frac{\partial X_0}{\partial \mathbf{e}} = \frac{(\Delta\hat{\boldsymbol{\Psi}} : \mathbf{X}_n^{s,e})}{\|\Delta\hat{\boldsymbol{\Psi}}\|} \frac{\partial b}{\partial \mathbf{e}} + \frac{b}{\|\Delta\hat{\boldsymbol{\Psi}}\|} \frac{\partial \mathbf{X}_n^{s,e}}{\partial \mathbf{e}} \Delta\hat{\boldsymbol{\Psi}} + b \left(\frac{\partial}{\partial \mathbf{e}} \frac{\Delta\hat{\boldsymbol{\Psi}}}{\|\Delta\hat{\boldsymbol{\Psi}}\|} \right) \mathbf{X}_n^{s,e} + X_{0,n} \frac{\partial a}{\partial \mathbf{e}} \qquad (5.447)$$

which is readily calculated in view of the previous derivations in this section.

Finally, with respect to the derivative of the backstress α for an elastoplastic step, it holds

$$\begin{aligned}
\frac{\partial \boldsymbol{\alpha}}{\partial \mathbf{e}} &= \left(H_{kin} \frac{\partial \Delta\mathbf{e}^p}{\partial \mathbf{e}} - \frac{1}{2} H_{nl} \boldsymbol{\alpha}_n \otimes \frac{\partial \Delta\gamma}{\partial \mathbf{e}} \right) \left(1 + \frac{1}{2} H_{nl} \Delta\gamma \right)^{-1} \\
&\quad - \frac{H_{nl}}{2} \left(1 + \frac{1}{2} H_{nl} \Delta\gamma \right)^{-2} \left[H_{kin} \Delta\mathbf{e}^p + \left(1 - \frac{1}{2} H_{nl} \Delta\gamma \right) \boldsymbol{\alpha}_n \right] \otimes \frac{\partial \Delta\gamma}{\partial \mathbf{e}}
\end{aligned}$$

where

$$\Delta \mathbf{e}^p = \frac{1}{2}\Delta\gamma\left(\frac{\mathbf{X}^s}{X_0} + \frac{\mathbf{X}^s_n}{X_{0,n}}\right) \tag{5.448}$$

$$\frac{\partial \Delta\gamma}{\partial \mathbf{e}} = \begin{cases} q\dfrac{\sigma_{y,0}}{H_{iso}} X_0^{q-1}\dfrac{\partial X_0}{\partial \mathbf{e}} & \text{if } H_{iso} = 0 \\ \\ \dfrac{\sigma_{y,0}}{2G_1}\dfrac{X_{0,n}}{X_0}\dfrac{\partial X_0}{\partial \mathbf{e}} & \text{if } H_{iso} \neq 0 \end{cases} \tag{5.449}$$

$$\frac{\partial \Delta \mathbf{e}^p}{\partial \mathbf{e}} = \frac{1}{2}\Delta\gamma\frac{\partial}{\partial \mathbf{e}}\left(\frac{\mathbf{X}^s}{X_0}\right) + \frac{1}{2}\left[\left(\frac{\mathbf{X}^s}{X_0} + \frac{\mathbf{X}^s_n}{X_{0,n}}\right)\otimes\frac{\partial \Delta\gamma}{\partial \mathbf{e}}\right] \tag{5.450}$$

$$\frac{\partial}{\partial \mathbf{e}}\left(\frac{\mathbf{X}^s}{X_0}\right) = \frac{1}{X_0}\frac{\partial \mathbf{X}^s}{\partial \mathbf{e}} - \frac{1}{X_0^2}\left(\mathbf{X}^s \otimes \frac{\partial X_0}{\partial \mathbf{e}}\right) \tag{5.451}$$

5.12.5 Brief review of the numerical properties of the ESC^{2}nl method

The presented ESC^{2}nl method satisfies the following algorithmical properties:

Yield consistency. As shown in (5.380), in the framework of formulation (5.376) the yield condition becomes

$$\|\mathbf{X}^s\|^2 = X_0^2 \tag{5.452}$$

at the end of all plastic steps. Following the same line of thought reported in Section 5.8.1, it can be immediately shown that such condition is fullfilled by the ESC^{2}nl scheme.

Second-order accuracy. Following standard calculations, namely a Taylor expansion in time, it can be proved that the truncation error of the ESC^{2}nl method is of order $(\Delta t)^2$, where Δt is the time step size. Therefore the scheme is second-order accurate, which guarantees a very reduced error at small time steps.

Exactness in case of no hardening. If $H_{iso} = H_{nl} = H_{kin} = 0$, provided $\mathbf{e}(t)$ is piecewise constant, the matrix in (5.376) is constant during each time step. As a consequence, the evolution problem (5.376) is integrated exactly by the exponential-based method presented. Therefore, whenever $H_{iso} = H_{nl} = H_{kin} = 0$, no error is introduced by the scheme in strain driven histories with piecewise linear strain tensors. Although this property does not imply exactness in the general mixed stress-strain driven case, it is reflected in a very good error behavior (see [10] for a brief discussion on this point).

Remark 5.12.5 *Stability of the method is, from the theoretical viewpoint, still to be addressed. This is for sure a point which should be further investigated.*

Chapter 6

Numerical tests

Introduzione

In questo capitolo vengono presentati alcuni test numerici relativi agli algoritmi di integrazione per modelli di plasticità J_2 analizzati nel precedente Capitolo 5. I test numerici hanno un duplice scopo. Il primo è quello di fornire un confronto in termini di precisione dei diversi schemi di integrazione considerati. Il secondo è quello di validare le proprietà numeriche dimostrate nel capitolo precedente con riferimento particolare alla famiglia degli algoritmi di integrazione a base esponenziale. Le analisi summenzionate vengono sviluppate attraverso test numerici di tipo diverso. In particolare, si presentano i risultati inerenti storie di carico puntuali a controllo misto deformazioni-tensioni e risultati relativi a problemi a valori iniziali e dati al bordo posti su continui tridimensionali.

Il capitolo è suddiviso in tre sezioni ed organizzato nel modo seguente. La Sezione 6.2 presenta il set-up delle diverse prove numeriche riportate nel capitolo. Vengono qui introdotti i dettagli inerenti le strategie risolutive e di implementazione algoritmica adottate, nonchè le diverse misure d'errore utilizzate a seconda della prova considerata. La Sezione 6.3 riguarda il confronto numerico degli algoritmi di integrazione del modello costitutivo J_2 con incrudimento isotropo e cinematico lineare (modello LP). La Sezione 6.4 riguarda il confronto numerico degli algoritmi di integrazione del modello costitutivo J_2 con incrudimento isotropo e cinematico lineare ed incrudimento cinematico non lineare (modello NLK). Alcuni dei risultati presentati in questo capitolo sono tratti da [6, 7, 8, 11, 12].

6.1 Introduction

In this chapter we present a set of numerical tests on the integration algorithms for J_2 elastoplastic models analyzed in Chapter 5. The numerical tests have a double scope. First, they are intended to provide a comparison in terms of precision between the different considered integration schemes. On the other hand, the numerical tests aim to validate the numerical properties and results found in the previous chapter with particular emphasis to the exponential-based integration algorithms family. The above mentioned analyses are carried out through different kinds of numerical tests. In particular, we present results relative to pointwise mixed stress-strain loading histories and results relative to initial boundary value problems on three-dimensional material bodies.

The chapter is divided in three sections and is organized as follows. Section 6.2 is concerned with the setup of the numerical tests reported in the present chapter. In this section the details inherent the solution strategies and the algorithmic implementation adopted in the tests together with the different error measures are introduced. Section 6.3 is devoted to the comparison of the numerical schemes which apply to the J_2 constitutive model with linear isotropic and kinematic hadening (LP model). Section 6.4 is devoted to the comparison of the numerical schemes which apply to the J_2 constitutive model with linear isotropic and kinematic hardening and nonlinear kinematic hardening (NLK model). Some of the results which are shown in this chapter are taken from some works among which we cite [6, 7, 8, 11, 12].

6.2 Numerical tests setup

This section is devoted to the setup of the numerical tests presented in the following sections. There are three different kinds of numerical tests. First, we consider mixed stress-strain loading histories for a material point. The object of this test is to study the accuracy granted by the method with respect to the computation of the stress-strain asset. Second, we show a set of iso-error maps [69, 70] in order to evaluate the algorithm precision using different time discretizations. Finally, we present two classical initial boundary value problems, which we study to analyze the algorithm reliability on a practical engineering problem.

As a result of the above numerical tests, we carry out a detailed comparison of the presented methods in terms of precision, accuracy and in terms of specific properties shown by each method. The pointwise tests and the iso-error maps are performed with the aid of the CE-Driver code [15], the initial boundary

value problem is solved using FEAP [73]. Each test is described in detail as follows.

6.2.1 Mixed stress-strain loading histories

We consider three biaxial non-proportional stress-strain loading histories defined on the reference time interval $[0, T]$, with $T = 7$ s. The considered loading histories are obtained assuming to control two strain components and four stress components, respectively, i.e.

Problem 1:	ε_{11}	σ_{22}	σ_{33}	ε_{12}	σ_{13}	σ_{23}
Problem 2:	ε_{11}	ε_{22}	σ_{33}	σ_{12}	σ_{13}	σ_{23}
Problem 3:	ε_{11}	σ_{22}	σ_{33}	ε_{12}	σ_{13}	σ_{23}

For each history we require that all the controlled stress components are identically equal to zero, while the strains are varied proportionally to

$$\varepsilon_{y,mono} = \sqrt{\frac{3}{2}}\frac{\sigma_{y,0}}{E} \tag{6.1}$$

which represents the first yielding strain value in a uniaxial loading history. A graphical representation of the varying quantities is given in Figure 6.1.

Instantaneous error

Lacking the analytical solutions of the problems under investigation, we compute the "exact" solutions using a reference scheme (BE for the LP model, BEnl for the NLK model) with a very fine time discretization, corresponding to 100000 steps per second ($\Delta t = 0.00001$ s). The "exact" solutions are compared with the "numerical" ones, corresponding respectively to 10, 20 and 40 steps per second ($\Delta t = 0.1$ s, 0.05 s, 0.025 s) and computed with each one of the compared algorithms.

The error is evaluated separately for the stress and the strain introducing the following relative norms:

$$E_n^{\boldsymbol{\sigma}} = \frac{\|\boldsymbol{\sigma}_n - \boldsymbol{\sigma}_n^{ex}\|}{\sigma_{y,n}} \qquad E_n^{\boldsymbol{\varepsilon}} = 2G\frac{\|\boldsymbol{\varepsilon}_n - \boldsymbol{\varepsilon}_n^{ex}\|}{\sigma_{y,n}} \tag{6.2}$$

where $\|\cdot\|$ indicates the usual euclidean norm and $\sigma_{y,n}$ is the yield surface radius at time t_n. In (6.2), $\boldsymbol{\sigma}_n$ and $\boldsymbol{\varepsilon}_n$ as well as $\boldsymbol{\sigma}_n^{ex}$ and $\boldsymbol{\varepsilon}_n^{ex}$ are respectively the stress and strain "numerical" and "exact" solution at time t_n.

Pb. 1

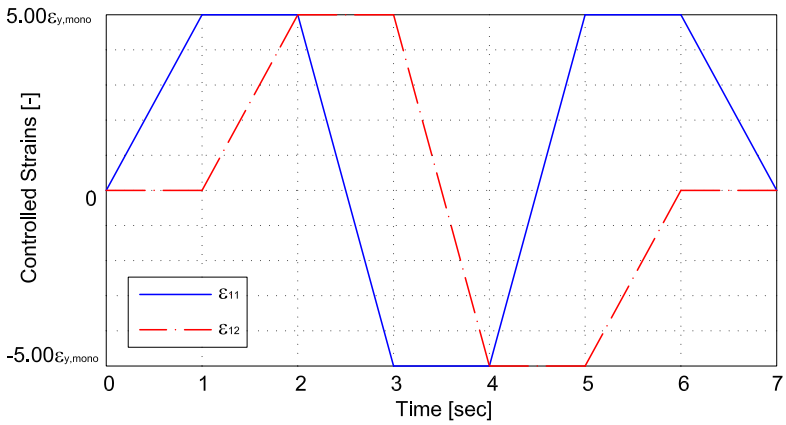

Pb. 2

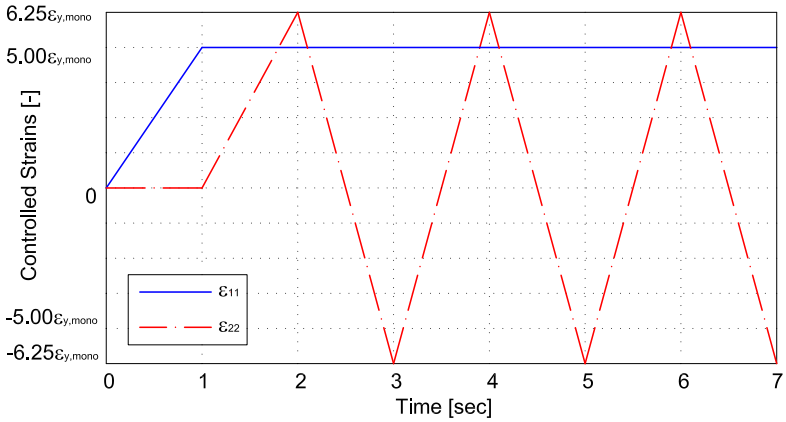

Pb. 3

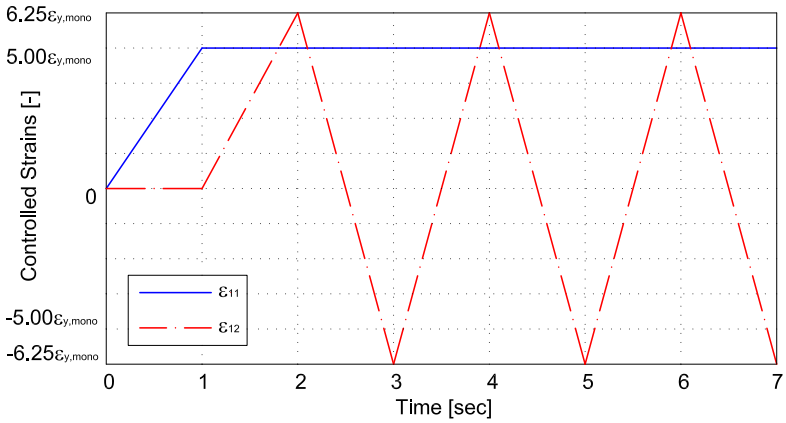

Figure 6.1: Pointwise stress-strain tests. Mixed stress-strain loading histories for Problem 1, Problem 2 and Problem 3.

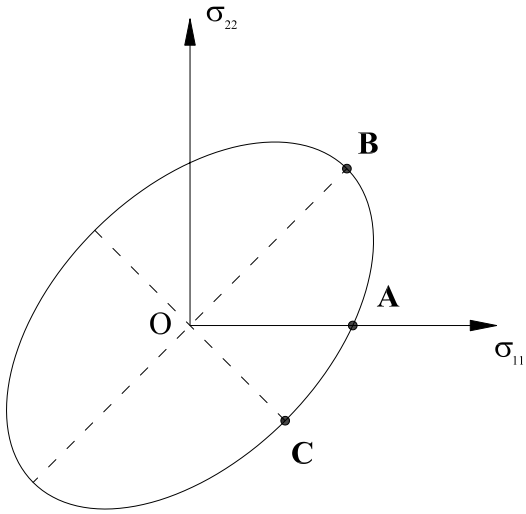

Figure 6.2: Plane stress von-Mises yield surface representation in principal stresses plane. State 1 choices for iso-error maps plots.

Total error

In order to further investigate the rate of convergence of the compared methods, we also introduce the average total error as the ℓ^1 norm in time of the absolute error:

$$E_T^{\boldsymbol{\sigma}} = \sum_{n=1}^{N} \frac{\Delta t}{T} \frac{\|\boldsymbol{\sigma}_n - \boldsymbol{\sigma}_n^{ex}\|}{\sigma_{y,n}} \qquad E_T^{\boldsymbol{\varepsilon}} = \sum_{n=1}^{N} 2G \frac{\Delta t}{T} \frac{\|\boldsymbol{\varepsilon}_n - \boldsymbol{\varepsilon}_n^{ex}\|}{\sigma_{y,n}} \tag{6.3}$$

6.2.2 Iso-error maps

Iso-error maps are commonly adopted in the literature [51, 63, 64, 69] as a systematic tool to test the accuracy of plasticity integration algorithms. In particular, iso-error maps provide a clear evaluation of the integration algorithm accuracy when a large time discretization is adopted in solving particular piecewise mixed stress-strain loading histories. Each loading history considered in this chapter is set up by controlling the ε_{11} and ε_{22} strain components and requiring that all the remaining stresses are equal to zero. The evolution in time of the controlled quantities is piecewise linear and can be divided in two distinct phases defined as follows (see Table 6.1). Phase 1 consists of a

Table 6.1: Benchmark mixed stress-strain history for iso-error maps computation.

	Time [s]	ε_{11}	ε_{22}	σ_{33}	σ_{12}	σ_{13}	σ_{23}
State 0	t=0	0	0	0	0	0	0
State 1	t=1	$\varepsilon_{11,y}$	$\varepsilon_{22,y}$	0	0	0	0
State 2	t=2	$\varepsilon_{y,11} + \Delta\varepsilon_{11}$	$\varepsilon_{y,22} + \Delta\varepsilon_{22}$	0	0	0	0

Table 6.2: Iso-error maps. Choices for the State 1 point on the yield surface.

	$\varepsilon_{11,y}$	$\varepsilon_{22,y}$	σ_{33}	σ_{12}	σ_{13}	σ_{23}
State 1-A	$\varepsilon_{y,mono}$	$-\nu\varepsilon_{y,mono}$	0	0	0	0
State 1-B	$(1-\nu)\varepsilon_{y,mono}$	$\varepsilon_{y,mono}$	0	0	0	0
State 1-C	$\frac{(1+\nu)}{3}\varepsilon_{y,mono}$	$-\frac{(1+\nu)}{3}\varepsilon_{y,mono}$	0	0	0	0

purely elastic path and proceeds from the zero stress and strain state (State 0) to a specific state on the yield surface (State 1) given in terms of the yield strain components $\varepsilon_{11,y}$ and $\varepsilon_{22,y}$. Phase 2 is a purely plastic path which starts from State 1 and leads to a final state (State 2) given in terms of the strain increments $\Delta\varepsilon_{11}$ and $\Delta\varepsilon_{22}$.

In this analysis, we consider three different choices of State 1, corresponding to plane states of stress on the yield surface [69], labeled **A**, **B** and **C** respectively, represented in Figure 6.2 and corresponding to uniaxial, biaxial and pure shear states. Each State 1 is expressed in Table 6.2 in terms of the quantity $\varepsilon_{y,mono}$ (uniaxial yield strain) already defined in (6.1) according to

$$\begin{aligned} \varepsilon_{11} &= \varepsilon_{11,y} \\ \varepsilon_{22} &= \varepsilon_{22,y} \end{aligned}$$

For each choice of State 1, we consider a State 2 defined as

$$\begin{aligned} \varepsilon_{11} &= \varepsilon_{11,y} + \Delta\varepsilon_{11} \\ \varepsilon_{22} &= \varepsilon_{22,y} + \Delta\varepsilon_{22} \end{aligned}$$

We solve a total of 60×60 mixed stress-strain histories for each State 1, corresponding to the following sets of normalized strain increments (see Figures

6.15-6.17 for instance)

$$\frac{\Delta\varepsilon_{11}}{\varepsilon_{11,y}} = 0.0, 0.1, 0.2, ..., 6.0$$
$$\frac{\Delta\varepsilon_{22}}{\varepsilon_{22,y}} = 0.0, 0.1, 0.2, ..., 6.0$$

This subdivision leads to a total of 3600 computed mixed stress-strain histories and to an equal number of calculated relative error values. According to [69, 72], as an error measure, we adopt the following expression

$$E^{\sigma}_{iso} = \frac{\|\boldsymbol{\sigma} - \boldsymbol{\sigma}^{ex}\|}{\|\boldsymbol{\sigma}^{ex}\|} \tag{6.4}$$

where $\boldsymbol{\sigma}$ is the final stress tensor, computed with a single time step discretization between State 1 and State 2, whereas $\boldsymbol{\sigma}^{ex}$ corresponds to an "exact" solution adopting a very fine time step between State 1 and State 2.

6.2.3 Initial boundary value problems

We consider two three-dimensional thin rectangular perforated strips, subjected to uniaxial extension in a plane strain state [69]. The first strip has a circular hole in the center, while the second one has an elliptical hole. Both strips have three planes of symmetry and in Figure 6.4 we show one quarter of the domain for each of the two strips. The geometric lenghts referred to Figure 6.4 are

$$B = 100 \text{ mm} \quad H = 180 \text{ mm} \quad R_0 = 50 \text{ mm} \quad H_0 = 10 \text{ mm} \quad B_0 = 50 \text{ mm}$$

while the thickness is 10 mm.

Initially the strip results undeformed and unstressed. The problem loading history results symmetric with respect to the three symmetry planes of the strip, hence we can refer to a single quarter of the domain and define the following equivalent problem. The loading history, which is represented in Figure 6.3, is composed of a first phase (1 s), in which, the strip is stretched assigning a top side vertical displacement δ_{max} and a second phase (1 s) in which the imposed displacement is set back to 0 mm. We set $\delta_{max} = 1$ mm. We assume to block the horizontal displacement on the left side and to block the vertical displacement on the bottom side of the strip. The remaining boundary sides are stress free. In the analysis we consider Material 2 as done for the iso-error map tests. We solve the boundary value problem using the

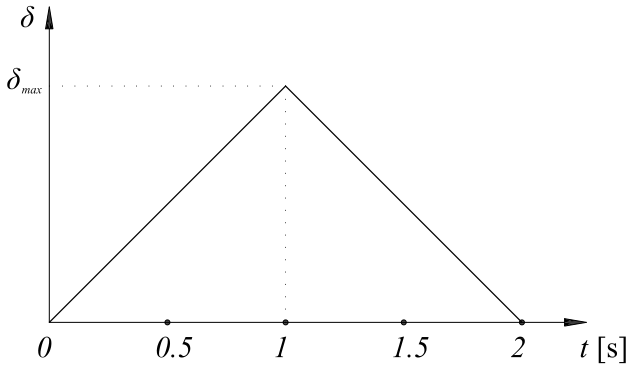

Figure 6.3: Initial boundary value problem. Loading history of imposed displacement on the top side of the strip and indication of L^2 norm error plot instants.

finite element code FEAP [73], in which the considered integration methods are implemented. The mesh is composed of N_{el} finite elements (displacement-based four-node SOLID2D elements adopting a four point Gauss quadrature rule [73]). The following results refer to a mesh with $N_{el} = 192$ as can be observed in Figure 6.5.

The comparison between the methods is carried out by evaluating the following L^2 norm error on stress and strain which makes use of stress and strain output at Gauss quadrature points

$$\tilde{E}^{\boldsymbol{\sigma}} = \sqrt{\frac{\int_\Omega \parallel \boldsymbol{\sigma}_n - \boldsymbol{\sigma}_n^{ex} \parallel^2}{\int_\Omega \parallel \boldsymbol{\sigma}_n^{ex} \parallel^2}} \approx \sqrt{\frac{\sum_{n=1}^{N_{el}} \sum_{q=1}^{4} w_{nq} \parallel \boldsymbol{\sigma}_{nq} - \boldsymbol{\sigma}_{nq}^{ex} \parallel^2}{\sum_{n=1}^{N_{el}} \sum_{q=1}^{4} w_{nq} \parallel \boldsymbol{\sigma}_{nq}^{ex} \parallel^2}} \tag{6.5}$$

$$\tilde{E}^{\boldsymbol{\varepsilon}} = \sqrt{\frac{\int_\Omega \parallel \boldsymbol{\varepsilon}_n - \boldsymbol{\varepsilon}_n^{ex} \parallel^2}{\int_\Omega \parallel \boldsymbol{\varepsilon}_n^{ex} \parallel^2}} \approx \sqrt{\frac{\sum_{n=1}^{N_{el}} \sum_{q=1}^{4} w_{nq} \parallel \varepsilon_{nq} - \varepsilon_{nq}^{ex} \parallel^2}{\sum_{n=1}^{N_{el}} \sum_{q=1}^{4} w_{nq} \parallel \varepsilon_{nq}^{ex} \parallel^2}} \tag{6.6}$$

In the above formulas, the indexes n and q respectively refer to the element number and quadrature point number, while w_{nq} is the qth quadrature point Gauss weight of the nth element. The quantities $\boldsymbol{\sigma}_{nq}$ and $\boldsymbol{\varepsilon}_{nq}$ are, respectively, the "numerical" stress and strain tensors calculated via the three integration schemes adopting a prescribed time step Δt, while $\boldsymbol{\sigma}_{nq}^{ex}$ and $\boldsymbol{\varepsilon}_{nq}^{ex}$ are the corresponding "exact" quantities evaluated with the reference scheme (BE for the LP model, BEnl for the NLK model) using an overkilling time step size. In the following tests we have chosen three different time steps sizes, respectively

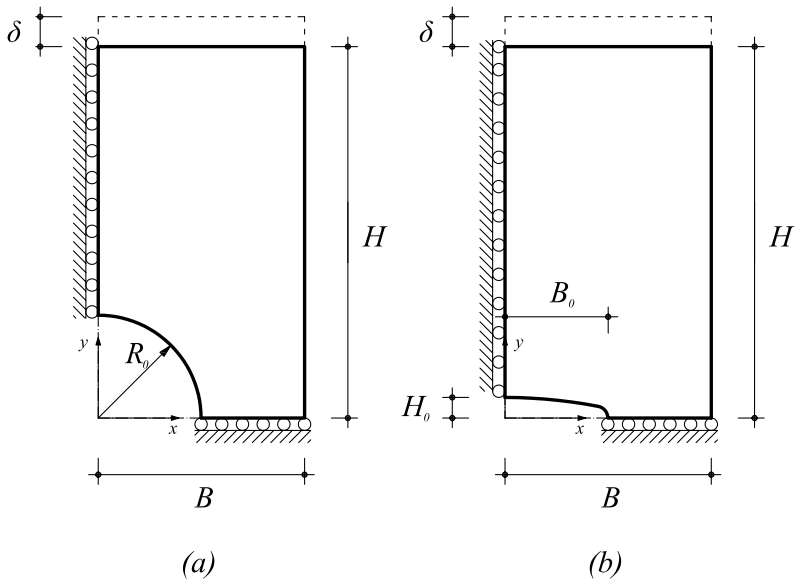

Figure 6.4: Boundary value problems. Strips with circular and elliptical holes: geometry and imposed displacements for a single quarter of the strips.

$\Delta t_1 = 0.05$ s, $\Delta t_2 = 0.025$ s, $\Delta t_3 = 0.0125$ s. The norms (6.5) and (6.6) are evaluated and plotted at four different instants ($t = 0.5$ s, $t = 1.0$ s, $t = 1.5$ s, $t = 2.0$ s) of the loading history (see Figure 6.3) with the three discretizations described above.

6.2.4 Material parameters

In the following analyses we consider five sets of material constants

- Material 1 [17]

$$\begin{array}{lll} E = 100 \quad \text{MPa} & \nu = 0.3 & \\ \sigma_{y,0} = 15 \quad \text{MPa} & H_{kin} = 10 \quad \text{MPa} & H_{iso} = 10 \quad \text{MPa} \\ \bar{\sigma}_{y,0} = \sigma_{y,0}/E = 0.15 & \bar{H}_{kin} = H_{kin}/E = 0.1 & \bar{H}_{iso} = H_{iso}/E = 0.1 \end{array}$$

- Material 2 [69]

$$\begin{array}{lll} E = 30000 \quad \text{MPa} & \nu = 0.3 & \\ \sigma_{y,0} = 3 \quad \text{MPa} & H_{kin} = 0 \quad \text{MPa} & H_{iso} = 0 \quad \text{MPa} \\ \bar{\sigma}_{y,0} = \sigma_{y,0}/E = 0.0001 & \bar{H}_{kin} = H_{kin}/E = 0 & \bar{H}_{iso} = H_{iso}/E = 0 \end{array}$$

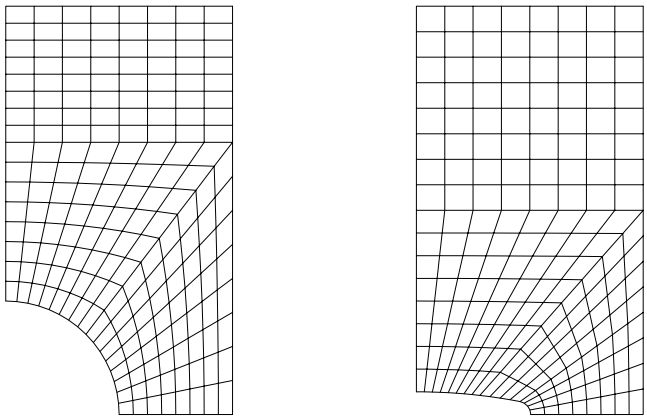

Figure 6.5: Strips with circular and elliptical holes: plane projection of the adopted meshes

- Material 3 [79]

$$\begin{array}{lll} E = 7000 \quad \text{MPa} & \nu = 0.3 & \\ \sigma_{y,0} = 24.3 \quad \text{MPa} & H_{kin} = 0 \quad \text{MPa} & H_{iso} = 225 \quad \text{MPa} \\ \bar{\sigma}_{y,0} = \sigma_{y,0}/E = 0.0034 & \bar{H}_{kin} = H_{kin}/E = 0 & \bar{H}_{iso} = H_{iso}/E = 0.032 \end{array}$$

- Material 4 [74]

$$\begin{array}{lll} E = 2 \times 10^5 \quad \text{MPa} & \nu = 0.3 & \sigma_{y,0} = 2 \times 10^2 \quad \text{MPa} \\ H_{iso} = 0 \quad \text{MPa} & H_{kin} = 2 \times 10^4 \quad \text{MPa} & H_{nl} = 50 \\ \bar{H}_{iso} = H_{iso}/E = 0 & \bar{H}_{kin} = H_{kin}/E = 10^{-1} & \bar{H}_{nl} = H_{nl}/E = 2.5 \times 10^{-4} \end{array}$$

- Material 5 [74]

$$\begin{array}{lll} E = 2 \times 10^5 \quad \text{MPa} & \nu = 0.3 & \sigma_{y,0} = 2 \times 10^2 \quad \text{MPa} \\ H_{iso} = 6 \times 10^3 \ \text{MPa} & H_{kin} = 2 \times 10^4 \ \text{MPa} & H_{nl} = 50 \\ \bar{H}_{iso} = H_{iso}/E = 3 \times 10^{-2} & \bar{H}_{kin} = H_{kin}/E = 10^{-1} & \bar{H}_{nl} = H_{nl}/E = 2.5 \times 10^{-4} \end{array}$$

Finally, we recall that the Young Modulus E and the Poisson ratio ν uniquely determine the constants K and G as follows

$$K = \frac{E}{3(1-2\nu)} \qquad G = \frac{E}{2(1+\nu)}$$

6.3 Numerical tests on the LP model

In this section we present the numerical tests on the integration algorithms discussed in Sections 5.3-5.7 which apply to the LP model. In what follows we systematically adopt the following acronyms for the tested algorithms:

- **BE** Bacward Euler return map method (Section 5.3)
- **MPT** Midpoint return map method (Section 5.4)
- **ENN** Exp. Non-symm. Non-cons. method (Section 5.5)
- **ENC** Exp. Non-symm. Cons. method (Section 5.6)
- **ESC** Exp. Symm. Cons. method (Section 5.7)
- **ESC**^{2} Exp. Symm. Cons. 2nd-order accurate method (Section 5.7)

6.3.1 Mixed stress-strain loading histories

The pointwise stress-strain tests are divided in two parts. First, we present a set of instantaneous error plots (Figures 6.6-6.9) corresponding to Problem 1 and to Problem 2 solved with the first-order accurate BE and ESC methods and with the exponential-based non-symmetric ENN and ENC methods, respectively with Material 1 and Material 2. Then, in Figures 6.10-6.13, we present the corresponding instantaneous error plots obtained with the quadratic methods MPT, ENC and ESC^2. This splitting is done in order to appreciate clearly the comparison in terms of precision between algorithms sharing the same order of accuracy.

From the error plots, we can extract the following comments

- The ESC and the BE methods perform similarly in terms of error, although in general the ESC seems slightly better. As the step size is reduced, both methods seem to converge with linear accuracy, i.e. the error seems to be divided by 2 every time we double the number of steps (error goes as Δt).

- The non symmetric methods ENN and ENC show practically the same error levels for all the considered stress-strain histories. These methods perform decisively better than the ESC and BE algorithms. The order of accuracy is 2 in this case and the error is roughly divided by 4 every time we double the number of steps (error goes as $(\Delta t)^2$).

- The performance of the MPT and the ENC methods are comparable. The MPT algorithm provides exact solutions for the case of proportional loading. Finally, as the step size is reduced, both methods converge quadratically, i.e. the error is divided by 4 every time the number of steps is doubled (the error goes as Δt^2).

- The new symmetric method ESC^2 grants relatively lower error levels than the MPT and ESC algorithms for all the considered stress-strain histories. Also in this case, the numerical solution is exact for proportional loading conditions and the error decreases quadratically with respect to the time step size.

We omit, for brevity's sake, to provide the error plots regarding the remaining load histories since they would lead to conclusions similar to those given in the above points.

Then, in Figure 6.14 we plot the total error expressed by Equation (6.3) versus the number of time steps in logarithmic scale for the six methods BE, MPT, ENN, ENC, ESC and ESC^2 for Problem 1 with Material 1. The quadratic convergence of the MPT, ENN, ENC and ESC^2 methods with respect to the linear convergence of the other algorithms can be clearly appreciated. It is remarkable that this error measurement qualifies the new optimal ESC^2 scheme as the most precise within the set of the tested algorithms, since it presents the lowest error levels both for the stress and the strain computation.

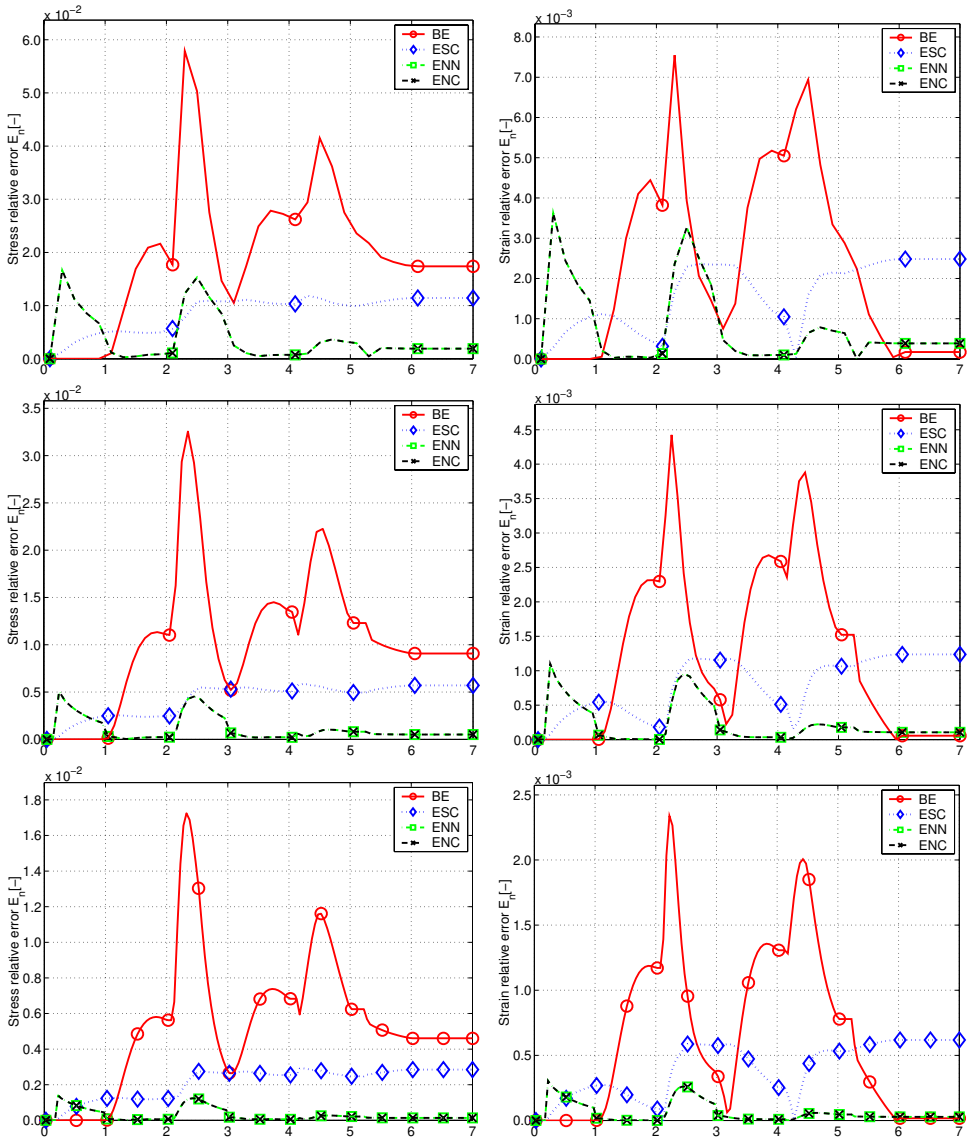

Figure 6.6: Mixed stress-strain loading histories: Problem 1 with Material 1. Stress and strain error for $\Delta t = 0.1$ s, $\Delta t = 0.05$ s, $\Delta t = 0.025$ s

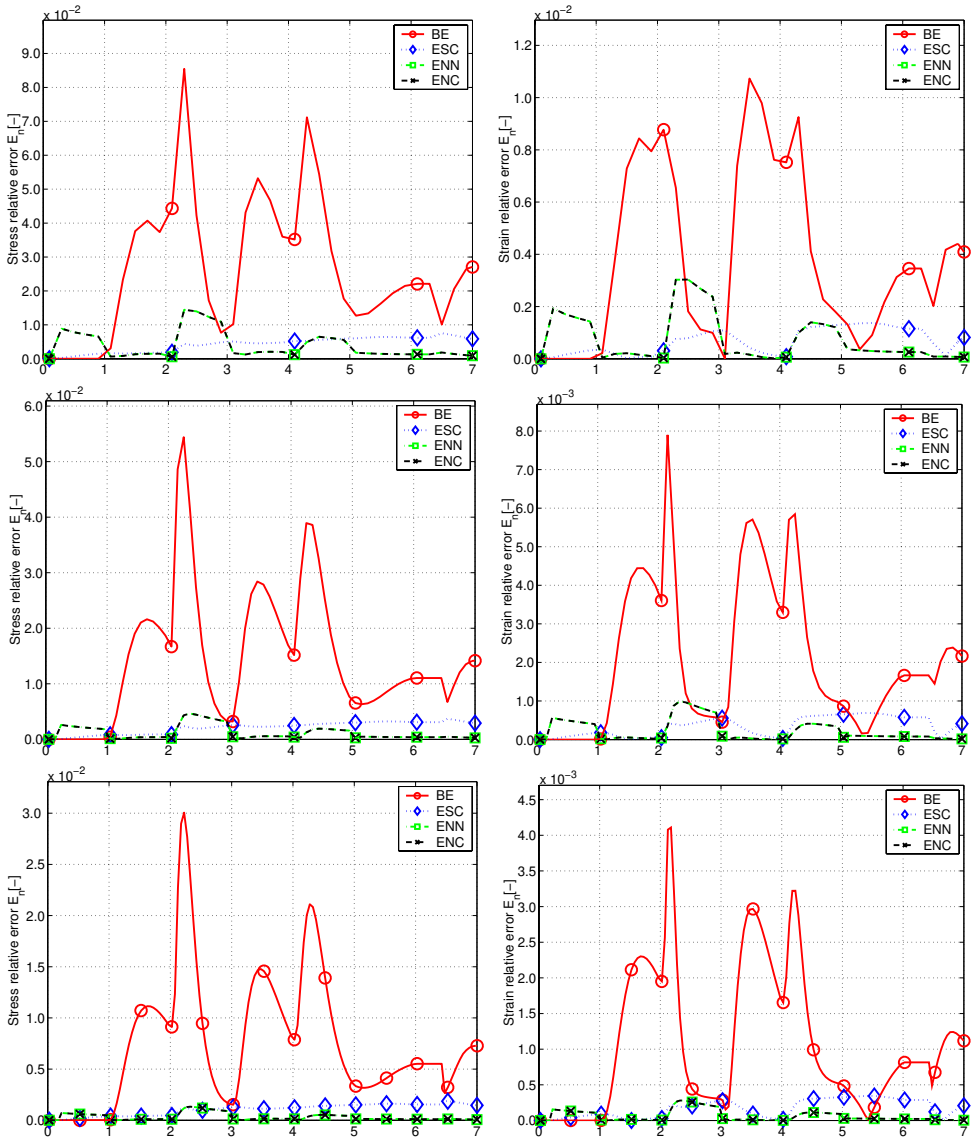

Figure 6.7: Mixed stress-strain loading histories: Problem 1 with Material 2. Stress and strain error for $\Delta t = 0.1$ s, $\Delta t = 0.05$ s, $\Delta t = 0.025$ s

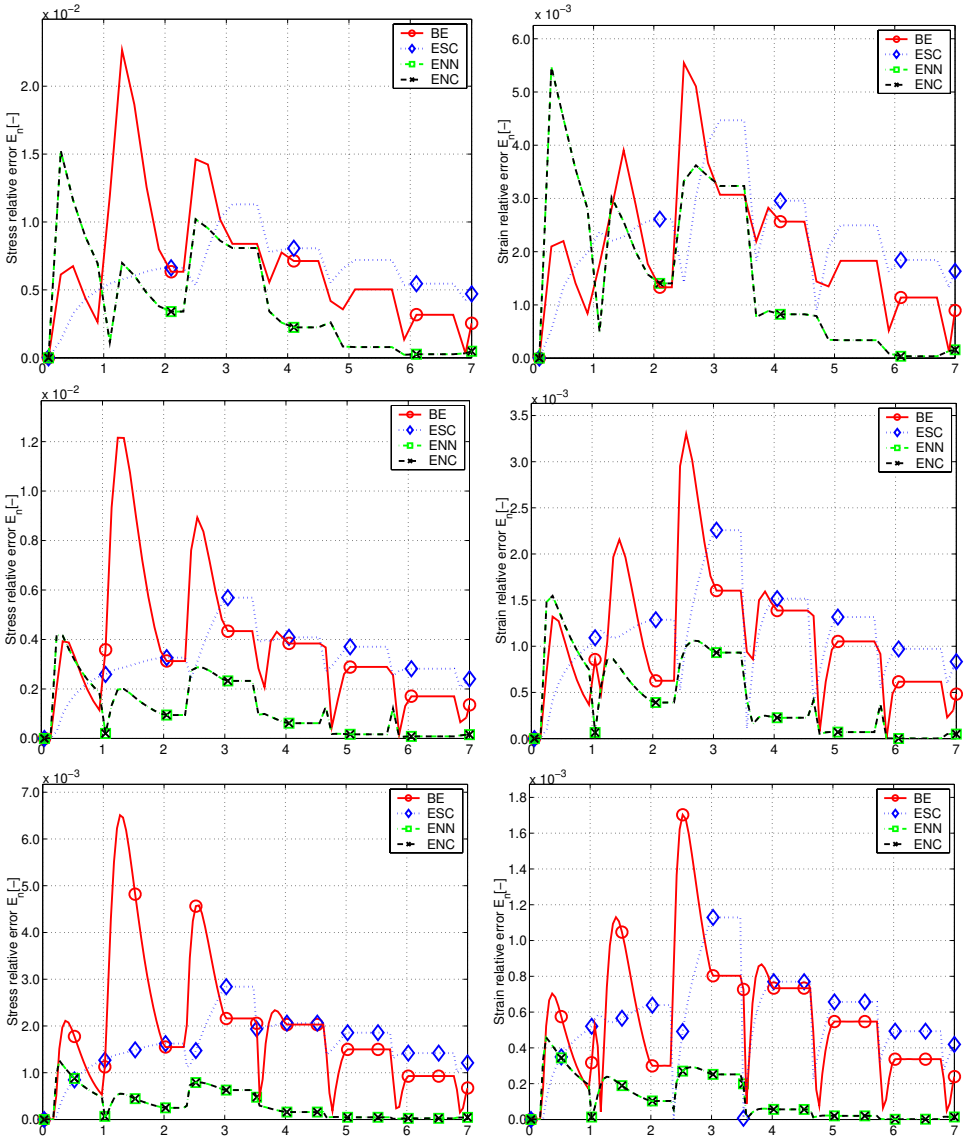

Figure 6.8: Mixed stress-strain loading histories: Problem 2 with Material 1. Stress and strain error for $\Delta t = 0.1$ s, $\Delta t = 0.05$ s, $\Delta t = 0.025$ s

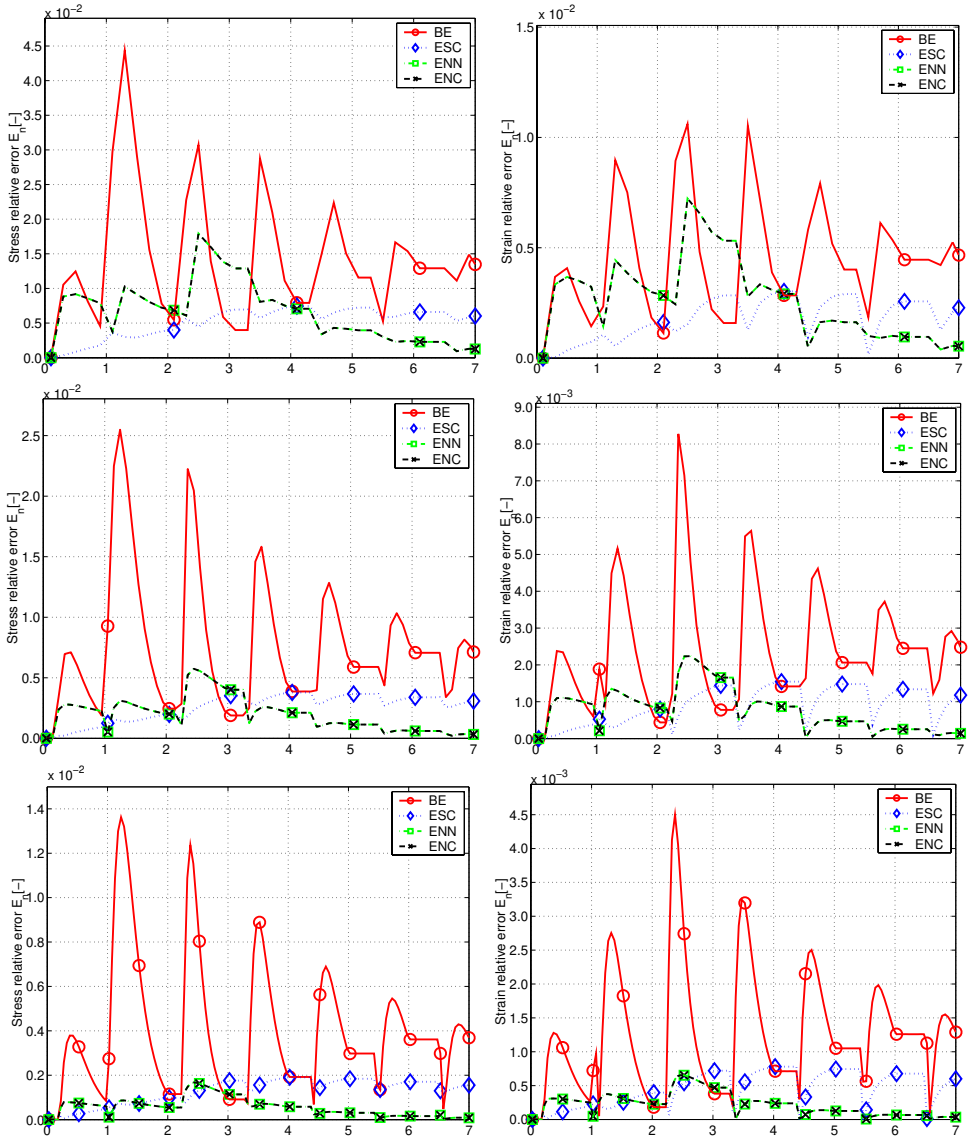

Figure 6.9: Mixed stress-strain loading histories: Problem 2 with Material 2. Stress and strain error for $\Delta t = 0.1$ s, $\Delta t = 0.05$ s, $\Delta t = 0.025$ s

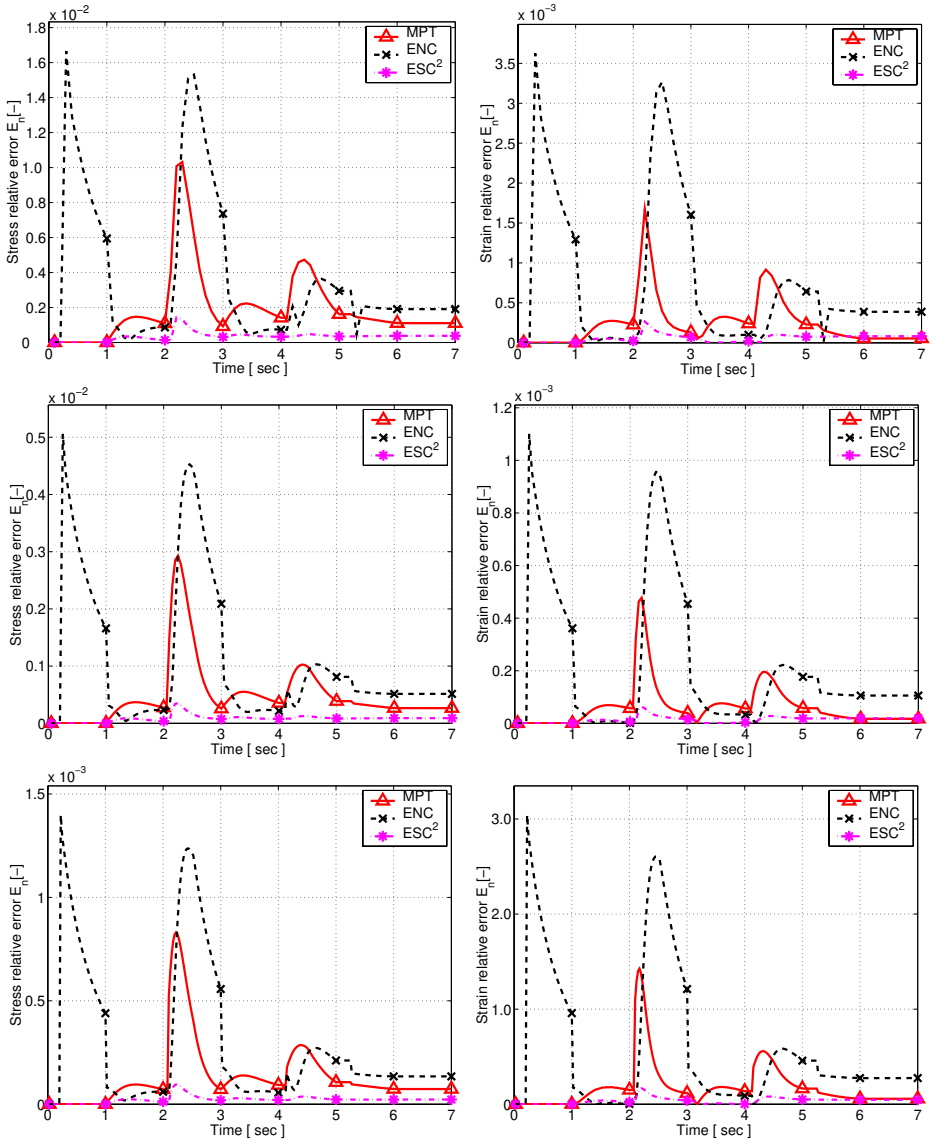

Figure 6.10: Mixed stress-strain loading histories: Problem 1 with Material 1. Stress and strain error for $\Delta t = 0.1$ s, $\Delta t = 0.05$ s, $\Delta t = 0.025$ s

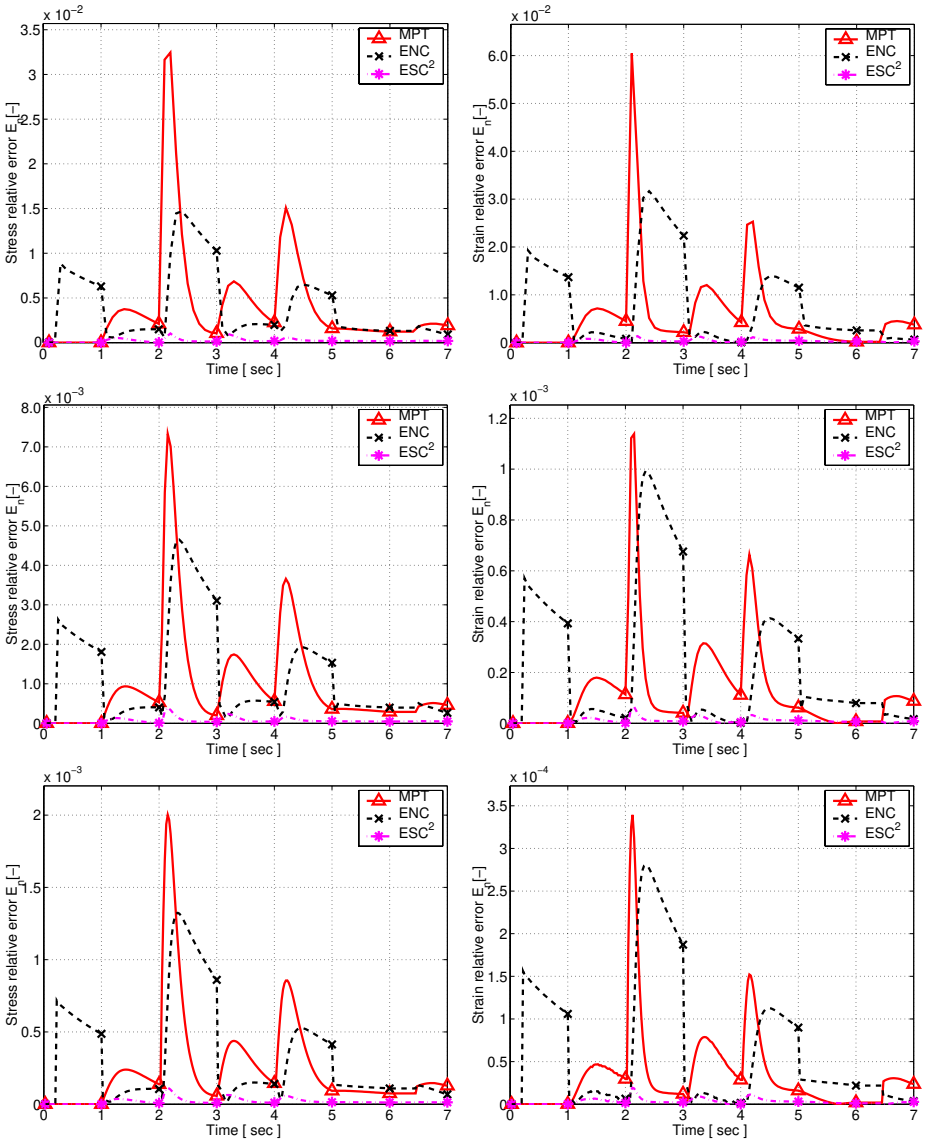

Figure 6.11: Mixed stress-strain loading histories: Problem 1 with Material 2. Stress and strain error for $\Delta t = 0.1$ s, $\Delta t = 0.05$ s, $\Delta t = 0.025$ s

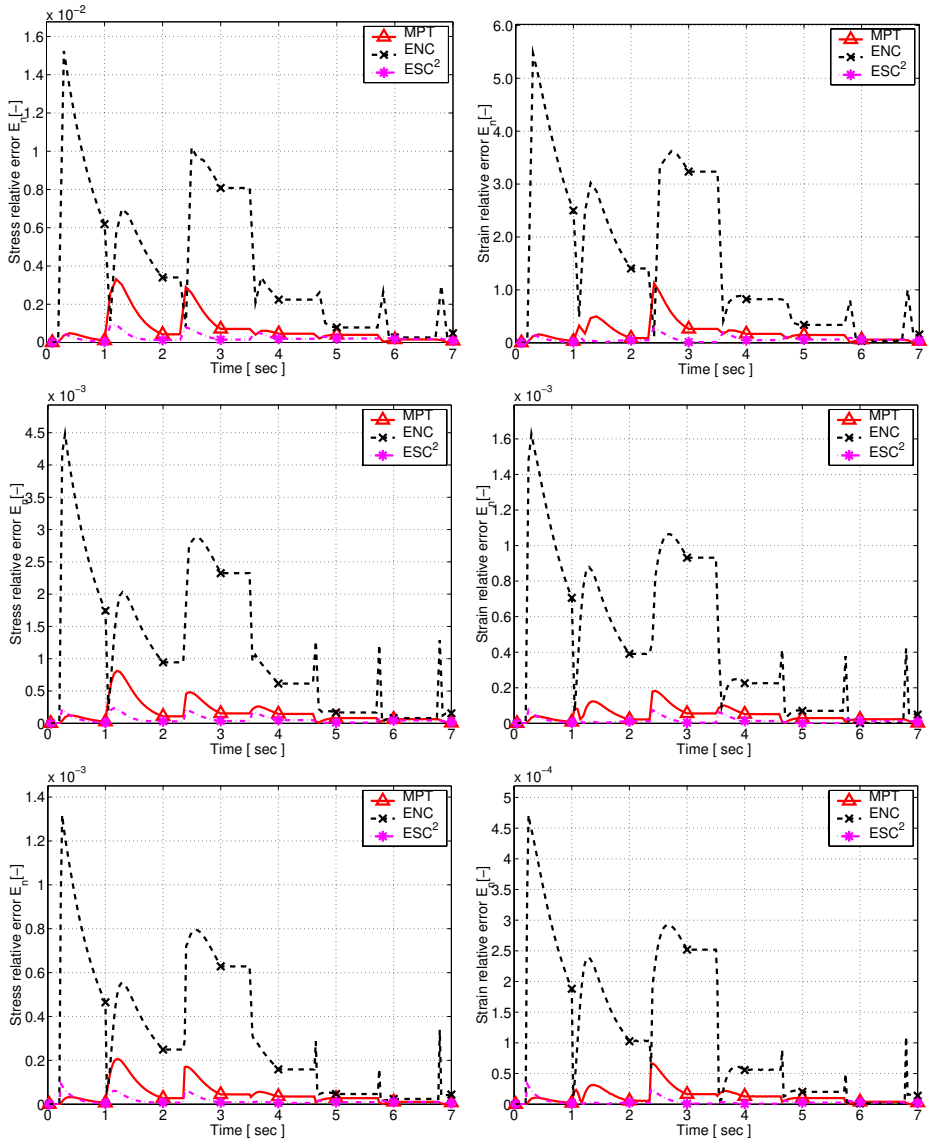

Figure 6.12: Mixed stress-strain loading histories: Problem 2 with Material 1. Stress and strain error for $\Delta t = 0.1$ s, $\Delta t = 0.05$ s, $\Delta t = 0.025$ s

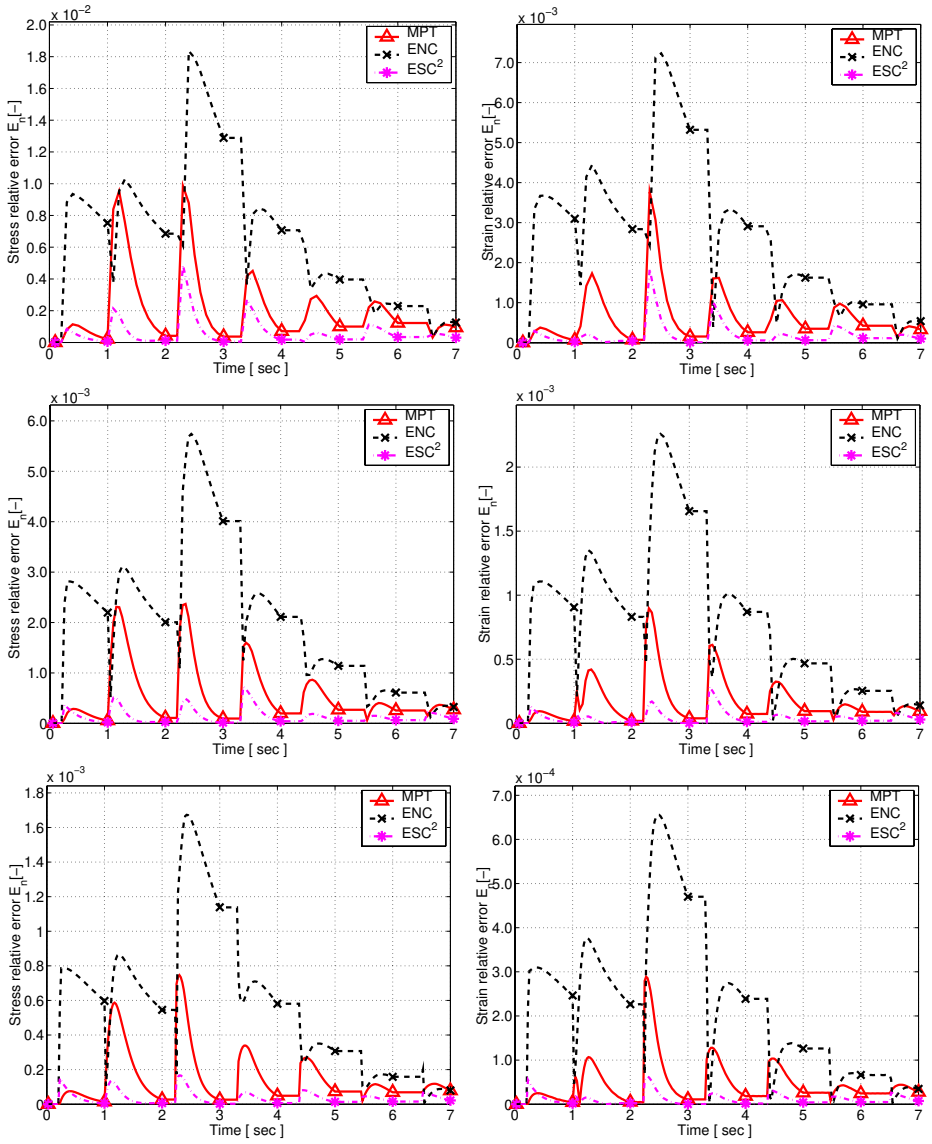

Figure 6.13: Mixed stress-strain loading histories: Problem 2 with Material 2. Stress and strain error for $\Delta t = 0.1$ s, $\Delta t = 0.05$ s, $\Delta t = 0.025$ s

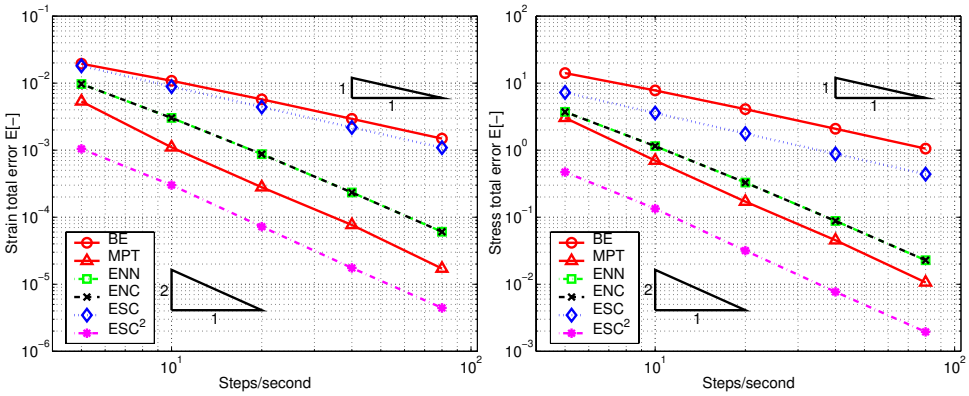

Figure 6.14: Pointwise stress-strain tests. Problem 1 with Material 1. Stress and strain total error versus number of steps per second.

6.3.2 Iso-error maps

In this section we present the iso-error maps corresponding to the three initial State 1 on the yield surface (cf. Table 6.2) and compare the precision levels granted by the BE, MPT and ESC^2 integration algorithms, respectively. All the calculations refer to Material 2.

The total error range is subdivided in ten equally spaced levels according to which the iso-curves are drawn in Figures 6.15-6.17. Each iso-curve is indicated by a proper error label while the thick continuous line represents the zero-level error stress-strain histories (i.e. proportional loading histories). For the sake of completeness, aside from each map we also report the maximum error value computed on the grid adopted for the computation of the iso-error map.

Observing Figures 6.15-6.17, we recognize that the ESC^2 scheme produces more precise solutions in terms of stresses if compared to the BE and MPT algorithms. Even for "large" strain increments the new exponential-based procedure reveals low levels of error compared with the other two methods. Such a result seems to be rather interesting since it suggests robustness of the integration scheme for practical application of the integration procedure in a finite element analysis of boundary value problems. It is also worth noting that the BE scheme, which has linear accuracy, is more precise than the quadratic MPT algorithm for large strain increments. In this sense the ESC^2 method turns out to be the most reliable within the three methods, since it is quadratic and mantains good behavior also for large time steps.

A further observation is that, although $H_{iso} = 0$, the exponential-based algorithm presents a non zero error. This apparently erroneous behavior is due to the fact that we have assumed a mixed stress-strain history and not a completely strain driven one (see Reference [11] for a deeper discussion of this point).

Remark 6.3.1 It is noted that even with a non zero value of isotropic hardening the ESC^2 scheme still produces more precise results for large time discretizations than both the BE and MPT scheme. The reader is referred to [7] where a wide set of iso-error maps regarding this particular case confirm the better performance of the exponential-based method.

6.3.3 Initial boundary value problems

In this section we report the L^2 norm error (6.5)-(6.6) obtained with the BE, ENC, ESC, MPT and ESC^2 integration algorithms, respectively, for the solution of the initial boundary value problems presented in Section 6.2.3. The results are summarized in Table 6.3 and Table 6.4 which report the norm error at different instants during the loading history for the tested algorithms.

As expected, Table 6.3 and Table 6.4 show that the BE, ENC and ESC algorithms grant first-order accuracy while the MPT and ESC^2 are second-order accurate schemes. The tests indicate that the quadratic algorithms are far more precise than the linear ones, both for the stress and the strain computation. The quadratically accurate ESC^2 algorithm results globally more precise than the MPT.

BE

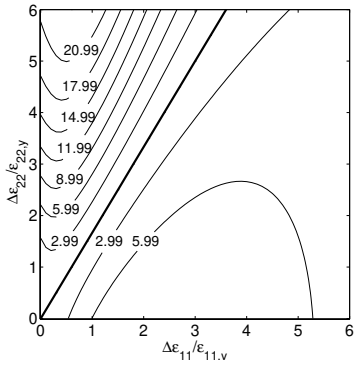

$E^{\sigma}_{iso,max} = 23.99\%$

MPT

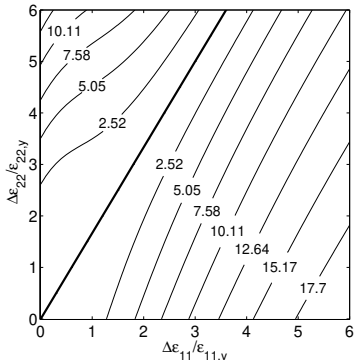

$E^{\sigma}_{iso,max} = 20.22\%$

ESC^2

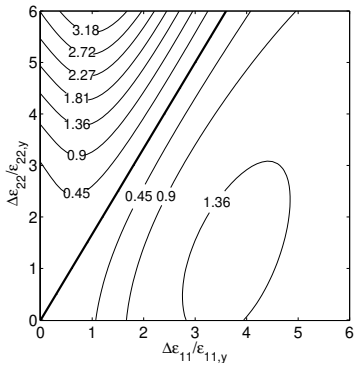

$E^{\sigma}_{iso,max} = 3.63\%$

Figure 6.15: Comparison between backward Euler (**BE**), midpoint (**MPT**) and the new exponential-based scheme (**ESC**^{2}). Iso-error maps for yield surface State 1 - **A** with Material 2 and indication of the maximum stress error level.

BE

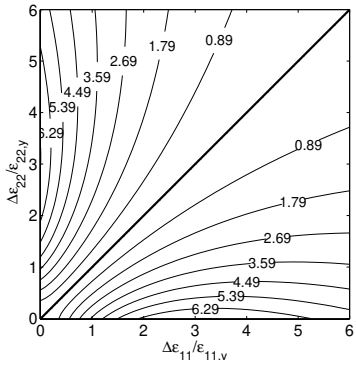

$E^{\sigma}_{iso,max} = 7.18\%$

MPT

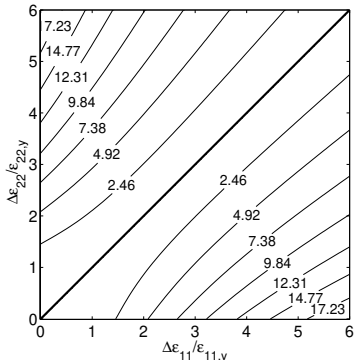

$E^{\sigma}_{iso,max} = 19.69\%$

ESC^2

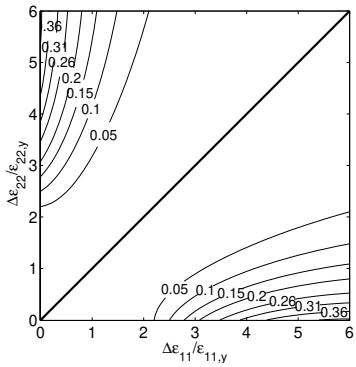

$E^{\sigma}_{iso,max} = 0.41\%$

Figure 6.16: Comparison between backward Euler (**BE**), midpoint (**MPT**) and the new exponential-based scheme (**ESC**^{2}). Iso-error maps for yield surface State 1 - **B** with Material 2 and indication of the maximum stress error level.

BE

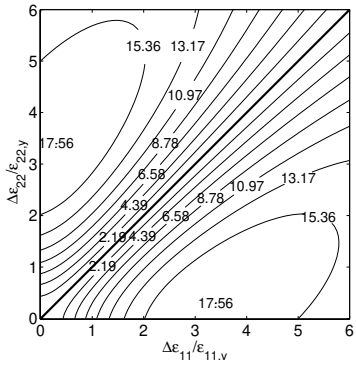

$E^{\sigma}_{iso,max} = 19.74\%$

MPT

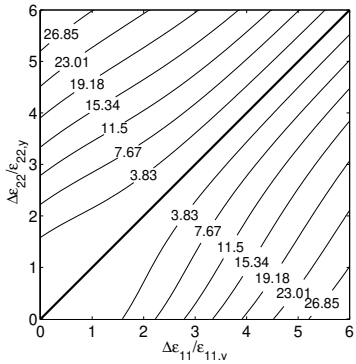

$E^{\sigma}_{iso,max} = 30.69\%$

ESC^2

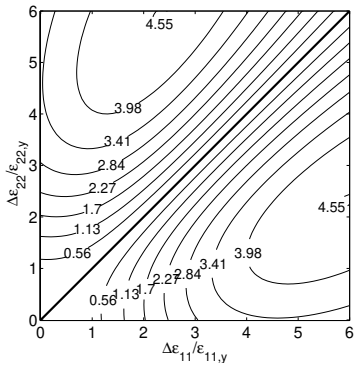

$E^{\sigma}_{iso,max} = 5.12\%$

Figure 6.17: Comparison between backward Euler (**BE**), midpoint (**MPT**) and the new exponential-based scheme (**ESC**^{2}). Iso-error maps for yield surface State 1 - **C** with material 2 and indication of the maximum stress error level.

Table 6.3: Initial boundary value problems. Extension of rectangular strip with circular hole. Stress and strain L^2 norm errors with Material 3 at $t = 0.5$ s,$t = 1.0$ s,$t = 1.5$ s,$t = 2.0$ s for BE, ENC, ESC, MPT and ESC^2 schemes

$\tilde{E}$	Δt	BE	ENC	ESC	MPT	ESC^2
				$t = 0.5$ s		
$\tilde{E}^{\boldsymbol{\sigma}}$	Δt_1	1.81×10^{-3}	1.15×10^{-3}	1.18×10^{-4}	1.36×10^{-4}	1.03×10^{-4}
	Δt_2	9.62×10^{-4}	3.26×10^{-4}	5.12×10^{-5}	3.24×10^{-5}	2.67×10^{-5}
	Δt_3	4.96×10^{-4}	9.09×10^{-5}	2.76×10^{-5}	9.27×10^{-6}	7.11×10^{-6}
$\tilde{E}^{\boldsymbol{\epsilon}}$	Δt_1	2.31×10^{-3}	2.08×10^{-3}	2.80×10^{-4}	3.02×10^{-4}	9.92×10^{-5}
	Δt_2	1.24×10^{-3}	5.91×10^{-4}	1.20×10^{-4}	7.44×10^{-5}	2.12×10^{-5}
	Δt_3	6.42×10^{-4}	1.62×10^{-4}	6.42×10^{-5}	2.31×10^{-5}	8.90×10^{-6}
				$t = 1.0$ s		
$\tilde{E}^{\boldsymbol{\sigma}}$	Δt_1	3.07×10^{-3}	1.94×10^{-3}	6.32×10^{-4}	1.26×10^{-4}	1.11×10^{-4}
	Δt_2	1.58×10^{-3}	5.17×10^{-4}	3.13×10^{-4}	3.05×10^{-5}	2.55×10^{-5}
	Δt_3	8.00×10^{-4}	1.32×10^{-4}	1.56×10^{-4}	7.81×10^{-6}	6.58×10^{-6}
$\tilde{E}^{\boldsymbol{\epsilon}}$	Δt_1	2.57×10^{-3}	2.99×10^{-3}	1.40×10^{-3}	2.86×10^{-4}	2.96×10^{-4}
	Δt_2	1.29×10^{-3}	8.12×10^{-4}	6.69×10^{-4}	5.87×10^{-5}	6.22×10^{-5}
	Δt_3	6.53×10^{-4}	2.03×10^{-4}	3.30×10^{-4}	1.64×10^{-5}	1.69×10^{-5}
				$t = 1.5$ s		
$\tilde{E}^{\boldsymbol{\sigma}}$	Δt_1	9.61×10^{-3}	6.10×10^{-3}	1.94×10^{-3}	2.31×10^{-1}	3.61×10^{-4}
	Δt_2	1.14×10^{-1}	1.14×10^{-1}	1.16×10^{-1}	1.15×10^{-1}	1.15×10^{-1}
	Δt_3	5.72×10^{-2}	5.74×10^{-2}	5.81×10^{-2}	5.78×10^{-2}	5.78×10^{-2}
$\tilde{E}^{\boldsymbol{\epsilon}}$	Δt_1	3.64×10^{-3}	4.23×10^{-3}	1.98×10^{-3}	5.23×10^{-2}	4.19×10^{-4}
	Δt_2	2.61×10^{-2}	2.63×10^{-2}	2.61×10^{-2}	2.61×10^{-2}	2.61×10^{-2}
	Δt_3	1.30×10^{-2}	1.31×10^{-2}	1.30×10^{-2}	1.30×10^{-2}	1.30×10^{-2}
				$t = 2.0$ s		
$\tilde{E}^{\boldsymbol{\sigma}}$	Δt_1	6.46×10^{-3}	3.40×10^{-3}	1.14×10^{-3}	2.92×10^{-4}	2.20×10^{-4}
	Δt_2	3.35×10^{-3}	9.06×10^{-4}	5.68×10^{-4}	6.98×10^{-5}	5.05×10^{-5}
	Δt_3	1.70×10^{-3}	2.31×10^{-4}	2.83×10^{-4}	1.78×10^{-5}	1.28×10^{-5}
$\tilde{E}^{\boldsymbol{\epsilon}}$	Δt_1	6.38×10^{-3}	5.64×10^{-3}	2.31×10^{-3}	5.27×10^{-4}	6.16×10^{-4}
	Δt_2	3.24×10^{-3}	1.51×10^{-3}	1.12×10^{-3}	1.07×10^{-4}	1.30×10^{-4}
	Δt_3	1.63×10^{-3}	3.79×10^{-4}	5.56×10^{-4}	2.98×10^{-5}	3.46×10^{-5}

Table 6.4: Initial boundary value problems. Extension of rectangular strip with elliptical hole. Stress and strain L^2 norm errors with Material at $t = 0.5$ s,$t = 1.0$ s,$t = 1.5$ s,$t = 2.0$ s for BE, ENC, ESC, MPT and ESC^2 schemes

$\tilde{E}$	Δt	BE	ENC	ESC	MPT	ESC^2
				$t = 0.5$ s		
$\tilde{E}^{\boldsymbol{\sigma}}$	Δt_1	2.72×10^{-3}	2.10×10^{-3}	2.60×10^{-4}	2.05×10^{-4}	2.21×10^{-4}
	Δt_2	1.43×10^{-3}	6.47×10^{-4}	1.05×10^{-4}	5.19×10^{-5}	5.45×10^{-5}
	Δt_3	7.38×10^{-4}	1.72×10^{-4}	5.24×10^{-5}	1.56×10^{-5}	1.64×10^{-5}
$\tilde{E}^{\boldsymbol{\epsilon}}$	Δt_1	2.93×10^{-3}	4.18×10^{-3}	6.74×10^{-4}	5.26×10^{-4}	3.58×10^{-4}
	Δt_2	1.59×10^{-3}	1.29×10^{-3}	2.65×10^{-4}	1.24×10^{-4}	8.19×10^{-5}
	Δt_3	8.27×10^{-4}	3.45×10^{-4}	1.26×10^{-4}	3.66×10^{-5}	2.62×10^{-5}
				$t = 1.0$ s		
$\tilde{E}^{\boldsymbol{\sigma}}$	Δt_1	3.65×10^{-3}	2.60×10^{-3}	1.10×10^{-3}	1.33×10^{-4}	2.66×10^{-4}
	Δt_2	1.86×10^{-3}	7.18×10^{-4}	5.30×10^{-4}	3.42×10^{-5}	6.68×10^{-5}
	Δt_3	9.45×10^{-4}	1.91×10^{-4}	2.60×10^{-4}	8.74×10^{-6}	1.67×10^{-5}
$\tilde{E}^{\boldsymbol{\epsilon}}$	Δt_1	6.04×10^{-3}	4.15×10^{-3}	2.12×10^{-3}	2.31×10^{-1}	3.61×10^{-4}
	Δt_2	3.05×10^{-3}	1.13×10^{-3}	1.02×10^{-3}	1.15×10^{-1}	1.15×10^{-1}
	Δt_3	5.72×10^{-2}	5.74×10^{-2}	5.81×10^{-2}	5.78×10^{-2}	5.78×10^{-2}
				$t = 1.5$ s		
$\tilde{E}^{\boldsymbol{\sigma}}$	Δt_1	8.50×10^{-3}	6.09×10^{-3}	2.56×10^{-3}	1.63×10^{-3}	6.27×10^{-4}
	Δt_2	8.08×10^{-2}	8.04×10^{-2}	8.24×10^{-2}	8.17×10^{-2}	8.17×10^{-2}
	Δt_3	4.03×10^{-2}	4.05×10^{-2}	4.12×10^{-2}	4.08×10^{-2}	4.08×10^{-2}
$\tilde{E}^{\boldsymbol{\epsilon}}$	Δt_1	7.88×10^{-3}	5.42×10^{-3}	2.76×10^{-3}	3.91×10^{-2}	8.89×10^{-4}
	Δt_2	1.92×10^{-2}	1.98×10^{-2}	1.93×10^{-2}	1.95×10^{-2}	1.95×10^{-2}
	Δt_3	9.61×10^{-3}	9.83×10^{-3}	9.66×10^{-3}	9.77×10^{-3}	9.76×10^{-3}
				$t = 2.0$ s		
$\tilde{E}^{\boldsymbol{\sigma}}$	Δt_1	8.05×10^{-3}	4.67×10^{-3}	1.85×10^{-3}	3.38×10^{-4}	4.95×10^{-4}
	Δt_2	4.16×10^{-3}	1.27×10^{-3}	9.33×10^{-4}	8.10×10^{-5}	1.21×10^{-4}
	Δt_3	2.11×10^{-3}	3.37×10^{-4}	4.70×10^{-4}	2.11×10^{-5}	3.07×10^{-5}
$\tilde{E}^{\boldsymbol{\epsilon}}$	Δt_1	1.21×10^{-2}	7.66×10^{-3}	3.21×10^{-3}	3.47×10^{-4}	1.25×10^{-3}
	Δt_2	6.16×10^{-3}	2.06×10^{-3}	1.70×10^{-3}	8.72×10^{-5}	3.05×10^{-4}
	Δt_3	3.10×10^{-3}	5.43×10^{-4}	8.80×10^{-4}	2.31×10^{-5}	7.81×10^{-5}

6.4 Numerical tests on the NLK model

In this section we present the numerical tests on the integration algorithms discussed in Sections 5.10-5.12 which apply to the NLK model. In what follows we systematically adopt the following acronyms for the tested algorithms:

- **BEnl** Bacward Euler return map method (Section 5.10)
- **MPTnl** Midpoint return map method (Section 5.11)
- **ESC^{2}nl** Exp. Symm. Cons. 2nd-order accurate method (Section 5.12)

6.4.1 Mixed stress-strain loading histories

The pointwise stress-strain tests are divided in two parts. First, we present a set of instantaneous error plots (Figures 6.18-6.21) corresponding to Problem 1 and to Problem 2 solved with the BEnl, MPTnl and ESC^{2}nl methods, respectively with Material 4 and Material 5. Then in Figures 6.22-6.25, we present the corresponding instantaneous error plots obtained with the quadratic methods MPTnl and ESC^{2}nl. This splitting is done in order to appreciate clearly the comparison in terms of precision between the MPTnl and the ESC^{2}nl algorithm. It is evident from the presented error plots that

- The BEnl method is linearly accurate, that is the error is proportional to the step size Δt, while both the MPTnl and ESC^{2}nl are quadratically accurate, that is the error is proportional to the square of Δt.

- The performance of the MPTnl and ESC^{2}nl methods are globally comparable. As the loading history evolves the exponential-based method seems to produce lower error levels than the midpoint algorithm when there is a direction change in the driving input (the dashed line peaks on the error plots are usually higher than the dash-dot line peaks). On the other hand, in most cases it is observed that the MPTnl algorithm error levels decrease more rapidly after the change of direction peaks than in the case of the ESC^{2}nl method.

- The two second-order accurate methods ESC^{2}nl and MPTnl perform decisively better than the linearly accurate BEnl, for all the considered stress-strain histories.

  In Figure 6.26 we plot the total error expressed by (6.3) versus the number of time steps in logarithmic scale for the three methods BEnl, MPTnl

and ESC^{2}nl for Problem 1 with Material 4. The quadratic convergence of the MPTnl and ESC^{2}nl methods, with respect to the linear one of the BEnl algorithm is still evident. Moreover, the quadratic methods show significantly lower error levels with respect to the ones granted by the linear method. The ESC^{2}nl method results more precise in stress computation than the MPT, while their strain error levels are practically equal.

6.4.2 Iso-error maps

In this section we present the iso-error maps corresponding to the three initial State 1 on the yield surface (cf. Table 6.2) and compare the precision levels granted by the BEnl, MPTnl and ESC^{2}nl integration algorithms, respectively. All the calculations refer to Material 5.

The total error range is subdivided in ten equally spaced levels according to which the iso-curves are drawn in Figures 6.27-6.29. Each iso-curve is indicated by a proper error label while the thick continuous line represents the couples of strain increments values corresponding to proportional loading histories starting from state 1. For the sake of completeness, aside from each map we also report the maximum error value computed on the grid adopted for the computation of the iso-error map. Observing Figures 6.27-6.29 we can derive the following conclusions

- the ESC^{2}nl scheme shows better performances than both the BEnl and MPTnl algorithms for every considered starting yield State **1-A**, **1-B** and **1-C**. Even for "large" strain increments the new exponential-based procedure reveals low levels of error compared with the other two methods in all the examined cases.

- In general the BEnl scheme presents lower error levels for large strain increments than the MPTnl method. This result is in agreement with the general observation that lower order methods perform better than higher order ones for large time steps.

- None of the algorithms presents a zero error level along proportional loading paths (thick black lines, Figures 6.27-6.29). This is due to the fact that we have taken into account a nonlinear kinematic hardening mechanism. However, in the vicinity of the thick black lines the exponential-based method seems to be more accurate than the other schemes.

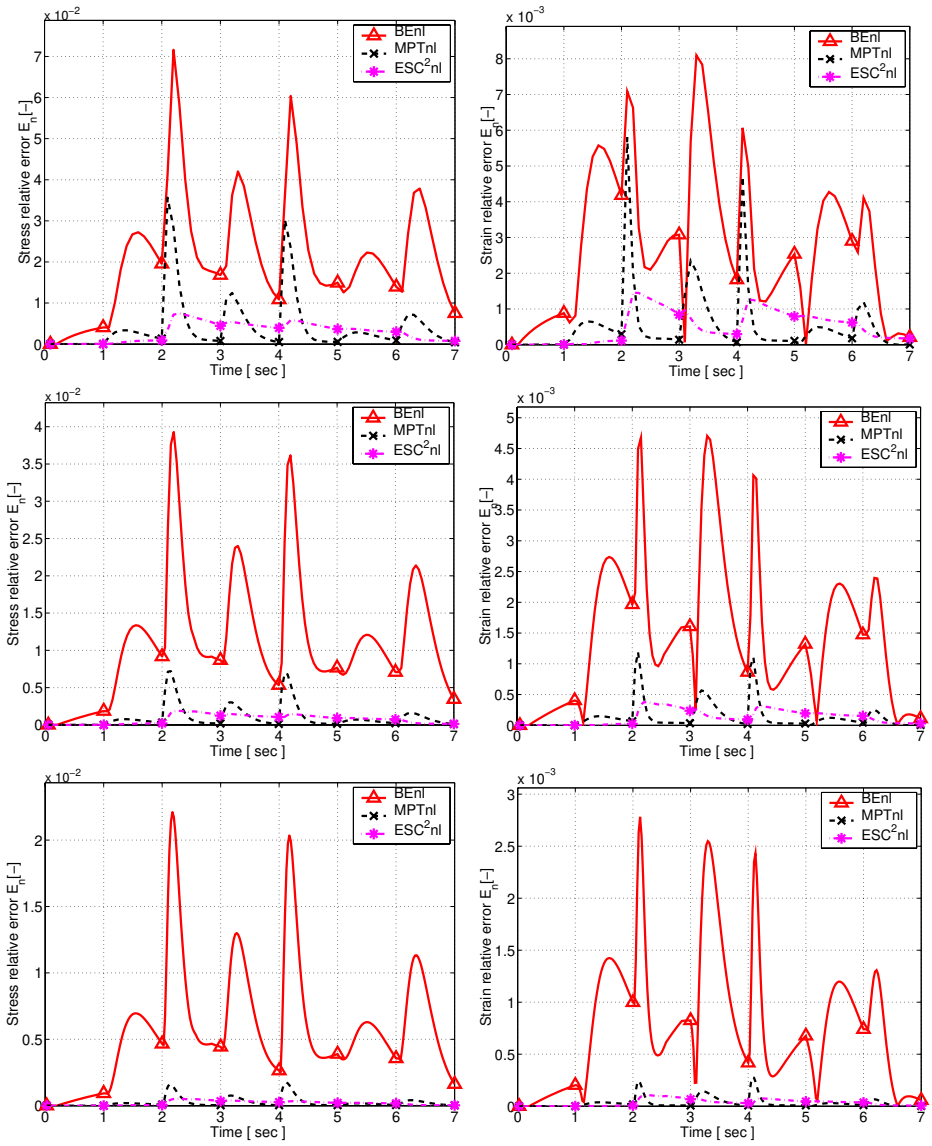

Figure 6.18: Mixed stress-strain loading histories: Problem 1 with Material 4. Stress and strain error for $\Delta t = 0.1$ s, $\Delta t = 0.05$ s, $\Delta t = 0.025$ s

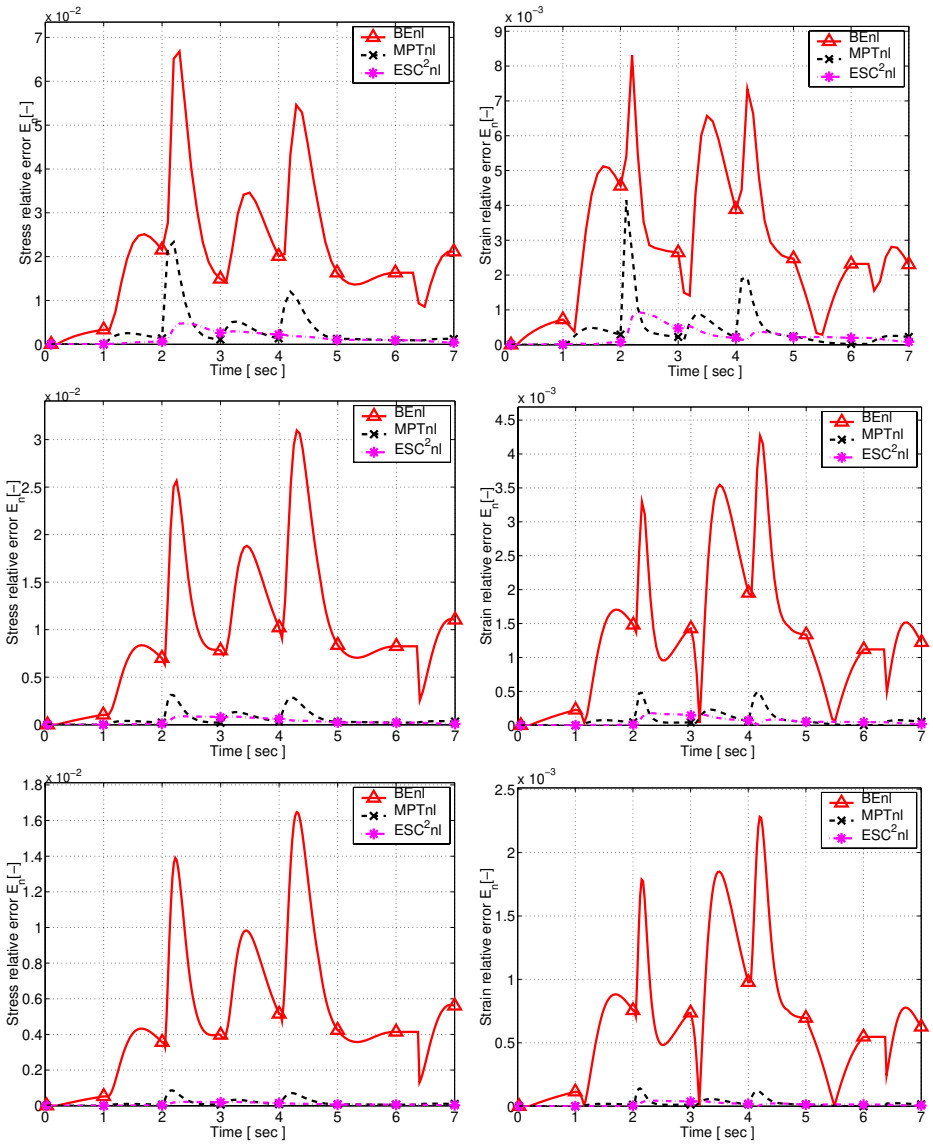

Figure 6.19: Mixed stress-strain loading histories: Problem 1 with Material 5. Stress and strain error for $\Delta t = 0.1$ s, $\Delta t = 0.05$ s, $\Delta t = 0.025$ s

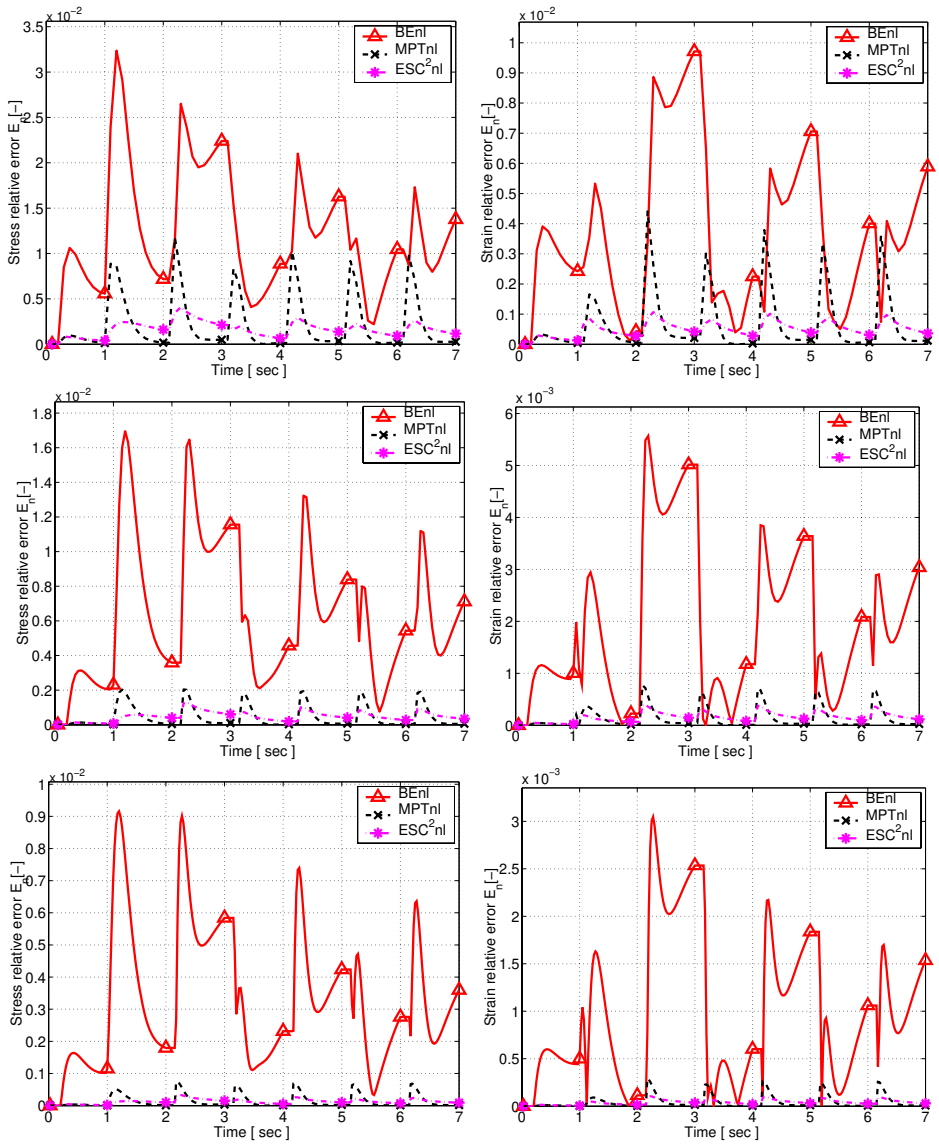

Figure 6.20: Mixed stress-strain loading histories: Problem 2 with Material 4. Stress and strain error for $\Delta t = 0.1$ s, $\Delta t = 0.05$ s, $\Delta t = 0.025$ s

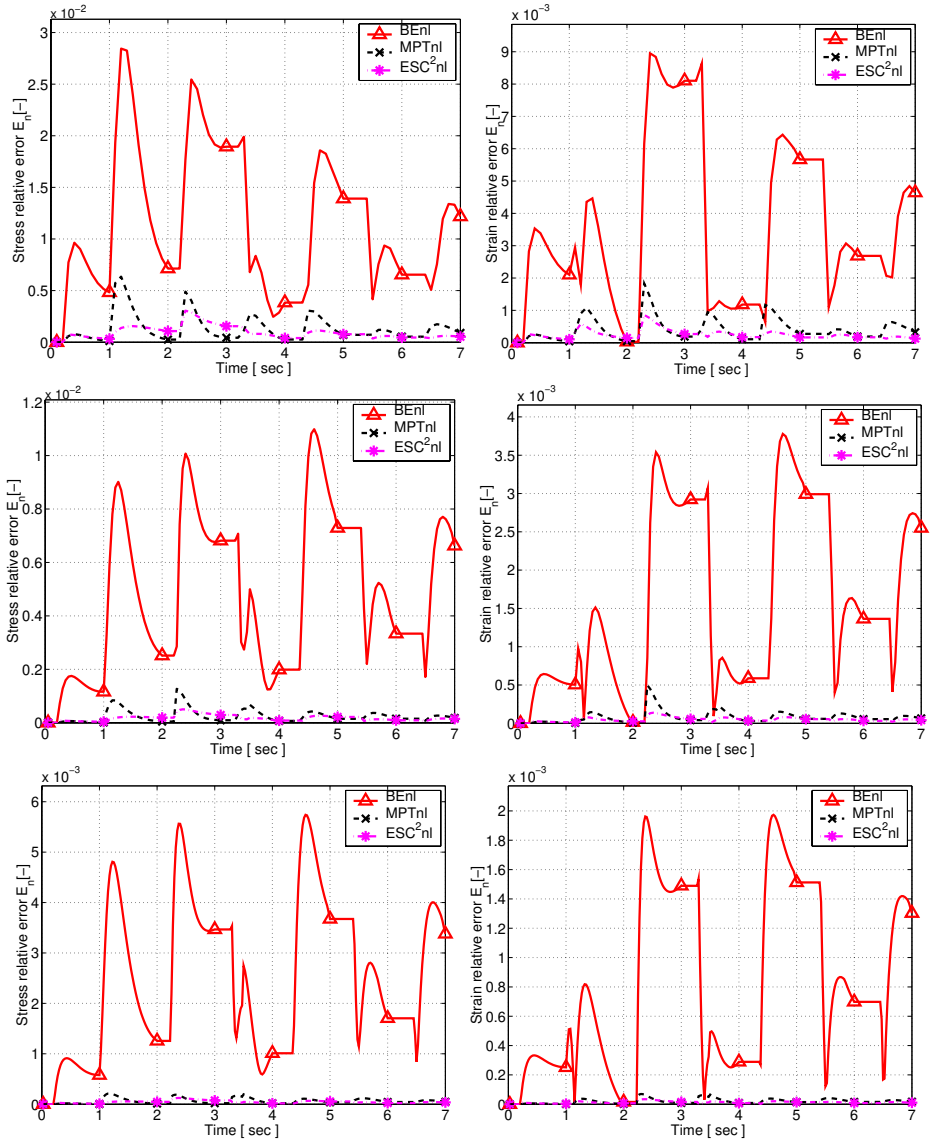

Figure 6.21: Mixed stress-strain loading histories: Problem 2 with Material 5. Stress and strain error for $\Delta t = 0.1$ s, $\Delta t = 0.05$ s, $\Delta t = 0.025$ s

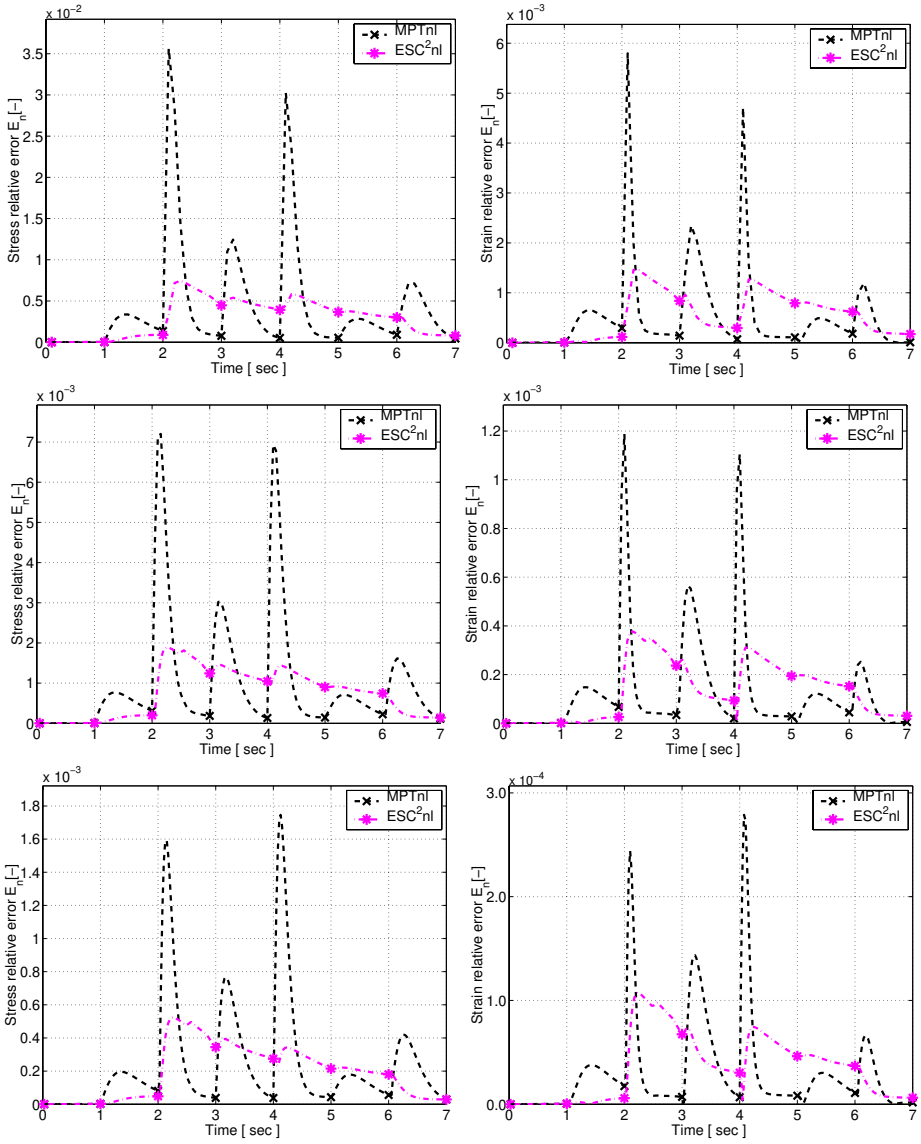

Figure 6.22: Mixed stress-strain loading histories: Problem 1 with Material 4. Stress and strain error for $\Delta t = 0.1$ s, $\Delta t = 0.05$ s, $\Delta t = 0.025$ s

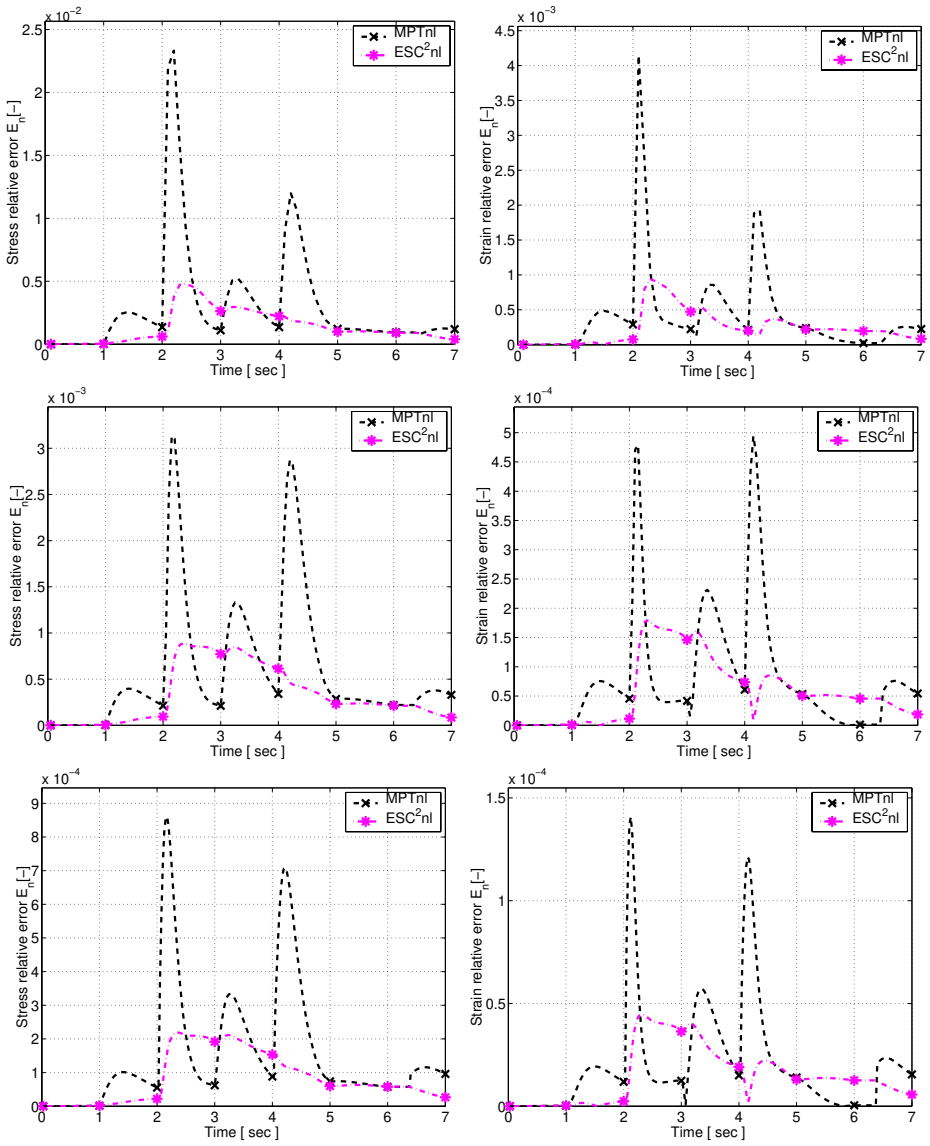

Figure 6.23: Mixed stress-strain loading histories: Problem 1 with Material 5. Stress and strain error for $\Delta t = 0.1$ s, $\Delta t = 0.05$ s, $\Delta t = 0.025$ s

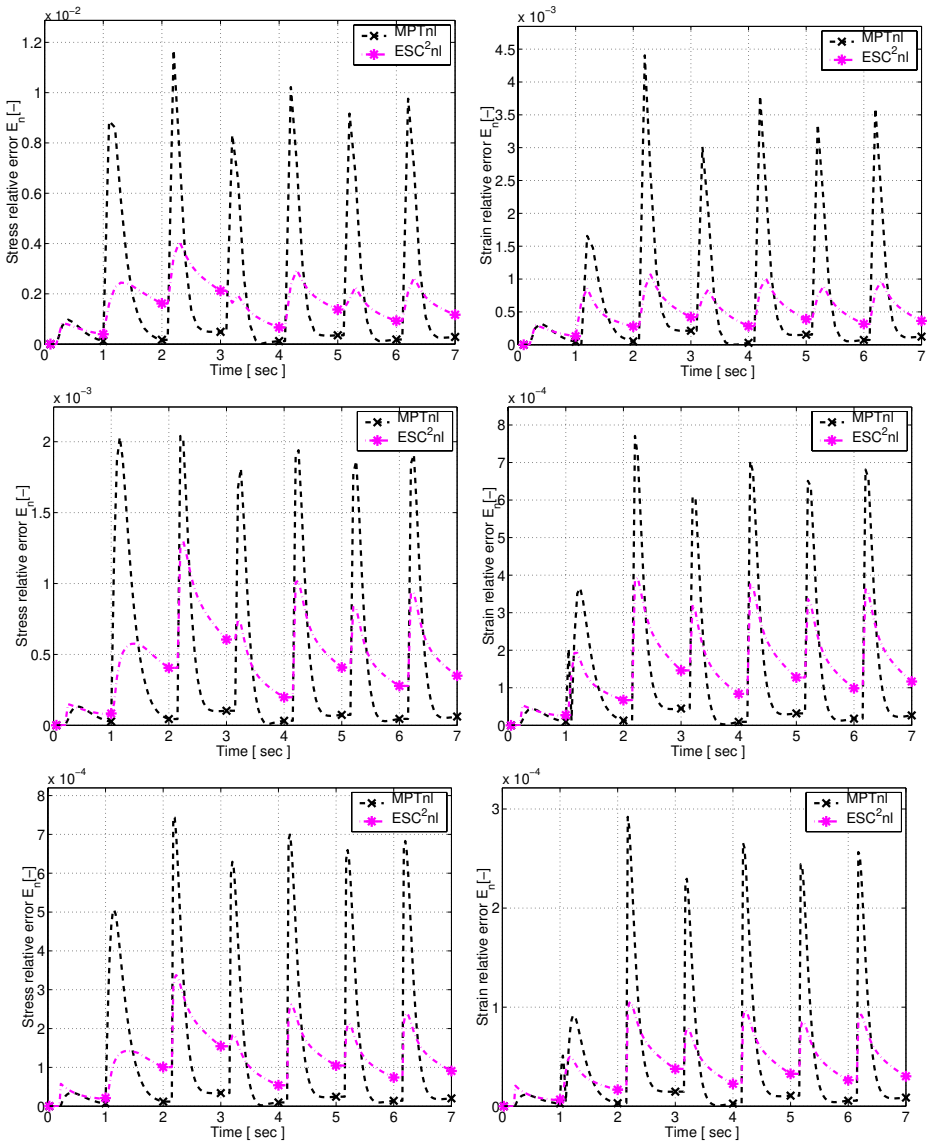

Figure 6.24: Mixed stress-strain loading histories: Problem 2 with Material 4. Stress and strain error for $\Delta t = 0.1$ s, $\Delta t = 0.05$ s, $\Delta t = 0.025$ s

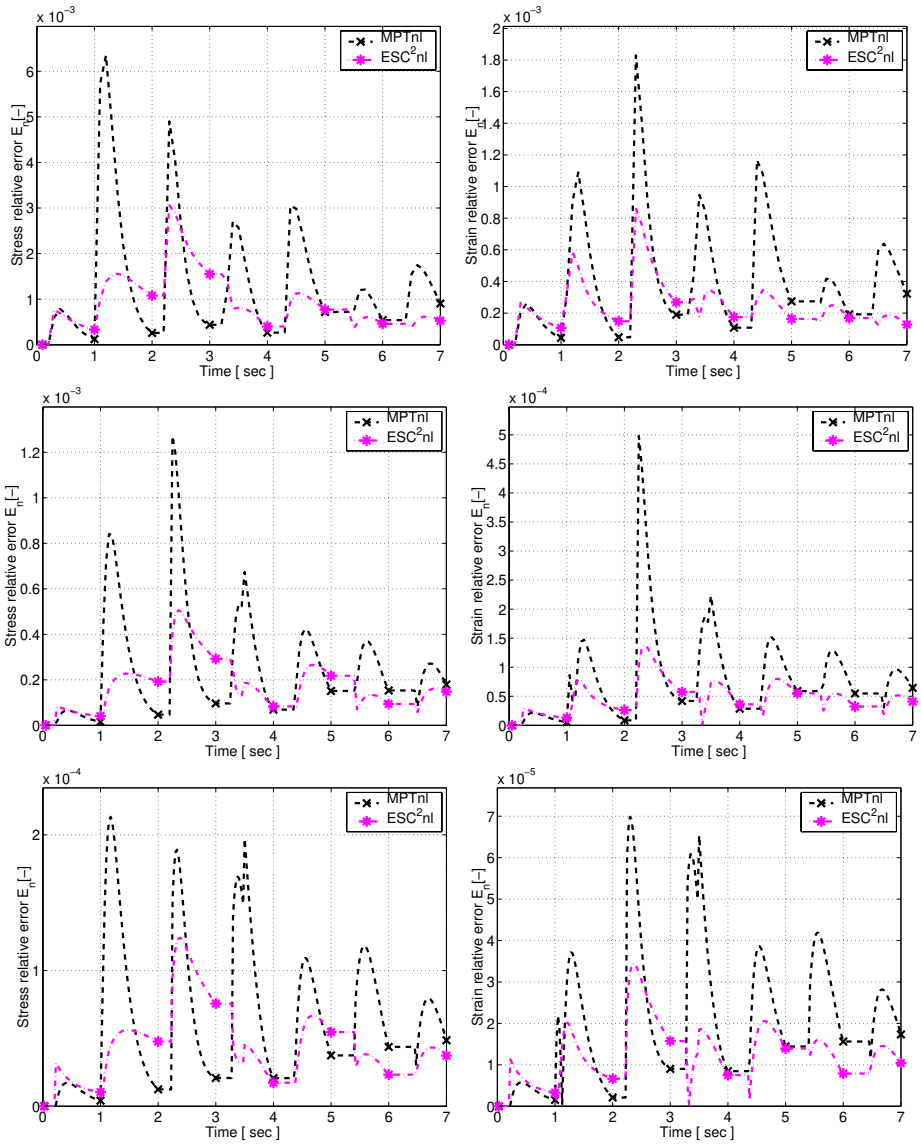

Figure 6.25: Mixed stress-strain loading histories: Problem 2 with Material 5. Stress and strain error for $\Delta t = 0.1$ s, $\Delta t = 0.05$ s, $\Delta t = 0.025$ s

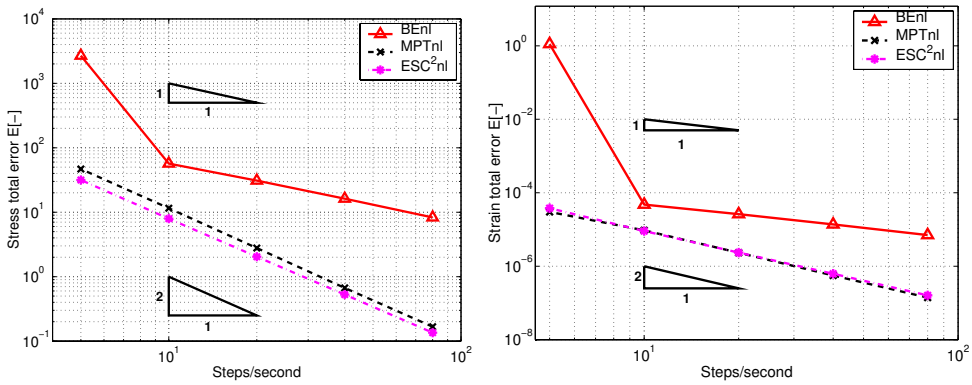

Figure 6.26: Pointwise stress-strain tests. Problem 1 with Material 4. Stress and strain total error versus number of steps per second.

6.4.3 Initial boundary value problems

In this section we report the L^2 norm error (6.5)-(6.6) obtained with the BEnl, MPTnl and ESC^{2}nl integration algorithms, respectively, for the solution of the initial boundary value problems presented in Section 6.2.3. The results are summarized in Table 6.5 and Table 6.6, which report the norm error at different instants during the loading history for the tested algorithms.

We may observe in Table 6.5 and Table 6.6 that the BEnl shows a first order of accuracy while the MPTnl and ESC^{2}nl are second-order accurate schemes. As shown in the tests, the quadratic algorithms are far more precise than the linear one, both for the stress and the strain computation. The quadratically accurate MPTnl and ESC^{2}nl algorithms result globally comparable in terms of precision.

Summarizing, the midpoint and the exponential-based scheme seem to behave very similarly. The higher peaks shown by the midpoint method in the pointwise error graphs, seem to reveal a better behavior of the ESC^{2}nl scheme whenever there is a crossing of the yield surface. Apart this difference, looking at the iso-error maps and the boundary value problem tests, it seems that the error behaviors of the two schemes are quite similar both for small and large time step size.

BEnl

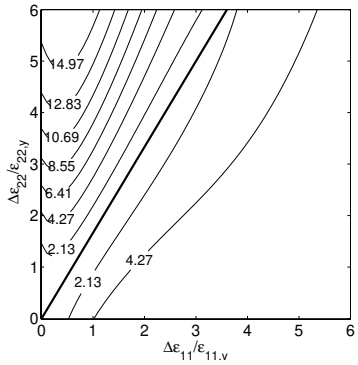

$E^{\sigma}_{iso,max} = 17.11\%$

MPTnl

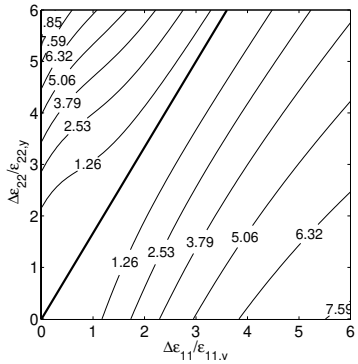

$E^{\sigma}_{iso,max} = 8.85\%$

ESC^{2}nl

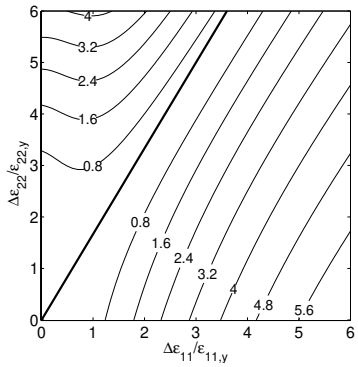

$E^{\sigma}_{iso,max} = 6.40\%$

Figure 6.27: Comparison between return map (**BEnl**), midpoint (**MPTnl**) and the new exponential-based scheme (**ESC^{2}nl**). Iso-error maps for yield surface State 1 - **A** with Material 5 and indication of the maximum stress error level.

BEnl

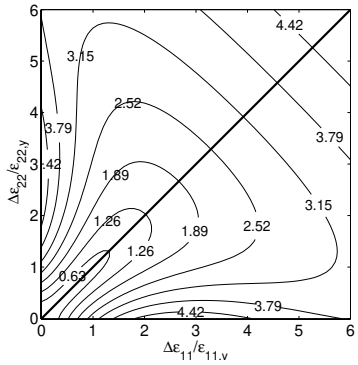

$E^{\sigma}_{iso,max} = 4.42\%$

MPTnl

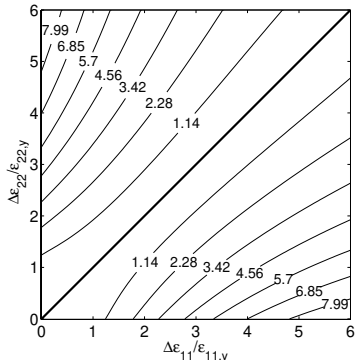

$E^{\sigma}_{iso,max} = 7.99\%$

ESC^{2}nl

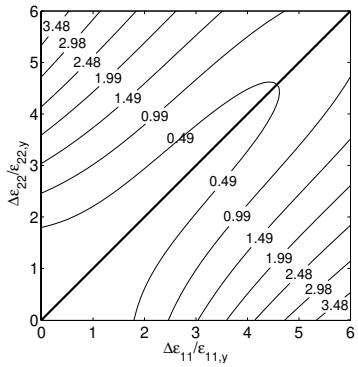

$E^{\sigma}_{iso,max} = 3.98\%$

Figure 6.28: Comparison between return map (**BEnl**), midpoint (**MPTnl**) and the new exponential-based scheme (**ESC^{2}nl**). Iso-error maps for yield surface State 1 - **B** with Material 5 and indication of the maximum stress error level.

BEnl

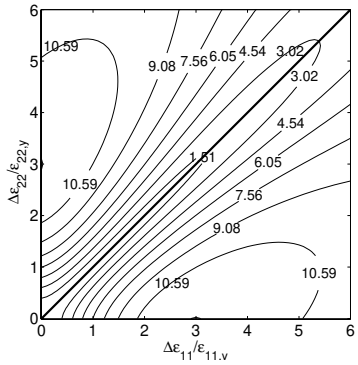

$E^{\sigma}_{iso,max} = 12.10\%$

MPTnl

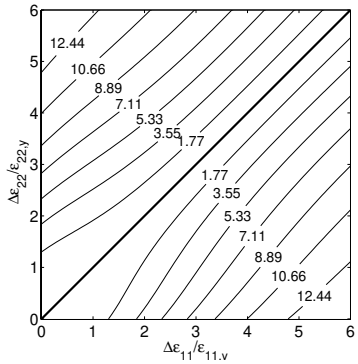

$E^{\sigma}_{iso,max} = 14.21\%$

ESC^{2}nl

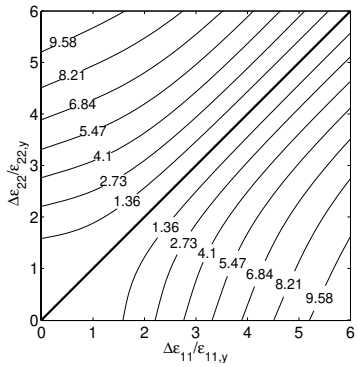

$E^{\sigma}_{iso,max} = 10.94\%$

Figure 6.29: Comparison between return map (**BEnl**), midpoint (**MPTnl**) and the new exponential-based scheme (**ESC^{2}nl**). Iso-error maps for yield surface State 1 - **C** with Material 5 and indication of the maximum stress error level.

Table 6.5: Initial boundary value problems. Extension of rectangular strip with circular hole. Stress and strain L^2 norm errors with Material 5 at $t = 0.5$ s,$t = 1.0$ s,$t = 1.5$ s,$t = 2.0$ s for BEnl, MPTnl and ESC^{2}nl schemes.

$\tilde{E}$	Δt	BEnl	MPTnl	ESC^{2}nl
			$t = 0.5$	
$\tilde{E}^{\boldsymbol{\sigma}}$	Δt_1	4.41×10^{-3}	2.27×10^{-4}	3.95×10^{-4}
	Δt_2	2.27×10^{-3}	6.11×10^{-5}	1.04×10^{-4}
	Δt_3	1.15×10^{-3}	1.61×10^{-5}	2.61×10^{-5}
$\tilde{E}^{\boldsymbol{\epsilon}}$	Δt_1	3.72×10^{-3}	5.83×10^{-4}	6.44×10^{-4}
	Δt_2	1.91×10^{-3}	1.52×10^{-4}	1.62×10^{-4}
	Δt_3	9.65×10^{-4}	3.94×10^{-5}	4.15×10^{-5}
			$t = 1.0$	
$\tilde{E}^{\boldsymbol{\sigma}}$	Δt_1	3.33×10^{-3}	6.87×10^{-5}	1.86×10^{-4}
	Δt_2	1.69×10^{-3}	1.84×10^{-5}	4.95×10^{-5}
	Δt_3	8.48×10^{-4}	4.92×10^{-6}	1.25×10^{-5}
$\tilde{E}^{\boldsymbol{\epsilon}}$	Δt_1	2.74×10^{-3}	1.97×10^{-4}	2.52×10^{-4}
	Δt_2	1.40×10^{-3}	5.17×10^{-5}	6.34×10^{-5}
	Δt_3	7.05×10^{-4}	1.32×10^{-5}	1.63×10^{-5}
			$t = 1.5$	
$\tilde{E}^{\boldsymbol{\sigma}}$	Δt_1	1.48×10^{-2}	1.62×10^{-3}	7.50×10^{-4}
	Δt_2	7.98×10^{-3}	4.42×10^{-4}	1.86×10^{-4}
	Δt_3	4.17×10^{-3}	1.10×10^{-4}	4.51×10^{-5}
$\tilde{E}^{\boldsymbol{\epsilon}}$	Δt_1	3.13×10^{-3}	2.21×10^{-4}	3.04×10^{-4}
	Δt_2	1.54×10^{-3}	6.06×10^{-5}	7.08×10^{-5}
	Δt_3	7.63×10^{-4}	1.40×10^{-5}	1.92×10^{-5}
			$t = 2.0$	
$\tilde{E}^{\boldsymbol{\sigma}}$	Δt_1	5.05×10^{-3}	2.22×10^{-4}	2.14×10^{-4}
	Δt_2	2.57×10^{-3}	5.71×10^{-5}	5.15×10^{-5}
	Δt_3	1.29×10^{-3}	1.48×10^{-5}	1.24×10^{-5}
$\tilde{E}^{\boldsymbol{\epsilon}}$	Δt_1	8.08×10^{-3}	4.94×10^{-4}	9.74×10^{-4}
	Δt_2	4.16×10^{-3}	1.13×10^{-4}	2.30×10^{-4}
	Δt_3	2.10×10^{-3}	3.19×10^{-5}	6.45×10^{-5}

Table 6.6: Initial boundary value problems. Extension of rectangular strip with elliptical hole. Stress and strain L^2 norm errors with Material 5 at $t = 0.5$ s,$t = 1.0$ s,$t = 1.5$ s,$t = 2.0$ s for BEnl, MPTnl and ESC^{2}nl schemes.

$\tilde{E}$	Δt	BEnl	MPTnl	ESC^{2}nl
			$t = 0.5$	
$\tilde{E}^{\boldsymbol{\sigma}}$	Δt_1	4.48×10^{-3}	2.11×10^{-4}	7.10×10^{-4}
	Δt_2	2.30×10^{-3}	5.47×10^{-5}	1.83×10^{-4}
	Δt_3	1.16×10^{-3}	1.47×10^{-5}	4.65×10^{-5}
$\tilde{E}^{\boldsymbol{\epsilon}}$	Δt_1	5.56×10^{-3}	3.11×10^{-4}	1.44×10^{-3}
	Δt_2	2.83×10^{-3}	8.00×10^{-5}	3.83×10^{-4}
	Δt_3	1.42×10^{-3}	2.24×10^{-5}	9.76×10^{-5}
			$t = 1.0$	
$\tilde{E}^{\boldsymbol{\sigma}}$	Δt_1	3.22×10^{-3}	6.73×10^{-5}	3.91×10^{-4}
	Δt_2	1.63×10^{-3}	1.68×10^{-5}	1.01×10^{-4}
	Δt_3	8.22×10^{-4}	4.70×10^{-6}	2.59×10^{-5}
$\tilde{E}^{\boldsymbol{\epsilon}}$	Δt_1	4.21×10^{-3}	1.27×10^{-4}	6.93×10^{-4}
	Δt_2	2.13×10^{-3}	3.19×10^{-5}	1.82×10^{-4}
	Δt_3	1.07×10^{-3}	8.81×10^{-6}	4.63×10^{-5}
			$t = 1.5$	
$\tilde{E}^{\boldsymbol{\sigma}}$	Δt_1	1.21×10^{-2}	1.22×10^{-3}	9.39×10^{-4}
	Δt_2	6.52×10^{-3}	3.26×10^{-4}	2.44×10^{-4}
	Δt_3	3.39×10^{-3}	8.74×10^{-5}	6.15×10^{-5}
$\tilde{E}^{\boldsymbol{\epsilon}}$	Δt_1	4.72×10^{-3}	2.00×10^{-4}	8.27×10^{-4}
	Δt_2	2.34×10^{-3}	5.20×10^{-5}	2.24×10^{-4}
	Δt_3	1.16×10^{-3}	1.46×10^{-5}	5.66×10^{-5}
			$t = 2.0$	
$\tilde{E}^{\boldsymbol{\sigma}}$	Δt_1	5.22×10^{-3}	2.17×10^{-4}	3.71×10^{-4}
	Δt_2	2.66×10^{-3}	5.65×10^{-5}	9.65×10^{-5}
	Δt_3	1.34×10^{-3}	1.50×10^{-5}	2.40×10^{-5}
$\tilde{E}^{\boldsymbol{\epsilon}}$	Δt_1	9.58×10^{-3}	5.04×10^{-4}	2.30×10^{-3}
	Δt_2	4.90×10^{-3}	1.31×10^{-4}	6.38×10^{-4}
	Δt_3	2.46×10^{-3}	3.88×10^{-5}	1.62×10^{-4}

Appendix A

Results from Functional Analysis

A.1 Generalities

In what follows it is assumed that reader is familiar to the notions and the properties of vector spaces. All vector spaces considered in the following will be defined over the field of real numbers.

Normed spaces and Banach spaces

Let V be a vector space. A *seminorm* on V is a map $|\cdot| \rightarrow \mathcal{R}^+$ that is subadditive and positively homogenous, i.e. it satisfies the properties

$$|u+v| \leq |u| + |v|, \quad |\alpha v| = |\alpha|\,|v| \quad \forall u, v \in V, \quad \forall \alpha \in \mathcal{R} \tag{A.1}$$

The above properties imply that $|0| = 0$ and $|v| \geq 0$ for all $v \in V$. A norm $\|\cdot\|$ on V is a special seminorm which is positive definite, i.e. it satisfies

$$\| v \| = 0 \text{ iff } v = 0 \tag{A.2}$$

If $\|\cdot\|$ is a norm on V, the pair $(V, \|\cdot\|)$ is called a *normed space*. Commonly, a normed space $(V, \|\cdot\|)$ is identified by the sole vector space V when there is no confusion about the norm defined on it. The norm function $\|\cdot\|$ can be interpreted as a generalization of the absolute value for the space of real numbers and thus is seen as a measure of the length of a vector $v \in V$ or equivalently of the distance between v and the null vector of V. Accordingly, the expression $\| u - v \|$ returns the distance between two points u and v of V.

Two distinct norms $\|\cdot\|_1$ and $\|\cdot\|_2$ defined over the same space V are said to be *equivalent* if there exist two strictly positive constants c_1 and c_2 such

that

$$c_1 \parallel v \parallel_1 \leq \parallel v \parallel_2 \leq c_2 \parallel v \parallel_1 \tag{A.3}$$

A well known property is that any two norms defined on a finite-dimensional vector space are equivalent. By contrast, this is not true in an infinite-dimensional space. The above notions are recalled since in the analysis of boundary value problems a common technique is that of establishing estimates using some norm equivalent to the conventional norm of the function space for the problem.

A sequence $\{v_n\}$ in a normed space V *converges* (strongly) to a vector $v \in V$ if and only if $\lim_{n\to\infty} \parallel v_n - v \parallel = 0$. This occurrence is indicated by $v_n \to v$ or by saying that v is the (strong) limit of the sequence $\{v_n\}$. Given two equivalent norms $\parallel \cdot \parallel_1$ and $\parallel \cdot \parallel_2$ defined over the space V, it can be shown that a sequence $\{v_n\} \subset V$ converges to a vector $v \in V$ in the norm $\parallel \cdot \parallel_1$ if and only if it converges to v in the norm $\parallel \cdot \parallel_2$.

A subset A of V is said to be *closed* in V if any converging sequence of elements of A has its limit in A. The *closure* $\bar{A}$ of A is the smallest closed set of V containing A; in other words, we may say that $\bar{A}$ is obtained by adding to A its "boundary points". The set A is *dense* in V if for every $v \in V$ there exists a sequence $\{v_n\}$ in A such that $v_n \to v$, or, equivalently, if $\bar{A} = V$. The set A is said to be *bounded* if there exists a positve constant M such that $\parallel v \parallel \leq M$ for every $v \in V$.

A *Cauchy sequence* in V is a sequence $\{v_n\}$ of elements of V such that for any $\varepsilon > 0$, there exists an integer $N(\varepsilon)$ such that, for all n and m larger than $N(\varepsilon)$, $\parallel v_n - v_m \parallel < \varepsilon$. This property simply means that the elements of the sequence are restricted to an arbitrarily small region of the space, provided that we consider elements of sufficiently high rank. Indeed, all convergent sequences are Cauchy sequences, while the converse is not true. A *Banach space* A is a normed vector space which is *complete*, i.e. in which all Cauchy sequences converge strongly to an element of the space. We have then the following proposition that relates the properties of completeness and closedness in normed spaces.

Proposition A.1.1 *A subset of a Banach space is complete if and only if it is closed.*

Linear operators and linear functionals

Let V and W be vector spaces. Let $L : V \to W$ be a map from V to W, also called an *operator*. The operator L is said to be linear if it is additive and

homogeneous, that is, if for all $u, v \in V$ and $\alpha \in \mathcal{R}$, it holds

$$\begin{aligned} L(u+v) &= L(u) + L(v) \\ L(\alpha v) &= \alpha L(v) \end{aligned}$$

Commonly the action of L on v is denoted with Lv instead of $L(v)$. If the space W coincides with $\mathcal{R}$, then L is called a *functional*.

The *range* $\mathcal{R}(L)$ and the *kernel* or *null space* $\mathcal{N}(L)$ of L are subspaces of W and V, defined respectively by

$$\mathcal{R}(L) = \{w \in W : w = L(v) \text{ for some } v \in V\}$$
$$\mathcal{N}(L) = \{v \in V : L(v) = 0\}$$

meaning that $\mathcal{R}(L)$ represents the set of images under the mapping L, while the null space $\mathcal{N}(L)$ is given by the elements in V which are mapped to the zero element of W.

If V and W are normed vector spaces and L is a map from V into W, then L is said to be *continuous* if to any converging sequence $v_n \to v$ in V there corresponds the converging sequence $L(v_n) \to L(v)$ in W. The map L is said to be *bounded* if for any $r > 0$, there exists a constant $R \geq 0$ such that

$$\| L(v) \| \leq R \quad \forall v \in V, \quad \text{s.t. } \| v \| \leq r$$

Any linear bounded operator L is characterized by the properties that

$$\| L(v) \| \leq M \| v \| \quad \forall v \in V \tag{A.4}$$

with M a nonnegative constant. It can be shown that a linear operator is continuous if and only if it is bounded.

Finally, the operator L will be said *Lipschitz continuous* if there exists a constant $c > 0$ such that

$$\| L(v_1) - L(v_2) \| \leq c \| v_1 - v_2 \| \quad \forall v_1, v_2 \in V$$

Lipschitz continuous operators are continuous, but the converse is not true in general. On the other hand, a linear operator is Lipschitz continuous if and only if it is continuous.

Bilinear forms

Given two vector spaces V and W, a map $b : V \times W \to \mathcal{R}$ is called a *bilinear form* if it is linear in each slot, that is, if it satisfies the following properties

$$b(\alpha v_1 + \beta v_2, w) = \alpha b(v_1, w) + \beta b(v_2, w)$$
$$b(v, \alpha w_1 + \beta w_2) = \alpha b(v, w_1) + \beta b(v, w_2)$$

for any $v_1, v_2, v \in V$, $w_1, w_2, w \in W$ and $\alpha, \beta \in \mathcal{R}$.

A bilinear form $b : V \times W \to \mathcal{R}$ is said to be *continuous* if there exists a positive constant M such that

$$b(v, w) \leq M \parallel v \parallel_V \parallel w \parallel_W \quad \forall v \in V, \ \forall w \in W$$

In the case where $W = V$, the bilinear form is *symmetric* if

$$b(v_1, v_2) = b(v_2, v_1) \quad \forall v_1, v_2 \in V$$

while it is *V-elliptic* if there exists a constant $\alpha > 0$ such that

$$b(v, v) \geq \alpha \parallel v \parallel^2 \quad \forall v \in V$$

Isomorphisms and completions

A linear continuous map $L : V \to W$ which is both *injective*, i.e. one-to-one and *surjective*, which means $\mathcal{R}(L) = W$, is called an *isomorphism*.

Given a normed space V, its *completion* is a Banach space $\hat{V}$, which holds the property that there exists an isomorphism from V onto a dense subspace of $\hat{V}$. A classical example in this sense is the completion of the continuous function space $C([0, 1])$ in the norm $\parallel v \parallel_0 = (\int_0^1 |v(x)|^2 dx)^{1/2}$ which coincides with the Lebesgue space $L^2(0, 1)$ [41].

The space $\mathcal{L}(V, W)$. Dual space

Let V and W be normed spaces. The space of all bounded linear operators from V to W is denoted by $\mathcal{L}(V, W)$. The conventional or natural norm defined over the space $\mathcal{L}(V, W)$ is

$$\parallel L \parallel_{\mathcal{L}(V,W)} = \sup_{v \in V \setminus \{0\}} \frac{\parallel Lv \parallel_W}{\parallel v \parallel_V} = \sup_{\|v\|_V \leq 1} \parallel Lv \parallel_W \tag{A.5}$$

which is always a well-defined quantity as can be deduced from (A.4). It can be shown that the space $\mathcal{L}(V, W)$ endowed with the norm (A.5) is a Banach space if W is a Banach space.

The space $\mathcal{L}(V, \mathcal{R})$ of bounded linear functionals on V is defined as the *dual space* of V and is denoted by V'. It follows that, since $\mathcal{R}$ is complete, V' is a Banach space with the norm

$$\parallel L \parallel_{V'} = \sup_{\|v\|_V \leq 1} |Lv| \tag{A.6}$$

In the following, the symbol ℓ will be frequently used to indicate a bounded linear functional on a normed space V, while the image $\ell(v)$ of a vector $v \in V$ through ℓ, will be denoted by ${}_{V'}\langle \ell, v \rangle_V$ rather than $l(v)$. The map $\langle \cdot, \cdot \rangle : V' \times V \to \mathcal{R}$ is known as the *duality pairing* between V and V'. Some examples of duality will be addressed in Section A.2.1 in the context of the function space $L^p(\Omega)$. In the following, when there is no amboguity, we simply indicate with $\langle \cdot, \cdot \rangle$ the duality pairing between V' and V.

Monotone and strongly monotone operators

An operator $T : V \to V'$ is said to be *monotone* if

$$\langle T(u) - T(v), u - v \rangle \geq 0 \quad \forall u, v \in V$$

and it is said to be *strongly monotone* if there exists a constant $c > 0$ such that

$$\langle T(u) - T(v), u - v \rangle \geq c \parallel u - v \parallel^2 \quad \forall u, v \in V$$

Biduals and reflexivity

The dual V' of a normed space V is a Banach space and V' itself has a dual $V'' \equiv (V')'$, called the *bidual* of V. Of course, the bidual is a Banach space and it is possible to show that there exists a bounded linear operator J from V onto V'' that is one-to-one and also an *isometry*, i.e. $\parallel Jv \parallel = \parallel v \parallel, \forall v \in V$. It follows that V can be identified with a subspace $J(V)$ of V''. The normed space V is said to be *reflexive* if the following identity holds

$$J(V) = V'' \tag{A.7}$$

To indicate the above relationship we briefly write $V'' = V$. Indeed, a reflexive normed space is a Banach space. A classical example of a reflexive Banach space is provided by the space $L^p(\Omega)$ (see Section A.2.1) for $p \in (1, \infty)$ in which $\Omega \subset \mathcal{R}^d$ is an open set.

Weak convergence

Let V be a normed space and V' its dual. A sequence $\{v_n\} \subset V$ is said to *converge weakly* in V to v if

$$\lim_{n \to \infty} \langle \ell, v_n \rangle = \langle \ell, v \rangle \ \ \forall \ell \in V' \tag{A.8}$$

The above notion is indicated by the following notation

$$v_n \rightharpoonup v$$

It is noted that strong convergence implies weak convergence, while the converse is not true, with the only exception of finite-dimensional spaces for which the two kinds of convergence coincide.

Compactness and weak compactness

A subset V_1 of a normed space V is said to be (sequentially) *compact* if every bounded sequence in V_1 has a subsequence that converges in V_1. Likewise, V_1 is *weakly compact* if every bounded sequence in V_1 has a subsequence that converges weakly in V_1.

A linear operator $L : V \to W$ is said to be *compact* if the image under L of a bounded sequence in V contains a subsequence converging in W, that is, if $\{v_n\} \subset V$ is bounded, then there exists a subsequence $\{v_{n_j}\}$ and an element $w \in W$ such that $Lv_{n_j} \to w$ in W. If in the above definition strong convergence is replaced by weak convergence and $Lv_{n_j} \rightharpoonup w$ in W, then L is said to be *weakly compact*. Clearly, L is compact if and only if it maps bounded sets to compact sets. We have now the following important result

Theorem A.1.2 (Eberlein-Smulyan). *A reflexive Banach space V is weakly compact, that is, if $\{v_n\}$ is a bounded sequence of V, then it results possible to extract a subsequence of $\{v_n\}$ that converges weakly in V. If, furthermore, the limit v is independent of the subsequence extracted, then the whole sequence $\{v_n\}$ converges weakly to v.*

Embeddings

Let V and W be normed spaces with $V \subset W$. If there is a constant $c > 0$ such that

$$\| v \|_W \leq c \| v \|_V \quad \forall v \in V \tag{A.9}$$

we say that V is *continuously embedded* in W and write

$$V \hookrightarrow W$$

The property (A.9) can be interpreted in various ways, for instance it allows to state that the identity operator $I : V \to W$ is bounded or, equivalently, continuous. Moreover the continuous embedding of V into W implies that if $v_n \to v$ in V, then also $v_n \to v$ in W.

A subspace V is said to be *compactly embedded* in W if

$$v_n \rightharpoonup v \text{ in } V \text{ implies } v_n \to v \text{ in } W$$

This property is expressed in the form

$$V \hookrightarrow\hookrightarrow W$$

and is equivalent to the statement that the identity operator from V into W is compact [41].

The above embedding results will be useful in the next section when Sobolev spaces with different indices are compared.

Dual operators

Consider a couple of normed spaces V and W and their respective dual spaces V' and W'. Let A be a linear operator with domain $\mathcal{D}(A) \subset V$ and range in W. Given a vector $w' \in W'$, it can be shown that there exists a vector $v' \in V'$ such that

$$_{W'}\langle w', Av\rangle_W =_{V'} \langle v', v\rangle_V \quad \forall v \in \mathcal{D}(A) \tag{A.10}$$

if and only if $\mathcal{D}(A)$ is dense in V. If this is the case, then v' is uniquely determined by w'. When $\mathcal{D}(A)$ coincides with V, then the above reasoning defines a linear operator A' from W' to V' such that $A'w' = v'$. The operator A' is called the *dual* operator of A and is such that the following statement holds

$$_{W'}\langle w', Av\rangle_W =_{V'} \langle A'w', v\rangle_V \quad \forall v \in V, \ \forall w' \in W'$$

If $\mathcal{D}(A) = V$ and A is bounded, then A' is also bounded and

$$\| A' \| = \| A \|$$

We have now the following important theorem which illustrates further relationships existing between dual operators.

Theorem A.1.3 (Closed Range Theorem). *Let V and W be two Banach spaces and let A be a bounded linear operator from V to W with dual operator A'. Then the following statements are equivalent:*

- $\mathcal{R}(A)$ *is closed in* W
- $\mathcal{R}(A')$ *is closed in* V'

- $\mathcal{R}(A) = [\mathrm{Ker}A']^\circ \equiv \{w \in W : \ \langle \ell, w\rangle = 0 \quad \forall \ell \in \mathrm{Ker}A'\}$
- $\mathcal{R}(A') = [\mathrm{Ker}A]^\circ \equiv \{\ell \in V' : \ \langle \ell, v\rangle = 0 \quad \forall v \in \mathrm{Ker}A\}$

The next result follows directly from the closed range theorem

Corollary A.1.4 *The following results hold:*

- $\mathcal{R}(A) = W$ iff there exists a constant c such that $\| A'\ell \|_{V'} \geq c_1 \| \ell \|_{W'}$ $\forall \ell \in W'$
- $\mathcal{R}(A') = V'$ iff there exists a constant c such that $\| Av \|_W \geq c_2 \| v \|_V$ $\forall v \in V$

The Babuška-Brezzi condition for bilinear forms

Let $b : V \times W \to \mathcal{R}$ be a continuous bilinear form, that is there exists a constant $\alpha_b > 0$ such that

$$|b(v, w)| \leq \alpha_b \| v \|_V \| w \|_W \quad \forall v \in V, \ \forall w \in W \tag{A.11}$$

The bilinear form $b(\cdot, \cdot)$ is said to satisfy the Babuška-Brezzi condition if there exists a constant $\beta_b > 0$ such that

$$\sup_{w \in W \setminus \{0\}} \frac{|b(v, w)|}{\| w \|_W} \geq \beta_b \| v \|_V \quad \forall v \in V \tag{A.12}$$

The following theorem establishes the relationship between the Babuška-Brezzi condition and the closed range theorem [18, 22].

Theorem A.1.5 *Let $b : V \times W \to \mathcal{R}$ be a continuous bilinear form which defines bounded linear operators $B : V \to W'$ and $B' : W \to V'$, according to*

$$b(v, w) =_{W'} \langle Bv, w\rangle_W =_{V'} \langle B'w, v\rangle_V \quad \forall v \in V, \ w \in W$$

With the above hypotheses, the following statements are equivalent

- *The bilinear form $b(\cdot, \cdot)$ satisfies the Babuška-Brezzi condition (A.12)*
- *The operator B is an isomorphism from $(\mathrm{Ker}B)^\circ$ onto W', where*
$$\mathrm{Ker}B = \{v \in V : \ b(v, w) = 0 \quad \forall w \in W\}$$
- *The operator B' is an isomorphism from W onto $(\mathrm{Ker}B)^\circ$, where*
$$(KerB)^\circ = \{\ell \in V' : \ \langle \ell, v\rangle = 0 \quad \forall v \in \mathrm{Ker}B\}$$

The Babuška-Brezzi condition is the crucial key-point in the analysis of mixed or saddle-point variational problems like those related to the formulation of the elastoplastic boundary value problem addressed in Chapter 3.

Inner products and Hilbert spaces

An inner product is a generalization of the ordinary vector scalar product in $\mathcal{R}^d$ to an arbitrary vector space. Let V be a vector space. An *inner product* on V is a symmetric positive-definite bilinear form $(\cdot,\cdot) : V \times V \to \mathcal{R}$, namely such that

$$\begin{aligned}
(u,v) &= (v,u) \quad \forall u,v \in V \\
(\alpha u_1 + \beta u_2, v) &= \alpha(u_1,v) + \beta(u_2,v) \quad \forall u_1,u_2,v \in V,\ \forall \alpha,\beta \in \mathcal{R} \\
(v,v) &\geq 0 \quad \forall v \in V, \text{ and } (v,v) = 0 \Leftrightarrow v = 0
\end{aligned}$$

An *inner product space* is a vector space endowed with an inner product. When the definition of the inner product $(\cdot,\cdot)$ is clear, we will briefly denote the inner product space with V.

From the definition above it follows immediately that any inner product space is a normed space with the norm

$$\| v \| = (v,v)^{1/2}$$

A complete inner product space is called a *Hilbert space*. It is evident that any Hilbert space is a Banach space with the norm induced by its inner product.

Consider now the following classical results on inner product and Hilbert spaces.

Theorem A.1.6 (Cauchy-Schwartz Inequality). *Given an inner product space V, it holds*

$$|(u,v)| \leq \| u \| \| v \| \quad \forall u,v \in V$$

Theorem A.1.7 (Riesz Representation Theorem). *Any Hilbert space V can be identified with its dual V' by means of an isometric isomorphism. More precisely, for any $\ell \in V'$ there exists a unique $u \in V$ such that*

$$\begin{aligned}
\langle \ell, v \rangle &= (u,v) \quad \forall v \in V \\
\| \ell \|_{V'} &= \| u \|_V
\end{aligned}$$

On the other hand, for any $u \in V$, the mapping $v \mapsto (u,v)$ determines an element $\ell \in V'$ such that $\| \ell \|_{V'} = \| u \|_V$

From the last theorem it follows immediately that a Hilbert space can be identified with its bidual as well. Therefore, we have the following

Corollary A.1.8 *Every Hilbert space is reflexive.*

Now combining the statements of Theorem A.1.7 and Corollary A.1.8 it is found that in a Hilbert space every bounded sequence has a weakly convergent subsequence. We have thus the property that on an inner product space V

$$v_n \rightharpoonup v \Rightarrow \| v \| \leq \lim_{n\to\infty} \inf \| v_n \|$$

which can be equivalently stated by saying that the norm function $\| \cdot \|$ of an inner product space is weakly l.s.c. The last proposition can be proved simply by checking that for a fixed $w \in V$, the mapping $v \mapsto (w, v)$ defines a bounded and continuous functional on V and thus

$$\| v \|^2 = (v, v) = \lim_{n\to\infty} (v, v_n) \leq \| v \| \lim_{n\to\infty} \inf \| v_n \|$$

The last property will be frequently used in Section 3.3.

We now present a well-known fundamental result which comes into play in proving the unique solvability of elliptic variational problems

Theorem A.1.9 (Lax-Milgram Lemma). *Let V be a Hilbert space. Given a continuous and V-elliptic bilinear form $b : V \times V \to \mathcal{R}$ and a bounded linear function $\ell : V \to \mathcal{R}$, the following (variational) problem*

$$\begin{gathered} \text{Find } \mathrm{u} \in \mathrm{V} \text{ such that} \\ b(u, v) = \langle \ell, v \rangle \quad \forall v \in V \end{gathered}$$

has a unique solution. Furthermore, there exists a positive constant c independent of ℓ such that

$$\| u \|_V \leq c \| \ell \|_{V'}$$

We now introduce a result from the theory of monotone operators which will be useful in Section 3.2 for proving the well-posedness of a particular initial boundary value problem of elastoplastic equilibrium.

Theorem A.1.10 *Assume that V is a Hilbert space and that $T : V \to V'$ is a strongly monotone and Lipschitz continuous operator. Then for any $\ell \in V'$, the equation $T(u) = \ell$ has a unique solution $u \in V$.*

Theorem A.1.11 (Projection Theorem). *Let K be a nonempty closed convex subset of a Hilbert space V and let $u \in V$. Then there exists a unique element $u_0 \in K$ such that*

$$\| u - u_0 \| = \min_{v \in K} \| u - v \|$$

The element u_0 is referred to as the projection $P(u)$ of u on K and is characterized by the following property

$$(u - u_0, v - u_0) \leq 0 \quad \forall v \in K$$

From the last characterization of the projection operator it is immediate to verify that the projection operator is nonexpansive, i.e. it satisfies

$$\| P(u) - P(v) \| \leq \| u - v \| \quad \forall u, v \in V$$

and monotone, that is

$$(P(u) - P(v), u - v) \geq 0 \quad \forall u, v \in V$$

Corollary A.1.12 *If K is a closed subspace of a Hilbert space V, then for any $u \in V$ there exists a unique element $u_0 \in K$ such that*

$$(u - u_0, v) = 0 \quad \forall u \in K$$

The map $u \mapsto Pu = u_0$ is linear and defines an orthogonal projection onto K

A.2 Function spaces

A.2.1 The spaces $C^m(\Omega)$, $C^m(\bar{\Omega})$ and $L^p(\Omega)$

In the following we will be referring as usual at spaces defined over a bounded domain $\Omega \subset \mathcal{R}^3$. Before entering the discussion on function spaces and related properties, we find it useful here to give some introductory notions on multi-index notation.

Multi-index notation

Let $\mathbb{Z}_+^d$ be the set of all ordered d-tuples of nonnegative integers. A member of $\mathbb{Z}_+^d$ will be referred to with a greek letter α or β, with

$$\alpha = (\alpha_1, \alpha_2, ..., \alpha_d)$$

where each component α_i denotes a nonnegative integer.

The sum of all elements in α will be written as $|\alpha| = \alpha_1 + \alpha_2 + \cdots + \alpha_d$ and will be called the length of the *multi-index* α. We indicate with $D^\alpha v$ the partial derivative of a vector v

$$D^\alpha v = \frac{\partial^{|\alpha|} v}{\partial x_1^{\alpha_1}, \partial x_2^{\alpha_2}, \cdots, \partial x_d^{\alpha_d}}$$

In this manner, if $|\alpha| = m$, then $D^\alpha v$ indicates one of the mth-order partial derivatives of v For instance, set $\alpha = (1, 0, 3) \in \mathbb{Z}_+^3$, with $|\alpha| = 4$. In this case we have

$$D^\alpha v = \frac{\partial^4 v}{\partial x_1^{\alpha_1} \partial x_2^{\alpha_2} \partial x_3^{\alpha_3}} = \frac{\partial^4 v}{\partial x_1^1, \partial x_2^0 \partial x_3^3} = \frac{\partial^4 v}{\partial x_1 \partial x_3^3}$$

The space of continuous and continuously differentiable functions

The space of all real-valued continuous functions defined over Ω is indicated by $C(\Omega)$. Being Ω an open set, a function of $C(\Omega)$ is not necessarily bounded; therefore we denote the space of *bounded and uniformly continuous* functions on Ω by $C(\bar{\Omega})$. Such notation follows from the property of bounded and uniformly continuous functions on Ω which have a unique continuous extension to $\bar{\Omega}$. It can be shown that the space $C(\bar{\Omega})$ is a Banach space when equipped with the norm

$$\| v \|_{C(\bar{\Omega})} = \sup\{|v(\mathbf{x})| : \mathbf{x} \in \Omega\} \equiv \max\{|v(\mathbf{x})| : \mathbf{x} \in \bar{\Omega}\}$$

The space $C^m(\Omega)$, with m a nonnegaive integer, is defined as the set of all real-valued functions on Ω which are continuous together with their derivatives of order less than or equal to m. Thus

$$C^m(\Omega) = \{v \in C(\Omega) : D^{\boldsymbol{\alpha}} v \in C(\Omega) \ \forall \alpha \in \mathbb{Z}_+^d \text{ with } |\alpha| \leq \mathrm{m}\}$$

and, as done before,

$$C^m(\bar{\Omega}) = \{v \in C(\bar{\Omega}) : D^{\boldsymbol{\alpha}} v \in C(\bar{\Omega}) \ \forall \alpha \in \mathbb{Z}_+^d \text{ with } |\alpha| \leq \mathrm{m}\}$$

In the sequel, for brevity, the spaces $C^0(\Omega)$ and $C^0(\bar{\Omega})$ will be indicated with $C(\Omega)$ and $C(\bar{\Omega})$, respectively.

The space $C^m(\bar{\Omega})$ can be endowed with the following seminorm

$$|v|_{C^m(\bar{\Omega})} = \sum_{|\alpha|=m} \| D^\alpha v \|_{C(\bar{\Omega})}$$

and it becomes a Banach space when equipped with the following norm

$$\| v \|_{C^m(\bar{\Omega})} = \sum_{j=0}^{m} |v|_{C^j(\bar{\Omega})} = \sum_{|\alpha| \leq m} \| D^\alpha v \|_{C(\bar{\Omega})}$$

According to the previous definitions the spaces of infinitely differentiable real-valued continuous functions on Ω and of infinitely differentiable bounded uniformly continuous functions over $\bar{\Omega}$ are respectively defined as

$$C^\infty(\Omega) = \{v \in C(\Omega) : v \in C^m(\Omega) \ \forall m \in \mathbb{Z}_+\}$$

and

$$C^{\infty}(\bar{\Omega}) = \{v \in C(\bar{\Omega}) : \ v \in C^{m}(\bar{\Omega}) \ \forall m \in \mathbb{Z}_{+}\}$$

Hölder spaces

A function $v : \Omega \to \mathcal{R}$ is said to be Lipschitz continuous if there exists a constant c such that

$$|v(\mathbf{x}) - v(\mathbf{y})| \leq c|\mathbf{x} - \mathbf{y}| \quad \forall \mathbf{x}, \mathbf{y} \in \Omega$$

while it is said to be Hölder continuous with exponent $\beta \in (0, 1]$ if there exists a constant $c > 0$ such that

$$|v(\mathbf{x}) - v(\mathbf{y})| \leq c|\mathbf{x} - \mathbf{y}|^{\beta} \quad \forall \mathbf{x}, \mathbf{y} \in \Omega$$

The space of Hölder continuous function of $C(\bar{\Omega})$ with exponent β is indicated with $C^{0,\beta}(\bar{\Omega})$ and, if endowed with the norm

$$\| v \|_{C^{0,\beta}(\bar{\Omega})} = \| v \|_{C(\bar{\Omega})} + \sup \left\{ \frac{|v(\mathbf{x}) - v(\mathbf{y})|}{|\mathbf{x} - \mathbf{y}|^{\beta}} : \ \mathbf{x}, \mathbf{y} \in \Omega, \ \mathbf{x} \neq \mathbf{y} \right\}$$

this space is shown to be a Banach space. Finally, given a nonnegative integer m and a real $\beta \in (0, 1]$, we have the following Hölder space

$$C^{m,\beta}(\bar{\Omega}) = \{v \in C^{m}(\bar{\Omega}) : \ D^{\alpha} v \in C^{0,\beta}(\bar{\Omega}) \ \forall \alpha \in \mathbb{Z}_{+}^{d} \ \text{with} \ |\alpha| = \mathrm{m}\}$$

which becomes a Banach space if it is endowed with the norm

$$\| v \|_{C^{m,\beta}(\bar{\Omega})} = \| v \|_{C^{m}(\bar{\Omega})} + \sum_{|\alpha| = m} \sup \left\{ \frac{|D^{\alpha} v(\mathbf{x}) - D^{\alpha} v(\mathbf{y})|}{|\mathbf{x} - \mathbf{y}|^{\beta}} : \ \mathbf{x}, \mathbf{y} \in \Omega, \ \mathbf{x} \neq \mathbf{y} \right\}$$

The spaces $L^{p}(\Omega)$

For any number $p \in [1, \infty)$, we denote by $L^{p}(\Omega)$ the space of (equivalence classes of) measurable functions v for which

$$\int_{\Omega} |v(\mathbf{x})|^{p} dx < \infty$$

where integration is understood to be in the sense of Lebesgue. The space $L^{p}(\Omega)$ is a Banach space when it is endowed with the norm

$$\| v \|_{0,p,\Omega} = \left(\int_{\Omega} |v(\mathbf{x})|^{p} dx \right)^{1/p} \tag{A.13}$$

The reason for including the zero in the subscript of the notation $\| \cdot \|_{0,p,\Omega}$ will be clarified soon when the Sobolev spaces are introduced. Instead, when there is no confusion, the domain symbol Ω will be omitted by the subscript of the natural norm on $L^p(\Omega)$ and since in many applications we will be dealing especially with the space $L^2(\Omega)$, for such a case the norm (A.13) will simply be expressed by $\| \cdot \|_0$ rather than by $\| \cdot \|_{0,2}$.

The function $\| \cdot \|_{0,p}$ is a norm only when it is understood that the argument represents an equivalence class of functions, that is two function belong to the same class if they are equal almost everywhere (a.e. in the sequel), which means they are equal everywhere except on a subset of Ω of Lebesgue measure zero.

The definition of the spaces $L^p(\Omega)$ can be generalized to account for the case $p = \infty$ with the aid of the following notion. The essential supremum (denoted by ess sup) of any measurable function v is defined as

$$\operatorname*{ess\,sup}_{x\in\Omega} v(x) = \inf\{M \in (-\infty, \infty] : \ v(x) \leq M \ \text{ a.e. in } \Omega\}$$

The function v is said to be *essentially bounded above* if $\operatorname{ess\,sup}_\Omega v < \infty$. Similarly, we may define the essential infimum of a function and provide the pertinent notion of essentially boundedness below. Joining the two statements, if v is both essentially bounded above and below then v is said to be *essentially bounded*.

With the above positions it is natural to define the space

$$L^\infty(\Omega) = \{v : \Omega \to \mathcal{R} : \ v \text{ is essentially bounded on } \Omega\}$$

which can be shown to be a Banach space when equipped with the following norm

$$\| v \|_{0,\infty,\Omega} = \operatorname*{ess\,sup}_{x\in\Omega} |v(x)|$$

We note that all continuous functions on a bounded closed set are bounded, thus

$$C(\bar{\Omega}) \hookrightarrow L^\infty(\Omega)$$

Furthermore, the space $L^2(\Omega)$ is an inner product space (then a Hilbert space) if endowed with the inner product

$$(u, v)_{0,\Omega} = \int_\Omega u(\mathbf{x})v(\mathbf{x})dx$$

which in fact defines the norm $\| \cdot \|_{0,2,\Omega}$.

Consider now a function v defined over Ω. The function $v \in L^p_{\text{loc}}(\Omega)$ (the space of functions whose p^{th}-order powers are locally integrable functions) if for any proper subset $\Omega' \subset\subset \Omega$, $v \in L^p(\Omega')$.

From the above definitions, two important results are drawn.

Theorem A.2.1

- (The Minkowski Inequality) If $u, v \in L^p(\Omega)$, $1 \leq p \leq \infty$, then $u + v \in L^p(\Omega)$ and

$$\| u + v \|_{0,p} \leq \| u \|_{0,p} + \| v \|_{0,p}$$

- (The Hölder Inequality) If p, q and r are reals satusfying $p, q, r \geq 1$ and $p^{-1} + q^{-1} = r^{-1}$. Suppose that $u \in L^p(\Omega)$ and $v \in L^q(\Omega)$. Then $uv \in L^r(\Omega)$ and

$$\| uv \|_{0,r} \leq \| u \|_{0,p} \| v \|_{0,q}$$

  When $p = q = 2$, the Hölder inequality reduces to the Cauchy-Schwartz inequality

$$\| uv \|_{0,2} \leq \| u \|_{0,2} \| v \|_{0,2} \quad \forall u, v \in L^2(\Omega)$$

Dual spaces and reflexivity

We define the dual exponent q of $p \in [1, \infty)$ by $1/p + 1/q = 1$ (taking $q = \infty$ when $p = 1$). The topological dual of $L^p(\Omega)$, indicated with $(L^p(\Omega))'$ is defined to be $L^q(\Omega)$. It follows immediately from the last definition that $L^2(\Omega)$ can be identified with its dual space. For $1 < p < \infty$, we also have

$$L^p(\Omega) = (L^q(\Omega))' = (L^p(\Omega))''$$

which implies that the spaces $L^p(\Omega)$ are reflexive for $1 < p < \infty$.

The spaces $L^1(\Omega)$ and $L^\infty(\Omega)$ are not reflexive, but it is still possible to identify the latter with the dual of the former in view of the following expression

$$L^\infty(\Omega) = (L^1(\Omega))'$$

Conversely, $L^1(\Omega)$ can be identified only with a proper subspace of $(L^\infty(\Omega))'$.

A.2.2 Sobolev spaces

Lipschitz domains

Given a point $\mathbf{x} = (x_1, x_2, ..., x_d) \in \mathcal{R}^d$, consider

$$y = x_d \quad \text{and} \quad \hat{\mathbf{x}} = (x_1, x_2, ..., x_{d-1}) \in \mathcal{R}^{d-1}$$

An open set $\Omega \subset \mathcal{R}^d$ is said to have *Lipschitz-continuous boundary* Γ if there exist two constant $\alpha > 0$ and $\beta > 0$, a finite number of *local* coordinate systems $(\hat{\mathbf{x}}^m, y^m)$ and local maps $f^m, m = 1, ..., M$, that are Lipschitz-continuous on their respective domains of definition $\{\hat{\mathbf{x}}^m : \ |\hat{\mathbf{x}}^m| \leq \alpha\}$ such that

$$\Gamma = \cup_{m=1}^{M} \{(\hat{\mathbf{x}}^m, y^m) : \ y^m = f^m(\hat{\mathbf{x}}^m), \ |\hat{\mathbf{x}}^m| \leq \alpha\}$$

and for $m = 1, ..., M$

$$\begin{aligned} \{(\hat{\mathbf{x}}^m, y^m) \ &: \ f^m(\hat{\mathbf{x}}^m) < y^m < f^m(\hat{\mathbf{x}}^m) + \beta, |\hat{\mathbf{x}}^m| \leq \alpha\} \subset \Omega \\ \{(\hat{\mathbf{x}}^m, y^m) \ &: \ f^m(\hat{\mathbf{x}}^m) - \beta < y^m < f^m(\hat{\mathbf{x}}^m), |\hat{\mathbf{x}}^m| \leq \alpha\} \subset \mathcal{R}^d \backslash \bar{\Omega} \end{aligned}$$

More in general, we say that the boundary is of class X if the functions f^m are of class X and that it is *smooth* if $X = C^\infty$.

In what follows, with a slight simplification of terminology, we will always assume that Ω is "a Lipschitz domain" meaning by that that its boundary is in fact Lipschitz-continuous.

Distributions

The notion of differentiability can be extended also to non-differentiable functions by means of the definition and of the properties of distributions.

We define $C_0^\infty(\Omega)$ the space of *smooth functions with compact support*, which is the set of all the functions in $C^\infty(\Omega)$ vanishing outside a compact subset of Ω. In particular, we may say that any $\phi \in C_0^\infty(\Omega)$ vanishes in a neighborhood of the boundary Γ of Ω.

The space of functions with compact support is not characterized by a "standard" norm topology; nevertheless we can define convergence in the following manner. A sequence $\{\phi_k\} \in C_0^\infty(\Omega)$ is said to converge to ϕ in $C_0^\infty(\Omega)$ if

- there exists a compact set K in Ω such that ϕ_k vanishes outside K for any k

and

- for each multi-index α, $D^\alpha \phi_k \to D^\alpha \phi$ uniformly in Ω

The space $C_0^\infty(\Omega)$ equipped with the last notion of convergence is called the *space of test functions* and is denoted by $\mathcal{D}(\Omega)$.

A *distribution* on Ω is a continuous linear functional on $\mathcal{D}(\Omega)$, that is a linear functional ℓ on $\mathcal{D}(\Omega)$ satisfying the condition

$$\phi_k \to \phi \text{ in } \mathcal{D}(\Omega) \text{ implies } \langle \ell, \phi_k \rangle \to \langle \ell, \phi \rangle$$

Clearly, the space of distribution on Ω is indicated by $\mathcal{D}'(\Omega)$.

Any *locally integrable* $u \in L^1_{\text{loc}}(\Omega)$ may be identified with a distribution, in the sense that there exists a unique distribution ℓ_u for which

$$\langle \ell_u, \phi \rangle = \int_\Omega u\phi \, dx \quad \forall \phi \in \mathcal{D}(\Omega)$$

In this case we indicate with u both the function itself and the associated distribution.

With an appropriate extension of the classical Green's formula it is possible to define derivatives of any order for distributions. Indeed, given $u \in \mathcal{D}'(\Omega)$ and a multi-index α with $|\alpha| = m$, the (distributional) derivative $D^\alpha u$ of u is a distribution defined by

$$\langle D^\alpha \, u, \phi \rangle = (-1)^m \langle u, D^\alpha \, \phi \rangle \quad \forall \phi \in \mathcal{D}(\Omega)$$

When u is an $m-$times continuously differentiable function, the distributional derivative $D^\alpha u$ coincides with the classical m^{th}-order derivative.

The Sobolev spaces $W^{m,p}(\Omega)$

For any nonnegative integer m and real number $p \geq 1$ or $p = \infty$, we define the *Sobolev space* as [2]

$$W^{m,p}(\Omega) = \{v \in L^p(\Omega) : \; D^\alpha v \in L^p(\Omega) \; \forall \alpha \in \mathbb{Z}_+^d \text{ with } |\alpha| \leq m\}$$

with the derivatives intended in the distributional sense. The spaces $W^{m,p}(\Omega)$, if equipped with the norms

$$\| \, v \, \|_{m,p,\Omega} = \left(\sum_{|\alpha| \leq m} \| \, D^\alpha v \, \|_{0,p,\Omega}^p \right)^{1/p} \qquad 1 \leq p < \infty \tag{A.14}$$

and

$$\| \, v \, \|_{m,\infty,\Omega} = \sup_{|\alpha| \leq m} \| \, D^\alpha v \, \|_{0,\infty,\Omega} \qquad p = \infty \tag{A.15}$$

become a Banach spaces. The seminorms which are defined on the Sobolev spaces $W^{m,p}(\Omega)$ are respectively

$$|v|_{m,p,\Omega} = \left(\sum_{|\alpha|=m} \| D^\alpha v \|_{0,p,\Omega}^p \right)^{1/p} \qquad 1 \leq p < \infty$$

and

$$|v|_{m,\infty,\Omega} = \sup_{|\alpha|=m} \| D^\alpha v \|_{0,\infty,\Omega} \qquad p = \infty$$

Furthermore, it can be shown that the space $W^{m,p}(\Omega)$ is reflexive if and only if $1 < p < \infty$ and it is noted that $W^{0,p}(\Omega) = L^p(\Omega)$.

When $p = 2$, $W^{m,2}(\Omega)$ may be endowed with an inner product. Setting $W^{m,2}(\Omega) \equiv H^m(\Omega)$ the following results an inner product on this space

$$(u, v)_{m,\Omega} = \sum_{|\alpha| \leq m} (D^\alpha u, D^\alpha v)_{0,\Omega}$$

where, as usual, $(\cdot, \cdot)_{0,\Omega}$ stands for the $L^2(\Omega)$ inner product. With this inner product, $H^m(\Omega)$ is a Hilbert space. The corresponding norm will be denoted by $\| \cdot \|_{m,2,\Omega}$ or briefly by $\| \cdot \|_{m,\Omega}$ or even by $\| \cdot \|_m$ when there is no danger of confusion.

By the definition of norm over the Sobolev spaces (A.14) and (A.15) it follows that convergence in $W^{m,p}(\Omega)$ of a sequence $\{v_l\}_{l=1}^\infty$ to a function v is expressed by the following condition

$$D^\alpha v_l \to D^\alpha v \quad \text{in} \quad L^p(\Omega) \ \forall \alpha \in \mathbb{Z}_+^d \ \text{with} \ |\alpha| \leq m$$

with a similar result for weak convergence in $W^{m,p}(\Omega)$.

The following theorem provides a number of properties regarding embeddings and inclusions about Sobolev spaces of different order

Theorem A.2.2 *The following statements ar valid*

- $W^{m,p}(\Omega) \hookrightarrow\hookrightarrow W^{k,p}(\Omega)$ *if* $m > k$
- $\mathcal{D}(\Omega) \subset W^{m,p}(\Omega)$
- $C^m(\bar{\Omega}) \hookrightarrow W^{m,p}(\Omega)$
- $C^\infty(\bar{\Omega}) \cap W^{m,p}(\Omega)$ *is dense in* $W^{m,p}(\Omega)$*; in other words, a function in* $W^{m,p}(\Omega)$ *can be approximated by a sequence of functions smooth up to the boundary*
- (Sobolev compact embedding) If $k < m - d/p$ with $1 \leq p \leq \infty$, then $W^{m,p}(\Omega) \hookrightarrow\hookrightarrow C^k(\bar{\Omega})$; in particular, $W^{m,p}(\Omega) \hookrightarrow\hookrightarrow C^k(\bar{\Omega})$

The space $W^{s,p}(\Gamma)$ for noninteger s

Consider a bounded domain $\Omega \subset \mathcal{R}^d$ $(d \geq 2)$ with Lipschitz boundary Γ. Suppose that $1 \leq p < \infty$ and $\sigma \in (0,1)$. For a function $v \in L^p(\Gamma)$, set

$$F_\sigma(v) = \int_{\Gamma\times\Gamma} \frac{|v(\mathbf{x}) - v(\mathbf{y})|^p}{|\mathbf{x}-\mathbf{y}|^{d-1+\sigma p}}\, ds(\mathbf{x})\, ds(\mathbf{y})$$

and

$$\| v \|_{\sigma,p,\Gamma} = \left(\int_\Gamma |v)|^p ds + F_\sigma(v) \right)^{1/p}$$

Then $W^{\sigma,p}(\Gamma)$ is defined to be the space of functions $v \in L^p(\Gamma)$ for which $\| v \|_{\sigma,p,\Gamma} < \infty$. This is a Banach space with the norm $\| v \|_{\sigma,p,\Gamma}$ and it is reflexive for $1 < p < \infty$.

More generally, for $s = m + \sigma$ with $m \in \mathbb{Z}_+$ and $\sigma \in (0,1)$, the space $W^{s,p}(\Gamma)$ is defined in a similar way, namely it consists of the functions v such that any tangential derivatives of order less that or equal to m of the function v belong to $L^p(\Gamma)$ and any tangential derivative $D^\alpha v$ of order $|\alpha| = m$ satisfies $F_\sigma(D^\alpha v) < \infty$.

Trace theorems

The well-defined boundary value taken by a uniformly continuous function v on a bounded domain Ω with boundary Γ is usually denoted by $v|_\Gamma$. This idea can be equivalently stated introducing a map γ, called *trace operator*, which maps each $v \in C(\bar{\Omega})$ into its boundary value $\gamma v = v|_\Gamma$, which in turn results a function belonging to $C(\Gamma)$. The above concept is not equally straightforward for functions $v \in W^{m,p}(\Omega)$: the restriction of v to Γ need not make sense, since Γ is a set of measure zero and two functions in $W^{m,p}(\Omega)$ are identified if they are equal a.e. Nevertheless, an extension of the definition of trace operator for functions of $C(\bar{\Omega})$ is still possible even for functions in $W^{m,p}(\Omega)$. This concept will be illustrated by the following theorem.

Theorem A.2.3 (Trace Theorem). *Assume that $1 \leq p \leq \infty$ and $m > 1/p$. Then there exists a unique bounded linear surjective mapping $\gamma : W^{m,p}(\Omega) \to W^{m-1/p,p}(\Gamma)$ such that $\gamma v = v|_\Gamma$ when $v \in W^{m,p}(\Omega) \cap C(\bar{\Omega})$.*

In later developments, when it is assumed that the trace γv of a Sobolev function v is known on the boundary, we will simply write v in the place of γv.

We now intend to use the trace theorem to investigate the notion of higher-order normal derivative of a function on its boundary. It is in fact known that the tangential derivative of a function is completely defined if the function itself is known along a boundary.

Let $\mathbf{n} = (n_1, n_2, ..., n_d)^T$ be the outward unit normal vector to the boundary Γ of Ω, assumed smooth. The kth-order normal derivative of a function $v \in C^k(\bar{\Omega})$ is defined by

$$\frac{\partial^k v}{\partial n^k} \equiv n_{i_1} \cdots n_{i_k} \frac{\partial^k v}{\partial x_{i_1} \cdots \partial x_{i_k}}$$

The following theorem states the possible extendibility of the last definition to functions of certain Sobolev spaces

Theorem A.2.4 (Second Trace Theorem). *Assume that Ω is a bounded open set with a $C^{k,1}$ boundary Γ. Assume that $1 \leq p \leq \infty$ and $m > k + 1/p$. Then there exists unique bounded linear and surjective mappings $\gamma_j : W^{m,p}(\Omega) \to W^{m-j-1/p,p}(\Gamma)$ $(j = 0, 1, ..., k)$ such that $\gamma_j v = (\partial^j v/\partial n^j)|_\Gamma$ when $v \in W^{m,p}(\Omega) \cap C^{k,1}(\bar{\Omega})$.*

It is remarkable that the ranges of the trace operators are proper subsets of $L^p(\Gamma)$. Moreover, it can be shown that $W^{m-j-1/p,p}(\Gamma)$ is dense in $L^p(\Gamma)$, for $j = 0, 1, ..., k$.

The space $W_0^{m,p}(\Gamma)$

Bearing in mind the above definitions of trace operator, it is now possible to consider those particular subspaces of Sobolev spaces which contains functions vanishing on the boundary. To this end we define the space

$$W_0^{m,p}(\Omega) = \{w \in W^{m,p}(\Omega) : \ \gamma_j v = 0 \text{ for } j < m - 1/p\}$$

which, equivalently, can be defined by

$$W_0^{m,p}(\Omega) = \text{ the closure of } C_0^\infty \text{ in } W^{m,p}(\Omega)$$

It is rather simple to see that any function in $W_0^{m,p}(\Omega)$ can be approximated by a sequence of $C_0^\infty(\Omega)$ functions with respect to the norm of $W^{m,p}(\Omega)$.

Applying the second trace theorem it can be shown that $W_0^{m,p}(\Omega)$ is a closed subspace of $W^{m,p}(\Omega)$. When $p = 2$, we have $H_0^m(\Omega)$ replace $W_0^{m,2}(\Omega)$ and in the case $m = 1$ we write

$$H_0^1(\Omega) = \{v \in H^1(\Omega) : \ v = 0 \text{ a.e. on } \Gamma\}$$

Equivalent norms

The following result can be used to construct different equivalent norms (see definition (A.3)) on Sobolev spaces. Before proceeding we briefly recall that over the Sobolev space $W^{k,p}(\Omega)$ we have the following seminorm

$$|v|_{k,p,\Omega} = \left(\int_\Omega \sum_{|\alpha|=k} |D^\alpha v)|^p dx \right)^{1/p}$$

Theorem A.2.5 (Equivalent norm theorem). *Let Ω be an open, bounded, connected set in $\mathcal{R}^d$ with a Lipschitz boundary, $k \geq 1$, $1 \leq p < \infty$. Assume that $f_j : W^{k,p}(\Omega) \to \mathcal{R}$, $1 \leq j \leq J$, are seminorms on $W^{k,p}(\Omega)$ satisfying the following conditions:*

- (H_1) $0 \leq f_j(v) \leq c \parallel v \parallel_{k,p,\Omega} \quad \forall v \in W^{k,p}(\Omega) \quad 1 \leq j \leq J$
- (H_2) *if v is a polynomial of degree less than or equivalent to $k-1$ and $f_j(v) = 0$, $1 \leq j \leq J$, then $v = 0$*

Then the quantity

$$\parallel v \parallel = |v|_{k,p,\Omega} + \sum_{j=1}^{J} f_j(v)$$

or

$$\parallel v \parallel = \left(|v|^p_{k,p,\Omega} + \sum_{j=1}^{J} f_j(v)^p \right)^{1/p}$$

defines a norm on $W^{k,p}(\Omega)$, which is equivalent to the norm $\parallel v \parallel_{k,p,\Omega}$.

The interested reader is referred to [41] for a complete proof of the last statement. Here, we focus our attention on some important consequences of Theorem A.2.5. Consider for instance the case $k = 1, p = 2, J = 1$, which imply

$$f_1(v) = \int_{\partial\Omega} |v| ds$$

Applying the equivalent norm theorem we derive that there exists a positive constant c, depending only on Ω, such that it holds

$$\parallel v \parallel_{1,\Omega} \leq c|v|_{1,\Omega} \quad \forall v \in H^1_0(\Omega) \tag{A.16}$$

The above result is usually referred to as the Poincaré-Friedrichs inequality and it implies that the seminorm $|\cdot|_1$ is a norm on $H_0^1(\Omega)$, equivalent to the usual $H^1(\Omega)$-norm.

Also, if Γ_0 indicates an open, nonempty subset of the boundary Γ, then there exists a constant $c > 0$, depending only on Ω, such that

$$\| v \|_{1,\Omega} \leq c|v|_{1,\Omega} \quad \forall v \in H^1_{\Gamma_0}(\Omega) \tag{A.17}$$

where it is implicitly assumed that

$$H^1_{\Gamma_0}(\Omega) = \{v \in H^1(\Omega) : \ v = 0 \text{ a.e. on } \Gamma_0\}$$

The above inequality is derivable also by application of the equivalent norm theorem with $K = 1, p = 2, J = 1$ and taking

$$f_1(v) = \int_{\Gamma_0} |v| ds$$

Korn's first inequality

We now present a classical result of function spaces theory which is frequently recalled in the mathematical developments carried out in the treatment of elasticity and elastoplasticity arguments.

Let Ω be a nonempty, open, bounded and connected set in $\mathcal{R}^3$ with a Lipschitz boundary. Given a function $\mathbf{u} \in [H^1(\Omega)]^3$, it is possible to extract the corresponding linearized strain tensor applying the definition (1.3). Thus, it can be shown that there exists a constant $c > 0$ depending on Ω only, such that

$$\| \mathbf{u} \|^2_{[H^1(\Omega)]^3} \leq c \int_\Omega |\boldsymbol{\varepsilon}(\mathbf{u})|^2 dx \quad \forall \mathbf{u} \in [H^1_0(\Omega)]^3 \tag{A.18}$$

The above statement can be proved first for $C_0^\infty(\Omega)$ functions by an integration by parts technique (if we use the equivalent norm $\| \nabla\cdot \|_{[L^2(\Omega)]^3}$ in the space $[H^1_0(\Omega)]^3$) and then extended to $[H^1_0(\Omega)]^3$ by a density argument. The inequality (A.18) is a special case of the more general Korn's first inequality [26]

$$\| \mathbf{u} \|^2_{[H^1(\Omega)]^3} \leq c \int_\Omega |\boldsymbol{\varepsilon}(\mathbf{u})|^2 dx \quad \forall \mathbf{u} \in [H^1_{\Gamma_0}(\Omega)]^3 \tag{A.19}$$

where Γ_0 is a measurable subset of $\partial\Omega$ with meas $(\Gamma_0) > 0$ and

$$[H^1_{\Gamma_0}(\Omega)]^3 = \{\mathbf{v} \in [H^1(\Omega)]^3 : \mathbf{v} = \mathbf{0} \text{ a.e. on } \Gamma_0\}$$

The space $W^{-m,p}(\Omega)$

Let m be a positive integer, p a real number satisfying $1 \leq p < \infty$ and q the conjugate number of p, i.e. $q = (1 - 1/p)^{-1}$ if $1 < p < \infty$ and $q = \infty$ if $p = 1$. Then, $W^{-m,q}(\Omega)$ is defined to be the dual space of $W_0^{m,p}(\Omega)$. Since $\mathcal{D}(\Omega)$ is dense in $W_0^{m,p}(\Omega)$, it follows that $W^{-m,q}(\Omega) \subset \mathcal{D}'(\Omega)$ which is to say that $W^{-m,q}(\Omega)$ is a space of distributions. With respect to the last property, we have the following explicative result

Theorem A.2.6 *A distribution ℓ belongs to $W^{-m,q}(\Omega)$ if and only if it can be expressed in the form*

$$\ell = \sum_{|\alpha| \leq m} D^\alpha u_\alpha$$

where u_α are functions in $L^q(\Omega)$.

A frequently recurring space with negative index is $H^{-1}(\Omega)$, the dual space of $H_0^1(\Omega)$. Given any function $f \in L^2(\Omega)$, we can define the dual function of f as the $H^{-1}(\Omega)$ function ℓ applying the following relation

$$\langle \ell, v \rangle = \int_\Omega f v dx \quad \forall v \in H_0^1 \Omega$$

Hence f and ℓ can be identified. The duality pairing $\langle f, v \rangle$ on $H^{-1}(\Omega) \times H_0^1(\Omega)$ defined by the above relation is usually denoted by $\int_\Omega f v dx$.

A.2.3 Spaces of vector-valued functions

When dealing with the mathematical treatment of initial-boundary value problems, it is useful to interpret functions of space and time as mappings from a time interval onto a Banach space such as the ones discussed earlier.

Consider now a Banach space X and a positive real number T. We define the space $C^m([0,T];X)$ $(m = 0, 1, ...)$ to be the set of all continuous functions v from $[0,T]$ to X that have continuous derivatives of order less or equal to m. This is a Banach space when endowed with the norm

$$\| v \|_{C^m([0,T];X)} = \sum_{k=0}^{m} \max_{0 \leq t \leq T} \| v^{(k)}(t) \|_X$$

where $v^{(k)}(t)$ is defined as the kth time derivative of v. When $m = 0$, we simply write $C([0,T];X)$.

We define the Lebesgue space $L^p(0,T;X)$, for $1 \leq p < \infty$, as the set of all the measurable functions v from $[0,T]$ to X which satisfy the following limitation

$$\| v \|_{L^p(0,T;X)} = \left(\int_0^T \| v(t) \|_X^p \, dt \right)^{1/p} < \infty$$

The space $L^p(0,T;X)$ becomes a Banach space when equipped with the norm $\| v \|_{L^p(0,T;X)}$, which is to be understood in the sense that the members represent equivalent classes of functions that are equal a.e. on $(0,T)$.

The extension of this definition to include the limit case $p = \infty$ is obtained in the usual manner. The space $L^\infty(0,T;X)$ will be defined as the set of all measurable functions v from $[0,T]$ to X that are essentially bounded. This space is endowed with the following norm

$$\| v \|_{L^\infty(0,T;X)} \equiv \text{ess} \sup_{0 \leq t \leq T} \| v(t) \|_X$$

which makes it a Banach space.

If X is a Hilbert space with inner product $(\cdot,\cdot)_X$, then $L^2(0,T;X)$ is a Hilbert space with the inner product

$$(u,v)_{L^2(0,T;X)} = \int_0^T (u(t), v(t))_X \, dt$$

We now give a crucial result for the spaces just discussed

Theorem A.2.7 *Let $m \in \mathbb{N}$, and $1 \leq p \leq \infty$. Then the following statements hold*

- *$C([0,T];X)$ is dense in $L^p(0,T;X)$ and the embedding is continuous*
- *if $X \hookrightarrow Y$, then $L^p(0,T;X) \hookrightarrow L^q(0,T;Y)$ for $1 \leq q \leq p \leq \infty$*

Let X' be the topological dual of a separable normed space X. Then for $1 < p < \infty$ the dual space of $L^p(0,T;X)$ is given by

$$[L^p(0,T;X)]' = L^q(0,T;X')' \quad \textit{with} \quad \frac{1}{p} + \frac{1}{q} = 1 \tag{A.20}$$

Furthermore, if X is reflexive, then so is $L^p(0,T;X)$.

Following the same reasonings used to define the generalized derivatives of distributions, it is now possible to introduce the notion of differentiability

with respect to time for functions belonging to $L^p(0,T;X)$. We start again considering the following integration by parts rule

$$\int_0^T \phi^{(m)}(t)v(t)dt = (-1)^m \int_0^T \phi(t)v^{(m)}(t)dt$$

which is valid for all functions $\phi \in C_0^\infty(0,T)$ and $v \in C^m([0,T];X)$ and where $(\cdot)^{(m)} \equiv d^m(\cdot)/dt^m$. Thus, a function $v \in L^1_{\text{loc}}(0,T;X)$ is said to possess an mth-order *generalized derivative* if there exists a function $w \in L^1_{\text{loc}}(0,T;Y)$ such that

$$\int_0^T \phi^{(m)}(t)v(t)dt = (-1)^m \int_0^T \phi(t)w(t)dt \quad \forall \phi \in C_0^\infty(0,T) \tag{A.21}$$

where X and Y are appropriate Banach spaces. When (A.21) holds, we write $w = v^{(m)}$. In the relevant case where $X = Y = \mathcal{R}$ and $v \in C^m(0,T)$, the last definition returns exactly the classical integration by parts formula. An important Lemma on generalized derivatives is now in order

Lemma A.2.8 *Let V be a reflexive Banach space and H a Hilbert space with the property that $V \hookrightarrow H \hookrightarrow V'$, the continuous embedding $V \hookrightarrow H$ being dense. Let $1 \leq p, q \leq \infty$, with $1/p + 1/q = 1$. Then any function $u \in L^p(0,T;V)$ possesses a unique generalized derivative $u^{(m)} \in L^q(0,T;V')$ if and only if there is a function $w \in L^q(0,T;V')$ such that*

$$\int_0^T (u(t),v)_H \phi^{(m)}(t)dt = (-1)^m \int_0^T \phi(t)\langle w(t),v\rangle_{V'\times V} dt$$

for all $v \in V$, $\phi \in C_0^\infty(0,T)$. Then $u^{(m)} = w$ and for almost all $t \in (0,T)$ it holds

$$\frac{d^m}{dt^m}(u(t),v)_H = \langle w(t),v\rangle_{V'\times V} \quad \forall v \in V$$

For an integer $m \geq 0$ and a real number $p \geq 1$, we define the space $W^{m,p}(0,T;X)$ as the set of functions $f \in L^p(0,T;X)$ such that $f^{(i)} \in L^p(0,T;X)$ $, i \leq m$. This space becomes a Banach space once endowed with the norm

$$\| f \|_{W^{m,p}(0,T;X)} = \left\{ \sum_{i=0}^m \| f^{(i)} \|^p_{L^p(0,T;X)} \right\}^{1/p}$$

For brevity, in the case where $p = 2$ we will use the notation $H^m(0,T;X)$ instead of $W^{m,2}(0,T;X)$. If X is a Hilbert space, $H^m(0,T;X)$ is a Hilbert

space too with the following inner product

$$(f,g)_{H^m(0,T;X)} = \int_0^T \sum_{i=0}^{m} \left(f^{(i)}(t), g^{(i)}(t)\right)_X dt$$

Moreover, we present the following fundamental inequality

$$\| f(t) - f(s) \| \leq \int_s^t \| \dot{f}(\tau) \|_X \, d\tau \tag{A.22}$$

which is valid for any $s < t$ and any $f \in W^{1,p}(0,T;X)$ and $p \geq 1$. It is also worth recalling the continuous embedding property

$$H^1(0,T;X) \hookrightarrow C([0,T];X) \tag{A.23}$$

which authorizes to state that there exists a constant $c > 0$ such that

$$\| v \|_{C([0,T];X)} \leq c \| v \|_{H^1(0,T;X)} \quad \forall v \in H^1(0,T;X)$$

Finally we introduce the property

$$C^\infty([0,T];X) \text{ is dense in } H^1(0,T;X) \tag{A.24}$$

which will become useful in the sequel

A theorem of Lebesgue

The following result becomes crucial in proving the existence of a solution for an abstract variational inequality (see Theorem 3.2.1, Section 3.2).

Theorem A.2.9 *Let X be a normed space and $f \in L^1(a,b;X)$. Then we have*

$$\lim_{h\to 0} \frac{1}{h} \int_{t_0}^{t_0+h} \| f(t) - f(t_0) \|_X \, dt = 0 \quad \textit{for almost all } t_0 \in (a,b)$$

The theorem implies

$$\lim_{h\to 0} \frac{1}{h} \int_{t_0}^{t_0+h} f(t)dt = f(t_0) \quad \text{for almost all } t_0 \in (a,b)$$

where the limit is understood in the sense of the norm on X, i.e.

$$\lim_{h\to 0} \left\| \frac{1}{h} \int_{t_0}^{t_0+h} f(t)dt - f(t_0) \right\|_X = 0 \quad \text{for almost all } t_0 \in (a,b)$$

Appendix B

Elements of Theory of Variational Inequalities

B.1 Variational formulation of elliptic boundary value problems

Elliptic boundary value problems

Let Ω be a bounded subset in $\mathcal{R}^d$ with a Lipschitz continuous boundary Γ. The unit outward normal vector $\mathbf{n} = (n_1, n_2, ..., n_d)$ exists a.e. on Γ and we will denote the normal derivative of a function u on Γ by $\partial u/\partial n$.

The following equations

$$\begin{aligned} -\Delta u &= f \quad \text{in } \Omega \\ u &= 0 \quad \text{on } \Gamma \end{aligned} \tag{B.1}$$

define the well-known Poisson boundary value problem with homogeneous Dirichlet boundary conditions. Here Δ denotes the Laplacian operator, defined by $\sum_{i=1}^{d} \partial^2 u/\partial x_i$.

A classical solution of problem (B.1) is a smooth function $u \in C^2(\Omega) \cap C(\bar{\Omega})$ which satisfies the differential equation $(\text{B.1})_1$ and the boundary condition $(\text{B.1})_2$ pointwise. Accordingly, f must be a $C(\Omega)$ function even if this further condition by itself does not assure the existence of a classical solution of the problem in argument.

A weak formulation in such cases as the one that has just been reviewed is sought properly in order to avoid the high smoothness requirement of the solution. As soon as this (possibly unrealistic) restriction is removed, it becomes straightforward to draw existence consideration for a (weak) solution.

The procedure that we are going to present now is a classical one in deriving a weak formulation of a b.v.p. Let us assume for one moment that problem (B.1) does have a classical solution $u \in C^2(\Omega) \cap C(\bar{\Omega})$. Multiplying the differential equation $(\text{B.1})_1$ by an arbitrary smooth test function $v \in C_0^\infty(\Omega)$ and integrating over Ω, we obtain

$$-\int_\Omega \Delta u \, v \, dx = \int_\Omega f \, v \, dx$$

Performing an integration by parts and bearing in mind that $v = 0$ on Γ, the preceding equation leads to

$$\int_\Omega \nabla u \cdot \nabla v \, dx = \int_\Omega f \, v \, dx \tag{B.2}$$

The relation (B.2) has been deduced hypothesizing $u \in C^2(\Omega) \cap C(\bar{\Omega})$ and $v \in C_0^\infty(\Omega)$, even if suffices that $u, v \in H^1(\Omega)$ and that $f \in L^2(\Omega)$ for it to make sense. Moreover, since $H_0^1(\Omega)$ constitutes the closure of $C_0^\infty(\Omega)$ in $H^1(\Omega)$, the integrals in (B.2) are well defined for any $v \in H_0^1(\Omega)$. Meanwhile, the solution u is sought in the space $H_0^1(\Omega)$, which allows to rewrite the weak formulation of the original problem as

$$u \in H_0^1(\Omega), \quad \int_\Omega \nabla u \cdot \nabla v dx = \int_\Omega f \, v \, dx \quad \forall v \in H_0^1(\Omega) \tag{B.3}$$

Interpreting the integral at the right hand side of (B.3) as the duality pairing $\langle f, v \rangle$ between $H_0^{-1}(\Omega)$ and $H_0^1(\Omega)$, it is sufficient to require $f \in H^{-1}(\Omega)$ rather than $f \in L^2(\Omega)$. It is thus demonstrated that if u is a classical solution of the problem (B.1), then u is also a solution of its weak formulation (B.3).

Instead, if u is a "weak" solution of (B.1) with the additional regularity $u \in C^2(\Omega) \cap C(\bar{\Omega})$, then for any $v \in C_0^\infty(\Omega) \subset H_0^1(\Omega)$, in view of (B.3) we have

$$\int_\Omega (-\Delta u - f) v \, dx \quad \forall v \in H_0^1(\Omega)$$

which is to say $-\Delta u = f$ in Ω, or equivalently u satisfies the strong form of the boundary value problem (B.1). Clearly, u satisfies the homogeneous boundary condition pointwise. It is then shown how a weak solution of (B.3) with additional regularity is also a classical solution of the boundary value problem (B.1). When the property $u \in C^2(\Omega) \cap c(\bar{\Omega})$ is not granted, we will say that u formally solves the boundary problem (B.1).

Let us consider $V = H_0^1(\Omega)$ and let $a(\cdot, \cdot) : V \times V \to \mathcal{R}$ be a bilinear form defined by

$$a(u, v) = \int_\Omega \nabla u \cdot \nabla v \, dx \quad \text{for } u, v \in V$$

while $\ell : V \to \mathcal{R}$ denotes the linear functional given by the duality pairing

$$\langle \ell, v \rangle = \int_\Omega f\, v\, dx \quad \forall v \in V$$

With these hypotheses, the weak formulation of the problem becomes

$$u \in V, \;\; a(u, v) = \langle \ell, v \rangle \quad \forall v \in V \tag{B.4}$$

Recalling the Poincaré-Friedrichs inequality (A.16) we recognize that the bilinear form $a(\cdot, \cdot)$ is V-elliptic and continuous, while the functional ℓ is bounded and linear. Hence, by the Lax-Milgram lemma (Theorem A.1.9), the problem (B.4) has a unique solution $u \in V$.

A formulation of the initial boundary value problem as the one given by (B.1) is usually referred to as a classical or strong formulation. Indeed, a formulation of the same problem in the form of (B.4) will be called a variational or weak formulation, in that the solution to be sought need belong only to $H_0^1(\Omega)$ and thus to be less regular. Nevertheless, for a solution u of (B.1) to make sense, it is required that $u \in C^2(\Omega) \cap C(\bar{\Omega})$.

Some remarks on the equivalence between the strong and weak formulations of boundary value problems are now in order. We have shown that under suitable hypotheses, the classical local formulation (B.1) of a boundary value problem is equivalent to the weak or variational formulation (B.4) of the same problem. It is anyway worth pointing out that the natural way of stating a boundary value problem which models a physical process is accomplished through the statement of an integral balance law. It is then by admitting sufficient smoothness of the quantities involved in the integrals appearing in the balance law that it is possible to obtain the differential or punctual formulation of the problem. It is therefore logical to ask wether there is any tie between the integral balance law of a process and the weak formulation arising from the boundary value problem-type formulation arising by the modeling of the same phenomenon. The answer is affirmative, as shown in [3], provided some specific requirements are satisfied in the weak formulation itself. Therefore we may say that indeed the most natural way of formulating a boundary valued problem from a mathematical standpoint is that of passing through a properly formulated weak or variational statement of the problem.

Now suppose that the problem (B.1) is stated by means of a nonhomogeneous-type Dirichlet boundary conditions, namely suppose for instance that instead of $(\text{B.1})_2$ we are left with

$$u = g \quad \text{on } \Gamma \tag{B.5}$$

with $g \in H^{1/2}(\Gamma)$ a known function. Since there is a surjective application from $H^1(\Omega)$ onto $H^{1/2}(\Gamma)$ (Theorem A.2.3) there also exists a function $G \in H^1(\Omega)$ such that $\gamma G = g$. Then, setting

$$u = w + G$$

the original problem may be restated as the one of finding a function w such that

$$\begin{aligned} -\Delta w &= f + \Delta G \quad \text{in } \Omega \\ w &= 0 \qquad\quad\ \ \text{on } \Gamma \end{aligned}$$

Noting that $f + \Delta G$ belongs to $H^{-1}(\Omega)$, it is possible to obtain a weak formulation of the above boundary value problem, which in fact reads: find $w \in H_0^1(\Omega)$ such that

$$\int_\Omega \nabla w \cdot \nabla v dx = \int_\Omega (fv - \nabla G \cdot \nabla v) dx \ \ \forall v \in H_0^1(\Omega)$$

The strategy adopted guarantees a way to work with homogeneous Dirichlet boundary conditions and thus, for convenience, we will assume from now on to consider only problems with such boundary assignments.

The next problem

$$\begin{aligned} -\Delta u + u &= f \quad \text{in } \Omega \\ \frac{\partial u}{\partial n} &= g \quad \text{on } \Gamma \end{aligned} \tag{B.6}$$

goes by the name of *Neumann* problem. Assuming that $f \in L^2(\Omega)$, $g \in L^2(\Omega)$, the right space in which to state the above problem in weak form is $H^1(\Omega)$. Multiplying (B.6) by an arbitrary smooth test function $v \in C^\infty(\bar{\Omega})$ and integrating both sides over the domain Ω, once applied the integration by parts rule, one obtains

$$\int_\Omega (\nabla u \cdot \nabla v + u\, v)\, dx = \int_\Omega f\, v\, dx + \int_\Gamma \frac{\partial u}{\partial n} v\, ds$$

The above equation can be furtherly modified introducing the Neumann boundary condition $(B.6)_2$ into the last integral over Γ to become

$$\int_\Omega (\nabla u \cdot \nabla v + u\, v)\, dx = \int_\Omega f\, v\, dx + \int_\Gamma g\, v\, ds \quad \forall v \in C^\infty(\bar{\Omega})$$

Being $C^\infty(\bar{\Omega})$ dense in $H^1(\Omega)$ and being the trace operator γ a continuous application from $H^1(\Omega)$ to $L^2(\Gamma)$, we may pose the weak formulation of (B.6) in the following form: find a function $u \in H^1(\Omega)$ such that

$$\int_\Omega (\nabla u \cdot \nabla v + u\, v)\, dx = \int_\Omega f\, v\, dx + \int_\Gamma g\, v\, ds \quad \forall v \in H^1(\Omega) \tag{B.7}$$

Setting

$$a(u,v) = \int_\Omega (\nabla u \cdot \nabla v + u\, v)\, dx$$

and

$$\langle \ell, v \rangle = \int_\Omega f\, v\, dx + \int_\Gamma g\, v\, ds$$

(B.7) reads

$$u \in V, \;\; a(u,v) = \langle \ell, v \rangle \quad \forall v \in V \tag{B.8}$$

where $V = H^1(\Omega)$.

At this stage, the Lax-Milgram lemma provides uniqueness of solution for the weak problem (B.8).

As a final remark it is noted that a classical solution $u \in C^2(\Omega) \cap C^1(\bar{\Omega})$ of the problem (B.6) is also the solution of the weak formulation (B.8) and on the other hand a solution u of (B.8) which additionally belongs to $C^2(\Omega) \cap C^1(\bar{\Omega})$ constitutes a strong solution of the boundary value problem (B.6).

In a straightforward manner it is possible to deal with mixed boundary conditions. Let us now consider the problem

$$\begin{aligned} -\Delta u + u &= f \quad \text{in } \Omega \\ u &= 0 \quad \text{on } \Gamma_D \\ \frac{\partial u}{\partial n} &= g \quad \text{on } \Gamma_N \end{aligned} \tag{B.9}$$

where Γ_D and Γ_N are open sets such that $\partial\Omega = \bar{\Gamma}_D \cup \bar{\Gamma}_N$, plus $\Gamma_D \cap \Gamma_N = \varnothing$. Defining

$$V \equiv H^1_{\Gamma_D}(\Omega) = \left\{ v \in H^1(\Omega) : v = 0 \text{ on } \Gamma_D \right\} \tag{B.10}$$

which is the natural space in which seeking a weak solution of the problem (B.9), we are left with

$$u \in V, \;\; a(u,v) = \langle \ell, v \rangle \quad \forall v \in V \tag{B.11}$$

where

$$a(u,v) = \int_\Omega (\nabla u \cdot \nabla v + u\, v)\, dx$$

and

$$\langle \ell, v \rangle = \int_\Omega f\, v\, dx + \int_{\Gamma_N} g\, v\, ds$$

Sufficient assumptions on the data for the applicability of the Lax-Milgram lemma are $f \in L^2(\Omega)$ and $g \in L^2(\Gamma_N)$. Under these hypotheses, uniqueness of the solution of (B.11) is guaranteed.

Linear elasticity equilibrium boundary value problem

We now intend to discuss the issue of existence and uniqueness of the fundamental equilibrium boundary value problem of linear elasticity. The equations governing the equilibrium of linear elastic bodies (Chapter 1) are here briefly recalled for the reader's convenience. Given a bounded domain Ω in $\mathcal{R}^3$, with a Lipschitz continuous boundary Γ, the static behavior of the three-dimensional elastic body Ω constituted of linear elastic material are

- equation of equilibrium $\quad -\operatorname{div}\boldsymbol{\sigma} = \mathbf{f}$
- elastic constitutive equation $\quad \boldsymbol{\sigma} = \mathbb{C}\boldsymbol{\varepsilon}(\mathbf{u})$
- strain-displacement relation $\quad \boldsymbol{\varepsilon}(\mathbf{u}) = \dfrac{1}{2}\Big[\nabla\mathbf{u} + (\nabla\mathbf{u})^T\Big]$

(B.12)

with the following boundary conditions

- $$\mathbf{u} = \mathbf{0} \quad \text{on} \quad \Gamma_u \tag{B.13}$$
- $$\boldsymbol{\sigma}\mathbf{n} = \mathbf{g} \quad \text{on} \quad \Gamma_g$$

It is assumed that the boundary Γ is divided into two complementary parts $\bar{\Gamma}_u$ and $\bar{\Gamma}_g$ with Γ_u and Γ_g open sets such that $\Gamma_u \cap \Gamma_g = \varnothing$ and $\Gamma_u \neq \varnothing$.

In order to find the weak formulation of problem (B.12) with boundary conditions (B.13) we first introduce the space of admissible displacements V which satisfy a-priori the displacement-type boundary conditions $(\text{B.13})_2$

$$V = [H^1_{\Gamma_u}(\Omega)]^d \equiv \{\mathbf{v} = (v_i) : \ v_i \in H^1(\Omega), \ v_i = 0 \ \text{on} \ \Gamma_u, \ 1 \le i \le d\}$$

Combining Equations $(B.12)_{1-2}$ to eliminate the stress $\boldsymbol{\sigma}$ we are left with

$$-\text{div}\,[\mathbb{C}(\boldsymbol{\varepsilon}(\mathbf{u}))] = \mathbf{f} \quad \text{in } \Omega$$

The next step is set forth multiplying the last equation by an arbitrary element $\mathbf{v} \in V$, integrating over Ω the resulting relation and substituting the last boundary condition $(B.13)_2$. Finally, applying as usual the integration by parts rule, one obtains

$$a(\mathbf{u}, \mathbf{v}) = \langle \boldsymbol{\ell}, \mathbf{v} \rangle \quad \forall \mathbf{v} \in V \tag{B.14}$$

where

$$a(\mathbf{u}, \mathbf{v}) = \int_\Omega \mathbb{C}\boldsymbol{\varepsilon}(\mathbf{u}) : \boldsymbol{\varepsilon}(\mathbf{v}) dx \tag{B.15}$$

and

$$\langle \boldsymbol{\ell}, \mathbf{v} \rangle = \int_\Omega \mathbf{f} \cdot \mathbf{v} dx + \int_{\Gamma_g} \mathbf{g} \cdot \mathbf{v} ds \tag{B.16}$$

It is now easy to verify that both the bilinear form (B.15) and the linear functional (B.16) are continuous and that $a(\cdot, \cdot)$ is also V-elliptic. This last property follows immediately from the assumption that $\mathbb{C}$ is pointwise stable (see (1.68)) and the use of Korn's inequality. Thus the Lax-Milgram lemma grants the following results

Theorem B.1.1 *The problem defined by Equations* (B.14-B.16) has a unique solution $\mathbf{u} \in V$ under the above stated hypotheses. Furthermore, there exists a constant $c > 0$ such that

$$\| \mathbf{u} \|_V \leq c \left(\| \mathbf{f} \|_{L^2(\Omega)} + \| \mathbf{g} \|_{L^2(\Gamma_g)} \right) \tag{B.17}$$

Minimization problems

A boundary value problem of the form (B.4) can be shown to be equivalent, under certain assumptions, to a minimization problem. In fact, if the bilinear form $a(\cdot, \cdot)$ is symmetric, a solution $v \in V$ which minimizes the functional $J : V \to \mathcal{R}$

$$J(v) = \frac{1}{2} a(v, v) - \langle \ell, v \rangle$$

satisfies also (B.4). Moreover, if $a(\cdot, \cdot)$ is also V-elliptic, a solution of (B.4) is also a minimizer of $J(\cdot)$. Thus, under the stated assumptions, the weak formulation and the minimization problem are equivalent and the existence of

a unique minimizer of J may be inferred from the unique solvability of the weak formulation proved by the Lax-Milgram lemma.

In more general minimization problems regarding functionals with non-symmetric bilinear forms, the following result provides a means to show uniqueness and solvability. For a complete proof, which is here omitted for brevity, the reader is referred to [41].

Proposition B.1.2 *Let X be a reflexive Banach space, K be a nonempty, closed, convex subset of X and f a proper, convex, l.s.c. functional on K. Assume that*

$$f(x) \to \infty \quad as \quad \| x \|_X \to \infty, \;\; x \in K \tag{B.18}$$

Then there exists $x_0 \in K$ such that

$$f(x_0) = \min_{x \in K} f(x)$$

If f is strictly convex on K, then the solution x_0 is unique.

Mixed variational problems

The problems of the kind of the one analyzed in the following can be regarded as an extension of the standard elliptic variational problem expressed by (B.4). In some cases, the above generalization results by the introduction of new auxiliary variables of the problem either as a complication of the modeling of the physical phenomenon underneath the problem itself or as a means to eliminate constraints of the problem.

If Q denotes the space of the new problem variables, then the cartesian product $V \times Q$ becomes the new space on which the problem is formulated. Assuming $a(\cdot,\cdot)$ a bilinear form on V as before and $b(\cdot,\cdot) : V \times Q \to \mathcal{R}$ another bilinear form and ℓ and m linear functionals defined respectively on V and on Q, then the problem under consideration is one of finding the functions $u \in V$ and $p \in Q$ such that

$$\begin{aligned} a(u,v) + b(v,p) &= {}_V\langle \ell, v \rangle_V \quad \forall v \in V \\ b(u,q) &= {}_{QV}\langle m, q \rangle_{QV} \quad \forall q \in Q \end{aligned} \tag{B.19}$$

The above problem in weak form is usually referred to as *saddle-point problem* because whenever $a(\cdot,\cdot)$ is a symmetric bilinear form it can be shown to be equivalent to the saddle-point or *minimax* problem of finding $(u,p) \in V \times Q$ such that

$$L(u,q) \le L(u,p) \le L(v,p) \quad \forall v \in V, q \in Q$$

with $L(v,q) = \frac{1}{2}a(v,v) + b(v,q) - \langle \ell, v\rangle - \langle m, q\rangle$. Though, it is to be pointed out that not every mixed problem can be posed in the form of a saddle point problem, hence the formulation (B.19) remains the more general and will in fact be the most frequently adopted in subsequent developments.

Let us now treat the example of the linear elasticity problem (B.12) in mixed form. Choosing the new variable as the stress tensor $\boldsymbol{\sigma}$, we may multiply the equilibrium equation $(\text{B.12})_1$ by an arbitrary function $\mathbf{v} \in V = \left[H^1_{\Gamma_u}(\Omega)\right]^d$, integrate the resulting equation over Ω, perform the integration by parts rule and use the mixed boundary condition (B.13) to obtain

$$\int_\Omega \boldsymbol{\sigma} : \boldsymbol{\varepsilon}(\mathbf{v})\, dx = \int_\Omega \mathbf{f}\cdot\mathbf{v}\, dx + \int_{\Gamma_g} \mathbf{g}\cdot\mathbf{v}\, ds \quad \forall \mathbf{v} \in V \tag{B.20}$$

We here introduce the space of *admissible stresses*, defined as

$$Q = [L^2(\Omega)]^{d\times d}_{sym} \equiv \left\{ \boldsymbol{\tau} \in [L^2(\Omega)]^{d\times d} : \ \tau_{ij} = \tau_{ji}, \ 1 \le i,j \le d \right\}$$

The second constitutive equation $(\text{B.12})_2$ can then be written in the form

$$\boldsymbol{\varepsilon}(\mathbf{u}) = \mathbb{A}\boldsymbol{\sigma}$$

where $\mathbb{A} = \mathbb{C}^{-1}$ is the elastic compliance tensor. Taking the scalar product of the above relation with an arbitrary admissible stress tensor $\boldsymbol{\tau} \in Q$ and integrating on the domain Ω we are lead to

$$\int_\Omega \mathbb{A}\boldsymbol{\sigma} : \boldsymbol{\tau}\, dx - \int_\Omega \boldsymbol{\varepsilon}(\mathbf{u}) : \boldsymbol{\tau}\, dx = 0 \quad \forall \boldsymbol{\tau} \in Q \tag{B.21}$$

Equations (B.20) and (B.21) can be recast in compact form to give the variational formulation of the problem of finding the pair $(\mathbf{u}, \boldsymbol{\sigma}) \in V \times Q$ satisfying

$$\begin{aligned} a(\boldsymbol{\sigma}, \boldsymbol{\tau}) + b(\boldsymbol{\tau}, \mathbf{u}) &= 0 \quad \forall \boldsymbol{\tau} \in Q \\ b(\boldsymbol{\sigma}, \mathbf{v}) &= \langle \boldsymbol{\ell}, \mathbf{v}\rangle \quad \forall \mathbf{v} \in V \end{aligned} \tag{B.22}$$

with the following positions

$$\begin{aligned} a(\boldsymbol{\sigma}, \boldsymbol{\tau}) &= \int_\Omega \mathbb{A}\boldsymbol{\sigma} : \boldsymbol{\tau}\, dx \\ b(\boldsymbol{\tau}, \mathbf{v}) &= -\int_\Omega \boldsymbol{\varepsilon}(\mathbf{v}) : \boldsymbol{\tau}\, dx \\ \langle \boldsymbol{\ell}, \boldsymbol{\tau}\rangle &= \int_\Omega \mathbf{f}\cdot\mathbf{v}\, dx + \int_{\Gamma_g} \mathbf{g}\cdot\mathbf{v}\, ds \end{aligned} \tag{B.23}$$

The fundamental question of well-posedness of the above mixed problem clearly relies on the choices of the spaces V and Q and on the properties of the bilinear forms $a(\cdot,\cdot)$ and $b(\cdot,\cdot)$. Assuming that both bilinear forms are continuous, i.e.

$$\begin{aligned} |a(u,v)| &\leq \| a \| \| u \| \| v \| \quad \forall u,v \in V \\ |b(v,q)| &\leq \| b \| \| v \| \| q \| \quad \forall v \in V, q \in Q \end{aligned} \tag{B.24}$$

it is possible to define bounded linear operators $A : V \to V'$, $B : V \to Q'$ and $B' : Q \to V'$ such that

$$\begin{aligned} \langle Au, v\rangle &= a(u,v) \quad \forall u,v \in V \\ \langle Bv, q\rangle &= \langle B'q, v\rangle = b(v,q) \quad \forall v \in V, q \in Q \end{aligned} \tag{B.25}$$

The kernels Ker$B$ and KerB' are therefore defined by

$$\begin{aligned} \mathrm{Ker}B &= \{v \in V : \ b(v,q) = 0 \ \forall q \in Q\} \\ \mathrm{Ker}B' &= \{q \in Q : \ b(v,q) = 0 \ \forall v \in V\} \end{aligned} \tag{B.26}$$

Under the above positions, the following result addressing the existence issue holds

Theorem B.1.3 (Babuška [18], Brezzi, [22]). *Let V and Q be Banach spaces. Suppose that the bilinear form $a(\cdot,\cdot)$ is symmetric, continuous and* Ker$B$-elliptic. Furthermore, suppose that $b(\cdot,\cdot)$ is continuous and that there exists a constant $\beta > 0$ such that

$$\sup_{v \in V} \frac{b(v,q)}{\| v \|} \geq \beta \| q \|_{Q \backslash \mathrm{Ker}B'} \quad \forall q \in Q \tag{B.27}$$

Then there exists a solution (u,p) of problem (B.19) for any $\ell \in V'$ and $m \in Q'$, with u being unique and p uniquely determined up to a member of KerB'.

In (B.27), the quotient norm $\| q \|_{Q \backslash \mathrm{Ker}B'}$ is defined by

$$\| q \|_{Q \backslash \mathrm{Ker}B'} = \inf_{q_0 \in \mathrm{Ker}B'} \| q + q_0 \|$$

Finally, it is easy to show that if meas$(\Gamma_u) \neq 0$, then the mixed variational problem of linear elasticity (B.22)-(B.23) satisfies Theorem B.1.3, with Ker$B' = \{\mathbf{0}\}$ and has therefore a unique solution.

B.2 Elliptic variational inequalities

There are several contributions in the literature to the theory of variational inequalities. Just to report a few of them, the reader is referred to [1, 31, 32, 34, 35, 36, 49, 50, 54, 65]. In this brief paragraph we aim to set the stage for the general form of an elliptic variational inequality (EVI in the following) and to present a sketch of the well-posedness and solvability issues of such a problem. Let us first consider the abstract of the EVI of the first kind. Given a real Hilbert space V endowed with its inner product $(\cdot,\cdot)$ and associated norm $\|\cdot\|$, define K as a subset of V. Let $a : V \times V \to \mathcal{R}$ be a continuous, V-elliptic bilinear form. Given a linear functional $\ell : V \to \mathcal{R}$, the problem under consideration is the one of finding $u \in K$ such that

$$a(u, v-u) \geq \langle \ell, v-u \rangle \quad \forall v \in K \tag{B.28}$$

In some cases EVI of the first kind are posed on convex subsets; moreover when the case is such that K is a subspace of V, it is shown that the problem (B.28) becomes a variational equation.

Theorem B.2.1 [54] Let V be a real Hilbert space, $a : V \times V \to R$ a continuous, V-elliptic bilinear form, $\ell : V \to R$ a bounded linear functional and $K \subset V$ a nonempty, closed and convex set. Then the EVI (B.28) has a unique solution $u \in K$.

The proof of the above theorem is not reported here and can be found in [41]. Indeed we have also the following useful result.

Theorem B.2.2 (Banach Fixed-Point Theorem) *Let X be a Banach space. Assume that $f : X \to X$ is a contractive mapping, that is, for some $\kappa \in [0, 1)$*

$$\| f(x) - f(y) \| \leq \kappa \| x - y \| \quad \forall x, y \in X$$

Then f possesses a unique fixed point $x \in X$, $f(x) = x$.

It is noted however that Theorem B.2.1 is a generalization of the Lax-Milgram lemma.

The second class of variational inequalities treated in this Appendix are characterized by the presence of nondifferentiable functions. These inequalities are usually referred to as of the second kind. To begin this investigation we may consider, in addition to the above defined bilinear form $a(\cdot,\cdot)$ and linear functional ℓ the following proper, convex, lower semicontinuous functional j :

$V \to \bar{\mathcal{R}}$ (see Chapter 2 for the pertinent definitions), which is not assumed to be differentiable. Then we define the problem of finding a function $u \in V$ that satisfies

$$a(u, v-u) + j(v) - j(u) \geq \langle \ell, v-u \rangle \quad \forall v \in V \tag{B.29}$$

as an EVI of the second kind.

The key difference between an EVI of the first kind and one of the second kind lies in the fact that the former is an inequality stating the formulation of a problem on a convex subset rather than on the whole space, while the latter is an inequality due to the presence of a nondifferentiable term $j(\cdot)$.

The following important theorem states the requirements for the unique solvability of an EVI of the second kind.

Theorem B.2.3 *Let V be a real Hilbert space, $a : V \times V \to \mathcal{R}$ a continuous, V-elliptic bilinear form, $\ell : V \to \mathcal{R}$ bounded linear functional on V and $j : V \to \bar{\mathcal{R}}$ a proper, convex, l.s.c. functional on V. Then the EVI of the second kind (B.29) has a unique solution.*

A thorough derivation of the above fundamental result is achievable in [41] and is therefore omitted here for brevity.

B.3 Parabolic variational inequalities

Parabolic variational inequalities result from problem formulations very similar to those presented in the preceding section, except for the presence of time as an independent variable of the problem. In the following, some basic definitions and results are presented with reference to such a kind of variational inequalities.

Let V and H be real Hilbert spaces such that $V \subset H$ and V is dense in H. We identify H with its dual space H'. Let K be a nonempty, closed, convex subset of V. Let A be a linear continuous operator from V to V' such that there exists a constant $\alpha > 0$ for which $\langle Av, v \rangle \geq \alpha \parallel v \parallel_V^2 \ \forall v \in V$. The position $a(u, v) = \langle Au, v \rangle$ defines a bilinear form $a : V \times V \to \mathcal{R}$ that is continuous and V-elliptic. Let $f \in L^2(0, T; V')$ for some time interval $[0, T]$ and suppose that the time derivative $\dot{f} \in L^2(0, T; V')$. Finally, let $u_0 \in K$ be a given initial value. Then a parabolic variational inequality of the first kind is a problem of the following form: find a function $u \in L^2(0, T; V)$ with $\dot{u} \in L^2(0, T; V)$ and $u(0) = u_0$ such that for almost all (a.a.) $t \in [0, T]$, $u(t) \in K$ and

$$(\dot{u}(t), v - u(t)) + a(u(t), v - u(t)) \geq \langle f(t), v - u(t) \rangle \quad \forall v \in K \tag{B.30}$$

We have the following result [36]

Theorem B.3.1 *In addition to the above assumptions, assume further that $f(0) - Au_0 \in H$. Then the parabolic variational inequality of the first kind (B.30) has a unique solution. Furthermore, it holds*

$$u, \dot{u} \in L^2(0,T;V) \cap L^\infty(0,T;H)$$

An illustrative exemplification of a problem corresponding to a parabolic variational inequality which can be found in [31] is the following. Introduce a functional $j : V \to \bar{\mathcal{R}}$ which is proper, convex and l.s.c. and such that there exists a family of differentiable functions j_k on V which satisfy the following three conditions:

- $$\int_0^T j_k(v(t))dt \to \int_0^T j(v(t))dt \text{ for any} v \in L^2(0,T;V)$$
- there is a sequence u_k bounded in V such that $j_k'(u_k) = 0$ for any k
- if $v_k \rightharpoonup v, \dot{v}_k \rightharpoonup \dot{v}$ in $L^2(0,T;V)$ and $\int_0^T j_k(v_k)dt$ is bounded from above, then

$$\lim_{k\to\infty} \inf \int_0^T j_k(v_k)dt \geq \int_0^T j(v)dt$$

The bilinear form a will be taken to be coercive, i.e.

$$a(v,v) + \lambda \parallel v \parallel_H^2 \geq \alpha \parallel v \parallel_V^2 \quad \forall v \in V$$

for some constants $\lambda \geq 0$ and $\alpha > 0$. Finally, it is also assumed that $j(u_0) \in \mathcal{R}$ and that there exists a sequence $\{u_{0k}\}$ such that $u_{0k} \to u_0$ in V and $\parallel Au_{0k} + j_k'(u_{0k}) \parallel_H$ is bounded.

Theorem B.3.2 *Under the above assumptions, there exists a unique solution to the problem of finding a function $u \in L^2(0,T;V)$ with $\partial u/\partial t \in L^2(0,T;V')$ and $u(0) = u_0$ such that for a.a. $t \in [0,T]$*

$$(\dot{u}(t), v - u(t)) + a(u(t), v - u(t)) + j(v) - j(u(t)) \geq \langle f(t), v - u(t)\rangle \quad \forall v \in V \tag{B.31}$$

Furthermore, $\dot{u} \in L^2(0,T;V) \cap L^\infty(0,T;H)$.

If we define, respectively,

$$\mathcal{K} = \left\{v : \ v \in L^2(0,T;V), \ \dot{v} \in L^2(0,T;V'), \ v(t) \in K \ a.a. \ t \in [0,T]\right\}$$

and

$$\mathcal{K}_{u_0} = \{v : \ v \in \mathcal{K}, \ v(0) = u_0\}$$

with u_0 a given function in H, it is then possible to restate the problems (B.30) and (B.31) in the following unified form

$$u \in \mathcal{K}_{u_0}, \ \int_0^T (\dot{u}, v-u)dt + \int_0^T [a(u, v-u) + j(v) - j(u)]dt \geq \int_0^T \langle f, v-u\rangle dt \ \ \forall v \in \mathcal{K} \tag{B.32}$$

which has a local counterpart of the type

$$\begin{aligned} u \in \mathcal{K}_{u_0}, \ \ (\dot{u}(t), v-u(t)) + a(u(t), v-u(t)) + j(v) - j(u(t)) \geq \\ \langle f(t), v-u(t)\rangle \quad \forall v \in K, \text{ for a.a. } t \in [0,T] \end{aligned} \tag{B.33}$$

It is probably worth presenting also the following variational formulation of the problem under consideration which does not require the assumptions on $f(0)$ and u_0 appearing in Theorem B.3.1 and on the nondifferentiable functional j stated in Theorem B.3.2. The problem becomes now the one of finding $u \in L^2(0,T;V)$ with $u(t) \in K$ for a.a. $t \in [0,T]$ such that

$$\int_0^T (\dot{v}, v-u)dt + \int_0^T [a(u, v-u) + j(v) - j(u)]dt \geq \int_0^T \langle f, v-u\rangle dt \quad \forall v \in \mathcal{K}_{u_0} \tag{B.34}$$

The solution to problem (B.32) satisfies (B.34) but the converse does not hold true. We have indeed the following result on the weak formulation (B.34) which is found in [36]

Theorem B.3.3 *Let K be a nonempty closed convex subset of V, with $u_0 \in K$. Let $a : V \times V \to \mathcal{R}$ be a bilinear elliptic form on V and $j : K \to \mathcal{R}$ a convex l.s.c. functional with the property that $|\int_0^T j(v)dt| < \infty$ for any $v \in L^2(0,T;K)$. Then, for any $f \in L^2(0,T;V')$, there exists a unique function $u \in L^2(0,T;V)$ with $u(t) \in K$ for a.a $t \in [0,T]$ such that (B.34) is satisfied.*

Results on the regularity of solutions to parabolic variational inequalities are very useful in accurately predicting the convergence orders of numerical approximations. Let us therefore consider the following theorem [21] which is a key result in this context.

Theorem B.3.4 *For the problem (B.30) in which $H = L^2(\Omega)$, $V = H_0^1(\Omega)$,*

$$a(u,v) = \int_\Omega \nabla u \cdot \nabla v \, dx, \quad \langle f, v \rangle = \int_\Omega f \, v \, dx,$$

and $K = \{v \in H_0^1(\Omega) : \ v \geq 0 \ a.e. \ on \ \Omega\}$, assume that

$$f \in C([0,T]; L^\infty(\Omega)), \ \dot{f} \in L^2([0,T]; L^\infty(\Omega))$$

and

$$u_0 \in W^{2,\infty}(\Omega) \cap K$$

Then there exists a unique solution to (B.30) satisfying

$$u \in L^2([0,T]; H^2(\Omega)), \ \ \dot{u} \in L^2([0,T]; H_0^1(\Omega)) \cap L^\infty([0,T]; L^\infty(\Omega))$$

and

$$\left(\frac{\partial u^+(t)}{\partial t}, v - u(t) \right) + a(u(t), v - u(t)) \geq \langle f(t), v - u(t) \rangle$$

for all $v \in K$, $t \in [0,T]$, where $\partial u^+(t)/\partial t$ denotes the right-hand derivative of u with respect to t.

List of Figures

List of Tables

Bibliography

[1] S. Agmon, *Lectures on Elliptic Boundary Value Problems*, Van Nostrand, Princeton, NJ, 1965.

[2] R.A. Adams, *Sobolev Spaces*, Academic Press, New York, 1975.

[3] S.S. Antman, *Nonlinear Problems of Elasticity*, Springer-Verlag, New York, 1995.

[4] F. Armero, *Elastoplastic and Viscoplastic Deformations in Solids and Structures*, in Encyclopedia of Computational Mechanics, pp. 227-266, Stein E., de Borst R., Hughes T.J.R. (eds.), John Wiley & Sons, Chichester, 2004.

[5] P.J. Armstrong, C.O. Frederick *A mathematical representation of the multiaxial Bauschinger effect*, CEGB Report RD/B/N731, Central Electricity Generating Board, 1966.

[6] E. Artioli, F. Auricchio, L. Beirão da Veiga, *A new integration scheme for von-Mises plasticity: numerical investigations*, Proceedings XV Italian Conference on Computational Mechanics, Genova 21-23 June, 2004.

[7] E. Artioli, F. Auricchio, L. Beirão da Veiga, *A new integration algorithm for the von-Mises elasto-plastic model*, Proceedings Colloquium Lagrangianum, Springer, Venice 21-23 December, 2004.

[8] E. Artioli, F. Auricchio, L. Beirão da Veiga, *Integration schemes for von-Mises plasticity models based on exponential maps: numerical investigations and theoretical considerations*, Int. J. Num. Meth. Eng., **64**, 1133-1165, 2005.

[9] E. Artioli, F. Auricchio, L. Beirão da Veiga, *Exponential-based integration algorithms for von-Mises plasticity with linear hardening. Part I: presentation of a novel "optimal" scheme and extensive numerical investigations*, Technical Report, I.M.A.T.I.-C.N.R., Pavia, 2005.

[10] E. Artioli, F. Auricchio, L. Beirão da Veiga, *Exponential-based integration algorithms for von-Mises plasticity with linear hardening. Part II: a theoretical analysis on consistency, accuracy and stability*, Technical Report, I.M.A.T.I.-C.N.R., Pavia, 2005.

[11] E. Artioli, F. Auricchio, L. Beirão da Veiga, *A novel "optimal" exponential-based integration algorithm for von-Mises plasticity with linear hardening: Theoretical analysis on yield consistency, accuracy, convergence and numerical investigations*, Int. J. Num. Meth. Eng., **67**, 449-498, 2006.

[12] E. Artioli, F. Auricchio, L. Beirão da Veiga, *Second-order accurate integration algorithms for von-Mises plasticity with a nonlinear kinematic hardening mechanism*, submitted for publication, 2006.

[13] E. Artioli, F. Auricchio, L. Beirão da Veiga, *A comparison of midpoint integration algorithms for von-Mises plasticity with nonlinear kinematic hardening*, submitted for publication, 2006.

[14] F. Auricchio, *Mechanics of Solid Materials: theoretical and computational aspects*, Lecture Notes, 2001.

[15] F.Auricchio, *Ce-driver*, Technical report, Dipartimento di Meccanica Strutturale - University of Pavia, 2001. Manual prepared for the European School of Advanced Studies of Seismik Risk Reduction.

[16] F. Auricchio, L. Beirão da Veiga, *On a new integration scheme for von-Mises plasticity with linear hardening*, Int. J. Num. Meth. Engrg., **56**, 1375-1396, 2003.

[17] F. Auricchio, R.L. Taylor, *Two material models for cyclic plasticity: nonlinear kinematic hardening and generalized plasticity*, Int. J. Plast., **1**: 65-98, 1995.

[18] I. Babuška, *The finite element method with Lagrangian multipliers*, Numer. Math., **20**: 179-192, 1973.

[19] K.J. Bathe, *Finite Element Procedures*, Englewood-Cliffs, NJ, 1996.

[20] J. Bonet, R.D. Wood *Nonlinear Continuum Mechanics for Finite Element Analysis*, Cambridge University press, Cambridge, 1997.

[21] H. Brezis, *Problèmes unilateraux*, J. Math. Pures et Appl. , **51**: 1-168, 1972.

[22] F. Brezzi, *On the existence, uniqueness and approximation of saddle-point problems arising from Lagrange multipliers*, RAIRO Anal. Numèr., R-2, **8**: 129-151, 1974.

[23] J.L. Chaboche, O. Jung, *Application of a kinematic hardening viscoplasticity model with thresholds to the residual stress relaxation*, Int. J. Plast., **13**: 785-807, 1998.

[24] J.L. Chaboche, N. El Mayas, P. Paulmier, *Modélisation thermodynamique des phénomènes de viscoplasticité, restauration et vieillissement*, C.R. Acad. Sci. Paris, **320**(II): 9-16, 1998.

[25] P. Chadwick, *Continuum Mechanics: Concise Theory and Problems*, George Allen & Unwin, London, 1976.

[26] P.G. Ciarlet, *The Finite Element Method for Elliptic Problems*, North Holland, Amsterdam, 1978.

[27] P.G. Ciarlet, *Mathematical Elasticity, Vol. I: Three-Dimensional Elasticity*, North Holland, Amsterdam, 1988.

[28] B. Coleman, M. Gurtin, *Thermodynamics with internal state variables*, J. Chem. Phys., **47**: 597-613, 1967.

[29] G.P. Del Piero, *Representation theorems of hemitropic and transversely isotropic tensor functions*, J. Elast., **51**: 43-71, 1998.

[30] D.C. Drucker, *A more fundamental approach to plastic stress-strain relations*, in Proc. 1st US National Congress of Applied Mechanics, ASME, New York, 1951, 487-491.

[31] G. Duvaut, J.L. Lions, *Inequalities in Mechanics and Physiscs*, Springer-Verlag, Berlin, 1976.

[32] L.C. Evans, *Partial Differential Equations*, Berkeley Mathematics Lecture Notes, Volume 3, 1994.

[33] R.A. Eve, B.D. Reddy, R.T Rockafellar, *An internal variable theory of elastoplasticity based on the maximum plastic work inequality*, Quart. Appl. Math., **48**: 59-83, 1990.

[34] A. Friedman, *Variational Principles and Free-Boundary Problems*, John Wiley & Sons, New York, 1982.

[35] R. Glowinski, *Numerical Methods for Nonlinear Variational Problems*, Springer-Verlag, New York, 1984.

[36] R. Glowinski, J.L. Lions, R. Trémolières, *Numerical Analysis of Variational Inequaities*, North-Holland, Amsterdam, 1981.

[37] M.E. Gurtin, *Modern Continuum Thermodynamics*, in Academic Press, New York, 1981.

[38] M.E. Gurtin, *An Introduction to Continuum Mechanics*,in Mechanics Today, 168-210, S. Nemat-Nasser, ed., Pergamon, Oxford, 1974.

[39] E. Hairer, S.P. Norsett, G.Wanner, *Solving Ordinary Differential Equations I : Nonstiff Problems*, Springer-Verlag, Berlin, 1987.

[40] B. Halpen, Q.S. Nguyen, *Sur les matèriaux standards gènèralisès*, J. Mec., **14**: 39-63, 1975.

[41] W. Han, B. Daya Reddy, *Plasticity: Mathematical Theory and Numerical Analysis*, Springer-Verlag, New York, 1999.

[42] W. Han, B. Daya Reddy, G.C. Schroeder, *Qualitative and numerical analysis of quasistatic problems in elastoplasticity*, SIAM J. Numer. Anal., **34**: 143-177, 1997.

[43] R. Hill, *Constitutive dual potentials in classical plasticity*, J. Mech. Phys. Solids, **35**, 39-63, 1987.

[44] H.K. Hong, C.S. Liu, *Internal symmetry in bilinear elastoplasticity*, Int. J. Nonl. Mech., **34**, 279-288, 1999.

[45] H.K. Hong, C.S. Liu, *Internal symmetry in the constitutive model of perfect elastoplasticity*, Int. J. Nonl. Mech., **35**, 447-466, 2000.

[46] H.K. Hong, C.S. Liu, *Some physical models with Minkowski spacetime structure and Lorentz group symmetry*, Int. J. Nonl. Mech., **36**, 1075-1084, 2001.

[47] H.K. Hong, C.S. Liu, *Lorentz group on Minkowski spacetime for construction of the two basic principles of plasticity*, Int. J. Nonl. Mech., **36**, 679-686, 2001.

[48] T.J.R. Hughes, *The Finite Element Method*, Prentice-Hall, Englewood Cliffs, N.J., 1978.

[49] N. Kikuchi, J.T. Oden, *Contact Problems in Elasticity: A Study of Variational Inequalities and Finite Element Methods*, SIAM, Philadelphia, 1988.

[50] D. Kinderlehrer, G. Stampacchia, *An Introduction to Variational Inequalities and Their Applications*, Academic Press, New York, 1980.

[51] R.D. Krieg, D.B. Krieg, *Accuracies of numerical solution methods for the elastic-perfectly plastic model*, J. Press. Vess. Tech., Transaction of ASME, **99**, 510-515, 1977.

[52] J.D. Lambert, *Computational Methods in Ordinary Differential Equations*, Wiley, Chirchester, 1991.

[53] J. Lemaitre, J.L. Chaboche, *Mechanics of Solid Materials*, Cambridge University Press, Cambridge, 1990.

[54] J.L. Lions, G. Stampacchia, *Variational inequalities*, Comm. Pure Appl. Math., **20**: 493-519, 1967.

[55] C.S. Liu, *Cone of non-linear dynamical system and group preserving schemes*, Int. J. Nonl. Mech., **36**, 1047-1068, 2001.

[56] J. Lubliner, *On the thermodynamics foundations of non-linear solid mechanics*, Int. J. Nonl. Mech., **7**: 237-254, 1972.

[57] J. Lubliner, *Plasticity Theory*, Macmillan, New York, 1990.

[58] D.G. Luenberger, *Linear and Nonlinear Programming*, Addinson-Wesley Publishing Company, Reading, Massachusets, 1984.

[59] G. Maenchen, S. Sack, *The tensor code*, in Methods in computational physics, ed. B. Alder, vol. 3, 181-210, Academic Press, 1964.

[60] J.E. Marsden, T.J.R. Hughes*Mathematical Foundations of Elasticity*, Prentice-Hall, New Jersey, 1983.

[61] J.B. Martin, *Plasticity: Fundamentals and General Results*, MIT Press, Cambridge, Mass., 1975.

[62] J.T. Oden, *Finite elements: an introduction*, Handbook for Numerical Analysis, vol. II, 3-15, Ciarlet P.G. and Lions J.L. (eds.), North-Holland, Amsterdam, 1991.

[63] M. Ortiz, E.P. Popov, *Accuracy and stability of integration algorithms for elastoplastic constitutive relations*, Int. J. Num. Meth. Engrg., **21**, 1561-1576, 1985.

[64] M. Ortiz, J. C. Simo, *An analysis of a new class of integration integration algorithms for elastoplastic constitutive relations*, Int. J. Num. Meth. Engrg., **23**: 353-366, 1986.

[65] P.D. Panagiotopoulos, *Inequality Problems in Mechanics and Applications*, Birkhäuser, Boston, 1985.

[66] W. Prager, *A new method of analyzing stress and strain in work-hardening plastic solids*, J. Appl. Mech., **23**, 493-496, 1956.

[67] M. Ristinmaa, J. Tryding, *Exact integration of constitutive equations in elasto-plasticity*, Int. J. Num. Meth. Engrg., **36**, 2525-2544, 1993.

[68] J.C. Simo, S. Govindjee, *Non-linear B-stability and symmetry preserving return mapping algorithms for plasticity and visco-plasticity*, Int. J. Num. Meth. Eng., **31**, 151-176, 1991.

[69] J.C. Simo, *Numerical Analysis of Classical Plasticity*, in Handbook for Numerical Analysis, vol. IV, 183-499, Ciarlet P.G. and Lions J.J. (eds.), Elsevier, Amsterdam, 1998.

[70] J.C. Simo, T.J.R. Hughes, *Computational Inelasticity*, Springer-Verlag, New York, 1998.

[71] J.C. Simo, R.L. Taylor, *Consistent tangent operators for rate independent elasto-plasticity*, Comput. Meth. Appl. Mech. Eng., **48**: 101-118, 1985.

[72] J.C. Simo, R.L. Taylor, *A return mapping algorithm for plane stress elastoplasticity*, Int. J. Num. Meth. Eng., **22**: 649-670, 1986.

[73] R.L. Taylor, *A finite-element analysis program*, University of California at Berkeley, http://www.ce.berkeley.edu/rlt, 2003.

[74] Ch. Tsakmakis, A. Willuweit, *A comparative study of kinematic hardening rules at finite deformations*, Int. J. Nonl. Mech., **39**: 539-554, 2004.

[75] C.C. Wang, C. Truesdell, *Introduction to Rational Elasticity*, Nordhoff, Leyden, 1973.

[76] M.L. Wilkins, *Calculation of elastic plastic flow*, in Methods in computational physics, ed. B. Alder, vol. 3, 211-263, Academic Press, 1964.

[77] P.J. Yoder, R.G. Whirley, *On the numerical implementation of elasto-plastic models*, J. Appl. Mech., **51**, 283-288, 1984.

[78] H. Ziegler, *A modification of Prager's hardening rule*, Quart. Appl. Math., **17**, 55-65, 1959.

[79] O.C. Zienkiewicz, R.L. Taylor, *The Finite Element Method*, vol. II, McGraw Hill, New York, 2002.